APPENDIX A
EVALUATION MODEL INPUT AND ANALYSIS GUIDELINES

The guidelines for input preparation are included in this appendix. All of the relevant input choices are discussed for the codes involved in the RLBLOCA analysis. The guidelines are separated into those pertaining to the steady state plant model and those that describe the case by case inputs which comprise the uncertainty analysis. Sample problems for Westinghouse 3-loop and 4-loop plants and a CE 2x4 plant are presented in Appendix B to show the behavior of the different plant types, and to demonstrate the capability of the analysis process to address the various plant differences.

A.1 *Base Input Model Guidelines*

The base input model guidelines are provided in the following subsections. This section contains technical guidance for preparation of the standardized S-RELAP5 base input model for realistic large break loss-of-coolant accident (RLBLOCA) analysis of Westinghouse 3- and 4-loop pressurized water reactors (PWR) and Combustion Engineering (CE) 2x4 loop PWRs that exhibit a characteristic bottom-up reflood (i.e., plants with cold leg ECC injection). S-RELAP5 is the primary tool for RLBLOCA analysis. This guideline is provided for the development of RLBLOCA input models only.

This guideline follows the S-RELAP5 modeling conventions for licensing calculations as developed by the RELAP5 Modeling Review Team. The instructions are based on the requirements of the AREVA RLBLOCA methodology. An input file prepared strictly within the provisions of this guideline will be applicable to RLBLOCA analyses.

A.1.1 Guideline Purpose

This guideline describes the input requirements for the AREVA RLBLOCA evaluation methodology. An evaluation methodology is the calculational framework for evaluating the behavior of a reactor system during a postulated transient or design basis accident. It consists of all the necessary information required to derive the final figures of merit (i.e., peak clad temperature and other factors involved in RLBLOCA analyses) from the S-RELAP5 code and its sub-code kernels COPERNIC and ICECON, including

- Field equation formulation (mass, momentum, and energy).
- Phenomenological constitutive models (e.g., various heat and mass transfer models).
- Procedures for treating code input arising from plant geometry and the assumed plant state at transient initiation.
- Procedures for performing calculations.
- Procedures for post-processing code output.

This guideline was developed to define the requirements for addressing the third bullet above. Specifically, the purpose of this guideline is to establish a consistent approach for the following parameters:

- Nodalization.
- Heat structure definition.
- Component modeling.
- Code correlation selections.
- Control variable and trip definition and use.
- Material properties.
- Initialization.

A.1.2 Guideline Philosophy

Evaluation models supporting the performance of emergency core cooling systems provide an estimate of the safety margin associated with the given plant design, fuel configuration, and operational constraints. The term "estimate" implies uncertainty. Sources of uncertainty come from both the physical structure of the plant and the numerical simulation. With the development of the Code Scaling, Applicability, and Uncertainty (CSAU) methodology, the U.S. NRC recognized the practical limits, including uncertainty, that exist in performing large break LOCA analyses for nuclear power plants.

With regard to nodalization, the CSAU methodology states the following (from Reference A-1):

> "The plant model must be nodalized finely enough to represent both the important phenomena and design characteristics of the [Nuclear Power Plant] but coarsely enough to remain economical."
>
> "Thus, the preferred path is to establish a standard [Nuclear Power Plant] nodalization for the subsequent analysis. This minimizes or removes nodalization, and the freedom to manipulate noding, as a contributor to uncertainty."
>
> "Therefore, a nodalization selection procedure defines the minimum noding needed to capture the important phenomena."
>
> "This procedure starts with analyst experience in previous code assessment and application studies and any documented nodalization studies. Next, nodalization studies are performed during the simulation of separate- and integral-effects code data comparisons. Finally, an iterative process using the [Nuclear Power Plant] model is employed to determine sufficiency of the NPP model nodalization."

Inherent in these quotes is the assumption that engineering judgment will be applied to determine the degree of nodalization resolution that is necessary while still being practical. It is a goal of these guidelines to specify any application of engineering judgment incorporated into the RLBLOCA methodology, along with the mechanistic rules required to achieve the following goals:

- Discriminate key structure characteristics.

- Obtain acceptable steady-state agreement with plant.
- Preserve dominant phenomena.
- Maintain reasonable computational economics.
- Maintain scalability.
- Assure accuracy, numerical stability, and convergence.

The modeling task is a mathematical mapping from the physical system to the computational framework of the evaluation model. It is recognized that different approaches to this task can yield different results. For this reason, the pedigree of the evaluation methodology relies on a consistent approach to the modeling task. Because of the complexity of nuclear power plants and design variations between like plants, the concept of a "standard nuclear power plant nodalization" requires clarification. Nodalization has traditionally referred to the mathematical representation of the physical system. This is simply the most recognizable interpretation. This guideline considers the "standard NPP nodalization" to include all computer code input necessary to represent the physical plant, and any engineered features influencing plant performance. These include trips and control systems, component dynamics (e.g., pumps), neutronic definition, fuel state description, and ECCS performance. In addition, the S-RELAP5 code includes flags and other plant-independent input for specific phenomenological code models.

This guideline recognizes that, outside the reactor coolant system, a "standard model" cannot apply to plant-to-plant variations without great simplification. These areas include the containment and the emergency core cooling system. For RLBLOCA analyses these areas are considered boundary conditions. Boundary condition models are to be designed according to the best information the utility customers can provide. It is acceptable, and may be necessary, to incorporate some conservatism to accommodate any uncertainties related to incomplete physical data.

As stated in Section A.1.1, this guideline has been developed to address the "Procedures for treating code input arising from plant geometry and the assumed plant state at transient initiation". The primary challenge in developing a guideline for this purpose is defining procedures that apply plant-to-plant and accommodate various levels of available information. A workable strategy to satisfy these practical constraints requires guidelines that provide the flexibility for engineering judgment, with some effort to anticipate the likely problem areas and to prepare procedures that explicitly account for such problems. To the extent possible, this guideline fulfills this strategy.

Accommodating engineering judgment may appear to leave the methodology vulnerable to analyst interpretation; however, the methodology has been developed considering the importance of the key phenomena influencing the acceptance criteria measures. For those phenomena not demonstrating a strong influence on these measures, a best-estimate approach is taken by considering any available information. Similarly, the relationship of modeling specifics to phenomena can be assessed providing a reasonable engineering judgment. The integrity of the methodology is built on a risk-informed approach (CSAU), emphasizing the primary contributors influencing clad temperatures, but regulations require a method of control over input development. For this reason, much of the task of S-RELAP5 model development has been computer automated. Key design parameters are compiled into a database, and that information is used by an automation program to generate an S-RELAP5 RLBLOCA input file. The automation applies rules that comply with guideline rules provided in this document. Quality assurance will then rely on review of the database and the use of the proper automation code, along with its user input.

A.1.3 Guideline Scope

This input prescription document includes technical issues associated with sound engineering practice, such as nodalization, heat structure definition, and hydraulic loss coefficients), as well as non-technical issues, such as numbering schemes and initial conditions consistent with sound quality practice.

A.1.3.1 Technical Expressions

- Heat structure – A heat conductor (thermal energy source/sink) connected to a hydrodynamic volume.
- Hydrodynamic junction – A connection between hydrodynamic volumes; characterized primarily by vector properties.
- Hydrodynamic volume (also control volume) – A geometric division of a plant model that contains working fluid; characterized primarily by scalar properties.
- Leakage (also bypass) – Flow paths that allow coolant flow to bypass the active core region without going through the fuel; also the fraction of coolant flow that is distributed to leakage paths.

A.1.3.2 Description

This guideline has been developed to satisfy the CSAU Evaluation Methodology (Reference A-1), Step 8: Nuclear Power Plant Nodalization Definition. The general philosophy emphasized in this methodology is presented in Section 9. While no calculational results appear in this document, the information provided here reflects these criteria as demonstrated through numerous S-RELAP5 calculations.

A few approaches are available for demonstrating code stability, convergence, and consistency. In any numerical process, the fidelity of the calculation is dependent on the modeled physics, model nodalization and execution. The presence of approximations in these calculations (e.g., the use of a well-known correlation to approximate the heat transfer coefficient between the rods and coolant) makes the demonstration of code stability, convergence, and consistency difficult to quantify without making conservative assumptions in physical models. Consistent with the CSAU methodology, non-deterministic methods can be applied in this situation without yielding to conservative assumptions. The challenge of this approach is the necessity to quantify model and code uncertainty, and then later apply this statistically in the final determination of the safety parameters limited by regulatory restrictions.

The adequacy of a nodalization is also measured in the ability of the model to capture specific and integral phenomena. This can be quantified by code assessment through the use of data from test facilities and analytical problems with known solutions. This is also advised in Reference A-1.

Key features of the methodology include the following:

- [
  ]
- [
  ]
- [
  ]
- [
  ]

A.1.3.3 Data Sources

The AREVA RLBLOCA automation package shall be used for all analyses. The automation package accesses plant design parameters to calculate key model parameters and creates the COPERNIC and S-RELAP5 input. The database relies heavily on design information from the plant, such as drawings or other verified data sources. In addition, a Plant Parameters Document (PPD) may contain parameters used in safety analyses that describe the configuration of a given plant and that could potentially change from cycle to cycle. Where a PPD exists for the plant being analyzed, the PPD will be used by the analyst as the key information resource.

A.1.3.4 Computer Codes

RLBLOCA calculations will be performed with S-RELAP5. A COPERNIC calculation will be performed to establish the initial fuel rod properties to be used in the S-RELAP5 calculations.

A.1.3.5 Required Input Information

The analyst responsible for developing a plant model will have the following items and information available:

- Plant design information (e.g., drawings or other verified data sources), including all information showing reactor cooling system- related piping and components, ECCS piping from accumulators/SITs and high-pressure and low-pressure injection pumps, secondary side drawings of the steam generators inlet piping and outlet piping to the main steam isolation valve, and reactor vessel drawings (including internal structure).
- Containment volume and surface areas.
- RCS pump data.
- Plant/cycle-specific parameters document.
- Fuel specification document.

- Cycle-specific neutronics input for safety analysis.
- Data on reactor protection system and the engineered safety features actuation system.
- S-RELAP5-, COPERNIC- and ICECON-related documentation.
- References supporting this guideline (handbooks for form loss coefficient calculation, code input manuals, material property references, etc.).

A.1.3.6 Instructions for S-RELAP5 Input

This section contains detailed instructions for preparation and use of the AREVA RLBLOCA code suite. Though the discussion focuses primarily on the S-RELAP5 input data requirements in Reference A-2, instructions are also provided for modeling a fuel rod for COPERNIC burnup analysis, and for modeling a containment using the ICECON-formatted input file. The first section addresses general modeling conventions and parameters. These instructions provide explicit definitions for flag parameters and provide methods for evaluating geometric information. The second section examines each system component explicitly and defines nodalization and any unique modeling conventions. The remaining sections address reactor kinetics, controls and trips, material properties, transient modeling, fuel rod model and containment mode.

A.1.3.6.1 General Modeling Conventions and Parameters

A.1.3.6.1.1 Nodalization

The component numbers identified in Table A-1 are recommended for S-RELAP5 nodalization of the PWR plants. Nodalization schemes must be consistent among different plants, and the component number for the same component should be the same for all plant input models.

Table A-1 Nodalization Numbering for Westinghouse PWR Plants

The nodalization numbering system follows a fixed pattern that has been established based on experience. This system reduces error, is easy to understand, minimizes confusion, allows treatment of 3- and 4-loop plants, as well as CE 2x4 plants, and maintains flexibility to accommodate plant-to-plant differences. Note that, by default, the pressurizer is modeled as being attached to Loop 1. If modeled in a different loop, the first digit of the pressurizer and surgeline components should be changed to correspond to that loop number. For CE 2x4 plants the descriptions for component numbers differ from Westinghouse plants, as shown in Table A-2.

Table A-2 Nodalization Numbering Differences for CE PWR Plants

Specific numbering guidelines are provided in later sections. These are provided for the same reasons as those provided for the general numbering scheme in Table A-1 and Table A-2. It is conceivable that as a result of complex plant geometry, the numbering guidelines may be too constraining. For such circumstances, deviations are acceptable.

The CSAU approach provides latitude in defining modeling rules, based on engineering judgment, of the significance a particular modeling decision has on the calculation of clad temperatures. The input prescription provided reflects the collective years of experience of both AREVA analysts, and the international community of RELAP5 users. At a fundamental level, the technical basis relies on this considerable experience base, and the input prescription reflects consistency from previous LOCA applications of S-RELAP5 and RELAP5, in general.

Clad temperature sensitivity to variations in modeling was examined during the development of the AREVA RLBLOCA methodology. In keeping with the philosophy of the CSAU process, this effort was focused on certain key components of the reactor system. These components were chosen based on their potential influence on the dominant LBLOCA phenomena identified in the RLBLOCA Process Identification and Ranking Table (PIRT) (Table 5-1). It is these areas that are highlighted in this section. For each of these specific areas, a discussion, supported by either physical arguments or by sensitivity studies, is provided stating why the given prescription is acceptable.

Inherent in the simulation of complex systems is the inability to produce a modeling strategy that eliminates code uncertainty associated with nodalization. It is, however, possible to calculate code uncertainties associated with both phenomena and nodalization given suitable experimental data, by defining and "freezing" a nodalization methodology. The pedigree of the code uncertainty calculation then relies on consistent application of the "frozen" nodalization scheme.

Much of the knowledge captured in this guideline originates with the work performed by the INEL RELAP5 development team. The INEL RELAP5 user's guidelines (Reference A-3) were used as a starting point in the development of these guidelines. In general, the nodalization recommendations meet or exceed the level of detail recommended by the INEL.

References are made in this section to sensitivity studies performed during the development of the RLBLOCA methodology for the purpose of defining nodalization. A summary of these studies is provided in Appendix A of the Revision 0 versions of Reference A-4 and in Section 9).

A.1.3.6.1.2 Hydrodynamic Component Modeling

S-RELAP5 provides various component models to provide the analyst flexibility in building plant models. These include the PIPE, BRANCH, SNGLVOL, SNGLJUN, and specialty component models such as PUMP, VALVE, TMDPVOL, and TMDPJUN. Many of these component models can be used interchangeably without significant impact on calculation result. For example, a single volume can be modeled with a SNGLVOL, BRANCH, or 1-volume PIPE component. Though these guidelines provide the analyst some modeling discretion in this regard, the analyst should maintain a strict economy of component models.

The general conventions for use in modeling the hydrodynamic components are described in the following paragraphs. Exceptions to these conventions are highlighted in the component-specific descriptions provided in the latter subsections of this section.

Initial Condition Control Word (bt)

b = 0, No boron present, for all volumes.

t = 3, State is specified by pressure and temperature, for all single-phase volumes without noncondensables.

= 2, State is specified by pressure and quality, for all two-phase volumes without noncondensables, such as the pressurizer and volumes in the steam generator secondary.

= 4, Two-component equilibrium state (pressure, temperature, and quality), for all volumes with noncondensables, such as the upper portion of an accumulator/SIT.

Volume Control Word (input parameters u,m,f,e)

The upper plenum entrainment model (u=1) has been specifically developed to address expected upper plenum entrainment based on assessment of UPTF Tests 10 and 29. The model is described in Section 8.5.1.4. The model is enabled only in the upper plenum components.

[

]

[

]

Junction Control Word (input parameters f,v,c,a,h,s):

RLBLOCA applications must use the Homogeneous-Equilibrium Model for choked flow conditions. The code bias and uncertainty used in RLBLOCA analysis have been derived with this assumption. No other models may be used.

Junction Area and Loss Coefficients

[

]

For most junctions in the reactor vessel, RCS, and ECCS, setting junction areas to 0.0, which results in the use of the minimum area of the two adjacent volumes is equivalent to specifying the actual junction area. This may not be the case for bypass flow paths in the reactor vessel (e.g., downcomer to upper head). Sensitivity studies with S-RELAP5 have shown that code performance is more robust with these junction areas set to 0.0. S-RELAP5 robustness has shown a particular sensitivity to junction modeling for bypass flow paths connecting to or from the downcomer. For this reason, the methodology explicitly specifies these flow areas to be 0.0. To maintain modeling flexibility, junction flow areas may be specified according to need, although, using 0.0 is the recommended default.

For the abrupt area change option (a = 1 or a = 2), the code defines the junction area as the minimum area of the two adjacent volumes, regardless of any junction area specification, and defines the ratio of actual junction flow area (if input by users) to the code-defined junction flow area as throat ratio. (The throat ratio is 1.0 if the junction area is entered as 0.0). The throat ratio is used only when a critical flow condition is allowed ($c \neq 1$). For junctions with the choking flag enabled, the actual area is used when the flow is choked and the minimum of the two volume areas is used when the flow is unchoked. These junctions have the actual area of the junction specified in the input. All user-input form-loss coefficients have to be computed with respect to the code-defined junction flow area.

User-input form-loss coefficients are provided at the important flow restricting locations. Plant derived pressure drop data should be used when available. Form loss can be calculated using the following:

Compute velocity using the specified flow rate (typically in gpm) and the flow area:

$$v\left(\frac{ft}{s}\right) = \frac{Q(gpm)\cdot\frac{0.13368\ ft^3}{gal}}{A(ft^2)\cdot\frac{60\ s}{min}}$$

Using this velocity, compute the loss coefficient:

$$K = \frac{\Delta P}{\rho v^2/2} = \frac{2\cdot\Delta P(psi)\cdot\frac{144\ in^2}{ft^2}\cdot\frac{32.2\ ft\cdot lbm}{lbf\cdot s^2}}{\rho\left(\frac{lbm}{ft^3}\right)v^2\left(\frac{ft^2}{s^2}\right)}$$

where ρ is the saturated liquid density.

When plant differential pressures are not known, formations from Idelchik's Handbook of Hydraulic Resistance (Reference A-5), Crane's Flow of Fluids through Valves, Fittings and Pipes (Reference A-6), or other respected sources may be used to evaluate the loss coefficient. Formulations applying a Reynolds number dependence should not be considered unless explicitly specified elsewhere in this guideline (assume fully turbulent flow), since these require complicated control systems to evaluate the form loss, and do not significantly improve the accuracy of calculations. Examples of other sources are:

- The core, where product specific correlations for loss coefficients are used.
- Other parts of the system where manufacturer or utility supplied values are provided.

The loss coefficients for bypass flow paths are adjusted to produce utility-specified bypass flow rates. This can be achieved by trial and error or using control variables.

[ ]

The loss coefficients for the separator junctions and the junction connecting the downcomer and the boiler in the steam generator secondary side are adjusted to produce a specified steady-state generator level and recirculation ratio. Control variables may be used since the method of trial and error may be too cumbersome for this application.

Initial Flow/Velocity Control Word

= 0, Indicating the initial condition specifies velocity rather than flow.
= 1, Indicating the initial condition specifies flow rather than velocity.

Either option is acceptable.

Volume/Area/Length Specification

Hydrodynamic volumes are modeled by preserving, in terms of priority, lengths, fluid volume, and flow areas, respectively. This prioritizing can result in some unavoidable distortion of the volume-averaged flow area, but this is less important than preserving length or volumes, especially in LOCA analyses.

Numerical stability is improved when the volume length-to-diameter dimension is greater than 0.5. No restriction is imposed on a maximum length-to-diameter for numerical convergence; however, the nodalization described in this section implicitly defines the appropriate length-to-diameter to be applied for analyses.

Elevation Changes

Volume elevation changes are always entered for components. These are important in defining horizontal or vertical flow regime models used in S-RELAP5. Inclination angles are used only to indicate orientation: +90° for upwards, -90° for downwards, 0° for horizontal. Only the sign is then used by S-RELAP5 in the determination of which flow map to use (horizontal or vertical). The magnitude of the inclination angle is ignored.

Component Elevation Closure

Special care must be given to defining component data so that elevation closure is ensured based on plant physical data. Artificial adjustments to plant data are not allowed to arbitrarily force elevation closure.

Surface Roughness

A typical commercial steel pipe roughness value of 1.5×10^{-4} ft is used for all surfaces except for fuel rods, guide and instrument tubes (in the core), and steam generator tubes. Unless better information is available for these components, use a typical drawn tubing roughness value of 5.0×10^{-6} ft (Reference A-7).

Hydraulic Diameter

Hydraulic diameter is one of the important parameters for computing wall friction, interphase friction, interphase mass transfer, and wall heat transfer. It must be specified (entered, or correctly defaulted) for all volumes except the pump. For normal pipe flow, hydraulic diameter is just the pipe diameter. For more complicated geometry, such as within the reactor vessel, hydraulic diameter is evaluated using one of the following formulas: (4*flow area)/(wetted perimeter) or (4*volume)/(wetted surface area).

Initial Conditions

Approximate values for initial state conditions of volumes, and initial flow rates at junctions may be used for most components. Values close to the expected conditions are desirable but not required. Verification of these initial values is not required as long as the expected plant steady-state conditions are obtained after an S-RELAP5 steady-state run. Expected conditions must be specified, and carefully checked, for external sinks or sources such as time-dependent volumes and accumulators.

A.1.3.6.1.3 Control Variables and Trips

The extended numbering option (20600000 card) for trips and (20500000 9999 card) for control variables is used to provide added flexibility. Each control variable and trip has a unique component number, and the same number should be used for all plant input models. Associating control and trip numbers with the hydrodynamic component numbers is not required since it may not be practical to do so.

A.1.3.6.1.4 Heat Structures

In response to changes in fluid conditions during a LOCA, plant components and related structure will store and release thermal energy. While this source of thermal energy is significantly smaller than core power or even pump heat, for fluid conditions at or near saturation, heat structure energy storage and release can significantly alter the two-phase fluid conditions. The important PIRT-defined phenomena, including interfacial drag and heat transfer are, therefore, impacted. For this reason, heat structures must be defined anywhere their presence can significantly impact fluid conditions in the plant's RCS.

In relation to specific important PIRT-defined phenomena, heat structures in the RCS affect coolant subcooling, impacting the extent of post-CHF heat transfer in the core and, in some situations, reactor vessel inventory from downcomer boiling (i.e., hot wall effects). Heat structures in the containment, steam generator secondary and emergency core cooling system are in areas considered as boundary conditions. The objectives of these boundary conditions are met by focusing on how the boundary condition interfaces with the RCS. By convention, detailed models are acceptable and preferred; but, simpler models not including detailed heat structure modeling are also acceptable as long as they meet the requirements of the LOCA calculation. Specifically:

- [

]

- [

]

- [

]

Geometry Flag

= 1, Rectangular structure, e.g., upper and lower core plates.
= 2, Cylindrical structure, e.g., pipes and fuel rods.
= 3, Spherical structure, e.g., upper and lower head walls.

[ ] [

]

Initialization Flag

Because S-RELAP5 will initialize fuel rods based on a COPERNIC calculation, the initialization flag is automatically set to 0 in S-RELAP5 for these fuel rods models; hence, the value of this flag has no impact on calculations. Beyond a single iteration of the heat conduction equation, no steady-state initialization is performed for fuel rods; thus, setting this flag to 0 is consistent with what S-RELAP5 will calculate.

= 1, Heat conduction steady-state initialization enabled, for all heat structures.
= 0, Heat conduction steady-state initialization disabled for fuel rods.

Fuel Rod Model

Gap Conductance Model

= 4, COPERNIC fuel model.

Rupture Model

= 5, Fuel rod rupture model set to use the sampled swelling, rupture and relocation model.

Metal-Water Reaction

= 1, Use Cathcart-Pawel model, recommended for all rods.

Reflood Model

[

]

CHF Option

This option is not used. Do not enter any number for Word 9 and Word 10 on Card 1CCCG000.

Hydraulic Diameter for Heat Transfer

The hydraulic diameter for heat transfer computation defaults to the hydrodynamic volume value. Therefore, in general, it is unnecessary to include Cards 1CCCG801 - 1CCCG899 or Cards 1CCCG901 - 1CCCG999. For some special situations, Word 2 on these cards can be entered to specify a diameter for heat transfer that is different from the hydrodynamic diameter. One particular case occurs when the heat transfer to the steam generator secondary side requires a heat transfer diameter for the secondary side in order to produce specified plant steady-state conditions. An appropriate first estimate value for this case is the tube spacing distance. This value may then be adjusted to obtain the desired primary-to-secondary heat transfer.

Surface Area/Thickness Specification

Heat structures are modeled by preserving, in the following priority, surface area exposed to the fluid, geometry type, and thickness. Some distortion of the geometry type and thickness can occur, but it is less important than distortion of surface areas, especially for LOCA analyses. Surface area is preserved as accurately as is reasonable. If the heat conductors associated with a volume exist as separate pieces, they may be combined or lumped together to form a single piece.

Radial Mesh Points and Interval Lengths

As a one-dimensional code, the fidelity of S-RELAP5's numerical solution of thermal wave transients within heat structures is dependent only on radial nodalization. Nodalization and thermal wave propagation studies have demonstrated that the thermal wave front in very thick metal structures, such as the reactor vessel wall, will propagate only a fraction of the total thickness during the time period of interest for a LOCA. Accurate treatment of a varying structure thickness is of less importance than the surface area consideration and the thermal wave front penetration. To account for this, it is necessary to limit the node lengths in the metal structures and to place a sufficient number of nodes close to the fluid volume. For this reason nodalization of heat structures modeled for RLBLOCA analyses apply a progressive noding scheme.

Althoough there are no universal rules about nodalization schemes for heat conduction, the accuracy of numerical heat conduction simulations is dependent on time step and mesh spacing – but, time steps used in S-RELAP5 are based on processes with faster response times than heat conduction. The sensitivity studies performed for mesh spacing have validated the assertion that mesh spacing near the heat conductor's surface based on a Biot number of 1.0 is sufficient for all phases of a large break LOCA. The Biot number is expressed as:

$$Bi = \frac{h\,\Delta x}{k}$$

where Δx is the mesh spacing, h is the heat transfer coefficient and k is the thermal conductivity.

For common reactor vessel materials exposed to post-blowdown environment, this assumption is satisfied by using a surface mesh size of 0.025 ft or less. Note that during blowdown, conduction from passive heat structures is conduction limited; that is, conduction is unaffected by changes in fluid convection. The progressive mesh spacing scheme of doubling mesh sizes was evaluated by sensitivity studies and demonstrated to be as accurate as using uniform mesh spacing equivalent to the surface mesh spacing size. The heat structure nodalization used for all passive heat conductors in RLBLOCA analyses apply a mesh spacing finer than those evaluated through sensitivity studies. It follows that by applying the prescribed nodalization methodology, the simulation of heat removal from the downcomer or any other heat conductor represents an accurate and best-estimate simulation of the heat conduction process.

By convention, the minimum axial resolution for heat structures corresponds to one heat structure per hydraulic volume. Including more or fewer heat structures is acceptable; however, the proper partitioning of surface area to the hydraulic volume is more complicated. For this reason the recommended axial nodalization is provided to minimize the potential for errors.

The rule, as presented in this guideline, provides for some flexibility in modeling various geometries. The stated approach was applied during the development of the assessment suite used to support the RLBLOCA methodology. While it is unclear what effect finer nodalization would have on the key figure-of-merit, PCT, the uncertainty associated with heat conduction response, would be less. On that basis, the application of the RLBLOCA uncertainties derived based on this guideline's minimum requirements implicitly addresses finer nodalization. The conclusion drawn by previous experience is that, at this resolution, nodalization is a very minor contributor to clad temperature uncertainty. In fact, within this range of modeling, the influence on PCT is assessed to be negligible. Nonetheless, the RLBLOCA automation suite has been developed to apply a consistent heat structure nodalization to assure that mechanistic independent reproduction is possible for RLBLOCA production calculations. Heat structures are modeled for all major RCS conductors (or metals). The minimum resolution for heat structure nodalization corresponds to one heat structure per hydraulic volume. Additional resolution may be required for some components. Heat structure numbers should correspond as closely as possible to the related component numbers. A description of recommended input conventions is presented in the following paragraphs.

The following recommendations define a minimum resolution. Finer nodalization is acceptable; however, analysis-to-analysis consistency will ensure reproducibility and satisfy 10 CFR 50.46 rules.

Fuel Rods

[

]

Steam Generator Tubes

Because the tube walls between the primary side and the secondary side are very thin, two uniformly spaced intervals (three mesh points) are sufficient.

Passive Heat Conductors

For vessel walls with stainless steel cladding, the general rule is two uniformly spaced intervals in the cladding, intervals of approximately 0.02-ft in length for the next three intervals, and a minimum of three, uniformly spaced intervals for the rest of the wall. Examples are reactor vessel, steam generator vessel, steam generator plena, and pressurizer vessels.

For other heat conductors, place three relatively fine intervals close to the surface contacting the fluid volume. For conductors with one insulated side, the first two intervals from the hydrodynamic volume contact surface are uniformly spaced with a thickness of 0.01 ft. The next one or two intervals are approximately 0.02 ft thick, and the rest of the region is divided into a minimum of three uniformly spaced intervals.

For conductors thicker than 0.05 ft with both sides contacting hydro volumes, place two 0.01 ft intervals on both ends (sides). If the middle region is large (> 0.06 ft), assign a minimum of three intervals with the outside intervals (i.e., closest to the surface) approximately 0.02 ft (consistent with the guidelines for insulated heat structures). For a small middle region (< 0.06 ft), use a maximum interval of 0.02 ft with no minimum number of intervals.

A maximum interval of 0.01 ft should be used for thin conductors less than about 0.05 ft thick.

Composition Data

The absolute value of this quantity is the composition number, and it must be identical to the material property table number. The sign indicates whether the region over which this composition is applied is to be included or excluded from the volume-averaged temperature computation. If it is positive, the region is included, and if it is negative, the region is not included. The option to exclude regions from the volume-average temperature integration serves to limit the integration to fuel regions only for use in reactivity feedback calculations. Gap and cladding regions are not included in this case. If the gap conductance model is used, only one interval may be used for the gap region.

A.1.3.6.1.5 Methodology Option

The S-RELAP5 input Card 100 (Problem Type and Option) contains a methodology option in Word 3. This input must be set to PWRLBRV2 to activate various models and options in the code that are required per Reference A-4. [

]

A.1.3.6.2 Component Modeling

The model constituents of S-RELAP5 code represent idealized volume components and component-to-component representations, idealized heat structures and heat structure-to-component representations. As such, complex geometry may need to be approximated. For these situations, approximations applying standard methods within the scope of these guidelines are acceptable. The RLBLOCA automation tool provides a consistent and traceable method for input file creation and should always be used for production calculations.

This section describes the thermal-hydraulic models for the pressurizer and the associated surge line, RCS piping and pumps, steam generators, the reactor vessel, and the ECCS. Statements related to minimum nodalization requirements for heat structures are provided to correspond with the expected hydraulic modeling.

The nodalization of the reactor coolant system loops is the empirical result from the INEL RELAP5 development team (Reference A-3) and AREVA user experience. The few significant deviations between AREVA and INEL guidelines are described as follows.

A.1.3.6.2.1 Pressurizer and Surge Line

This section describes the modeling of the pressurizer vessel and surge line. The spray valves, heaters, safety valves, and pilot/power-operated relief valves (PORVs) are not required for the RLBLOCA analysis. [

]

Pressurizer Vessel

The pressurizer vessel is modeled as follows (see Figure A-2):

- [

  ] the height of each hemispherical volume is the actual height or may be approximated as the radius of the hemisphere.
- Vessel height is maintained.
- Hydraulic diameter is evaluated individually for each volume or is approximated as the diameter of the cylindrical region for all volumes.

- A minimum of one heat structure per control volume is used to model the vessel wall to correspond to the [ ] volumes used to model the hydraulic volume.
- Modeling of the pressurizer heaters is unnecessary.

The pressurizer is always connected to primary loop number 1 by default. This is done to facilitate the use of automation tools, but it may be desirable to connect it to another loop to correspond to plant configuration. Note that the broken cold leg must be in the same loop as that containing the pressurizer. This increases the probability that pressurizer fluid will leave via the break, rather than be available to the core.

The pipe is oriented upward, which means that the first volume is at the bottom. For steady-state initialization, a steam source volume is connected to the top volume to maintain the system pressure. Additionally, a liquid source volume is connected to the bottom volume to maintain the liquid level. These two volumes, and associated junctions, are deleted, or the flows are shut off during the transient (restart) calculation.

Pressurizer Surgeline

The surgeline is modeled as follows:

- [ ] An acceptable model is one that, at a minimum, preserves flow length, area, volume, elevation and any relevant form losses.
- A minimum of one heat structure per control volume is used to model the surgeline pipe wall.
- The surgeline-pressurizer nozzle form loss is modeled with a [ ] This may be obtained from plant data, an approximation of the form-loss from Idelchik (Reference A-5), or other appropriate formulas.
- [ ]

- The surgeline-hot leg connection is modeled as a cross-flow junction. However, if exceptions can be justified (e.g., unique physical orientation), then a normal junction can be applied. [

]

- The surgeline-hot leg connection is a tee. The loss coefficient for a tee connection is variable, depending on the relative flow rates in the main and branch lines. To accurately model the loss, the control variable input for loss coefficient computation can be used. One control variable can be used for both forward and reverse coefficients, since, depending on the flow direction, only one coefficient is used at a time to compute the pressure loss. The formula for the loss coefficient control variable can be found in many fluid dynamics handbooks, but the formula by

[ ]

is preferred, based on user experience.

A.1.3.6.2.2 Reactor Coolant System Piping

The RCS loop piping is divided into the hot legs, crossover legs, and cold legs. The configuration for these components is included in Figure A-2.

Hot Leg Piping

Since the hot leg nozzle from the reactor vessel and the hot leg nozzle connection to the steam generator inlet plenum do not have a constant ID, the modeled volume of the hot leg will not exactly match the actual volume. Because this small deviation will have a negligible effect on overall coolant inventory, it has a negligible effect on clad temperatures. This simplification has been done to facilitate automation. The hot leg section extends from the core barrel interface to the entrance of the steam generator inlet plenum. This includes the vessel outlet nozzle, steam generator inlet nozzle, and the piping between them. The hot leg is modeled with a five-volume pipe component. Other key points include the following:

- The steam generator inlet nozzle and upward bend is modeled as the [

  ]

- [

  ]

- [

  ]

- [

  ]

- The pressurizer surgeline is connected to the hot leg of Loop 1 by default, regardless of which loop contains the connection in the plant drawings. Since within the RCS all loops are identical, the actual loop number is of no consequence. It is placed in Loop 1 for standardization and automation tasks, however it may be connected to the same loop as in the plant if desired. Note that the broken cold leg must be in the same loop as that containing the pressurizer. [

  ] The exact connection position is not critical.

- [

]

- A minimum of one heat structure per control volume is used to represent the pipe wall. The vessel outlet and steam generator inlet nozzles are approximated as having the same thickness as the hot leg piping.

Crossover Leg Piping

The crossover leg piping consists of piping from the steam generator outlet plenum to the pump, including the steam generator outlet nozzle but excluding the pump suction nozzle. Note that for CE 2x4 plants, two crossover legs begin from a single steam generator. Guidelines for the crossover leg piping segments are as follows:

- The crossover leg is modeled by a pipe component with [ ] volumes. [

]

- [

]

- The elevation of the centerline of the horizontal segment relative to the reactor vessel nozzle centerline is input as the actual elevation difference.
- Loss coefficients for the bends are to be included.
- A minimum of one heat structure per control volume is used to represent the pipe wall. Steam generator and pump nozzles are approximated as having the same thickness as the crossover leg piping.

Pump Model

It is generally considered that for limiting large break LOCAs, after pump coastdown the influence of the pump on clad temperatures rapidly diminishes as coolant flashes and exits the cold leg. For this reason, and since the break spectrum treats break sizes down to the SBLOCA range, the pump model is inherited from the SBLOCA methodology (Reference A-11). Nonetheless, the objective of pump modeling for RLBLOCA applications is to capture the appropriate amount of liquid below and above the cold leg and to capture the elevation at which liquid fallback would occur. While still a minor contributor to clad temperature response, liquid fallback may influence clad temperatures in two ways: 1) loss of coolant available to the core and, 2) potential steam binding.

Type B pumps (see bullet list following the discussion in this section) call for the discharge volume BRANCH component to be modeled with an elevation change equal to two times the weir or spillway height. The two times height compensates for the gravity/2 term in S-RELAP5, which comes from the finite differencing between cell center to cell center.

Following a pump trip or loss of AC power, pump coastdown will be determined by the moment of inertia, the friction torque, and the interaction (through the homologous curves) between the pumped fluid and the impeller. While the moment of inertia can be typically found from standard pump data, frictional torque is rarely provided. The frictional torque model is best described as a curve fit derived from pump-specific coastdown data. The guideline recommendation for frictional torque parameters is a "rule-of-thumb" based on the original INEL guideline (the RLBLOCA rule-of-thumb conservatively applies 2.5 times more frictional torque than the INEL model); nonetheless, many "acceptable" curve fits are considered possible based on code-to-data comparisons. This rule-of-thumb has demonstrated reasonable pump-coastdown agreement for Westinghouse 93 and 93A pumps. Clad temperatures are phenomenologically sensitive to pump coastdown in its influence on steam binding and break flow. Variation in pump coastdown characteristics generally causes the steam binding and break flow effects on PCT to be counter to one another. That is, higher pump flow will remove more coolant from the RCS and decrease steam binding influences, while lower pump flow will remove less coolant from the RCS and increase steam binding influences. For this reason, it is impossible to make a general conclusion about the clad temperature sensitivity to this parameter. For RLBLOCA analyses pump coastdown dynamics should be assessed for reasonableness

The general pump model of RELAP5/MOD3 is used in S-RELAP5. This model also includes the CE-EPRI pump performance degradation data (Reference A-9). The CE-EPRI pump two-phase degradation test results are based on pumps that are similar to PWR reactor coolant pumps (RCPs). The CE-EPRI data also include torque degradation data represented as a torque multiplier, which is a function of void fraction only. These data are incorporated through the input to S-RELAP5. The guidelines for modeling the reactor coolant pumps are as follows:

- Pumps will vary from plant-to-plant. For modeling purposes two generalized pump types have been identified. The distinction is based on the elevation of the spillway at the pump impeller exit. Pumps with this spillway above the cold leg centerline are to be considered Type A and pumps with this spillway at or below the cold leg centerline are to be considered Type B. The Westinghouse 93 pump is modeled as a Type A; while the Westinghouse 93A pump is modeled as a Type B. It is conceivable that the following guidelines addressing these two pump types are not generally applicable. [

]

- Both pump types are modeled in two sections. [

]

- [

] In addition, the node elevations and displacements will preserve the reactor coolant pump height and volume.

- [

]

- [ ] specify volume either explicitly or by specifying the area that corresponds to the total volume. The hydraulic diameter of the [ ] component may be approximated as that of the downstream cold leg piping.

- [

]

- [

]

- Parameters on Card CCC0301 supply key information that tells S-RELAP5 where to find data describing pump dynamics. Words 1 through 3 can take the pump component number to pump data used in defining another pump. Otherwise, abide by the following instructions:
  - W1: S-RELAP5 contains built-in, single-phase homologous data for a Bingham Pump Company pump and a Westinghouse Electric Corporation pump type 93. If the RCS pumps in the plant correspond to one of these pump types, the built-in data can be used. If these pump models do not correspond to the actual pumps in the plant, appropriate homologous curves must be supplied by the user. By demonstrating reasonable agreement of simulated coastdown characteristics with plant flow coastdown data, one of the built-in pumps may be used.
  - W2 and W3: The EPRI two-phase pump degradation model is used. This requires that -2 be entered for the two-phase index (W2), and that the EPRI head difference curves, torque difference curves, and torque difference multiplier table be input (W3 = 0).
  - W4: No pump motor torque table is used; enter -1 for word 4 on card CCC0301.
  - W5: A simple two-point "time-dependent" pump rotational velocity table is included, as needed by the pump speed control system, by entering 0. The actually table is entered on cards CCC6100 - CCC6199. The search variable for this table is defined by a control system (see Section A.1.3.6.4.2) and the two points in the table sufficiently bound expected behavior of the control system.
  - W6: A trip number is supplied identifying whether the pump is powered.
  - [ ]

- By convention, the RCPs frictional torque is modeled as a quadratic function of rotational velocity. It is recommended that the TF0 and TF2 frictional torque coefficients be initially set to [ ] of the rated torque value, while TF1 and TF3 are set to [

  ] If better information is available, an alternative representation may be used with no guideline-directed constraints on the four frictional torque model parameters.

- A minimum of one heat structure per control volume is used to represent the pump [ ] The complex geometry of the pump prohibits precise modeling; hence, reasonable approximations may be made. For consistency, the automation tool will represent the pump casing by a cylindrical heat structure with [

  ] By applying this approach, the actual metal mass of the pump will be greater than that accounted for by simply using the pump casing thickness, since the thermal masses of the impeller, shaft, and bearings are ignored. However, the difference is compensated by the assumption in calculating surface area factor of a long cylindrical flow path instead of the actual pump torus. The left radial boundary is assumed to be the inner radius of the crossover leg piping. The right radial boundary is then determined by adding the pump casing thickness.

Cold Leg Piping

A coarse broken loop cold leg nodalization has been empirically demonstrated to improve stability of water property estimations, which is particularly important near the break for calculating the maximum mass flux (i.e., choking). The cold leg section extends from the RCP discharge to and including the reactor vessel inlet nozzle. The cold legs in all loops are modeled identically. The modeling guidelines are as follows:

- The cold leg piping is nodalized as [ ] pipe components separated at the point corresponding to the modeled break plane location in the broken loop. The break plane is located downstream of the last emergency core cooling injection location.

- [

  ] If multiple emergency core cooling injection locations exist, they are all modeled at the point of the first injection location (nearest the pump). If the first emergency core cooling injection location is different for different loops, the averaged location over all loops is used. Emergency core cooling injection is connected to the inlet of the [ ]

- The last volume in the cold leg is given the length of the reactor vessel inlet nozzle. The flow area or fluid volume of this volume is adjusted to account for the taper in the inlet nozzle, calculated from a standard formula for the volume of a frustum of a right circular cone:

$$V_{nozzle} = \frac{\pi}{3} h\left(r^2 + rr' + r'^2\right)$$

  where h is the length of the nozzle, r is the radius of the cold leg opening at the inner vessel wall, and r′ is the cold leg radius.

- [

  ]

- [

  ]

- The cold leg connection to the downcomer is modeled with the junction orientation from each cold leg to the downcomer. Each of these junctions is a [

]

The junction area is that of the cold leg opening at the vessel wall.

- A minimum of one heat structure per control volume is used to represent the pipe wall. The reactor vessel inlet and pump outlet nozzles are approximated as having the same thickness as the cold leg wall.
- For the specific case of an internal pipe junction with no area change and no specified loss coefficient, note that "a=0" is an additional exception to the "a=2" convention (or "rule") for a multiple junctions connecting to a single volume face. Pipe component number 150 represents one of the RCS cold legs. [

] Page 6-2 of the S-RELAP5 user manual (Reference A-2) presents cross flow and time-dependent junctions as the only (currently recognized) exceptions to using "a=2" for junctions involved in multiple connections.

[

]

- [

]

A.1.3.6.2.3 Steam Generator

The basic steam generator model is shown in Figure A-2 and Figure A-3.

Steam Generator Primary Side

The Wallis parameters used for the steam generator inlet CCFL model have been derived from UPTF small break LOCA test 11 (Section 8.2.9.7). These values are typically unimportant for large break LOCA, but since this methodology examines breaks near the small break range, these values are retained in this methodology. The guidelines for modeling the primary side are as follows:

- The inlet/outlet plena are each modeled as a BRANCH component with two junctions. For the inlet side, these connect from the hot leg and to the tubes. On the outlet side, these connect from the tubes and to the crossover leg. A third junction is required in the outlet plenum for a CE plant as there are two crossover legs connected to each outlet plenum.
- [

]
- [

]

- The characterization of the inlet and outlet plena is to be identical. The volume of the plena can either be entered directly (if supplied by the utility), or calculated as one-fourth of the volume of a sphere minus relevant internals. The volume length and elevation is set to the elevation difference between the location of the inlet nozzle and the bottom of the tubesheet. The junction flow area is input as 0.

- The tube region is modeled using a pipe component with [

  ] The inlet and outlet tubesheet regions are each modeled as an additional volume at the beginning and end of the same pipe component, also with a + or -90° orientation. The total length of the active tube portion of the pipe preserves the total secondary side tube surface area from the plant data. For plants with steam generators having an axial economizer, the number of volumes in the active tube length may be increased by two (one up and one down) because of the longer tube length.

- A minimum of [ ] heat structures are to be used to model steam generator metal mass in contact with primary side volumes. This corresponds to one heat structure per hydraulic volume (plena and tubes), plus one heat structure modeling the partition between the inlet and outlet plena.

- The inlet and outlet plena heat structures (2) are modeled in spherical geometry. The surface area factor is approximately 0.25 (i.e., corresponding to one-quarter of a sphere less the partition plate volume).

- A heat structure component is used to model the partition wall between the inlet and outlet plena. It is represented by a rectangular heat structure with one axial node. The left side is connected to the inlet plenum and the right side is connected to the outlet plenum. The surface area of each side of the structure is the area of a semi-circle with a radius equal to the inside radius of the plenum.

- The tubesheet heat structure is modeled as a plate with a thickness greater than two feet for simulating heat storage. There are two separate structures for each generator: one attached to the inlet tubesheet region and one to the outlet tubesheet region. This region is modeled in cylindrical geometry with the left radial boundary at the inner radius of a single U-tube. This side is in contact with the primary side volume. The total surface area in contact with the primary side is modeled as best-estimate and the component total mass and material composition is applied in deriving the radial nodalization. The volume of the tubesheet associated with each tube must consider the tube array configuration (rectangular or triangular). There are no connections to the secondary coolant volumes.

- The tube region heat structures [ ] are modeled in cylindrical geometry with a left radial boundary at the inner radius of a single U-tube in contact with a primary side volume and a right boundary at the outer radius in contact with a secondary side volume.

- Typical drawn tube surface roughness is used (5.0×10^{-6} ft) unless a known value is available.

Steam Generator Secondary Side

The role of the steam generator during a large break is dominated by its contribution to steam binding. Modeling rapid isolation of the steam generator, thus minimizing heat transfer to the secondary side, is considered a bounding assumption in terms of the effect of steam generator modeling and related dynamics influencing steam binding. In general, large break LOCA is statistically insensitive to steam generator secondary nodalization. For this reason, the secondary sides of the steam generators can be modeled identically (in any plant-specific input file). Concessions can be made for unique designs (such as generators with axial economizers) to account for significantly longer tube length. This approach will also improve control system response during initialization.

A simplified, generalized model of the steam generator secondary side has been chosen. Pre-heaters are not modeled explicitly, although the model is revised to capture the behavior of a steam generator with an axial economizer. Likewise, although there are typically a primary and a secondary steam separator, only one separator component is used in the model. The added complexity of modeling these features does not improve the accuracy of the simulations. The guidelines for modeling the steam generator secondary side are as follows (see Figure A-3):

- The downcomer is divided into [ ] volumes. [

  ] For steam generators with feedwater nozzles along this length, the nozzle is modeled as a normal junction at the location closest to the actual feedwater injection elevation.

- The boiler region at the elevations of the U-tubes is modeled as a pipe with [

  ]

- The primary separators (swirl vane, boiler exit) are modeled as a BRANCH component, not a separator component. The physical height and elevation of the swirl-vane separators is maintained in the BRANCH component.

- The secondary separators and dryers are modeled as a SEPARATR component. All liquid that recirculates back to the downcomer is assumed to pass through the separator liquid return junction. Initial estimates for the VOVER and VUNDER parameters are [

  ]

- A separator drain may be modeled as a single volume spanning the length of the primary separators. If used, the liquid return junction from the SEPARATR component is connected to the inlet of the separator drain component. The outlet of the separator drain must connect to the downcomer. This component may be necessary to achieve sufficient code agreement with the steam generator data at steady-state, full power conditions.

- The steam dome is modeled as one volume.

- The steam exit piping from the steam dome to the main steam isolation valves (MSIVs) is modeled using an equivalent length for all the loops; however, using the exact average length is not required for RLBLOCA analysis. The steam line ends with a VALVE component (servo valve SRVVLV) connection to a TMDPVOL. The steam flow control system is applied to each of these valve components. This steam flow control system is used in the model initialization to obtain the desired primary side temperature.

- Appropriate leak paths may be included as necessary to achieve sufficient code agreement with the steam generator data at steady-state, full power conditions. Use an area of 0.0 and adjust form losses to tune code results to the desired state. (Note: "desired state" may include parameters other than plant-supplied data such as steam separator void fraction, which has shown sensitivity to the presence of certain leak flow paths.)

- [

]

- To facilitate steady-state initialization, a control variable may be defined adjusting the loss coefficients on the junction between the downcomer and the boiler to obtain the specified steam generator level. The difference between the current and specified levels is used to adjust the loss coefficients evaluated by the control variable. The control variable must be deleted or disabled in the restart run for the transient calculation. An acceptable alternative to an initialization controller to obtain the target level would be one to obtain a target initial mass. Adjustments must be made to the junction loss coefficients to obtain both an initial level and mass within acceptable tolerances of the target values.
- To facilitate steady-state initialization, a control variable may be defined adjusting the loss coefficients on the liquid return junction of the separator (the second junction) to obtain the specified steam generator recirculation ratio. The difference between the current and specified recirculation ratio is used to adjust the loss coefficients evaluated by the control variable. The control variable must be deleted or disabled in the restart run for the transient calculation.
- Main and auxiliary feedwater flows are modeled with TMDPVOL and TMDPJUN components. The connection to the downcomer is at the elevation of the main feedwater nozzle or feed sparger ring. It is possible that for many RLBLOCA analyses, auxiliary feedwater is not activated. If this can be determined, then modeling of the auxiliary feedwater system is optional.

- Locations of level taps are identified to satisfy control system requirements. The SG water level is calculated in control variables as a [

]

A.1.3.6.2.4 Reactor Vessel

The reactor vessel model represents a major departure from past RELAP5-based modeling. This is primarily the byproduct of the TWODEE component created specifically for S-RELAP5. Extensive calculational investigation has been performed to support the model described in this guideline.

The reactor vessel model for RLBLOCA analysis is shown in Figure A-4. It specifies the use of the TWODEE-A component for modeling the downcomer (axial, azimuthal), and a TWODEE component for modeling the core (axial, radial) and the upper plenum (axial, radial) regions. This allows a more realistic calculation of the asymmetrical flows during blowdown and reflood in both the core and RCS piping.

Reactor Vessel Downcomer

A number of sensitivity studies have been done in evaluating the acceptability of the downcomer nodalization. The primary phenomenological concerns are downcomer boiling and CCFL. This model was further assessed during NRC review of the RLBLOCA methodology. The response to the Request for Additional Information #27 provides considerable technical support for this model (Reference A-10).

The reactor downcomer is modeled for RLBLOCA analysis using a two-dimensional (axial and azimuthal) (TWODEE-A) component to simulate the asymmetrical flows that occur during the LOCA. The azimuthal configuration is dependent on the vessel geometry and is defined to physically simulate the unique configuration of the inlet/outlet nozzles. Typical inlet nozzle downcomer configurations are shown in Figure A-5 for Westinghouse 3-loop and 4-loop and Combustion Engineering (CE) 2x4 loop vessel configurations.

[

]

- [

]

[

]

[ ]

- Axial junction loss coefficients in the downcomer are calculated based on the standard area change relationships from Reference A-5, [

]

- Azimuthal junction loss coefficients are calculated based on the Reference A-5, Diagram 6-1 formulation for a curved rectangular duct. The duct height is the axial height of the downcomer volume, the duct width is the radial downcomer width, and the duct length is the arc length between the centers of the adjacent azimuthal volumes.
- [

]

- [

]

  - To prevent asymmetric steady-state flows in the downcomer, each top level downcomer volume must be connected to the upper head.
  - Flow areas are set to 0.0 (causing the code to select the minimum of the connected volume flow areas), and the loss coefficients are identical for each of these junctions. The loss coefficient must be tuned to obtain the specified bypass flow rate manually or by using a control variable.
- The junctions between the downcomer and lower plenum are external to the downcomer component and have downcomer volumes as from-volumes.
- One heat structure for each fluid volume, or a minimum of [ ] heat structures are used to model the reactor vessel wall for a Westinghouse 3-loop plant. A minimum of [ ] heat structures are used to model the reactor vessel wall for a 4-loop plant or for a CE plant. The left boundary of each structure is connected to a separate downcomer hydraulic volume. The right boundary is insulated. Appropriate simplification and approximation can be applied. The area of the wall at the nozzle belt region is appropriately reduced to account for the openings of the hot and cold legs.

- One heat structure for each fluid volume, or a minimum of [ ] heat structures is used to model the thermal shield or neutron pads along the active length of the core for a Westinghouse 3-loop and Westinghouse 4-loop or CE plant, respectively. The downcomer hydraulic volume will provide both the left and right boundaries, with each structure connected to a separate downcomer volume at the active core elevations. Appropriate simplification and approximation can be applied (e.g., lumping thermal shield/neutron pads and core barrel are acceptable when the gap between them is very small). Additional heat structures may be added to model extensions of the thermal shield/neutron pads beyond the active length of the core. A few plants are known to have neither thermal shields, nor neutron pads. This heat structure is neglected for this situation.

- One heat structure is used to model each distinct region of the core barrel for all plants. A distinct region is one with a unique volume number in contact with the barrel, keeping in mind that both the downcomer and the upper plenum are TWODEE components, each volume of which has a separate heat structure if in contact with the barrel. This will typically result in [ ] separate structures for a Westinghouse 3-loop plant and [ ] structures for a 4-loop or CE plant. The construction is complicated by the fact that the elevation of volume boundaries on either side of the barrel do not coincide in the upper plenum region. The left boundary spans from the lower plenum to the baffle region to the upper plenum. The right boundary spans the downcomer. Appropriate simplification and approximation can be applied.

[

]

The cold legs enter the downcomer at the [ ] axial level. The MULTJUN containing the cold leg connections must have the junction areas calculated from the diameter of the cold leg opening at the reactor vessel wall, and has loss coefficients calculated from an appropriate physical situation such as a piping exit with the flow directed against a baffle from Reference A-5, Diagram 11-7 (forward loss) or Diagram 3-5 (reverse loss).

Lower Vessel

A set of sensitivity studies was done to evaluate the lower head nodalization. Previous lower vessel modeling studies with RELAP5-based codes have recommended either very coarse nodalization or a nodalization including a dead-end volume at the bottom of the lower head. AREVA concluded that these configurations could adversely influence LBLOCA calculations and chose between a 3-node model and a TWODEE component model. Both models were studied using UPTF Test 6 data and with convergence studies using the 3-loop sample problem of Revision 0. [

]

The lower vessel includes all volumes from the bottom of the active fuel to the bottom of the lower head and is divided into three regions: lower plenum, lower head, and downcomer extension. The essential features of this model are:

- Lower plenum region extending from the bottom of the active fuel down to the bottom of the casting support location for the lower support plate or support dome at the core barrel. It is modeled as a single volume (i.e., SNGLVOL or BRANCH component).

- Lower head region extends from the bottom of the lower support plate to the bottom of the vessel. It is modeled as a PIPE component with two volumes. [

]

- Downcomer extension region extending from the bottom of the lower support plate to the top of the lower head's bottom volume. It is modeled as a [

]

- [

]

- The lower nozzle loss coefficient is applied at the junctions connecting to the active core region. Since the core is an upward oriented two-dimensional component, the from-volume of these core connection junctions is the lower plenum volume.
- A minimum of [ ] heat structures are used to model the lower head vessel walls. [

]

- Hydraulic diameter is calculated by assuming the 4*fluid volume/(surface area) relationship. It considers the surface area of the vessel walls and major internals including the lower core plate, lower support plate or casting, support columns, guide tubes, and lower unheated rods.

- A minimum of [ ] heat structures are used to represent the major lower vessel internals, including lower head plates (base plate and instrumentation tie plates, [ ] support and guide tube/instrument columns [( ] lower support plate or support casting [ ] lower plenum remainder (e.g., diffuser; [ ] The last structure may include the lower core plate, support and guide tube portion in the lower plenum, and unheated rods. CE plants will also have a flow skirt heat structure that connects to both the downcomer extension and upper lower head fluid volumes. Depending on the information available, simplification and approximation may be necessary.

[
]

Baffle Bypass Region

A bypass path is included to account for the flow in the core baffle region. In some plants, this section may be a negligible leakage path, so this component may be neglected. In other cases, the modeling guidelines for this region are as follows:

- The region is modeled using a [ ] PIPE component.
- The lower junction is connected to the top of the lower plenum volume.
- Depending on the plant type, this region may be connected as either a downcomer bypass with the top junctions connected to the downcomer third level volumes, or as a core bypass with the top junction connected to the upper plenum volume. The bottom junction is at the lower plenum.

- For the case of a downcomer bypass,
  - The component is oriented downward and the length of the first volume may be adjusted to have correct elevation change for a cross-flow connection from the downcomer two-dimensional component.
  - [

    ]
  - The junction area from the downcomer to the bypass are set to 0.0 and form losses adjusted to get proper flow and equal liquid velocities between the parallel junctions.
- The core baffle (including internals) is modeled with a minimum of [ ] cylindrical heat structures (one per peripheral core control volume). The left and right boundaries are connected to the baffle bypass and the outer region of the core, respectively. Portions of the core baffle may extend into the lower plenum and the unheated core exit region.
- The hydraulic diameter and loss coefficient can be obtained from the geometrical conditions, but accuracy is not critical because the form-loss coefficients may be adjusted during steady-state initialization to give the proper bypass flow rate.
- [

  ]

Control Rod Guide Tube/Instrument Tube Bypass Region/Upper Head Injection Columns

This region represents the core bypass through the fuel assembly control rod guide tubes and instrument tubes. The guidelines are as follows:

- The region is modeled using a [ ] pipe component in each radial core ring. This separation is necessary to prevent any nonrealistic flow patterns resulting from asymmetric modeling. The flow area is the cross-sectional area of all guide and/or instrument tubes in the particular radial core ring.
- The tube walls are modeled as a heat structure connected to both the active core and bypass volumes.
- The hydraulic diameter is chosen as the inside diameter of a single guide tube/instrument tube.
- By convention, the CCFL parameters at the bypass exit are set to be [ ] The tops of the bypass volumes are connected to the unheated volume from the appropriate two-dimensional core channel in a manner that best represents the physical configuration. Cross-flow junctions are acceptable to ensure that the bypass guide tube elevation is accurately modeled. [ ]
- An initial value for the form-loss coefficient at the inlet to and the outlet from the bypass can be estimated from the nominal core pressure drop, but this value is not significant since it is adjusted during steady-state initialization to give the proper bypass flow rate through the region. [ ]
- [ ]

- The number of heat structures per guide and/or instrument tube correspond to the number of axial volumes in the core. The left boundary is connected to the guide and/or instrument tube and the right boundary is connected to the hydraulic volumes in the appropriate core region. For plants designed with guide bars instead of guide tubes, heat structures representing guide bars on an assembly's periphery are included as a separate heat structure modeled with the number of axial nodes that corresponds with the core TWODEE component.

- [

]

A subset of Westinghouse 4-loop plants were originally designed for a portion of ECCS to be delivered directly to the top of the reactor vessel. While this feature has been disabled by plant modifications to cap the associated piping connections, a "left over" feature is the presence of hollow Upper Head Injection (UHI) support columns within the reactor vessel. In addition, the Control Rod Guide Tube (CRGT) structures in the upper internals, these UHI columns provide a separate flow path through the Upper Support Plate, from the Upper Head to the bottom of the Upper Plenum.

Each PIPE component representing the UHI columns would have [ ] nodes and extend from the bottom of the Upper Plenum to the middle of the bottom node of the Upper Head. [

]

[

]

Each junction at the bottom of the column is "from" the inlet of the bottom node of the Upper Plenum "to" the inlet of the bottom node of the UHI column. The "inlet" to "inlet" connection (and the choice of a "normal" junction) places the junction at the appropriate elevation at the top of the Upper Core Plate. Even though the nozzle at the bottom of the UHI column may extend slightly lower (below the plane of the top surface of the upper core plate), the connection to the Upper Plenum has the advantage of avoiding any change to current core exit [

]

Core Region

Core axial nodalization is based on sensitivity studies using the FLECHT-SEASET Test 31504.

[

]

[

]

Because axial power shapes are replaced for RLBLOCA analyses, any reasonable shape is acceptable for the base input file.

[

]

This region extends from the bottom of the active core to the top of the upper core plate. The region is nodalized as [

] as shown in Figure A-6 and Figure A-7. [

] The component is oriented upward. The first [ ] axial levels cover the entire active core region, and an additional volume covers the unheated end of the fuel rods, upper assembly nozzles, and upper core plate. A sample nodalization of an AREVA fuel assembly with HTP spacers is shown in Figure A-8. This component has [ ] axial volumes and [ ] junctions. Key hydrodynamic modeling features include the following:

- [

]

- Use the default for the axial junction flow areas (input zero) and use the gap flow area between regions as the y-direction junction flow area (accounting for the expected number of assembly faces between each radial ring). Also use default junction flow area at the top unheated region (input zero). The following function is acceptable for defining the total gap area between core regions, other approaches providing a more precise estimate are also considered acceptable:

$$gap = N_{sides}\, dx\, (N_{rod} - 1)\, (Pitch_{rod} - D_{rod})$$

Where *dx* is the volume height, N_{rod} is the number of rods on a assembly side, and N_{sides} is the effective number of assembly sides that define the gap.

- The hydraulic diameter of the axial nodes is that of the fuel assembly, which means it includes both fuel pins and guide tube (or bar) and/or instrument tubes. For an assembly with fuel pins and similar guide or instrument tubes only, the follow expression is applied:

$$D_h = \frac{4A_{flow}}{P_w} = \frac{4\left(Pitch_{ass}{}^2 - \#_{rods}\,\pi\left(\frac{OD_{clad}}{2}\right)^2 - \#_{gt}\,\pi\left(\frac{OD_{gt}}{2}\right)^2 \right)}{\#_{rods}\,\pi OD_{clad} + \#_{gt}\,\pi OD_{gt}}$$

where *gt* refers to guide tube (or bar) and/or instrument tubes.

The hydraulic diameter in the y-direction can be calculated as

$$D_{h,y} = 4\frac{(Pitch_{rod} - D_{rod})}{2}$$

[

]

- [

]

- For AREVA-built assemblies, proprietary formulas describing the form-loss coefficients of key assembly components (such as spacers, tie-plates), or component groupings (such as inlet/outlet regions) are likely to be available. The loss coefficients are assigned to the nearest modeled junction, including the inlet and outlet junctions attached to this TWODEE core component. These parameters may be adjusted during steady-state initialization to match best-estimate core pressure drop information.

- Radial loss coefficients in the core region may be calculated using formulations for tube banks, [

]

- A MULTJUN is used to model the core exit junctions for the core regions other than the hot assembly. For all plants, the to-volume for exit junctions (external to the two-dimensional component) is the bottom volume of the upper plenum TWODEE component and the junction flag is [

]

- The exit junction from the first radial ring is modeled independently from the other core-to-upper-plenum junctions. This is modeled with a SNGLJUN component and connects the hot assembly ring to the [

]

- [

]

- [

  ]

- [

  ]

- In a mixed core configuration (fuel assemblies from two fuel vendors) the most probable configuration would be a checkerboard pattern of fresh and burnt fuel around the hot assembly and surrounding assemblies. In the outer periphery, only burnt fuel would be expected. The balance of the fresh fuel assemblies will fall in the average assembly region. [

  ]

- The analysis of mixed cores must consider the phenomenological impact of assembly pressure drop differences. This relates to differences in flow area and form losses. The recommended approach is to model the hot assembly with the highest pressure drop (may or may not be an AREVA product) and then weight the flow areas and form losses in other regions by the expected ratio of assembly types in each region. [

  ]

- A minimum of [ ] heat structures are used to model the unheated core, upper assembly nozzle, and upper core plate (i.e., the top axial level). The unheated core and upper assembly nozzle have connections to both the left and right boundaries. The upper core plate will connect to the top core level on the left and the bottom upper plenum region on the right.

- A minimum of [ ] fuel "rods" are used to model the active core: [

] The heat structure modeling conventions for fuel rods described in Section A.1.3.6.1.4 are used for the fuel rods. Axially, each rod has [ ] heat structures of equal length per hydraulic volume [

] This information must also be present in the COPERNIC model.

[

] Additional guidelines for the fuel rod heat structures are as follows:

- [

]

- [

]

- The Cathcart-Pawel metal-water reaction model is activated by setting the metal-water reaction flag = 1.

- [

]

- Appropriate reference associating the COPERNIC rod number to a specific rod heat structure is necessary. This is done on heat structure card 1CCCG004. Words 1 through 4 are required for this card. Only W1 and W4 are important for LBLOCA simulation.

- An energy deposition factor or gamma smearing factor of [ ] for all modeled rods in the base input file.

- Reasonable and representative power fractions should be provided in the source data cards (1CCCG701). Core and radial power peaking factors (F_q and $F_{\Delta h}$) may be useful parameters to aid in the generation of axial and radial power profiles. Since the power profiles used in the base model are replaced by sampled power profiles during an analysis, this is not an absolute requirement.

- For plants licensed to an LHGR core power limit rather than an F_q limit (i.e., CE plants), analysts must calculate the corresponding F_q "TechSpec" value. The value will depend on the total fuel rod active length. Though the presence of shield assemblies and part- or reduced-length fuel rods must be considered in this calculation, explicit modeling of the unique shield assembly characteristics is not appropriate.

- [

]

- [

]

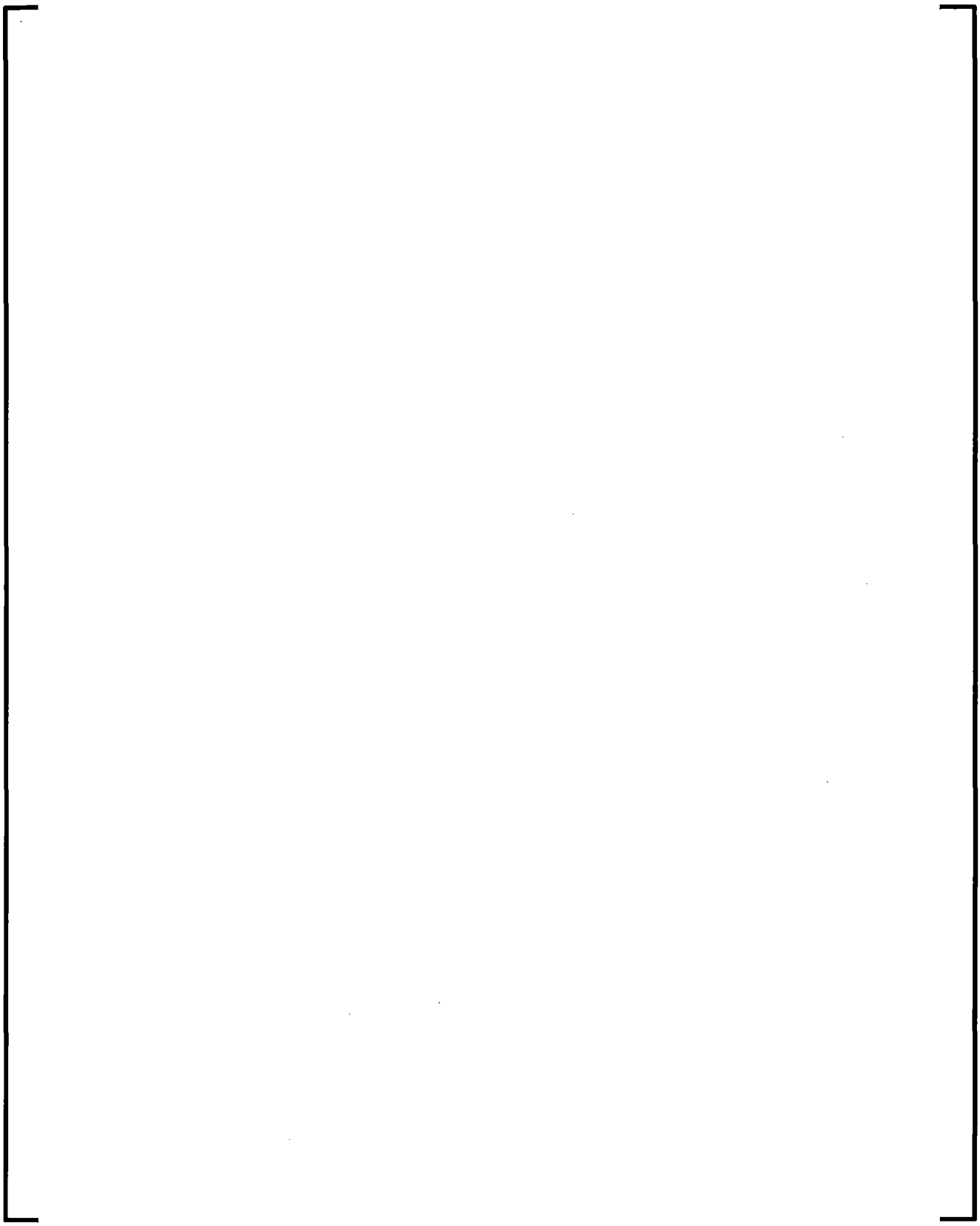

[

]

Vessel Upper Plenum

The upper plenum nodalization is the result of sensitivity studies comparing a single volume, a single TWODEE component with three rings, a single TWODEE component with four rings, and the two TWODEE components with three rings each. [

]

This region extends from the top of the upper core plate to the top of the upper support plate. In some PWRs, the upper head fluid volume extends below the core support ledge (i.e., inverted "top hat" upper support plate). For these types of plants this volume is included in the upper head. The upper plenum region may contain plates, flow mixers, support columns, and guide tube assemblies or shrouds. The region is modeled as a [ ] volume TWODEE component.

In some Westinghouse plants (especially 3-loop) an asymmetry of flow into the upper plenum can exist. Flow from the core can either travel directly into the upper plenum or travel through a support column or mixer vane (i.e., a standpipe) and then into the middle of the upper plenum. [

] The bottom axial level in the TWODEE component representing the open hole is reserved to absorb a cross-flow connection from the guide tubes. S-RELAP5 allows only one cross-flow connection to any individual volume in a TWODEE component.

[

]

The general guidelines are as follows:

- The TWODEE component is oriented upward. [

]

- [

]

- [

]

- [

]

- Hydraulic diameter is calculated for each axial level assuming the fluid 4*volume/(surface area) relationship. It should consider the volume and surface area of the upper plenum skirt and major internal components including the upper support plate, hollow support columns, guide tube assemblies or shrouds, mixer vanes, and other support structures. [

]

- Connection from the upper plenum to hot legs is modeled as normal junctions from the relevant outer faces of the upper plenum TWODEE components to the inlet face of the hot leg volumes. [

]

- [

]

- Flow across the upper support plate [ ] may be modeled with a normal junction between the top-level upper plenum volumes and the bottom upper head volume. To model this flow path, include a junction connecting all top-level volumes to the upper head. This is required to ensure symmetry of fluid during steady-state.
- A minimum of [ ] cylindrical heat structures is used to represent the mixer vanes and hollow support columns, if present. [

]

- A minimum of [ ] slab heat structures is used to represent the upper plenum skirt. The left boundary connects to the outer region of the upper plenum TWODEE component. [

]

- As necessary, cylindrical heat structures are used to represent significant solid support column structures in the upper plenum. These structures are insulated on the left boundary and connected to the relevant hydraulic volumes on the right boundary.

Upper Head

The vessel upper head (closure head) region extends from the top of the upper support plate to the top of the vessel closure head. The guidelines are as follows:

- Three structural variations, describing the upper support plate are common among PWRs: flat plate, top hat, and inverted top hat. [

]

- The downcomer bypass flow paths (spray nozzles) are connected at the bottom end of the component [

] Junction connections are made to each top-level downcomer volume to ensure symmetric downcomer streamlines.

- Upper head wall and internal structures are modeled (Refer to Section A.1.3.6.1.4 on heat structure modeling).

Guide Tubes/Control Element Assembly Shrouds

Because of a limitation in S-RELAP5, guide tube assemblies or assembly shrouds must connect in cross flow to the bottom axial volume in the TWODEE component representing the [ ] The TWODEE component allows for only one cross flow connection from each specified volume and no normal junctions for internal volumes.

The top end of the guide tube assemblies or assembly shrouds will connect at an internal junction of the upper head; however, the connection code differs for the outermost guide tube assembly model. This is done to facilitate fluid mixing in the upper head by preventing the existence of a dead-end volume.

This region represents the guide tube assemblies or, for CE plants, control element assembly shrouds through the upper plenum to the upper head. The guidelines are as follows:

- The region is modeled using [

  ] The upper plenum volume is designated as the "from volume" in cross flow, i.e., set the flag s = 2. The guide tube assembly (or assembly shroud) model extends from the upper plenum into the upper head, [

  ] (see Figure A-9, Figure A-11, or Figure A-12). The flow area is the cross-sectional area of all guide tube assemblies in the particular radial core ring.
- The hydraulic diameter is calculated by the usual formulas.

- For hot head plants (those with upper head temperatures close to the hot leg temperature), the form-loss coefficient at the inlet to and the outlet from the bypass is adjusted during steady-state initialization to give the proper upper-head temperature. For cold head plants (those with upper head temperatures at or near the cold leg temperature), the form-loss coefficient at the center of the bypass volumes is adjusted uniformly [

  ] This adjustment will force the upper head temperature to the cold leg temperature and would be acceptable in the steady state calculation. [

  ] Since the flow paths can be reasonably complicated, especially for the guide tubes, it is acceptable to bias the nominal values high in order to be conservative. Biasing the values high would serve to limit the steam venting path in the LOCA, which is accepted to be conservative.

- Connect the top of the guide tube assemblies or shrouds at the junction [

  ]

- [ ]

- Each guide tube assembly or shroud is modeled with a minimum of [

]

A.1.3.6.2.5 Emergency Core Cooling System

The heat structures in the ECCS lines and the [ ] within the accumulator/SIT lines provided in these guidelines have been shown to improve numerical robustness to the rapid depressurization transient. Without these additions, water property errors are more likely. Since the purpose of the heat structures is to provide a thermal lag to the fluid condition to prevent freezing and code problems, the details of these heat structures are not considered to be important. A reasonable representation is acceptable.

Since the accumulator/SIT initial condition is a sampled parameter in RLBLOCA analysis, initial conditions within the ECCS provided in the base input do not require rigid derivation. While the initial conditions in the accumulator/SIT discharge piping and other safety injection piping are not sampled parameters, their contribution to the overall ECCS flow is typically below 10% of the total injected ECCS coolant mass which is considered to have minor importance for RLBLOCA analyses.

In general, the RWST temperature for safety injection phenomenologically contributes to both coolant subcooling and cold-leg/downcomer condensation such that the overall influence on clad temperatures is lessened. Nonetheless, in responding to the NRC in support of their review of the RLBLOCA methodology, downcomer boiling was characterized as being sensitive to ECCS subcooling. To address this phenomenological affect, RWST temperature is set to a maximum value (e.g., Technical Specifications). This condition has also been shown to improve code robustness by lessoning the likelihood of freezing in the ECCS piping for certain plants.

Emergency core cooling systems may vary significantly from plant to plant. Most plants have separate systems for high pressure injection, low pressure injection, and accumulators/SITs. With regard to LOCA, the pumped safety injection designs can be modeled as simple flow boundary conditions (using TMDPVOL and TMDPJUN components); however, to sufficiently capture the effects of the accumulator/SIT cover-gas (typically, this is nitrogen) on the transient response, the accumulator/SIT is modeled explicitly. Many high and low pressure injection systems branch from a common header. From this header to the injection locations, the piping losses can vary significantly. For this reason, this boundary condition must consider the uncertainty associated with flow split. It is common practice to use a bounding low value for the expected flow from these systems. This may be done from a separate flow split network analysis; however, most utilities have performed these analyses and can provide this ECCS performance information. As an alternative, a more detailed ECCS model may be used that will provide a best-estimate calculation of the flow split.

Some plants tee the pumped injection systems into an accumulator/SIT line. There is some inherent uncertainty associated with the dynamics of these two systems. For that reason it is recommended that the ECCS systems model be similar in detail to the nodalization as shown in Figure A-13 (a 3-loop plant is shown; add a line for 4-loop plants). In this nodalization, the flow split of the low-pressure safety injection to the loops is computed by the code and any adverse interaction between the two systems (LPSI and accumulator/SIT) can be simulated. An SI network that ties into an accumulator network may introduce a concern over SI backflow into the accumulator piping. Analysts need to consider this possibility when developing an ECCS model.

The additional guidelines are as follows:

- The accumulator/SIT is modeled as a [ ] volume PIPE component, consisting of the following elements:
  - [

]

- On some accumulators/SITs, the exit piping is attached on the side of the accumulator/SIT. It is assumed for RLBLOCA analyses that only the accumulator/SIT liquid volume at and above the elevation of the exit nozzle will actually exit from the accumulator/SIT during an LBLOCA.
- ECCS piping is nodalized with resolution corresponding to the dominant form losses (i.e., bends and valves). The model includes the check valve that separates low- and high-pressure regions in the accumulator/SIT lines. [

]

- Initial conditions within the ECCS piping may be set to nominal values. If, during model shakedown, the freezing is observed in the ECCS piping, it is recommended that initial temperature values be biased high to avoid this problem.
- RWST temperature for pumped safety injection is set equal to the [

]

- [

]

- The overall elevation change and form losses within the ECCS piping are modeled.
- Flow characteristics of the high- and low-pressure safety injection systems are modeled using time-dependent volumes and junctions.
- Heat structures must be modeled for the accumulator/SIT vessel and piping walls (Refer to Section A.1.3.6.1.4 on heat structure modeling).

A.1.3.6.3 Reactor Kinetics

The reactor kinetics model is used for RLBLOCA. General guidelines for reactor kinetics parameters in the base and transient input files are as follows:

- The point kinetics with separable feedback option is used.
- Fission product decay is to include actinides (GAMMA-AC option).

- The initial reactor power is entered for the rated total power.
- Initial reactivity is set to 0.0 dollars.
- The base input file will use an EOC nominal value consistent with minimizing reactivity which is conservative for LOCA.
- [

]

- Fissions per initial fissile atom for the neutron capture model is not included in the steady state base model. This parameter is only used in transient calculations.
- The 1979 ANS fission product standard data (Reference A-13) for U^{235} is used (option ANS79-1). The uncertainty reported for the ANS-79 decay heat model is applied in all RLBLOCA analyses. It is therefore the only appropriate choice for this input parameter in the base input files.
- The reactivity feedback weighting-factor for a particular volume is equivalent to the volume fraction (volume of individual cell/total core volume).
- Doppler feedback weighting factor for a particular heat structure is equivalent to the heat structure surface area fraction.
- [

]

- Scram is not modeled in RLBLOCA analyses.

The kinetics input must be entered in both steady-state and transient runs. For the steady-state run, only the first three cards (Cards 30000000, 30000001, and 30000002) are required,but the density and Doppler reactivity tables, and the weighting factors must not be entered. The transient run requires a complete set of kinetics input data.

A.1.3.6.4 Control Variables and Trips

This section describes system monitoring control variables, steady-state initialization aids, and reactor trips, which are needed or are useful in LOCA calculations. As a methodology based on the principles of "Code Scaling, Uncertainty and Applicability" (Reference A-1), an AREVA RLBLOCA analysis distinguishes uncertainty between phenomenological influences (e.g., film boiling heat transfer and stored energy), and plant operational influences (e.g., pressurizer level and accumulator/SIT pressure). In these separate domains, the uncertainty will be treated differently in RLBLOCA analyses. The emphasis of any CSAU methodology is focused on the assessment of phenomenological uncertainty. In addition, a CSAU-based methodology recognizes a hierarchical relationship among phenomena influencing the key figure-of-merit (i.e., the peak clad temperature). During development of the AREVA RLBLOCA methodology, this hierarchical relationship was first established by the development of a Phenomena Identification and Ranking Table (PIRT) (Table 5-1), and then quantified by a series of sensitivity studies performed in EMF-2103 Revision 0 (Reference A-4).

For those phenomena identified as important, code bias and uncertainty were evaluated using experimental test data from a diverse set of experiments. Instrument uncertainty was inherent in all tests was, but no effort was made to remove this uncertainty to improve code-to-data agreement. Instead, this uncertainty represents a component of the final uncertainty values determined for the statistically ranged parameters applied in the methodology. A benefit of accepting this additional uncertainty is that the population of plant states and operational ranges into the computer models does not need to include measurement uncertainty. While it is acceptable to explicitly apply this uncertainty in parameter ranges, to do so is double accounting for measurement uncertainty and, hence, conservative.

A.1.3.6.4.1 System Monitoring Control Variables

The following control variables can be present for monitoring of various parameters, or to provide derived values for trip functions (others are certainly permitted):

- Reactor downcomer (collapsed) liquid levels.
- Core liquid levels.
- Reactor vessel liquid levels.
- Pressurizer liquid level.
- Steam generator tubes up-flow side liquid level.
- Steam generator tubes down-flow side liquid level.
- Loop seal up-flow side liquid level.
- Loop seal down-flow side liquid level.
- Steam generator (secondary side) liquid level with respect to pressure taps.
- Reactor downcomer mass.
- Core mass.
- Total reactor vessel mass.
- Cold leg mass.
- Hot leg mass.
- Pressurizer and surge line mass.
- Total primary system mass.
- Total steam generator secondary system mass.
- Net power to the hydraulic volumes in the core and core bypass.
- Net power to the steam generator boiler.
- Steam generator secondary side recirculation ratio.
- Reflood emergency core cooling injection rate.

A.1.3.6.4.2 Steady-State Initialization Aids

To facilitate efficient steady-state initialization, the following control systems may be used. These systems generally do not model actual plant control systems but are present only to accelerate the convergence to a desired steady-state condition of the plant. These controllers must be disabled for the transient calculation.

Reactor Coolant System Flow (Pump) Control

A control system that varies pump speed is used to attain a target loop flow rate, which, in turn, determines a target temperature difference between cold leg and hot leg.

Primary Pressure Control

To hold the primary pressure at a target value, a time-dependent volume is connected to the pressurizer steam space (the top volume) using a VALVE component that must be closed or deleted in the transient calculation.

Pressurizer Liquid Level Control

A liquid source connected to the bottom of the pressurizer is used to fill or drain liquid for maintaining the pressurizer level at a target value. This source must also be disabled in the transient calculation.

Power Level Control

Reactor kinetics model without feedback reactivity is used to maintain a preset initial power level. The feedback is added in the transient calculation.

Steam Generator Feedwater Flow Control

The feed flow rate is varied to maintain a target steam generator secondary side mass.

Steam Generator Steam Flow Control

The steam generator steam flow rate is varied to maintain a target vessel average or cold leg temperature. Equal steam flow and feedwater flow is established from this and the above control. The control system is applied to the MSIV. In an actual plant, a turbine control valve downstream of the MSIV and the common header provided for the steam lines would perform this function; however, that portion of the plant is not modeled for RLBLOCA applications. This constraint requires that a control system be constructed for each MSIV modeled (rather than just one that would exist in an actual plant).

Steam Generator Recirculation Ratio Control

Control variable input for the form-loss coefficient of the separator liquid return junction (the second junction of the separator component) is used to get a target recirculation ratio by varying the form-loss coefficient. It is required to delete or disable the control variables for the form-loss coefficients in the transient run input.

Steam Generator Liquid Level Control

With the control variable input for the form-loss coefficient of the connection junction between the downcomer and boiler, a target steam generator liquid level can be obtained by varying the form-loss coefficient. It is required that the control variables for the form-loss coefficients be deleted or disabled in the transient run input.

Primary System Bypass Flow Paths

The target mass flow rates for various bypass flow paths in the primary system may be obtained by manually adjusting the form-loss coefficients or by setting up control variables for evaluating the form-loss coefficients.

A.1.3.6.4.3 Trips

Required trips for large break LOCA are relatively few. The primary plant trips may be classified as either Reactor Protection System (RPS) trips or Engineered Safety Features Actuation System (ESFAS) trips. Additional trips are necessary to facilitate the simulation. Trips are defined by modeling measured variables. These variables are modeled using calculated variables from volumes as close as possible to the actual plant measurement locations. Sensor and instrumentation delays are included either explicitly (e.g., control lag or lead/lag) or by an effective time delay. Customers may prefer to qualify plant instrumentation by including measurement uncertainty in trip setpoints. Although not required by the RLBLOCA methodology, the inclusion of this uncertainty is acceptable.

Reactor Protection System Trips

For LBLOCA, only the low pressurizer pressure trip causes a reactor trip to be activated. While RLBLOCA analyses do not take credit for reactor scram, this trip is used by other trip and control systems.

Engineered Safety Features Actuation System

The various ESFAS functions included in the S-RELAP5 RLBLOCA input model are:

- Safety Injection Initiation - actuated by:
  - Low pressurizer pressure, or
  - High containment pressure.
- Turbine Trip and Main Feedwater Isolation - actuated by:
  - Reactor scram, or
  - Conservatively assumed to occur at start of transient.

- Auxiliary Feedwater Initiation – actuation of the auxiliary feedwater is not anticipated during an LBLOCA; however, this system may be needed for specialized model shakedown tests associated with the steady-state initialization process. It is typically actuated by low-low steam generator level.

Non-RPS and Non-ESFAS Trips

Several other non-RPS trips may be present in the input model to perform various control functions. These include:

- A master steady-state trip (true for steady-state, false during transient run). This automatically disables all steady-state initialization aids for the transient run.
- RCP trips – A trip card for each pump is supplied to de-energize the pumps at a specified time during the transient. Unlike Appendix K-based evaluation methodologies, RLBLOCA provides for the possibility that there is no loss of offsite power.
- [

]

A.1.3.6.5 Material Properties

The following material property tables are included in the S-RELAP5 steady-state input file:

- UO_2 (fuel).
- Zircaloy-2, Zircaloy-4, or M5® (cladding).
- Stainless steel (Type 304 or 316) (RCS or vessel internals).
- Carbon steel (RCS or vessel internals).
- Helium (fuel/clad gap).
- Inconel (Type 600 or 690) (RCS or vessel internals).
- SA-508 or SA-533 Class 3A steel (steam generator tubesheets).

Material property tables for the fuel, gap, and cladding must be present even through the COPERNIC fuel model is to be incorporated into the calculation. The accuracy of these tables is to be confirmed for a particular analysis. If additional materials are required, new tables can be appended to the current list.

For the COPERNIC fuel model, the properties of fuel rod materials (UO2, M5®, and gap fill gas) are evaluated from the COPERNIC calculation and then read by S-RELAP5. In this case the material properties entered by users are used only for the unheated portion of the fuel rods if they are modeled, or they may be needed to satisfy certain input requirements.

A.1.3.6.6 Steady-State Initialization

Certain plant specific parameters must be approximated in the base input file prior to steady-state initialization. These include bypass flow rates, upper head temperature, and steam generator secondary steam heat transfer rate (via feedwater temperature, pressure, liquid level, and recirculation ratio). In addition, best-estimate pressure drop information may be used to refine form-loss values. This is often done to validate steam generator, core, and vessel pressure drops.

Geometry and inherent limits of finite difference computer codes to model heat exchanger heat transfer make steam generator initialization a particular challenge. Analysts are expected to make an effort to best match plant data on the key steam generator parameters: steam dome pressure, main steam flows, main feedwater flows, and steam generator mass. [

]

Steam generator pressure, liquid level, and recirculation ratio are parameters that reflect the proper distribution of liquid in the steam generator, but since this is of less importance for the LBLOCA simulation, steady-state results within a 10% tolerance for these parameters are acceptable. Errors larger than this tolerance may either be contributing to, or resulting from problems with the steady-state controllers.

Bypass flow rates include spray nozzles (downcomer to upper head), baffle bypass (downcomer to lower plenum or lower plenum to upper plenum), core guide tubes (or guide bar) (lower plenum to upper plenum), and upper plenum guide tube (or guide bar) assemblies or assembly shrouds (upper plenum to upper head). The mass flow rates for these bypasses are available from plant data. Using these values, form losses at entrance and exit junctions may be varied to match the plant data. This is done for all of these bypass paths, with the exception of the upper plenum guide tube assemblies. No attempt is made to match available plant data. Form losses on these guide tube are adjusted to uniformly match upper head temperature.

The primary and secondary sides of the U-tubes are thermally connected through a heat structure for each tube volume. S-RELAP5 will underpredict the primary to secondary heat transfer rate in the steam generator in most applications. This is partly due to inherent characteristics of the heat transfer correlations, and partly due to steam generator features, which are not included in the model (such as two-dimensional heat transfer in the tubesheet, and ignoring tube baffles and support plates). Existing control systems will try to achieve the proper primary side fluid characteristics,, but poor primary-to-secondary heat transfer rate may undermine these controllers. Heat transfer rate is related to the tight coupling between steam pressure and steam generator liquid level. Changing the secondary side heat structure heated-hydraulic diameter can be used by the analyst to best match expected steady-state conditions, and to optimize the performance of the controllers. Experience has shown that using a value equal to the distance between tube walls (tube pitch - tube outer diameter) will provide a good initial estimate. Adjustments to main feedwater temperature and secondary backpressure (within reasonable uncertainty ranges) are also acceptable to achieve the targeted steam generator performance.

Steam generator heat transfer and feed and steam flows are highly dependent on the steam generator recirculation ratio. Recirculation ratio is the ratio of the liquid fallback from the separator to the steam flow. An analyst can modify this by adjusting form losses at the inlet of the boiler region and/or at the liquid fallback junction in the separator model. If the steam generator recirculation ratio is initialized by a control system adjusting the form loss, the final value providing the correct recirculation ratio is included in the steady-state input model and the controller disabled.

If data that describe reactor coolant pump coastdown are available, pump frictional torque coefficients may be adjusted to obtain the proper flow coastdown characteristics.

Steady state conditions exist when:

- The net RCS heat generation rate (core power plus RC pump heat minus losses) exactly matches primary to secondary heat transfer across the steam generators, and,
- Liquid and vapor mass inventories are relatively constant.

The following variables must be within acceptable tolerances prior to initiating a transient calculation:

Primary Coolant System	**Secondary System**
Core Power	Steam Generator Pressure
RCS Thot, Tcold, Tavg	Main Steam Flows
RCS Loop Flows	Main Feedwater Flows
Pressurizer Pressure	Steam Generator Mass
Pressurizer Level	
Core Bypass Flow Rates	

Upon successful initialization to the desired conditions, the steady state run is restarted in the transient mode. The master steady-state trip is set to false which disables all of the initialization aids. A steady-state run of [ ] seconds (minimum) is made with the steady-state controllers on and then an additional [ ] seconds (minimum) with the controllers off to demonstrate a "null" transient showing that the model is at steady-state conditions. If steady-state conditions are maintained, transient analyses can then be made with the model.

A.1.3.6.7 Transient Model

The transient restart model includes the break model, deletion of steady-state controllers, fuel rod reflood data, trips for safety injection delay, and transient reactor kinetics. These are discussed in the guideline for running the uncertainty analysis (Section A.2). A brief overview is given as follows.

A.1.3.6.8 Break Model

Two break configurations must be considered when performing licensing safety analyses: the double-ended guillotine break (DEGB), and the double-ended split break (DESB). In the RLBLOCA methodology, the DEGB assumes the complete severing of a cold leg pipe to the extent that no fluid can pass from the pump to the reactor vessel. All water at the break flows into the containment. The DESB assumes a break along the pipe wall and fluid exiting the RCS in a direction normal to the pipe wall. Section A.2.5.12.4 below contains discussion on determination of the break parameters.

In theory, DESBs only have to be examined up to an area equivalent to 100% of the pipe area. Beyond that size, the choke plane will move to the inside of the pipe and the break will behave in a manner similar to a DEGB. Although it may be argued that a cross-flow junction is a more appropriate way to model the DESB, at intermediate and small breaks, the Courant limit can be violated. Since S-RELAP5 only tests for Courant violations along normal pathways, it is possible for S-RELAP5 to become numerically unstable with this configuration.

In RLBLOCA analyses with S-RELAP5, the DEGB break nodalization is shown in

[

]

The containment volume is modeled as [

] These volumes are added in the base input deck, but the break junctions are not added until the creation of the transient input deck.

A.1.3.6.9 Simulation Control

The steady-state calculation begins with a short period of time step sizes that is smaller than those used later in the calculation. The primary concern addressed by using the smaller time steps for a short time period is a reduction in the likelihood that certain hot assembly heat structures will move beyond critical heat flux. Since the initial conditions provided to a steady-state S-RELAP5 calculation are approximate, an artificial transient occurs at the start of the calculation. For calculations having core heat structures approaching 16 kW/ft, inadvertent CHF conditions resulting from this artificial transient have been observed. Decreasing time steps early in the steady-state calculation have shown to eliminate this problem. Because for plants not approaching 16 kW/ft, CHF is much less likely, reducing the period of short time steps provides improved economy without impact on the steady-state calculation.

[

]

A.1.3.6.9.1 Time Step

Time step sensitivity studies have been performed to identify an appropriate time step for RLBLOCA calculations. The maximum analysis time step is the following (smaller time step are acceptable):

[ ]

The smaller time step size for the first [ ] seconds is needed for initialization of the COPERNIC models within S-RELAP5. If numerical difficulties are observed, the period of the smaller time step size can be extended.

[

]

The transient time step sizes are discussed in Section A.2.5.18.2.

Because plant systems and designs vary, convergence using the maximum transient time step size is not guaranteed. This may be the result of Courant limit violation or other modeling limitations. The analyst must investigate solution convergence and the Courant limit criteria, and modify the time step sequence as necessary. S-RELAP5 will reduce the time step based on a set of numerical methods criteria (including Courant limit violation), but the S-RELAP5 has been observed to lose robustness and fidelity when used in this manner. In addition, because the Courant limit can vary over time, the optimal time step may be a function of time itself.

The conclusion of the transient will coincide with whole core quench. To demonstrate sustained cooling, the limiting case is expected to run a minimum of 100 s beyond whole core quench. Control systems can be developed to identify these conditions and terminate S-RELAP5 appropriately.

A.1.3.6.9.2 Deletion of Steady-State Controllers

The following controllers may need to be deleted or disabled, if present:

- Steam generator mass (feedwater flow) controller.
- Cold leg temperature controller (secondary steam flow).
- Pressurizer pressure controller, pressurizer level controller, pump controllers.
- Form loss controllers used to control steam generator recirculation rate.

For the steam generator recirculation rate controllers, it may be useful to first perform a scoping calculation to determine the steady-state form losses. These values can then be hardwired into the model and the controller can be removed from the steady-state model with replacement cards. Applying this approach may be necessary to support calculations in which some fraction of the steam generator tubes are plugged.

Since many of the control systems applied to secondary side components are used to adjust conditions on the primary side, it may not be possible to program both the primary side control and the realistic secondary side control functions for the main steam and feedwater valves. [

]

A.1.3.6.9.3 Reflood Option

[

]

A.1.3.6.9.4 RLBLOCA Option

[

]

Card 100, Problem Type and Option:

Word	Description	Value
W3(A)	PWR Realistic LBLOCA with penalties.	PWRLBRV2

A.1.3.6.10 Reactor Kinetics

The importance of reactor kinetics parameters on the prediction of clad temperatures is not specified in the AREVA RLBLOCA PIRT. This is neglected because reactor shutdown is a basic assumption for an LBLOCA analysis and since it is assured by the core voiding that occurs following an LBLOCA. Conservative choice of reactor kinetics parameters can delay the eventual reactor shutdown, but, by definition, reactor is shutdown by the end of blowdown, which approximately corresponds to the time of minimum reactor vessel inventory.

[

] Since RLBLOCA calculations using S-RELAP5 apply the point kinetics model, a spurious return to criticality is possible and has been observed. [

]

The transient reactor kinetics model requires input needed to describe any reactivity feedback mechanisms expected during a large break LOCA. The point kinetics model for S-RELAP5 allows reactivity feedback from scram, moderator density, and fuel temperature (Doppler).

Justification of a reactor scram is nontrivial. Hydraulic forces within the core during an LBLOCA may act to impede and delay the insertion of control rods/elements following a reactor trip. A best estimate of control rod insertion dynamics requires examination of these "LOCA-loads" on the control rods/elements and the surrounding structure. For PWRs operating with a negative moderator density reactivity worth, such an analysis is unnecessary, since the reactor will shutdown naturally as the reactor vessel depressurizes and significant voiding occurs in the core. As previously stated, for LBLOCAs this process will happen by the end of blowdown. Since reactor shutdown is ensured by core moderator voiding, the modeling of reactor scram is unnecessary.

Taking credit for a reactor scram is not considered in RLBLOCA applications. This assumption is made to show that the reactor shuts down on moderator voiding. [

]

Also required for a transient is Word 7 on Card 30000001. This parameter is set to -1.0 to apply the neutron capture correction factor which is a time dependent ratio applied to decay heat. Using a negative number prescribes S-RELAP5 to use the hardwired correction factor table. Note that this parameter must not be set in a steady-state calculation.

A.1.3.7 Instructions for COPERNIC Input

The static COPERNIC parameters (i.e., not time- or burnup-dependent) are based primarily on AREVA mechanical specifications of the fuel. For this reason, best-estimate values should be available for these parameters. Nonetheless, while PCTs are strongly influenced by burnup, scoping studies have shown that within the normal range of uncertainty, variation of most COPERNIC parameters have only a small effect on PCT.

COPERNIC is the preferred fuel rod code to be used for all Zirconium clad fuel. This guideline section highlights the unique code input requirements for performing an RLBLOCA analysis using COPERNIC.

Application of the COPERNIC code is for the generation of best-estimate fuel rod properties to be used in the S-RELAP5 RLBLOCA calculation. The COPERNIC Theory and Users Manual (Reference A-8) should be consulted for a description of input.

[ ] much of the input must be generated dynamically. Instruction for creating this input is presented in the RLBLOCA Analysis Guideline (Section A.2.5.16.1 below). Nonetheless, it is necessary to have a base COPERNIC model to initialize the S-RELAP5 model. Automation tools are provided to create this input.

This base input model can be developed by following the COPERNIC input description given in Reference A-8. Use best-estimate or analysis values as recommended in this manual or fuel design specifications. [

] The LOCA analyst should be aware that the axial power profile shapes used in the COPERNIC input inherit certain assumptions that may make entry for some input parameters unnecessary [ ]

It is required for identical radial fuel pin nodalizations to be used for COPERNIC fuel rod models and their corresponding S-RELAP5 heat structures. Since COPERNIC uses a relatively complex method of equal area radial nodalization, it is recommended that COPERNIC be nodalized first, and then the results of that nodalization be copied to the corresponding S-RELAP5 heat structure. The actual COPERNIC nodalization can be found in the ftn21 file generated by COPERNIC. A search on "Radius =" leads to a list of the nodal radii (mm) within the pellet. No listing of cladding radii is provided, but using equally spaced radii within the cladding will give an acceptable result.

All COPERNIC rod models must have the same axial nodalization, but that nodalization does not need to be the same as that in the S-RELAP5 heat structures representing the fuel rods. S-RELAP5 will automatically detect the axial nodalization used in the COPERNIC model, and will map data between the COPERNIC and heat structure models accordingly. A reduction in the number of COPERNIC axial levels will result in reduced S-RELAP5 execution time.

A separate COPERNIC run must be performed for each rod type to be modeled, and a separate restart file saved for each rod type at the relevant exposure time. The creation of a restart file is specified by setting variable IREDEM/OPT to 1, and by setting variable NMRDM/OPT to the macro time step number at which the restart file will be dumped. The restart file from each run is originally written to file ftn12. These files must be renamed with names of the form copernic.dxxx, where the rod number xxx = 001, 002, 003, etc. Currently, a maximum of 99 COPERNIC fuel rods may be used.

Card 300, COPERNIC Execution Frequency

The S-RELAP5 input card 300 is used to specify the number of S-RELAP5 maximum size time steps that occur between each execution of the COPERNIC subcode. For the steady state analysis, this must occur frequently as the problem is being initialized, then less often as the fuel rod parameters reach their steady state values. A control system can be used to implement a variable number of steps between COPERNIC executions. The following input is used in the steady state model:

```
300  -299  1
```

This indicates that control variable 299 will provide the execution frequency, and that the S-RELAP5 heat structures will be initialized with the data transfer file value of fuel rod cladding temperature at the core inlet. The missing final word on this input card uses the default of zero, indicating that the COPERNIC cracking and plastic strain model will be bypassed.

The control system used to supply the execution frequency should be similar to the following:

```
*
* Control Variable 0298  COPERNIC Read Frequency After 5 Seconds
*
20502980 COPREAD1 TRIPUNIT 50.000 0.0000 0
20502981 0300
*
* Control Variable 0299  COPERNIC Read Frequency
*
20502990 COPREAD STDFNCTN 1.0000 1.0000 0
20502991 MAX CNTRLVAR 0008
20502992    CNTRLVAR 0298
```

Control variable 0298 is a TRIPUNIT CV monitoring a trip (300), which becomes true when the execution time is greater than 5 seconds. The scaling factor of 50.0 causes the output of this CV to be 50.0 when time is greater than five seconds. CV 0299 takes the maximum of the previous variable and another TRIPUNIT (0008), which has a value of 1.0 during steady state. Thus, the COPERNIC execution frequency is 1 (every S-RELAP5 maximum time step interval) up to five seconds, then every 50 steps thereafter.

Alternatively, the COPERNIC execution frequency may be specified in Word 8 on the time step cards.

The 300 card input for the transient analysis is:

```
300   50
```

which sets the frequency to every 50 steps during the transient.

Card 1CCCG001, Fuel Rod Model Option

Word	Description	Value
W1(I)	Gap Conductance Model Flag	[ ]

Card 1CCCG004, Fuel Rod Model Data (See Section 7.2.3, Reference A-2)

Word	Description	Value
W1(I)	COPERNIC Rod number	Must be same as *xxx* extension on corresponding *copernic.dxxx* file.
W2(I)	Fuel Rod Upper Plenum Boundary Coolant Volume Number	[ ]
W3(I)	Fuel Rod Lower Plenum Boundary Coolant Volume Number	Integer value must be supplied. Not used for COPERNIC rods.
W4(I)	Trip Number for Activating Transient Fuel Rod Plenum Temperature Model	Integer value must be supplied. Not used for COPERNIC rods.

Execute the S-RELAP5 steady state run with the appropriate number of copernic.dxxx files present in the submit directory. These COPERNIC files are not required for subsequent transient runs. All other files are used the same as previously. Minor edit and plot variables for fission gas pressure, fuel rod plenum temperature, and gap conductance are available for COPERNIC fuel rods.

A.1.3.8 Instructions for Containment Input

For large break LOCA analysis, the containment models in S-RELAP5 provide simulation of the expected pressure boundary condition. Containment pressure response is the direct result of mass and energy dynamics anticipated during the transient. As with modeling the ECCS, plant-to-plant variation of containment dynamics and the inconsistent availability of structural detail prevent a standardized approach to modeling minute design details. As a boundary condition influencing clad temperatures, best-practice containment modeling places an emphasis on the dominant systems for adding and removing mass and energy. It is well understood that lower containment pressure reduces coolant liquid subcooling and core reflood rates, which lead to higher clad temperatures. As with an ECCS model that minimizes coolant flow, minimizing containment pressure may be used to conservatively bound containment response models used in S-RELAP5. If serious discrepancies in transient behavior exist, other containment parameters may need to be changed to capture model uncertainty not associated with heat removal by passive heat structures.

In the RLBLOCA methodology RWST temperature for containment sprays is decoupled from the RWST temperature for safety injection. Since RWST temperature for containment sprays is not considered to be an important parameter for LOCA analyses, setting this parameter to nominal is acceptable. If conservatism is requested by a customer, low RWST temperature will theoretically reduce containment back pressure. Lower containment pressure is usually correlated to higher clad temperatures.

Containment volume guidelines for ice condenser plants have been developed with the strategy to maximize the effectiveness of the ice condenser cooling system. [

]

Upper door and sump drain fluid temperatures are explicitly provided in input for ice condenser containments. The values for these parameters were derived from data from the Westinghouse Waltz Mill Ice Condenser Blowdown Facility. The use of this data is an inherent part of the legacy ICECON containment methodology and is originally presented in AREVA documentation in Reference A-14. These values reflect a conservative bias designed to minimize the partial pressure of air (i.e., air mass) by maximizing the vapor pressure.

Code modules from the ICECON containment analysis code have been implemented in the S-RELAP5 code for RLBLOCA applications. As described in Section A.1.3.6.8, the containment models are applied when the 20900000 S-RELAP5/ICECON Component Connection Data card is appended to an S-RELAP5 transient input file as shown in Appendix A of Reference A-2. This card supplies the identification of the break junctions and the containment time-dependent volumes. In addition to the 20900000 card in S-RELAP5, S-RELAP5 requires a separate containment input file provided in the format of the ICECON computer code (which is based on the CONTEMPT code, Reference A-15). The explanation for creating input describing a plant's containment for use in S-RELAP5 is given in Reference A-14. Some guidelines for best-estimate analyses are given in Section 7.11 of Reference A-14. An automated input generator, AUTOICECON is available to produce the input file.

For new models, the analyst should recognize that the LBLOCA transient has a relatively short duration. As such, many heat transfer processes modeled with the containment models in S-RELAP5 have long time constants that net very little effect on containment pressure. For this reason, the analyst is encouraged to focus on modeling the dominant mass and energy addition and removal systems when developing a plant-specific containment model. For those relatively unimportant parameters representative or reasonable analysis values may be applied. [

]

The use of the ICECON module in S-RELAP5 inherits a few code model changes that prevent older ICECON or CONTEMPT input files from functioning without modification in an RLBLOCA analysis. [

] Upon validation of supporting references, the physical containment description (including volume and heat structure information), from previously developed ICECON or CONTEMPT containment model (as used in an Appendix K analysis), are considered valid for RLBLOCA applications. Heat structure nodalization will still comply with the mesh size limit specified in this section.

The remainder of this section provides general guidance for developing a containment input model. These guidelines define the basic requirements for a new containment model for RLBLOCA applications. More detail in the area of heat structure definition, is acceptable, but additional detail beyond that specified in these guidelines is not required for RLBLOCA analyses.

Nominal values are used for non-critical parameters in the descriptions below. A reasonable value is acceptable.

A.1.3.8.1 General Control Card 11001

Word	Variable	Description	Value
W1-R	TFNL	Problem end time	10.0 (value overridden by S-RELAP5)
W2-I	NSL	Number of heat conducting structures	Plant/model specific
W3-I	NPSOPT	Pressure suppression model	0, drywell containment
W4-R	TAIR	Initial outside air temperature (°F)	[ ]
W5-R	PAIR	Initial outside air absolute pressure (psia or Pa)	[ ]
W6-R	HUMO	Initial outside air humidity (0.0 to 1.0)	[ ]
W7-R	TCONT	Constant temperature (°F) when type 0 is specified for heat structure bulk temperature control on 1YY400 cards	[ ]
W8-W13		For best-estimate calculations assume:	0.0
W14	ASUMPV	Active sump volume in drywell compartment (ft3)	[ ]

A.1.3.8.2 Compartment Description Card 10XX1

For plants with only a dry containment, this is card number 10031. For ice containment plants use card 10031 for the lower compartment, use card 10021 for the upper compartment, and use 10041 for the dead end volumes.

Word	Variable	Description	Value
W1-R	VOL[b]	Total compartment volume (ft^3)	[ ]
W2-R	VOLL	Volume of liquid pool on floor (ft^3)	0.0
W3-R	TV	Temperature of vapor region (°F)	[ ]
W4-R	TL	Temperature of liquid pool region (°F)	[ ]
W5-R	PRT	Total compartment absolute pressure (psia). For ice condenser plants, lower compartment and ice chest pressures should be set to ensure that there is no flow to the ice chest at time zero (setting them equal is acceptable).	[ ]
W6-R	HUM	Relative humidity of vapor region	[ ]
W7-R	ASURF	Horizontal cross-sectional area of compartment (ft^2). Deadend volumes, by convention, may apply a value of 1.0.	[ ]
W8-R	CHTC	Film heat transfer coefficient multiplier for sensible heat transfer between the liquid pool and vapor region	[ ]
W9-R	CMTC	Mass transfer multiplier for evaporation model	[ ]

A.1.3.8.3 Heat Exchanger Description Cards 800 and 850

These cards are used to describe any heat exchangers used to treat liquid collected in the sump that will be used by a containment spray system.

Word	Variable	Description	Value
W1-I	IHEX	Type of heat exchanger	[ ]
W2-R	HEX(1)	Heat exchanger surface area (ft^2)	[ ]
W3-R	HEX(2)	Overall heat exchanger heat transfer coefficient (Btu/hr-ft^2-°F)	[ ]
W4-R	HEX(3)	Heat exchanger coolant inlet temperature (°F)	[ ]
W5-R	HEX(4)	Heat exchanger coolant flow rate (lbm/s)	[ ]
W6-R	HEX(5)	Drywell pressure at which spray system is activated (psia)	[ ]
W7-R	HEX(6)	Drywell pressure at which spray system is shut off Cards 8XX	[ ]

A.1.3.8.4 Heat Exchanger and Outside Flow Table Cards 8XX

These cards are used to describe the anticipated dynamics of the primary containment spray systems during the LOCA transient. It is assumed that at most two spray systems are available; however, the generality of the input description allows for other unique spray configurations. The input is provided relative to time into the transient. The "fractions of flow obtained from" parameters do not have to add up to 1.0; the remaining is from outside water (see W10).

[

]

Word	Variable	Description	Value
W1-R	AWA(1)	Time (s)	[ ]
W2-R	AWA(2)	Flow rate (lbm/s)	[ ]
W3-R	AWA(3)	Spray efficiency	[ ]
W4-R	AWA(4)	Fraction of flow directed to drywell (or lower compartment) spray	[ ]
W5-R	AWA(5)	Fraction of flow directed to upper compartment spray	[ ]
W6-R	AWA(6)	Fraction of flow directed to primary system	[ ]
W7-R	AWA(7)	Fraction of flow directed to drywell (or lower compartment) liquid region	[ ]
W8-R	AWA(8)	Fraction of flow obtained from drywell (or lower compartment) liquid-region	[ ]
W9-R	AWA(9)	Fraction of flow obtained from upper compartment liquid region	[ ]
W10-R	AWA(I0)	Temperature of outside water (°F)	[ ]

A.1.3.8.5 Fan Cooler Control Card 2000, 20XX

[

]

Card 2000

Word	Variable	Description	Value
W1-R	TFAN(1)	Starting time for fan cooler system (s)	[ ]
W2-R	TFAN(2)	Ending time for fan cooler system (s)	[ ]

Card 20XX

Word	Variable	Description	Value
W1-R	FNC(1)	Temperature (°F)	Independent parameter
W2-R	FNCL(2)	Energy addition rate (Btu/s)	[ ]

[ ]

A.1.3.8.6 Timestep Control Cards, 9000, 90XX

Because S-RELAP5 controls time step within the normal S-RELAP5 input, the W1 on 9000 and W1 and W2 on the 90XX cards are ignored during execution. Nonetheless, they are required for input check. The remaining parameters are discretionary.

Card 9000

Word	Variable	Description	Value
W1-A	UNITT	Time units	SEC

Card 90XX

Word	Variable	Description	Value
W1-R	TX(1)	Interval end of time (s, per card 9000)	1.0
W2-R	TX(2)	Timestep length (s, per card 9000)	0.005
W3-I	IT(1)	Printout frequency for heat-conducting structures	0
W4-I	IT(2)	Printout frequency for pressure, temperatures, masses, …	200
W5-I	IT(3)	Printout frequency for plots	20

A.1.3.8.7 Blowdown Control Cards 300, 3XX

S-RELAP5 controls the blowdown mass and energy addition, but these cards are required for input check.

Card 300

Word	Variable	Description	Value
W1-A	UNITT	input time unit	SEC
W2-A	UNITM	unit for input mass addition rate	LBM/SEC
W3-A	UNITH	unit for input enthalpy	BTU/LBM

Card 301

Word	Variable	Description	Value
W1-R	MADD(1)	Time (s, per card 300) Non-critical (legacy) parameter, explicitly handled by S-RELAP5	0.0
W2-R	MADD(2)	Water addition rate (lbm/s, per card 300)	0.0
W3-R	MADD(3)	Enthalpy of water (Btu/lbm, per card 300)	0.0

Card 302

Word	Variable	Description	Value
W1-R	MADD(1)	Time (s, per card 300)[a]	1.0E6
W2-R	MADD(2)	Water addition rate (lbm/s, per card 300)	0.0
W3-R	MADD(3)	Enthalpy of water (Btu/lbm, per card 300)	0.0

A.1.3.8.8 Heat-Conducting Structures Cards 1YY000, 1YY001, 1YY1XX

Due to the large thickness of some containment structure and components, heat structures modeled in this compartment may be constructed using node lengths up to a factor of 10 greater than the guidelines provided in Section A.1.3.6.1.4 for S-RELAP5 heat structures (i.e., mesh spaces ≤ 0.2 ft). For particularly large structures in which the code modeling limits are challenged, larger mesh spacing is allowed as long as the first 1 ft of material is modeled with a mesh spacing of ≤ 0.2 ft. Analyst choice of geometry type in certain circumstances may be subjective. The important measures to be preserved are total surface area and total mass.

Cards 1YY000, Heat slab descriptive text. Enclose in double quotes ("). Up to 73 characters including quotes.

Cards 1YY001

Word	Variable	Description	Value
W1-I	N	Total number of mesh points	Must correspond to the total number provided on the 1YY1XX cards
W2-I	L	Number of regions	# of different materials in structure
W3-I	IGEOM	Geometry type	0, slab; 1, cylindrical; 2, sphere
W4-R	XO	Coordinate of left boundary	0.0
W5-R	FF	Power factor	0.0
W6-R	DELAY	Delay time until source is started (s)	0.0
W7-R	ARA	Heat-transfer surface multiplier	[ ]
W8-I	NCMPH(1)	Left side compartment number	Appropriate compartment or 0
W9-I	NCMPH(2)	Right side compartment number	Appropriate compartment or 0

Cards 1YY1XX, mesh spacing cards (heat structure nodalization)

Word	Variable	Description	Value
W1-I	NS	The number of intervals in the first region	Apply above guideline
W2-R	UB	The value of the spatial coordinate on the right boundary of the first region (ft)	Apply above guideline

Repeat W1 and W2 for each modeled region (W2 on card 1YY001).

A.1.3.8.9 Material Overlay Cards 1YY2XX

Material number corresponds to the material described on Cards 4100XX.

Word	Variable	Description	Value
W1-I	ITS	Material number for Region 1	See Cards 4100XX

A.1.3.8.10 Source Space-Dependence Cards 1YY300, 1YY3XX

These cards are input as zero; however, cards 1YY3XX are optional.

A.1.3.8.11 Heat Conductor Boundary Condition Cards 1YY400

Word	Variable	Description	Value
W1-I	BTO(1)	Heat-transfer coefficient control for left boundary. 0 for insulated boundary, 2 for steam condensation	0 or 2
W2-I	BTO(2)	Heat-transfer coefficient control for left boundary.	0 or 2
W3-I	BTN(1)	The same as Word 1 except for the right boundary.	0 or 2
W4-I	BTN(2)	The same as Word 2 except for the right boundary.	0 or 2

A.1.3.8.12 Material Property Cards 4100XX

Word	Variable	Description	Value
W1-R	TUCVHC(1)	Thermal conductivity for Material 1. (Btu/hr-ft-°F).	[ ]
W2-R	TUCVHC(2)	Volumetric heat capacity for Material 1 (Btu/hr-ft-°F).	[ ]

A.1.3.8.13 Uchida Heat Transfer Multiplier Card 12002

[

]

A.1.3.8.14 Ice Condenser Cards 6XXXX

The ice condenser modeling in S-RELAP5 requires detailed structural description.

[

]

Card 60000. Ice Compartment Description

Word	Variable	Description	Value
W1-I	NDOORS	Number of lower doors leading to ice	[ ]
W2-R	FALD	Fully open area (ft^2) of a single lower door	[ ]
W3-R	AUD	Area of a single upper door	[ ]
W4-R	VLP	Ice condenser lower plenum volume (ft^3) (per a single door)	[ ]
W5-R	VUP	Ice condenser upper plenum volume (ft^3) (per a single door)	[ ]
W6-R	AFLOW	Flow area (ft^2) of ice bay passage corresponding to a single door	[ ]
W7-R	AICE	Effective cross sectional area (ft^2) of ice corresponding to a single door	[ ]

Card 60100. Ice Condenser Flow Loss Coefficients

Word	Variable	Description	Value
W1-R	KLP	Lower compartment to ice passages	[ ]
W2-R	KUP	Ice passage to upper compartment	[ ]
W3-R	KIO	Through ice bay full of ice	[ ]
W4-R	KIZ	Through ice bay empty of ice	[ ]

Card 60200. Ice Compartment Initial Conditions

Word	Variable	Description	Value
W1-R	MICE	Total mass of ice (lbm)	[ ]
W2-R	ZICE	Length of ice column (ft)	[ ]
W3-R	TICE	Temperature of ice (°F)	[ ]
W4-R	PIC	Pressure of ice compartment (psia)	[ ]

Card 60300. Ice-Covered Structures

Word	Variable	Description	Value
W1-R	MCOND	Mass (lbm) of structure initially covered by ice	[ ]
W2-R	UCOND	Structure heat capacity (Btu/lbm-F)	[ ]

Card 60400. Recirculation Fan

Word	Variable	Description	Value
W1-R	AFANF	Fan flow area (ft^2) in forward direction	[ ]
W2-R	KFANF	Loss coefficient in forward direction	[ ]
W3-R	AFANR	Fan flow area (ft^2) in reverse direction	[ ]
W4-R	KFANR	Loss coefficient in reverse direction	[ ]
W5-R	TSRFAN	Start time (s) for recirculation fan	[ ]

Card 604XX. Recirculation Fan Pressure vs. Flow Table

Word	Variable	Description	Value
W1-R	WRFAN(1)	Pressure (psi)	[ ]
W2-R	WRFAN(2)	Flow (ft^3/min)	[ ]

Additional cards as needed

Card 60500. Time Units

Word	Variable	Description	Value
W1-A	UNITT	HR or S	SEC

Cards 606yy. Upper Door Temperatures

Word	Variable	Description	Value
W1-R	TUPDR(1)	Time (s, per card 60500)	[ ]
W2-R	TUPDR(2)	Temperature (°F)	[ ]
W3-R	TUPDR(3)	Time (s, per card 60500)	[ ]
W4-R	TUPDR(4)	Temperature (°F)	[ ]

Code numerical stability may require a temperature ramp for the first 1 s.

Card 60650. Warm Up Time Interval (hr or s)

Word	Variable	Description	Value
W1-A	TSTARW	Warm up time interval (s)	[ ]

Cards 607yy. Sump Temperatures

Word	Variable	Description	Value
W1-R	TSUMP(1)	Time (s, per card 60500)	[ ]
W2-R	TSUMP(2)	Temperature (°F)	[ ]
W3-R	TSUMP(3)	Time (s, per card 60500)	[ ]
W4-R	TSUMP(4)	Temperature (°F)	[ ]
W5-R	TSUMP(5)	Time (s, per card 60500)	[ ]
W6-R	TSUMP(6)	Temperature (°F)	[ ]
W7-R	TSUMP(7)	Time (s, per card 60500)	[ ]
W8-R	TSUMP(8)	Temperature (°F)	[ ]

Code numerical stability may require a temperature ramp for the first 1 s.

Card 60800. Sump Drain Information

Word	Variable	Description	Value
W1-R	ADRAIN	Exit area (ft^2) of sump drain pipe	[ ]
W2-R	DRAINK	Loss coefficient of sump drain pipe	[ ]
W3-R	DOORL	Width of single lower door (ft)	[ ]
W4-R	DHIGH	Distance of drain exit to lower door (ft)	[ ]
W5-R	SUMPM	Initial mass of water in sump (lbm) (per single lower door)	[ ]
W6-R	SUMPU	Initial internal energy of water in sump (Btu) (per single lower door)	[ ]
W7-R	EFFBLD	Heat transfer efficiency of drain water (Time < TBLD)	[ ]
W8-R	TBLD	Time end of blowdown	[ ]
W9-R	EFFREF	Heat transfer efficiency of drain water (TBLD < Time < TFLD)	[ ]
W10-R	EFFFLD	Heat transfer efficiency of drain water (Time > TFLD)	[ ]
W11-R	TFLD	Time start of reflood	[ ]

Card 609xx. Sump Drain Height-Volume Relationship

Word	Variable	Description	Value
W1-R	SUMPH	Sump height (ft) relative to drain exit	[ ]
W2-R	SUMPV	Sump volume (ft^3) includes drain line	[ ]

A.1.3.8.15 Unused Cards

- Decay power cards 1XX
- Metal-water reaction cards 2XX
- All mass and energy addition cards 4XX, 5XX, 6XX, 7XX, and 9XX
- Outside air condition cards 10XX
- Tagami-Uchida condensing heat transfer coefficient parameters card 12001

- Steady-state special bulk temperature card 1YY410
- All leakage cards 3XXXX
- Miscellaneous or time dependent heat transfer cards 4200XX, 4300XX, and 4400XX
- Containment junction inertias and solution convergence card 62000

A.1.3.9 Documentation

Analytical documentation of the S-RELAP5 RLBLOCA input model prepared under this guideline will reference the guideline by document number and revision. The documentation will contain the following items:

- Referable sources of all input data.
- Steady-state runs to initialize the plant model and control systems.
- Exceptions to the provisions of this guideline.

Additional detail may be included at the analyst's discretion.

A.2 *Uncertainty Analysis Guidelines*

AREVA NP Inc. (AREVA) has developed Revision 3 of the methodology for evaluation of a realistic large-break loss-of-coolant-accident (RLBLOCA) analysis for pressurized water reactors (PWRs). This methodology is applicable to Westinghouse 3- and 4-loop designs, Combustion Engineering 2x4 and AREVA 3 and 4-loop designs with the common characteristics: recirculation (U-tube) steam generators, initial ECCS injection into cold legs and fuel assemblies of up to [ ] feet in length.

A.2.1 Purpose

The purpose of this guideline is to establish a consistent approach for performing the RLBLOCA analysis using the fuel rod code COPERNIC and S-RELAP5 to address low-enriched-uranium (LEU) fuel performance and thermal-hydraulic phenomena respectively.

A.2.2 Scope

This guideline covers technical issues such as input generation and analysis procedures as well as the reporting format to be used. This report provides guidance on how to perform an RLBLOCA analysis using the methodology as described in this Topical Report and input models built as described in Section A.1.

Sections 3.0, 4.0, and 5.0 discuss major decisions and Section 9 discusses the major assumptions associated with the application of the methodology. Additional assumptions are inherent in the development of the sample problems provided in Appendix B. Clarification will be provided about how the decisions or assumption are translated to the calculation procedure.

Computer programs have been developed to automate the creation of the models, to create input for COPERNIC and S-RELAP5 and to perform the RLBLOCA uncertainty analysis. Due the nature of the RLBLOCA calculations and the amount of data required to develop models and perform the calculations and the volume of data generated by the calculations it is imperative that the analyst use the automation tools to maintain consistency in application of the RLBLOCA methodology.

A.2.3 Definitions and Descriptions

A.2.3.1 Blowdown, Refill and Reflood Definition

For the purpose of applying the RLBLOCA methodology, the three phases of the LBLOCA are defined as:

- Blowdown – The blowdown phase of the LOCA is defined as the time period from initiation of the break, until flow from the accumulators or safety injection tanks begins.
- Refill – The refill phase of the LOCA begins when the accumulators or SITs begin injecting and continues, until the mixture level in the vessel refills the lower plenum and begins to flow into the heated core region.

- Reflood – The reflood phase of the transient begins when the lower plenum fills and ECC begins flowing into the bottom of the active core and continues until the temperature transient throughout the core has been terminated. At that time, the LOCA stored energy and decay heat are being removed and the LOCA has been reduced to an issue of maintaining long-term cooling.

A.2.3.2 Required Sample Size

Table A-3 shows the UTLs and defines the limiting values for each criterion as a function of sample size for the RLBLOCA methodology. For the AREVA RLBLOCA uncertainty analysis, [ ] cases is the [

]

Table A-3 [

]

A.2.3.3 Random Number Generator

The statistical nature of this RLBLOCA methodology requires the ability to randomly sample plant operational states and phenomenological conditions. For this reason, the RLBLOCA analyst must have a validated random number generator available. Random number generators are available on most computers or workstations, and provide non-negative floating point values uniformly distributed over the interval [0.0, 1.0). The symbol "[" indicates 0.0 is included in the sampled interval. The symbol ")" indicates 1.0 is not included in the interval. Automated calculations on the Linux workstation use [ ] to generate pseudo-random numbers for the uncertainty analysis.

A.2.3.4 Random Number Sequence

In order to randomly vary the input data for each case, a unique series of random numbers must be generated for each case.

Using the pseudo-random number generator functions, a series of random numbers can be generated and recorded to calculate the input for each case of the uncertainty analysis. This sequence of numbers must be generated in such a way that the sequence is repeatable and is not repeated within the number of cases executed for the analysis.

[ ] The array of required random numbers is shown in Table A-19, along with the variable with which each random number is associated. Note that not all of the random values are used for sampling, but generating two random numbers for each sampled parameter allows for a change in the PDF used for that parameter without a change in the random number sequence order or the total number of random numbers required.

Allowing for a change in the PDF for a parameter without necessitating a change in random number sequence will maintain the same values (given the same initial random number seed is used) for all parameters currently varied as part of the uncertainty analysis.

A.2.3.5 Random Sequence Seed

Random number generators found on most computers or workstations provide a means for supplying an initialization entry point or seed to the random number sequence. Use of a user supplied seed provides a mechanism for reproducing a series of random numbers.

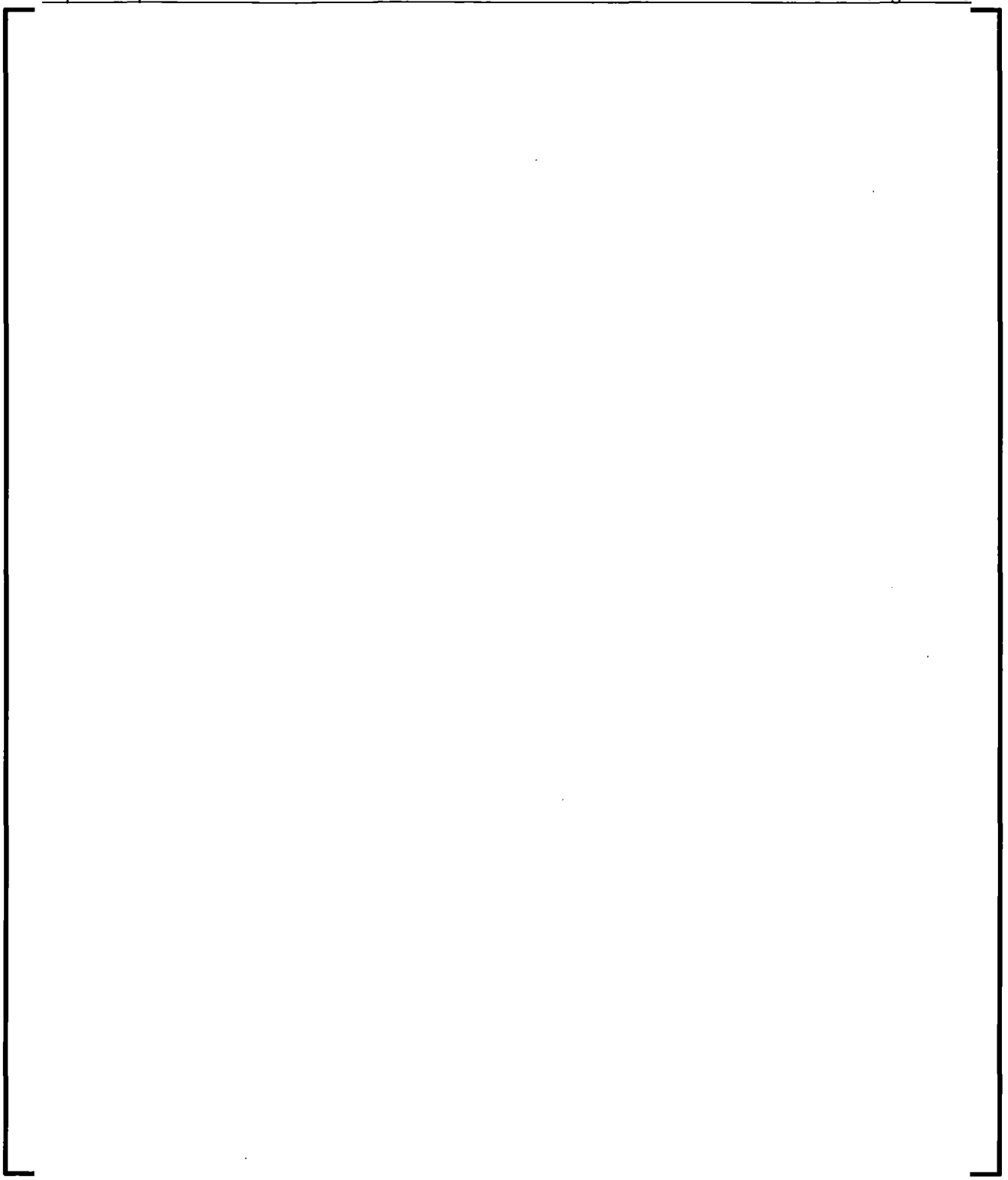

A.2.3.6 Probability Distributions Functions (PDFs)

Using random numbers uniformly distributed over the interval [0.0,1.0) allows these values to be mapped to other PDFs. For the RLBLOCA uncertainty analysis, the common probability distributions to be applied to parameter uncertainty ranges are binary, uniform between two arbitrary numbers, and Gaussian (normal). Additional PDFs may be defined, depending on the characteristics of the input data being modeled.

For the purpose of automating calculations, two random numbers are selected for the sampling each parameter in order to maintain reproducibility of the random number sequence because the Gaussian PDF requires two random numbers.

A.2.3.6.1 Binary PMF

The binary PMF produces a value of either 0 or 1. Using the floating point random number generator, the binary PMF is defined as:

```
int(random1 + 0.5)
```

0.5 is added to the floating point number produced by the random number generator so that, upon truncating the number to an integer, a value of 0 or 1 is produced. Random values in the interval of [0.0, 0.5) are truncated to 0 and random values in the interval of [0.5, 1.0) are truncated to 1.

A.2.3.6.2 Uniform PDF

A uniform PDF ensures an equal probability of selecting any given value over a specified range. Using the floating point random number generator, the uniform PDF ranging between the upper bound and lower bound is defined as:

```
lower_bound + random1 * ( upper_bound - lower_bound )
```

A.2.3.6.3 Gaussian (Normal) PDF

A Gaussian PDF is the natural limit to the convolution of many random events. Using the floating point random number generator, this PDF is defined using the Box-Muller transform (Reference A-16):

$$\eta + \sigma * \sqrt{-2 * \ln(\text{random1})} * \cos(2 * \pi * \text{random2})$$

Where η is the mean and σ is the standard deviation.

A.2.3.6.4 Log-Normal PDF

The log-normal PDF provides a distribution for variables whose natural logarithm is normally distributed. Using the floating point random number generator, the log-normal PDF is defined as:

$$\exp\left(\eta + \sigma * \sqrt{-2 * \ln(\text{random1})} * \cos(2 * \pi * \text{random2})\right)$$

Where η is the mean and σ is the standard deviation.

A.2.3.6.5 Film Boiling Multipliers

[

]

A.2.3.6.5.1 FILMBL and DFFBHTC

[

]

A.2.3.6.5.2 PDF of FILMBL and DFFBHTC

[

]

[

]

Table A-4 Film Boiling Multiplier

[	
	]

Table A-5 Dispersed Flow Film Boiling Multiplier

[	
	]

A.2.3.7 Uncertainty Parameters and Ranges

In RLBLOCA uncertainty analyses the parameters to be sampled are identified as either "Model Parameters" or "Plant Parameters". The distinction between these parameters is the way in which each sampling range is defined. The sampling ranges for model parameters have been predetermined for all RLBLOCA uncertainty analyses as an integral part of the methodology. The sampling ranges for the plant parameters are plant- and analysis-specific.

Table A-6 Uncertainty Parameters and PDFs

A.2.3.7.1 Model Parameter Ranges

Table A-7 summarizes the model parameters that must be applied in every RLBLOCA analysis.

Table A-7 Model Parameter Uncertainty Ranges

[

]

Table A-8 Phenomenological Model Parameters

[

[

]

A.2.3.7.2 Plant Parameter Ranges

Table A-6 defines the plant parameters required for the uncertainty analysis and Table A-12 identifies the plant and calculation specific data required for each of the plant parameters. Completion of Table A-12 prior to the uncertainty analysis defines the PDF and data range for each of the plant parameters specified in Table A-6.

A.2.3.8 Uncertainty Analysis Case

A single uncertainty analysis case is depicted in Figure A-1. For a single case, the required computational order is to calculate fuel rod properties with COPERNIC, followed by an S-RELAP5 steady-state initialization calculation at the sampled conditions, and finally an S-RELAP5 LBLOCA transient calculation is performed restarting from the sampled steady-state conditions.

The fuel rod code (COPERNIC) provides pertinent fuel rod properties at the sampled time in cycle through output file(s) the fuel rod code creates to be read by S-RELAP5. During steady-state initialization, S-RELAP5 processes the fuel rod code output files and performs the steady-state calculation using the plant base model input. The S-RELAP5 transient calculation restarts the steady-state calculation using the input read from the LBLOCA transient input and the containment model input. The key RLBLOCA results are retrieved from the S-RELAP5 transient calculation output files.

A.2.3.9 Key Results

For each of the uncertainty cases, the values for S-RELAP5 rod number and associated PCT, total hydrogen generated, % total oxidation and % oxidation maximum are all read from the S-RELAP5 output. For the rod with the highest PCT temperature the values for the time of PCT, axial node of PCT and total transient time are also read from the transient output file.

A.2.3.10 Corrosion Adjustment

The % local oxidation read from S-RELAP5 must be adjusted to account for the initial operational oxidation.

[

]

[

]

A.2.3.11 Statistical Evaluation

As previously explained, the methodology has the advantage of being able to treat a large number of parameters by randomly varying each parameter in each single calculation. This random selection process is repeated to define a large number of RLBLOCA calculations, all of which are then run.

The key results are read for each of the RLBLOCA calculations and the values for PCT, Maximum Local Oxidation, and Core-Wide Oxidation are saved for each case. The values for PCT, % Maximum Local Oxidation and % Core-Wide Oxidation are then set to the PCT_i, MLO_i, and CWO_i for each case respectively.

[

]

Table A-9 Example Statistical Evaluation Data

[

]

A.2.3.12 Limiting Case

For the RLBLOCA uncertainty analysis the [ ] cases (see Section A.2.3.2), however this does not preclude analyses performed with different sample sizes. [

]

A.2.4 Analytical methodology

The RLBLOCA methodology is supported by the discussions and references provided in previous sections of this document. It is the object of the methodology to conform to with the philosophy expressed by the CSAU Evaluation Methodology, Reference A-1.

This guideline will assist the analyst in satisfying the CSAU Evaluation Methodology; Steps 12-14. Application of these steps will provide a statement of the key acceptance criteria parameters and the overall uncertainty associated with those parameters. Adherence to the CSAU approach will assure that the calculations or total uncertainties are quantifiable.

Application of the RLBLOCA methodology is discussed in Appendix B. Examples of the application of the methodology can be viewed in the sample problems discussed in that appendix.

A.2.4.1 Major Assumptions

The following sections define major assumptions used in the RLBLOCA uncertainty analyses.

A.2.4.1.1 Worst Single Failure

For the 3- and 4-loop sample problems (also applicable to CE plants), the worst single failure assumption conservatively couples the two most probable failures: [

]

When the loss of offsite power is chosen, a time delay for startup of diesel generators and the safety injection system is applied. Technical specification values for the delay times are to be used.

AREVA has performed sensitivity studies on maximum versus minimum ECCS injection to determine if a loss of one train of ECCS is a conservative assumption for the single failure. [

]

[

]

A.2.4.1.2 Break Location

The break location is modeled between the pump discharge and the reactor vessel within the RCS loop containing the pressurizer.

A.2.4.2 Determination of Offsite Power Limiting Condition

Reference A-17, Appendix A, GDC-35 requires that abundant emergency core cooling shall be provided both with or without the availability of off-site power. [

]

A.2.4.3 RLBLOCA Uncertainty Analysis

Since the RLBLOCA methodology is a statistics-based methodology, the application does not involve the evaluation of many different deterministic calculations. Instead a number of calculations are performed with the parameters defined as explained in Section 9.4 varied randomly over the specified uncertainty range. This random sampling process is repeated for a number of calculations, all of which are run to obtain key results.

A.2.4.4 Computer Codes

The COPERNIC computer code is used to predict fuel rod performance with respect to fuel rod mechanical design. The computer code S-RELAP5 is used to simulate the RLBLOCA transient. Table A-10 lists the codes used for the uncertainty analysis.

Table A-10: Analysis Codes

Computer Code	Description
COPERNIC	Fuel rod performance code for M5® fuel.
S-RELAP5	System and transient analysis.

Section A.2.2 states computer codes have been developed to automate application of the RLBLOCA methodology. Table A-11 provides a list of these codes.

Table A-11: Automation Computer Codes

Computer Code	Description
AUTOR5BASE_REV3	Develop S-RELAP5 model base deck for use in RLBLOCA analysis
AUTOICECON	Develop S-RELAP5 containment model for use in RLBLOCA analysis transient calculation
AUTOROD	Provide fuel rod performance data for steady-state initialization of S-RELAP5 base deck
AUTORLBLOCA_REV3	Perform the RLBLOCA analysis

A.2.5 Analysis Input Requirements

This section provides instructions for preparing input for an RLBLOCA analysis. Prior to the performing the uncertainty analysis the analyst must obtain information to build the fuel rod model, S-RELAP5 model, containment model, and plant parameter uncertainty ranges. It is expected that the analysis responsible for performing the RLBLOCA analysis and using this guideline will have the following information readily available for the plant being analyzed:

- COPERNIC fuel rod model.
- S-RELAP5 base model.
- ICECON containment model.
- Neutronics Input to RLBLOCA.
- Assembly dimensions and description for fuel type to be analyzed.

- Core design data.
- Plant licensing parameters.
- Plant operating parameters.
- ECCS, RCS, pressurizer, vessel parameters.
- Uncertainty ranges for plant parameters.
- Fixed code versions.
- Automation database data.

A.2.5.1 Fuel Rod Model

The RLBLOCA uncertainty analysis requires a fuel rod model created as described in Section A.2.5.16.2 for use with COPERNIC.

When using automation tools, the fuel rod model is automatically generated for each case of the uncertainty analysis using data supplied through the automation databases. Therefore, no fuel rod base deck is required for the automated analysis.

A.2.5.2 S-RELAP5 Base Model (Base Deck)

The RLBLOCA uncertainty analysis requires an S-RELAP5 model built as described in Section A.1.3.6. This model must be initialized to an approximation of steady-state conditions as defined in Section A.1.3.6.6.

For the uncertainty analysis, input cards will be appended to the base deck based to set the sampled PIRT parameter conditions and a calculation will be run to initialize the base deck back to steady-state at the sampled conditions. Following the steady-state calculation an S-RELAP5 input deck is created to supply the sampled PIRT parameter conditions required for the transient portion of the calculation.

The S-RELAP5 base deck is file location is provided through the use of the automation plant database record defined by component *autor5base* and parameter *basedeck_rlbloca_ss*.

A.2.5.3 ICECON Containment Model

The RLBLOCA uncertainty analysis requires a containment model built as described in Section A.1.3.8. The ICECON input deck is modified prior to its use in the transient portion of the calculation to include the randomly sampled containment volume and containment temperature.

The containment model is provided through the use of the automation plant database record defined by component *autoicecon* and parameter *rlbloca_icecon_deck*.

A.2.5.4 Neutronics Input to RLBLOCA

The neutronics inputs to RLBLOCA are provided to AUTORLBLOCA_REV3 through the automation plant database components *autosar* and *neutronics*.

A.2.5.5 Additional Data

The remaining database data required for the uncertainty analysis can be obtained from plant parameter documents, fuel design drawings, plant drawings, plant technical specifications or other verified documentation.

A.2.5.6 Plant Parameters Uncertainty Ranges

The analyst must obtain the uncertainty range and PDFs for the 'plant' parameters defined in Table A-6. The following table provides the analyst with a list of parameter ranges that must be set prior to the RLBLOCA uncertainty analysis can be performed.

Table A-12: Plant Parameter Uncertainty Variables Required

The plant uncertainty variable ranges are provided through the use of the automation plant database table defined by component *plant_licensing_parameters* and parameter *uncert_rlbloca_plant.tab*.

A.2.5.7 Fixed Code Versions

Code versions for COPERNIC and S-RELAP5 must be obtained and verified for use prior to performing the uncertainty analysis.

The applicable code versions are provided through the use of the automation PWR methods database records defined by the component *pwr_methods* and parameters *copernic_version, srelap5_rlbloca_version.*

The code version for AUTORLBLOCA_REV3 that will perform the uncertainty analysis is also defined in the automation PWR methods database records defined by the component *pwr_methods* and parameter *autorlbloca_rev3_version*.

A.2.5.8 Automation Database Data

The automation codes read all required data from the plant and methods databases.

A.2.5.9 Results From Previous Uncertainty Analysis

The results of previous uncertainty analysis are to be reviewed prior to and following the uncertainty analysis being performed. The analysis will verify that changes to the S-RELAP5 base deck, ICECON base deck and input files created between analyses are correct and expected.

RLBLOCA Uncertainty Analysis

For the uncertainty analysis each of the parameters identified in Table A-6 are randomly varied for a number of cases that simulates the LOCA at the sampled conditions. The process is repeated for a number of cases and produces results the simultaneously bound the PCT, MLO and CWO with 95 percent coverage and 95 percent confidence.

The uncertainty analysis can be summarized by the following primary tasks: data initialization, random number generation, parameter sampling, calculating time dependent data, creating input files, executing calculations, processing output, performing statistical analysis, summarizing output and reporting limiting case information. These are discussed in the following sections.

A.2.5.10 Data Initialization

A.2.5.10.1 Keyword Based Input

The KBI file for AUTORLBLOCA_REV3 provides information specific to the uncertainty analysis being performed and includes listing of the databases to be used for the analysis, setting input execution options and providing information for the calculation file to be created.

A.2.5.10.2 Database Data

Prior to performing the calculations the analysis must verify that the correct methods and plant databases are named in the KBI input file.

A.2.5.10.2.1Reactor-Specific Input Options

Plant Specific Nomenclature

Special considerations may be required for reactor vendors or for unique plant types.

Throughout this guideline and the calculation file created by AUTORLBLOCA_REV3 many references to the global peaking factor, F_Q, are made. [

]

Containment Type

Containment type options are triggered by the plant database record defined by component containment and parameter type. This database record specifies the containment type as one of the following options: (a) dry (b) sub-atmospheric or (c) ice condenser type containment. [

]

[

]

Upper Head Type

Two types of plants exist with respect to regulation of upper head temperature, hot head and cold head plants. Section A.1.3.6.2.4 discusses each and the treatment of the associated form-loss coefficients.

Upper head type options are triggered by the plant database records defined by component *reactor_vessel* and parameters *upper_head_type* and *uhi_column_hole_id*. The parameter *upper_head_type* defines the plants having a hot or cold upper head. The existence of the parameter *uhi_column_hole_id* triggers the writing of additional input cards to the S-RELAP5-TR calculation input file for the upper head injection columns. Note that the original functionality of ECCS injection to the upper head through these columns has been disabled. The hollow columns do, however, provide a drain path for the fluid in the upper head.

Nomenclature and Terminology

Plant specific terminology may be required in the document created by the automation tools. The analyst is responsible for verifying, making additions or making corrections for plant specific terminology in the calculation notebooks produced by the automation tools.

A.2.5.10.3 Power History Data

The power history data are created according to the relevant PWR engineering guideline and the file names for the relevant power history data are read from the plant database record with component *neutronics* and parameters *power_history.tab* for the

[

]

All power history data must be provided in the format defined in the engineering guidelines and shown below.

Power History Data File Example

The subsections that follow describe the creation of a "Rod Identification Table" (RIT) that is used in the automated uncertainty analysis. The data used in the creation of the RIT are either read directly from or calculated from data provided in power history files.

A.2.5.10.3.1Power History Data Filter

This section describes the data read from the power history files. An example of power history data is provided in the previous section.

The variables in Table A-13 are read from the database records previously mentioned. They are not read directly from the power history data. The UO_2 enrichment and Gad loading are typically part of the rod history file name.

Table A-13 Power History Data Files

Variable	Description	Units
ph_file	power history file name	no units
ph_file_enr	rod UO2 enrichment	w/o
ph_file_gad	rod Gad loading	%

The values for the variables listed in Table A-14 are read from the power history data. These data are not manipulated in any way.

Table A-14 Power History Data Values Read from File

[

]

[

]

[

]

A.2.5.10.3.2Power History Data Calculations

The values for the variables listed in Table A-15 are calculated from data read from the power history data and other database data. These data are not found in the power history file.

Table A-15 Power History Calculated Values

[ ]

Additionally, the values for the variables listed in Table A-16 are calculated from data read from the power history data and other database data. These data are not found in the power history file and are calculated by the automation process for use in the uncertainty analysis.

Table A-16: Power History Calculated Values

[

]

Using the data read from the power history file and the data calculated from the power history file a summary is produced for each unique power history file. An example of this summary is shown below.

AUTORLBLOCA_REV3 Created Power History Summary File Example

[ ]

A.2.5.10.3.3Power History Data – Uncertainty Analysis Variables

The example below shows the power history data retained by the automation process for use with the uncertainty analysis. Table A-17 defines variables to be used in the description of calculated data throughout this report.

AUTORLBLOCA_REV3 Created Sorted Summary File Example

Table A-17: Power History Calculated Values

[

]

A.2.5.10.3.4Power History Data - Sort

[

]

A.2.5.10.4 Axial Power Data

The axial data file names are read from the plant database record with component *autosar* and parameter *rlbloca_axials.tab*. This database record contains the archived file location in cstor for the axial files.

[

]

An example of single axial power shape file is shown below.

Axial Power Data File Example

[

]

A.2.5.10.5 Radial Power Data

The radial power data file names are read from the plant database record with component *autosar* and parameter *rlbloca_radials.tab*. Radial power profiles are provided for the cycle being analyzed.

[

]

The radial power maps include the assembly power for all assemblies. There is no requirement to distinguish between fresh, once-burned or other burned fuel within the radial power maps. An example is shown below.

Radial Power Data File Example

```
* Full-Core Assembly Power Distribution Map at Cycle Exposure 100 MWd/MTU
*
TABLE00
{
     .     .     .     .     .     . 0.268 0.326 0.267     .     .     .     .     .     .
     .     .     .     . 0.327 0.601 0.989 1.003 0.990 0.600 0.326     .     .     .     .
     .     .     . 0.496 1.069 1.221 1.201 1.155 1.202 1.215 1.065 0.495     .     .     .
     .     . 0.495 1.069 1.274 1.169 1.230 1.202 1.220 1.163 1.267 1.069 0.496     .     .
     . 0.326 1.065 1.267 1.270 1.272 1.288 1.290 1.283 1.267 1.270 1.274 1.069 0.327     .
     . 0.600 1.215 1.163 1.267 1.145 1.182 1.113 1.183 1.145 1.272 1.169 1.221 0.601     .
 0.267 0.990 1.202 1.220 1.283 1.183 1.085 1.174 1.085 1.182 1.288 1.230 1.201 0.989 0.268
 0.326 1.003 1.155 1.202 1.290 1.113 1.174 1.159 1.174 1.113 1.290 1.202 1.155 1.003 0.326
 0.268 0.989 1.201 1.230 1.288 1.182 1.085 1.174 1.085 1.183 1.283 1.220 1.202 0.990 0.267
     . 0.601 1.221 1.169 1.272 1.145 1.183 1.113 1.182 1.145 1.267 1.163 1.215 0.600     .
     . 0.327 1.069 1.274 1.270 1.267 1.283 1.290 1.288 1.272 1.270 1.267 1.065 0.326     .
     .     . 0.496 1.069 1.267 1.163 1.220 1.202 1.230 1.169 1.274 1.069 0.495     .     .
     .     .     . 0.495 1.065 1.215 1.202 1.155 1.201 1.221 1.069 0.496     .     .     .
     .     .     .     . 0.326 0.600 0.990 1.003 0.989 0.601 0.327     .     .     .     .
     .     .     .     .     .     . 0.267 0.326 0.268     .     .     .     .     .     .
}
```

[ ]

A.2.5.10.6 Core Power

The core power for the uncertainty analysis is calculated using the data read from the plant database record [

]

A.2.5.10.7 Technical Specification Global Peaking Factor, F_Q

The technical specification global peaking factor, F_Q, is read from the plant database record with component *plant_licensing_parameter* and component *fq_ts*. The value of the tech spec global peaking factor remains constant throughout the uncertainty analysis.

Within this document, the technical specification global peaking factor value will be referred to as: $F_Q^{TechSpec}$

A.2.5.10.8 Technical Specification Hot Channel Peaking Factor, FΔH

The technical specification $F_{\Delta H}$ is read from the from the plant database table with component *plant_licensing_parameter* and component *fdh_limit_ts.tab* at 100% power.

[

]

Within this document, the technical specification hot channel peaking factor value will be referred to as: $F_{\Delta H}^{Tech\ Spec}$

A.2.5.10.9 Fuel Rod Heat Structures

Table A-18 identifies the heat structure numbers defined for the S-RELAP5 base deck core regions. The heat structure numbers are used for a number of replacement (modset) cards used in the uncertainty analysis.

Table A-18 S-RELAP5 Rod Heat Structure

[

]

[

]

A.2.5.10.10 Cutback Factors

[

]

[

]

A.2.5.10.11 Model Parameter Ranges

The model parameter ranges are fixed according to the data in Table A-7, except for the initial stored energy range. [

] Table A-7 lists the values for use with COPERNIC.

[

]

A.2.5.10.12 Plant Parameter Ranges

The plant parameter ranges are read from the database record with component *plant_licensing_parameters* and parameter *uncert_rlbloca_plant.tab* (see Table A-12). The ranges for the plant parameter variables remain constant throughout the uncertainty analysis.

A.2.5.11 Random Number Sequence

The random number sequence for the uncertainty analysis must be composed of a unique sequence of random numbers.

A.2.5.11.1 First Case Seed

A seed must be supplied for the first case of the uncertainty analysis. [

]

A.2.5.11.2 Random Number Sequence

Once the seed is set for the subsequent case, [ ] additional random numbers are generated to randomly vary the PIRT parameters. Table A-19 provides a list of the sampled parameters and the random numbers associated with each parameter. The random numbers are used to calculate fuel rod code and S-RELAP5 input for the sampled parameters.

Table A-19 Random Number Sequence

[

]

A.2.5.12 Model Parameter Sampling

The modeling parameters are sampled for each case. The ranges and PDF are constant for the entire analysis. The following section defines how the sampled value for each modeling parameter is calculated. Unless noted otherwise, the lower and upper bounds or the mean and standard deviation are defined in Table A-7.

A.2.5.12.1 Time In Cycle

[

]

The lower and upper bound are determined as described in Section A.2.5.10.11.1.

[

]

A.2.5.12.2 Sampled Global Peaking Factor, F_Q

[

]

The lower and upper bounds are determined as described in Section A.2.5.10.11.2.

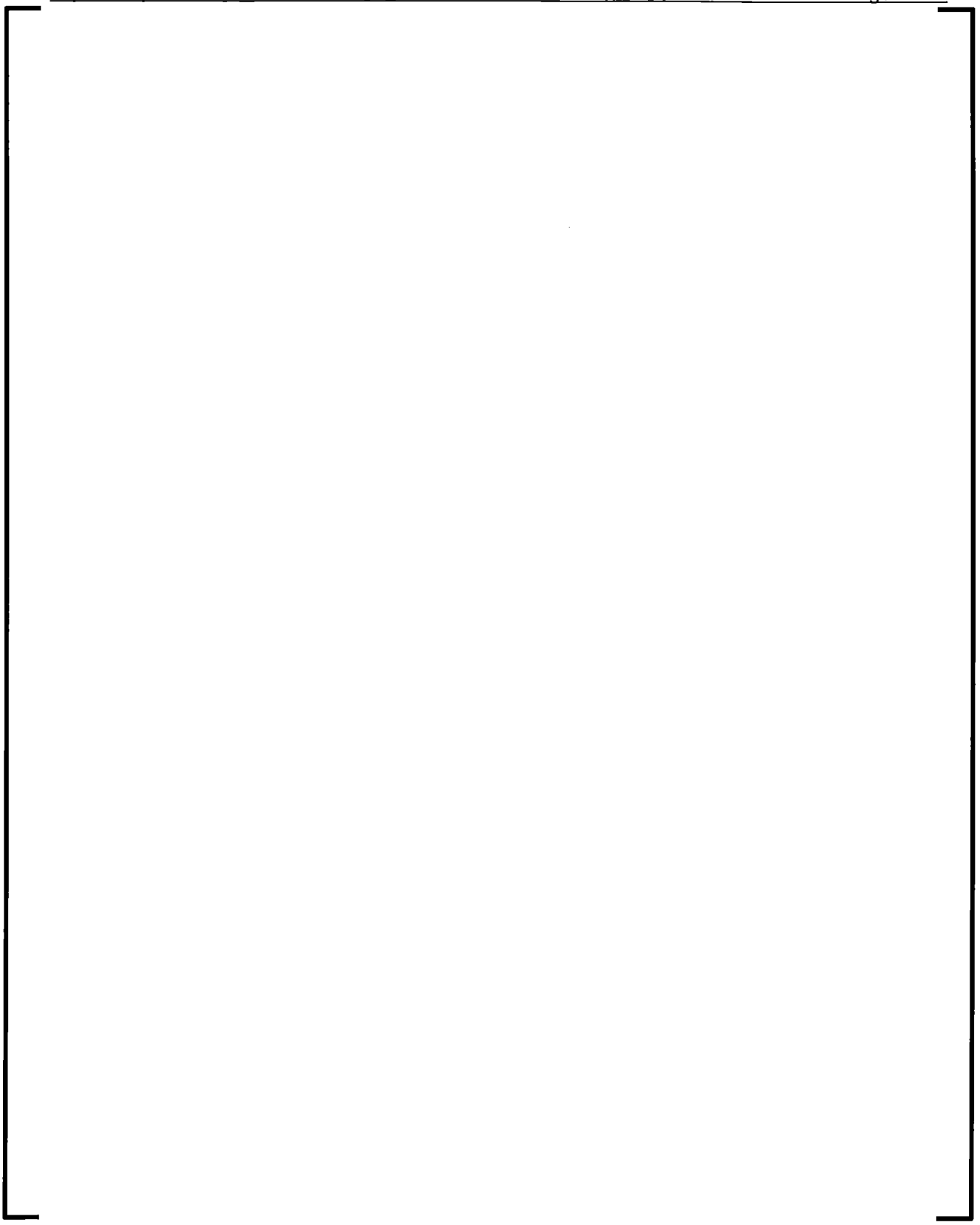

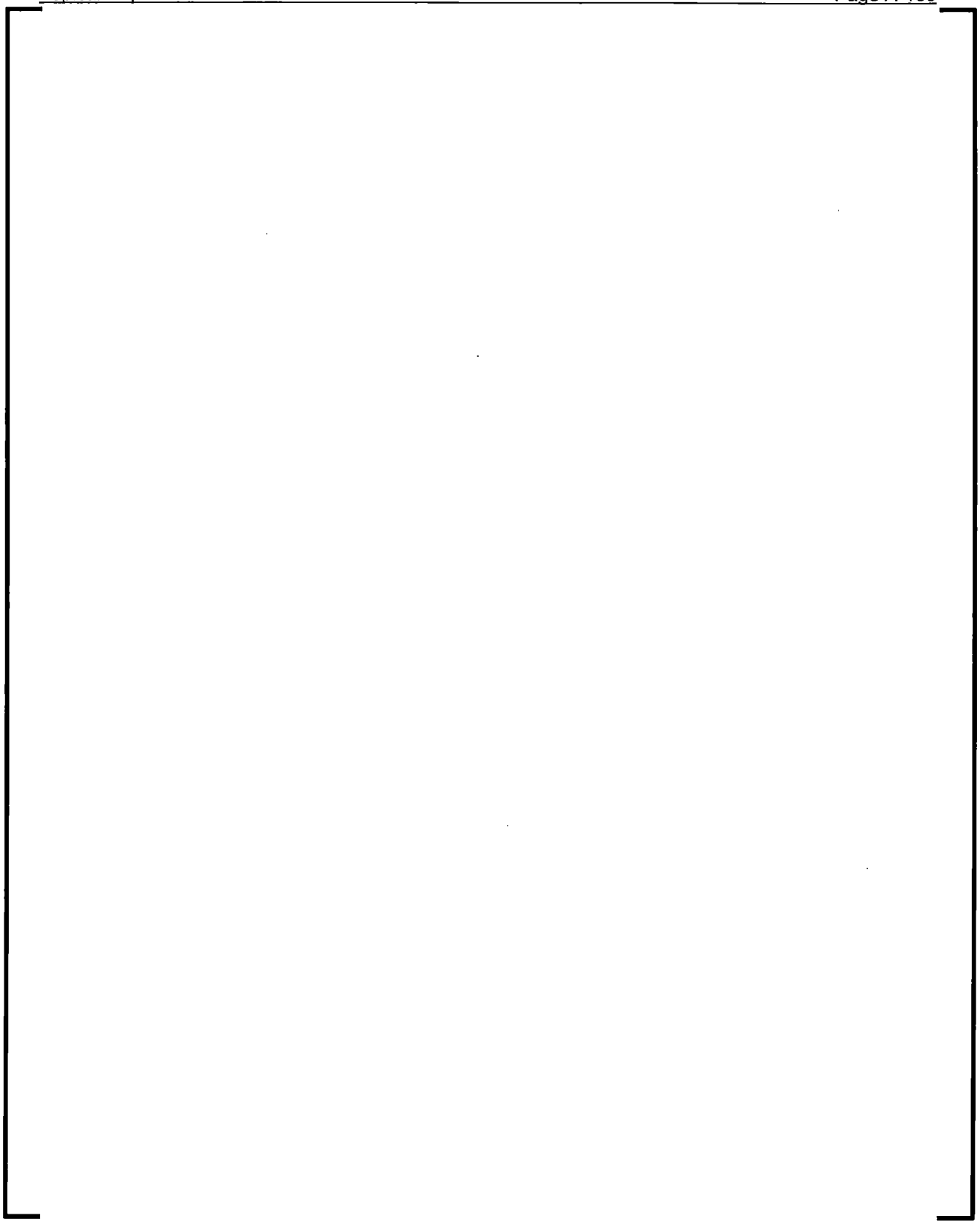

A.2.5.13 Plant Parameters

Each plant parameter is sampled according to the PDF defined for the uncertainty analysis as described in Section A.2.5.6. The calculation of each parameter is discussed in the sections that follow.

Note that the lower bound or mean and upper bound or standard deviations are defined in Table A-12.

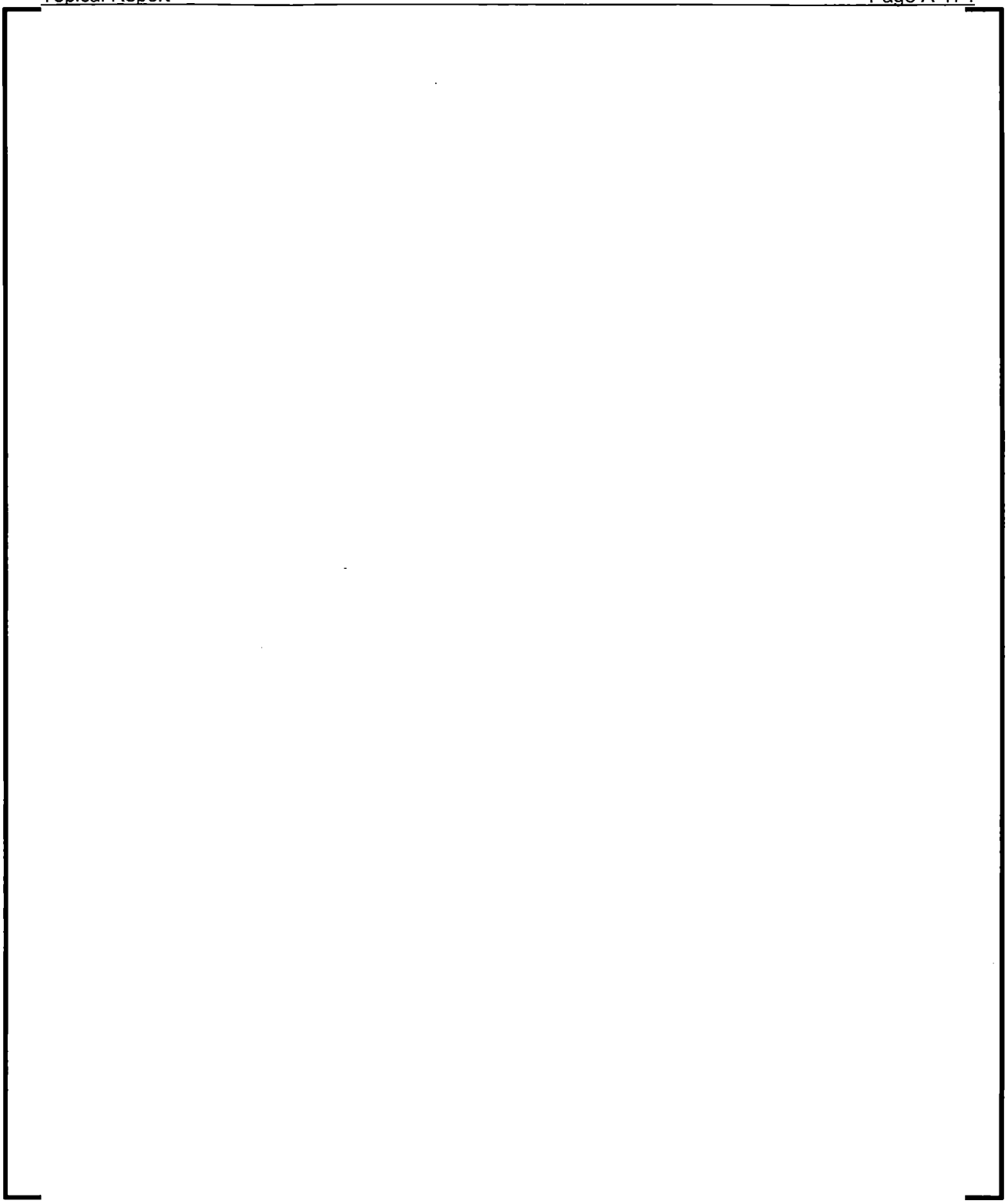

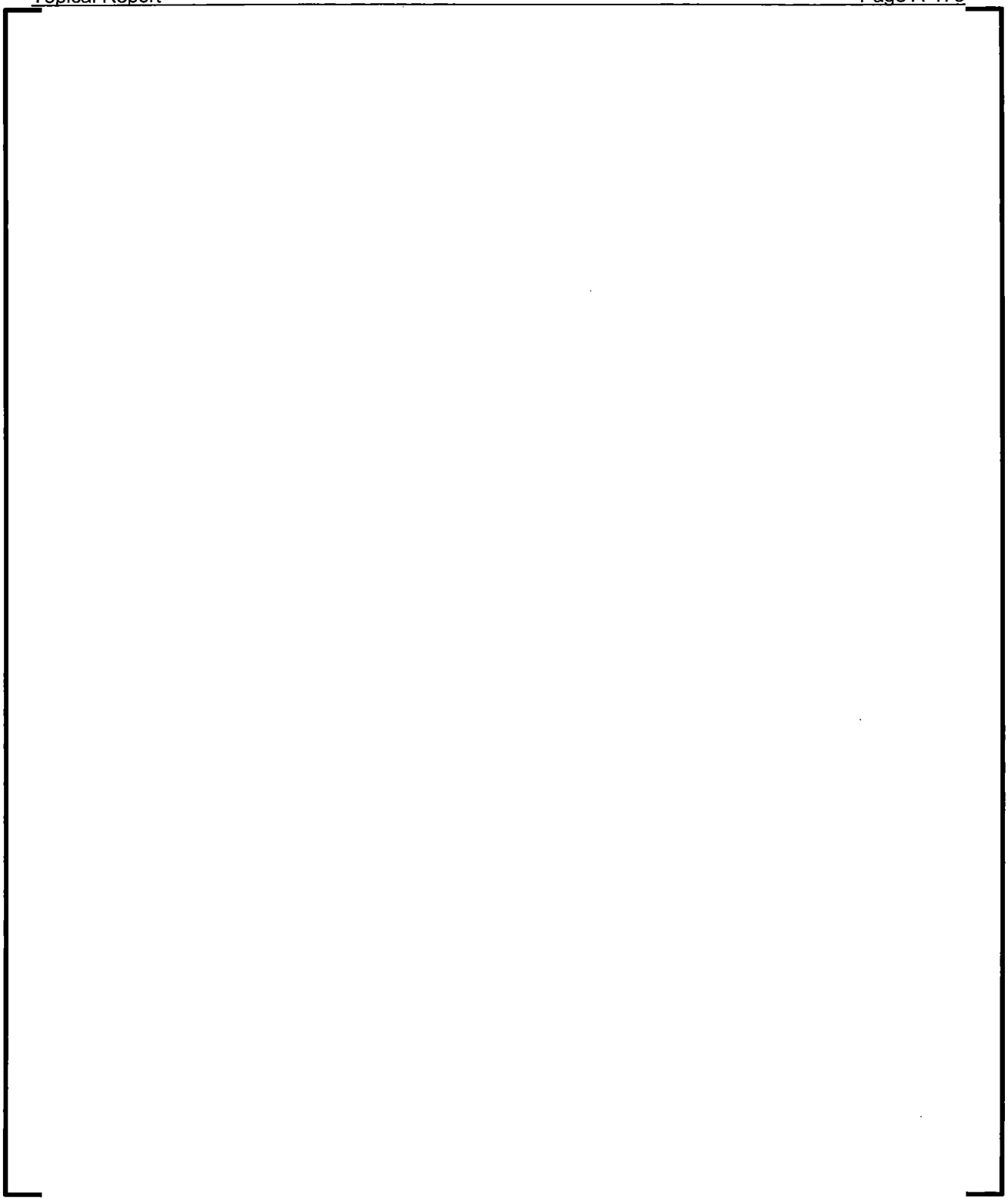

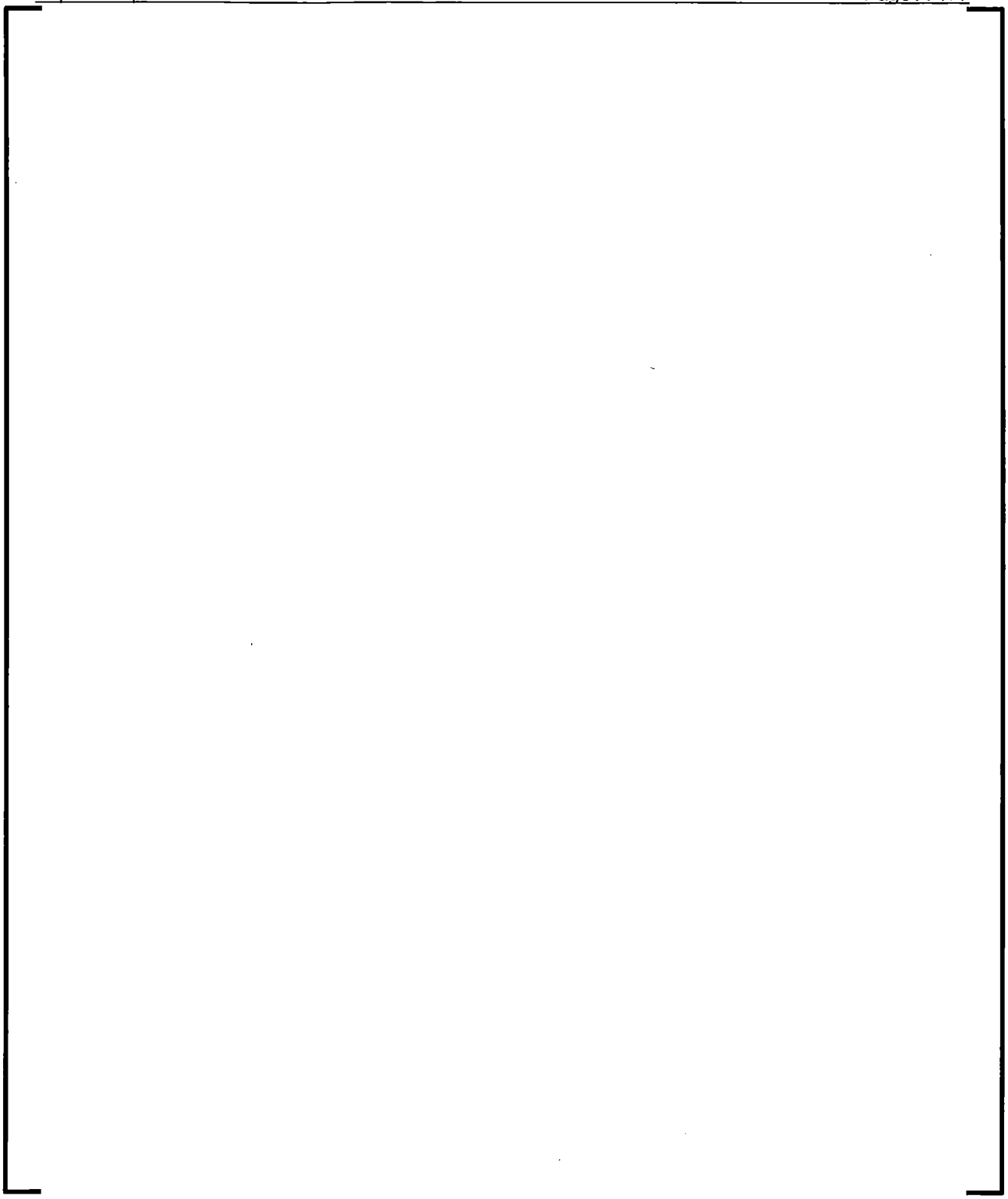

[redacted]

[redacted]

A.2.5.15 Radial Power Factor Calculation

The radial power peaking factors are used to partition the power among the modeled fuel rod regions defined in Table A-20.

Table A-20: Radial Power Peaking Factors

The number of fuel rods must be calculated for each region, so that the power in each region is normalized to the number of rods in the core. Table A-20 identifies the variable used for the number of rods in each region, for the equations used to calculate the radial power fractions for each region in the sections that follow.

The total number of assemblies in the core ($Assy_{Core}$) is read from the plant database record with component core_design and parameter num_assy. The number of fuel rods per assembly ($Rods_{Assy}$) is read from the plant database record with component *assembly_** and parameter *assy_num_rods_fuel*.

[redacted]

A.2.5.16 Fuel Rod Input

The static fuel rod parameters (i.e., not time- or burnup-dependent) are based primarily on mechanical specifications for the fuel rod and assembly. For this reason, best-estimate values are need for these parameters. Nonetheless, while PCTs are strongly influenced by burnup, scoping studies have shown that within the normal range of uncertainty, variation of most fuel rod parameters have only a small effect on PCT.

The fuel rod model for COPERNIC is discussed in the following sections. Default input is used where not specifically mentioned.

Mechanical assembly, rod and pellet data are read from the automation database records with components *assembly_"suffix"* and *core_design*, where the assembly *"suffix"* is set by the database record with component *core_design* and parameter *hot_assy_fuel_type*. The term *"assembly_"* will be used throughout this section and will refer to the hot assembly fuel type.

A.2.5.16.1 COPERNIC Modeling Assumptions

Three regions are required for COPERNIC pellet input. These three regions are: (1) an upper blanket, (2) lower blanket and (3) enriched fuel region. The blanket regions surround the enriched fuel region.

Name lists and input variables omitted from the guidelines below either default to COPERNIC default values, or are deemed not necessary for the purposes of RLBLOCA uncertainty analysis.

A.2.5.16.2 COPERNIC Model Input

The COPERNIC fuel rod calculation is actually split into two calculations. First, the COPERNIC preprocessor, COPRE, is executed to process a free-format input file and produce a fixed-format input file for COPERNIC. The following sections define the COPRE pre-processor input required for the COPERNIC RLBLOCA uncertainty analysis fuel rod model.

Name lists and input variables omitted from the guidelines below either default to COPERNIC default values, or are deemed not necessary for the RLBLOCA uncertainty analysis fuel rod model

A.2.5.16.2.1Physical Models

The &OPT name list input will be identical for each case of an uncertainty analysis.

&OPT	**Physical Model Input**
ICORRO	*waterside corrosion model input option* [ ]
IREDEM	*restart option* [ ]
M3	*number of axial slices set to 24*
NMRDM	*restart macro-time step number* [ ]

A.2.5.16.2.2Material Properties

The &MAT name list input will be identical for each case of an uncertainty analysis.

&MAT	**Material Properties**
IWERKB	*fuel properties* [ ]
IWERKB(1,4)	*strain due to swelling (solid + gaseous)* [ ]
IWERKB(1,6)	*fuel thermal conductivity* [ ]
IWERKH	*cladding properties* [ ]
IWERKH(2)	*Young's modulus* [ ]
IWERKH(3)	*Poisson's ratio* [ ]

IWERKH(4)	*axial growth before fuel-cladding interaction* [ ]
IWERKH(5)	*thermal expansion* [ ]
IWERKH(6)	*thermal conductivity* [ ]
IWERKH(7)	*all5 low and high stress creep model* [ ]
IWERKH(8)	*yield strength* [ ]
IWERKH(9)	*rupture strain* [ ]
IWERKH(13)	*specific heat* [ ]
IWERKH(14)	*density* [ ]
IWERKH(16)	*melting temperature* [ ]
IWERKH(18)	*emissivity* [ ]
IWERKK	*coolant properties* *set to 1 for AREVA water properties*

A.2.5.16.2.3Model Coefficients Selected

The &COEF name list input will be identical for each case of an uncertainty analysis.

&COEFF	**Model Coefficients Selected**
FHEAT	*fission energy fraction generating heat in the fuel rod (fraction)* [ ]
IEXCEL	*EXCEL output option, 0 = do not print, 1 = print slice L results on file *.xls* *set to 24*0*

A.2.5.16.2.4Fuel Rod Characteristics

The &CARA name list input will be identical for each case of an uncertainty analysis.

&CARA	**Fuel Rod Characteristics**
AOPL	*multiplier to adjust upper plenum volume (fraction)* [ ]
CANF	*fill gas composition (fraction)* [ ]
HHREF	*reference heights of axials slices in the cladding (mm)* [ ]
IDAX	*array of M3 values with binary index to indicate if a slice is redefined or not* [ ]
PI0EIN	*fill gas pressure (MPa)* [ ]
TI0EIN	*fill gas temperature (°C)* [ ]
UPLVG	*lower plenum volume (mm^3)* [ ]

A.2.5.16.2.5Pellet Characteristics

A set of &DAX cards must be input for an upper and lower blanket region, and a middle region representing the fuel region. The &DAX name list input will be identical for each case of an uncertainty analysis.

&DAX	**Pellet Characteristics**
M1	*number of radial coarse rings in the fuel rod (fuel and cladding)* [ ]
M1H	*number of radial coarse rings inside the cladding* [ ]
M2	*number of fine radial nodes inside each coarse ring* [ ]
IFALL	*variable defining the geometry for the fuel rod analyzed* [ ]
DICI	*cladding inner diameter (mm)* [ ]
DIFI	*pellet inner diameter (mm)* [ ]
DOCI	*cladding outer diameter (mm)* [ ]
DOFI	*pellet outer diameter (mm)* [ ]
DRMAX	*resintering density increase (%)* [ ]
ENR35	*Uranium enrichment, U^{235}, (%)* [ ]
ENRPU	*Plutonium enrichment (a non-zero entry indicates MOX fuel)* [ ]

HPELLT *pellet height (mm)*
[
]

IFRM *fuel pellet radial power distribution option*
[ ]

KORNGR *average fabrication grain size diameter in the fuel (mm)*
[ ]

OPOROS *as-fabricated open porosity (%)*
[ ]

PCHIP *pellet chip volume as percentage of pellet volume (%)*
[ ]

PDISH *ratio between the dish volume and the pellet volume (%)*
[
]

PGD2O3 *Gd_2O_3 weight content (%) for active fuel only*
[
]

POROSI *porosity of the fuel at the beginning of the calculation (%)*
[ ]

SWESOL *solid swelling rate (%)*
[ ]

[ ] COPERNIC built-in tables are used for the UO2 fuel regions, See input for *IFRM*. [
]

BFLRA *burnups for TFLRA data tables (required if IFRM=6)*

NBFLRA *number of BFLRA burnups used for TFLRA data table*

NFLRA *number of RFLRA radii used for TFLRA data tables*

RFLRA *radii for TFLRA data table*

TFLRA — *data table giving pellet radial power density distribution as a function of radius (RFLRA) and local burnup (BFLRA)*

A.2.5.16.2.6Irradiation History Characteristics

The &HISTO name list input will be different for each case of an uncertainty analysis.

&HISTO	**Irradiation History Characteristic**
NM	*number of macro time steps (<2000)* [ ]
NAXSM	*number of axial shapes* [ ]
NP	*array specifying the number of points for each axial shape contained in AXS array* [ ]
APEAK	*peaking factor for power and flux axial shapes* [ ]
DAL	*coolant subchannel equivalent hydraulic diameter (mm),* [

]

DCHL *coolant subchannel heating diameter (mm)*

[

]

FLUXL *fast neutron flux (neutrons/cm^2-s) for each time step*

[ ]

Input Calculations:

[

]

[

]

[

]

[

]

[

]

GKL *coolant mass flux (kg/m2-s)*
[

]

IAXOUT *slice by slice print-out options*
array of size M3 all set to 0, to not print output slice by slice

IHOLD *macro-time step option* [

]

IOUT *print-out option for each time step*
array of size NM with all values set to 1.0 to print output for each time step

JFLUXL *index that provides the axial shape of FLUXL for each time step*
[

]

JQL *index that provides the axial shape of QL for each time step*
[

]

PAL *coolant pressure (MPa)*
[

]

QL *linear heat rate (kW/m)*
[ ]

Input Calculations:

[

]

[

]

[

]

RAUBL *surface roughness of fuel (mm)*

[ ]

RAUHL *surface roughness of cladding (mm)*

[ ]

TETKIN *inlet coolant or outer cladding temperature (°C)*

[

]

TIME *irradiation history times (hours)*

Input Calculations:

[

]

AXS *values at the ZAXS elevations (arbitrary units)*

[

]

ZAXS *axial elevations (mm)*

[

]

[

]

[

]

[

]

[

]

A.2.5.17 Steady-State Model Input

An analysis and plant specific S-RELAP5 base model must be created according to the guidelines presented in Section A.1.3.6, and provided to the uncertainty analysis as described in Section A.2.5.2.

[

]

The base model and how each of these parameters is included in the S-RELAP5-SS model are discussed below.

A.2.5.17.1 Base Model

The S-RELAP5-SS uncertainty analysis base model must be created by AUTOR5BASE_REV3 (See Table A-10), and in compliance with the guidelines presented in Section A.1.3.6. The base model file archive location is read from the database record with component *autor5base* and parameter *basedeck_rlbloca_ss* and retrieved from the named location.

The sections that follow define the "modsets" that are used to append the sampled PIRT parameter information to the end of the base deck. Some of the modsets use duplicate input cards to overwrite data already found in the base deck, and some modsets use new cards not found in the base deck. These are identified by the leading card group number. Where LBLOCA uncertainty analysis multipliers are used, the cards starting with 130-139 are used with the line continuation character '+'. Since there is a limit of 10 sets of LBLOCA multiplier cards, and there is a limit to the number of line continuations per set of multiplier cards, some modsets are combined under a single set of LBLOCA multiplier cards in the base deck.

The following variables are used in the card groups specified in the following sections. The variables are identified once to avoid repetition.

Variable	Description
CCC	*component index*
G	*geometry index*
NN	*continuation card index*

A.2.5.17.2 Power Shape and Peaking Factor Comment Cards

[

]

[

]

[

]

A.2.5.17.3 Heat Source Modset

A heat structure is defined as a node of heat conductor, thermal energy source or sink, connected to a hydrodynamic volume.

This procedure presents a broad spectrum of possible radial power distributions biased conservatively based on trends observed in sensitivity studies. With the axial power shape and radial power peaking factors, the fuel rod heat structure card group 1CCCG7NN can be modified. The specific cards requiring change are as follows:

Card 1CCCG7NN	**Heat Structure Source Data Cards**
W1(I)	*source type.* [ ]
W2(R)	*Internal heat structure source multiplier.* [

]

[

]

[

]

[

]

The total number of rods in the core is calculated from the database records with component and parameters *core_design:num_assy* and *assembly_:assy_num_rods_fuel* as:

The total number of assemblies in the core ($Assy_{Core}$) is read from the plant database record with component core_design and parameter num_assy. The number of fuel rods per assembly ($Rods_{Assy}$) is read from the plant database record with component *assembly_** and parameter *assy_num_rods_fuel*. The total number of rods in the core is calculated as the product of these two values as:

$$Rods_{Core} = Assy_{Core} \times Rods_{Assy}$$

[

]

A.2.5.17.4 Core Power and Reactor Kinetics Modset

The core power and reactor kinetics information is added to the calculation within the card set describing reactor kinetics (i.e., 30000000 – 30099999 series) as follows:

Card 30000001 **Reactor Kinetics Information Card**

W1(A) *fission product decay type.*

[

]

W2(R) *total power. Power is entered in the units of watts regardless of the units standard chosen for the input model.*

[ ]

W3(R) *initial reactivity ($)*

[ ]

W4(R) *delay neutron fraction over prompt neutron generation time (1/s).*

[ ]

W5(R) *fission product yield factor.*

[ ]

W6(R) *U^{239} yield factor.*

[ ]

[

]

Card 13X	**LBLOCA Multiplier Card**
W1(I)	*Keyword. Enter "KLOSS"*
W2(I)	*Component number. Enter guide tube junction number (CCCJJ, CCC = component number and JJ = junction number).*
W3(R)	*Multiplier value. Enter sampled parameter value.*

[

]

Card 205NNNN0	**Control Variable Card**
W1(A)	*Alphanumeric name.*
W2(A)	*Control Component Type. Enter "CONSTANT".*
W3(R)	*Constant value. Enter sampled parameter value.*

[

]

The LBLOCA multiplier cards are defined as follows:

Card 13X	LBLOCA Multiplier Card
W1(A)	*Keyword. Enter "FUELK"*
W2(I)	*Heat structure-geometry number (CCCG).*
W3(R)	*Multiplier. Enter –1*control system number.*

[

]

Card 205NNNN0	Control Variable Card
W1(A)	*Alphanumeric name.*
W2(A)	*Control Component Type. Enter "CONSTANT".*
W3(R)	*Constant value. Enter sampled parameter value.*

[

]

Card 205NNNN0	**Control Variable Card**
W1(A)	*Alphanumeric name. Any description ok.*
W2(A)	*Control Component Type. Enter "CONSTANT".*
W3(R)	*Constant value. Enter sampled parameter value.*

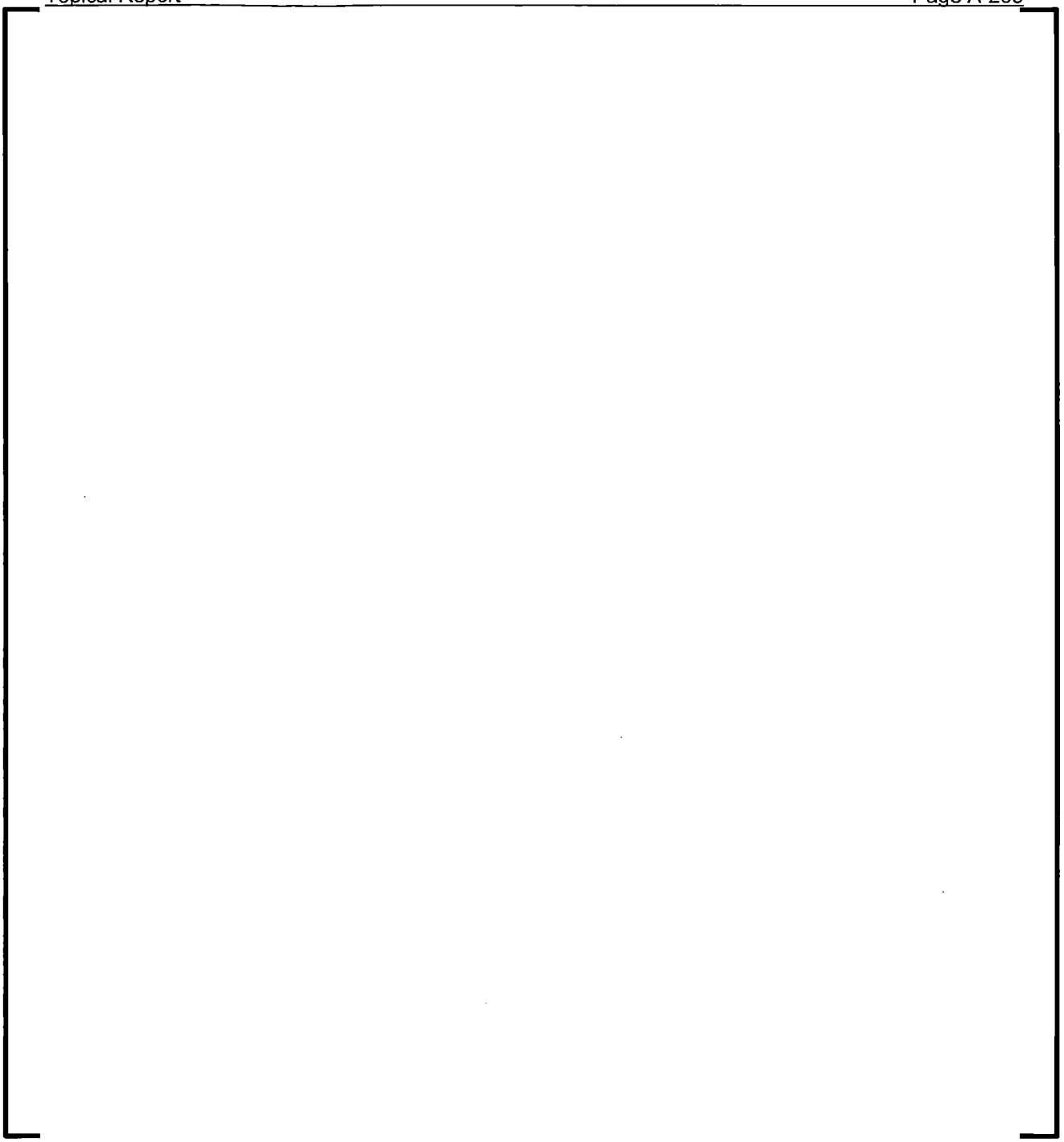

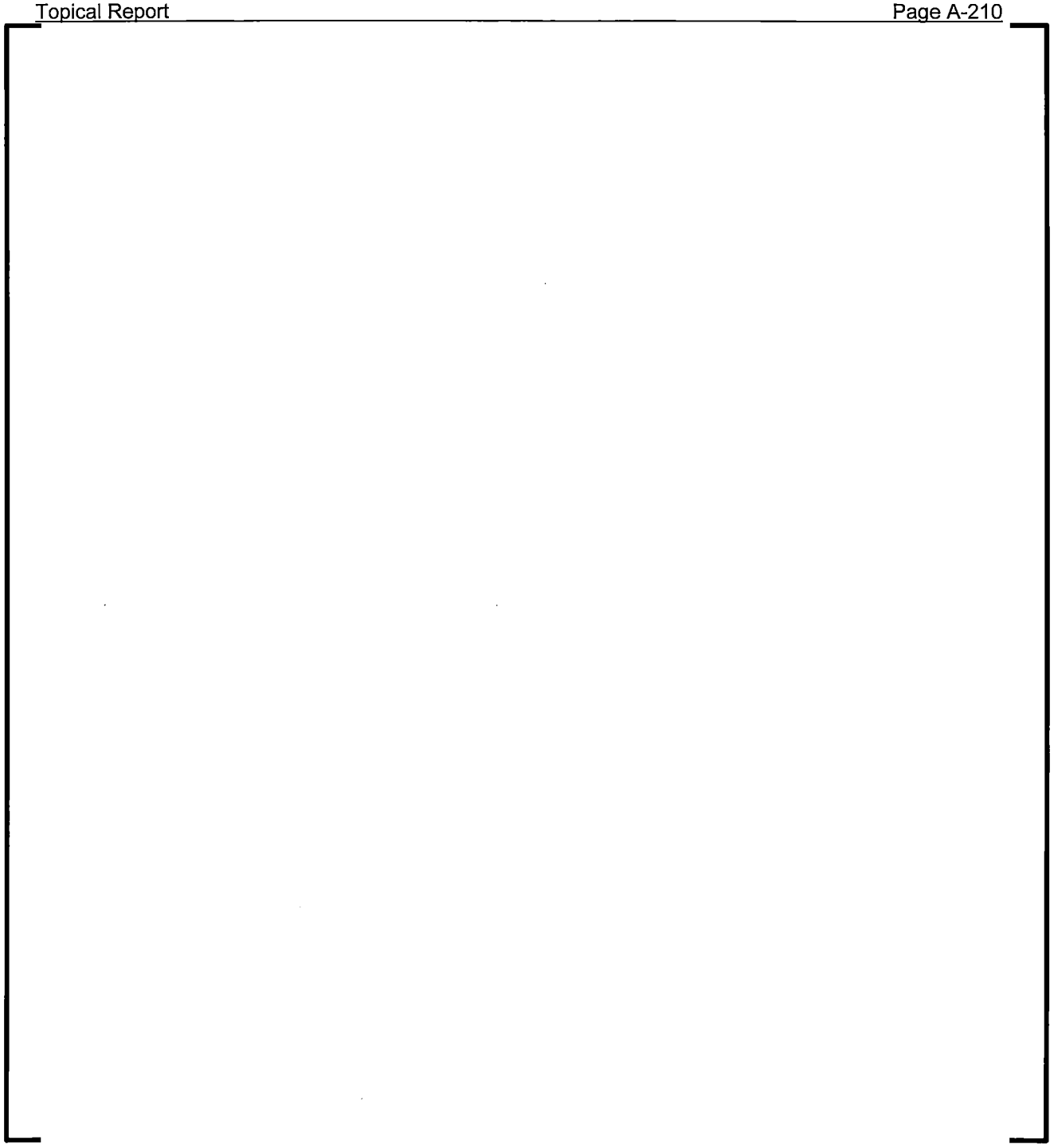

A.2.5.18 S-RELAP5 Transient Model Input

The S-RELAP5 transient calculations predict the key variables that must be used to address the LOCA/ECCS acceptance criteria. Because the modset cards for each S-RELAP5 transient input file are analysis and case dependent, a new file is created for each case.

[

]

A.2.5.18.1 Break System Modset

[

]

A.2.5.18.2 Time Step Control Modset

A time step control sensitivity was performed and used as a basis for the time step control modset. The time step control cards are entered using cards similar to the example mod set listed below.

[

]

A.2.5.18.3 COPERNIC Read Frequency Modset

The COPERNIC read frequency is set by the following 300 card to every 50 seconds for the S-RELAP5-TR calculations.

Example

```
*
* Set copernic read frequency to 50
*
300  50
*
```

A.2.5.18.4 Transient Trip Modset

[

]

Card 30000001 Reactor Kinetics Information Card

W2(R) *Total power.* [

]

W5(R) *Fission product power factor.* [

]

A.2.5.18.6 Initial Upper Head Temperature Modset

[

]

Card 13X	**LBLOCA Multiplier Card**
W1(I)	*Keyword. Enter "KLOSS"*
W2(I)	*Component number. Enter guide tube junction number (CCCJJ, CCC = component number and JJ = junction number).*
W3(R)	*Multiplier value. Enter sampled parameter value.*

[

]

A.2.5.18.7 Pressurizer Surgeline Critical Flow Modset

[

]

Card 13X	**LBLOCA Multiplier Card**
W1(A)	*Keyword. Enter "CFSUB"*
W2(I)	*Component number. Enter component-junction form (CCCJJ, CCC = component number and JJ = junction number).*
W3(R)	*Multiplier. Enter sampled parameter value.*

Card 13X	**LBLOCA Multiplier Card**
W1(A)	*Keyword. Enter "CF2PH"*
W2(I)	*Component number. Enter component-junction form (CCCJJ, CCC = component number and JJ = junction number).*
W3(R)	*Multiplier. Enter sampled parameter value.*

[

]

A.2.5.18.8 Film Boiling HTC Modset

[

]

[

]

A.2.5.18.9 Fuel Conductivity Modset

[

]

Card 13X	**LBLOCA Multiplier Card**
W1(A)	*Keyword. Enter "FUELK"*
W2(I)	*Heat structure-geometry number (CCCG).*
W3(R)	*Multiplier. Enter –1*control system number.*

[

]

A.2.5.18.10 Dispersed Film Boiling Modset

[

]

[redacted]

Card 13X	**LBLOCA Multiplier Card**
W1(A)	*Keyword. Enter "FIJ"*
W2(I)	*Component number (CCCJJ).*
W3(R)	*Multiplier. Enter bias parameter value.*

[redacted]

A.2.5.18.17 Minor Edits Modset

A number of minor edit cards are added to the S-RELAP5-TR input deck. These are inserted in the S-RELAP5-TR input deck to instruct S-RELAP5 to write minor edits to the restart-plot file (RSTPLT). Section 4.9 of Reference A-2 provides a list of variables that can optionally be written to the RSTPLT file through the use of 2080XXXX cards.

Card 2080XXXX	**Minor Edit Requests Card**
W1(A)	*Variable Code.*
W2(I)	*Parameter.*

Table A-22 details the minor edit requests created in the automated S-RELAP5-TR input deck.

Table A-22: Minor Edit Requests

A.2.5.18.18 ICECON Connection Data Modset

A containment (ICECON) model is developed according to Section A.1.3.8, and provided to the uncertainty analysis, as described in Section A.2.5.3

A.2.5.19 Containment Model Input

The S-RELAP5/ICECON containment input file is processed during (and only during) the S-RELAP5 transient calculation. A distinct containment model input file is also required for each transient calculation. [

]

A.2.5.20 Calculations

As described in Section A.2.3.2, calculations for the [ ] unique cases will be performed for the uncertainty analysis. For each case, the fuel rod code is executed first, followed by the S-RELAP5-SS calculation and concludes with the S-RELAP5-TR calculation.

A.2.5.20.1 Fuel Rod Code Calculations

A.2.5.20.1.1COPERNIC Calculation

The COPERNIC calculation is actually divided into two calculations for each rod heat structure: a COPRE input processing calculation, and a COPERNIC calculation.

The COPRE calculation must be checked to see if the file fort.09 is created, and has a non-zero size. This file is then passed to the COPERNIC calculation as its input file.

The following checks are performed to ensure that the COPERNIC calculation completed correctly.

The standard output file must exist and have length and the last line of the standard out output file must contain the phrase: "Total computer time used for this datacase =". Additionally, the file named "CONVTMP" must exist, and the file named "ftn21" must exist and have non-zero size. The ftn21 file is passed to S-RELAP5 for each rod in the model.

Table A-23 Single Case, Single Rod COPRE Calculation Input

File Name	Description
STARTING.DAT	COPRE input file

Table A-24: Single Case, Single Rod COPRE Calculation Output

File Name	Description
fort.09	COPERNIC input file

Table A-25: Single Case, Single Rod COPERNIC Calculation Input

File Name	Description
fort.09	COPERNIC input file (output from COPRE)

Table A-26 Single Case, Single Rod COPERNIC Calculation Output

File Name	Description
ftn12	binary data transfer file created by COPERNIC to be used with S-RELAP5
ftn18	COPERNIC standard output
ftn21	COPERNIC standard output

A.2.5.20.2 Steady-State S-RELAP5 Calculation

The steady-state calculation requires the base deck input with the case specific data appended to the file.

Table A-27 Single Case Steady-State Calculation Input

File Name	Description
INPUT	S-RELAP5-SS input file created from base deck and appended to by AUTORLBLOCA_REV3.

Table A-28 Single Case Steady-State Calculation Output

Filename	Description
OUTPUT	S-RELAP5-SS calculation standard output file
RSTPLT	S-RELAP5-SS calculation restart output file, used in S-RELAP5-TR calculation

A.2.5.20.3 Transient S-RELAP5 Calculation

The transient calculation requires a unique deck with case specific data, an ICECON input deck and the RSTPLT file generated in the S-RELAP5-SS calculation step.

Table A-29 Single Case Transient Calculation Input

File Name	Description
INPUT	S-RELAP5-TR input file created from base deck and appended to by AUTORLBLOCA_REV3.
ICEIN	S-RELAP5-TR ICECON input file created from base deck and appended to by AUTORLBLOCA_REV3.
RSTPLT	S-RELAP5-TR restart plot file created from steady-state calculation.

Table A-30 Single Case Transient Calculation Output

Filename	Description
OUTPUT	S-RELAP5-TR calculation standard output file
RSTPLT	S-RELAP5-TR restart plot file created from transient calculation
R5DMX	Demultiplexed plot file created by executing the utility r2dmx, for use with XMGR5 plotting utility

A.2.5.21 Results

No guideline exists for results that must be reported to the customer; however, due to the statistical nature of the RLBLOCA uncertainty analysis, there is a presentation of typical results is necessary, as well as a presentation of the calculated input parameters. The following sections identify results that are to be available in the uncertainty analysis calculation notebook.

A.2.5.21.1 Statistical Analysis

For each case, the S-RELAP5 standard output file is read and the values for the S-RELAP5 predicted PCT, MLO and CWO are determined. [

]

[

]

A.2.5.21.2 Rupture Results

[

]

A.2.5.22 Plots

A number of plots are necessary for reviewing and reporting results from the uncertainty analysis. These plots are described in the following sections, which identify a minimum set of plots that are created for each uncertainty analysis.

A.2.5.22.1 Operational Parameters

A number of plots are to be created to view key operation parameters for the limiting case. The plots to be generated are defined in Table A-31.

Table A-31: Key Operational Parameter Plots

A.2.5.22.1.12-D Scatter Plots

Scatter plots are provided for the limiting criteria (PCT, Total Oxidation, and Maximum Oxidation), as well as sampled and calculated parameters. The suggested plots for the analysis are listed in Table A-32.

Table A-32: Scatter Plot Parameters

[redacted]

±PCT is plotted versus time of PCT. The remaining parameters are compared to PCT (°F or C)

A.2.5.22.2 Fuel Temperature Trace Plots

A.2.5.22.2.1Fuel Rod Maximum Clad Surface Temperature Plots

Control variables are included in the S-RELAP5 base deck to calculate the maximum clad surface temperature for each the fresh and once-burned hot rods in the model.

Table A-33: Maximum Clad Surface Temperature Control Variables

[

]

A.2.5.22.2.2Maximum Clad Surface Temperature Plot – Hot Rods

The control variables in Table A-33 calculate the maximum clad surface temperature for each hot rod in the model. A plot containing the maximum clad surface temperature for each of the hot rods will be made available for all cases and for the limiting case the plot or plots are included in the results documented in the calculation notebook.

A.2.5.22.2.3Maximum Clad Surface Temperature Plot – All Rods

Control variable 654 is included in the model for the purpose of calculating the maximum clad surface temperature for all hot rods included in the model at each time step. A plot of control variable 654 is made available for all cases, and for the limiting case this plot is included in the results documented in the calculation notebook.

A.2.5.22.3 Limiting Case Plots

For the limiting case, the following plots are generated and included in the calculation notebook for the limiting case.

Table A-34: Limiting Case Plots

Description	Units	SI Units
Break flow	(lb_m / s) x 10^3	(kg / s) x 10^3
Core inlet mass flux	lb_m / (ft^2-s)	kg / (m^2-s)
Core outlet mass flux	lb_m / (ft^2-s)	kg / (m^2-s)
Pump void fraction	(-)	(-)
ECCS flows	lb_m / s	kg / s
Upper plenum pressure	psia	bar
Downcomer liquid level	ft	m
Lower vessel liquid level	ft	m
Core liquid level	ft	m
Containment and loop pressure	psia	bar
Pressure difference between upper plenum and downcomer	psia	bar

A.2.5.23 File Retention

Due to the number of files and size of some output files associated with the uncertainty analysis, it is not feasible to archive all input and output files used for the analysis. The following sections identify the files that must be archived for each analysis.

A.2.5.23.1 Input

The KBI file and the automation database files named in the KBI file must be archived in cstor with the calculation, or in the automation controlled directories.

A.2.5.23.2 Limiting Case

For the limiting case, the entire calculation directory, "/working_directory/*_case_directory_*/" must be archived.

A.2.5.23.3 Fuel Rod Calculation File Archival

Each COPERNIC calculation has a COPRE input file and output file, as well as the COPERNIC input and output files. For the COPRE calculation the input file named STARTING.DAT, and the output file fort.9 must be archived. For the COPERNIC portion of the calculation, the standard input file named INPUT, and the output files named ftn12 and ftn21 must be archived.

A.2.5.23.4 Steady-State S-RELAP5 Calculation

Only two files must be archived for the S-RELAP5-SS calculation. The standard input file named INPUT, and the standard output file named OUTPUT.

A.2.5.23.5 Transient S-RELAP5 Calculation

For the S-RELAP5-TR calculation, the standard input file named INPUT, and the ICECON input file named ICEIN, must be archived, as well as the standard output file named OUTPUT, and the resulting demux plot file created, R5DMX.

Figure A-1 Uncertainty Analysis Case Description

Figure A-2 Loop Nodalization Example

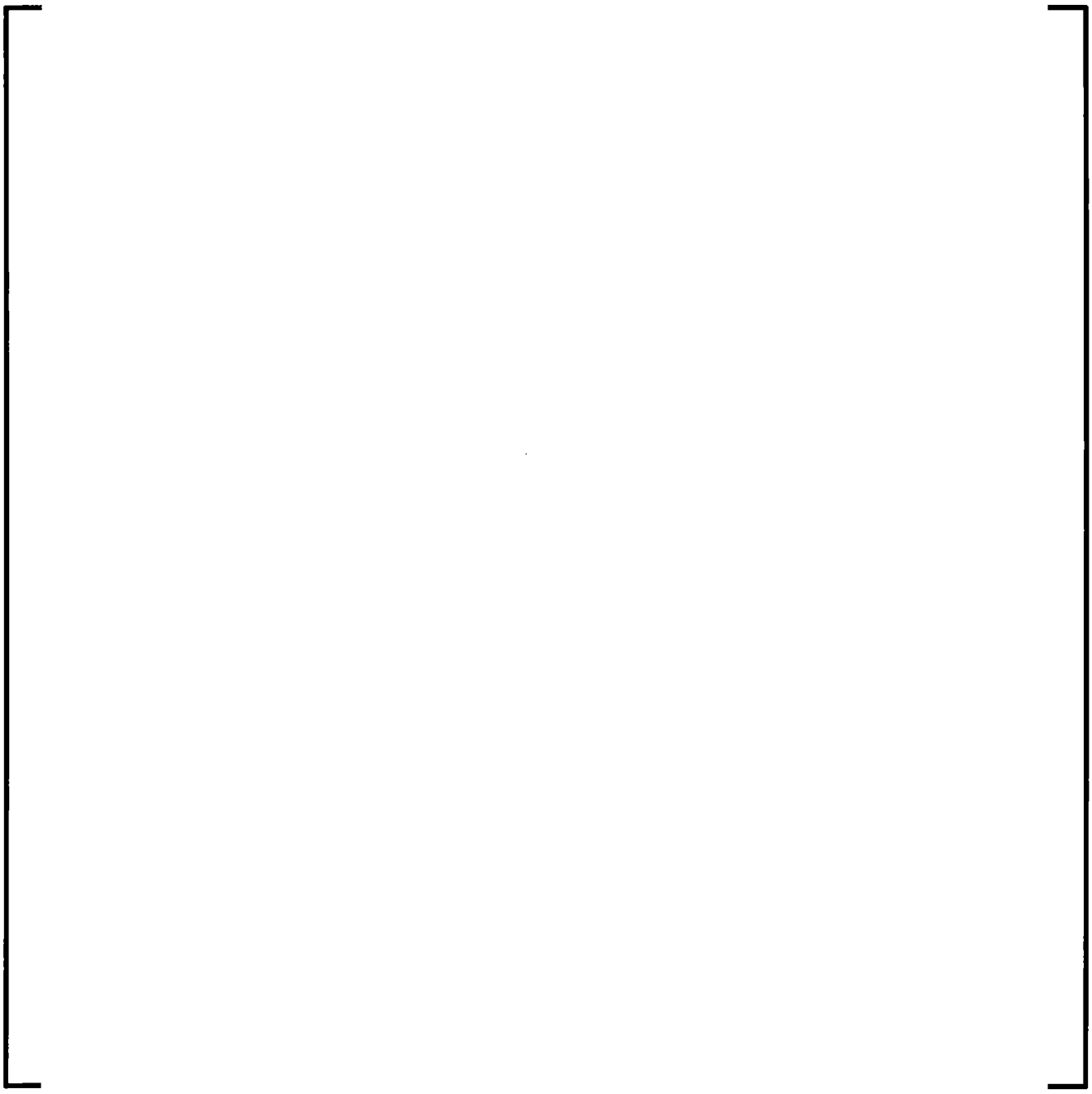

Figure A-3 Loop 1 Secondary Side Nodalization

Figure A-4 Reactor Vessel Nodalization Example (Downflow Baffle Case)

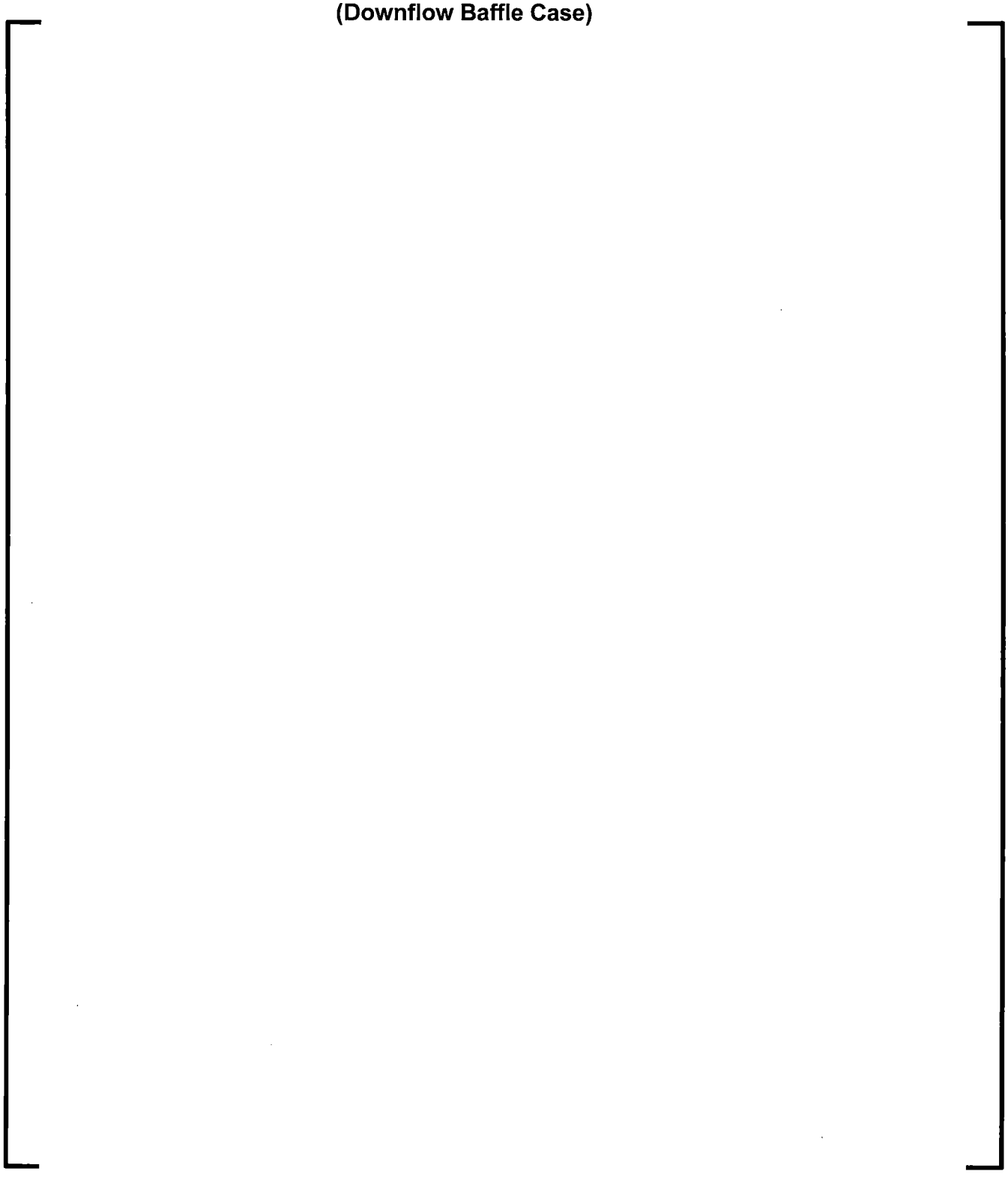

Figure A-5 Westinghouse 3- and 4-Loop and CE 2x4 Loop Plant Vessel Downcomer Configuration

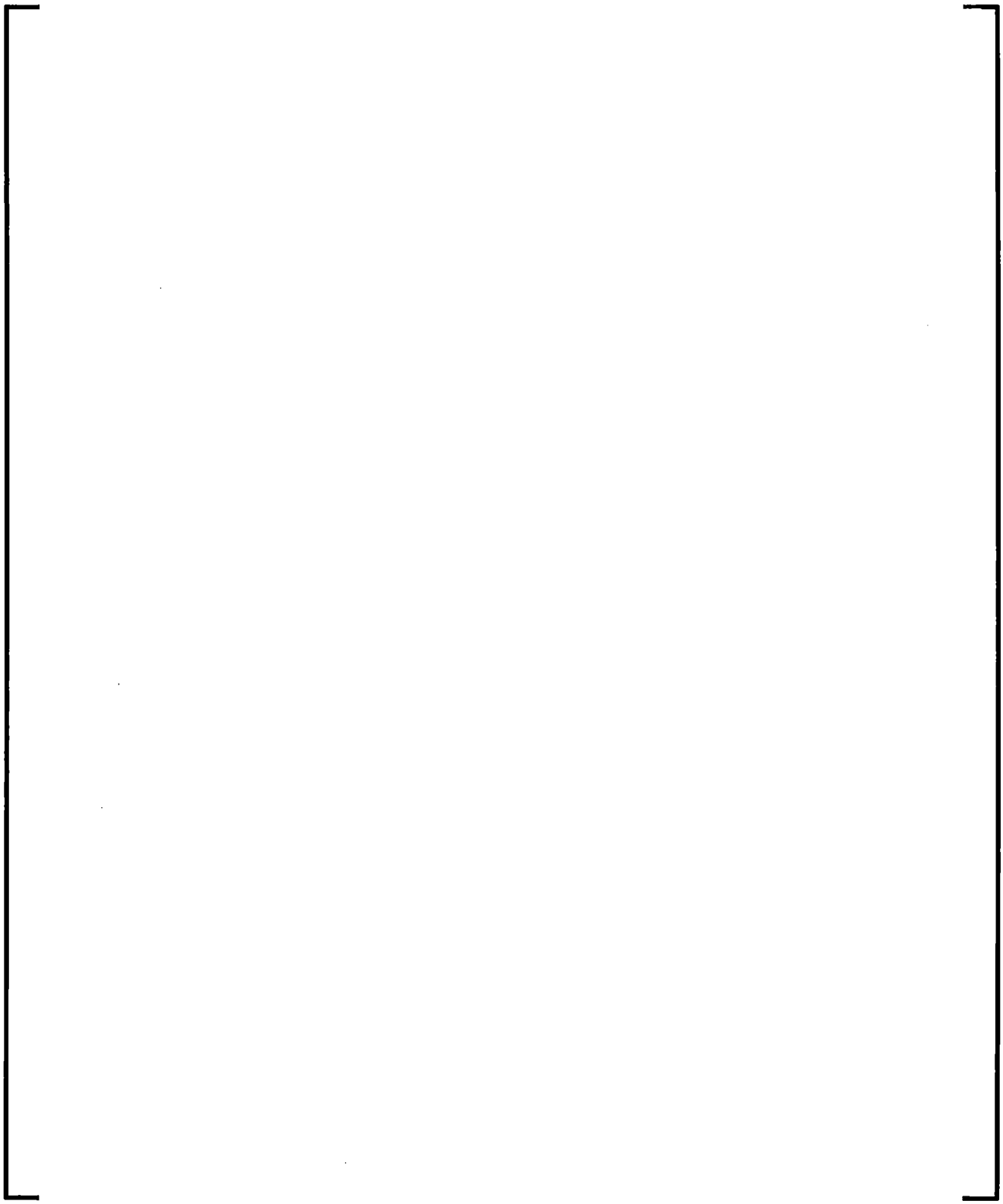

Figure A-6 Core Nodalization Example – Axial Plane (example)

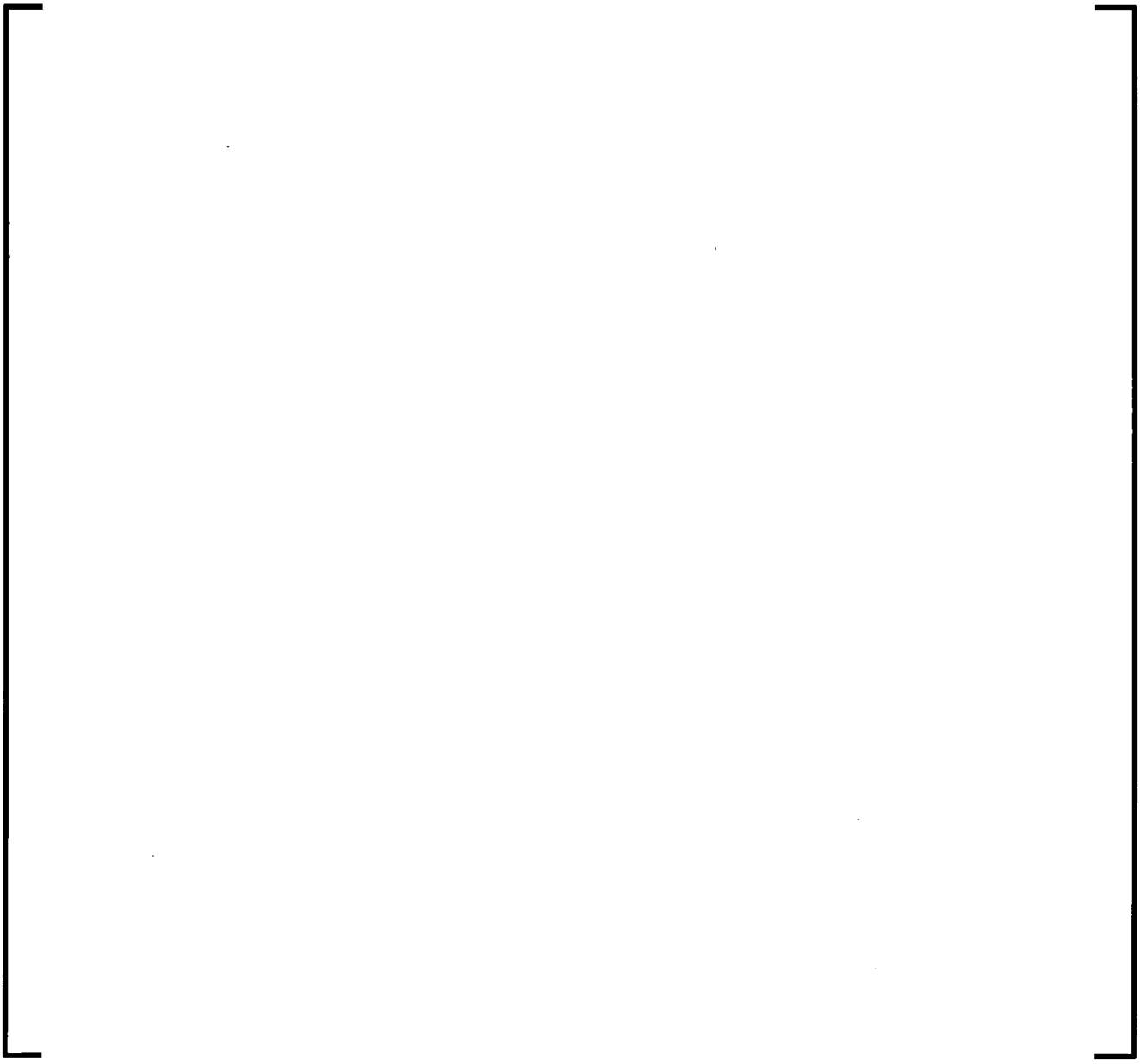

Figure A-7 Core Nodalization – Cross-Sectional Plane

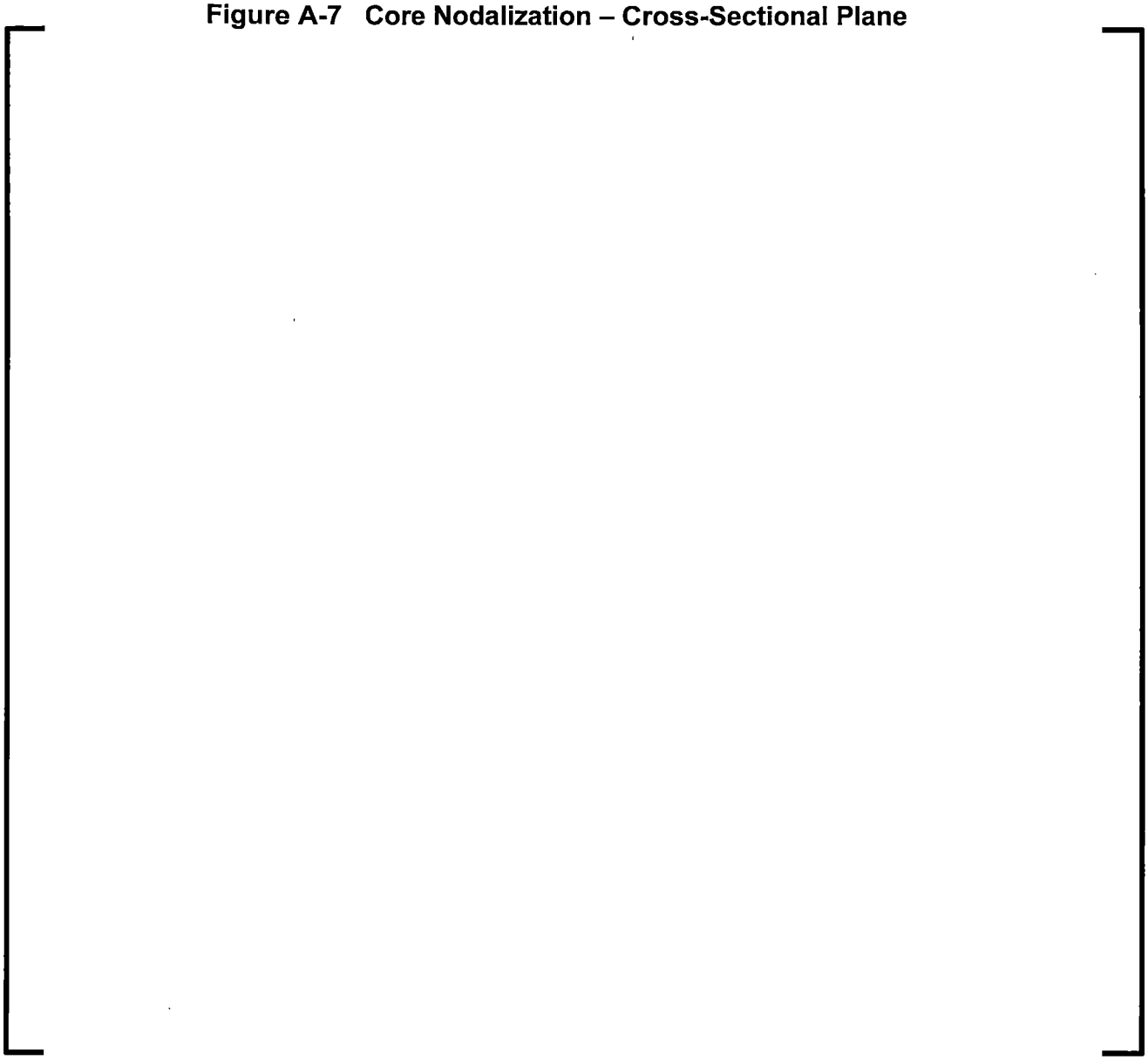

Figure A-8 Spacer and Node Locations Example for 23 Volume Core (example)

Figure A-9 Upper Plenum Nodalization – Axial Plane (for Plants with Mixer Vanes/Standpipes)

Figure A-10 Upper Plenum Nodalization – Cross-Sectional Plane (for Plants with Mixer Vanes/Standpipes)

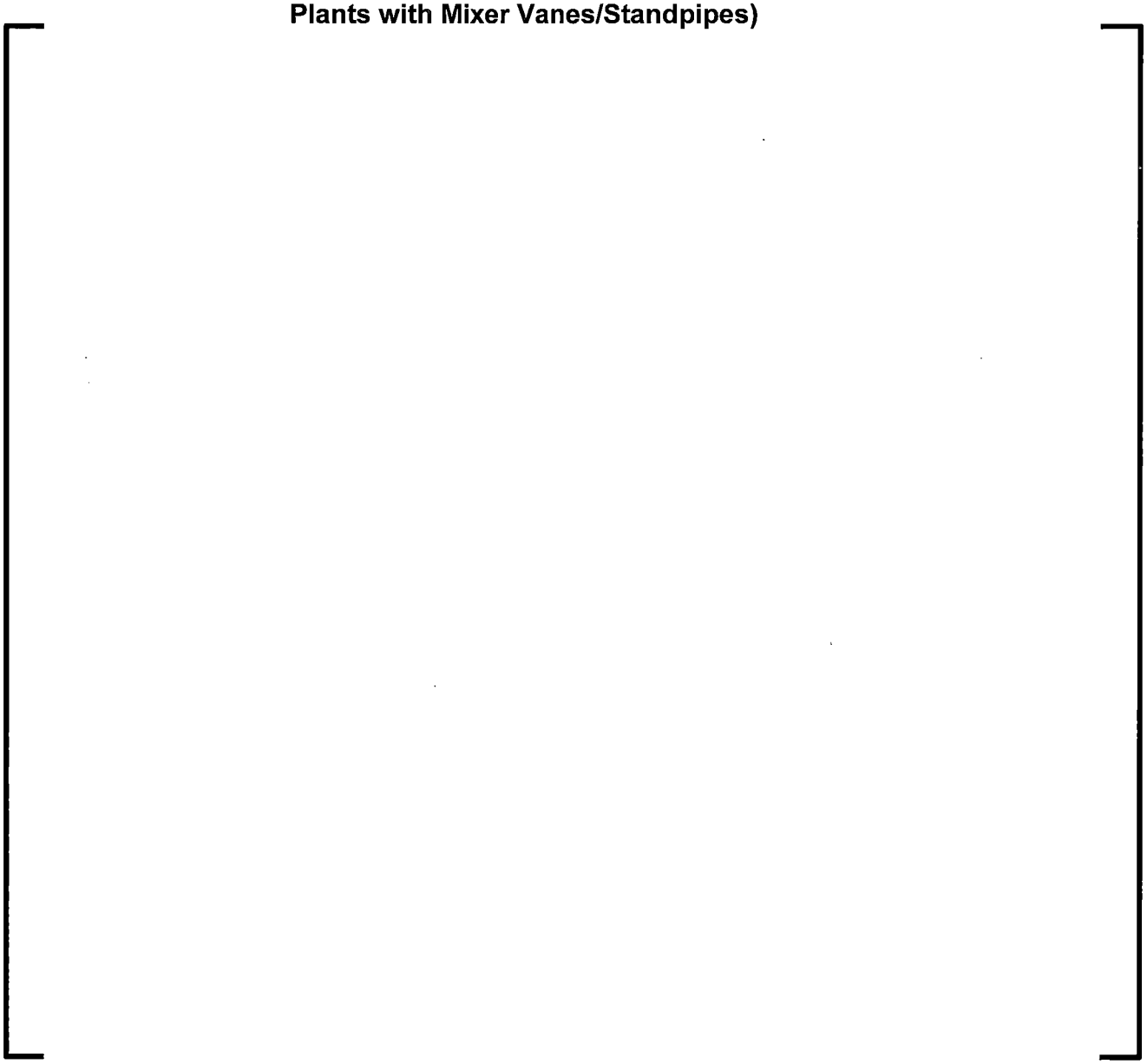

Figure A-11 Upper Plenum Nodalization – Axial Plane (for Plants with UHI Columns)

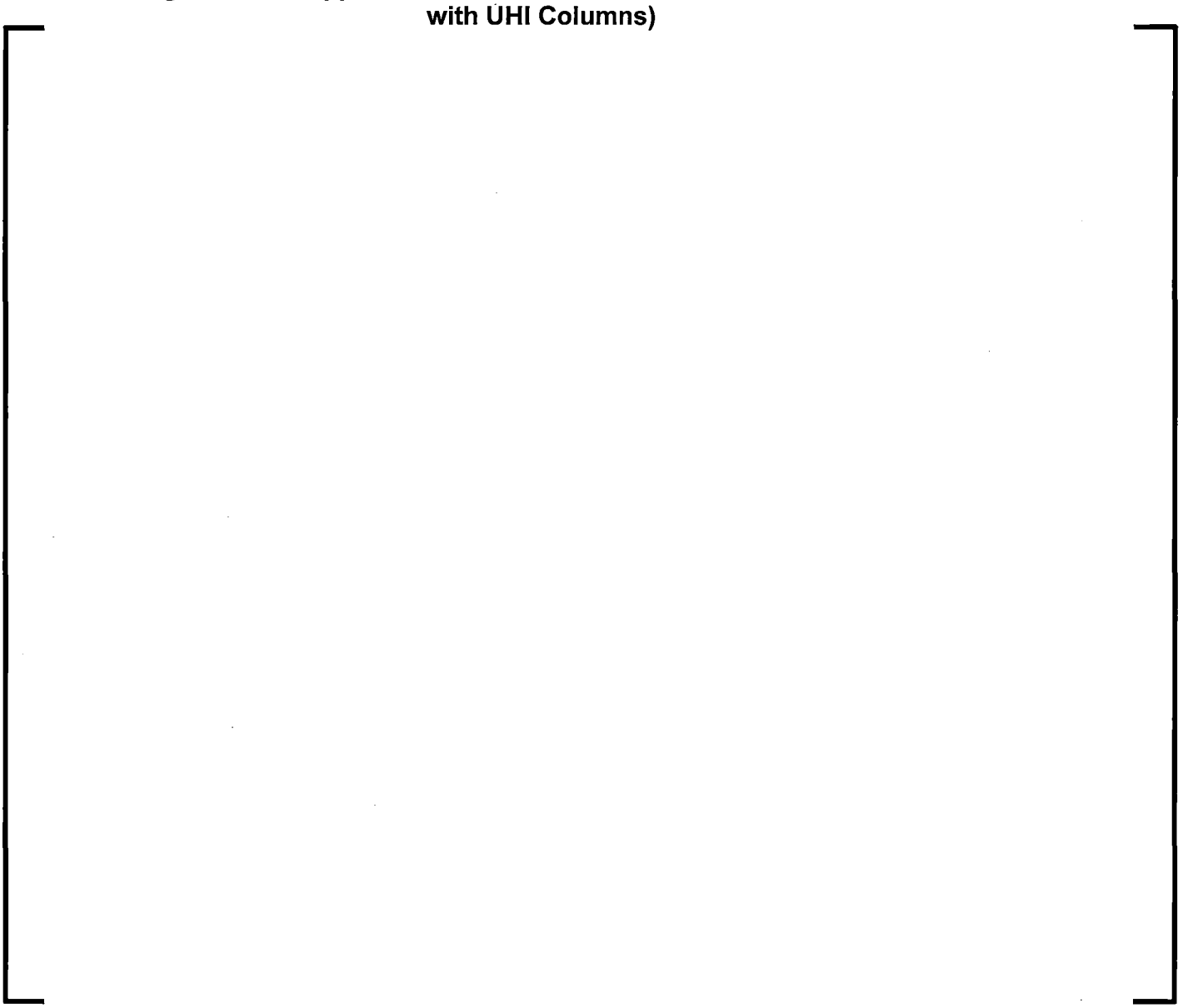

Figure A-12 Upper Plenum Nodalization – Axial Plane (for Plants without Mixer Vanes/Standpipes)

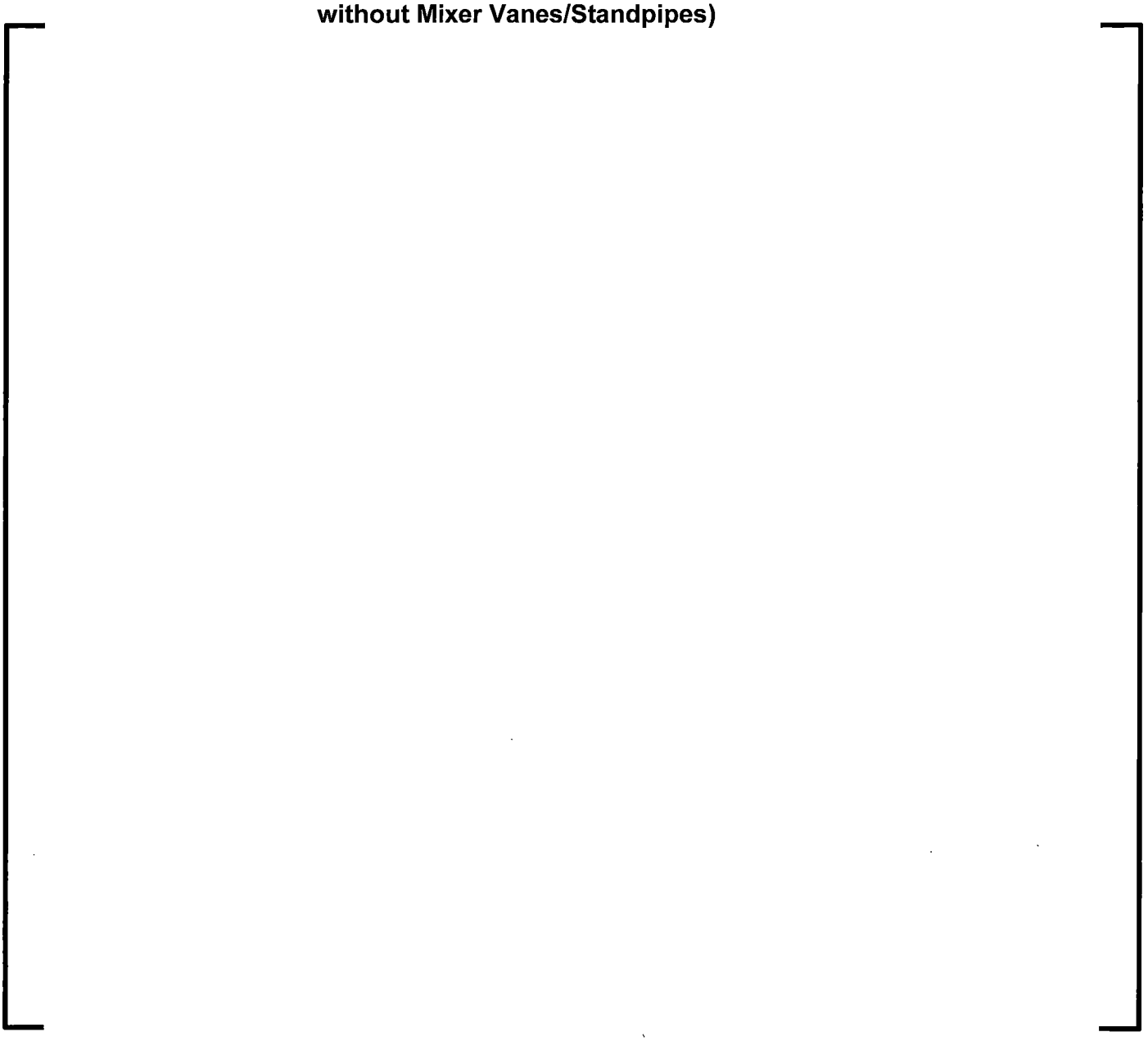

Figure A-13 Detailed Emergency Core Cooling System Nodalization Example

Figure A-14 Double-Ended Guillotine Break Nodalization

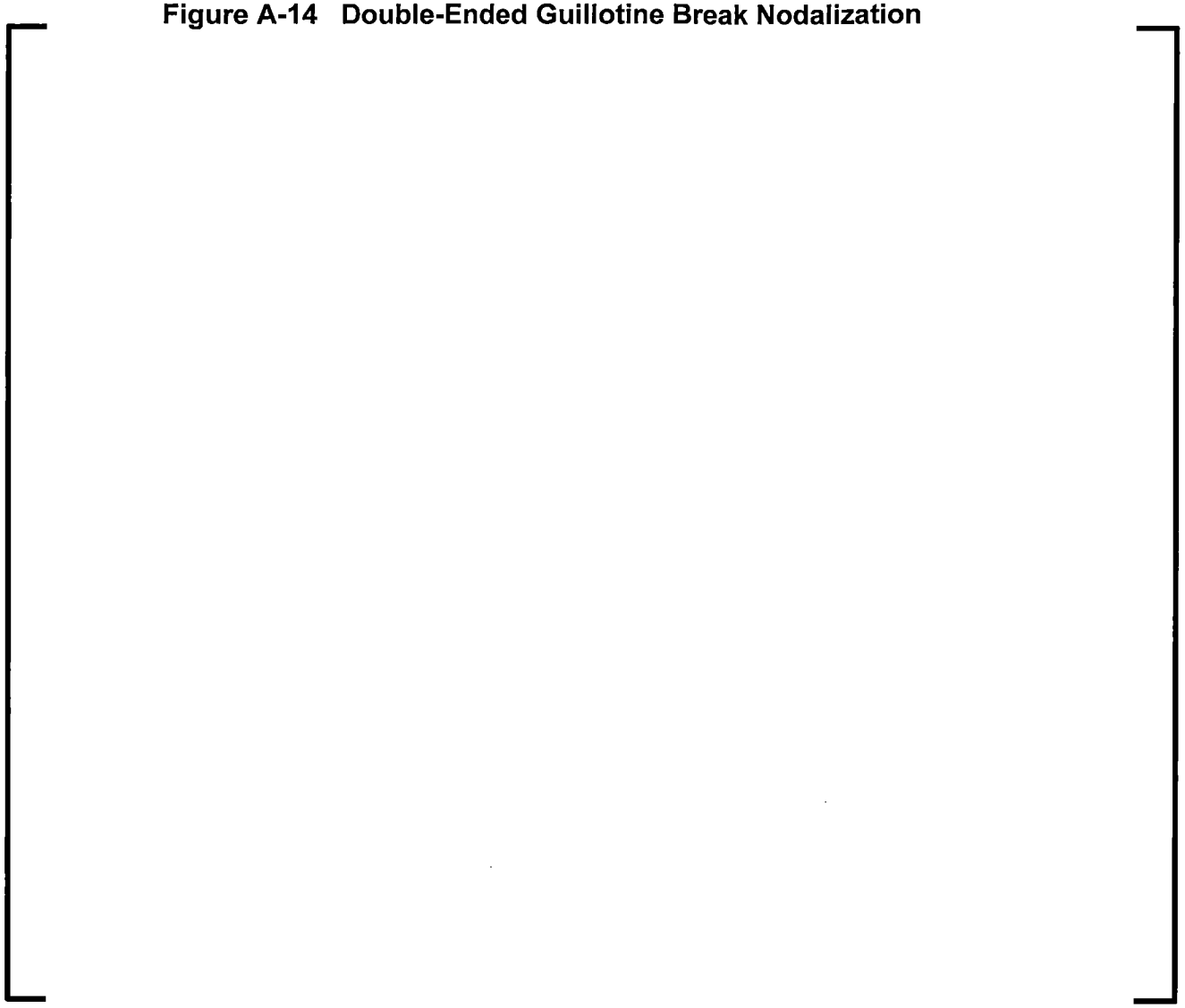

Figure A-15 Double-Ended Split Break Nodalization

A.3 *References*

A-1. Technical Program Group, "Quantifying Reactor Safety Margins," NUREG/CR-5249, EGG-2552, October 1989.

A-2. AREVA NP Inc. Document FS1-0011181, Revision 1.0, "FSQA-07 S-RELAP5 Input Data Requirements (User's Manual)," August 2013.

A-3. C. D. Fletcher, R. R. Schultz, "RELAP/MOD3 Code Manual: User's Guidelines," NUREG/CR-5535, INEL-95/0174, Volume 5, R1, August 1995.

A-4. AREVA NP Inc. Document EMF-2103 (P)(A) Revision 0, "Realistic Large Break LOCA Methodology for Pressurized Water Reactors," April 2003.

A-5. I. E. Idelchik, "Handbook of Hydraulic Resistance," Third Edition, Hemisphere Publishing Co., Washington, D.C., 1986.

A-6. Crane Co. Technical Paper No. 410, "Flow of Fluids Through Valves, Fittings, and Pipe," 1988.

A-7. L. F. Moody, "Friction Factors for Pipe Flow," Transactions of the ASME, 66, 8, November 1944, pp. 671-684.

A-8. AREVA NP Inc. Document 2A4-COPERNIC, Revision 0, "COPERNIC, Fuel Rod Computer Code, User's Manual," December 2001.

A-9. Electrical Power Research Institute, EPRI NP-1556, "Pump Two-Phase Performance Program", Volumes 1 through 8, September 1980.

A-10. AREVA NP Inc. Letter, NRC-02-062A(P), "Reponses to a Request for Additional Information on EMF-2103(P)", Revision 0, RLB LOCA Methodology for PWRs (TAC NO. MB2865)," December 20, 2002.

A-11. AREVA NP Inc. Document EMF-2328 (P)(A) Revision 0, "PWR Small Break LOCA Evaluation Model, S-RELAP5 Based," March 2001.

A-12. S. C. Yao L. E. Hochreiter, and W. J. Leech, "Heat-Transfer Augmentation in Rod Bundles Near Grid Spacers," Journal of Heat Transfer Volume 104, pp. 76-81, February 1982.

A-13. American National Standards Institute, "American National Standard for Decay Heat Power in Light Water Reactors," ANSI/ANS-5.1-1979, August 1979.

A-14. AREVA NP Inc. Document EMF-CC-39 (P) Revision 5, Supplement 1, "ICECON User's Manual," July 2007.

A-15. Wheat, Larry L., "CONTEMPT-LT A Computer Program for Predicting Containment Pressure-Temperature Response to a Loss-Of-Coolant-Accident," Aerojet Nuclear Company, TID-4500, ANCR-1219, June 1975.

A-16. Box, G.E.P, M.E. Muller, "A note on the generation of random normal deviates", Annals Math. Stat, Volume 29, pp. 610-611 (1958).

A-17. U.S. National Archives and Records Administration, Title 10–Energy, Code of Federal Regulations, Part 50, July 8, 2013.

A-18. [

]

A-19. [

]

APPENDIX B
SAMPLE PWR LICENSING ANALYSES

B.1 Introduction

This appendix provides sample RLBLOCA analyses for a Westinghouse 3- and 4-loop PWR and a Combustion Engineering 2x4 PWR. These sample analyses are presented to provide representative solutions to the RLBLOCA evaluation and the reporting or recording of such analyses. None of the sample problems are fully representative of any specific plant. The analyses contain hypothetical core designs for higher operating power and higher peaking factors than found in the current operating fleet. Each has been reviewed to assure that it offers an accurate representation of the RLBLOCA evaluation model findings and conclusions. The three sample analyses have AREVA fuel with M5® cladding and utilize the COPERNIC code for fuel calculations within S-RELAP5. [

]

RLBLOCA analyses, as illustrated by the sample analyses, are designed to support operation for a typical reload cycle. It also applies to subsequent cycles, unless changes in the Technical Specifications, Core Operating Limits Report, fuel design, plant hardware, or plant operation cause model input revisions.

Section B.1.1 describes the criteria that the RLBLOCA analyses will analyze. Section B.1.2 of this report describes the models used in the analysis. Section B.1.3 describes the GDC-35 limiting condition. Section B.1.4 describes the statistical evaluation and compliance to the acceptance criteria. Section B.1.5 discusses the application of heat transfer correlations. Section B.2 describes the 3-loop PWR plant analysis, Section B.3 describes the 4-loop PWR plant analysis, and Section B.4 describes the CE 2x4 PWR plant analysis.

B.1.1 Analysis

The purpose of the analysis is to verify typical technical specification peaking factor limits and the adequacy of the ECCS by demonstrating that the following 10 CFR 50.46(b) criteria are met:

- The calculated maximum fuel element cladding temperature shall not exceed 2200 °F.
- The calculated total oxidation of the cladding shall nowhere exceed 0.17 times the total cladding thickness before oxidation.
- The calculated total amount of hydrogen generated from the chemical reaction of the cladding with water or steam shall not exceed 0.01 times the hypothetical amount that would be generated if all of the metal in the cladding cylinders surrounding the fuel excluding the cladding surrounding the plenum volume were to react.

As discussed in Section 3.0, the two remaining 10 CFR 50.46(b) criteria require evaluations beyond the applicability of this methodology and are treated separately during plant evaluations.

B.1.2 Description of Analytical Models

The modeling of plant components is performed by following the guidelines presented in Appendix A and developed to ensure accurate accounting for physical dimensions and that the dominant phenomenon expected during a LBLOCA event are captured. The basic building block for modeling is the hydraulic volume for fluid paths and the heat structure for a heat transfer surface. In addition, special purpose components exist to represent specific components such as the pumps or the steam generator separators. All geometries are modeled at the resolution necessary to best resolve the flow field and the phenomena being modeled within practical computational limitations.

A typical calculation using S-RELAP5 begins with the establishment of a steady-state, initial condition with all loops intact. The input parameters and initial conditions for this steady-state calculation are chosen to reflect plant technical specifications or to match measured data. Specific parameters are discussed in Sections B.2.2, B.3.2, and B.4.2.

Following the establishment of an acceptable steady-state condition, the transient calculation is initiated by introducing a break into one of the loops. The evolution of the transient through blowdown, refill, and reflood is computed continuously using S-RELAP5. Containment pressure is calculated by the ICECON module within S-RELAP5.

A detailed assessment of the S-RELAP5 computer code was made through comparisons to experimental data, as documented in Section 8.0. These assessments were used to develop quantitative estimates of the ability of the code to predict key physical phenomena in a PWR LBLOCA. The final step of the best-estimate methodology is to combine all the uncertainties related to the code and plant parameters and estimate the PCT at 95 percent probability and 95 percent confidence. The steps taken to derive the PCT uncertainty estimate are summarized below:

1. Base Plant Input File Development

First, base COPERNIC and S-RELAP5 input files for the plant (including the containment input file) are developed. Code input development guidelines documented in Appendix A are applied to ensure that the model nodalization is consistent with the model nodalization used in the code validation.

2. Sampled Case Development

The statistical approach requires that many "sampled" cases be created and processed. For every set of input created, each "key LOCA parameter" is randomly sampled over a range established through code uncertainty assessment or expected operating limits (provided by plant technical specifications or data). Those parameters considered "key LOCA parameters" are listed in Table A-6. This list includes both parameters related to LOCA phenomena (based on the PIRT provided in Section 5.0) and to plant operating parameters. The uncertainty ranges associated with each of the model parameters are provided in Table A-7.

3. Determination of Adequacy of ECCS

The RLBLOCA methodology uses a non-parametric statistical approach to determine that the first three criteria of 10 CFR 50.46 (PCT, MLO, and CWO) are met with a probability of at least 95 percent with at least 95 percent confidence.

B.1.3 GDC-35 Limiting Condition Determination

[

]

B.1.4 Overall Statistical Compliance to Criteria

[

]

B.1.5 Application of Heat Transfer Correlations

During a transient simulation, different heat transfer correlations may be applied at any given time. The best way to demonstrate how the S-RELAP5 simulation of a LBLOCA is supported by correlation development and validation studies is to first identify (or map) the "simulation-space" and compare it to the "assessment-space." The assessment-space represents the combination of the applicability range from separate-effects investigation (i.e., correlation development or derivation), the expanded applicability range from uncertainty analysis, and validation from integral-effects benchmark calculations. The simulation-space is evaluated through the examination of the limiting calculations (in terms of PCT) for the 3- and 4-loop and CE sample problems for key correlation dependent parameters. The key parameters are defined as those engineered parameters that can be designed into a thermal-hydraulic test matrix. The most common engineered parameters used in thermal-hydraulic testing and correlation development

are pressure, power (in terms of LHGR, or heat flux), and mass flux (may also be given as Reynolds number or mass flow).

The comparison of the simulation-space and the assessment-space provides quantitative support to CSAU Step 6, Determination of Code Applicability (Reference B-1). As stated in Reference B-1, "if inadequacies are noted, they should be fully documented and, if possible, quantified." Ideally, the assessment-space will span the simulation-space; however, realistically, there will likely be holes in the assessment-space. To prioritize the effort in demonstrating adequate coverage, a PIRT for the LBLOCA has been presented in Section 5.0. This PIRT identified and ranked the relevant phenomena of importance for a LBLOCA. The important heat transfer regimes are nucleate boiling, CHF (DNB), transition boiling, and film boiling. It was the conclusion of the AREVA PIRT team that the other heat transfer regimes were either not present or had negligible impact on peak clad temperatures. In fact, it was concluded that nucleate boiling has a relatively low ranking during a LBLOCA event.

The best resource for information about the heat transfer regimes and their application can be found in Section 7.0. The selection logic for each heat transfer regime is presented in Figure 7-9 of this document. As a summary, Table B-1 highlights the heat transfer correlations used in S-RELAP5. Table B-12, Table B-19, and Table B-26 summarize the different heat transfer regimes, the heat transfer correlations used, and the approximate parameter ranges for the 3- and 4-loop and CE sample problems. The time ranges in this section are defined as used in Appendix K deterministic methods.

Time Period: Early Blowdown

Immediately following the postulated LBLOCA, portions of the core will, for a brief time, be in the nucleate boiling heat transfer regime until CHF is achieved. The duration of this period depends on the size of the break; however, for the typical limiting PCT break, this period will last only several seconds, at most. This period is more influenced by the CHF correlation, rather than the nucleate boiling heat transfer correlation, because CHF triggers the time of transition to the low heat transfer regimes (post-CHF). Table B-2 provides a comparison of simulation space against the range of applicability evaluated for the assessment-space for the CHF correlation.

S-RELAP5 Implementation of CHF

Early in the transient, heat transfer in the core rapidly advances to post-CHF conditions. Nonetheless, the Biasi correlation was assessed against the tests performed on the THTF at Oak Ridge National Laboratory and a bounding bias was determined for application in the RLBLOCA methodology. This study is presented in Section 8.4.4.

Table B-2 provides a comparison of simulation space against the range of applicability evaluated for the assessment-space for the Biasi CHF correlation. Note that the assessment-space includes three components as previously described: (1) the test conditions used in correlation development, (2) relevant uncertainty analysis, and (3) integral-effects validation.

Time Period: Blowdown

As the RCS depressurizes and CHF is reached in the core, vapor generation is rapid and the steam quality increases. This post-CHF period is characterized by film boiling, single-phase steam convection, and radiation (although radiation is not expected to be significant; hence, it does not appear in the PIRT). As long as the steam maintains some wetness, the total heat transfer includes all three heat transfer mechanisms; however, single-phase steam convection dominants heat transfer when void fractions are above about 0.90. Post-CHF heat transfer includes uncertainty not only from the application of the correlations, but also from contributions of interfacial drag and heat transfer phenomena. For this reason, total post-CHF heat transfer, rather than the individual correlations, is a statistically treated parameter. Table B-3 provides a comparison of the simulation-space and the range of applicability evaluated for the assessment-space for the film boiling correlation.

S-RELAP5 Implementation of Film Boiling Heat Transfer

Within S-RELAP5 both the modified Bromley and the Wong-Hochreiter correlation are used outside their derived range of applicability; however, applied statistical uncertainty on the total heat transfer provides the means for expanding the range of applicability. The primary deviations from the original range of applicability are:

[ ]

- [ ]

A discussion of the statistical treatment of total heat transfer is presented in Section 8.5.2.4. The uncertainty analysis applies data from the FLECHT-SEASET tests. The applicability of these tests was evaluated by analysis of the breadth of the data in terms of key correlation parameters and the density of the data in terms of the parameters for which the correlation is most sensitive, pressure and void fraction. [

] The IETs were initiated from full pressure conditions.

S-RELAP5 Implementation of Single-Phase Vapor Convection

Single-phase vapor heat transfer was assessed using the 161-rod bundle FLECHT-SEASET steam cooling tests (Section 8.2.4). The LOFT and Semiscale integral tests during the refill period and the separate effect assessments, including FLECHT-SEASET, CCTF and SCTF, during the early period of adiabatic heat-up were used to validate single-phase heat transfer at low flows.

Low flows that directionally oscillate are characteristic during refill in both the tests and the calculations. In LBLOCA calculations during vessel refill, vapor flow rates decelerate and directionally oscillate as a result of the transition to refill. This will last until the beginning of core reflood, which is a period typically less than 15 seconds. During this unsettled period, core flow will likely remain turbulent; however, vapor Reynolds numbers will be low.

In general, the S-RELAP5 results conservatively bound the measured results (higher clad temperatures). While the results of the assessments demonstrated that the Wong-Hochreiter correlation is adequate for post-blowdown periods during a LOCA (and lower Reynolds numbers), single-phase vapor heat transfer is treated implicitly in the evaluation of uncertainty in the total post-CHF heat transfer (see previous section).

S-RELAP5 Implementation of Radiation

Thermal radiation [ ] provides a significant contribution to the total heat transfer. The wall-to-fluid radiation is intrinsic to the heat

transfer model and is implicitly validated in all post-CHF assessments. The wall-to-structure component is activated through input and required a separate assessment of the performance of the model and a separate assessment of the rod-to-rod radiation model's implementation into the plant model.

Time Period: Refill

During the refill period, the RCS has nearly depressurized and the core region is devoid of coolant. Heat transfer in the core is almost all from single-phase vapor. As previously stated, single-phase vapor heat transfer is predicted using the Wong-Hochreiter correlation. The core conditions during this time are consistent with both the derived range of applicability and the FLECHT-SEASET steam cooling tests. While post-CHF total heat transfer is a statistically treated parameter, there is no bias or uncertainty applied when void fraction equals 1.0. As assessed from the FLECHT-SEASET steam cooling tests, the Wong-Hochreiter correlation is slightly conservative relative to the data. Analysis of the integral tests assessment cases support this finding.

Since the single-phase vapor heat transfer is a component of film boiling, refer to Table B-3 for a comparison of the simulation-space and the range of applicability evaluated for the assessment-space for the single-phase vapor heat transfer correlation.

Time Period: Reflood

By this time, the RCS pressure has established some equilibrium with the relative low pressure containment. ECCS coolant from the accumulator begins to reach the lower portions of the core and a definite two-phase mixture is present throughout the core region. With the constant supply of coolant, a quench front is established at the bottom of the core that slowly moves upward. At some point the coolant supply from the accumulator ends and core heat removal relies solely on that provided by the pumped injection safety systems. This may result in a late reflood heat up. Nonetheless, in time, this supply of coolant will be able to completely quench all the fuel rods in the core.

For the duration of this period, the heat structure nodes with the highest temperatures are removing heat by film boiling. Table B-3 provides a comparison of the simulation-space and the range of applicability evaluated for the film boiling assessment-space. This period ends with the fuel rod quenched, which will occur shortly after meeting the conditions for transition boiling.

S-RELAP5 Implementation of Reflood Heat Transfer

When core reflood is enabled in S-RELAP5 (provided in the input model), a heat transfer regime profile covering the entire boiling curve is established along the modeled heat structure. Proceeding from the bottom of the core, this will be single-phase liquid and/or nucleate boiling, transition boiling, and single-phase vapor and/or film boiling. The same heat transfer correlations apply that would apply otherwise; the only major difference is the forced mapping of the heat transfer profile that keys on the calculation of CHF wall temperature from the Modified Zuber CHF correlation.

The uncertainty and bias for the total post-CHF heat transfer includes data from FLECHT-SEASET simulations that modeled reflood heat transfer. The range of applicability was presented previously in the discussion of film boiling.

S-RELAP5 Implementation of Transition Boiling

In general, the application of the modified Chen correlation is within its range of applicability; however, system pressures will likely be lower than the 61 psia used in the derived range of applicability. In limiting RLBLOCA simulations (high clad temperatures), the PCT sensitivity to transition boiling is minimal. This is because the location of PCT in these limiting cases is well above the quench plane. Once heat transfer moves into the transition boiling regime, the feedback from the cooler cladding temperature enhances heat transfer rapidly and within seconds the heat transfer moves into the nucleate boiling regime. Considering the distance between the quench location and the PCT location, heat transfer below the quench front has little direct influence on PCT when there is no bulk boiling.

The results of several test validation problems including LOFT, CCTF and Semiscale, presented in Section 8.0, show that the quenching of the cladding occurs soon after the heat transfer regime is switched from film boiling to transition boiling. Therefore, the determination of the transition point is more important than the transition boiling heat transfer. For this reason, a T_{min} model defining the transition from film boiling to transition boiling is used in S-RELAP5.

Table B-4 provides a comparison of the simulation-space and the range of applicability evaluated for the assessment-space for the Modified Chen transition boiling correlation. [

]

Time Period: Long-Term Cooling

This period is characterized by single-phase liquid or nucleate boiling heat transfer. Peak clad temperatures are not influenced by this condition. Calculations are terminated after whole-core quench.

S-RELAP5 Implementation of Nucleate Boiling Heat Transfer

Since nucleate boiling is not considered to have a significant influence on clad temperatures, no formal assessment was performed. S-RELAP5 was assessed for the few high pressure boil-off tests presented in Section 8.0; however, the focus of these tests is the more dominant film boiling phenomena.

Table B-5 provides a comparison of the simulation-space and the range of applicability evaluated for the assessment-space for the Chen nucleate boiling correlation. [

]

Summary

As has been presented, individual correlations have been programmed into S-RELAP5; however, during a LBLOCA calculation multiple correlations will be employed simultaneously to calculate a total heat transfer during post-CHF conditions. In addition, correlations for interfacial phenomena will also influence this calculation. For this reason, it is the superposition of these individual correlations that becomes the post-CHF heat transfer correlation in S-RELAP5. The pedigree of this "correlation" relies on the range of applicability of the individual correlations, the range of applicability provided by the uncertainty analysis using FLECHT-SEASET datasets and the RLBLOCA analysis methodology, and the various benchmarks.

Table B-6 presents a collective summary of the coverage of the assessment-space provided in the discussion of the heat transfer regimes (including data provided in Table B-2 through Table B-5). This includes the derived range of applicability, the expanded range of applicability based on statistical treatment (the uncertainty analysis), and code-to-data comparisons. In general, the FLECHT-SEASET test-spaces, used to expand the range of applicability, encompass the original derived range of applicability. In addition, a number of integral test simulations were performed and are presented in Section 8.0. The integral tests, including LOFT, CCTF, SCTF, and Semiscale, provide the largest coverage of the assessment-space; that is, they were performed at typical LBLOCA conditions. The demonstration of acceptable agreement among these validation cases sufficiently completes the assessment-space and the assessment-space provides sufficient coverage over the simulation-space.

Table B-1 Identification of Heat Transfer Parameters during a Limiting LBLOCA Simulation

[ ]

Table B-2 Simulation and Application Space for CHF during Blowdown

Table B-3 Simulation and Application Space for Film Boiling Heat Transfer Including Thermal Radiation

[redacted]

Table B-4 Simulation and Application Space for Transition Boiling Heat Transfer

Table B-5 Simulation and Application Space for Nucleate Boiling Heat Transfer (late reflood)

Table B-6 Summary of Full Range of Applicability

B.2 Westinghouse 3-Loop PWR

B.2.1 Summary

The parameter specification for this analysis is provided in Table B-9. [

] The analysis addresses typical operational ranges or technical specification limits (whichever is applicable) with regard to pressurizer pressure and level; accumulator pressure, temperature (containment temperature), and level; core inlet temperature; core flow; containment pressure and temperature; and refueling water storage tank temperature. [

]

[

]

[

]

B.2.2 Plant Description and Summary of Analysis Parameters

The plant analysis presented in this section is a Westinghouse designed PWR, having three loops, each with a hot leg, a U-tube steam generator, and a cold leg with a RCP. The RCS also includes a pressurizer. The ECCS comprises three accumulators, one per loop, and one full train of LHSI and HHSI injection (after applying the single failure assumption). The HHSI and LHSI feed into common headers (cross connected) that are connected to the accumulator lines.

The S-RELAP5 model explicitly describes the RCS, reactor vessel, pressurizer, and ECCS back to the common LHSI header and accumulators. This model also describes the secondary-side steam generator that is instantaneously isolated (closed MSIV and feedwater trip) at the time of the break.

As described in Appendix A, many parameters associated with LBLOCA phenomenological uncertainties and plant operation ranges are sampled. A summary of those parameters sampled is given in Table A-6. The LBLOCA phenomenological uncertainties are provided in Table A-7. Values for process or operational parameters, including ranges of sampled process parameters, and fuel design parameters used in the analysis are given in Table B-7. Plant data are analyzed to develop uncertainties for the process parameters sampled in the analysis. Table B-8 presents a summary of the uncertainties used in the analysis. [

]

Where applicable, the sampled parameter ranges are based on technical specification limits. Plant data are used to define range boundaries for [

]

B.2.3 Realistic Large Break LOCA Results

[

]

Table B-9 is a summary of the major input parameters for the demonstration case. The results of the plant sample analyses are presented in Table B-10. The fraction of total hydrogen generated was not directly calculated; however, it is conservatively bounded by the calculated total percent oxidation, which is well below the 1-percent limit. The event times for the demonstration case can be found in Table B-11 and the heat transfer parameter range for the demonstration case is provided in Table B-12. [

]

[

] The analysis plots are shown in Figure B-2 through Figure B-19. Figure B-2 shows linear scatter plots of the key parameters sampled for all the cases. Parameter labels appear to the left of each individual plot. These figures illustrate the parameter ranges used in the analysis.

Figure B-3 and Figure B-4 show PCT scatter plots versus the time of PCT and versus break size [ ] The scatter plots for the maximum local oxidation and total core-wide oxidation [ ] are shown in Figure B-5 and Figure B-6, respectively. Figure B-7 through Figure B-18 show key parameters from the S-RELAP5 calculations for the demonstration case. Figure B-7 is the plot of PCT, independent of elevation. Figure B-19 compares the beginning of core recovery times [ ] to the BOCR time predicted using the MPR CCFL correlation. Note that Figure B-19 uses the total break area, while previous plots used break area per side.

B.2.4 Conclusions

[

]

Table B-7 3-Loop Westinghouse Plant Operating Range Supported by the RLBLOCA Analysis

	Event	Operating Range
1.0	**Plant Physical Description**	
	1.1 Fuel	
	a) Cladding outside diameter	
	b) Cladding inside diameter	
	c) Cladding thickness	
	d) Pellet outside diameter	
	e) Initial Pellet density	
	f) Active fuel length	
	g) Gd_2O_3 concentrations	
	1.2 RCS	
	a) Flow resistance	
	b) Pressurizer location	
	c) Hot assembly location	
	d) Hot assembly type	
	e) SG tube plugging	
2.0	**Plant Initial Operating Conditions**	
	2.1 Reactor Power	
	a) Analyzed reactor power	
	b) F_q	
	c) $F_{\Delta H}$	
	d) MTC	
	2.2 Fluid Conditions	
	a) Loop flow	
	b) RCS average temperature	
	c) Upper head temperature	
	d) Pressurizer pressure	
	e) Pressurizer level	
	f) Accumulator pressure	
	g) Accumulator liquid volume	
	h) Accumulator temperature	
	i) Accumulator resistance fL/D	
	j) Minimum ECCS boron	

1 Includes 4 percent measurement uncertainty.
2 Upper head temperature will change based on sampling of RCS temperature.

Table B-7 3-Loop Westinghouse Plant Operating Range Supported by the RLBLOCA Analysis (continued)

	Event	Operating Range
3.0	**Accident Boundary Conditions**	[
	a) Break location	
	b) Break type	
	c) Break size (each side, relative to cold leg pipe area)	
	d) Worst single-failure	
	e) Offsite power	
	f) ECCS pumped injection temperature	
	g) HHSI pump delay	
	h) LHSI pump delay	
	i) Containment pressure	
	j) Containment temperature	
	k) Containment sprays delay	
	l) Containment spray water temperature	
	m) LHSI Flow	]

Table B-7 3-Loop Westinghouse Plant Operating Range Supported by the RLBLOCA Analysis (continued)

Event	Operating Range
n) HHSI Flow	

Table B-8 3-Loop Westinghouse Statistical Distribution Used for Process Parameters

Parameter	Operational Uncertainty Distribution	Parameter Range	Measurement Uncertainty Distribution	Standard Deviation
Pressurizer Pressure (psig)				
Pressurizer Level (%)				
Accumulator Volume (ft^3)				
Accumulator Pressure (psia)				
Containment/Accumulator Temperature (°F)				
Containment Volume ($x10^6$ ft^3)				
Initial Flow Rate (Mlbm/hr)				
Initial Operating Temperature (°F)				

Table B-9 3-Loop Westinghouse Summary of Major Parameters for the Demonstration Case

Parameter	Value
Time in Cycle (hrs)	
Burnup (GWd/mtU)	
Core Power (MWt)	
Core Peaking (F_q)	
Radial Peak ($F_{\Delta H}$)	
Axial Offset	
Local Peaking (F_l)	
Break Type	
Break Size (ft^2/side)	
Offsite Power Availability	

Table B-10 3-Loop Westinghouse Compliance with 10 CFR 50.46

Table B-10 3-Loop Westinghouse Compliance with 10 CFR 50.46 (continued)

[
]

Table B-11 3-Loop Westinghouse Calculated Event Times for the Demonstration Case

Event	Time (sec)
Begin Analysis	
Break Opens	
RCP Trip	
SIAS Issued	
Start of Broken Loop Accumulator Injection	
Start of Intact Loop Accumulator Injection (Loop 2 and 3 respectively)	
Start of HHSI	
Start of Charging	
Beginning of Core Recovery (Beginning of Reflood)	
LHSI Available	
PCT Occurred	
Broken Loop LHSI Delivery Began	
Intact Loops LHSI Delivery Began (Loop 2 and 3 respectively)	
Broken Loop HHSI Delivery Began	
Intact Loops HHSI Delivery Began (Loop 2 and 3 respectively)	
Broken Loop Accumulator Emptied	
Intact Loop Accumulator Emptied (Loop 2 and 3 respectively)	
Transient Calculation Terminated	

Table B-12 Westinghouse 3-Loop Heat Transfer Parameters for the Demonstration Case

Time (s)						
LOCA Phase	Early Blowdown	Blowdown [1]	Refill	Reflood	Quench	Long Term Cooling
Heat Transfer Mode						
Heat Transfer Correlations						
Maximum LHGR (kW/ft)						
Pressure (psia)						
Core Inlet Mass Flux (lbm/s-ft2[2])						
Vapor Reynolds Number[3]						
Liquid Reynolds Number						
Vapor Prandtl Number						
Liquid Prandtl Number						
Vapor Superheat[4] (°F)						

1 End of Blowdown considered as beginning of refill.
2 Conservatively biased parameter
3 Not important in pre-CHF heat transfer
4 Vapor superheat is meaningless during blowdown and system depressurization

Table B-13 Westinghouse 3-Loop Fuel Rod Rupture Ranges of Parameters

[ ]

Parameter Name	Minimum Value	Maximum Value

Figure B-1 [ ]

Figure B-2 3-Loop Westinghouse Scatter Plot of Operational Parameters

[ ]

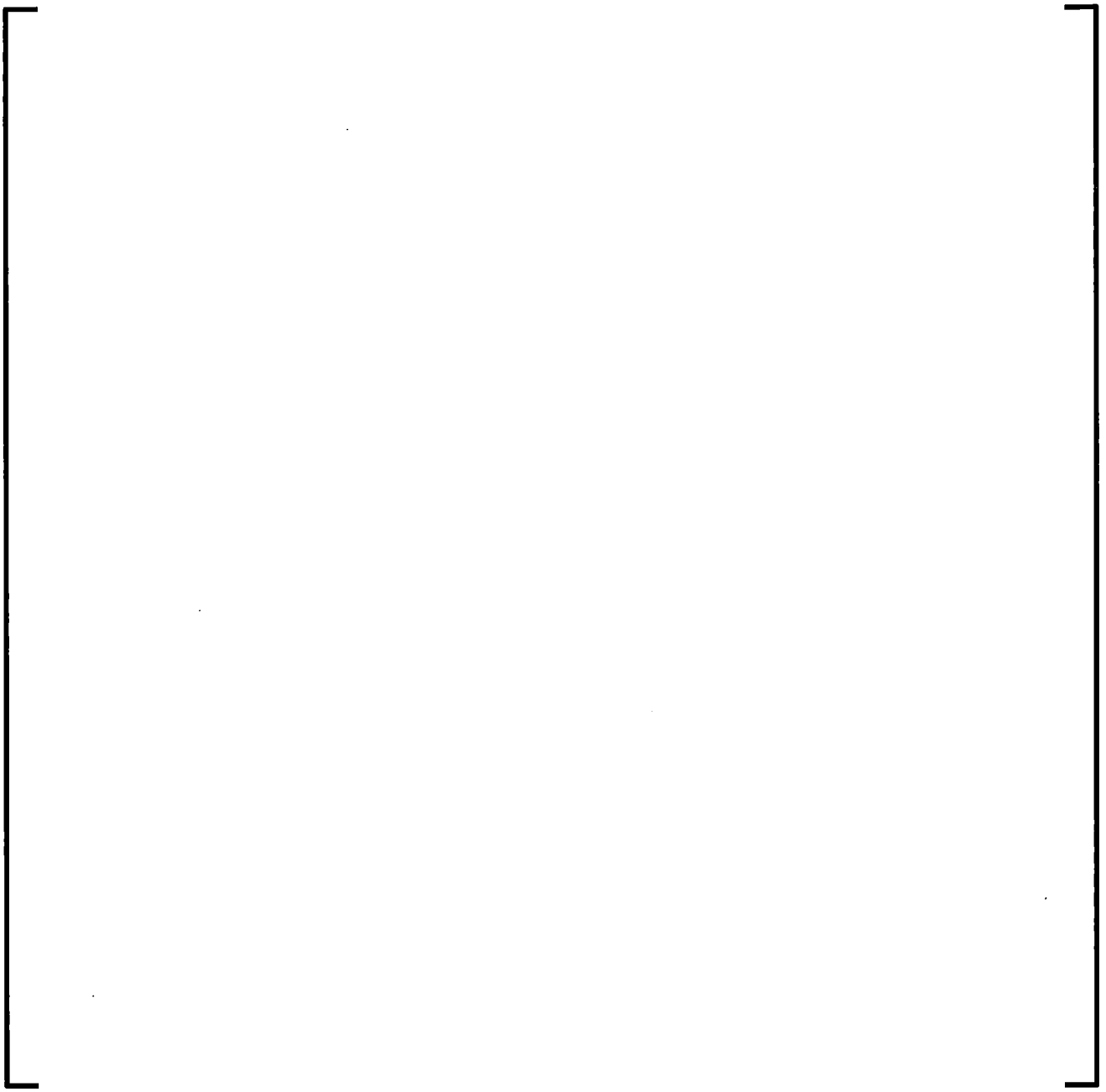

Figure B-2 3-Loop Westinghouse Scatter Plot of Operational Parameters [ ] (continued)

[ ]

Figure B-3 3-Loop Westinghouse PCT versus PCT Time Scatter Plot

[ ]

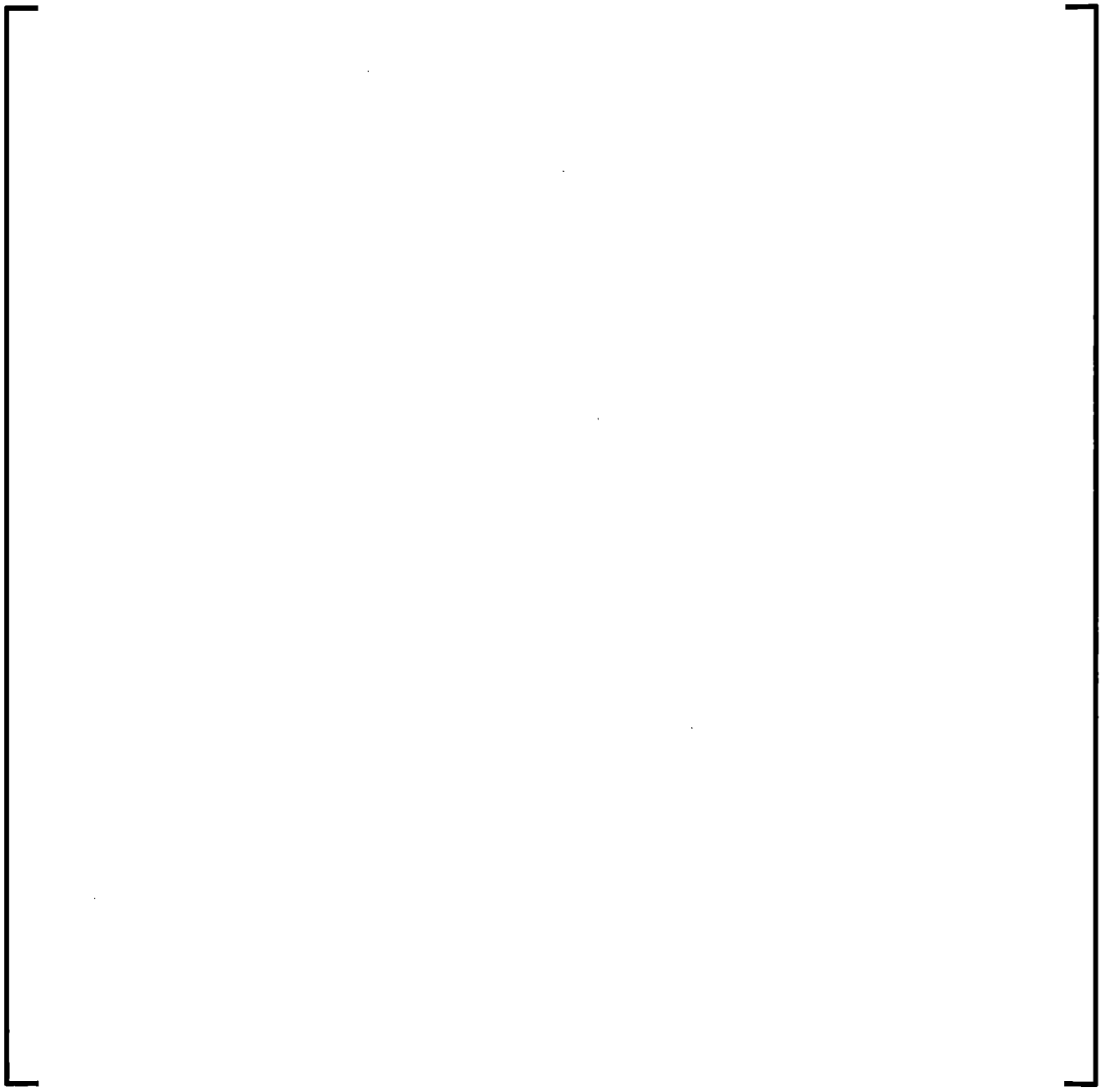

Figure B-4 3-Loop Westinghouse PCT versus Break Size Scatter Plot

[ ]

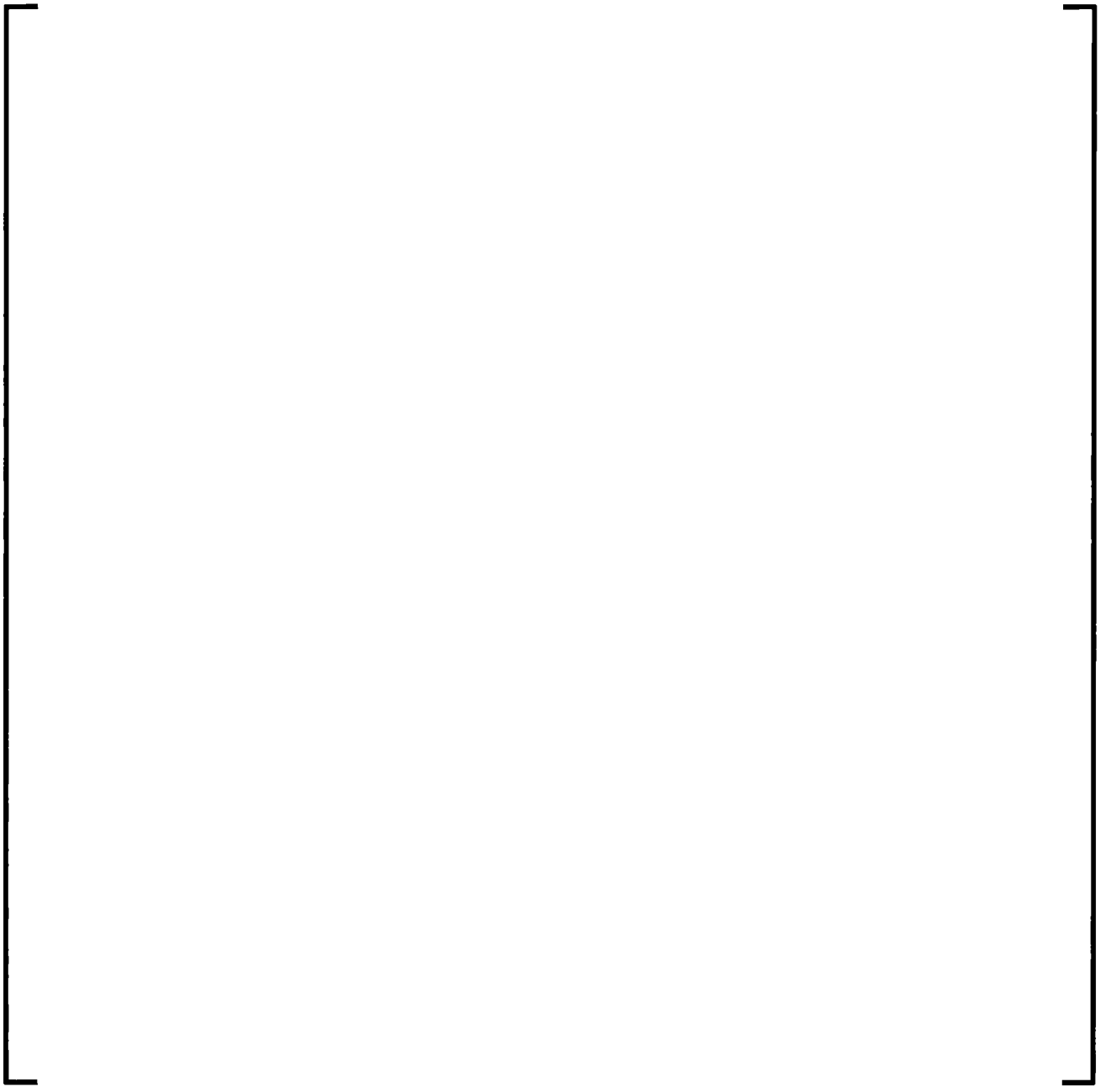

Figure B-5 3-Loop Westinghouse Maximum Local Oxidation versus PCT Scatter Plot [ ]

[ ]

Figure B-6 3-Loop Westinghouse Total Core-Wide Oxidation versus PCT Scatter Plot [ ]

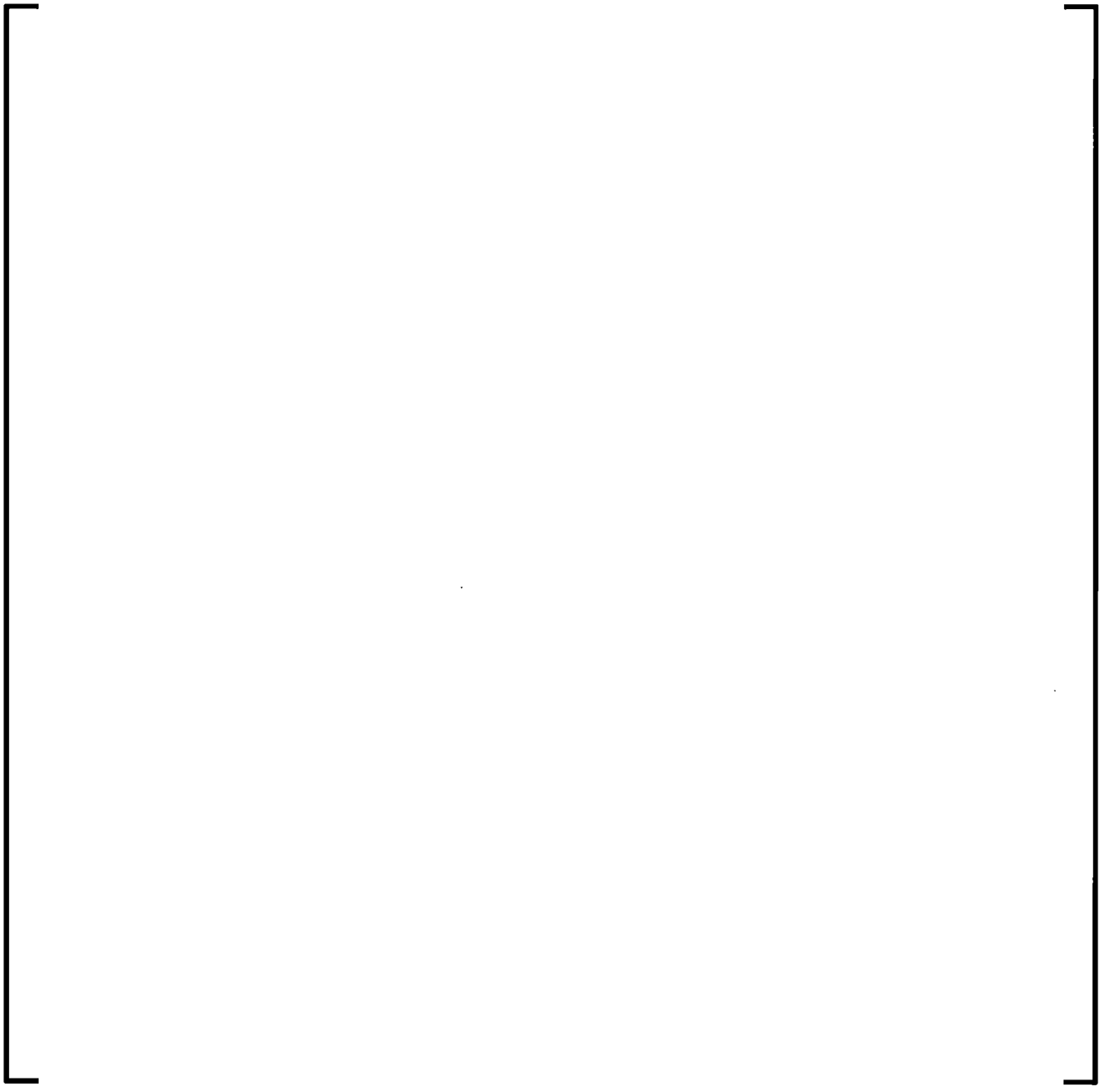

Figure B-7 3-Loop Westinghouse Peak Cladding Temperature (Independent of Elevation) for the Demonstration Case

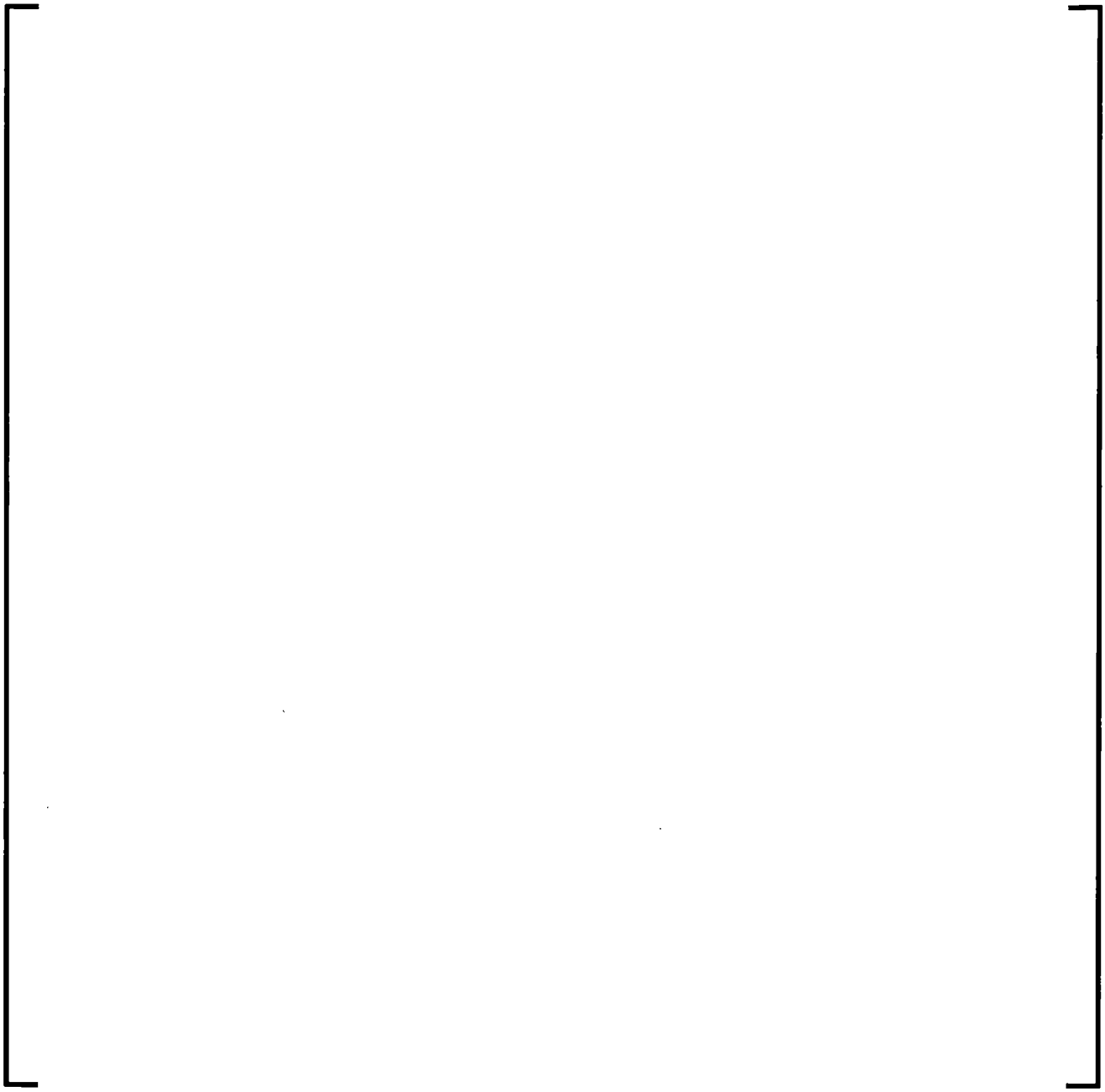

Figure B-8 3-Loop Westinghouse Break Flow for the Demonstration Case

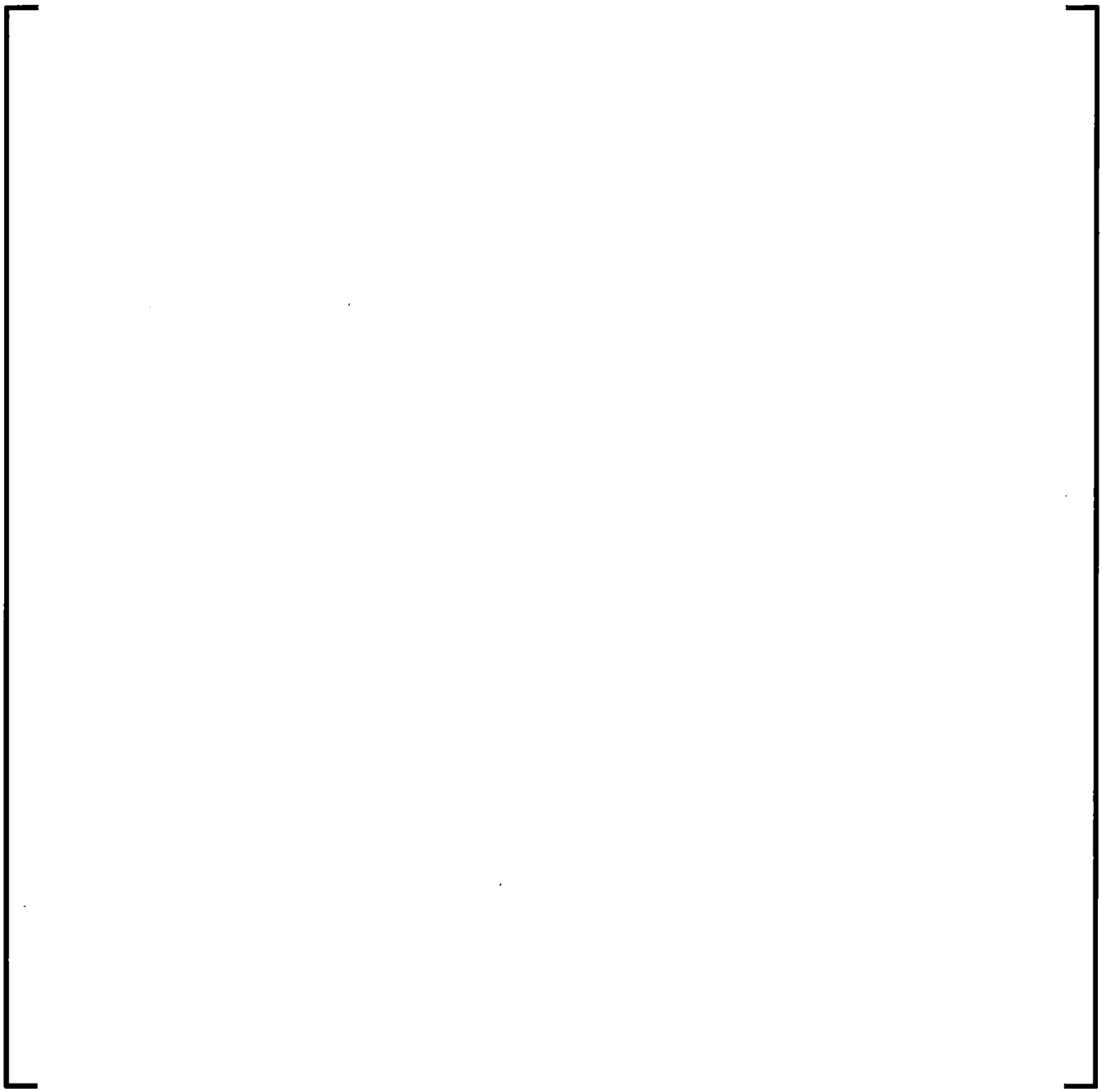

Figure B-9 3-Loop Westinghouse Core Inlet Mass Flux for the Demonstration Case

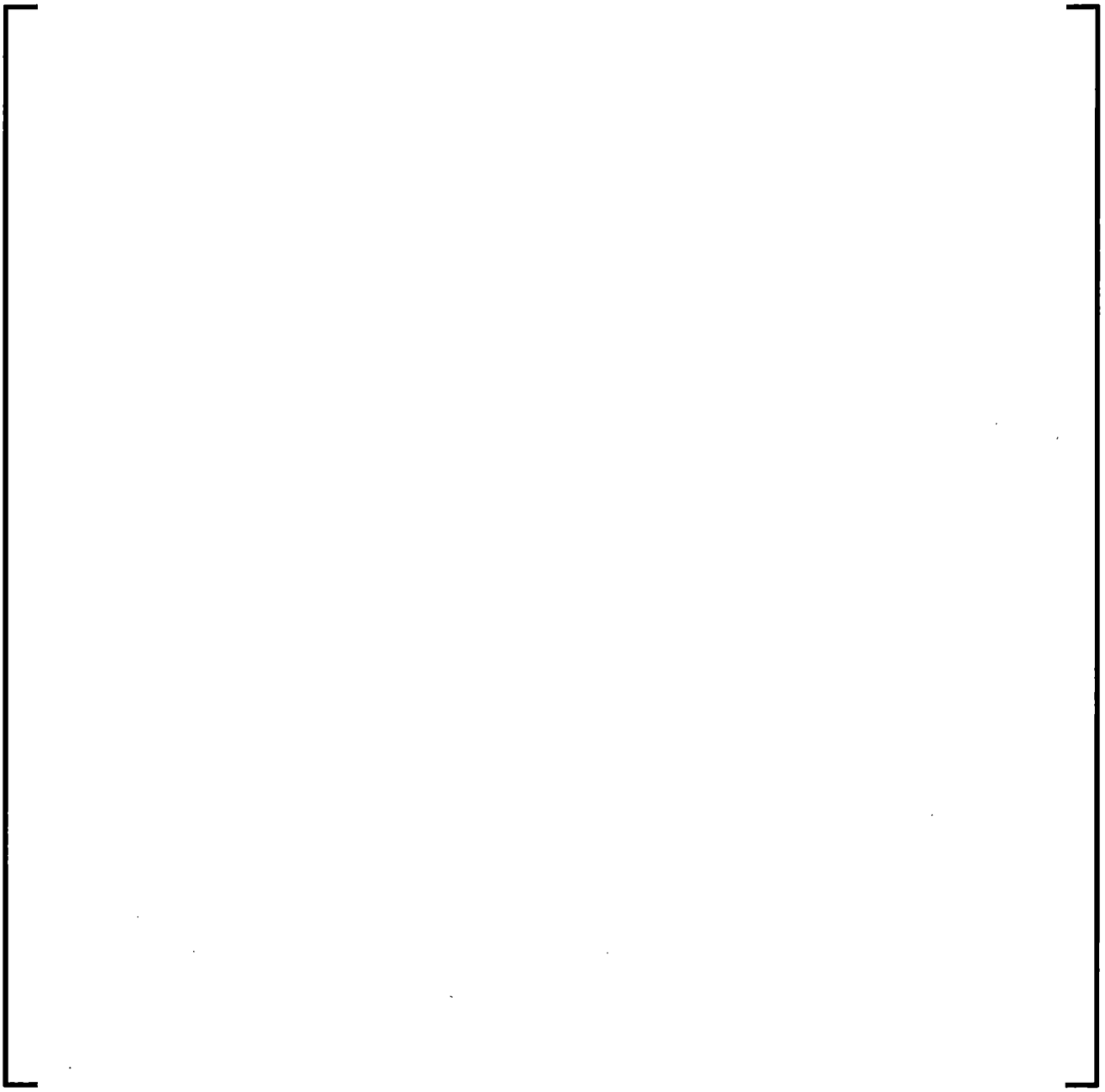

Figure B-10 3-Loop Westinghouse Core Outlet Mass Flux for the Demonstration Case

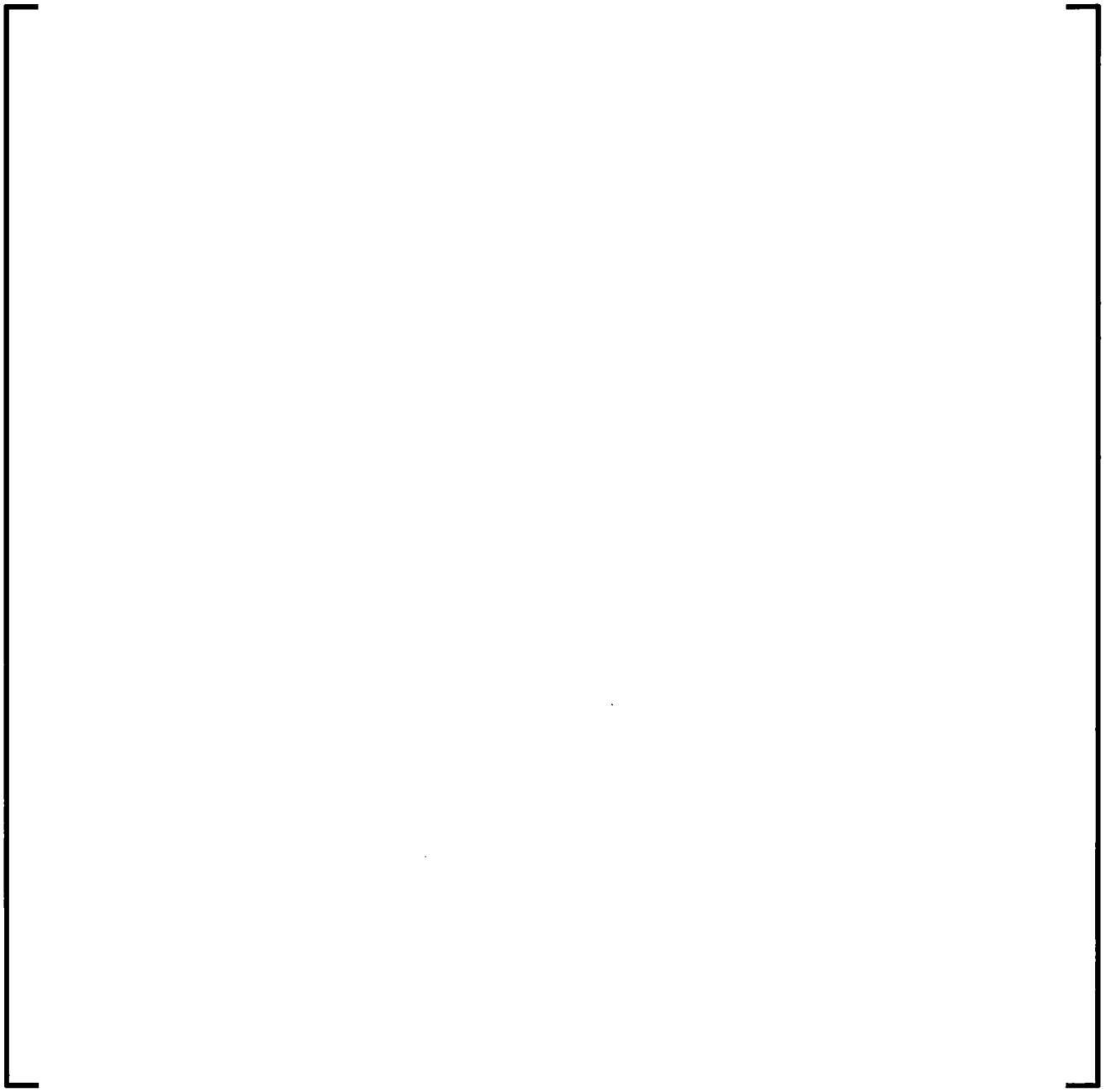

Figure B-11 3-Loop Westinghouse Void Fraction at RCS Pumps for the Demonstration Case

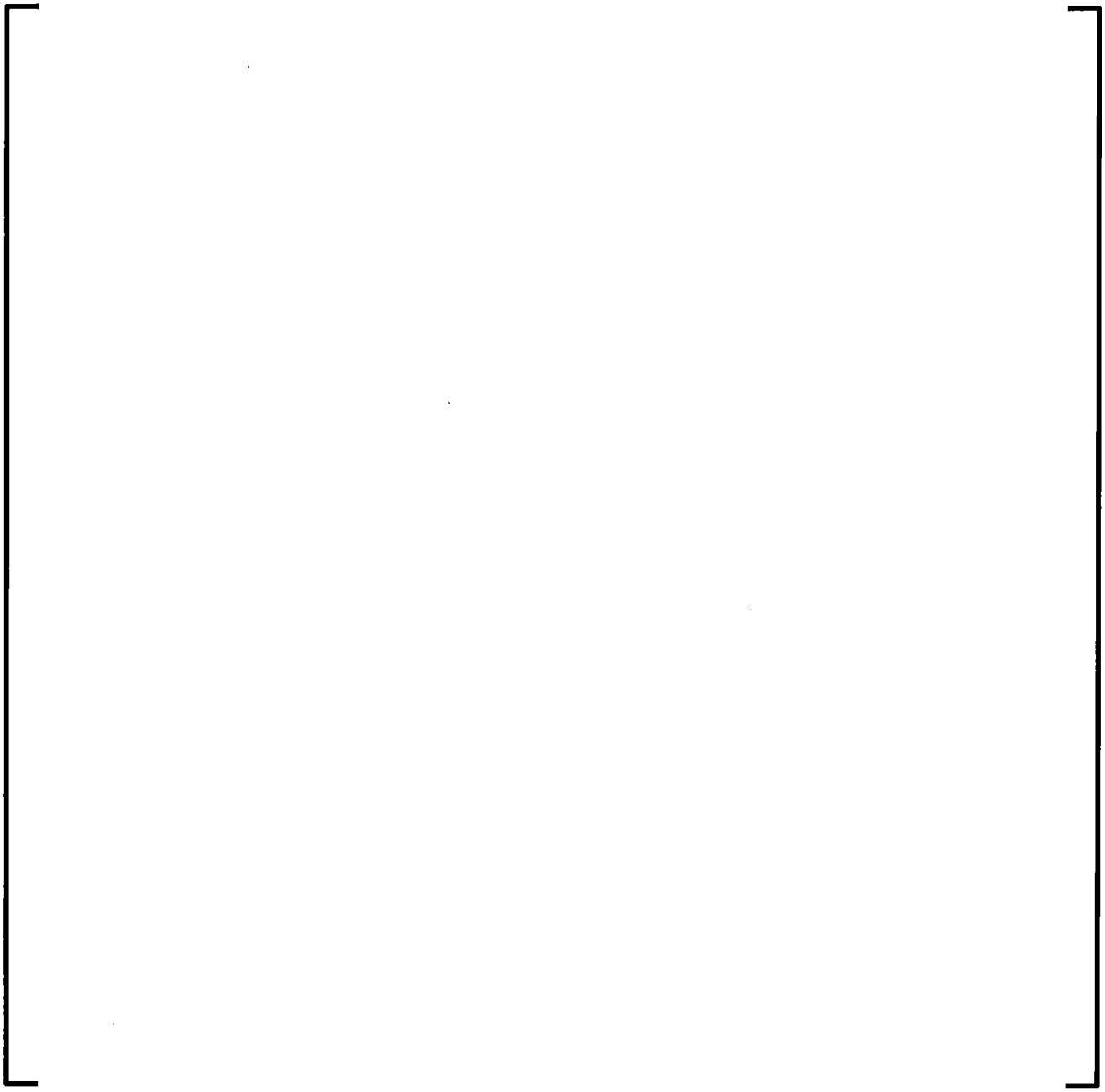

Figure B-12 3-Loop Westinghouse ECCS Flows (Includes Accumulator, Charging, SI and RHR) for the Demonstration Case

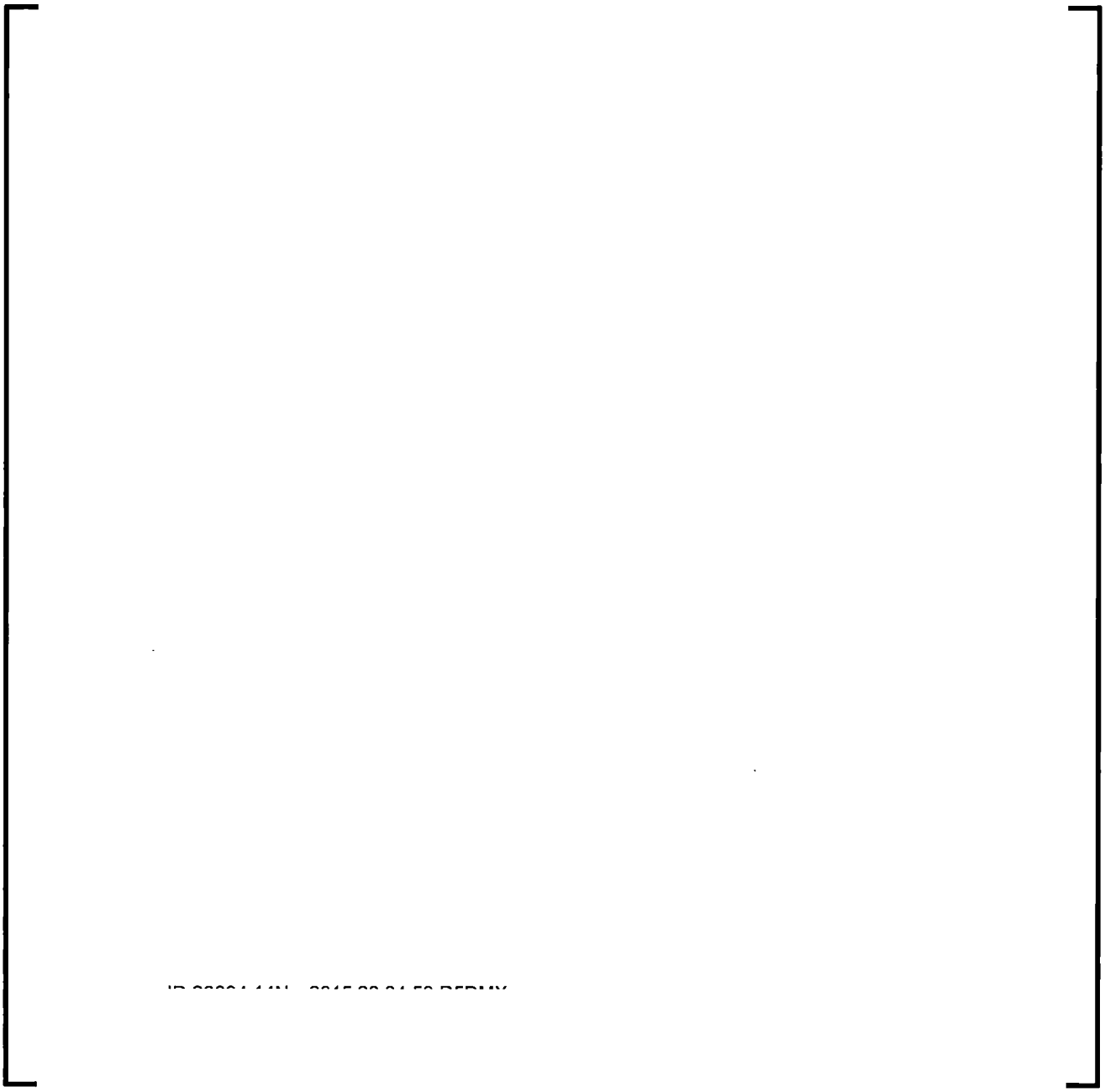

Figure B-13 3-Loop Westinghouse Upper Plenum Pressure for the Demonstration Case

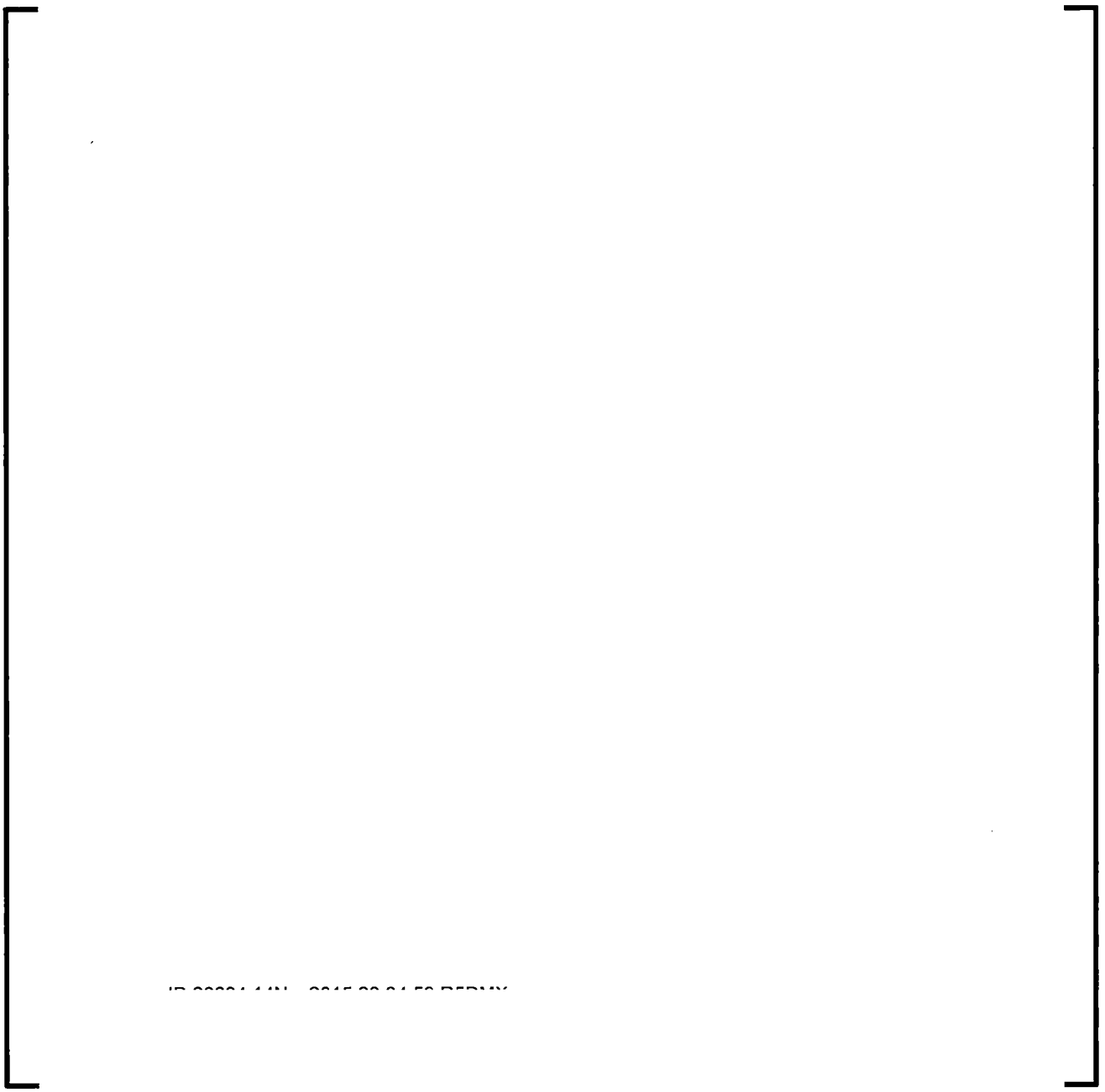

Figure B-14 3-Loop Westinghouse Collapsed Liquid Level in the Downcomer for the Demonstration Case

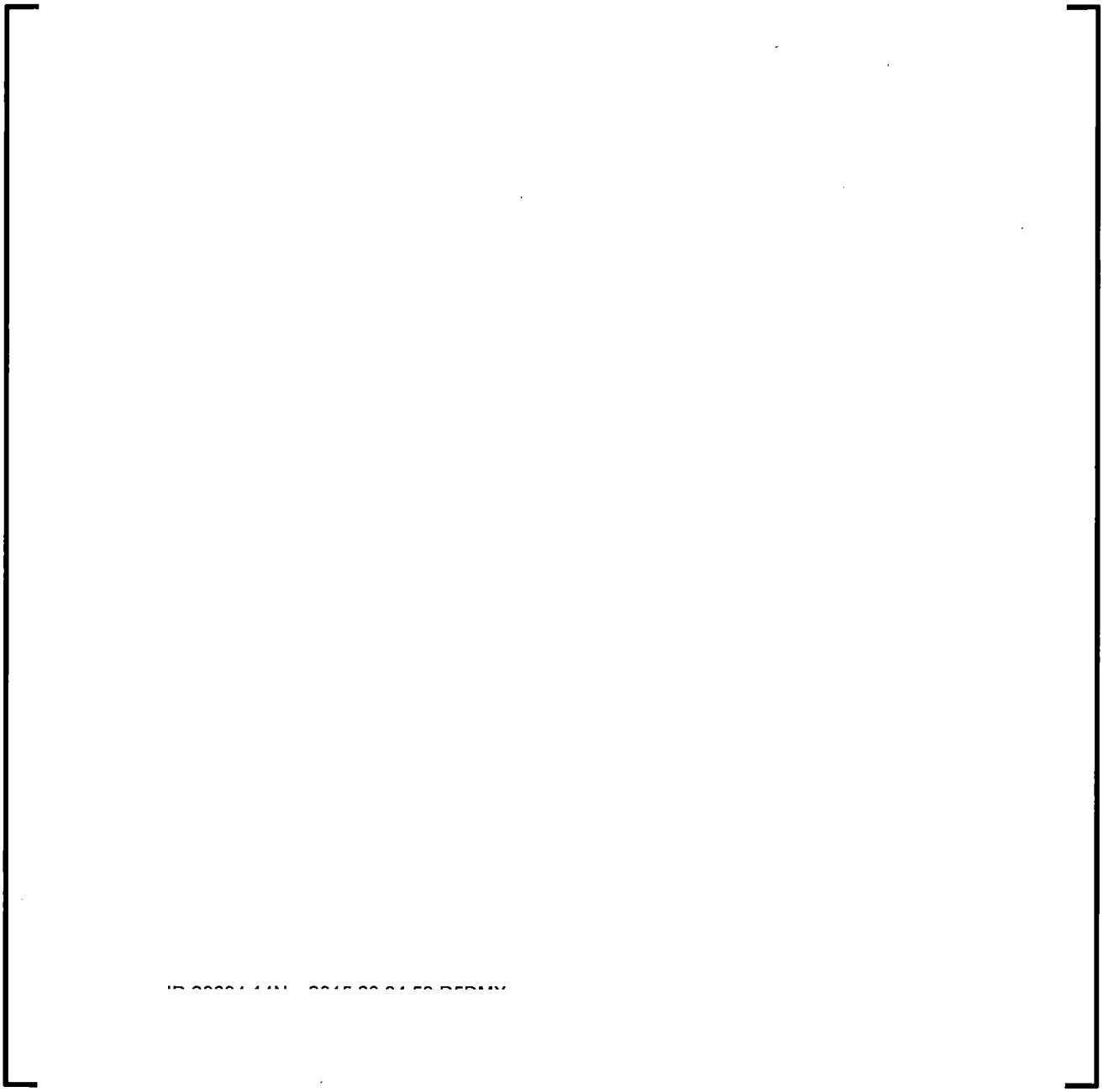

Figure B-15 3-Loop Westinghouse Collapsed Liquid Level in the Lower Plenum for the Demonstration Case

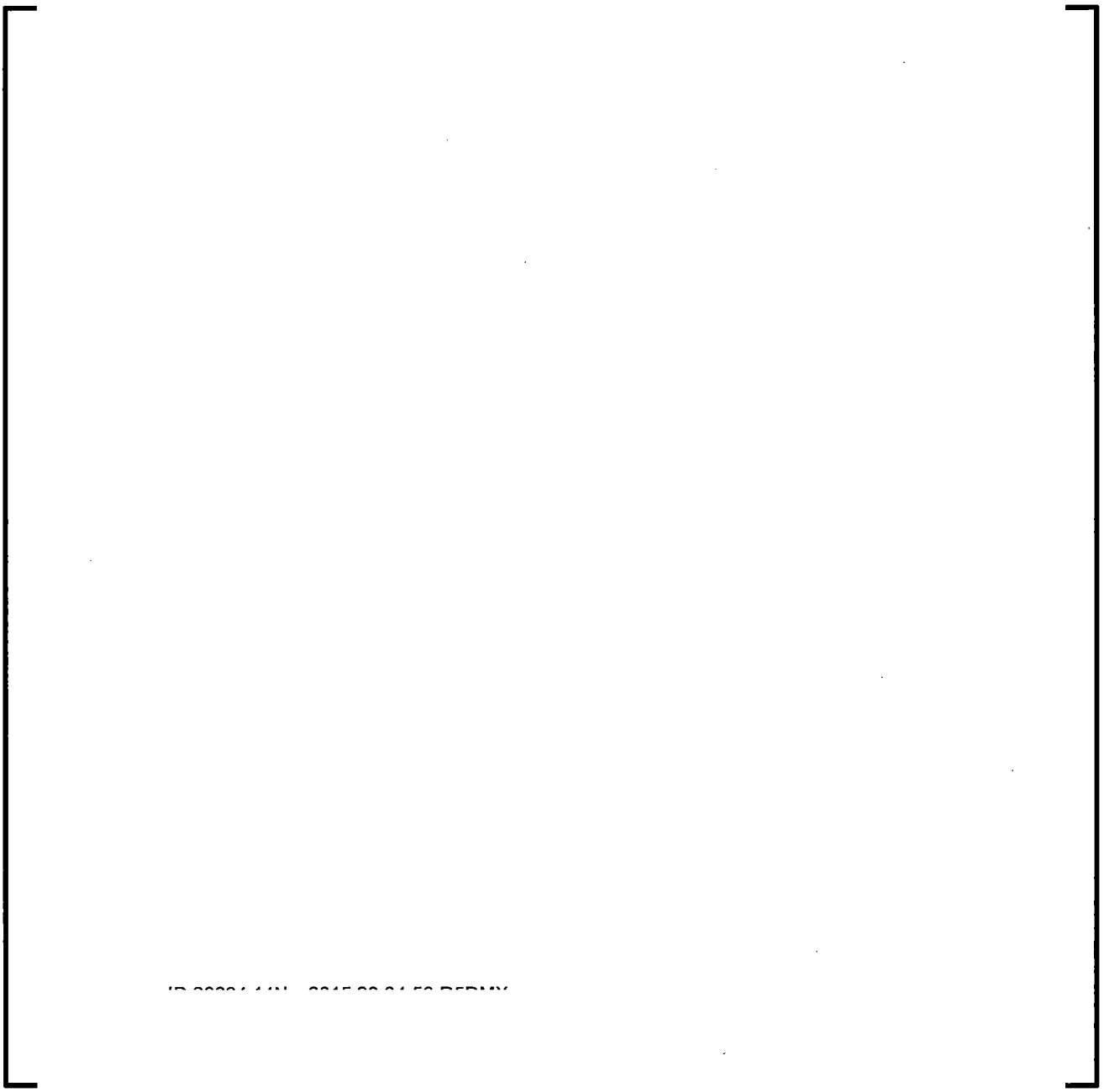

Figure B-16 3-Loop Westinghouse Collapsed Liquid Level in the Core for the Demonstration Case

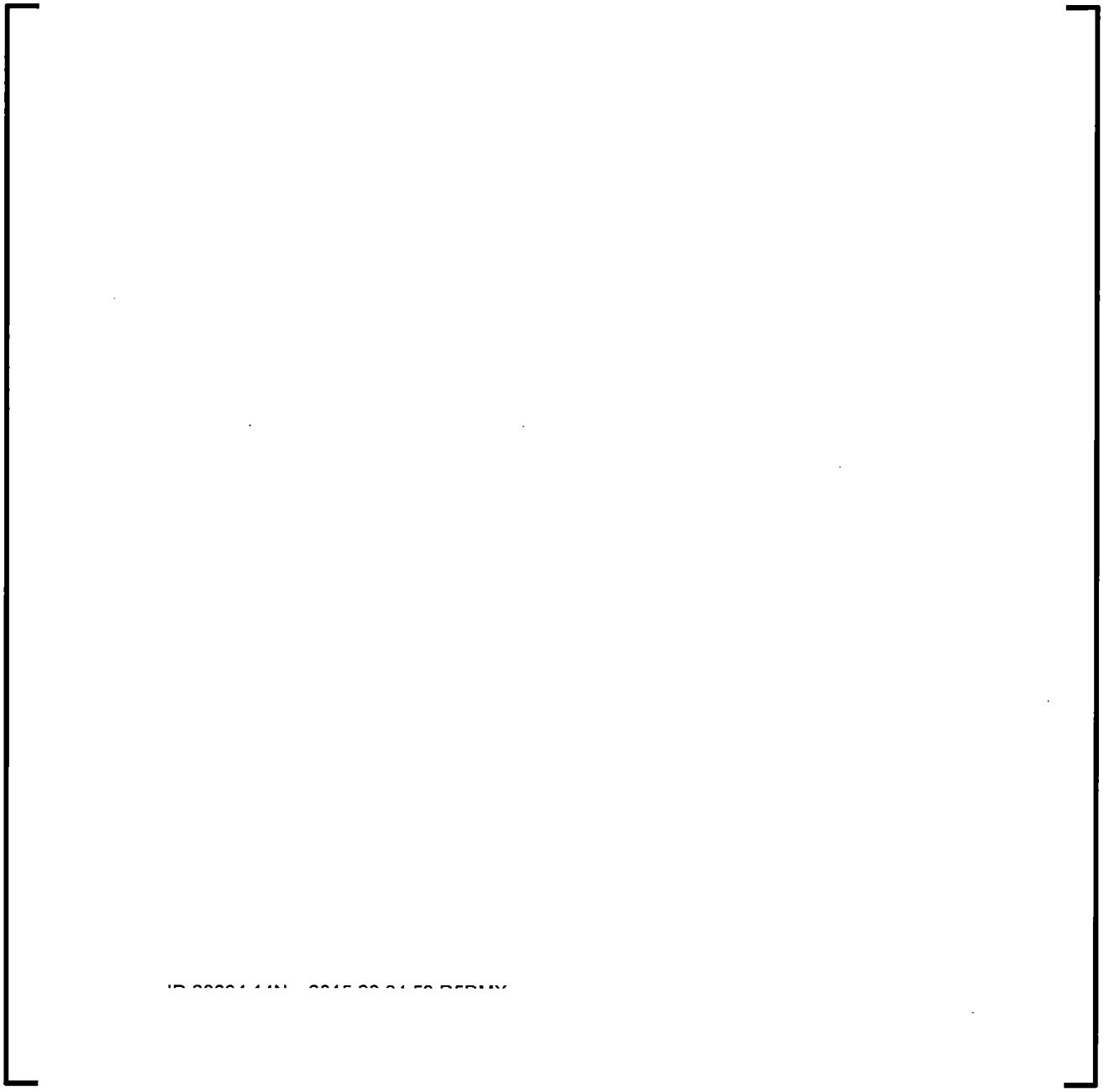

Figure B-17 3-Loop Westinghouse Containment and Loop Pressures for the Demonstration Case

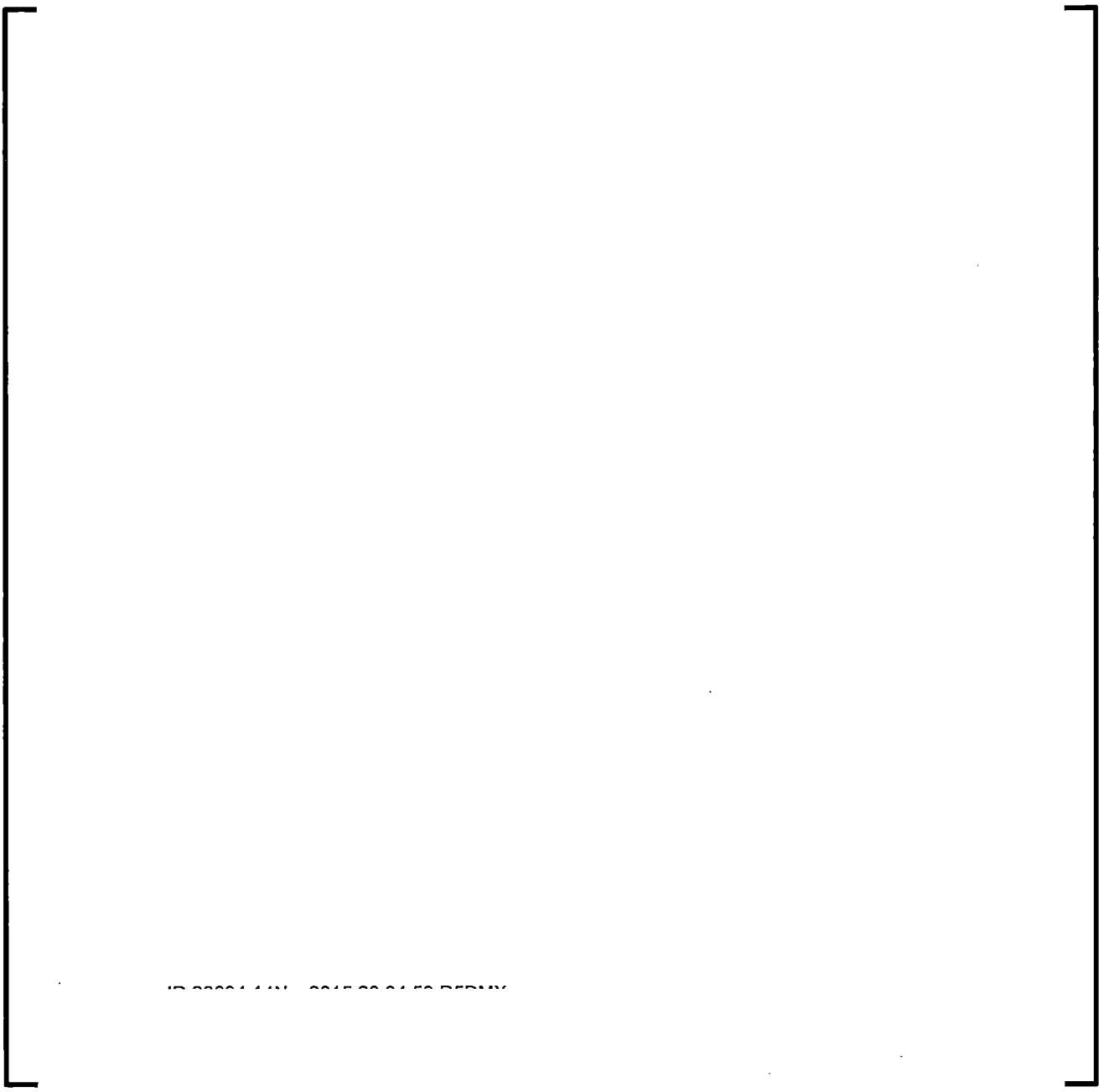

Figure B-18 3-Loop Westinghouse Pressure Difference between Upper Plenum and Downcomer for the Demonstration Case

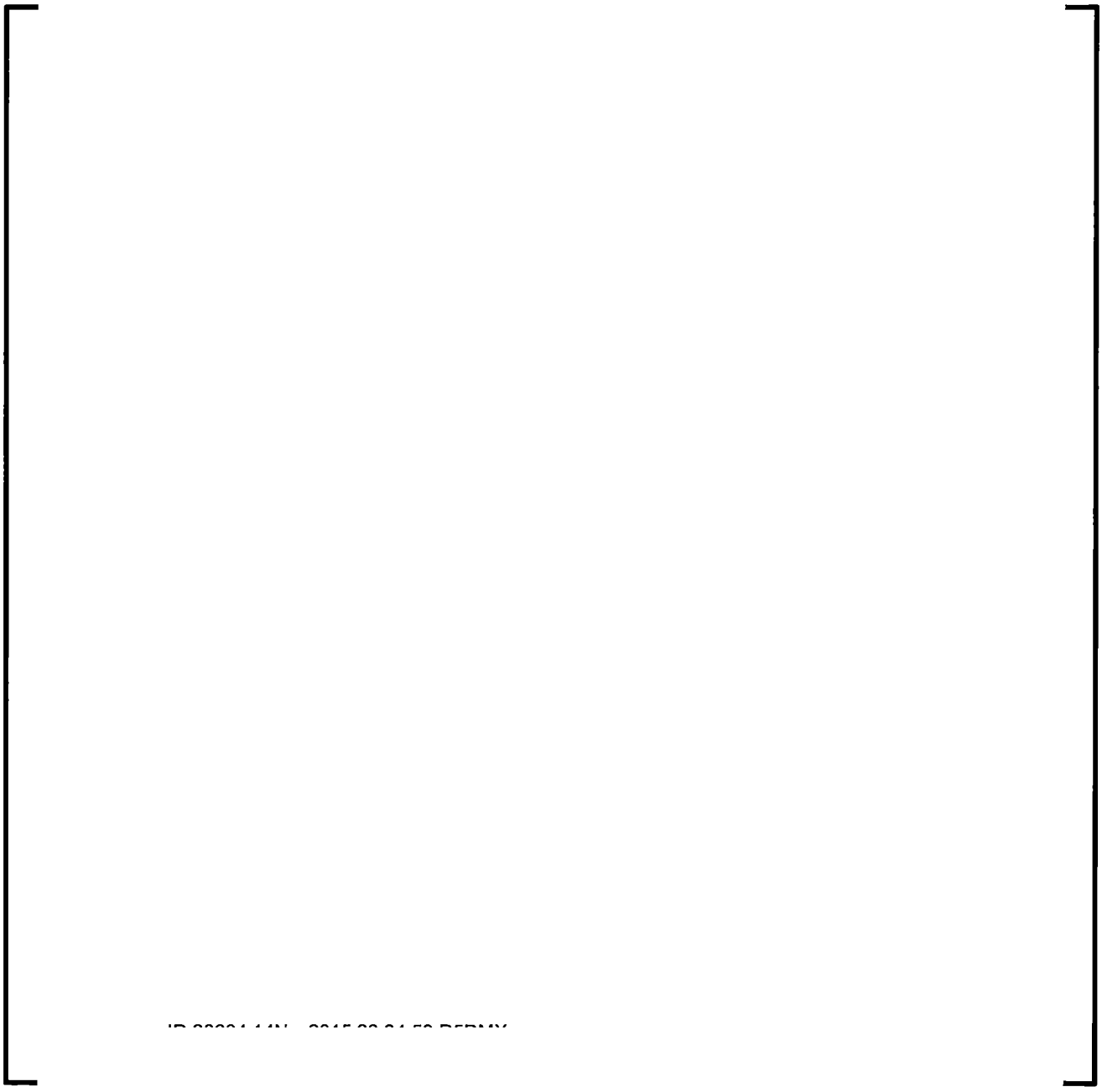

Figure B-19 3-Loop Westinghouse Validation of BOCR Time using MPR CCFL Correlation, [ ]

[ ]

B.3 Westinghouse 4-Loop PWR

B.3.1 Summary

The parameter specification for this analysis is provided in Table B-14. [

] This analysis also addresses typical operational ranges or technical specification limits (which ever is applicable) with regard to pressurizer pressure and level; accumulator pressure, temperature (containment temperature), and level; core inlet temperature; core flow; containment pressure and temperature; and refueling water storage tank temperature. [

]

[

]

[

]

B.3.2 Plant Description and Summary of Analysis Parameters

The plant analysis presented in this section is a Westinghouse designed pressurized water reactor (PWR), which has four loops, each with a hot leg, a U-tube steam generator, and a cold leg with a RCP. The RCS also includes one pressurizer. The ECCS includes one charging and one accumulator/SI/RHR injection path per RCS loop (after applying the single failure assumption). The SI and RHR feed into common headers which are connected to the accumulator lines. The charging pumps are also cross-connected.

The S-RELAP5 model explicitly describes the RCS, reactor vessel, pressurizer, and accumulator lines. The charging injection flows are connected to the RCS, and the SI and RHR injection flows are connected to the accumulator lines. This model also describes the secondary-side steam generator that is instantaneously isolated (closed MSIV and feedwater trip) at the time of the break.

As described in Appendix A, many parameters associated with LBLOCA phenomenological uncertainties and plant operation ranges are sampled. A summary of those parameters sampled is given in Table A-6. The LBLOCA phenomenological uncertainties are provided in Table A-7. Values for process or operational parameters, including ranges of sampled process parameters, and fuel design parameters used in the analysis are given in Table B-14. Plant data is analyzed to develop uncertainties for the process parameters sampled in the analyses. Table B-15 presents a summary of the uncertainties used in the analysis. [

]

Where applicable, the sampled parameter ranges are based on technical specification limits. Plant data are used to define range boundaries for [

]

B.3.3 Realistic Large Break LOCA Results

[

]

Table B-16 is a summary of the major parameters input parameters for the demonstration case. The results of the plant sample analyses are presented in Table B-17. The fraction of total hydrogen generated was not directly calculated; however, it is conservatively bounded by the calculated total percent oxidation, which is well below the 1-percent limit. The event times for the demonstration case can be found in Table B-18 and the heat transfer parameter range is provided in Table B-19. [

].

[

] The analysis plots are shown in Figure B-21 through Figure B-37. Figure B-21 shows linear scatter plots of the key parameters sampled for all the cases. Parameter labels appear to the left of each individual plot. These figures illustrate the parameter ranges used in the analysis.

Figure B-22 and Figure B-23 show PCT scatter plots versus the time of PCT and versus break size [ ] The scatter plots for the maximum local oxidation and total core-wide oxidation [ ] are shown in Figure B-24 and Figure B-25, respectively. Figure B-26 through Figure B-37 show key parameters from the S-RELAP5 calculations for the demonstration case. Figure B-26 is the plot of PCT, independent of elevation. [

] Note that Figure B-38 uses the total break area while previous plots used break area per side.

B.3.4 Conclusions

[

]

Table B-14 4-Loop Westinghouse Plant Operating Range Supported by the LOCA Analysis

	Event	Operating Range
1.0	**Plant Physical Description**	
	1.1 Fuel	
	a) Cladding outside diameter	
	b) Cladding inside diameter	
	c) Cladding thickness	
	d) Pellet outside diameter	
	e) Initial pellet density	
	f) Active fuel length	
	g) Gd_2O_3 concentrations	
	1.2 RCS	
	a) Flow resistance	
	b) Pressurizer location	
	c) Hot assembly location	
	d) Hot assembly type	
	e) SG tube plugging	
2.0	**Plant Initial Operating Conditions**	
	2.1 Reactor Power	
	a) Analyzed Reactor Power	
	b) F_q	
	c) $F_{\Delta H}$	
	d) MTC	
	2.2 Fluid Conditions	
	a) Loop flow	
	b) Core inlet temperature	
	c) Upper head temperature	
	d) Pressurizer pressure	
	e) Pressurizer level	

1 Includes 5 percent measurement uncertainty.
2 Upper head temperature will change based on sampling of RCS temperature.
3 Considers both representative plant data and includes ±30 psi measurement uncertainty.

Table B-14 4-Loop Westinghouse Plant Operating Range Supported by the LOCA Analysis (continued)

	Event	Operating Range
	f) Accumulator pressure	
	g) Accumulator liquid volume	
	h) Accumulator temperature	
	i) Accumulator fL/D	
	j) Minimum ECCS boron	
3.0	**Accident Boundary Conditions**	
	a) Break location	
	b) Break type	
	c) Break size (each side, relative to cold leg pipe area)	
	d) Worst single-failure	
	e) Offsite power	
	f) ECCS pumped injection temperature	
	g) Charging pump delay	
	h) SI pump delay	
	i) RHR pump delay	
	j) Containment pressure	
	k) Containment upper compartment temperature	
	l) Containment lower compartment temperature	
	m) Containment sprays delay	

Table B-14 4-Loop Westinghouse Plant Operating Range Supported by the LOCA Analysis (continued)

Event	Operating Range
n) Charging pump flow	
o) SI pump flow	
p) RHR pump flow	

Table B-15 4-Loop Westinghouse Statistical Distribution Used for Process Parameters

Parameter	Operational Uncertainty Distribution	Parameter Range	Measurement Uncertainty Distribution[1]	Standard Deviation
Pressurizer Pressure (psia)	[			]
Pressurizer Liquid Level (percent)				
Accumulator Liquid Volume (ft^3)				
Accumulator Pressure (psia)				
Containment Lower Compartment /Accumulator Temperature (°F)				
Containment Upper Compartment Temperature (°F)				
Containment Upper Volume (ft^3)				
Initial RCS Flow Rate (Mlbm/hr)				
Initial RCS Operating Temperature (Tavg) (°F)				

[1] All measurement uncertainties were incorporated into the operational ranges.

Table B-16 4-Loop Westinghouse Summary of Major Parameters for the Demonstration Case

Parameter	Value
Time in Cycle (hrs)	[ ]
Burnup (GWd/mtU)	
Core Power (MWt)	
Core Peaking (F_q)	
Radial Peak ($F_{\Delta h}$)	
Axial Offset	
Local Peaking (FI)	
Break Type	
Break Size (ft^2 / side)	
Offsite Power Availability	]

Table B-17 4-Loop Westinghouse Compliance with 10 CFR 50.46

Table B-17 4-Loop Westinghouse Compliance with 10 CFR 50.46 (continued)

[redacted]

Table B-18 4-Loop Westinghouse Calculated Event Times for the Demonstration Case

Event	Time (sec)
Begin Analysis	
Break Opens	
RCP Trip	
SIAS Issued	
Start of Broken Loop Accumulator Injection	
Start of Intact Loop Accumulator Injection (Loop 2, 3, and 4 respectively)	
Start of SI	
Start of CC	
Beginning of Core Recovery (Beginning of Reflood)	
RHR Available	
PCT Occurred (1921°F)	
Broken Loop RHR Delivery Began	
Intact Loops RHR Delivery Began (Loop 2, 3, and 4 respectively)	
Broken Loop SI Delivery Began	
Intact Loops SI Delivery Began (Loop 2, 3, and 4 respectively)	
Broken Loop Accumulator Emptied	
Intact Loop Accumulator Emptied (Loop 2, 3, and 4 respectively)	
Transient Calculation Terminated	

Table B-19 Westinghouse 4-Loop Heat Transfer Parameters for the Demonstration Case

Time (s)						
LOCA Phase	Early Blowdown	Blowdown [1]	Refill	Reflood	Quench	Long Term Cooling
Heat Transfer Mode						
Heat Transfer Correlations						
Maximum LHGR (kW/ft)						
Pressure (psia)						
Core Inlet Mass Flux (lbm/s-ft^2)						
Vapor[3] Reynolds Number						
Liquid Reynolds Number						
Vapor Prandtl Number						
Liquid Prandtl Number						
Vapor Superheat (°F)						

1 End of Blowdown considered as beginning of refill.
2 Conservatively biased parameter, as per the methodology
3 Not important in pre-CHF heat transfer.

Table B-20 Westinghouse 4-Loop Fuel Rod Rupture Ranges of Parameters [ ]

Figure B-20 [ ]

Figure B-21 4-Loop Westinghouse Scatter Plot of Operational Parameters

[ ]

Figure B-21 4-Loop Westinghouse Scatter Plot of Operational Parameters [ ] (continued)

[ ]

Figure B-22 4-Loop Westinghouse PCT versus PCT Time Scatter Plot

[ ]

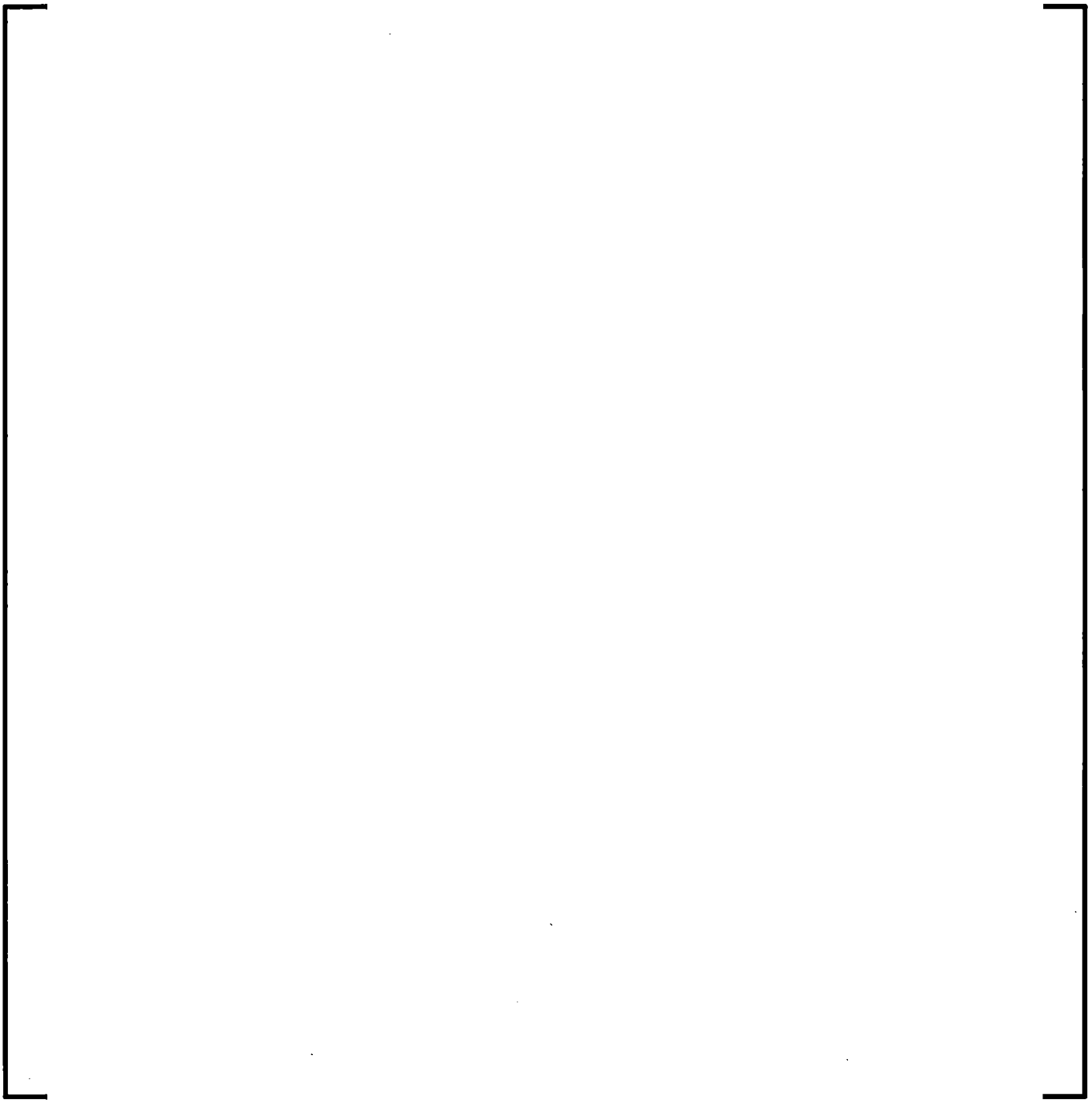

Figure B-23 4-Loop Westinghouse PCT versus Break Size Scatter Plot

[ ]

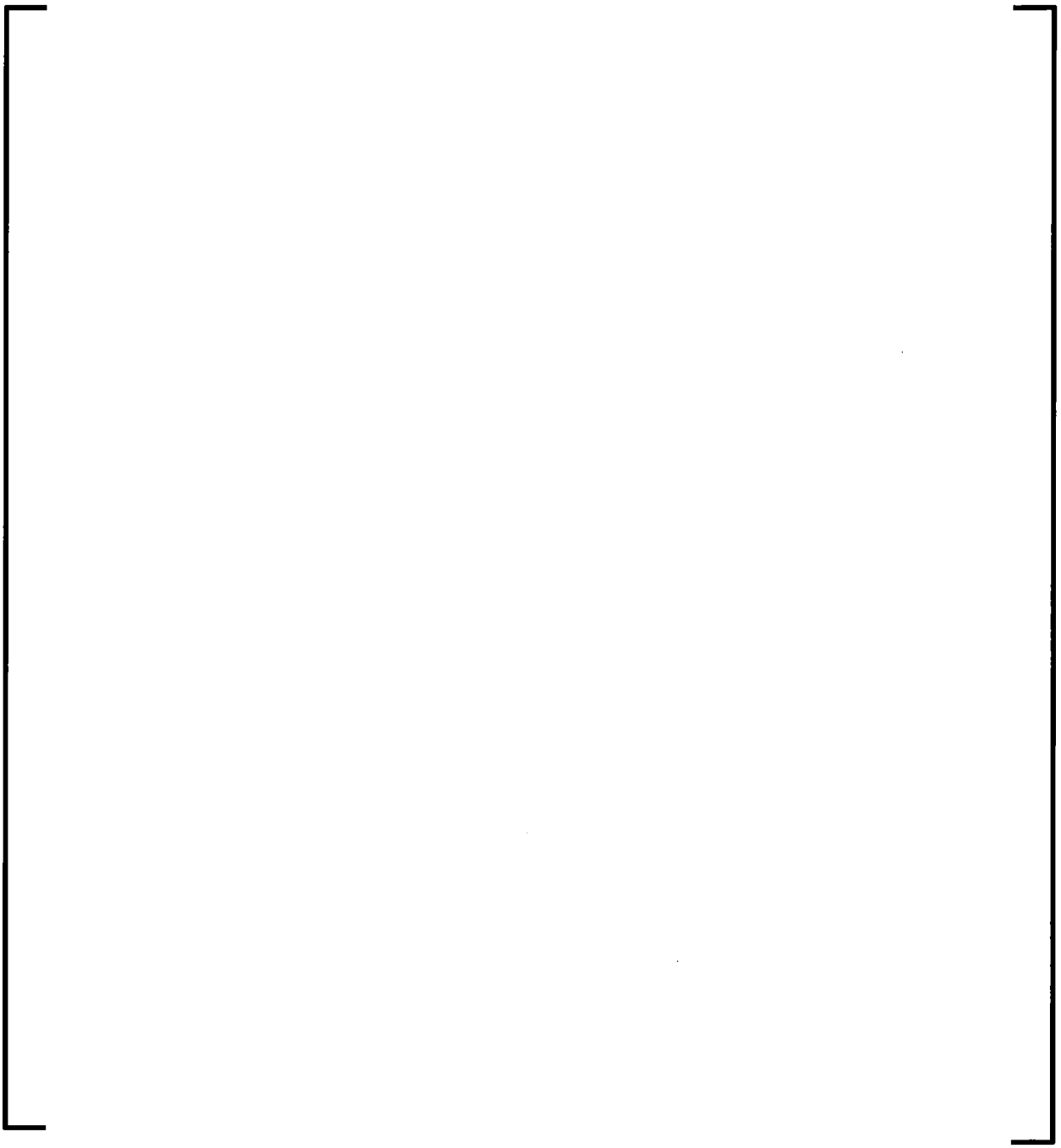

Figure B-24 4-Loop Westinghouse Maximum Oxidation versus PCT Scatter Plot [ ]

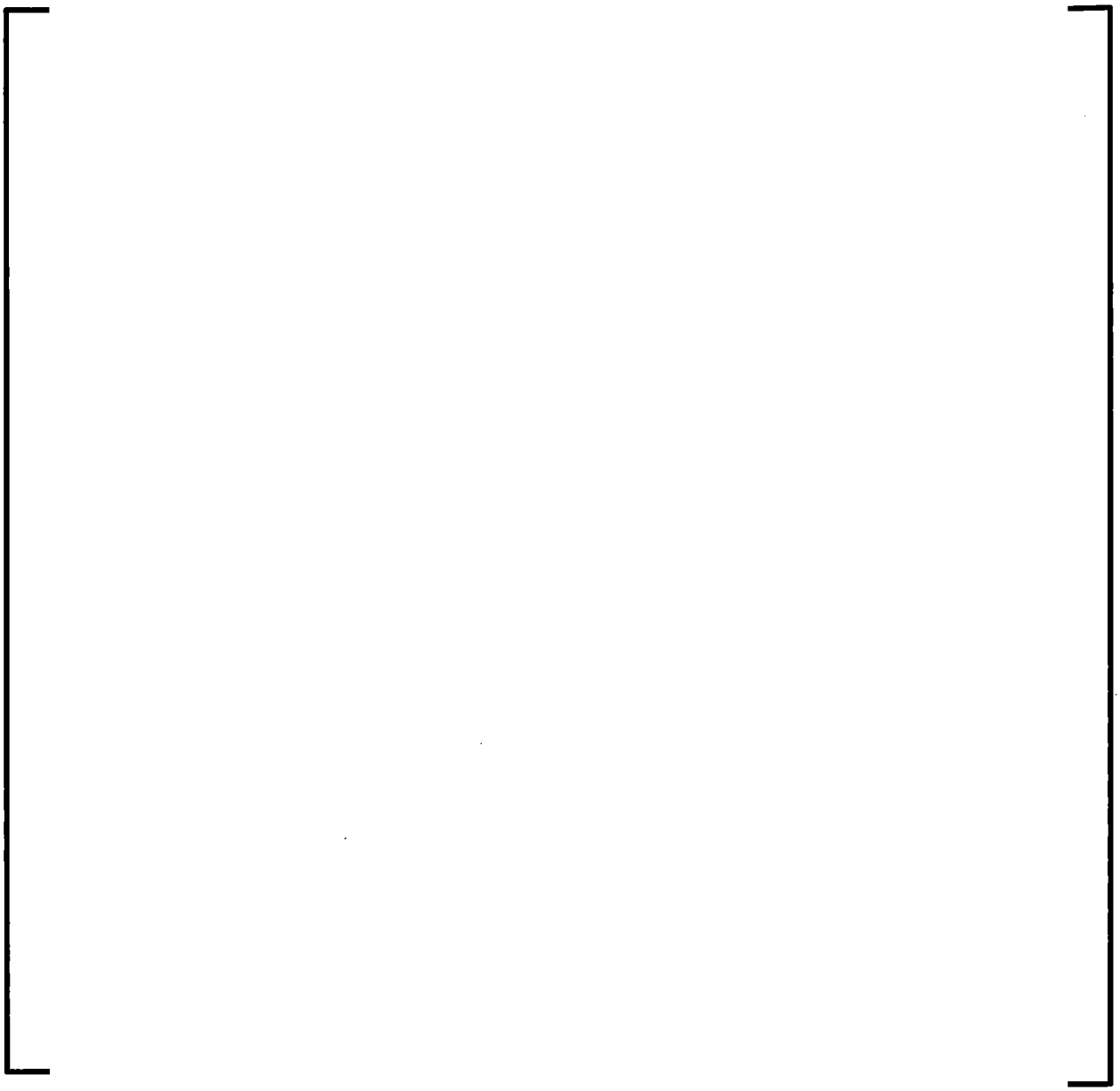

Figure B-25 4-Loop Westinghouse Total Core-Wide Oxidation versus PCT Scatter Plot [ ]

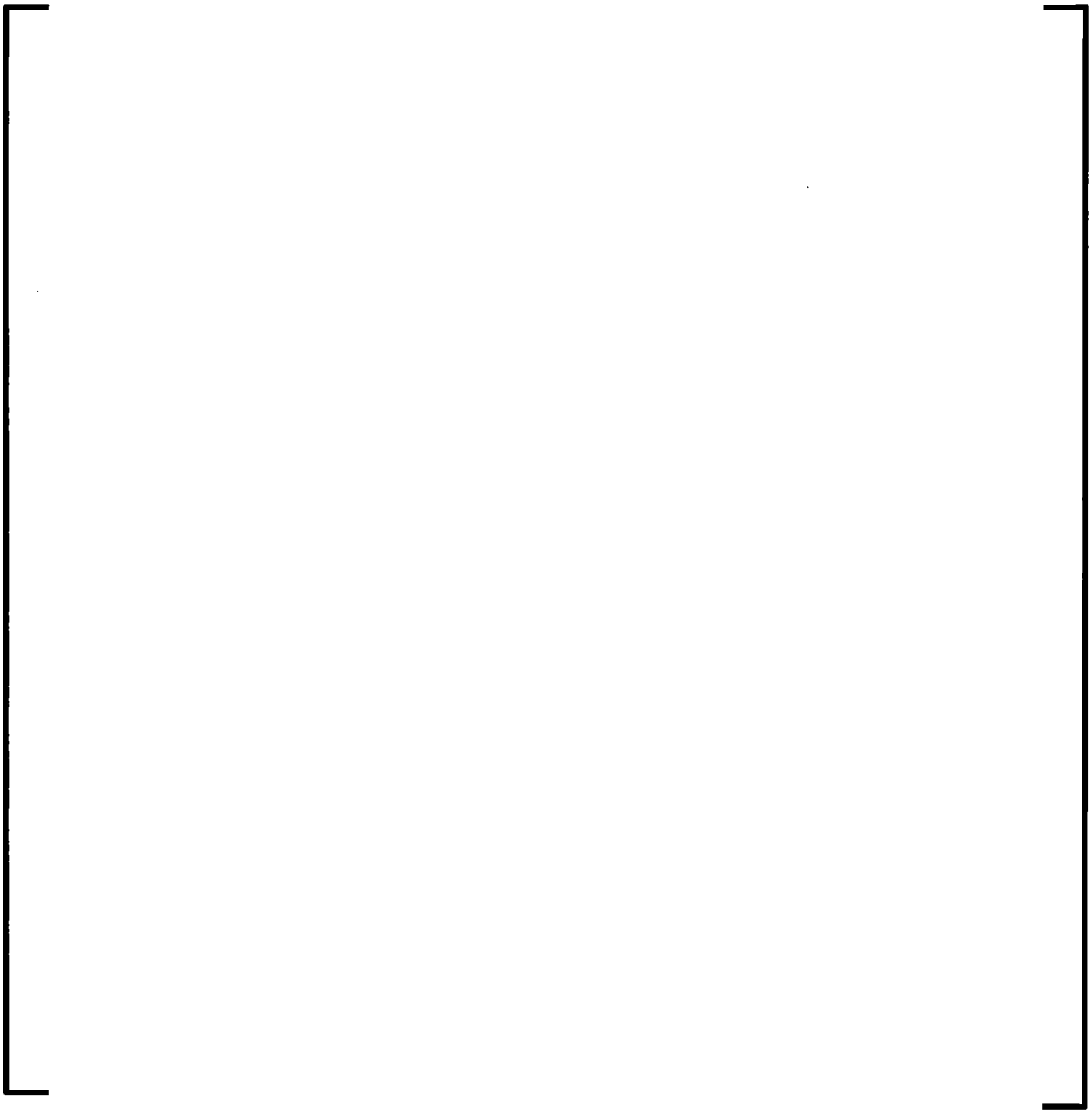

Figure B-26 4-Loop Westinghouse Peak Cladding Temperature (Independent of Elevation) for the Demonstration Case

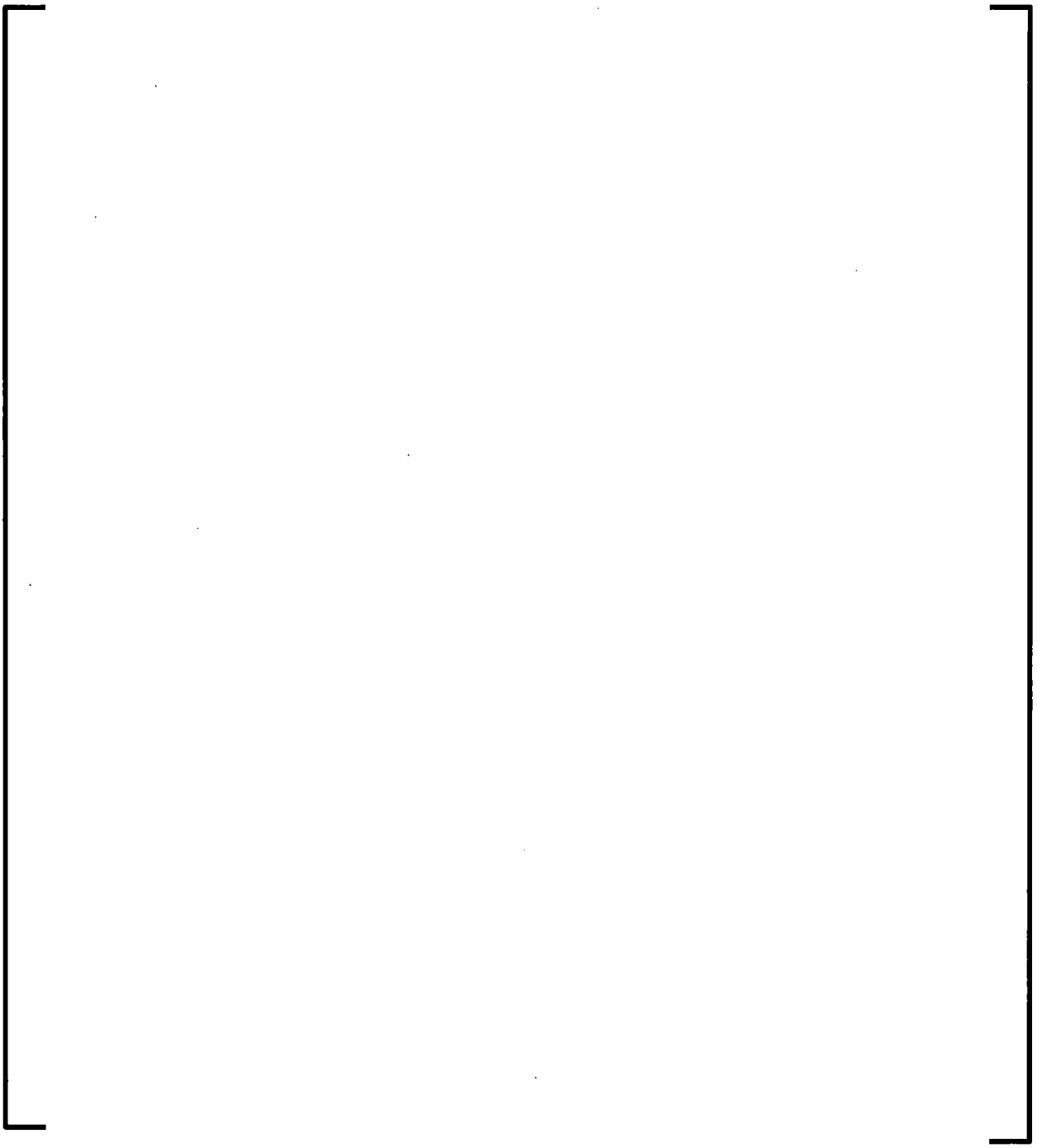

Figure B-27 4-Loop Westinghouse Break Flow for the Demonstration Case

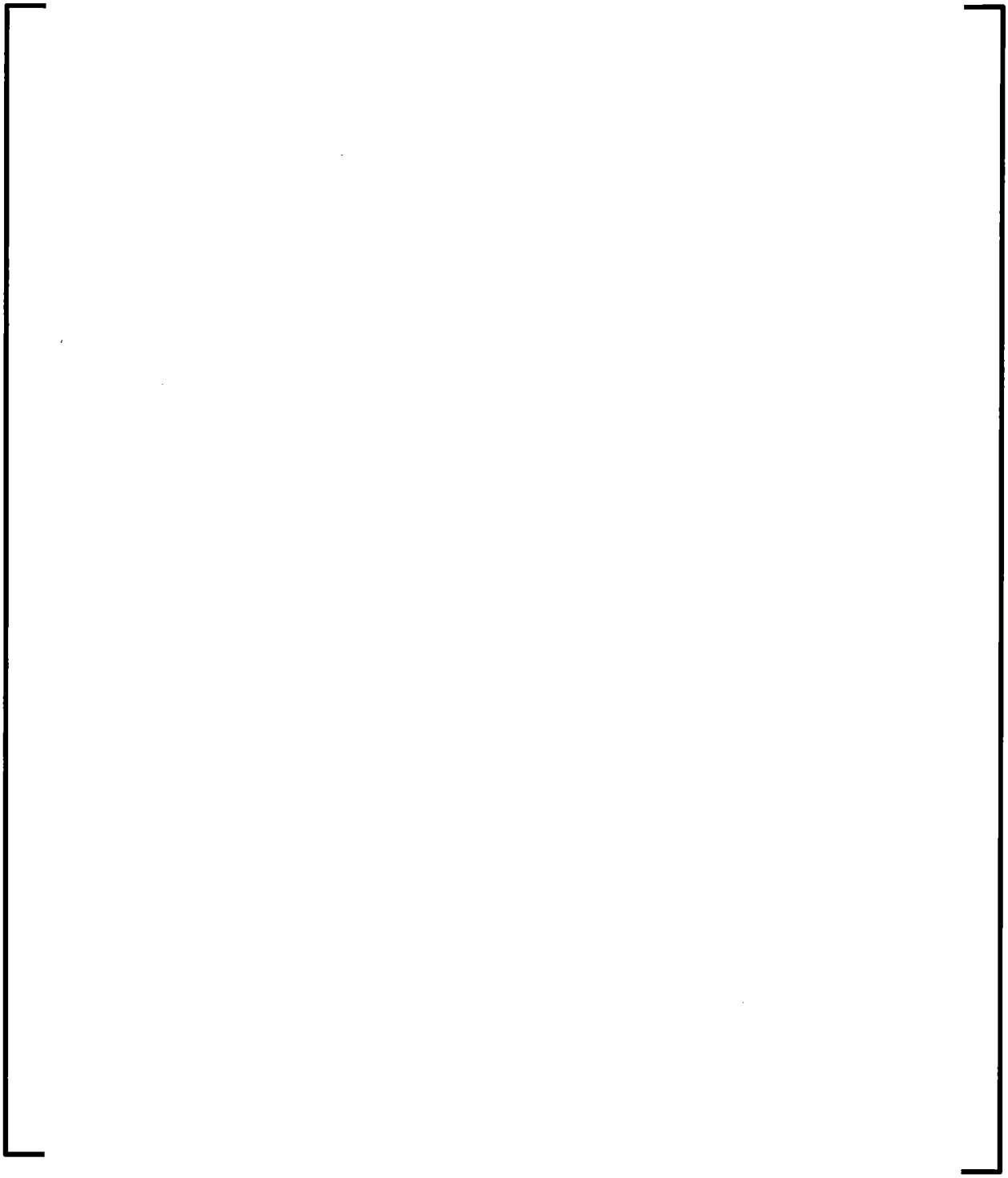

Figure B-28 4-Loop Westinghouse Core Inlet Mass Flux for the Demonstration Case

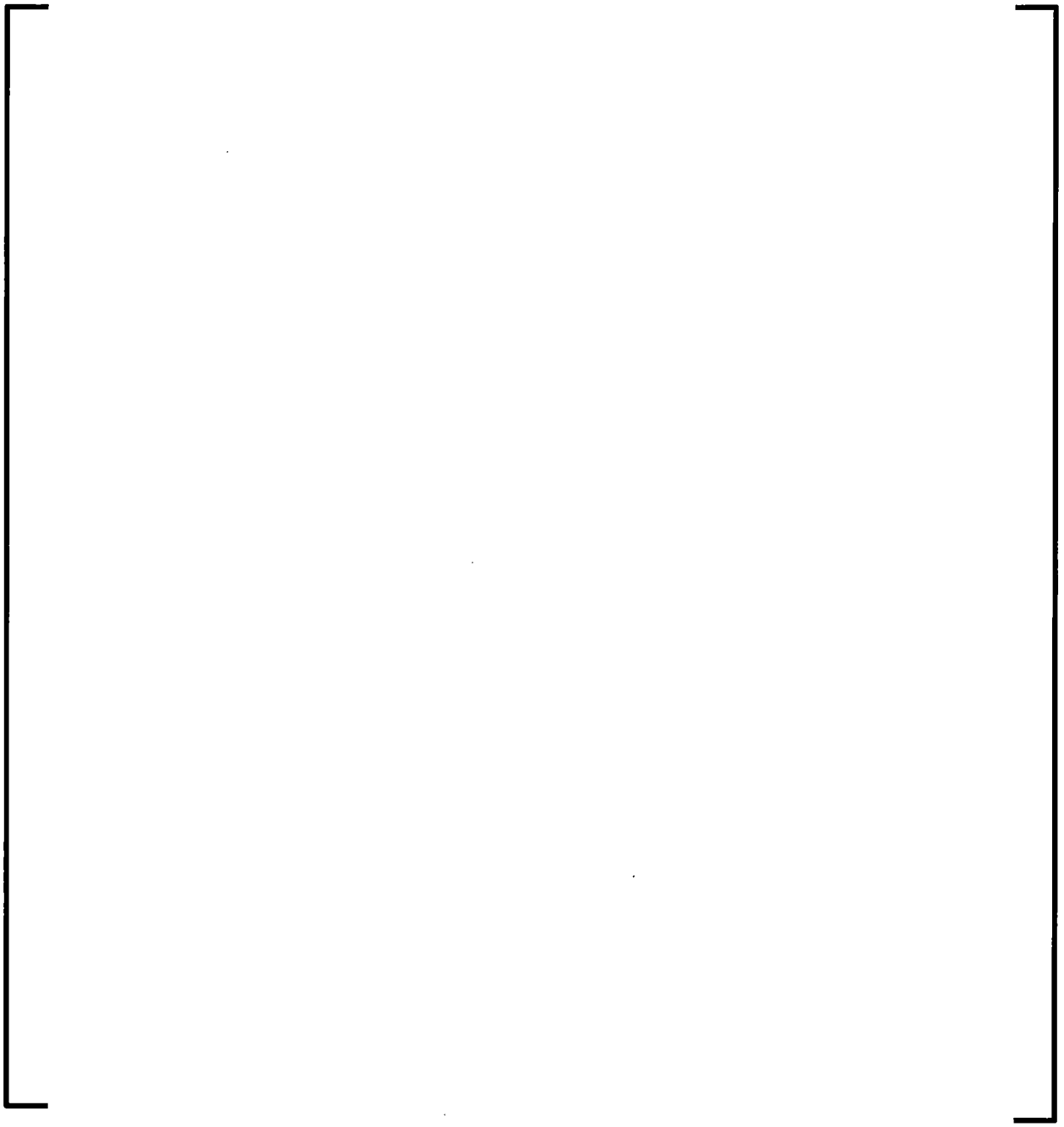

Figure B-29 4-Loop Westinghouse Core Outlet Mass Flux for the Demonstration Case

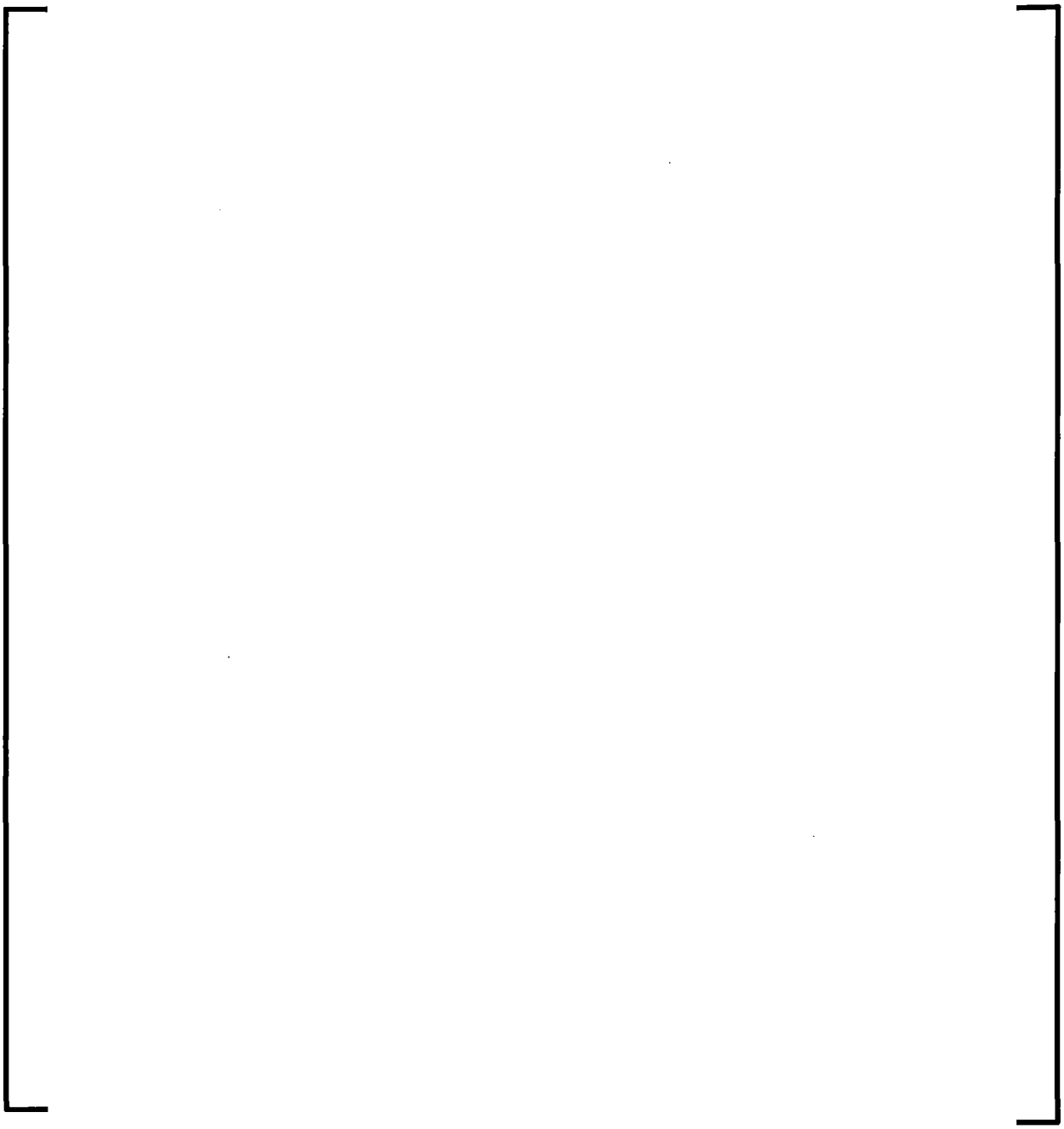

Figure B-30 4-Loop Westinghouse Void Fraction at RCS Pumps for the Demonstration Case

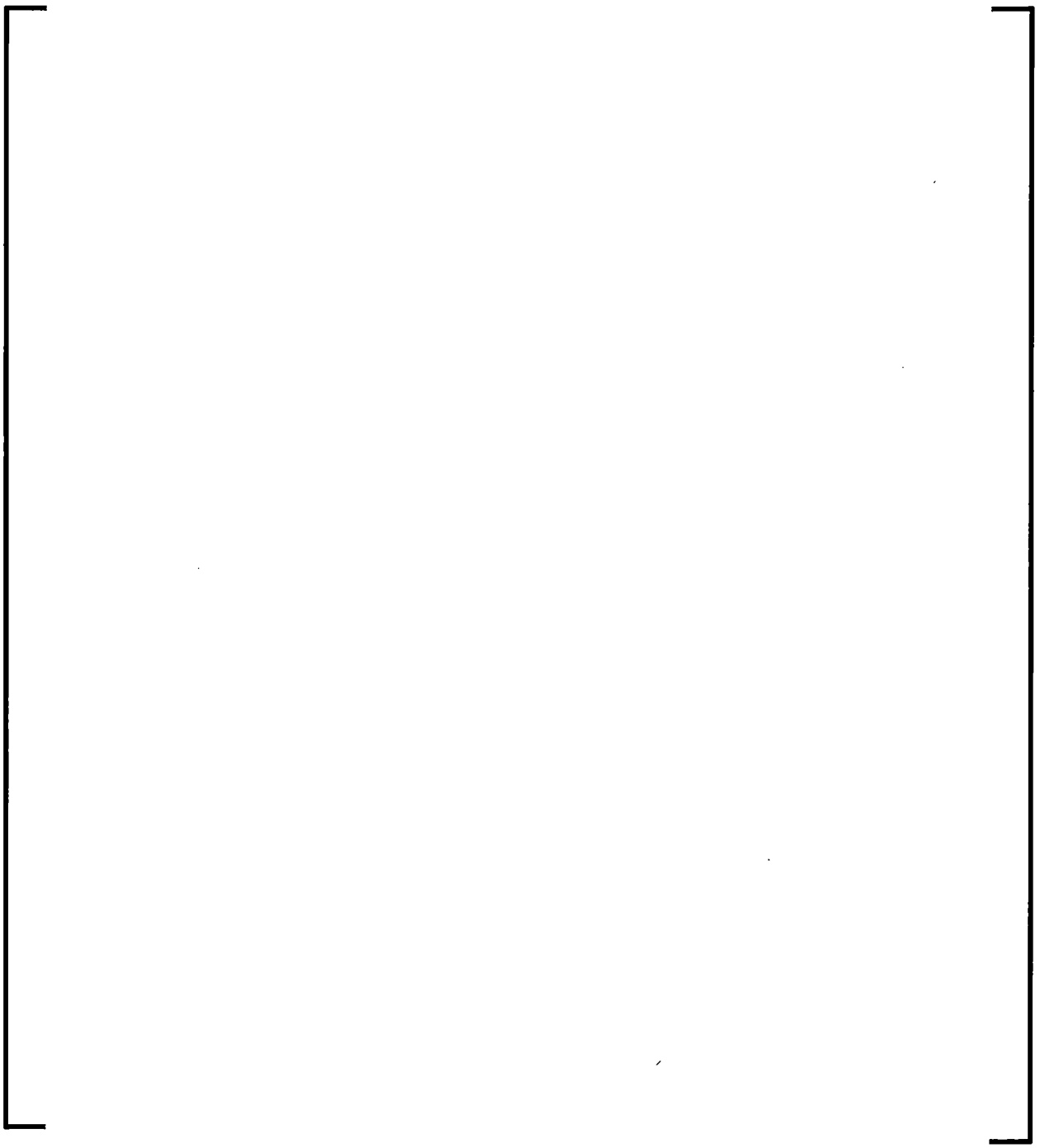

Figure B-31 4-Loop Westinghouse ECCS Flows (Includes Accumulator, Charging, SI and RHR) for the Demonstration Case

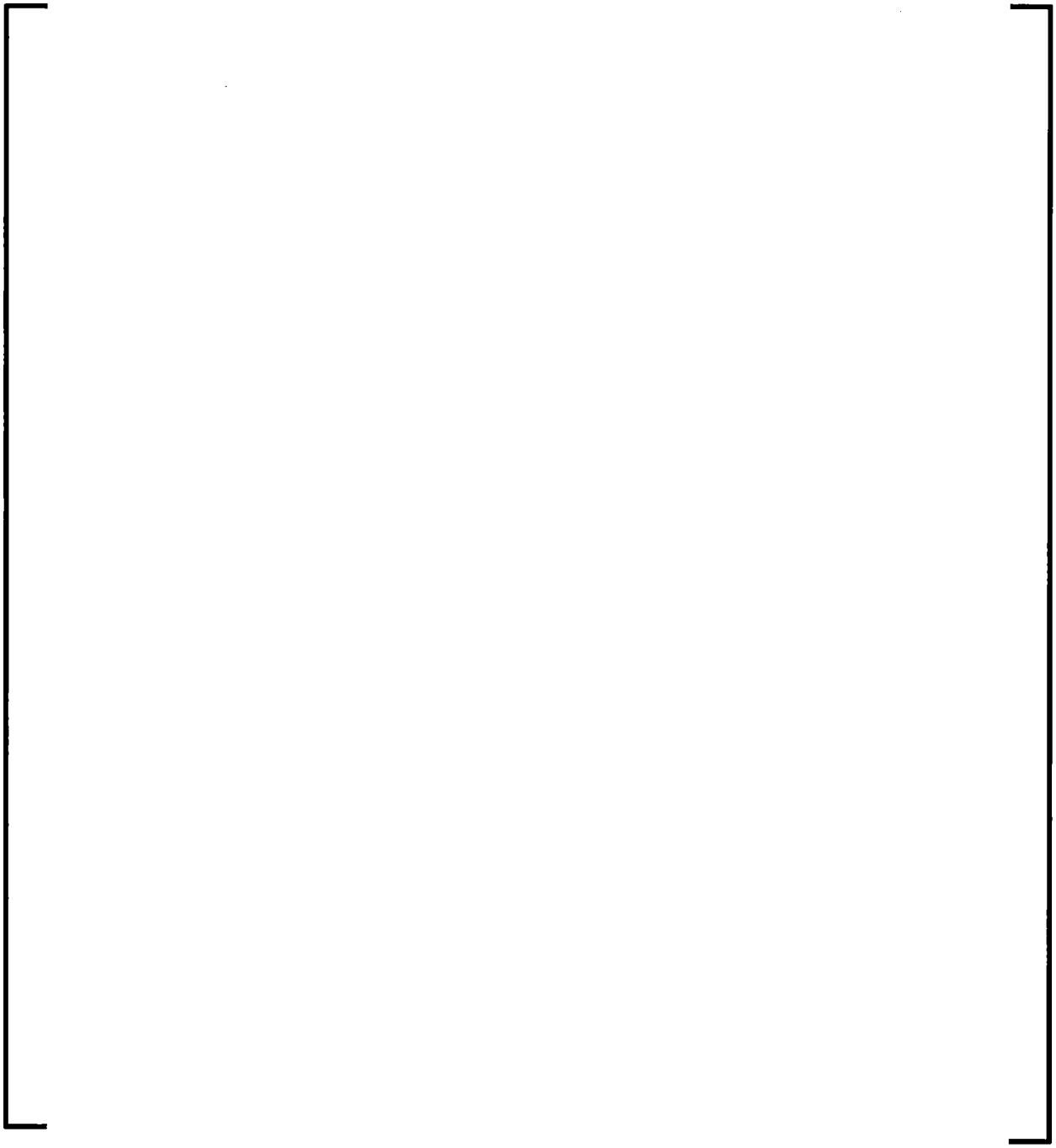

Figure B-32 4-Loop Westinghouse Upper Plenum Pressure for the Demonstration Case

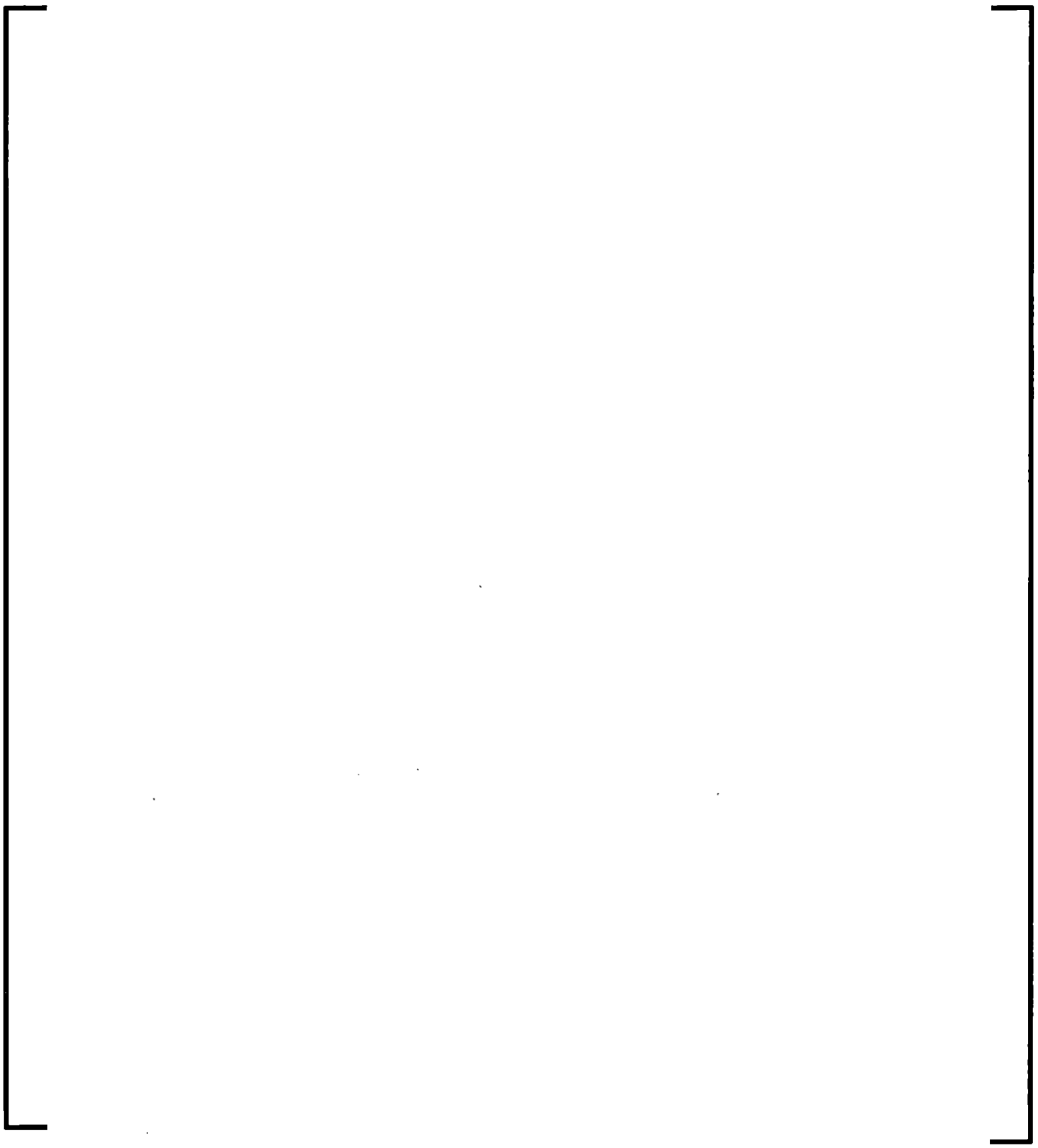

Figure B-33 4-Loop Westinghouse Collapsed Liquid Level in the Downcomer for the Demonstration Case

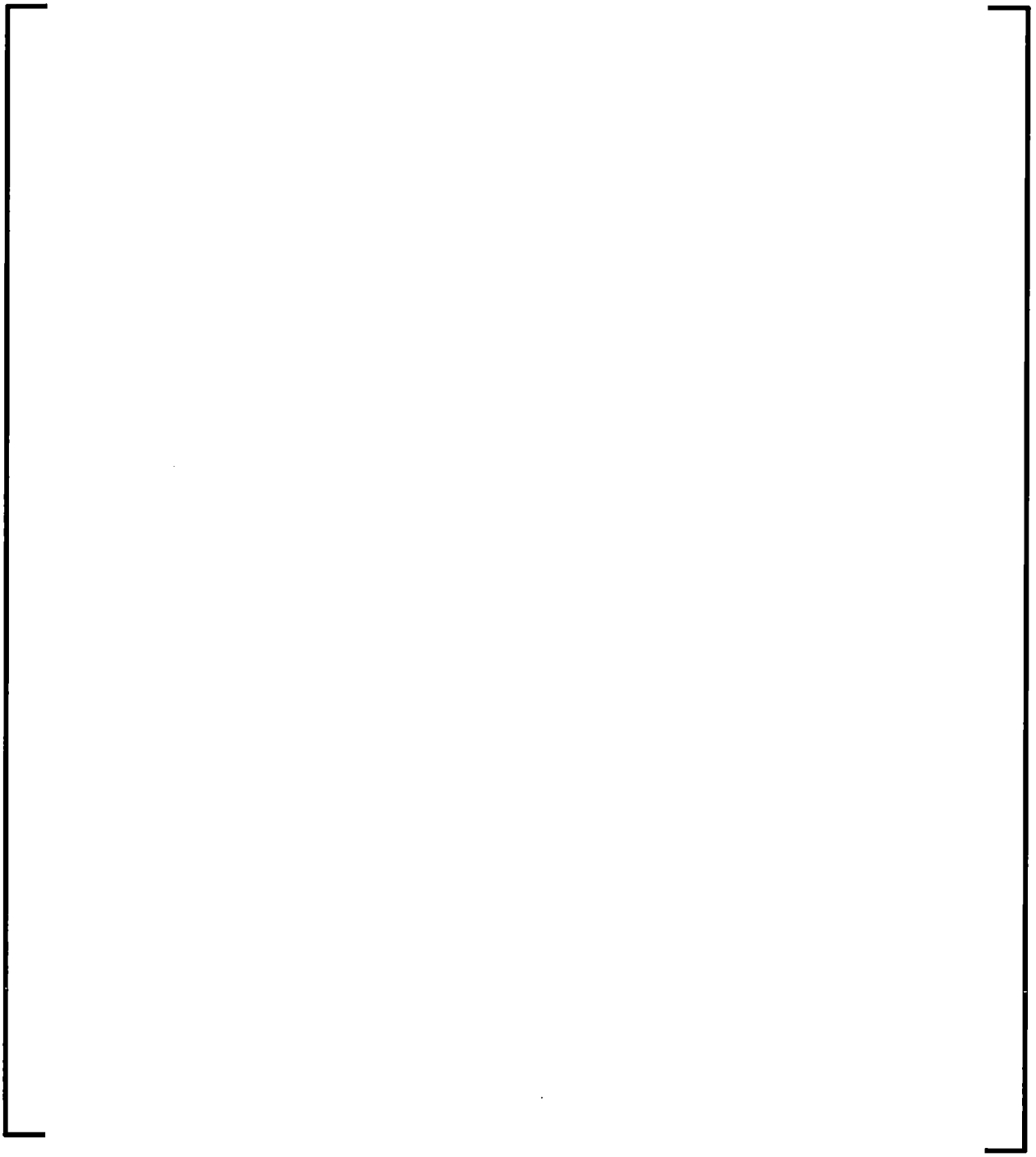

Figure B-34 4-Loop Westinghouse Collapsed Liquid Level in the Lower Plenum for the Demonstration Case

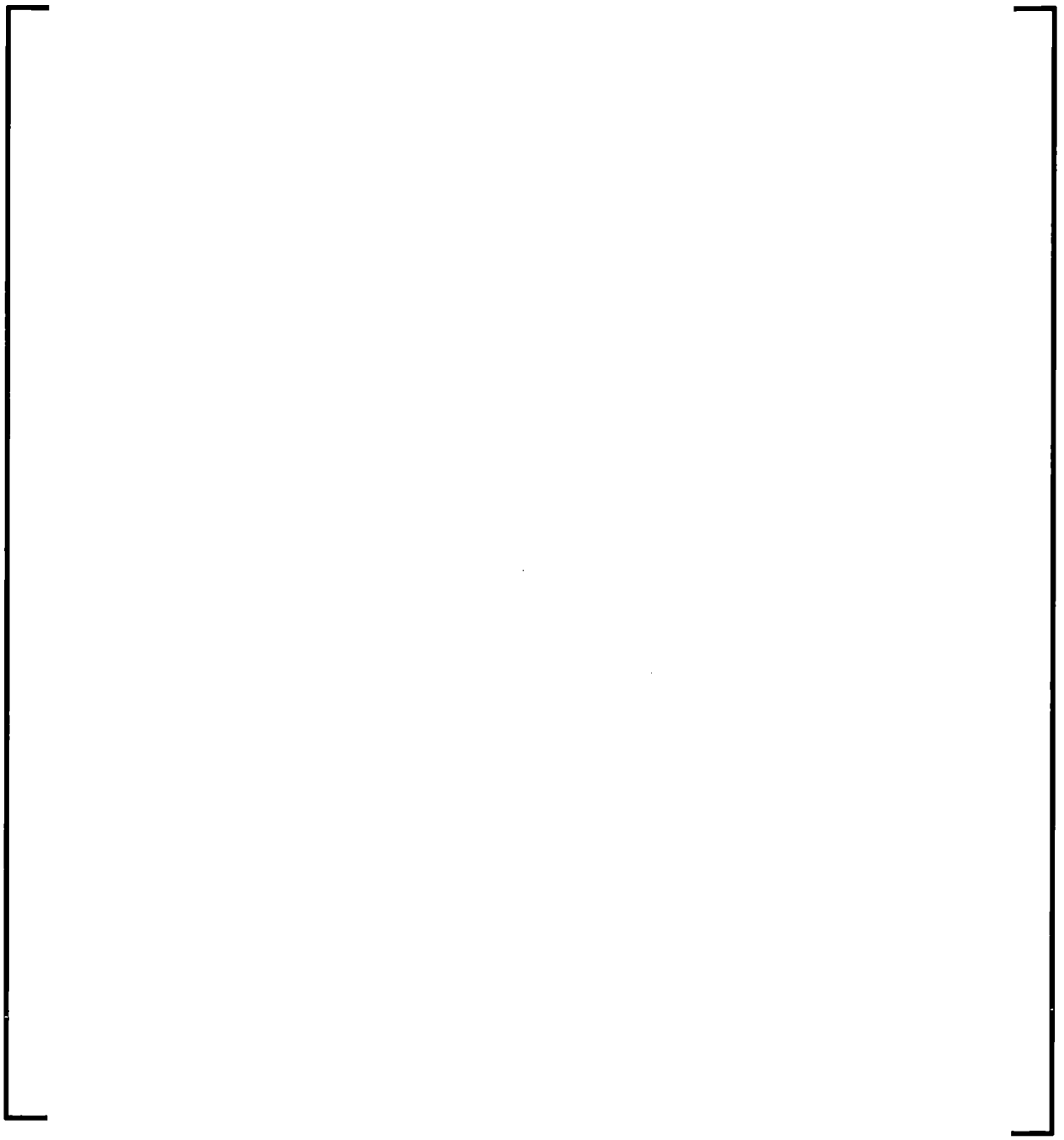

Figure B-35 4-Loop Westinghouse Collapsed Liquid Level in the Core for the Demonstration Case

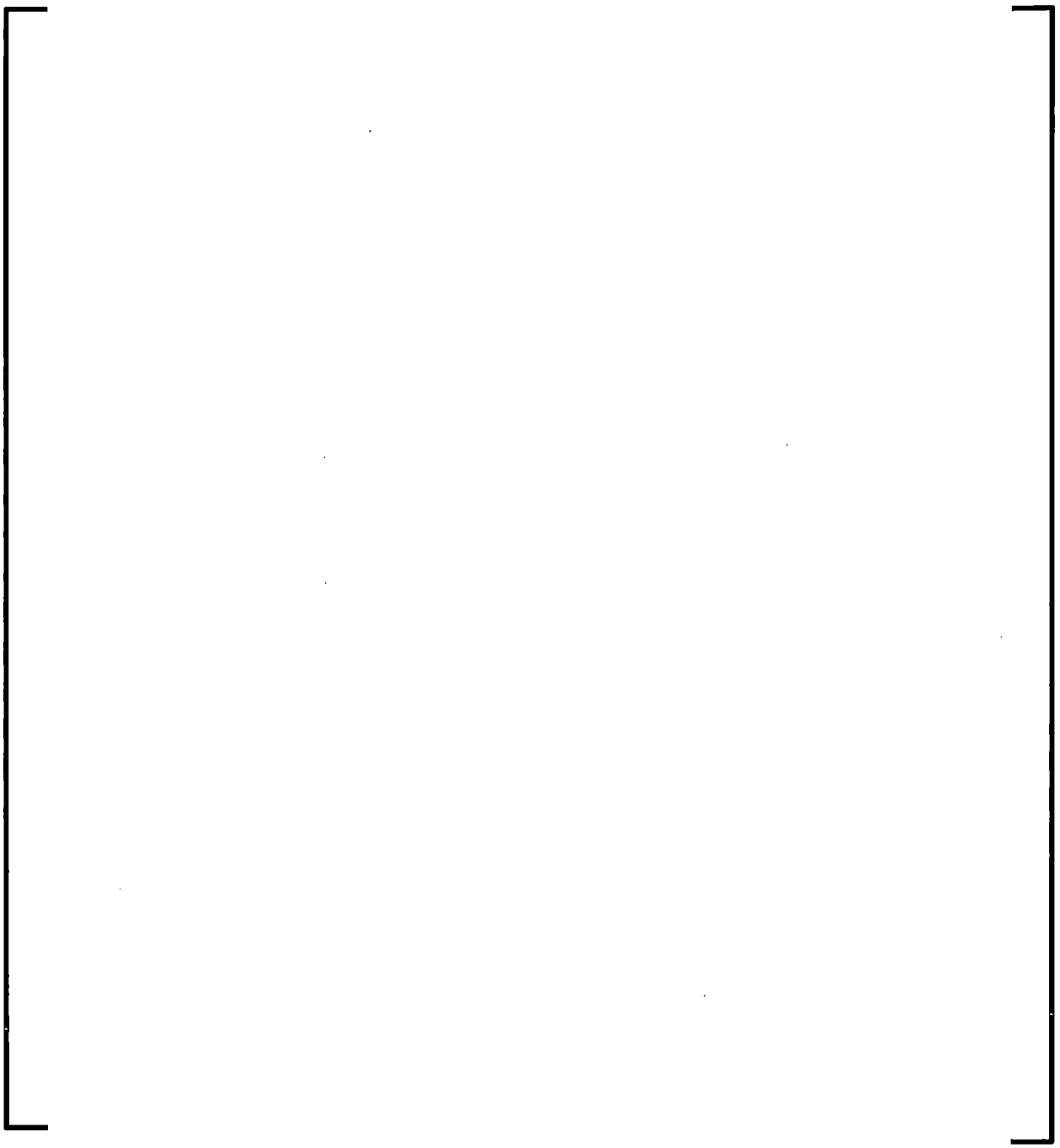

Figure B-36 4-Loop Westinghouse Containment and Loop Pressures for the Demonstration Case

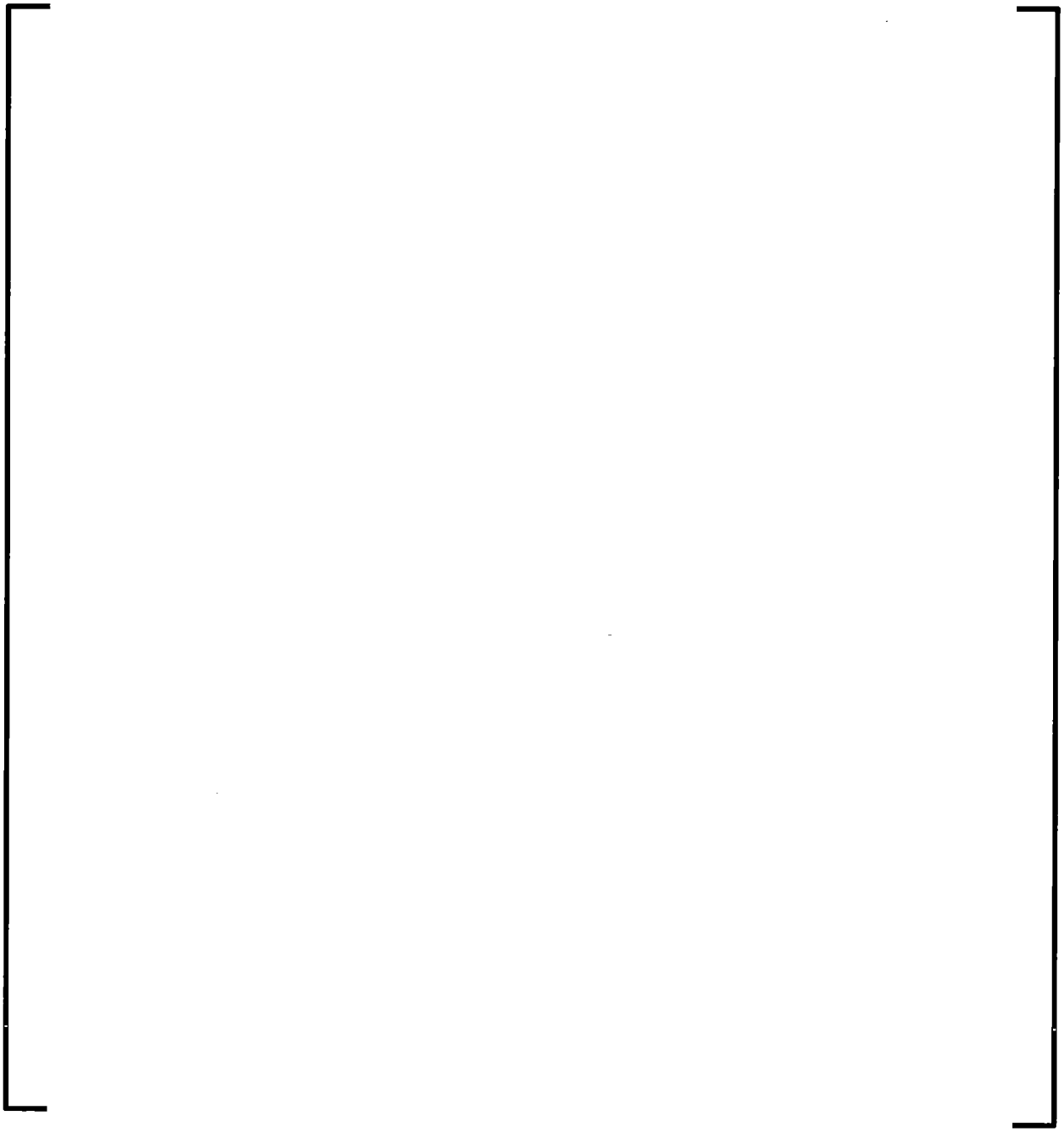

Figure B-37 4-Loop Westinghouse Pressure Difference between Upper Plenum and Downcomer

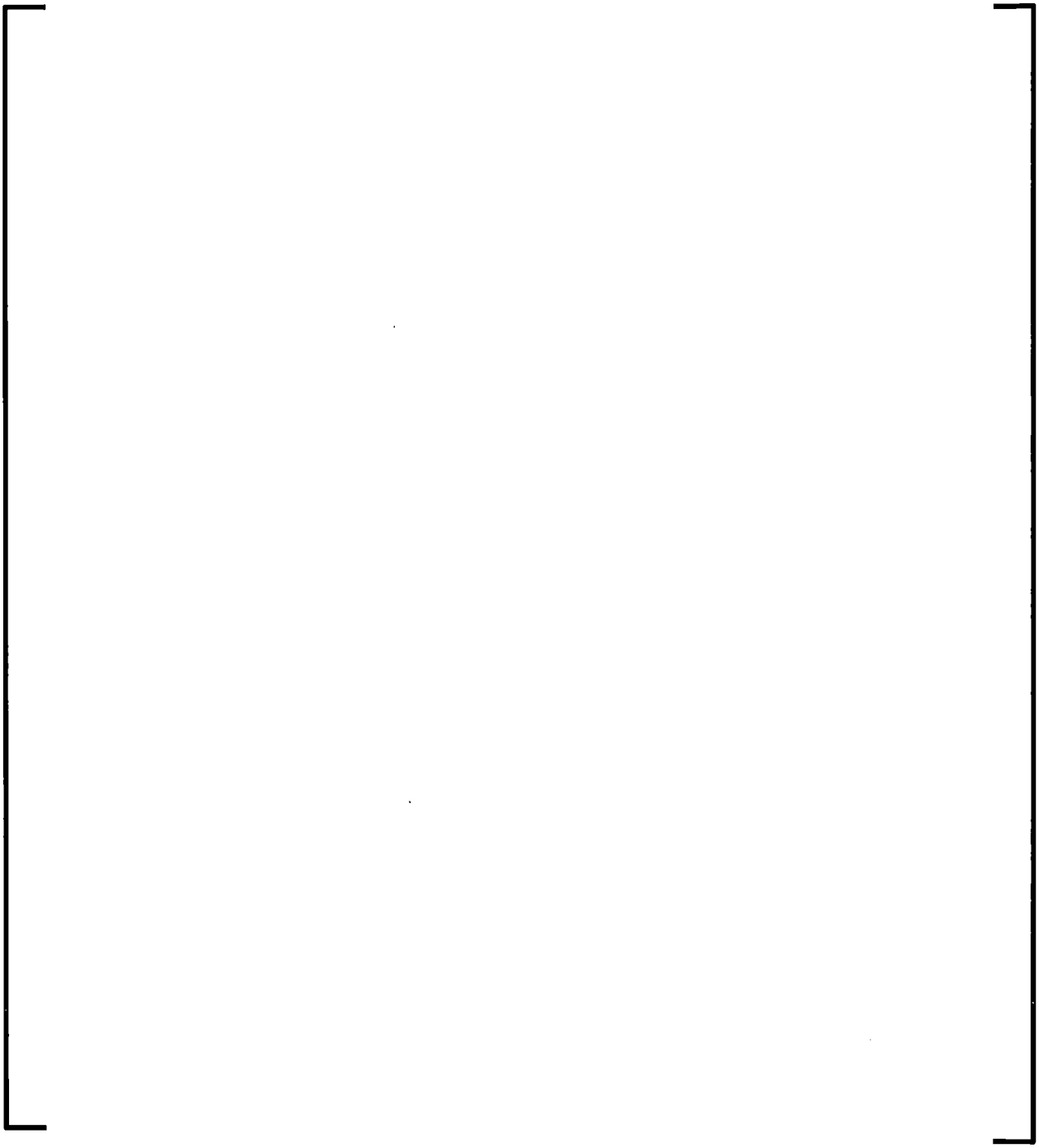

Figure B-38 4-Loop Westinghouse Validation of BOCR Time using MPR CCFL Correlation, [ ]

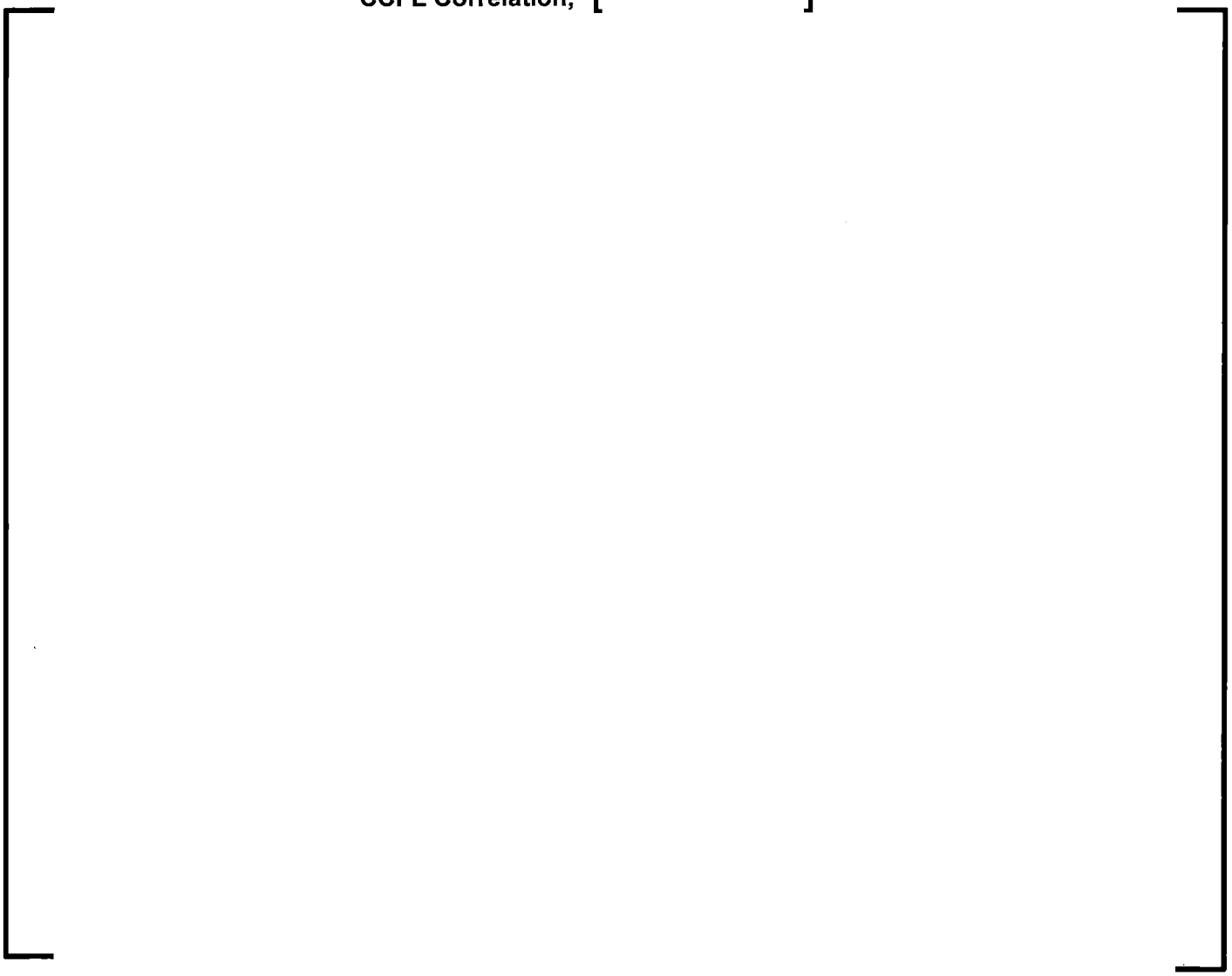

B.4 CE 2x4 PWR

B.4.1 Summary

The parameter specification for this analysis is provided in Table B-21. [

] This analysis also addresses typical operational ranges or technical specification limits (whichever is applicable) with regard to pressurizer pressure and level; SIT pressure, temperature (containment temperature), and level; core inlet temperature; core flow; containment pressure and temperature; and refueling water storage tank temperature. [

]

[

]

[

]

B.4.2 Plant Description and Summary of Analysis Parameters

The plant analysis presented in this report is for a CE-designed PWR, which has 2X4-loop arrangement. There are two hot legs each with a U-tube steam generator and four cold legs each with a RCP. The RCS includes one Pressurizer connected to a hot leg. The core contains 217 thermal-hydraulic compatible AREVA HTP 14X14 fuel assemblies with [

]. The ECCS includes one high pressure safety injection (HPSI), one LPSI and one SIT injection path per RCS loop. The break is modeled in the same loop as the pressurizer, as directed by the RLBLOCA methodology. The RLBLOCA transients are of sufficiently short duration that the switchover to sump cooling water (i.e., RAS) for ECCS pumped injection need not be considered.

The S-RELAP5 model explicitly describes the RCS, reactor vessel, Pressurizer, and ECCS. The ECCS includes a SIT path and a LPSI/HPSI path per RCS loop. The HPSI and LPSI feed into a common header that connects to each cold leg pipe downstream of the RCP discharge. The ECCS pumped injection is modeled as a table of flow versus backpressure. This model also describes the secondary-side steam generator that is instantaneously isolated (closed MSIV and feedwater trip) at the time of the break.

As described in Appendix A, many parameters associated with LBLOCA phenomenological uncertainties and plant operation ranges are sampled. A summary of those parameters sampled is given in Table A-6. The LBLOCA phenomenological uncertainties are provided in Table A-7. Values for process or operational parameters, including ranges of sampled process parameters, and fuel design parameters used in the analysis are given in Table B-21. Plant data are analyzed to develop uncertainties for the process parameters sampled in the analyses.

Table B-22 presents a summary of the uncertainties used in the analysis. [

]

Where applicable, the sampled parameter ranges are based on technical specification limits.

Plant data are used to define range boundaries for [

]

B.4.3 Realistic Large Break LOCA Results

[

]

Table B-23 is a summary of the major parameters for the demonstration case. The results of the plant sample analyses are presented in Table B-24. The fraction of total hydrogen generated was not directly calculated; however, it is conservatively bounded by the calculated total percent oxidation, which is well below the 1-percent limit. The event times for the demonstration case can be found in Table B-25. The heat transfer parameter range for the demonstration case is provided in Table B-26. Table B-27 [

]

[

] The analysis plots for the demonstration case are shown in Figure B–40 through Figure B–57. Figure B–40 shows linear scatter plots of the key parameters sampled for all the cases. Parameter labels appear to the left of each individual plot. These figures illustrate the parameter ranges used in the analysis.

Figure B–41 and Figure B–42 show PCT scatter plots versus the time of PCT and versus break size [ ] The scatter plots for the maximum local oxidation and total core-wide oxidation are shown in Figure B–43 and Figure B–44, respectively. Figure B–45 through Figure B–56 show key parameters from the S-RELAP5 calculations for the demonstration case. Figure B–45 is the plot of PCT, independent of elevation. Figure B–57 compares the beginning of core recovery times [ ] to the BOCR time predicted using the MPR CCFL correlation. Note that Figure B–57 uses the total break area, while previous plots used break area per side.

B.4.4 Conclusions

[

]

Table B-21 CE 2x4 Plant Operating Range Supported by the LOCA Analysis

	Event	Operating Range
1.0	**Plant Physical Description**	
	1.1 Fuel	
	a) Cladding outside diameter	
	b) Cladding inside diameter	
	c) Cladding thickness	
	d) Pellet outside diameter	
	e) Pellet density	
	f) Active fuel length	
	g) Gd_2O_3 concentrations	
	1.2 RCS	
	a) Flow resistance	
	b) Pressurizer location	
	c) Hot assembly location	
	d) Hot assembly type	
	e) SG tube plugging	
2.0	**Plant Initial Operating Conditions**	
	2.1 Reactor Power	
	a) Analyzed reactor power	
	b) LHR	
	c) F_q	
	d) F_r	
	2.2 Fluid Conditions	
	a) Loop flow	
	b) RCS Cold Leg temperature	
	c) Pressurizer pressure	
	d) Pressurizer level	
	e) SIT pressure	
	f) SIT liquid volume	
	g) SIT temperature	
	h) SIT resistance fL/D	
	i) Minimum ECCS boron	

[1] The radial power peaking for the hot rod includes 6 percent measurement uncertainty and 3.5 percent allowance for control rod insertion effect.

Table B-21 CE 2x4 Plant Operating Range Supported by the LOCA Analysis (continued)

	Event	Operating Range
3.0	**Accident Boundary Conditions**	
	a) Break location	
	b) Break type	
	c) Break size (each side, relative to cold leg pipe area)	
	d) Worst single-failure	
	e) Offsite power	
	f) ECCS pumped injection temperature	
	g) HPSI pump delay	
	h) LPSI pump delay	
	i) Containment pressure	
	j) Containment temperature	
	k) Containment sprays delay	
	l) Containment spray water temperature	
	m) LPSI Flow	

[1] Nominal containment pressure range is -0.7 to 0.5 psig. For RLBOCA, a reasonable value between this range is acceptable.

Table B-21 CE 2x4 Plant Operating Range Supported by the LOCA Analysis (continued)

Event	Operating Range
n) HPSI flow	

Table B-22 CE 2x4 Statistical Distribution Used for Process Parameters

Parameter	Operational Uncertainty Distribution	Parameter Range	Measurement Uncertainty Distribution	Standard Deviation
Pressurizer Pressure (psig)				
Pressurizer Level (%)				
SIT Volume (ft^3)				
SIT Pressure (psia)				
Containment/SIT Temperature (°F)				
Containment Volume ($x10^6$ ft^3)				
Initial Flow Rate (Mlbm/hr)				
Initial Operating Temperature (°F)				

Table B-23 CE 2x4 Summary of Major Parameters for the Demonstration Case

Parameter	Value
Time in Cycle (hrs)	
Burnup (GWd/mtU)	
Core Power (MWt)	
LHGR (kW/ft)	
Core Peaking (Equivalent F_q)	
Radial Peak ($F_{\Delta H}$)	
Axial Shape Index	
Local Peaking (F_I)	
Break Type	
Break Size (ft^2 / side)	
Offsite Power Availability	

Table B-24 CE 2x4 Compliance with 10 CFR 50.46

Table B-24 CE 2x4 Compliance with 10 CFR 50.46 (continued)

[ ]

Table B-25 CE 2x4 Calculated Event Times for the Demonstration Case

Event	Time (sec)
Begin Analysis	
Break Opens	
RCP Trip	
SIAS Issued	
Start of Broken Loop SIT Injection	
Start of Intact Loop SIT Injection (Loop 2, 3 and 4 respectively)	
PCT Occurred	
Start of HPSI	
Start of Charging	
Beginning of Core Recovery (Beginning of Reflood)	
LPSI Available	
Broken Loop LPSI Delivery Began	
Intact Loops LPSI Delivery Began (Loop 2, 3, and 4 respectively)	
Broken Loop HPSI Delivery Began	
Intact Loops HPSI Delivery Began (Loop 2, 3, and 4 respectively)	
Broken Loop SIT Emptied	
Intact Loop SIT Emptied (Loop 2, 3, and 4 respectively)	
Transient Calculation Terminated	

Table B-26 CE 2x4 Heat Transfer Parameters for the Demonstration Case

Time (s)						
LOCA Phase	Early Blowdown	Blowdown [1]	Refill	Reflood	Quench	Long Term Cooling
Heat Transfer Mode						
Heat Transfer Correlations						
Maximum LHGR (kW/ft)						
Pressure (psia)						
Core Inlet Mass Flux (lbm/s-ft^2)						
Vapor Reynolds Number[3]						
Liquid Reynolds Number						
Vapor Prandtl Number						
Liquid Prandtl Number						
Vapor Superheat[4] (°F)						

1 End of Blowdown considered as beginning of refill.
2 Conservatively biased per the methodology
3 Not important in pre-CHF heat transfer.
4 Vapor superheat is meaningless during blowdown and system depressurization.

Table B-27 CE 2x4 Fuel Rod Rupture Ranges of Parameters [ ]

Parameter Name	Minimum Value	Maximum Value
[		]

Figure B–39 [ ]

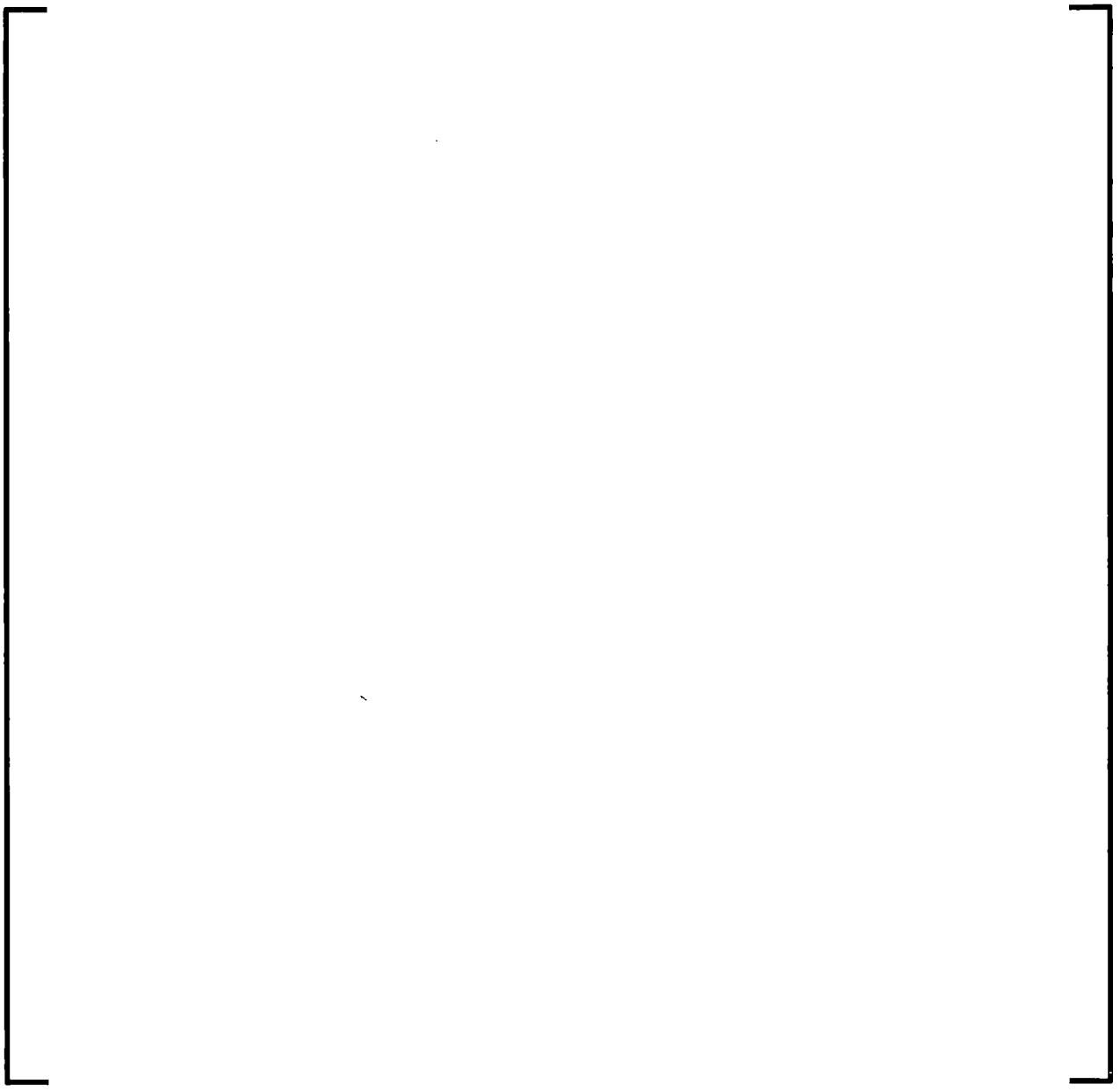

Figure B–40 CE 2x4 Scatter Plot of Operational Parameters [

]

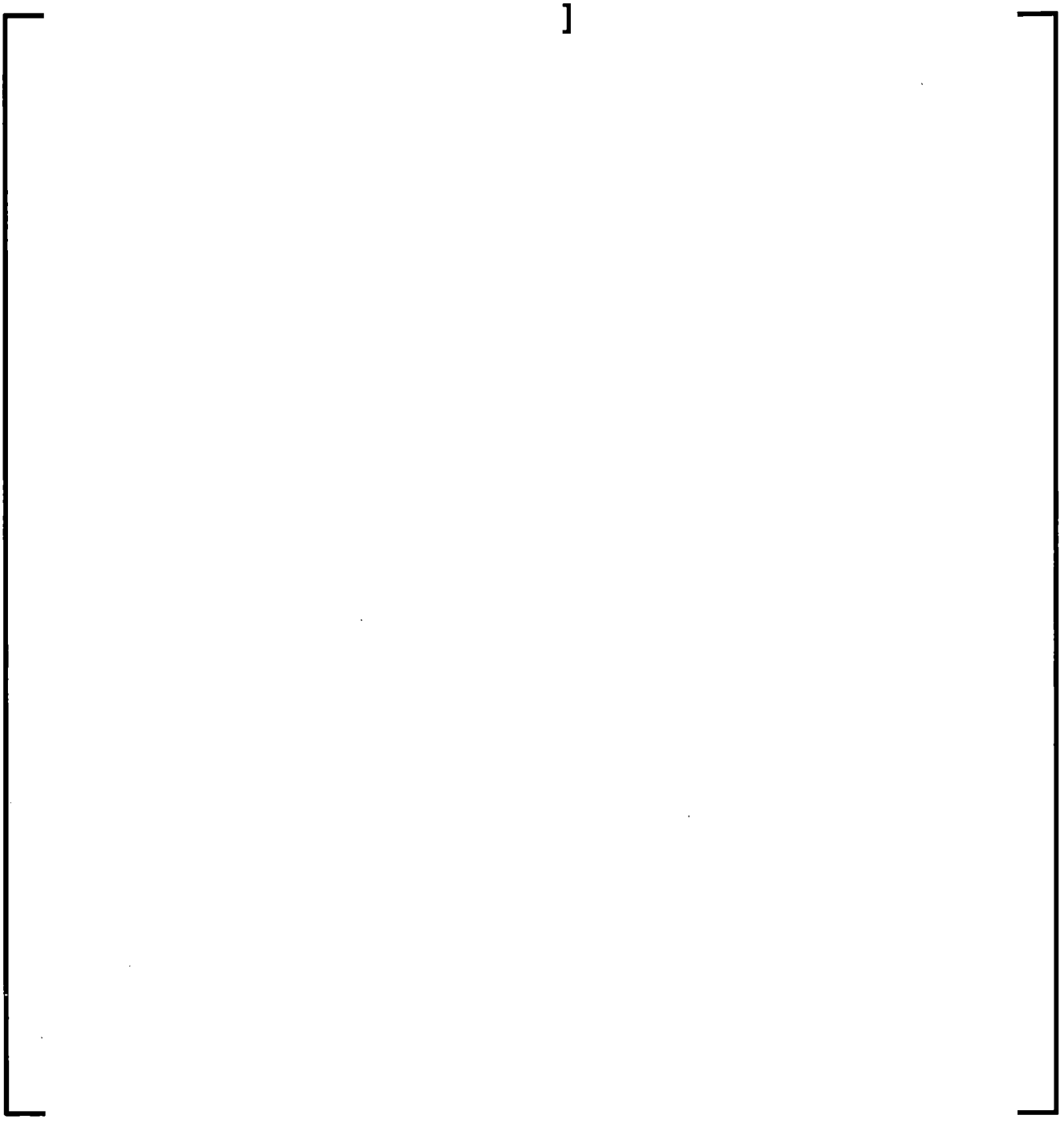

Figure B–40 CE 2x4 Scatter Plot of Operational Parameters [ ] (continued)

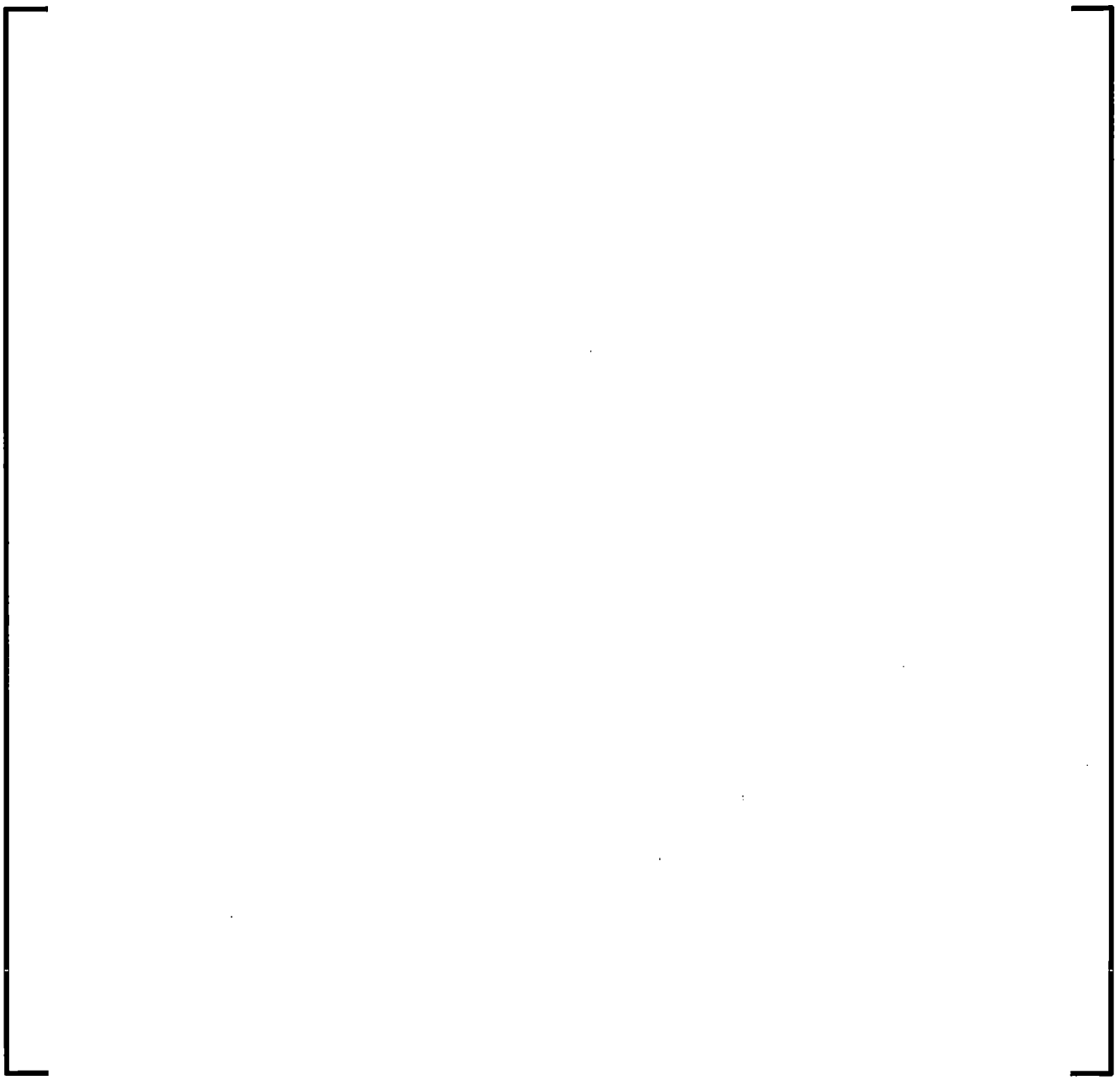

Figure B–41 CE 2x4 PCT versus PCT Time Scatter Plot

[ ]

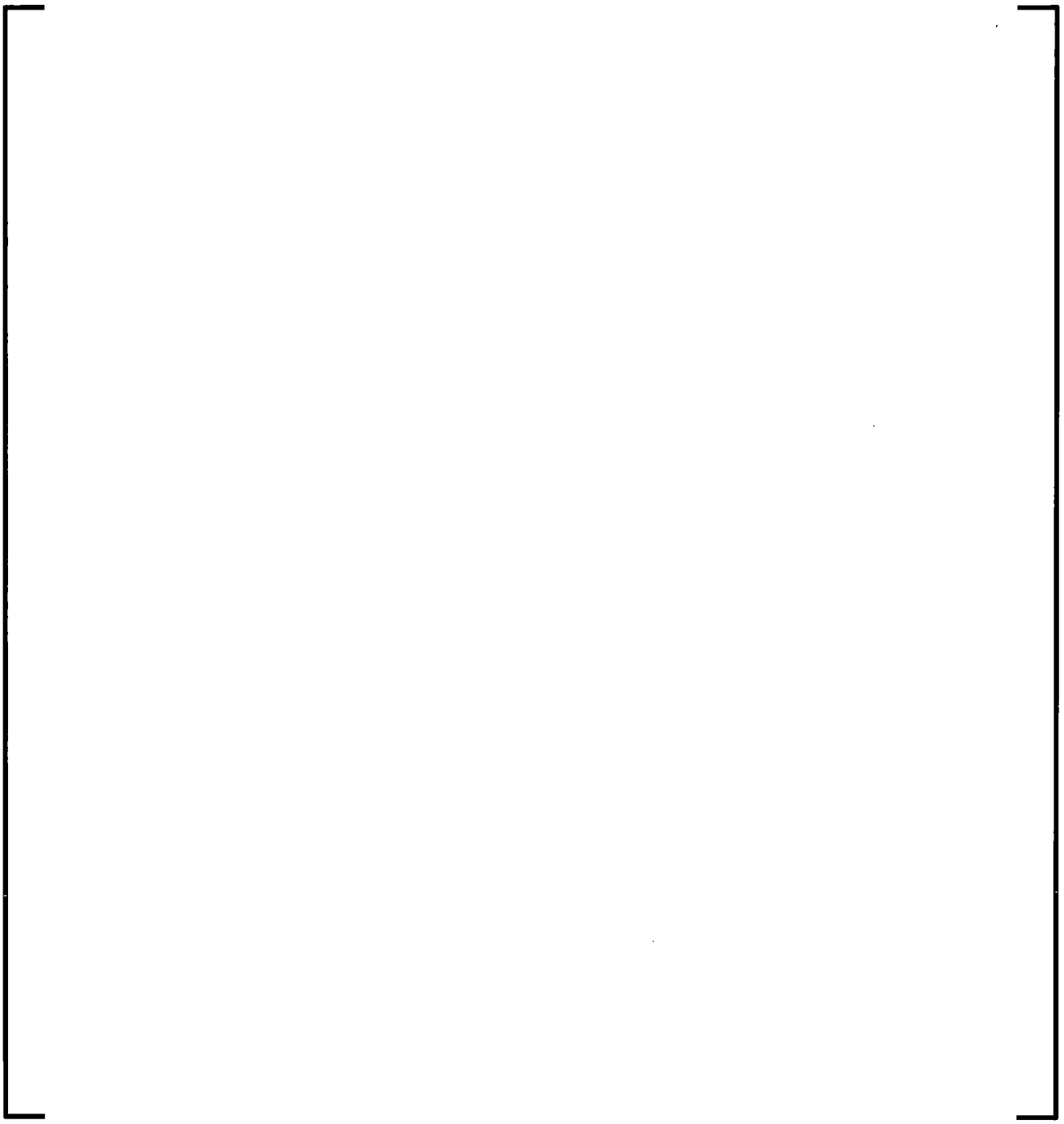

Figure B–42 CE 2x4 PCT versus Break Size Scatter Plot

[ ]

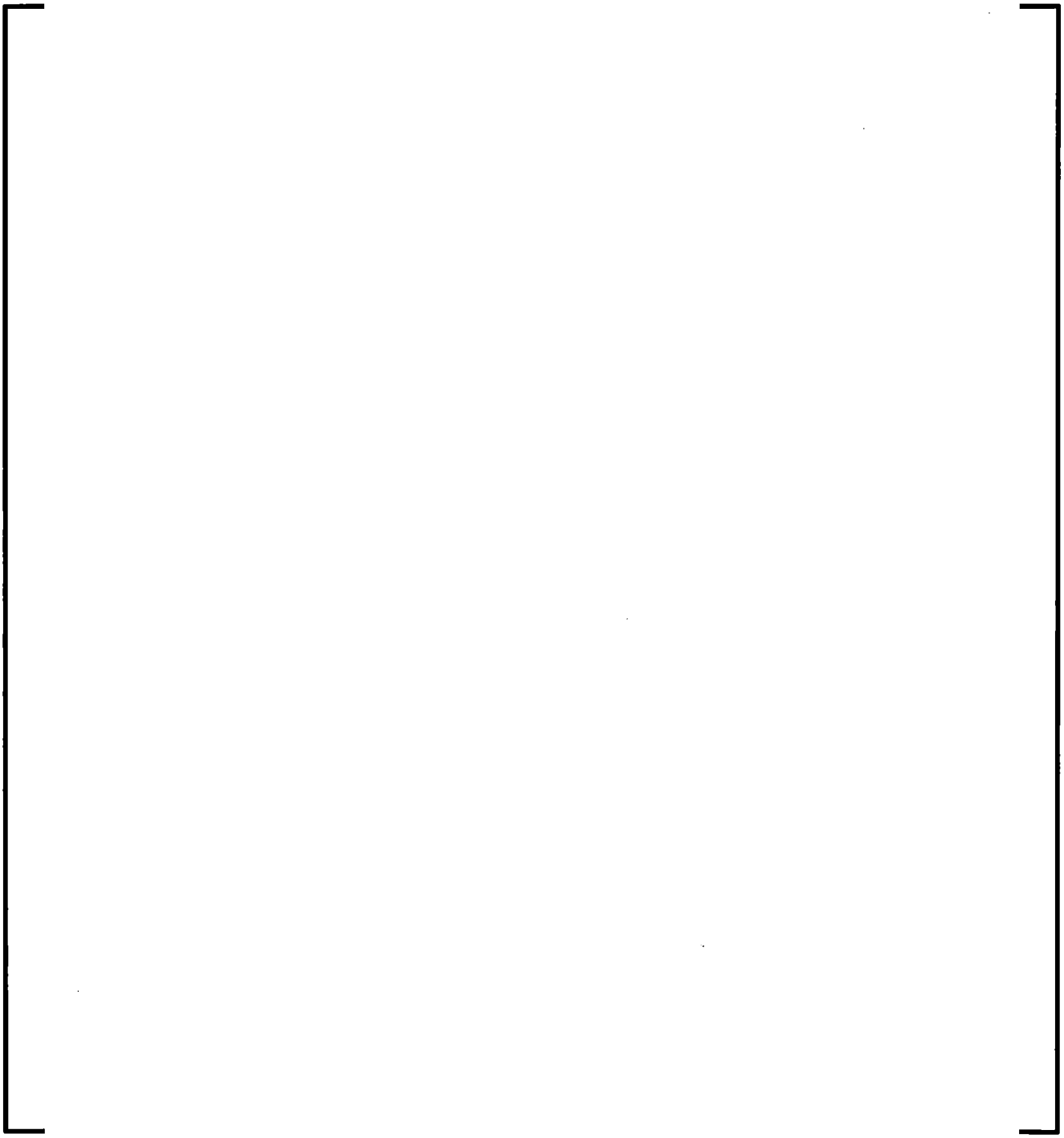

Figure B–43 CE 2x4 Maximum Local Oxidation versus PCT Scatter Plot

[ ]

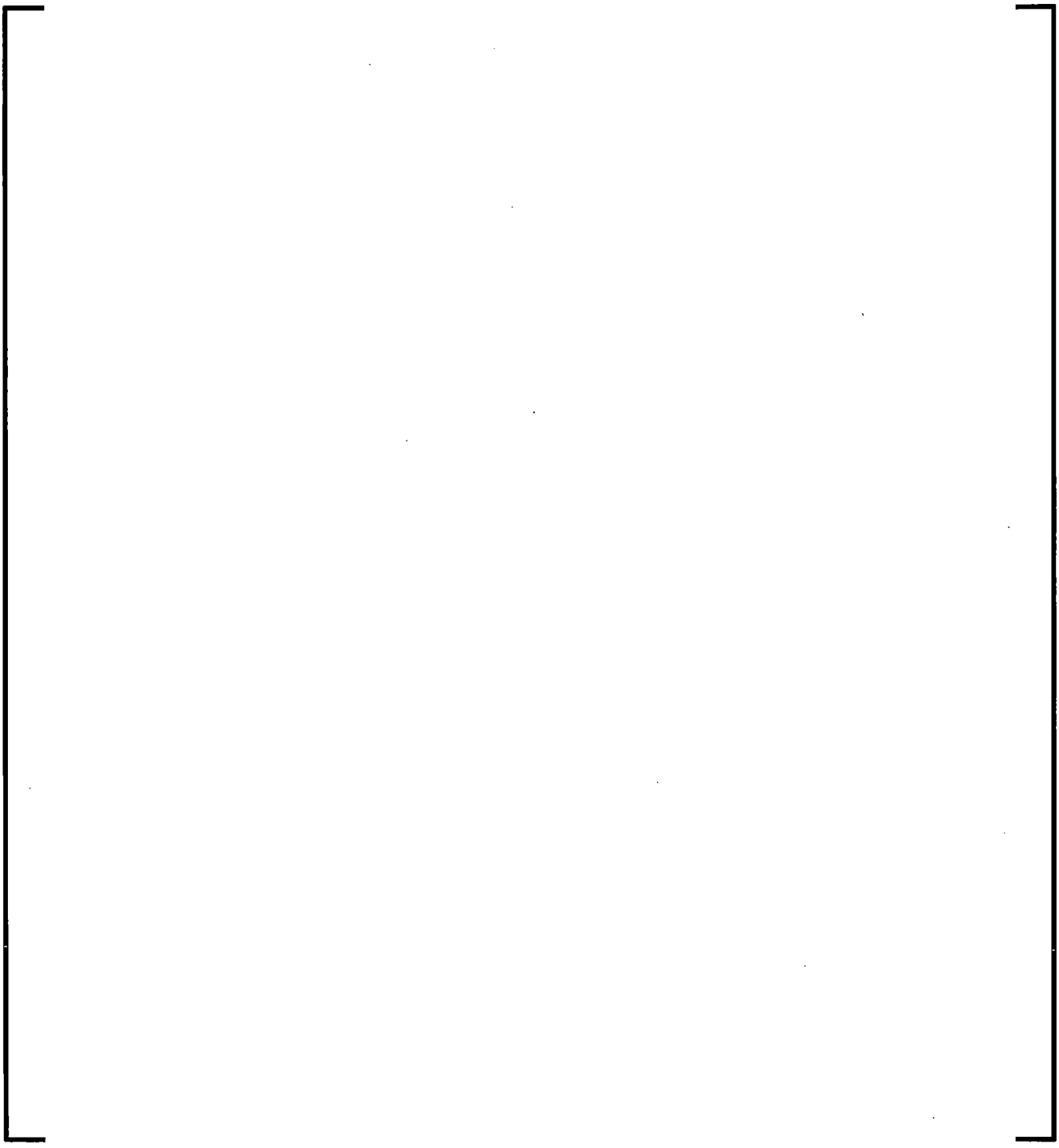

Figure B–44 CE 2x4 Total Oxidation versus PCT Scatter Plot

[ ]

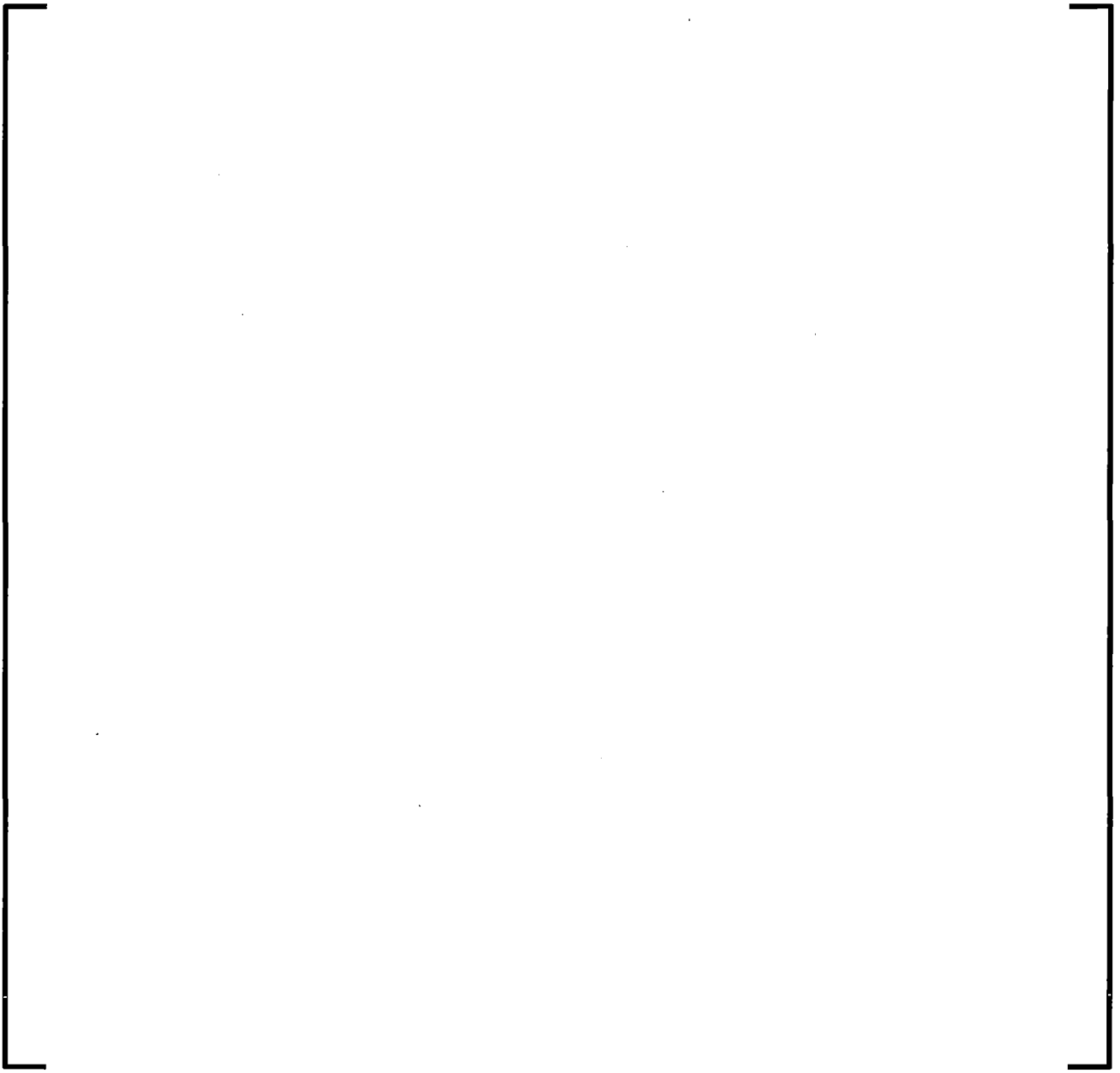

Figure B–45 CE 2x4 Peak Cladding Temperature (Independent of Elevation) for the Demonstration Case

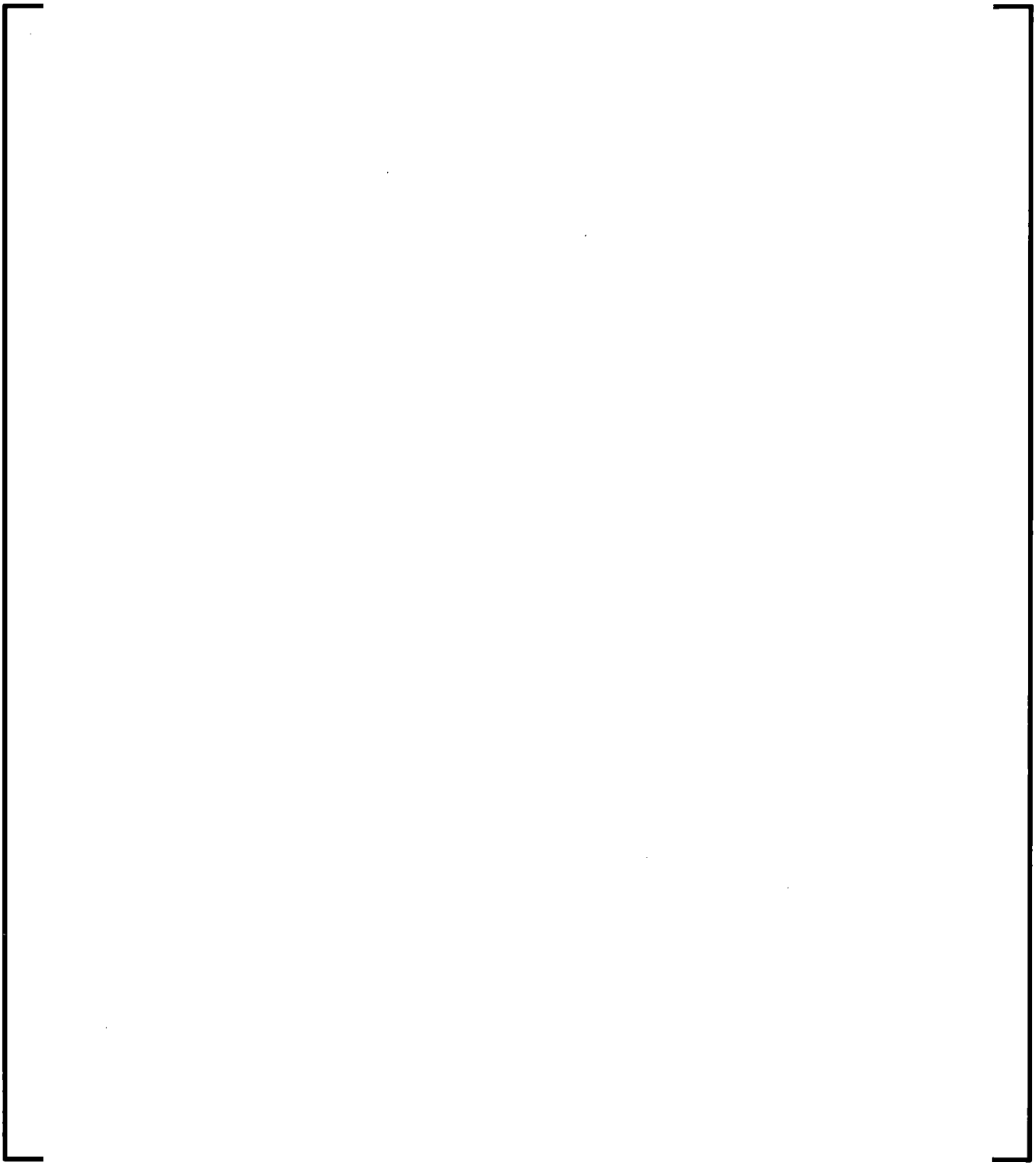

Figure B–46 CE 2x4 Break Flow for the Demonstration Case

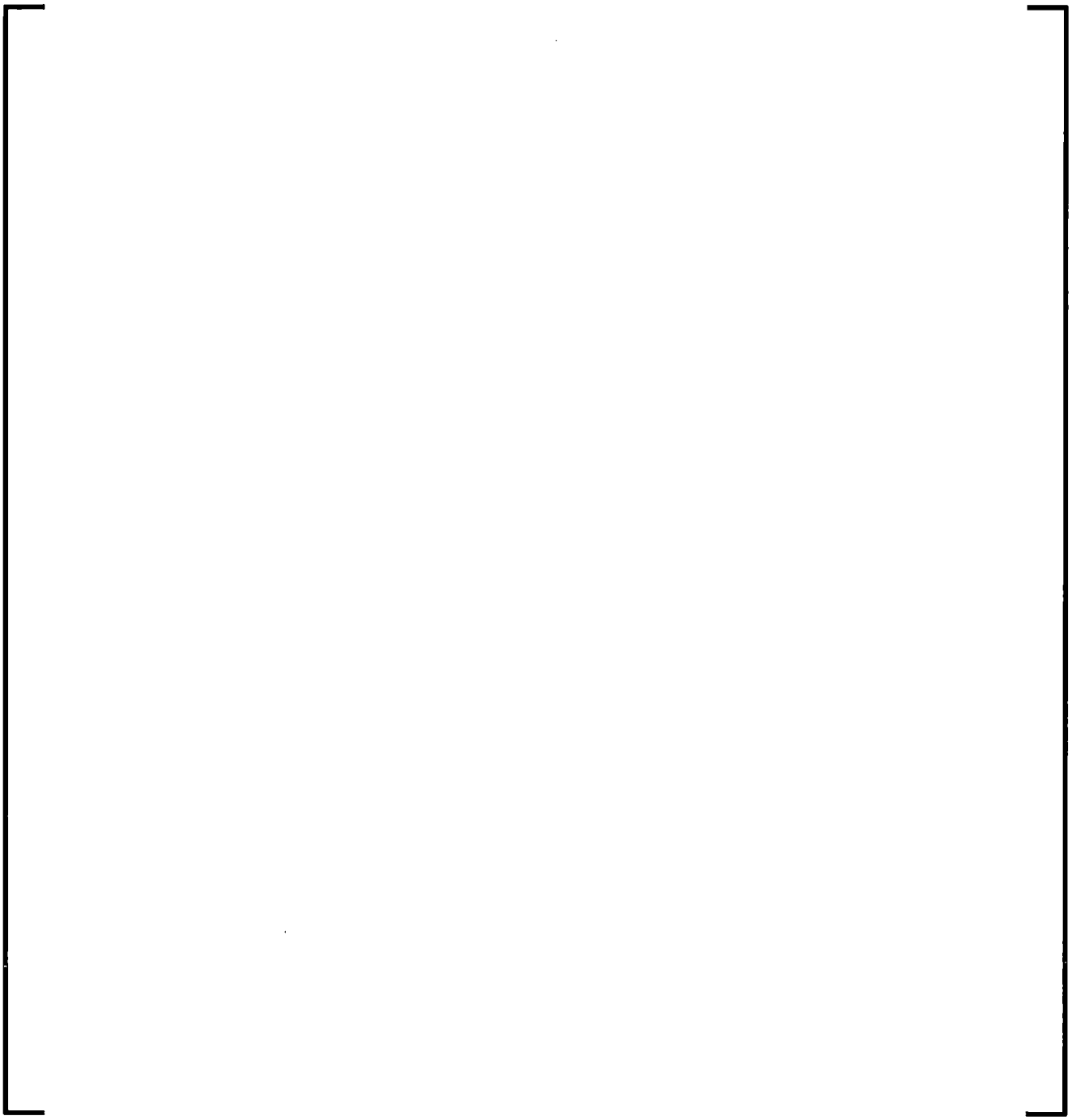

Figure B–47 CE 2x4 Core Inlet Mass Flux for the Demonstration Case

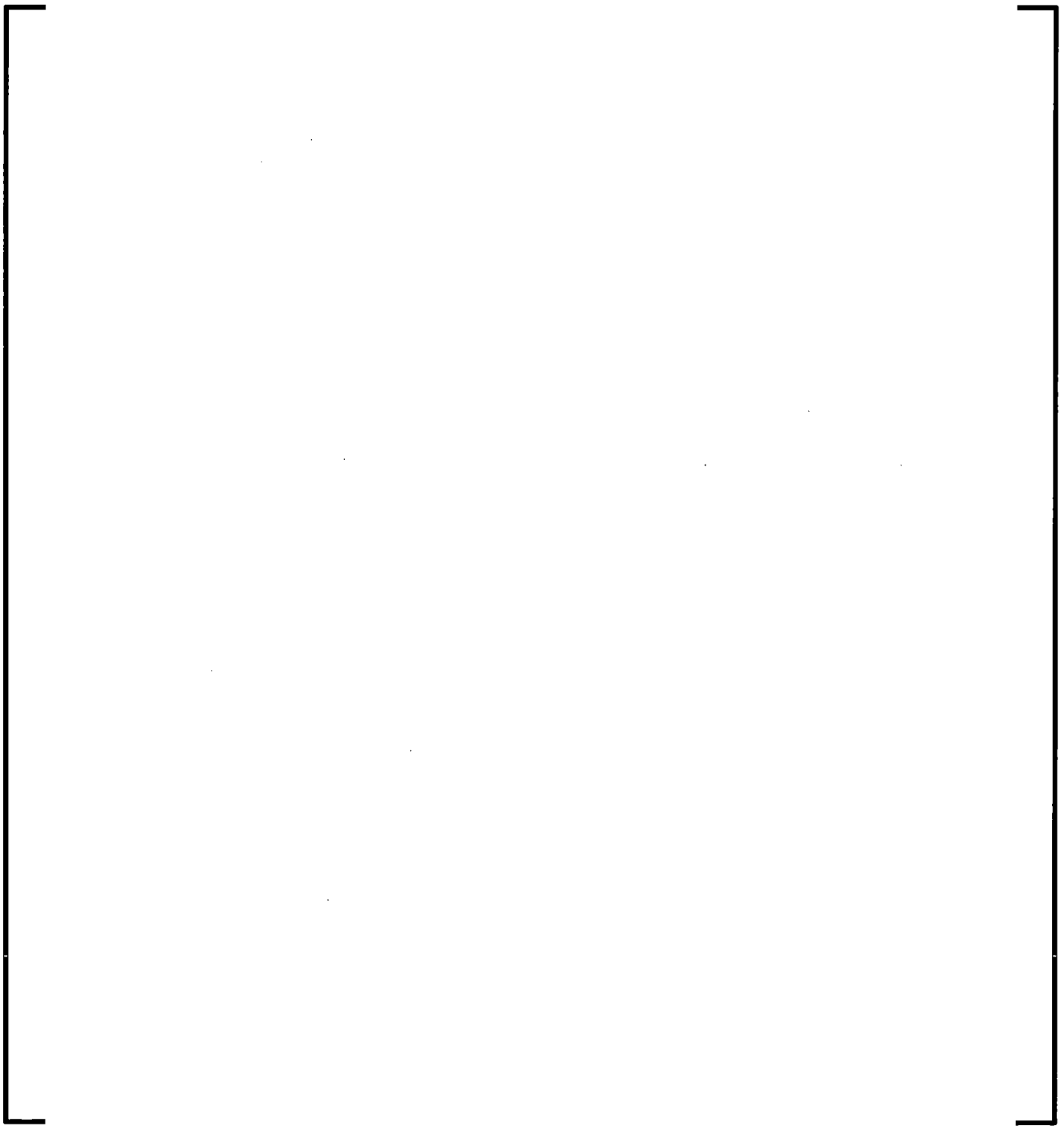

Figure B–48 CE 2x4 Core Outlet Mass Flux for the Demonstration Case

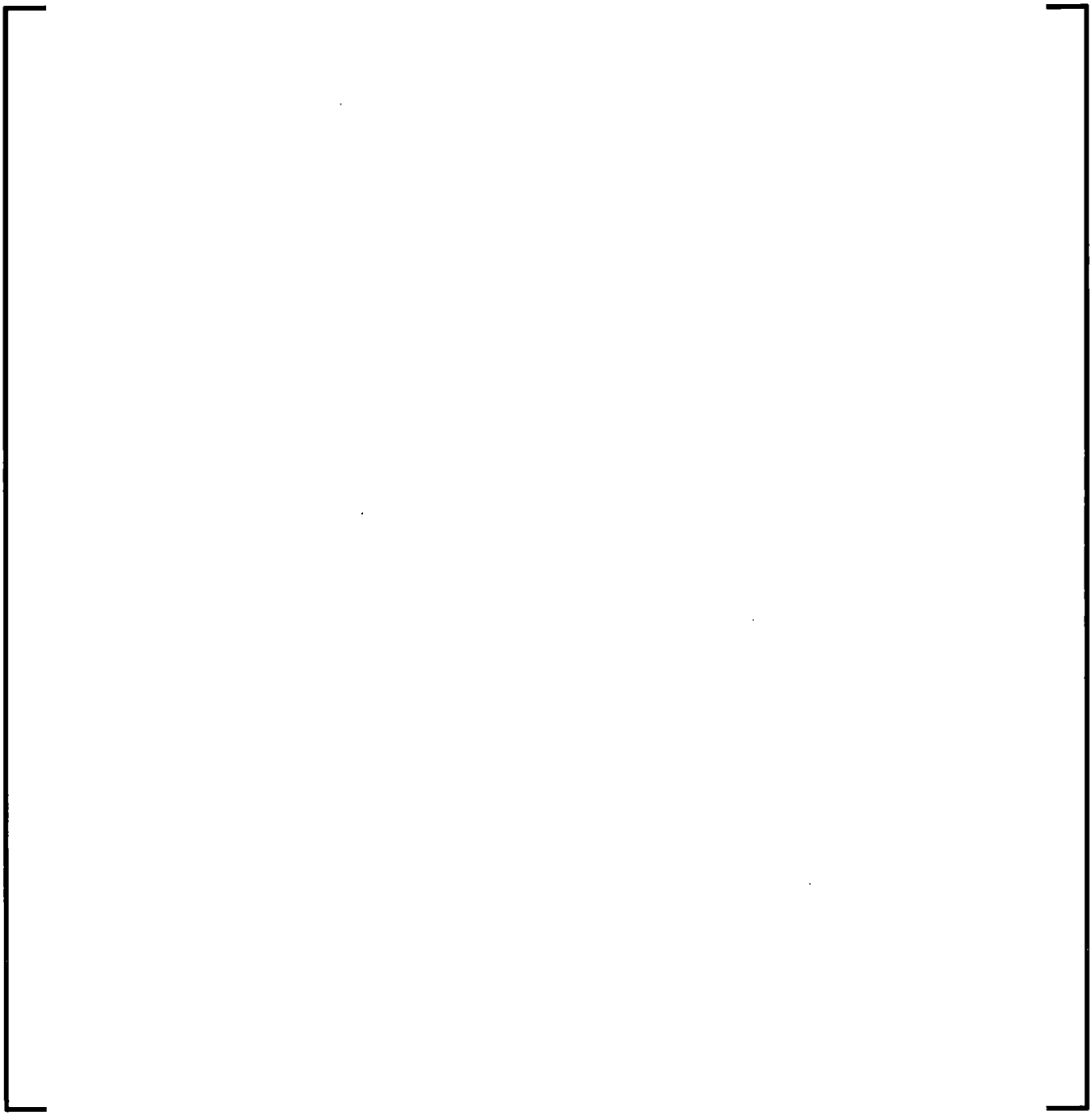

Figure B–49 CE 2x4 Void Fraction at RCS Pumps for the Demonstration Case

Figure B–50 CE 2x4 ECCS Flows (Includes SIT, Charging, SI and RHR) for the Demonstration Case

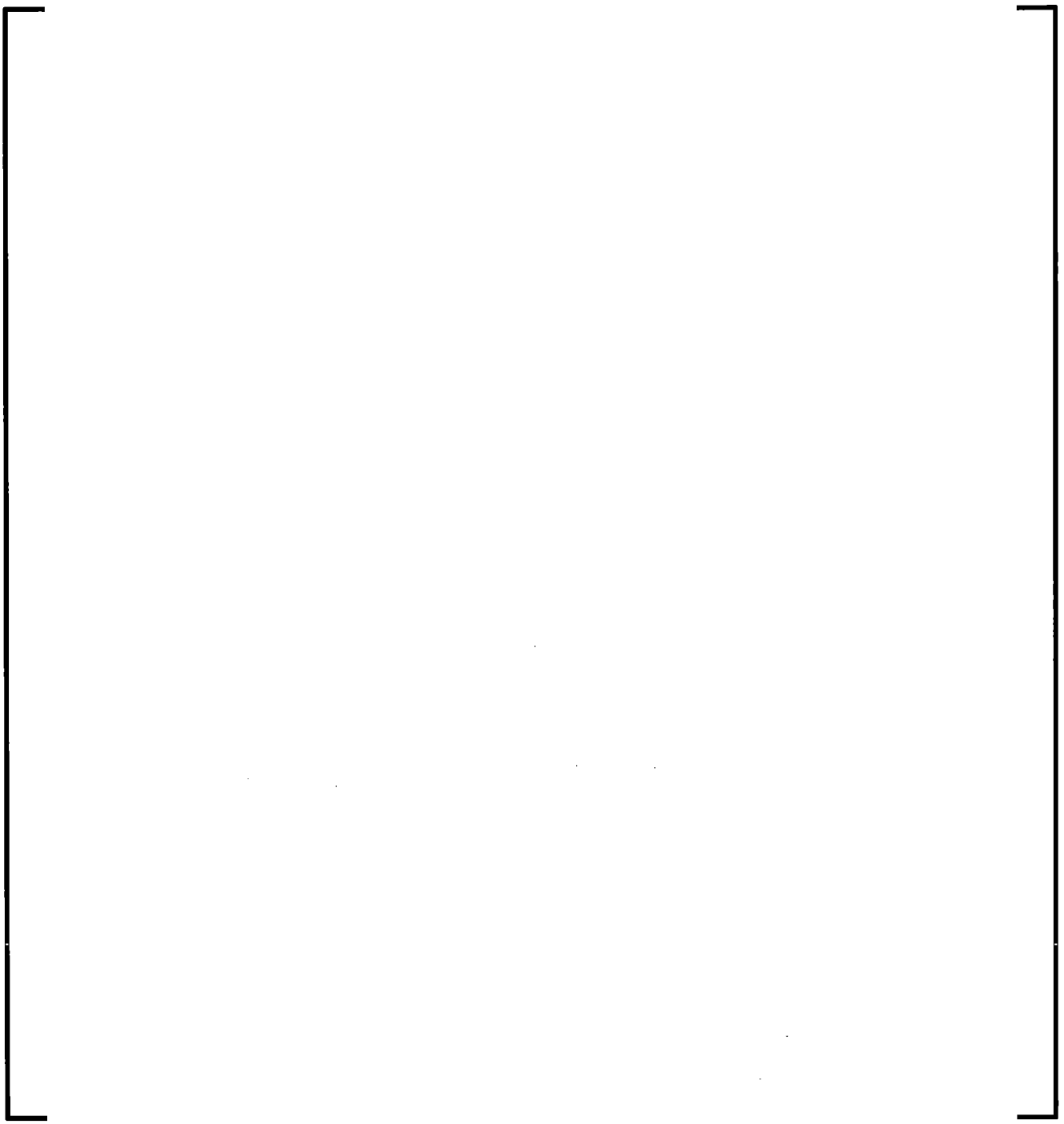

Figure B–51 CE 2x4 Upper Plenum Pressure for the Demonstration Case

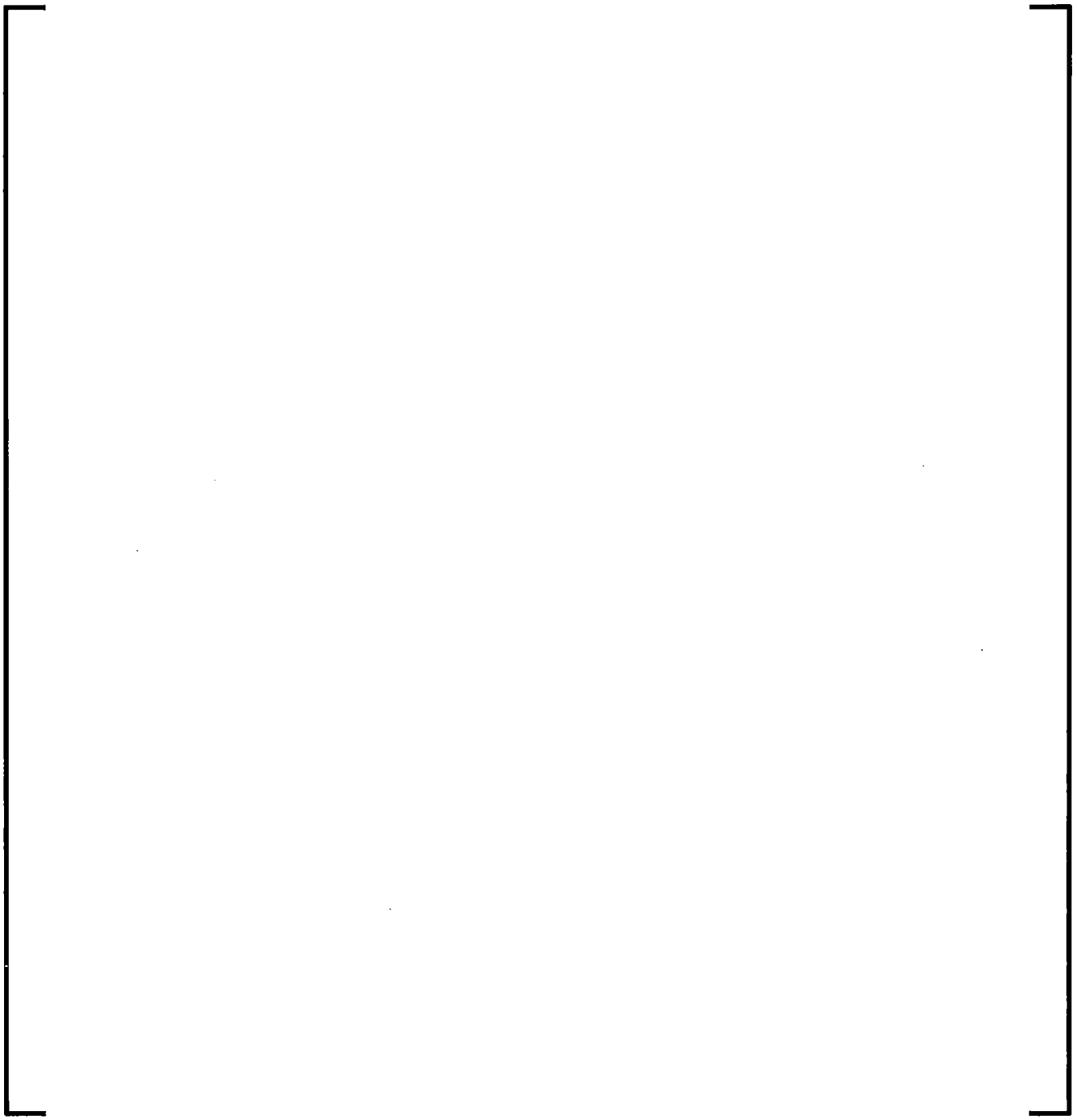

Figure B–52 CE 2x4 Collapsed Liquid Level in the Downcomer for the Demonstration Case

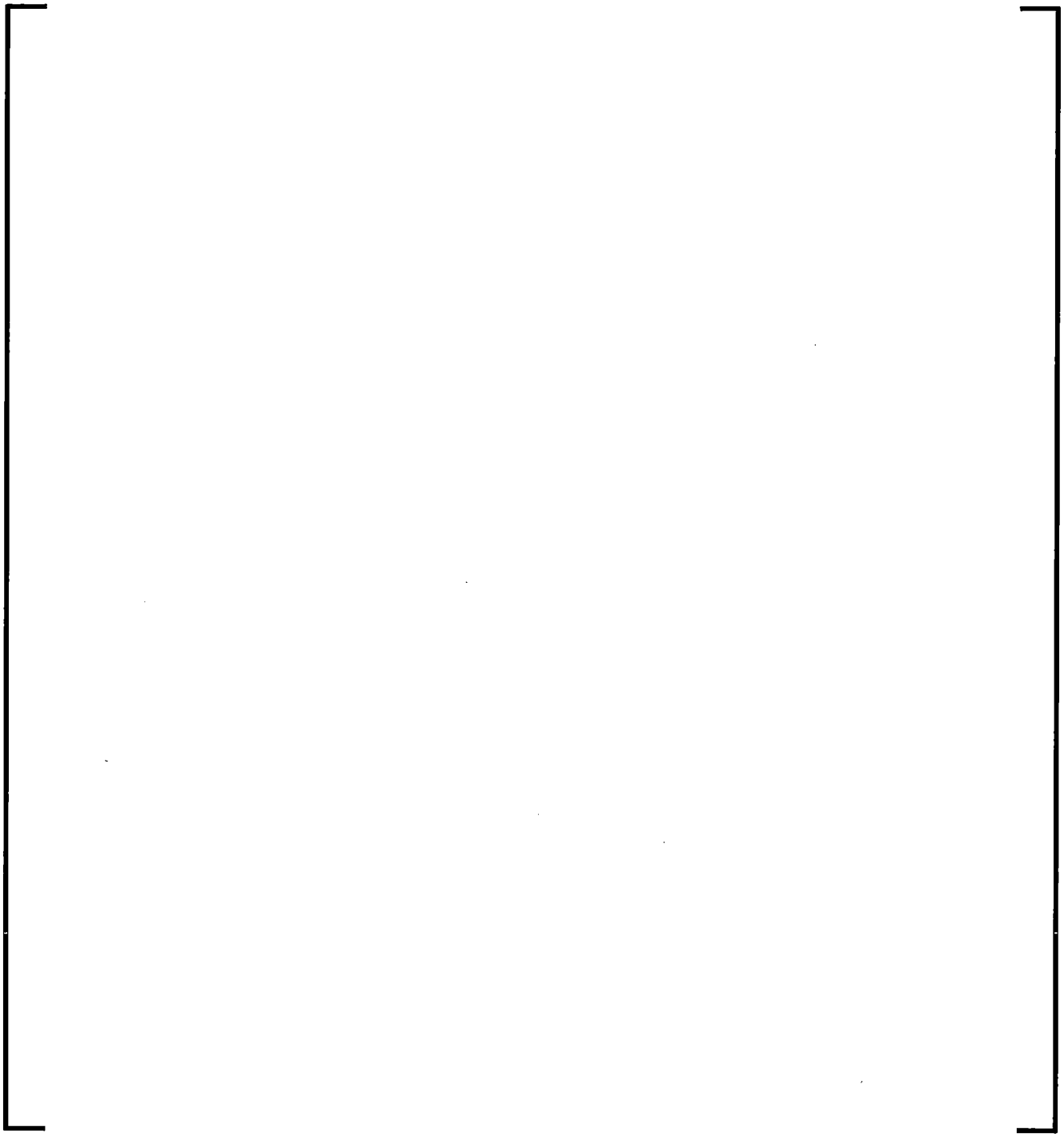

Figure B–53 CE 2x4 Collapsed Liquid Level in the Lower Plenum for the Demonstration Case

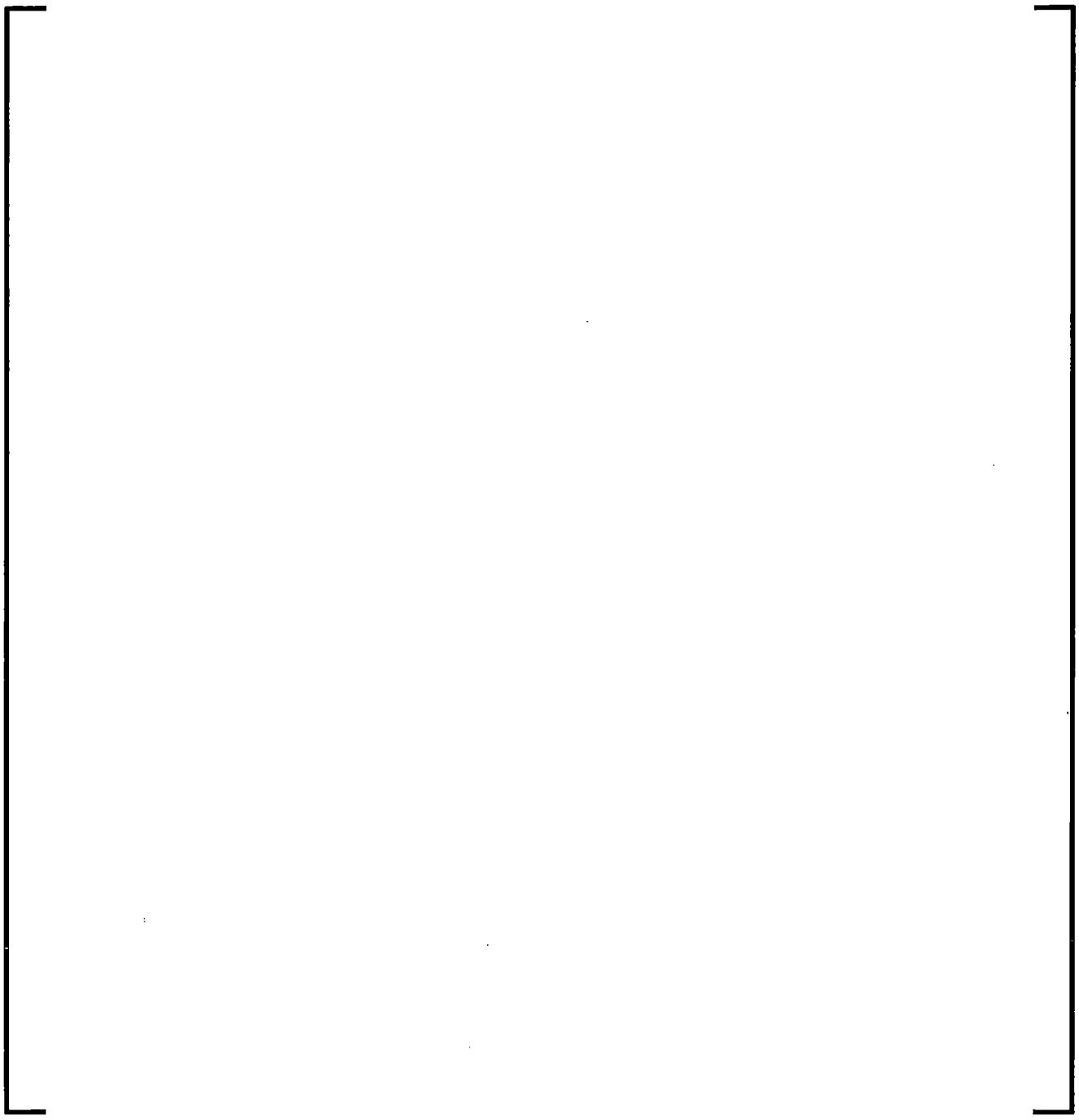

Figure B–54 CE 2x4 Collapsed Liquid Level in the Core for the Demonstration Case

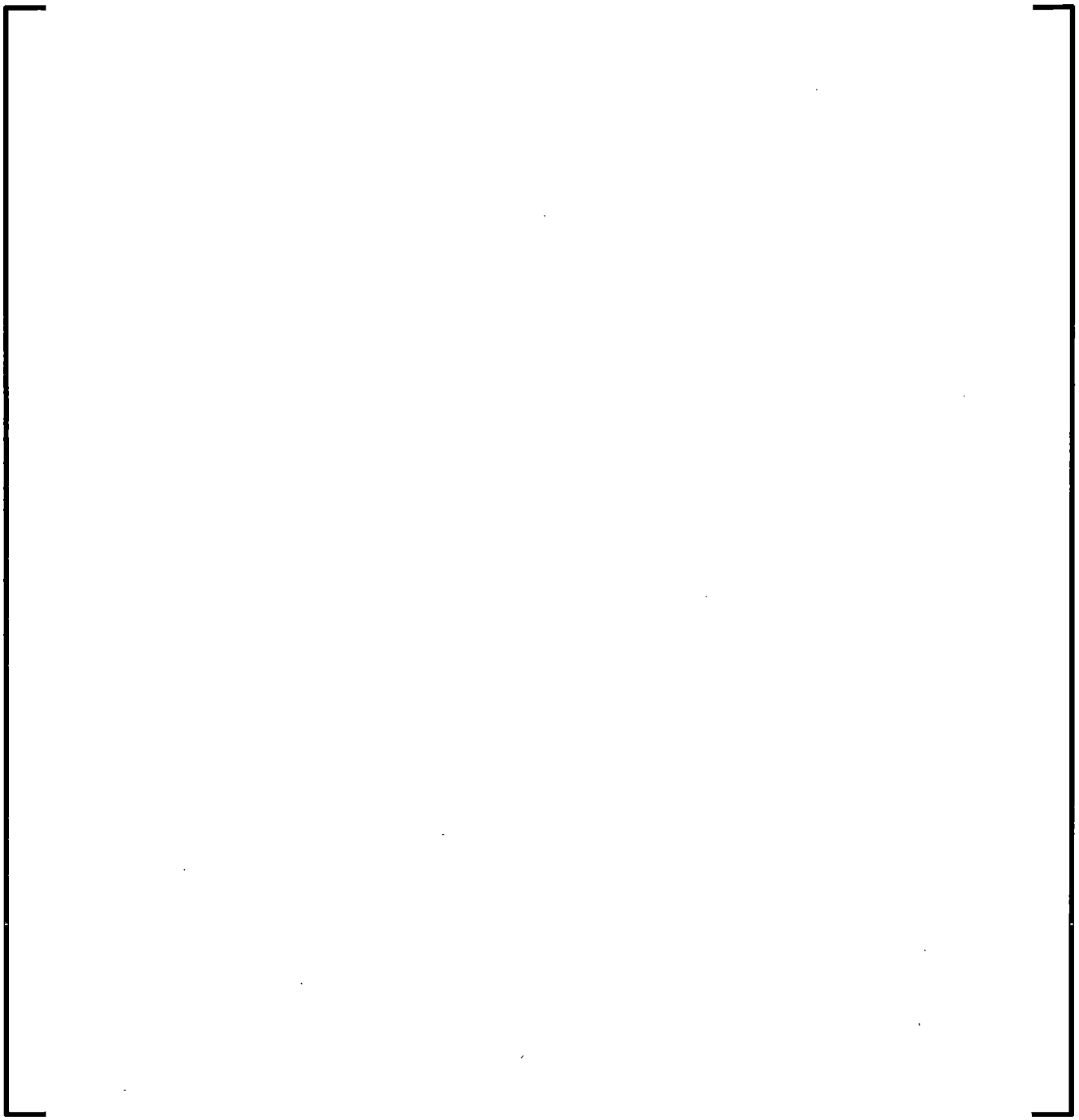

Figure B–55 CE 2x4 Containment and Loop Pressures for the Demonstration Case

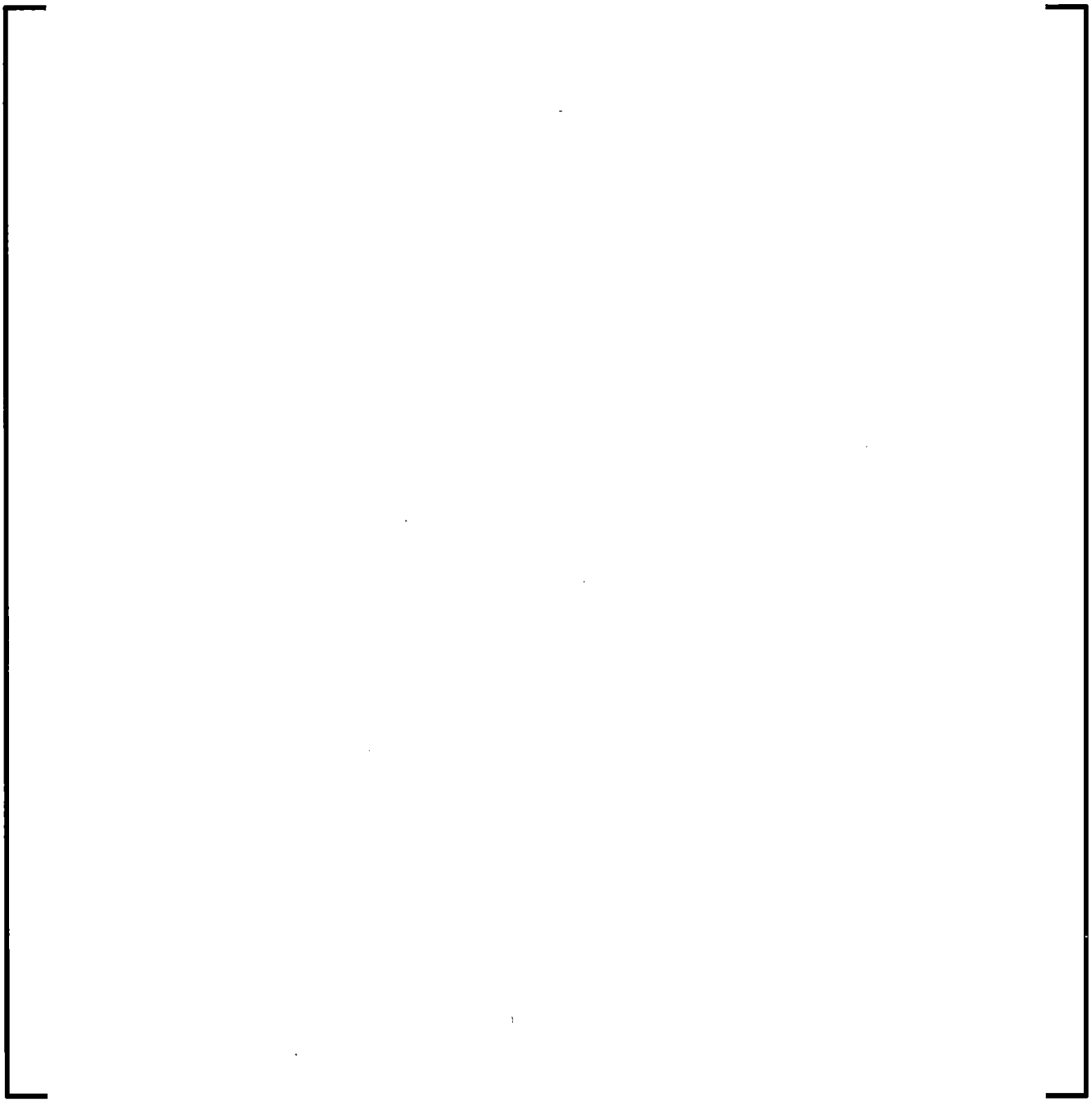

Figure B–56 CE 2x4 Pressure Difference between Upper Plenum and Downcomer for the Demonstration Case

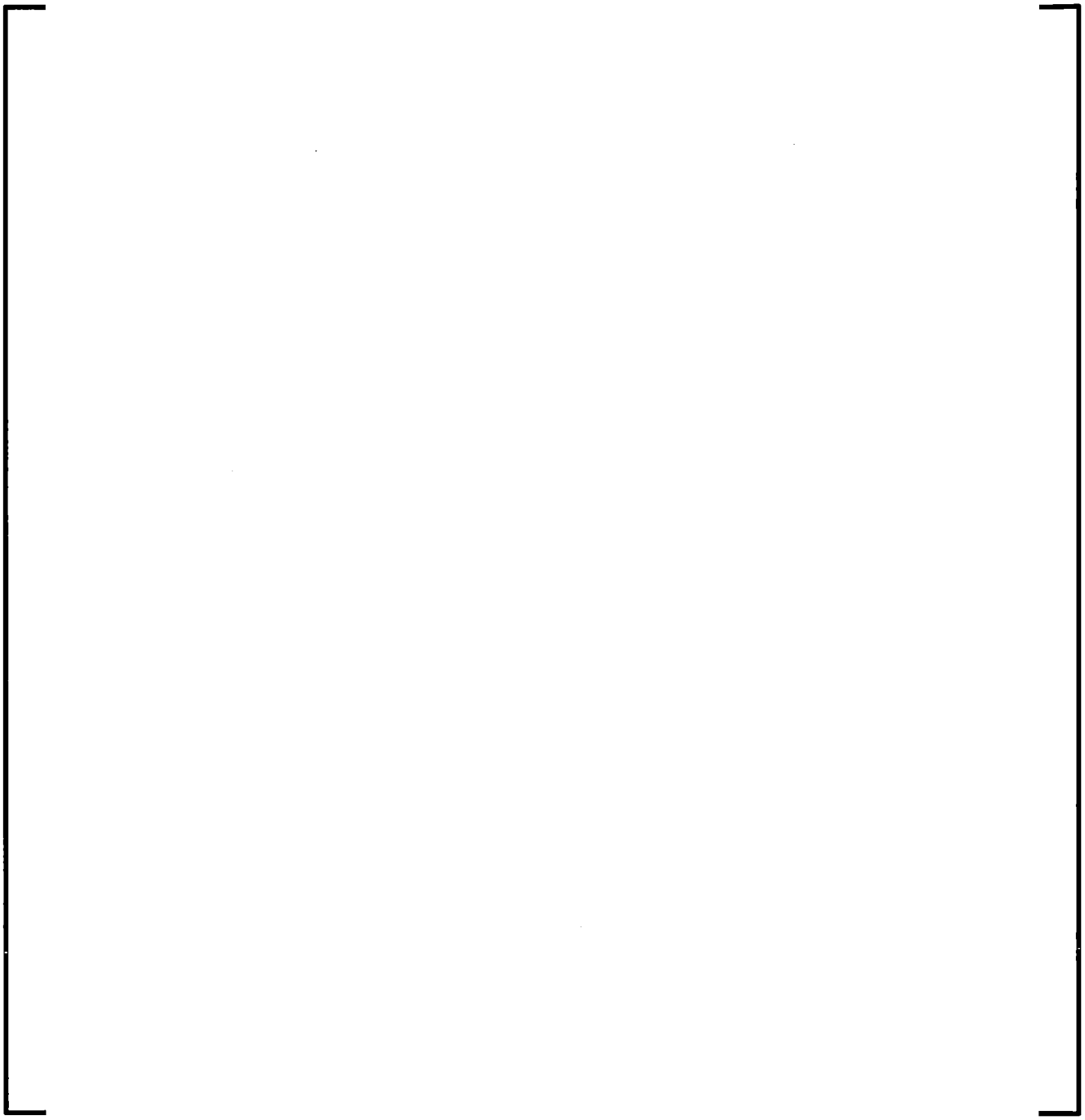

Figure B–57 CE 2x4 Validation of BOCR Time using MPR CCFL Correlation, [ ]

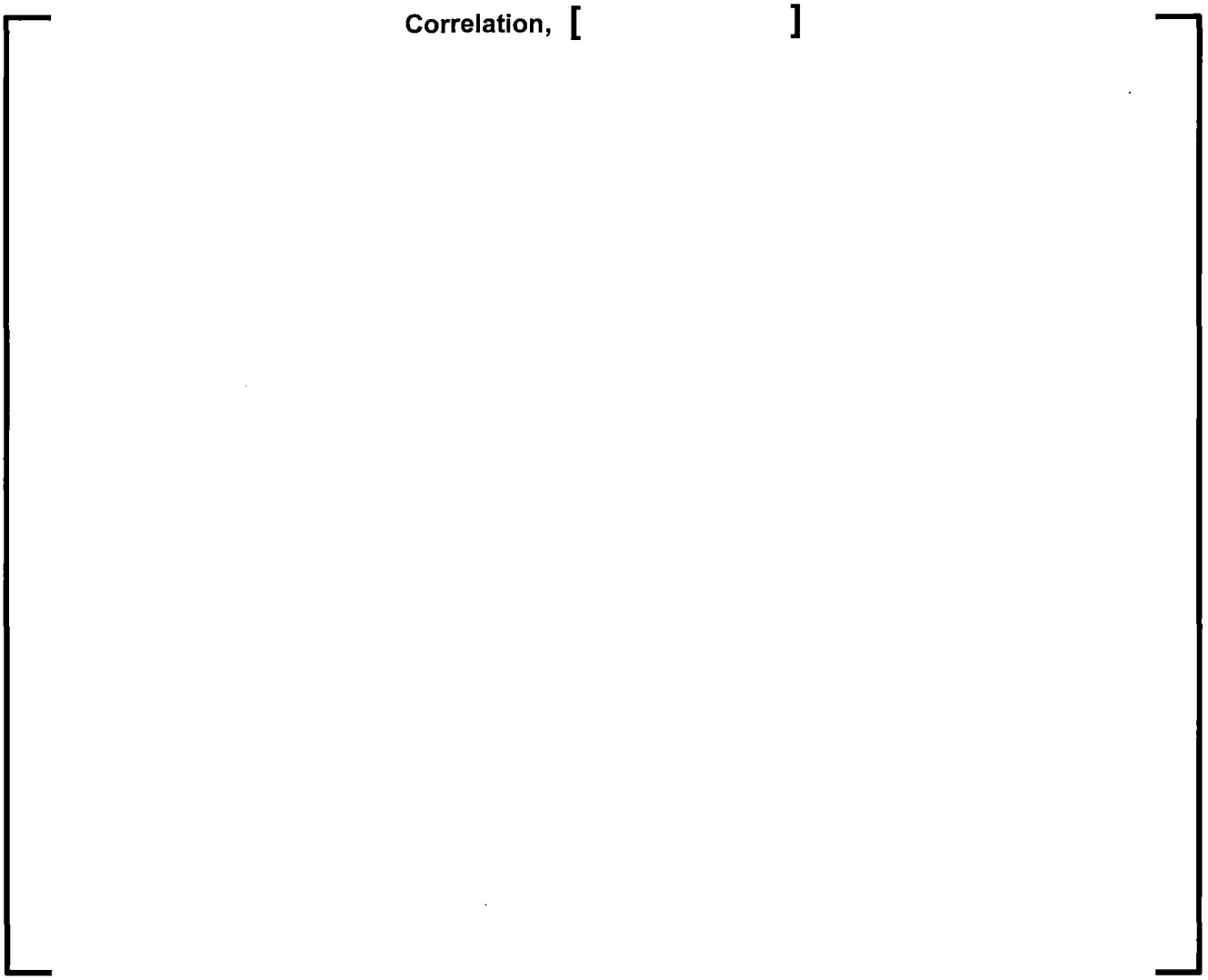

B.5 References

B-1 Technical Program Group, "Quantifying Reactor Safety Margins," NUREG/CR-5249, EGG-2552, October 1989.

B-2 F. W. Dittus and L. M. K. Boelter, "Heat Transfer in Automobile Radiators of the Tubular Type," Publications in Engineering, Volume 2, pp. 443-461, University of California, Berkeley, 1930.

B-3 J. C. Chen, "A Correlation for Boiling Heat Transfer to Saturated Fluids in Convective Flow, Process Design and Development," Volume 5, pp. 322-327, 1966.

B-4 N. Zuber, M. Tribus and J. W. Westwater, "Hydrodynamic Crisis in Pool Boiling of Saturated and Subcooled Liquid," 2nd International Heat Transfer Conference, Denver, Colorado, 1961.

B-5 Biasi, et al., "Studies on Burnout Part 3 - A New Correlation for Round Ducts and Uniform Heating and Its Comparison with World Data, Energia Nucleare," Volume 14, pp. 530-536, 1967.

B-6 J. C. Chen, R. K. Sundaram, F. T. Ozkaynak, "A Phenomenological Correlation for Post-CHF Heat Transfer," NUREG-0237, June 1977.

B-7 L. A. Bromley, "Heat Transfer in Stable Film Boiling," Chemical Engineering Progress Volume 46, pp. 221-227, 1950.

B-8 Wong, S. and Hochreiter, L. E., "Analysis of the FLECHT-SEASET Unblocked Bundle Steam Cooling and Boil-off Tests", January 1981, NUREG/CR-1533.

B-9 E. F. Carpenter and A. P. Colburn, "The Effect of Vapor Velocity on Condensation Inside Tubes," Proceedings of General Discussion on Heat Transfer, Institute Mechanical Engineering/American Society of Mechanical Engineers, pp. 20-26, 1951.

B-10 V. H. Ransom, et al., "RELAP5/MOD2 Code Manual," Volume 1: Code Structure, Systems Models, and Solution Methods, NUREG/CR-4312, EGG-2396, Revision 1, March 1987.

B-11 K. H. Sun, J. M. Gonzales-Santalo, and C. L. Tien, "Calculations of Combined Radiation and Convection Heat Transfer in Rod Bundles Under Emergency Cooling Conditions," Journal of Heat Transfer, pp. 414-420, 1976.

APPENDIX C
DISPOSITION OF EMF-2103 REVISION 0 SER RESTRICTIONS

The SER on EMF-2103, Revision 0 noted several limitations, concerns, and deficiencies resulting in restrictions on the methodology and the use of S-RELAP5. A disposition of each of these items, referred to as "SER Restrictions", is provided with each analysis performed with that methodology. Revision 3 addresses most of these items. This appendix describes the way in which this set of Revision 0 SER Restrictions has been addressed by the AREVA NP RLBLOCA Revision 3 methodology. These items are no longer restrictions on the methodology and an analysis-specific disposition of these particular items will not be provided for RLBLOCA applications with Revision 3.

C.1 *Model Applicability: 3- and 4-loop W&CE Plants*

The EMF-2103, Revision 0 SER restriction is as follows:

> *The model applies to 3 and 4 loop Westinghouse- and CE-designed nuclear steam systems.*

Section 1.0 of EMF-2103, Revision 3 states that the methodology specifically applies to Westinghouse 3- and 4-loop designs, Combustion Engineering (CE) 2x4 designs and AREVA 3- and 4-loop designs.

C.2 *Model Applicability: Bottom Reflood Plants*

The EMF-2103, Revision 0 SER restriction is as follows:

> *The model applies to bottom reflood plants only (cold side injection into the cold legs at the reactor coolant discharge piping).*

Section 1.0 of EMF-2103, Revision 3 states that the methodology specifically applies to plants with ECCS injection to the cold legs.

C.3 *Limitation on Top-down Quench*

The EMF-2103, Revision 0 SER restriction is as follows:

> *The reflood model applies to bottom-up quench behavior. If a top-down quench occurs, the model is to be justified or corrected to remove top quench. A top-down quench is characterized by the quench front moving from the top to the bottom of the hot assembly.*

[

]

C.4 *Long Term Cooling*

The EMF-2103, Revision 0 SER restriction is as follows:

> *The model does not determine whether Criterion 5 of 10 CFR 50.46, long term cooling, has been satisfied. This will be determined by each applicant or licensee as part of its application of this methodology.*

Section 3.0 of EMF-2103, Revision 3 explains that only first three criteria of 10 CFR 50.46 are addressed by this methodology. The remaining two criteria, coolable geometry and long-term cooling are treated separately during plant specific evaluations.

C.5 *Guidelines for Plant-specific Nodalization*

The EMF-2103, Revision 0 SER restriction is as follows:

> *Specific guidelines must be used to develop the plant-specific nodalization. Deviations from the reference plant must be addressed.*

Appendix A of EMF-2103, Revision 3 presents in an abridged format the model input development guidelines and the analysis guidelines as currently implemented in the internal AREVA calculation process for performing RLBLOCA licensing analyses. Any deviations from the development guidelines would require justification.

C.6 *Results Presentation*

The EMF-2103, Revision 0 SER restriction is as follows:

> *The licensee or applicant using the approved methodology must submit the results of the plant-specific analyses, including the calculated worst break size, PCT, and local and total oxidation.*

[

]

C.7 *M5 Cladding*

The EMF-2103, Revision 0 SER restriction is as follows:

> *Applicants or licensees wishing to apply the Framatome ANP realistic large break loss-of-coolant accident (RLBLOCA) methodology to M5 clad fuel must request an exemption for its use until the planned rulemaking to modify 10 CFR 50.46(a)(i) to include M5 cladding material has been completed.*

This SER requirement is related to a higher order regulation present in the Code of Federal Regulations. 10 CFR 50.46 states, "(a)(1)(i) Each boiling or pressurized light-water nuclear power reactor fueled with uranium oxide pellets within cylindrical zircaloy or ZIRLO cladding must be provided with an emergency core cooling system (ECCS) that must be designed so that its calculated cooling performance following postulated loss-of-coolant accidents conforms to the criteria set forth in paragraph (b) of this section." M5 cladding is not a form of zircaloy or ZIRLO and cannot be loaded into a U.S. licensed reactor without an exemption to this part of the Code. The use of M5 cladding is a licensee decision and the licensee is responsible for requesting the exemption. An SER restriction related to the higher order regulation is not needed on the evaluation model and the next revision of the regulation, 10 CFR 50.46(c) will include M5 cladding.

C.8 *Hot Leg to Downcomer Nozzle Gap*

The EMF-2103, Revision 0 SER restriction is as follows:

> *Framatome ANP has agreed that it is not to use nodalization with hot leg to downcomer nozzle gaps.*

As described in Section 9.1.4 and Appendix A, Section A.1.2.6.4.1 of EMF-2103, Revision 3 the hot leg to downcomer nozzle gaps are not modeled.

C.9 *Blowdown Rupture*

The EMF-2103, Revision 0 SER restriction is as follows:

> *If Framatome ANP applies the RLBLOCA methodology to plants using a higher planar linear heat generation rate (PLHGR) than used in the current analysis, or if the methodology is to be applied to an end-of-life analysis for which the pin pressure is significantly higher, then the need for a blowdown clad rupture model will be reevaluated. The evaluation may be based on relevant engineering experience and should be documented in either the RLBLOCA guideline or plant specific calculation file.*

[

]

APPENDIX D
TIME STEP SENSITIVITY

For the AREVA RLBLOCA methodology, solution convergence is demonstrated by performing sensitivity studies in which the calculation time step is varied for three appropriate plant designs. This approach demonstrates solution convergence while recognizing that a certain degree of variability is to be expected. This sensitivity study was performed in an earlier revision of EMF-2103 (Reference D-1), but the results and conclusions are equally applicable to EMF-2103, Revision 3.

This sensitivity study was performed by first regenerating steady-state plant analysis decks for three types of plants appropriate for this methodology, i.e., 3- and 4-loop Westinghouse designs, and a CE design. These decks were then brought to typical steady-state conditions, and a transient initiated with a DEG break with nominal parameters, other than decay heat. Each transient used 120 percent of nominal decay heat to drive the temperatures sufficiently high that code models would be challenged.

The recommended time step selection strategy is to set a single maximum time step during the portions of the transient of most significance to safety, that is, the blowdown, refill, and early reflood phases. The requested time step should then be increased during late reflood when the flooding phenomena are reasonably stable. This approach was found to provide a reasonable compromise between optimal numerical stability and run time. It should be noted that the time step requested by the user is actually the maximum time step allowed by the code for that time period, and that in fact the code will reduce the requested time step should instability be detected. The nominal or base case used a requested time step of 0.002 seconds from 0 to 400 seconds, and then 0.004 seconds from 400 to 600 seconds, 0.008 seconds from 600 to 800 seconds and 0.010 seconds beyond 800 seconds. Code convergence and stability at the nominal time step of 0.002 seconds were demonstrated by incrementally varying the time step from 0 to 400 seconds over a range from the nominal time step to an order of magnitude smaller.

[

] The nominal case for each of the designs noted in the time step sensitivity study was repeated with this new time step and it was determined that the code continued to proceed through the analysis with the requested time steps, indicating code stability, with a minor deviation at the time of quench at the core hot spot.

Figure D-1, Figure D-3, and Figure D-5 show the calculated PCTs from the 3-loop, 4-loop, and CE studies, respectively. S-RELAP5 shows stability and convergence for all design types during the blowdown period. During refill and early reflood, there is some noticeable divergence in the results; however this has little impact on the PCT.
Figure D-2, Figure D-4, and Figure D-6 show the variability about the mean PCT from the 3-loop, 4-loop, and CE studies, respectively. The data for these figures were generated by averaging the calculated PCTs for each design, and then calculating the maximum deviation, whether it is above or below the mean. As shown in these figures, the nominal variability for the 3-loop design is approximately 15 K (27 °F), the 4-loop design is approximately 12 K (21 °F), and the CE design is approximately 15 K (27 °F).

[

]

Figure D-1: Time Step Sensitivity of Westinghouse 3-Loop Analysis

Figure D-2: Variability of Westinghouse 3-Loop Analysis

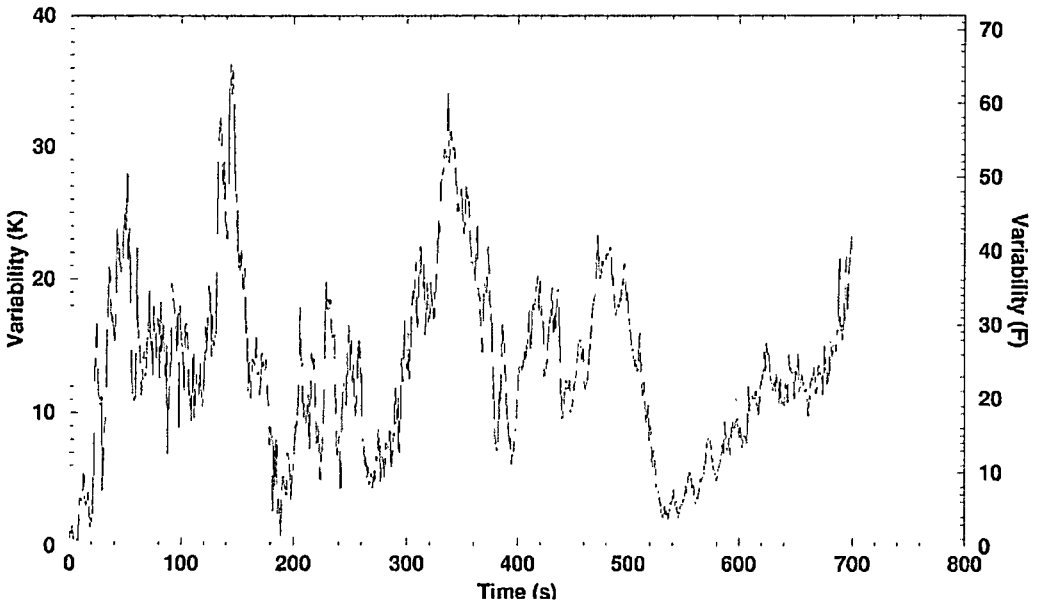

Figure D-3: Time Step Sensitivity of Westinghouse 4-Loop Analysis

Figure D-4: Variability of Westinghouse 4-Loop Analysis

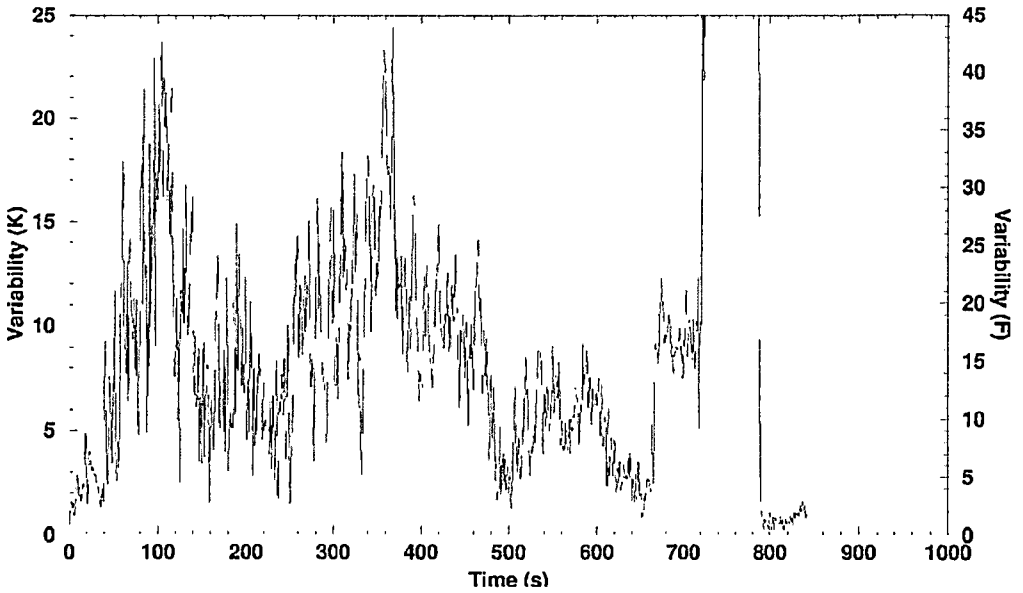

Figure D-5: Time Step Sensitivity of CE Analysis

Figure D-6: Variability of CE Analysis

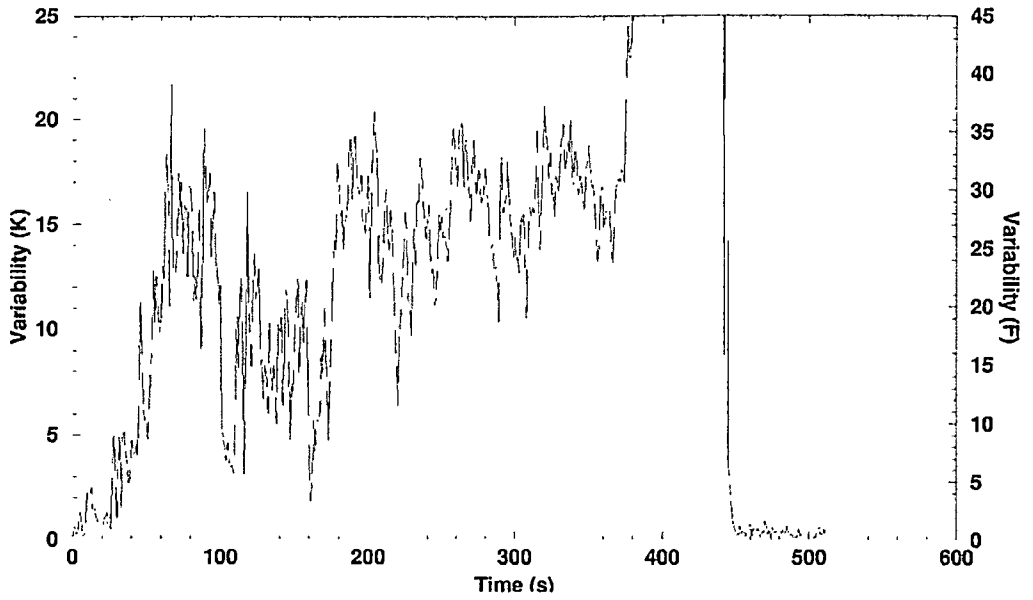

D-1 *References*

D-1 AREVA Document EMF-2103, Revision 2, "Realistic Large Break LOCA Methodology for Pressurized Water Reactors", November 2010 (ADAMS Accession No. ML110200553).

APPENDIX E
EMF 2103P-003: NRC REQUEST FOR ADDITIONAL INFORMATION (RAI) AND AREVA RESPONSES

List of Contents

1 Letter, Pedro Salas to NRC, Request for Review and Approval of EMF-2103(P), Revision 3, "Realistic Large Break LOCA Methodology for Pressurized Water Reactors," September 13, 2013.

2 Letter, Pedro Salas to NRC, Document to Support the NRC review of EMF-2103P, Revision 3, "Realistic Large Break LOCA Methodology for Pressurized Water Reactors," January 10, 2014.

3 Letter, Jonathan G. Rowley (NRC) to Pedro Salas (AREVA NP Inc.), "Request for additional information RE: AREVA NP Inc. (AREVA), Topical Report EMF-2103(P), Revision 3, "Realistic Large Break LOCA Methodology for Pressurized Water Reactors," (TAC NO. MF2904), November 20, 2014.

4 Letter, Pedro Salas to NRC, Response to Request for Additional Information Regarding EMF-2103(P), Revision 3, "PWR Realistic Large Break LOCA Methodology for Pressurized Water Reactors," January 16, 2015.

5 Letter, Pedro Salas to NRC, Errata and Revised Sample Problems for EMF-2103P, Revision 3, "Realistic Large Break LOCA Methodology for Pressurized Water Reactors," January 16, 2015.

6 NRC letter from J.G. Rowley (NRC) to G. Peters (AREVA), "Request for Additional Information Related to Review of AREVA NP Licensing Topical Report EMF-2103 Revision 3, Realistic Large Break LOCA Methodology for Pressurized Water Reactors" (ML15348A140), January 5, 2016.

7 Letter, Gary Peters to NRC, Response to First and Second Request for Additional Information Regarding EMF-2103(P), Revision 3, "PWR Realistic Large Break LOCA Methodology for Pressurized Water Reactors," February 16, 2016.

8 Letter, Gary Peters to NRC, Revised Pages for EMF-2103{P), Revision 3, "Realistic Large Break LOCA Methodology for Pressurized Water Reactors," February 19, 2016.

9 EMF-2103R3Q1P, Revision 0, "AREVA Response to First and Second Request for Additional Information EMF-2103 (P), Revision 3, 'Realistic Large Break LOCA Methodology for Pressurized Water Reactors'," February, 2016.

September 13, 2013
NRC:13:072

U.S. Nuclear Regulatory Commission
Document Control Desk
11555 Rockville Pike
Rockville, MD 20852

Request for Review and Approval of EMF-2103(P), Revision 3, "Realistic Large Break LOCA Methodology for Pressurized Water Reactors"

Ref. 1: Letter, James Kim (NRC) to Dominion Nuclear Connecticut, Inc., "Summary of July 17, 2013, Meeting with Dominion Nuclear Connecticut, Inc. and AREVA to Discuss Upgrade to AREVA Standard CE14 HTP Fuel Assembly," July 30, 2013 (ADAMS Accession No. ML13207A259).

AREVA NP Inc. (AREVA NP) requests the NRC's review and approval of the topical report EMF-2103(P), Revision 3, "Realistic Large Break LOCA Methodology for Pressurized Water Reactors," dated September 2013, for referencing in licensing actions. Revision 3 of this report supersedes and replaces all previous versions of this report.

This report presents a methodology for the realistic evaluation of a large break loss-of-coolant accident. The methodology consists of the advanced fuel performance code COPERNIC and the thermal-hydraulic system code, S-RELAP5. This revision comprises improvements in the methodology that enhance safety to the public. The specific improvements, such as treating fuel swelling, rupture, and relocation, are itemized in Attachment A. Section 9.4.1 of the report provides additional information describing how the methodology demonstrates compliance to the criteria of 10 CFR 50.46 with high probability.

The topical report EMF-2103(P), Revision 3, is part of AREVA NP's response to NRC Information Notice 2009-23: Nuclear Fuel Thermal Conductivity Degradation. This information notice states that previous fuel performance codes did not model the impact of irradiation on fuel thermal conductivity adequately. The COPERNIC fuel performance code in EMF-2103(P), Revision 3, contains a nuclear fuel thermal conductivity model which accurately reflects the impact of irradiation.

In previous revisions of EMF-2103(P), the documentation and supporting material was provided in four separate documents: EMF-2103(P), Revision 2 (the topical report itself); the corresponding Supplement 1 to EMF-2103(P), Revision 2; EMF-2100(P) (the S-RELAP5 models and correlations code manual) and; EMF-2102(P) (the code verification and validation document). The material in EMF-2103(P), Revision 3, has been reorganized into a structure to include this information in a single document to provide a comprehensive description of the evaluation model.

AREVA NP considers some of the material contained in the enclosed documents to be proprietary. As required by 10 CFR 2.390(b), an affidavit is enclosed to support the withholding of the information from public disclosure. Proprietary and non-proprietary versions of the report are found in Enclosures 1 and 2,

respectively. Enclosure 3 is the proprietary S-RELAP5 User's Input manual and Enclosure 4 is the notarized Affidavit.

AREVA NP is providing a table in Attachment A to call to the NRC's attention the changes in the Evaluation Models in EMF-2103(P), Revision 3.

In support of the Office of Nuclear Reactor Regulation's prioritization efforts, the prioritization scheme matrix is attached (refer to Attachment B).

There are no commitments contained within the enclosures to this letter.

AREVA NP requests NRC approval of this topical report by April 1, 2015 to support commercial reloads. Specifically, Dominion Generation intends to reference this topical report in their License Amendment Request for fuel upgrade activities at Millstone Power Station Unit 2, as presented to the NRC staff on July 17, 2013 (Reference 1). AREVA NP will contact the NRC with the intent of arranging a post-submittal meeting in October 2013. Additionally, any preliminary feedback from the staff prior to the October 2013 meeting would be appreciated.

If you have any questions related to this submittal, please contact Ms. Gayle F. Elliott, Product Licensing Manager at 434-832-3347 or by e-mail at gayle.elliott@areva.com.

Sincerely,

Pedro Salas, Director
Regulatory Affairs
AREVA NP Inc.

Attachments:

A. Changes to the RLBLOCA Evaluation Model (EM)
B. NRC Prioritization Matrix

Enclosures:

1. Proprietary Version of EMF-2103(P), Revision 3, "Realistic Large Break LOCA Methodology for Pressurized Water Reactors"
2. Non-Proprietary Version of EMF-2103(NP), Revision 3, "Realistic Large Break LOCA Methodology for Pressurized Water Reactors"
3. Proprietary Version of FSQA-07 – S-RELAP5 – 1.0 (FS1-0011181), "S-RELAP5 Input Data Requirements (User's Manual) PWR Version"
4. Notarized Affidavit

cc: J.A. Golla
J.G. Rowley
Project 728

Attachment A

Changes to RLBLOCA Evaluation Model (EM)				
Item	**Evaluation Model Element**	**Technical Upgrade**	**Comment**	**Discussed in EMF-2103, Rev. 3 Section**
1	Cold Leg Condensation Model	A more accurate modeling of the cold leg condensation during the pumped ECC injection phase resulting in near saturated fluid conditions at the downcomer entrance, which conservatively increases the potential for downcomer boiling.	An earlier version of this EM element of EMF-2103, Revision 3 has been reviewed and approved by the NRC in several LARs, most recently in Reference 1.	Presented in Section 7.6.7.2 and is assessed in Sections 8.2.1, 8.2.4, 8.4.1 and 8.4.4.
2	Second Cycle Fuel	The methodology has been upgraded such that a direct calculation of second cycle fuel performance is accomplished. This expands the range of evaluations and ensures that fuel experiencing its second burn will be evaluated and, if limiting, recognized as limiting.	These EM elements of EMF-2103, Revision 3 have been reviewed and approved by the NRC in several LARs, most recently in Reference 1.	Presented in Section 9.3.1.3
3	Break Modeling	The break modeling was altered from EMF-2103, Revision 0 to concur with the approach outlined in Regulatory Guide 1.157. The split versus double-ended break type is no longer related to break area.	These EM elements of EMF-2103, Revision 3 have been reviewed and approved by the NRC in several LARs, most recently in Reference 1.	Presented in Section 8.5.2.6.
4	Decay Heat Simulation	The decay heat calculation, which in EMF-2103, Revision 0 had been sampled according to the standard deviation presented in the 1979 ANS standard, has been replaced by a fixed, non-sampled, application of the 1979 standard.	These EM elements of EMF-2103, Revision 3 have been reviewed and approved by the NRC in several LARs, most recently in Reference 1.	Presented in Section 8.5.1.17.

Changes to RLBLOCA Evaluation Model (EM)				
Item	**Evaluation Model Element**	**Technical Upgrade**	**Comment**	**Discussed in EMF-2103, Rev. 3 Section**
5	Clarification of Single Failure	The documentation of the treatment of single failure within the evaluation model has been upgraded to clarify the approach.	These EM elements of EMF-2103, Revision 3 have been reviewed and approved by the NRC in several LARs, most recently in Reference 1.	Presented in Section A.2.4.1.1.
6	Sampling of Core Power	The methodology has been changed such that core power is treated deterministically using the nominal power plus uncertainty.	These EM elements of EMF-2103, Revision 3 have been reviewed and approved by the NRC in several LARs, most recently in Reference 1.	Presented in Section 3.1.3.2.2.
7	Forslund-Rohsenow Correlation	The Forslund-Rohsenow correlation is no longer used in determining the fuel cladding temperature. For the dispersed flow film boiling regime in the core, Wong-Hochreiter with enhancements replaces the use of Sleicher-Rouse. This alteration was adopted as a model improvement.	These EM elements of EMF-2103, Revision 3 have not yet been reviewed and approved by the NRC. This change was included in EMF-2103, Revision 2 (Reference 2).	Presented in Section 7.6.7.2 and is assessed in Sections 8.2.1, 8.2.4, 8.4.1 and 8.4.4.
8	Rod-to-Rod Radiation	A rod-to-rod radiation model has been incorporated into the methodology and the reflood heat transfer benchmarking has been redone.	These EM elements of EMF-2103, Revision 3 have not yet been reviewed and approved by the NRC. This change was included in EMF-2103, Revision 2 (Reference 2).	Presented in Section 7.6.8.2 and assessed in Sections 8.2.5, 8.5.2.4 and 8.6.2.1.

Changes to RLBLOCA Evaluation Model (EM)				
Item	**Evaluation Model Element**	**Technical Upgrade**	**Comment**	**Discussed in EMF-2103, Rev. 3 Section**
9	Statistical Evaluation	The statistical evaluation has been upgraded, with the application of the Tukey methodology, to provide a multi-variant evaluation.	These EM elements of EMF-2103, Revision 3 have not yet been reviewed and approved by the NRC. This change was included in EMF-2103, Revision 2 (Reference 2).	Presented in Section 9.4.1.
10	Fuel Performance Code	In response to NRC concerns over thermal conductivity degradation, the following change has been made. The COPERNIC fuel performance code has replaced RODEX3A as the source of fuel initial conditions. COPERNIC is NRC approved for application to M5 cladding and Revision 3 will request approval of the limited application of COPERNIC to Zircaloy 4 cladding for LOCA applications.	These EM elements of EMF-2103, Revision 3 have not yet been reviewed and approved by the NRC. This change was included in EMF-2103, Revision 2 (Reference 2).	Presented in Section 7.9 and assessed in Sections 8.3.1, 8.4.8, and 8.5.1.15.
11	Interfacial Drag Package	The interfacial drag package has been modified with improved logic for transition between flow regimes to cover a wider range of experimental data.	These EM elements of EMF-2103, Revision 3 have not yet been reviewed and approved by the NRC. This change was included in EMF-2103, Revision 2 (Reference 2).	Presented in Sections 7.5.2 and 7.5.4.

Changes to RLBLOCA Evaluation Model (EM)				
Item	**Evaluation Model Element**	**Technical Upgrade**	**Comment**	**Discussed in EMF-2103, Rev. 3 Section**
12	Reported Local Cladding Oxidation	The evaluation accounts for the interior transient oxidation of the ruptured cladding and adds the initial corrosion layer to the total transient oxidation for comparison with the maximum local oxidation criteria of 10 CFR 50.46.	These EM elements of EMF-2103, Revision 3 have not yet been reviewed and approved by the NRC. This change was included in EMF-2103, Revision 2 (Reference 2).	Presented in Section 9.2.
13	Treatment of GDC-35	GDC-35 states that the plant shall be able to mitigate design basis accidents with or without off site power available. The methodology does this by determining the most severe condition between these two configurations and then performing the RLBLOCA statistical analysis for the plant with off site power availability set to the most severe condition.	These EM elements of EMF-2103, Revision 3 have not yet been reviewed and approved by the NRC. This change was included in EMF-2103, Revision 2 (Reference 2).	Presented in Section A.2.4.2.
14	Interphase Heat Transfer	The interphase heat transfer for mist flow has been improved to obtain better agreement with separate effects reflood test data.	These EM elements of EMF-2103, Revision 3 have not yet been reviewed and approved by the NRC. This change was included in EMF-2103, Revision 2 (Reference 2).	Presented in Section 7.5.4.

Changes to RLBLOCA Evaluation Model (EM)				
Item	**Evaluation Model Element**	**Technical Upgrade**	**Comment**	**Discussed in EMF-2103, Rev. 3 Section**
15	SG Tube Inlet Interfacial Drag	Modification of the steam generator tube inlet interfacial drag as a result of an error correction to the level tracking model.	These EM elements of EMF-2103, Revision 3 have not yet been reviewed and approved by the NRC.	Presented in Sections 9 and 8.1.5.
16	Grid Spacer Droplet Breakup Heat Transfer Enhancement	A model to increase the heat transfer downstream of a grid spacer due to droplet breakup was added.	These EM elements of EMF-2103, Revision 3 have not yet been reviewed and approved by the NRC.	Presented in Sections 7.5.4.10.1, 8.2.3, and 8.4.1.
17	Fuel Swelling, Rupture, and Relocation (SRR)	A model for SRR based on a statistical approach for geometry and the evaluation of cooling for a fuel rod isolated from other ruptures has been added. This model improves the evaluation of fuel rod rupture during LOCA through a mechanistic approach.	These EM elements of EMF-2103, Revision 3 have not yet been reviewed and approved by the NRC.	Presented in Sections 7.9.3.3 and 8.5.2.11.
18	Steam Absorptivity	A change to the steam absorptivity was made and a conservative limit was set on the pressure in computing the vapor absorption coefficient.	These EM elements of EMF-2103, Revision 3 have not yet been reviewed and approved by the NRC.	Presented in Sections 7.6.8.1 and 8.1.5.
19	Core Nodalization	The core nodalization has been slightly changed to align the node boundaries with the bottom of the grid spacers, rather than the grid centerline.	These EM elements of EMF-2103, Revision 3 have not yet been reviewed and approved by the NRC.	Presented in Sections 9.0 and 8.1.5.

Attachment B

TR Prioritization Scheme Matrix for Metric and Resources			
Title: EMF-2103(P), Revision 3, "Realistic Large Break LOCA Methodology for Pressurized Water Reactors"			
Expect submitting FY	**TAC**	**PM**	**Today's Date: 9/13/2013**
Technical Review Division(s)		**Technical Review Branch(s)**	

Factors	Select the Criteria That the TR Satisfies	Points can be Assigned for Each Criteria	Assigned Points
TR Classification (Select one only)	Resolve Generic Safety Issue (GSI).	6	3
	Emergent NRC Technical Issue.	3	
	New technology improves safety.	2	
	TR Revision reflecting current requirements or analytical methods.	2	
	Standard TR.	1	
TR Applicability (Select one only)	Potential industry-wide applications.	3	2
	Potentially applicable to entire groups of licensees.	2	
	Intended for only partial groups of licensees.	1	
TR Implementation Certainty (Select one only)	Industry-wide Implementation expected.	3	2
	Expected implementation by an entire group of licensees (BWROG, PWROG, BWRVIP, etc.) who sponsored the TR.	2	
	Docketed intent by U.S. plant(s) but no formal LAR schedule yet.	1	
	No U.S. plant(s) have indicated strong intent on docket to implement yet.	0	
Tie to a LAR (Select if applicable)	A SE is requested by a certain date (less than two years) to support a licensing activity or renewal date (note it in Comments).	3	3
Review Progress (Points are cumulative as applicable)	Accepted for review.	0.3	0
	RAI issued.	0.5	0.5
	RAI responded.	1.2	0
	SE drafted.	2.0	0
Management (LT/ET) discretion adjustment		-3 to +3	
Total Points (Add the total points from each factor and total here):			10.5

Comments:

The 3 points for "TR Classification" is justified as the upgrades in EMF-2103(P) responds to all issues the NRC staff has raised on AREVA NP's Realistic LBLOCA methodology dating back to 2007. The upgrade also addresses the 2009 Thermal Conductivity Degradation issue with a more holistic correction through the incorporation of COPERNIC into the S-RELAP5 code.

The 2 points for "TR Applicability" are justified because AREVA NP could apply this methodology in a fuel transition for all PWRs except the B&W design and Westinghouse 2-loop design plants.

The 2 points for "TR Implementation Certainty" is justified as most of the US PWR customers that AREVA NP provides fuel have commitments written into their SERs which approved the use of "EMF-2103(P) Rev. 0 plus Transition Package" that will require the customer to upgrade the analysis of record when the next revision to EMF-2103(P) is approved.

The 3 points for "Tie to a LAR" is justified because Dominion met with the NRC and AREVA NP on July 17 and documented their intent to use EMF-2103(P) Revision 3 to support the Millstone 2 fuel upgrade.

The 0.5 points for "RAIs issued" is justified because RAIs were issued on October 23, 2012 for EMF-2103(P) Revision 2 by NRC Staff Reviewer Yuri Orechwa and forwarded to AREVA NP by Jonathan Rowley via email. The responses to his RAIs were incorporated into Section 9.4 of EMF-2103(P) Revision 3.

AFFIDAVIT

COMMONWEALTH OF VIRGINIA)
) ss.
CITY OF LYNCHBURG)

1. My name is Gayle F. Elliott. I am Manager, Product Licensing, for AREVA NP Inc. (AREVA NP) and as such I am authorized to execute this Affidavit.

2. I am familiar with the criteria applied by AREVA NP to determine whether certain AREVA NP information is proprietary. I am familiar with the policies established by AREVA NP to ensure the proper application of these criteria.

3. I am familiar with the AREVA NP information contained in the topical report titled "EMF-2103(P), Revision 3, 'Realistic Large Break LOCA Methodology for Pressurized Water Reactors'," dated September 2013 and referred to herein as "Document." Information contained in this Document has been classified by AREVA NP as proprietary in accordance with the policies established by AREVA NP for the control and protection of proprietary and confidential information.

4. This Document contains information of a proprietary and confidential nature and is of the type customarily held in confidence by AREVA NP and not made available to the public. Based on my experience, I am aware that other companies regard information of the kind contained in this Document as proprietary and confidential.

5. This Document has been made available to the U.S. Nuclear Regulatory Commission in confidence with the request that the information contained in this Document be withheld from public disclosure. The request for withholding of proprietary information is made in accordance with 10 CFR 2.390. The information for which withholding from disclosure is

requested qualifies under 10 CFR 2.390(a)(4) "Trade secrets and commercial or financial information":

6. The following criteria are customarily applied by AREVA NP to determine whether information should be classified as proprietary:

(a) The information reveals details of AREVA NP's research and development plans and programs or their results.

(b) Use of the information by a competitor would permit the competitor to significantly reduce its expenditures, in time or resources, to design, produce, or market a similar product or service.

(c) The information includes test data or analytical techniques concerning a process, methodology, or component, the application of which results in a competitive advantage for AREVA NP.

(d) The information reveals certain distinguishing aspects of a process, methodology, or component, the exclusive use of which provides a competitive advantage for AREVA NP in product optimization or marketability.

(e) The information is vital to a competitive advantage held by AREVA NP, would be helpful to competitors to AREVA NP, and would likely cause substantial harm to the competitive position of AREVA NP.

The information in the Document is considered proprietary for the reasons set forth in paragraphs 6(c) and 6(d) above.

7. In accordance with AREVA NP's policies governing the protection and control of information, proprietary information contained in this Document has been made available, on a limited basis, to others outside AREVA NP only as required and under suitable agreement providing for nondisclosure and limited use of the information.

8. AREVA NP policy requires that proprietary information be kept in a secured file or area and distributed on a need-to-know basis.

9. The foregoing statements are true and correct to the best of my knowledge, information, and belief.

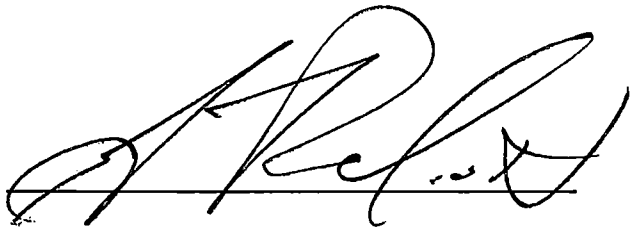

SUBSCRIBED before me this 13th day of September 2013.

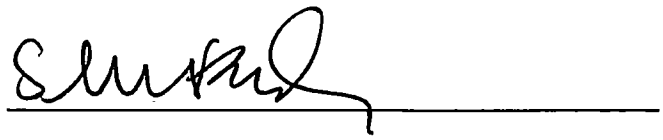

Sherry L. McFaden
NOTARY PUBLIC, COMMONWEALTH OF VIRGINIA
MY COMMISSION EXPIRES: 10/31/2014
Reg.#7079129

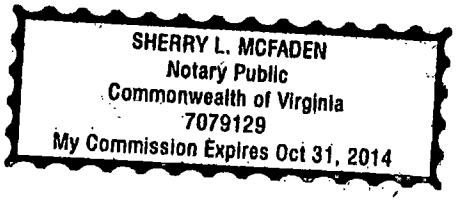

AREVA

January 10, 2014
NRC:14:001

U.S. Nuclear Regulatory Commission
Document Control Desk
11555 Rockville Pike
Rockville, MD 20852

Document to Support the NRC review of EMF-2103P, Revision 3, "Realistic Large Break LOCA Methodology for Pressurized Water Reactors"

Ref. 1: Letter, Pedro Salas (AREVA Inc.) to Document Control Desk (NRC), "Request for Review and Approval of EMF-2103P, Revision 3, 'Realistic Large Break LOCA Methodology for Pressurized Water Reactors'," NRC:13:072, September 13, 2013.

Ref. 2: Letter, Pedro Salas (AREVA Inc.) to Document Control Desk (NRC), "Information to Support the Request for Review and Approval of EMF-2103P, Revision 2, 'Realistic Large Break LOCA Methodology for Pressurized Water Reactors'," NRC:11:067, June 30, 2011.

In Reference 1, AREVA Inc. (AREVA) requested NRC's review and approval of the topical report EMF-2103P, Revision 3, "Realistic Large Break LOCA Methodology for Pressurized Water Reactors." During the post-submittal meeting held between AREVA and the NRC on October 31, 2013, the NRC requested additional information to support the review process of EMF-2103P, Revision 3; specifically, the NRC requested a copy of EMF-2100P, Revision 16, "S-RELAP5 Models and Correlations Code Manual."

In support of this request for additional information, a copy of EMF-2100P, Revision 16, "S-RELAP5 Models and Correlations Code Manual" is enclosed with this letter, which includes a summary of changes since AREVA provided Revision 14 in Reference 2 (Attachment A).

AREVA considers the material contained in the enclosed document to be proprietary. As required by 10 CFR 2.390(b), an affidavit is enclosed to support the withholding of the information from public disclosure. Only a proprietary version of the document is provided since it is considered proprietary in its entirely.

There are no commitments contained within the enclosures to this letter.

If you have any questions related to this submittal, please contact Ms. Gayle F. Elliott, Product Licensing Manager at 434-832-3347 or by e-mail at Gayle.Elliott@areva.com.

Sincerely,

Pedro Salas, Director
Regulatory Affairs
AREVA Inc.

cc: J. A. Golla
Project 728

Enclosures:

1. EMF-2100P, Revision 16,"S-RELAP5 Models and Correlations Code Manual," December 2011
2. Notarized Affidavit

Attachment:

1. Changes to Topical Report, EMF-2100, Revisions 15 and 16 subsequent to Revision 14

ATTACHMENT A
Changes to Topical Report, EMF-2100, Revisions 15 and 16 subsequent to Revision 14

Rev. 15 changes:

Item	Page	Description and Justification
1.	1-3	Modify item (5) to include droplet shatter cooling in conjunction with swelling and rupture.
2.	1-4	Modify item (10) to include fuel relocation with swelling and rupture.
3.	3-67 to 3-69	Added droplets shatter model discussion to 'Special Treatments' section.
4.	7-20	Added fuel relocation discussion.
5.	7-52	Corrected definitions of reacted zirconium thickness.
6.	7-96	Clarified definition of cladding deformation.

Rev. 16 changes:

Item	Page	Description and Justification
1.	2-65	Modify the criteria for water-packing scheme.
2.	3-11	Modify description of mixture level elimination.
3.	3-59	Typographical error correction.
4.	3-67 to 3-73	Inserted subsection headers for clarity.
5.	4-4	Included void criteria in Figure 4-1.
6.	4-24 to 4-30	Add Section 4.4.3 XL Correlations.
7.	4-30	Revised temperature correction factor (Equation 4.56).
8.	4-37	Revised temperature correction factor (Equation 4.77).
9.	4-38	Modify description of grid spacer enhancement.
10.	7-22 to 7-23	Revised and relocated fuel relocation section.
11.	7-95 to 7-96	Modified description of ballooning and rupture model for COPERNIC fuel model.

AFFIDAVIT

COMMONWEALTH OF VIRGINIA)
) ss.
CITY OF LYNCHBURG)

1. My name is Gayle F. Elliott. I am Manager, Product Licensing, for AREVA NP Inc. (AREVA NP) and as such I am authorized to execute this Affidavit.

2. I am familiar with the criteria applied by AREVA NP to determine whether certain AREVA NP information is proprietary. I am familiar with the policies established by AREVA NP to ensure the proper application of these criteria.

3. I am familiar with the AREVA NP information contained in EMF-2100P, Revision 16, "S-RELAP5 Models and Correlations Code Manual," dated December 2011, and referred to herein as "Document." Information contained in this Document has been classified by AREVA NP as proprietary in accordance with the policies established by AREVA NP for the control and protection of proprietary and confidential information.

4. This Document contains information of a proprietary and confidential nature and is of the type customarily held in confidence by AREVA NP and not made available to the public. Based on my experience, I am aware that other companies regard information of the kind contained in this Document as proprietary and confidential.

5. This Document has been made available to the U.S. Nuclear Regulatory Commission in confidence with the request that the information contained in this Document be withheld from public disclosure. The request for withholding of proprietary information is made in accordance with 10 CFR 2.390. The information for which withholding from disclosure is

requested qualifies under 10 CFR 2.390(a)(4) "Trade secrets and commercial or financial information."

6. The following criteria are customarily applied by AREVA NP to determine whether information should be classified as proprietary:

(a) The information reveals details of AREVA NP's research and development plans and programs or their results.

(b) Use of the information by a competitor would permit the competitor to significantly reduce its expenditures, in time or resources, to design, produce, or market a similar product or service.

(c) The information includes test data or analytical techniques concerning a process, methodology, or component, the application of which results in a competitive advantage for AREVA NP.

(d) The information reveals certain distinguishing aspects of a process, methodology, or component, the exclusive use of which provides a competitive advantage for AREVA NP in product optimization or marketability.

(e) The information is vital to a competitive advantage held by AREVA NP, would be helpful to competitors to AREVA NP, and would likely cause substantial harm to the competitive position of AREVA NP.

The information in this Document is considered proprietary for the reasons set forth in paragraphs 6(c) and 6(d) above.

7. In accordance with AREVA NP's policies governing the protection and control of information, proprietary information contained in this Document has been made available, on a limited basis, to others outside AREVA NP only as required and under suitable agreement providing for nondisclosure and limited use of the information.

8. AREVA NP policy requires that proprietary information be kept in a secured file or area and distributed on a need-to-know basis.

9. The foregoing statements are true and correct to the best of my knowledge, information, and belief.

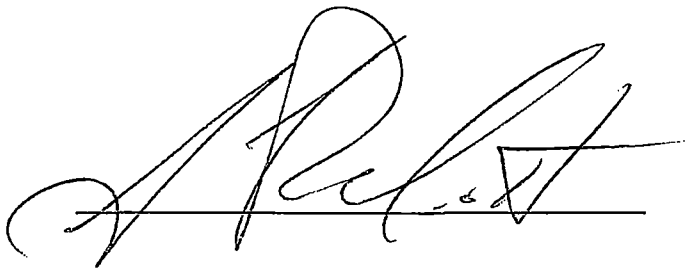

SUBSCRIBED before me this 10th

day of January, 2014.

Sherry L. McFaden
NOTARY PUBLIC, COMMONWEALTH OF VIRGINIA
MY COMMISSION EXPIRES: 10/31/14
Reg. # 7079129

SHERRY L. MCFADEN
Notary Public
Commonwealth of Virginia
7079129
My Commission Expires Oct 31, 2014

November 20, 2014

Mr. Pedro Salas, Manager
Corporate Regulatory Affairs
AREVA NP Inc.
3315 Old Forest Road
P.O. Box 10395
Lynchburg, VA 24506-0935

SUBJECT: REQUEST FOR ADDITIONAL INFORMATION RE: AREVA NP, INC. (AREVA) TOPICAL REPORT EMF-2103(P), REVISION 3, "REALISTIC LARGE BREAK LOCA [LOSS-OF-COOLANT ACCIDENT] METHODOLOGY FOR PRESSURIZED WATER REACTORS" (TAC NO. MF2904)

Dear Mr. Salas:

By letter dated September 13, 2013 (Agencywide Documents Access and Management System Accession No. ML13283A220), AREVA submitted for U.S. Nuclear Regulatory Commission (NRC) staff review Topical Report EMF-2103(P), Revision 3, "Realistic Large Break LOCA Methodology for Pressurized Water Reactors." Upon review of the information provided, the NRC staff has determined that additional information is needed to complete the review. On October 30, 2014, Gayle Elliott, AREVA Product Licensing Manager, and I agreed that the NRC staff will receive the response to the enclosed Request for Additional Information (RAI) questions within 90 days from the date of this letter.

If you have any questions regarding the enclosed RAI questions, please contact me at 301-415-4053.

Sincerely,

/RA/

Jonathan G. Rowley, Project Manager
Licensing Processes Branch
Division of Policy and Rulemaking
Office of Nuclear Reactor Regulation

Project No. 728

Enclosures:
1. RAI questions (Non-Proprietary)
2. RAI questions (Proprietary)

NOTICE: Enclosure 2 transmitted herewith contains Proprietary Information. When separated from Enclosure 2, this transmittal document is decontrolled.

Mr. Pedro Salas, Manager
Corporate Regulatory Affairs
AREVA NP Inc.
3315 Old Forest Road
P.O. Box 10395
Lynchburg, VA 24506-0935

SUBJECT: REQUEST FOR ADDITIONAL INFORMATION RE: AREVA NP, INC. (AREVA) TOPICAL REPORT EMF-2103(P), REVISION 3, "REALISTIC LARGE BREAK LOCA [LOSS-OF-COOLANT ACCIDENT] METHODOLOGY FOR PRESSURIZED WATER REACTORS" (TAC NO. MF2904)

Dear Mr. Salas:

By letter dated September 13, 2013 (Agencywide Documents Access and Management System Accession No. ML13283A220), AREVA submitted for U.S. Nuclear Regulatory Commission (NRC) staff review Topical Report EMF-2103(P), Revision 3, "Realistic Large Break LOCA Methodology for Pressurized Water Reactors." Upon review of the information provided, the NRC staff has determined that additional information is needed to complete the review. On October 30, 2014, Gayle Elliott, AREVA Product Licensing Manager, and I agreed that the NRC staff will receive the response to the enclosed Request for Additional Information (RAI) questions within 90 days from the date of this letter.

If you have any questions regarding the enclosed RAI questions, please contact me at 301-415-4053.

Sincerely,

/RA/

Jonathan G. Rowley, Project Manager
Licensing Processes Branch
Division of Policy and Rulemaking
Office of Nuclear Reactor Regulation

Project No. 728

Enclosures:
1. RAI questions (Non-Proprietary)
2. RAI questions (Proprietary)

NOTICE: Enclosure 2 transmitted herewith contains Proprietary Information. When separated from Enclosure 2, this transmittal document is decontrolled.

DISTRIBUTION:
See next page

ADAMS Accession Nos. ML14303A372 (Package); ML14303A377 (Cover letter); ML14303A385 (Prop RAIs); ML14303A382 (Non-Prop RAIs) **NRR-106**

OFFICE	PLPB/PM	PLPB/LA	SNPB/BC	PLPB/BC	PLPB/PM
NAME	JRowley	DHarrison	JDean	AMendiola	JRowley
DATE	10/30/14	11/5/14	11/18/14	11/20/14	11/20/14

OFFICIAL RECORD COPY

Letter to Pedro Salas from Jonathan Rowley dated November 20, 2014

SUBJECT: REQUEST FOR ADDITIONAL INFORMATION RE: AREVA NP, INC. TOPICAL REPORT EMF-2103(P), REVISION 3, "REALISTIC LARGE BREAK LOCA METHODOLOGY FOR PRESSURIZED WATER REACTORS" (TAC NO. MF2904)

DISTRIBUTION:
PUBLIC
RidsNrrDpr
JRowley
RidsNrrDss
LWard
RidsNrrDprPlpb
RidsNroOd
RidsNrrDssSnpb
JDean
BParks
RidsNrrLADHarrision
RidsOgcMailCenter
RidsAcrsAcnwMailCenter
RidsResOd
JLehning

January 16, 2015
NRC:15:001

U.S. Nuclear Regulatory Commission
Document Control Desk
11555 Rockville Pike
Rockville, MD 20852

Response to Request for Additional Information Regarding EMF-2103(P), Revision 3, "PWR Realistic Large Break LOCA Methodology for Pressurized Water Reactors"

Ref. 1: Letter, Pedro Salas (AREVA NP Inc.) to Document Control Desk (NRC), "Request for Review and Approval of EMF-2103(P), Revision 3, "PWR Realistic Large Break LOCA Methodology for Pressurized Water Reactors," NRC:13:072, September 13, 2013.

Ref. 2: Letter, Jonathan G. Rowley (NRC) to Pedro Salas (AREVA NP Inc.), "Request for additional information RE : AREVA NP Inc. (AREVA), Topical Report EMF-2103(P), Revision 3, "Realistic Large Break LOCA Methodology for Pressurized Water Reactors," (TAC NO. MF2904), November 20, 2014.

Ref. 3: Letter, Pedro Salas (AREVA Inc.) to Document Control Desk (NRC), "Errata Document to Support the NRC review of EMF-2103P, Revision 3, 'Realistic Large Break LOCA Methodology for Pressurized Water Reactors'," NRC:15:005, January 16, 2015.

AREVA Inc. (AREVA) requested the NRC's review and approval of the topical report EMF-2103(P), Revision 3, "PWR Realistic Large Break LOCA Methodology for Pressurized Water Reactors" in Reference 1. The NRC provided a Request for Additional Information (RAI) in Reference 2. The response to this RAI is enclosed with this letter.

Note that the response to RAI 20, 21, and 25 refer to the revised sample problems in the Appendix B of Topical Report EMF-2103, Revision 3. The revised sample problems set are provided in the ERRATA Letter submitted to the NRC in Reference 3.

AREVA considers some of the information contained in the enclosed document to be proprietary. As required by 10 CFR 2.390(b) an affidavit is enclosed to support the withholding of the information from public disclosure. Proprietary and non-proprietary versions of the RAI responses are enclosed.

Also enclosed with this letter is a compact disc. This CD is labeled "EMF-2103, Rev. 3 RAI-6 Additional Plots," and contains .eps files for additional FLECHT-SEASET cases as part of the RAI 6 response, as well as a PDF file describing what is on the disc.

Also enclosed with this letter are markups of EMF-2103, Revision 3 due to RAI responses. Proprietary and non-Proprietary versions of the markups to EMF-2103, Revision 3 are enclosed.

If you have any questions related to this information, please contact Gayle F. Elliott, Product Licensing Manager, by telephone at (434) 832-3347, or by e-mail at Gayle.Elliott@areva.com.

Sincerely,

Pedro Salas, Director
Licensing and Regulatory Affairs
AREVA Inc.

cc: J. G. Rowley
Project 728

Enclosures:

1. Proprietary version of "Response to NRC Request for Additional Information (RAI) Related to EMF-2103, 'PWR Realistic Large Break LOCA Methodology for Pressurized Water Reactors'."
2. Non-Proprietary version of "Response to NRC Request for Additional Information (RAI) Related to EMF-2103, 'PWR Realistic Large Break LOCA Methodology for Pressurized Water Reactors'."
3. Notarized Affidavit
4. Disc labeled "EMF-2103, Rev. 3 RAI-6 Additional Plots" containing additional plots
5. Markups to EMF-2103, Revision 3 due to RAI responses – Proprietary
6. Markups to EMF-2103, Revision 3 due to RAI responses – Non-Proprietary

AREVA

January 16, 2015
NRC:15:005

U.S. Nuclear Regulatory Commission
Document Control Desk
11555 Rockville Pike
Rockville, MD 20852

Errata and Revised Sample Problems for EMF-2103P, Revision 3, "Realistic Large Break LOCA Methodology for Pressurized Water Reactors"

Ref. 1: Letter, Pedro Salas (AREVA NP Inc.) to Document Control Desk (NRC), "Request for Review and Approval of EMF-2103P, Revision 3, "Realistic Large Break LOCA Methodology for Pressurized Water Reactors'," NRC:13:072, September 13, 2013

AREVA Inc. (AREVA) requested the NRC's review and approval of the topical report EMF-2103P, Revision 3, "Realistic Large Break LOCA Methodology for Pressurized Water Reactors" in Reference 1. Enclosed are revised pages to be inserted into EMF-2103(P) Revision 3. The revisions to these pages were developed to rectify minor editorial changes in the body of the document, and corrections to equations.

Sample problems were rerun to address condition reports that have been identified since the sample problems were last executed. The revised sample problems calculation results are provided in the attachments. The revised pages will be included in the approved versions of the proprietary and non-proprietary topical reports, which will be issued following NRC approval of the topical report. The revised pages do contain both proprietary and non-proprietary information, and are both enclosed as attachments.

AREVA considers some of the information contained in the enclosed document to be proprietary. As required by 10 CFR 2.390(b) an affidavit is enclosed to support the withholding of the information from public disclosure. Proprietary and non-proprietary versions of the document are enclosed.

If you have any questions related to this information, please contact Ms. Gayle F. Elliott, Product Licensing manager by telephone at (434) 832-3347, or by e-mail at Gayle.Elliott@areva.com.

Sincerely,

Pedro Salas, Director
Licensing and Regulatory Affairs
AREVA Inc.

cc: J. G. Rowley
Project 728

AREVA INC.

3315 Old Forest Road, Lynchburg, VA 24501
Tel.: 434 832 3000 - www.areva.com

Enclosures:

1. Proprietary version of EMF-2103P, Revision 3, "Realistic Large Break LOCA Methodology for Pressurized Water Reactors" Errata
2. Non-Proprietary version of EMF-2103P, Revision 3, "Realistic Large Break LOCA Methodology for Pressurized Water Reactors" Errata
3. Notarized Affidavit

January 5, 2016

Mr. Gary Peters, Director
Licensing and Regulatory Affairs
AREVA Inc.
3315 Old Forest Road
Lynchburg, VA 24501

SUBJECT: REQUEST FOR ADDITIONAL INFORMATION RE: AREVA NP, INC. TOPICAL REPORT EMF-2103(P), REVISION 3, "REALISTIC LARGE BREAK LOCA METHODOLOGY FOR PRESSURIZED WATER REACTORS" (TAC NO. MF2904)

Dear Mr. Peters:

By letter dated September 13, 2013 (Agencywide Documents Access and Management System Accession (ADAMS) No. ML13283A220), AREVA NP, Inc. (AREVA) submitted for U.S. Nuclear Regulatory Commission (NRC) staff review Topical Report EMF-2103(P), Revision 3, "Realistic Large Break LOCA [loss-of-coolant accident] Methodology for Pressurized Water Reactors." Upon review of the information provided, the NRC staff has determined that additional information is needed to complete the review.

Additionally, clarification is needed to the responses to previously issued Request for Additional Information (RAI) questions submitted by letter dated November 20, 2015 (ADAMS Accession No. ML14303A377).

On December 14, 2015, Gayle Elliott, AREVA Product Licensing Manager, and I agreed that the NRC staff will receive the response to the enclosed RAI questions within 30 days from the date of this letter.

NOTICE: The Enclosure transmitted herewith contains Proprietary Information. When separated from the Enclosure, this transmittal document is decontrolled.

If you have any questions regarding the enclosed RAI questions, please contact me at 301-415-4053.

Sincerely,

/RA/

Jonathan G. Rowley, Project Manager
Licensing Processes Branch
Division of Policy and Rulemaking
Office of Nuclear Reactor Regulation

Project No. 728

Enclosure:
RAI questions (Proprietary)

If you have any questions regarding the enclosed RAI questions, please contact me at 301-415-4053.

Sincerely,

/RA/

Jonathan G. Rowley, Project Manager
Licensing Processes Branch
Division of Policy and Rulemaking
Office of Nuclear Reactor Regulation

Project No. 728

Enclosure:
RAI questions (Proprietary)

DISTRIBUTION:

PUBLIC	RidsNrrDpr	JRowley	RidsNrrDss
LWard	RidsNrrDprPlpb	RidsNroOd	RidsNrrDssSnpb
JDean	BParks	RidsNrrLADHarrison	RidsOgcMailCenter
RidsACRS_MailCTR	RidsResOd	JLehning	

ADAMS Accession Nos.: ML15348A132 (Package); ML15348A140 (Letter); ML15348A145 (Prop RAIs); *concurred via e-mail **NRR-106**

OFFICE	PLPB/PM	PLPB/LA*	SNPB/BC	PLPB/BC	PLPB/PM
NAME	JRowley	DHarrison	(JWhitman for) JDean	KHsueh	JRowley
DATE	12/14/2015	12/22/2015	12/30/2015	01/04/2016	01/05/2016

OFFICIAL RECORD COPY

AREVA

February 16, 2016
NRC:16:005

U.S. Nuclear Regulatory Commission
Document Control Desk
11555 Rockville Pike
Rockville, MD 20852

Response to First and Second Request for Additional Information Regarding EMF-2103(P), Revision 3, "PWR Realistic Large Break LOCA Methodology for Pressurized Water Reactors"

AREVA Inc. (AREVA) requested the NRC's review and approval of the topical report EMF-2103(P), Revision 3, "PWR Realistic Large Break LOCA Methodology for Pressurized Water Reactors" in Reference 1. The NRC provided an initial Request for Additional Information (RAI) in Reference 2, and a second RAI in Reference 3. The combined response to these RAIs is provided in the enclosed document.

Please note that the responses to RAI questions 1 through 26 were previously submitted in Reference 4. Any changes to these previous responses are identified in the enclosed RAI response.

AREVA considers some of the information contained in the enclosed document to be proprietary. As required by 10 CFR 2.390(b), an affidavit is enclosed to support the withholding of the information from public disclosure. Proprietary and non-proprietary versions of the RAI responses are attached.

A complete set of proposed marked-up pages for the submitted topical report, inclusive of those previously sent in Reference 4, will be sent under a separate letter targeting February 19 for release.

If you have any questions related to this information, please contact Morris E. Byram, Product Licensing Manager, by telephone at (434) 832-4665, or by e-mail at Morris.Byram@areva.com.

Sincerely,

Gary Peters, Director
Licensing and Regulatory Affairs
AREVA Inc.

cc: J. G. Rowley
Project 728

AREVA INC.

3315 Old Forest Road, Lynchburg, VA 24501
Tel.: 434 832 3000 - www.areva.com

Ref. 1: Letter, Pedro Salas (AREVA NP Inc.) to Document Control Desk (NRC), "Request for Review and Approval of EMF-2103(P), Revision 3, 'PWR Realistic Large Break LOCA Methodology for Pressurized Water Reactors'," NRC:13:072, September 13, 2013.

Ref. 2: Letter, Jonathan G. Rowley (NRC) to Pedro Salas (AREVA NP Inc.), "Request for additional information RE : AREVA NP Inc. (AREVA), Topical Report EMF-2103(P), Revision 3, 'Realistic Large Break LOCA Methodology for Pressurized Water Reactors'," November 20, 2014.

Ref. 3: Letter, Jonathan G. Rowley (NRC) to Gary Peters (AREVA NP Inc.), "Request for Additional Information Related to Review of AREVA NP Licensing Topical Report EMF-2103 Revision 3, 'Realistic Large Break LOCA Methodology for Pressurized Water Reactors'," January 13, 2016.

Ref. 4: Letter, Pedro Salas (AREVA NP Inc.) to Document Control Desk (NEC), "Response to Request for Additional Information Regarding EMF-2103(P), Revision 3, 'PWR Realistic Large Break LOCA Methodology for Pressurized Water Reactors'," January 16, 2015.

Enclosures:

1. EMF-2103R3Q1P, Revision 0, Proprietary version of "Response to First and Second Requests for Additional Information for EMF-2103(P), Revision 3, ' Realistic Large Break LOCA Methodology for Pressurized Water Reactors'," February 2016.
2. EMF-2103R3Q1NP, Revision 0, Non-Proprietary version of "Response to First and Second Requests for Additional Information for EMF-2103(P), Revision 3, ' Realistic Large Break LOCA Methodology for Pressurized Water Reactors'," February 2016.
3. Notarized Affidavit

AREVA

February 19, 2016
NRC:16:006

U.S. Nuclear Regulatory Commission
Document Control Desk
11555 Rockville Pike
Rockville, MD 20852

Revised Pages for EMF-2103(P), Revision 3, "Realistic Large Break LOCA Methodology for Pressurized Water Reactors"

Ref. 1: Letter, Pedro Salas (AREVA NP Inc.) to Document Control Desk (NRC), "Request for Review and Approval of EMF-2103(P), Revision 3, 'PWR Realistic Large Break LOCA Methodology for Pressurized Water Reactors'," NRC:13:072, September 13, 2013.

Ref. 2: Letter, Gary Peters (AREVA NP Inc.) to Document Control Desk (NRC), "Response to First and Second Request for Additional Information Regarding EMF-2103(P), Revision 3, 'PWR Realistic Large Break LOCA Methodology for Pressurized Water Reactors'," February 16, 2016.

Ref. 3: Letter, Pedro Salas (AREVA NP Inc.) to Document Control Desk (NEC), "Errata and Revised Sample Problems for EMF-2103P, Revision 3, 'Realistic Large Break LOCA Methodology for Pressurized Water Reactors'," January 16, 2015.

AREVA Inc. (AREVA) requested the NRC's review and approval of the topical report EMF-2103(P), Revision 3, "PWR Realistic Large Break LOCA Methodology for Pressurized Water Reactors" in Reference 1. AREVA provided a complete set of RAI (Request for Additional Information) responses for this Reference 1 submittal in Reference 2.

A complete set of EMF-2103(P), Revision 3 marked-up pages is enclosed. The enclosed marked-up pages incorporate those previously submitted in Reference 3. The markups also include minor text corrections, including corrections to typographical errors and text inconsistencies. The initial page of the enclosure lists the changes and the nature of the changes to aid in the NRC's review.

AREVA considers some of the information contained in the enclosed document to be proprietary. As required by 10 CFR 2.390(b), an affidavit is enclosed to support the withholding of the information from public disclosure. Proprietary and Non-Proprietary versions of the marked-up pages are attached.

If you have any questions related to this information, please contact Morris E. Byram, Product Licensing Manager, by telephone at (434) 832-4665, or by e-mail at Morris.Byram@areva.com.

Sincerely,

Gary Peters, Director
Licensing and Regulatory Affairs
AREVA Inc.

cc: J. G. Rowley
Project 728

Enclosures:

1. Proprietary version of EMF-2103(P), Revision 3, "Realistic Large Break LOCA Methodology for Pressurized Water Reactors," Revised Pages.
2. Non-Proprietary version of EMF-2103(P), Revision 3, "Realistic Large Break LOCA Methodology for Pressurized Water Reactors," Revised Pages.
3. Notarized Affidavit

AREVA

Response to First and Second Request for Additional Information

EMF-2103R3Q1NP
Revision 0

EMF-2103 (P), Revision 3, "Realistic Large Break LOCA Methodology for Pressurized Water Reactors"

February 2016

AREVA Inc.

(c) 2016 AREVA Inc.

Nature of Changes

Item	Section(s) or Page(s)	Description and Justification
1	All	Initial Issue

Contents

Page

1.0 INTRODUCTION AND SUMMARY 1-1

2.0 REQUESTS FOR ADDITIONAL INFORMATION AND RESPONSES 2-1

2.1 RAI 1: 2-1
2.1.1 Statement of RAI 1 2-1
2.1.2 Response to RAI 1 2-1

2.2 RAI 2: 2-6
2.2.1 Statement of RAI 2 2-6
2.2.2 Response to RAI 2 2-8

2.3 RAI 3: 2-10
2.3.1 Statement of RAI 3 2-10
2.3.2 Response to RAI 3 2-10

2.4 RAI 4: 2-15
2.4.1 Statement of RAI 4 2-15
2.4.2 Response to RAI 4 2-15

2.5 RAI 5: 2-25
2.5.1 Statement of RAI 5 2-25
2.5.2 Response to RAI 5 2-25

2.6 RAI 6: 2-29
2.6.1 Statement of RAI 6 2-29
2.6.2 Response to RAI 6 2-30

2.7 RAI 7: 2-84
2.7.1 Statement of RAI 7 2-84
2.7.2 Response to RAI 7 2-84

2.8 RAI 8: 2-98
2.8.1 Statement of RAI 8 2-98
2.8.2 Response to RAI 8 2-99

2.9 RAI 9: 2-105
2.9.1 Statement of RAI 9 2-105
2.9.2 Response to RAI 9 2-105

2.10 RAI 10: 2-111
2.10.1 Statement of RAI 10 2-111
2.10.2 Response to RAI 10 2-111

2.11 RAI 11: 2-113
2.11.1 Statement of RAI 11 2-113
2.11.2 Response to RAI 11 2-113
2.12 RAI 12: 2-124
2.12.1 Statement of RAI 12 2-124
2.12.2 Response to RAI 12 2-124
2.13 RAI 13: 2-130
2.13.1 Statement of RAI 13 2-130
2.13.2 Response to RAI 13 2-130
2.14 RAI 14: 2-134
2.14.1 Statement of RAI 14 2-134
2.14.2 Response to RAI 14 2-134
2.15 RAI 15: 2-136
2.15.1 Statement of RAI 15 2-136
2.15.2 Response to RAI 15 2-136
2.16 RAI 16: 2-141
2.16.1 Statement of RAI 16 2-141
2.16.2 Response to RAI 16 2-141
2.17 RAI 17: 2-143
2.17.1 Statement of RAI 17 2-143
2.17.2 Response to RAI 17 2-143
2.18 RAI 18: 2-145
2.18.1 Statement of RAI 18 2-145
2.18.2 Response to RAI 18 2-145
2.19 RAI 19: 2-157
2.19.1 Statement of RAI 19 2-157
2.19.2 Response to RAI 19 2-157
2.20 RAI 20: 2-284
2.20.1 Statement of RAI 20 2-284
2.20.2 Response to RAI 20 2-284
2.21 RAI 21: 2-287
2.21.1 Statement of RAI 21 2-287
2.21.2 Response to RAI 21 2-290
2.21.3 Statement of Follow-Up to RAI 21 2-297
2.21.4 Response to Follow-up on RAI 21 2-298
2.22 RAI 22: 2-302
2.22.1 Statement of RAI 22 2-302

2.22.2 Statement of Follow-up on RAI 22 2-303
2.22.3 Response to RAI 22 2-304
2.23 RAI 23: 2-306
2.23.1 Statement of RAI 23 2-306
2.23.2 Follow-up on RAI 23 2-307
2.23.3 Response to RAI 23 2-308
2.24 Self-Initiated RAI 24: 2-313
2.24.1 Statement of RAI 24 2-313
2.24.2 Response to RAI 24 2-313
2.25 Self-Initiated RAI 25: 2-324
2.25.1 Statement of RAI 25 2-324
2.25.2 Response to RAI 25 2-324
2.26 Self-Initiated RAI 26: 2-330
2.26.1 Statement of RAI 26 2-330
2.26.2 Response to RAI 26 2-330
2.27 RAI 27: 2-332
2.27.1 Statement of RAI 27 2-332
2.27.2 Response to RAI 27 2-332
2.28 RAI 28: 2-338
2.28.1 Statement of RAI 28 2-338
2.28.2 Response to RAI 28 2-338
2.29 RAI 29: 2-346
2.29.1 Statement of RAI 29 2-346
2.29.2 Response to RAI 29 2-346
2.30 RAI 30: 2-349
2.30.1 Statement of RAI 30 2-349
2.30.2 Response to RAI 30 2-349
2.31 RAI 31: 2-352
2.31.1 Statement of RAI 31 2-352
2.31.2 Response to RAI 31 2-352
2.32 RAI 32: 2-360
2.32.1 Statement of RAI 32 2-360
2.32.2 Response to RAI 32 2-360
2.33 Self-Initiated RAI 33: 2-362
2.33.1 Statement of RAI 33 2-362
2.33.2 Response to RAI 33 2-362

2.34 Self-Initiated RAI 34: 2-364
2.34.1 Statement of RAI 34 2-364
2.34.2 Response to RAI 34 2-364
2.35 Self-Initiated RAI 35: 2-373
2.35.1 Statement of RAI 35 2-373
2.35.2 Response to RAI 35 2-373
3.0 REFERENCES 3-1

List of Tables

Table 2.1-1 Uncertainty Parameters and PDFs 2-4
Table 2.6-1 FLECHT SEASET, FLECHT Skewed Test Conditions 2-31
Table 2.6-2 Description of Delivered Parameters 2-32
Table 2.6-3 FLECHT SEASET Grid Elevations 2-33
Table 2.6-4 Cosine Profile Tests Heated Length Nodalization 2-34
Table 2.7-1 Uncertainty Parameters Ranges for CCTF Run 62 Uncertainty Analysis 2-89
Table 2.7-2 Summary of Random Sampled Values for the [ ] Cases in CCTF Test C2-4 Run 62 Uncertainty Analysis 2-90
Table 2.9-1 CE Heat Structures Subject to [ ] 2-107
Table 2.18-1 Comparison of 95/95 Limiting Cases 2-148
Table 2.18-2 Ranking of Top 5 Cases 2-154
Table 2.20-1 Comparison of Limiting Values LOOP vs. No LOOP 2-285
Table 2.21-1 Case Summary of Compliance with 10 CFR 50.46 2-291
Table 2.21-2 Characterization of 95/95 Set 2-291
Table 2.21-3 Numerical Examples of Results for Hypothetical Top 10 Cases 2-299
Table 2.21-4 Numerical Examples of Ranked Results for Hypothetical Top 10 Cases 2-300
Table 2.25-1 Overall Case PCT Comparison with and without T_g* Limitation 2-326
Table 2.28-1 Case Summary – W3 Sample Problem (PCT Rod) 2-342
Table 2.28-2 Results of Sensitivity Study (PCT Rod) 2-343
Table 2.34-1 FILMBL and DFFBHTC Heat Transfer Multipliers 2-367
Table 2.35-1 FILMBL and DFFBHTC Heat Transfer Multipliers 2-374
Table 2.35-2 PDF of FILMBL Heat Transfer Multiplier 2-374
Table 2.35-3 PDF of DFFBHTC Heat Transfer Multiplier 2-375
Table 2.35-4 FILMBL and DFFBHTC Heat Transfer Multipliers Used 2-376

List of Figures

Figure 2.3-1 Trend of Function [ ] 2-12
Figure 2.3-2 Comparison of PCT Function of Test Elevation [ ] 2-13
Figure 2.3-3 Comparison of PCT at 78 inch Elevation [ ] 2-14
Figure 2.4-1 Comparison of [ ] functions 2-18
Figure 2.4-2 Comparison of PCT Function of Test Elevation S-RELAP5 [ ] 2-19
Figure 2.4-3 Comparison of PCT at 78 inch Elevation S-RELAP5 [ ] 2-20
Figure 2.4-4 Trend of Function [ ] 2-22
Figure 2.4-5 Comparison of PCT Function of Test Elevation S-RELAP5 [ ] 2-23
Figure 2.4-6 Comparison of PCT at 78 inch Elevation S-RELAP5 [ ] 2-24
Figure 2.5-1 Comparison of PCT Function of Test Elevation (Minimum Droplet Size Sensitivity) 2-26
Figure 2.5-2 Comparison of PCT at 78 inch Elevation (Minimum Droplet Size Sensitivity) 2-27
Figure 2.6-1 FLECHT SEASET 31504 Convective HTC to vapor at PCT location (node 10) 2-35
Figure 2.6-2 FLECHT SEASET 31504 Interphase surface area multiplier at PCT location (node 10) 2-36
Figure 2.6-3 FLECHT SEASET 31504 Two-phase enhancement multiplier at PCT location (node 10) 2-37
Figure 2.6-4 FLECHT SEASET 31504 Radiation to vapor HTC at PCT location (node 10) 2-38
Figure 2.6-5 FLECHT SEASET 31504 Radiation to liquid HTC at PCT location (node 10) 2-39
Figure 2.6-6 FLECHT SEASET 31504 Vapor side interfacial HTC at PCT location (node 10) 2-40

Figure 2.6-7 FLECHT SEASET 31504 Droplet density at PCT location (node 10) 2-41
Figure 2.6-8 FLECHT SEASET 31504 Liquid and vapor temperatures at PCT location (node 10) 2-42
Figure 2.6-9 FLECHT SEASET 31504 Droplet diameter at PCT location (node 10) 2-43
Figure 2.6-10 FLECHT SEASET 31504 Rod to rod radiation HTC at PCT location (node 10) 2-44
Figure 2.6-11 FLECHT SEASET 31504 Fraction of Convection and Radiation at PCT location (node 10) 2-45
Figure 2.6-12 FLECHT SEASET 31504 Cladding temperature at PCT location (node 10) 2-46
Figure 2.6-13 FLECHT SEASET 31504 Liquid fraction at PCT location (node 10) 2-47
Figure 2.6-14 FLECHT SEASET 31504 Convective HTC to vapor below grid (node 12) 2-48
Figure 2.6-15 FLECHT SEASET 31504 Interphase surface area multiplier below grid (node 12) 2-49
Figure 2.6-16 FLECHT SEASET 31504 Two-phase enhancement multiplier below grid (node 12) 2-50
Figure 2.6-17 FLECHT SEASET 31504 Radiation to vapor HTC below grid (node 12) 2-51
Figure 2.6-18 FLECHT SEASET 31504 Radiation to liquid HTC below grid (node 12) 2-52
Figure 2.6-19 FLECHT SEASET 31504 Vapor side interfacial HTC below grid (node 12) 2-53
Figure 2.6-20 FLECHT SEASET 31504 Droplet density below grid (node 12)..... 2-54
Figure 2.6-21 FLECHT SEASET 31504 Liquid and vapor temperatures below grid (node 12) 2-55
Figure 2.6-22 FLECHT SEASET 31504 Droplet diameter below grid (node 12)..... 2-56
Figure 2.6-23 FLECHT SEASET 31504 Rod to rod radiation HTC below grid (node 12) 2-57
Figure 2.6-24 FLECHT SEASET 31504 Cladding temperature below grid (node 12) 2-58
Figure 2.6-25 FLECHT SEASET 31504 Liquid fraction below grid (node 12) 2-59
Figure 2.6-26 FLECHT SEASET 31504 Convective HTC to vapor at grid (node 13) 2-60

Figure 2.6-27 FLECHT SEASET 31504 Interphase surface area multiplier at grid (node 13) 2-61
Figure 2.6-28 FLECHT SEASET 31504 Two-phase enhancement multiplier at grid (node 13) 2-62
Figure 2.6-29 FLECHT SEASET 31504 Radiation to vapor HTC at grid (node 13) 2-63
Figure 2.6-30 FLECHT SEASET 31504 Radiation to liquid HTC at grid (node 13) 2-64
Figure 2.6-31 FLECHT SEASET 31504 Vapor side interfacial HTC at grid (node 13) 2-65
Figure 2.6-32 FLECHT SEASET 31504 Droplet density at grid (node 13) 2-66
Figure 2.6-33 FLECHT SEASET 31504 Liquid and vapor temperatures at grid (node 13) 2-67
Figure 2.6-34 FLECHT SEASET 31504 Droplet diameter at grid (node 13) 2-68
Figure 2.6-35 FLECHT SEASET 31504 Rod to rod radiation HTC at grid (node 13) 2-69
Figure 2.6-36 FLECHT SEASET 31504 Cladding temperature at grid (node 13) 2-70
Figure 2.6-37 FLECHT SEASET 31504 Liquid fraction at grid (node 13) 2-71
Figure 2.6-38 FLECHT SEASET 31504 Convective HTC to vapor above grid (node 14) 2-72
Figure 2.6-39 FLECHT SEASET 31504 Interphase surface area multiplier above grid (node 14) 2-73
Figure 2.6-40 FLECHT SEASET 31504 Two-phase enhancement multiplier above grid (node 14) 2-74
Figure 2.6-41 FLECHT SEASET 31504 Radiation to vapor HTC above grid (node 14) 2-75
Figure 2.6-42 FLECHT SEASET 31504 Radiation to liquid HTC above grid (node 14) 2-76
Figure 2.6-43 FLECHT SEASET 31504 Vapor side interfacial HTC above grid (node 14) 2-77
Figure 2.6-44 FLECHT SEASET 31504 Droplet density above grid (node 14) 2-78
Figure 2.6-45 FLECHT SEASET 31504 Liquid and vapor temperatures above grid (node 14) 2-79
Figure 2.6-46 FLECHT SEASET 31504 Droplet diameter above grid (node 14) 2-80
Figure 2.6-47 FLECHT SEASET 31504 Rod to rod radiation HTC above grid (node 14) 2-81

Figure 2.6-48 FLECHT SEASET 31504 Cladding temperature above grid (node 14) 2-82
Figure 2.6-49 FLECHT SEASET 31504 Liquid fraction above grid (node 14) 2-83
Figure 2.7-1 Scatter Plots of the Random Sampled Parameters for CCTF Test C2-4 Run 62 Uncertainty Analysis 2-90
Figure 2.7-2 CCTF Heater Rod (all dimensions in mm) 2-91
Figure 2.7-3 Rod 210 (BN) Calculated Temperatures Envelope vs. Measured Data at 6 ft. (1.83 m) Elevation for CCTF Test C2-4 Run 62 Uncertainty Analysis 2-92
Figure 2.7-4 Rod 210 (BN) Calculated Temperatures Envelope vs. Measured Data at 8 ft. (2.44 m) Elevation for CCTF Test C2-4 Run 62 Uncertainty Analysis 2-93
Figure 2.7-5 Rod 210 (BN) Calculated Temperatures Envelope vs. Measured Data at 10 ft. (3.05 m) Elevation for CCTF Test C2-4 Run 62 Uncertainty Analysis 2-94
Figure 2.7-6 Histogram of the predicted vs. measured peak temperatures at 6 ft. (1.83 m), 6.68 ft. (2.035 m), 8 ft. (2.44 m), and 10 ft. (3.05 m) elevation for CCTF Test C2-4 Run 62 Uncertainty Analysis 2-95
Figure 2.7-7 Peak Cladding Temperature vs. Elevation for Rod 210 (BN) for CCTF Test C2-4 Run 62 Uncertainty Analysis 2-96
Figure 2.7-8 Boxplot Illustration of the Distribution of Peak Cladding Temperature vs. Elevation for Rod 210 (BN) for CCTF Test C2-4 Run 62 Uncertainty Analysis 2-97
Figure 2.8-1 Flow and Heat Transfer Regimes during Reflood 2-100
Figure 2.8-2 FLECHT-SEASET Froth Level (Z_{froth}), Collapsed Liquid Level (Z_{Lf}), and Saturation Level (Z_{sat}) Data (Figure 5-1 from Reference 2.8.2) ... 2-101
Figure 2.9-1 RV Wall Temperatures 2-108
Figure 2.9-2 Reactor Vessel Wall Heat Transfer Mode 2-109
Figure 2.9-3 Impact of the Removal of the [ ] Heat Transfer on PCT 2-110
Figure 2.11-1 FLECHT-SEASET Steady State Temperature Distribution (60 inch Elevation) for the Wong-Hochreiter vapor convection correlation 2-117
Figure 2.11-2 FLECHT-SEASET Data/Calculated Temperature Comparison for the Wong-Hochreiter vapor convection correlation 2-118
Figure 2.11-3 FLECHT-SEASET Case Tests Exit Section Reynolds number for the Wong-Hochreiter vapor convection correlation 2-118

Figure 2.11-4 FLECHT-SEASET Steady State Temperature Distribution (60 in Elevation) for the Sleicher-Rouse vapor convection correlation 2-120
Figure 2.11-5 FLECHT-SEASET Data/Calculated Temperature Comparison for the Sleicher-Rouse vapor convection correlation 2-120
Figure 2.11-6 FLECHT-SEASET Case Tests Exit Section Reynolds number for the Sleicher-Rouse vapor convection correlation 2-121
Figure 2.12-1 Droplet Weber Number Determined from FLECHT Movies (Reference 2.12.5) 2-127
Figure 2.12-2 Peak Cladding Temperature Variations from the Base Case vs. Droplet Diameter (Reference 2.12.8) 2-128
Figure 2.18-1 Rod Thermal Radiation in FLECHT-SEASET Bundle and in a 17x17 FA 2-146
Figure 2.18-2 Peak Clad Node Temperature Comparison 2-149
Figure 2.18-3 Normalized Axial Factor Comparison 2-150
Figure 2.18-4 PCT Rod Temperature versus Elevation at Time of PCT 2-151
Figure 2.18-5 Comparison of PCT Margin for All Cases 2-152
Figure 2.18-6 PCT Versus Break Area 2-153
Figure 2.18-7 Peak Node Temperature for Top 5 PCT Cases 2-154
Figure 2.18-8 Reactor Vessel Mass for Top 5 PCT Cases 2-155
Figure 2.19-1 Influence of New Drag Package and Use of Wong-Hochreiter Bundle Option 2-160
Figure 2.19-2 Influence of Code Error Corrections 2-161
Figure 2.19-3 Influence of Core Re-nodalization 2-162
Figure 2.19-4 Influence of Grid Cooling Model 2-163
Figure 2.19-5 Influence of Rod-to-rod Radiation 2-164
Figure 2.19-6 FLECHT SEASET Test 31203, Max Clad Temperature 2-165
Figure 2.19-7 FLECHT SEASET Test 31203, Rod Surface Temperatures at 48 in 2-166
Figure 2.19-8 FLECHT SEASET Test 31203, Rod Surface Temperatures at 78 in 2-167
Figure 2.19-9 FLECHT SEASET Test 31203, Rod Surface Temperatures at 90 in 2-168
Figure 2.19-10 FLECHT SEASET Test 31203, Rod Surface Temperatures at 111 in 2-169

Figure 2.19-11 FLECHT SEASET Test 31203, Differential Pressure Between 72 in and 84 in 2-170
Figure 2.19-12 FLECHT SEASET Test 31203, Heat Transfer Coefficient 2-171
Figure 2.19-13 FLECHT SEASET Test 31203, Accumulated Water Mass in Test Section 2-172
Figure 2.19-14 FLECHT SEASET Test 31203, Total Liquid Carryover from Test Assembly 2-173
Figure 2.19-15 FLECHT SEASET Test 31203, Steam Temperatures at 72 in 2-174
Figure 2.19-16 FLECHT SEASET Test 31203, Steam Temperatures at 78 in 2-175
Figure 2.19-17 FLECHT SEASET Test 31203, Steam Temperatures at 84 in 2-176
Figure 2.19-18 FLECHT SEASET Test 31203, Steam Temperatures at 90 in 2-177
Figure 2.19-19 FLECHT SEASET Test 31203, Steam Temperatures at 96 in 2-178
Figure 2.19-20 FLECHT SEASET Test 31302, Max Clad Temperature 2-179
Figure 2.19-21 FLECHT SEASET Test 31302, Rod Surface Temperatures at 48 in 2-180
Figure 2.19-22 FLECHT SEASET Test 31302, Rod Surface Temperatures at 78 in 2-181
Figure 2.19-23 FLECHT SEASET Test 31302, Rod Surface Temperatures at 90 in 2-182
Figure 2.19-24 FLECHT SEASET Test 31302, Rod Surface Temperatures at 111 in 2-183
Figure 2.19-25 FLECHT SEASET Test 31302, Differential Pressure Between 72 in and 84 in 2-184
Figure 2.19-26 FLECHT SEASET Test 31302, Heat Transfer Coefficient 2-185
Figure 2.19-27 FLECHT SEASET Test 31302, Accumulated Water Mass in Test Section 2-186
Figure 2.19-28 FLECHT SEASET Test 31302, Total Liquid Carryover from Test Assembly 2-187
Figure 2.19-29 FLECHT SEASET Test 31302, Steam Temperatures at 72 in 2-188
Figure 2.19-30 FLECHT SEASET Test 31302, Steam Temperatures at 78 in 2-189
Figure 2.19-31 FLECHT SEASET Test 31302, Steam Temperatures at 84 in 2-190
Figure 2.19-32 FLECHT SEASET Test 31302, Steam Temperatures at 90 in 2-191
Figure 2.19-33 FLECHT SEASET Test 31302, Steam Temperatures at 96 in 2-192
Figure 2.19-34 FLECHT SEASET Test 31504, Max Clad Temperature 2-193

Figure 2.19-35 FLECHT SEASET Test 31504, Rod Surface Temperatures at 48 in 2-194
Figure 2.19-36 FLECHT SEASET Test 31504, Rod Surface Temperatures at 78 in 2-195
Figure 2.19-37 FLECHT SEASET Test 31504, Rod Surface Temperatures at 90 in 2-196
Figure 2.19-38 FLECHT SEASET Test 31504, Rod Surface Temperatures at 111 in 2-197
Figure 2.19-39 FLECHT SEASET Test 31504, Differential Pressure Between 72 in and 84 in 2-198
Figure 2.19-40 FLECHT SEASET Test 31504, Heat Transfer Coefficient 2-199
Figure 2.19-41 FLECHT SEASET Test 31504, Accumulated Water Mass in Test Section 2-200
Figure 2.19-42 FLECHT SEASET Test 31504, Total Liquid Carryover from Test Assembly 2-201
Figure 2.19-43 FLECHT SEASET Test 31504, Steam Temperatures at 72 in 2-202
Figure 2.19-44 FLECHT SEASET Test 31504, Steam Temperatures at 78 in 2-203
Figure 2.19-45 FLECHT SEASET Test 31504, Steam Temperatures at 84 in 2-204
Figure 2.19-46 FLECHT SEASET Test 31504, Steam Temperatures at 90 in 2-205
Figure 2.19-47 FLECHT SEASET Test 31504, Steam Temperatures at 96 in 2-206
Figure 2.19-48 FLECHT SEASET Test 31701, Max Clad Temperature 2-207
Figure 2.19-49 FLECHT SEASET Test 31701, Rod Surface Temperatures at 48 in 2-208
Figure 2.19-50 FLECHT SEASET Test 31701, Rod Surface Temperatures at 78 in 2-209
Figure 2.19-51 FLECHT SEASET Test 31701, Rod Surface Temperatures at 90 in 2-210
Figure 2.19-52 FLECHT SEASET Test 31701, Rod Surface Temperatures at 111 in 2-211
Figure 2.19-53 FLECHT SEASET Test 31701, Differential Pressure Between 72 in and 84 in 2-212
Figure 2.19-54 FLECHT SEASET Test 31701, Heat Transfer Coefficient 2-213
Figure 2.19-55 FLECHT SEASET Test 31701, Accumulated Water Mass in Test Section 2-214
Figure 2.19-56 FLECHT SEASET Test 31701, Total Liquid Carryover from Test Assembly 2-215

Figure 2.19-57 FLECHT SEASET Test 31701, Steam Temperatures at 72 in 2-216
Figure 2.19-58 FLECHT SEASET Test 31701, Steam Temperatures at 78 in 2-217
Figure 2.19-59 FLECHT SEASET Test 31701, Steam Temperatures at 84 in 2-218
Figure 2.19-60 FLECHT SEASET Test 31701, Steam Temperatures at 90 in 2-219
Figure 2.19-61 FLECHT SEASET Test 31701, Steam Temperatures at 96 in 2-220
Figure 2.19-62 FLECHT SEASET Test 31805, Max Clad Temperature 2-221
Figure 2.19-63 FLECHT SEASET Test 31805, Rod Surface Temperatures at 48 in 2-222
Figure 2.19-64 FLECHT SEASET Test 31805, Rod Surface Temperatures at 78 in 2-223
Figure 2.19-65 FLECHT SEASET Test 31805, Rod Surface Temperatures at 90 in 2-224
Figure 2.19-66 FLECHT SEASET Test 31805, Rod Surface Temperatures at 111 in 2-225
Figure 2.19-67 FLECHT SEASET Test 31805, Differential Pressure Between 72 in and 84 in 2-226
Figure 2.19-68 FLECHT SEASET Test 31805, Heat Transfer Coefficient 2-227
Figure 2.19-69 FLECHT SEASET Test 31805, Accumulated Water Mass in Test Section 2-228
Figure 2.19-70 FLECHT SEASET Test 31805, Total Liquid Carryover from Test Assembly 2-229
Figure 2.19-71 FLECHT SEASET Test 31805, Steam Temperatures at 72 in 2-230
Figure 2.19-72 FLECHT SEASET Test 31805, Steam Temperatures at 78 in 2-231
Figure 2.19-73 FLECHT SEASET Test 31805, Steam Temperatures at 84 in 2-232
Figure 2.19-74 FLECHT SEASET Test 31805, Steam Temperatures at 90 in 2-233
Figure 2.19-75 FLECHT SEASET Test 31805, Steam Temperatures at 96 in 2-234
Figure 2.19-76 FLECHT SEASET Test 32013, Max Clad Temperature 2-235
Figure 2.19-77 FLECHT SEASET Test 32013, Rod Surface Temperatures at 48 in 2-236
Figure 2.19-78 FLECHT SEASET Test 32013, Rod Surface Temperatures at 78 in 2-237
Figure 2.19-79 FLECHT SEASET Test 32013, Rod Surface Temperatures at 90 in 2-238
Figure 2.19-80 FLECHT SEASET Test 32013, Rod Surface Temperatures at 111 in 2-239

Figure 2.19-81 FLECHT SEASET Test 32013, Differential Pressure Between 72 in and 84 in 2-240
Figure 2.19-82 FLECHT SEASET Test 32013, Heat Transfer Coefficient 2-241
Figure 2.19-83 FLECHT SEASET Test 32013, Accumulated Water Mass in Test Section 2-242
Figure 2.19-84 FLECHT SEASET Test 32013, Total Liquid Carryover from Test Assembly 2-243
Figure 2.19-85 FLECHT SEASET Test 32013, Steam Temperatures at 72 in 2-244
Figure 2.19-86 FLECHT SEASET Test 32013, Steam Temperatures at 78 in 2-245
Figure 2.19-87 FLECHT SEASET Test 32013, Steam Temperatures at 84 in 2-246
Figure 2.19-88 FLECHT SEASET Test 32013, Steam Temperatures at 90 in 2-247
Figure 2.19-89 FLECHT SEASET Test 32013, Steam Temperatures at 96 in 2-248
Figure 2.19-90 FLECHT SEASET Test 34209, Max Clad Temperature 2-249
Figure 2.19-91 FLECHT SEASET Test 34209, Rod Surface Temperatures at 48 in 2-250
Figure 2.19-92 FLECHT SEASET Test 34209, Rod Surface Temperatures at 78 in 2-251
Figure 2.19-93 FLECHT SEASET Test 34209, Rod Surface Temperatures at 90 in 2-252
Figure 2.19-94 FLECHT SEASET Test 34209, Rod Surface Temperatures at 111 in 2-253
Figure 2.19-95 FLECHT SEASET Test 34209, Differential Pressure Between 72 in and 84 in 2-254
Figure 2.19-96 FLECHT SEASET Test 34209, Heat Transfer Coefficient 2-255
Figure 2.19-97 FLECHT SEASET Test 34209, Accumulated Water Mass in Test Section 2-256
Figure 2.19-98 FLECHT SEASET Test 34209, Total Liquid Carryover from Test Assembly 2-257
Figure 2.19-99 FLECHT SEASET Test 34209, Steam Temperatures at 72 in 2-258
Figure 2.19-100 FLECHT SEASET Test 34209, Steam Temperatures at 78 in 2-259
Figure 2.19-101 FLECHT SEASET Test 34209, Steam Temperatures at 84 in 2-260
Figure 2.19-102 FLECHT SEASET Test 34209, Steam Temperatures at 90 in 2-261
Figure 2.19-103 FLECHT SEASET Test 34209, Steam Temperatures at 96 in 2-262
Figure 2.19-104 FLECHT SEASET Test 32013, Max Clad Temperature with PVAB Limit 2-263

Figure 2.19-105 FLECHT SEASET Test 13609, Max Clad Temperature 2-264
Figure 2.19-106 FLECHT SEASET Test 13609, Rod Surface Temperatures at 36 in 2-265
Figure 2.19-107 FLECHT SEASET Test 13609, Rod Surface Temperatures at 60 in 2-266
Figure 2.19-108 FLECHT SEASET Test 13609, Rod Surface Temperatures at 84 in 2-267
Figure 2.19-109 FLECHT SEASET Test 13609, Rod Surface Temperatures at 108 in 2-268
Figure 2.19-110 FLECHT SEASET Test 13609, Differential Pressure Between 72 in and 84 in 2-269
Figure 2.19-111 FLECHT SEASET Test 13609, Heat Transfer Coefficient 2-270
Figure 2.19-112 FLECHT SEASET Test 13609, Accumulated Water Mass in Test Section 2-271
Figure 2.19-113 FLECHT SEASET Test 13609, Total Liquid Carryover from Test Assembly 2-272
Figure 2.19-114 FLECHT SEASET Test 13609, Steam Temperatures at 84 in 2-273
Figure 2.19-115 FLECHT SEASET Test 13914, Max Clad Temperature 2-274
Figure 2.19-116 FLECHT SEASET Test 13914, Rod Surface Temperatures at 36 in 2-275
Figure 2.19-117 FLECHT SEASET Test 13914, Rod Surface Temperatures at 60 in 2-276
Figure 2.19-118 FLECHT SEASET Test 13914, Rod Surface Temperatures at 84 in 2-277
Figure 2.19-119 FLECHT SEASET Test 13914, Rod Surface Temperatures at 108 in 2-278
Figure 2.19-120 FLECHT SEASET Test 13914, Differential Pressure Between 72 in and 84 in 2-279
Figure 2.19-121 FLECHT SEASET Test 13914, Heat Transfer Coefficient 2-280
Figure 2.19-122 FLECHT SEASET Test 13914, Accumulated Water Mass in Test Section 2-281
Figure 2.19-123 FLECHT SEASET Test 13914, Total Liquid Carryover from Test Assembly 2-282
Figure 2.19-124 FLECHT Skewed Test 13914, Steam Temperatures at 84 in 2-283
Figure 2.20-1 No LOOP versus LOOP Cases PCT Values 2-286
Figure 2.24-1 Measured and Predicted Void Fraction: THTF Test 3.09.10j 2-317

Figure 2.24-2 Measured and Predicted Void Fraction: THTF Test 3.09.10m 2-318
Figure 2.24-3 Measured and Predicted Vapor Temperature: THTF Test 3.09.10j . 2-319
Figure 2.24-4 Measured and Predicted Vapor Temperature: THTF Test 3.09.10m 2-320
Figure 2.24-5 Measured and Predicted Rod Surface Temperature: THTF Test 3.09.10j 2-321
Figure 2.24-6 Measured and Predicted Rod Surface Temperature: THTF Test 3.09.10m 2-322
Figure 2.25-1 W3 Case 039 – Limited T_g* Case vs. Sample Problem 2-327
Figure 2.25-2 W4 Case 138 – Limited T_g* Case vs. Sample Problem 2-328
Figure 2.25-3 CE Case 065 – Limited T_g* Case vs. Sample Problem 2-329
Figure 2.27-1 Rupture Temperature vs. Stress – Fast Ramp Rate (Fig. 2, Ref. 2.27.1) 2-334
Figure 2.27-2 Rupture Temperature vs. Stress – Various Ramp Rates (Fig. 3, Ref. 2.27.1) 2-335
Figure 2.27-3 Rupture Temperature vs. Stress – Slow Ramp Rate (Fig. K-5.11, Ref. 2.27.2) 2-336
Figure 2.27-4 Rupture Temperature vs. Stress – Fast Ramp Rate (Fig. K-5.12, Ref. 2.27.2) 2-337
Figure 2.28-1 Circumferential Strain vs. Rupture Temperature (Fig. 4 of Ref. 2.28.2) 2-340
Figure 2.28-2 M5 Slow Ramp Correlations with Supporting Rupture Strain Data (Figure 8.5-6 of Ref. 2.28.1) 2-341
Figure 2.28-3 M5 Fast Ramp Correlations with Supporting Rupture Strain Data (Figure 8.5-7 of Ref. 2.28.1) 2-342
Figure 2.28-4 [ ] 2-344
Figure 2.29-1 Maximum Diametrical Expansion vs. Temperature (Ref. 2.29.1) 2-347
Figure 2.30-1 Rupture Width vs. Rupture Length (Figure 4-56 of Ref. 2.30.2) 2-350
Figure 2.31-1 Schematic of Liquid Droplet Distribution around a Blockage during an ACHILLES Reflood Test (Fig. 10 in Reference 2.31.8) 2-355
Figure 2.31-2 Cladding Temperature and Internal Rod Pressure of a Burst Rod in REBEKA-6 Test (Figs. 7 and 8 in Reference 2.31.9) 2-356
Figure 2.31-3 Temperature and Pressure Transients of REBEKA-7 Rod Bundle (70% Blockage) (Fig. 13 in Reference 2.31.3) 2-357
Figure 2.31-4 Burst Strain vs. Azimuthal Temperature Difference (Fig.9 in Reference 2.31.3) 2-358

Figure 2.34-1 Flow and Heat Transfer Regimes during Reflood 2-364
Figure 2.34-2 Wet Wall Flow Regime Map (Figure 1 in Reference 2.34.2) 2-365
Figure 2.34-3 Vertical Flow Regime Map with Hatches Indicating Transition Regions..... 2-366
Figure 2.34-4 Combined FRIGG-2, FRIGG-3 and KATHY Void Distribution Tests Calculated Minus Measured Void Fraction..... 2-370

Nomenclature

Acronym	Definition
AOR	Analysis of Record
BN	Boron Nitride
CCTF	Cylindrical Core Test Facility
CE	Combustion Engineering
CL	Cold Leg
CRGT	Control Rod Guide Tube
CWO	Core Wide Oxidation
DESB or DEGB	Double Ended Split Break / Double Ended Guillotine Break
DFFB	Dispersed Flow Film Boiling
GC	Grid Cooling
GDC	Generic Design Criteria
GHF	Grid Turbulence Heat Transfer Enhancement Factor
γ_{RT}	Random number multiplier for rupture temperature
HT	Heat Transfer
HTC	Heat Transfer Coefficient
IET	Integral Effect Test
LBLOCA	Large Break Loss of Coolant Accident
LCO	Limited Conditions for Operation
LOOP	Loss Of Offsite Power
MLO	Maximum Local Oxidation
NRC	Nuclear Regulatory Commission
PCT	Peak Cladding Temp
PDF	Probability Distribution Function
PIRT	Process Identification and Ranking Table
PVAB	Pressure Limit on Absorptivity Coefficient
PWR	Pressurized Water Reactor
RAI	Request for Additional Information
RBHT	Rod Bundle Heat Transfer
RLBLOCA	Realistic Large Break Loss of Coolant Accident
RTR	Rod to Rod
RV	Reactor Vessel
SCC	Sub-Channel Cooling

SIT	Safety Injection Tank
THTF	Thermal-Hydraulic Test Facility
TR	Topical Report

1.0 INTRODUCTION AND SUMMARY

AREVA document EMF-2103(P), Revision 3, "Realistic Large Break LOCA Methodology for Pressurized Water Reactors" (Reference 1) was prepared by AREVA and subsequently submitted to the Nuclear Regulatory Commission (NRC). The NRC has issued Requests for Additional Information (RAIs) (Reference 2 and 3) on this submittal, and this report provides the answers to those RAIs.

RAI Questions 1 through 19 responses are identical to those sent to the NRC in Reference 4, with the exception of the addition of a missing Reference in RAI Question 18. Responses to RAI Questions 20 through 23 have been revised from those expressed in Reference 4 based on follow-up input. Responses to self-initiated RAI Questions 24 through 26 are identical to those submitted in Reference 4. RAI Question responses 27 to 32 are given in response to NRC questions in Reference 3. Self-initiated RAI Questions 33 through 35 and responses are submitted as supplemental information for NRC review.

References pertaining to a specific RAI response are listed within the RAI response. Overall report references are listed in Section 3.0 of this report.

2.0 REQUESTS FOR ADDITIONAL INFORMATION AND RESPONSES

2.1 RAI 1:

2.1.1 Statement of RAI 1

Please create a table with the following column entries for each parameter (including break size) that is treated as a random variable (or fixed/biased) in a run of the realistic large break LOCA (RLBLOCA) calculation. Include all phenomenological and plant sampled large break LOCA (LBLOCA) parameters as well.

A. The mathematical symbol used in the code for the parameter; listed in the order of its importance in the phenomena identification and ranking table.

B. The analytic expression of the correlation where the parameter appears.

C. A simple statement of the primary physical phenomenon that the parameter governs.

D. The probability density function from which random realizations of the parameter value are obtained for each code run.

E. The mean value of the parameter.

F. The variance of the parameter.

G. The limiting value

2.1.2 Response to RAI 1

This response is unchanged from the original response.

Table 5-1 of Reference 2.1.1 is the Phenomena Identification and Ranking Table (PIRT) used for AREVA Inc.'s (AREVA) RLBLOCA methodology. This table ranks the various phenomena in the blowdown, refill, and reflood phases. Section 8.5 of Reference 2.1.1 discusses how the methodology treats the PIRT phenomena. Section 8.5.1 of Reference 2.1.1 deals with important PIRT phenomena that are not treated statistically, while Section 8.5.2 of Reference 2.1.1 deals with important PIRT phenomena that are treated statistically. As such, Section 8.5.2 of Reference 2.1.1 is the most relevant section for the current discussion.

Unique mathematical symbols are not created for the parameters within the code. The code manual uses standard symbols and English names for the parameters requested. The case set run script uses long names in compliance with a structured programing approach. The code itself uses short names and acronyms in an attempt to meet some structured programing recommendations. Therefore, a table of symbols is not available or relevant to the RLBLOCA evaluation model as a whole.

Many sampled parameters are simple multipliers of the results of an analytical expression. Some are more like input parameters and enter into the calculations at many steps. Still others are binary selections, which determine which approach or table will be utilized in the calculation. Consequently, a unique response to the request for analytic expression is not able to be easily presented. However, Table 2.1-1 provides a listing of the relationship to the primary physical phenomena governed and is relates to this request (see Table 2.1-1 below).

Sections A.2.3.6 and A.2.3.7 of Reference 2.1.1 describe the uncertainty parameters, their ranges, and distributions as used in the RLBLOCA calculation. The sampled parameters are identified as either "Model Parameters" or "Plant Parameters." The distinction between these parameters is the way in which each sampling range and distribution is defined. The sampling ranges and distributions for model parameters have been predetermined for all RLBLOCA uncertainty analyses as an integral part of the methodology. The sampling ranges and distributions for the plant parameters are plant and analysis-specific and the characterization of the distributions are included in the applications reports.

Section A.2.3.6 of Reference 2.1.1 describes the five probability density function types that are used to map the sampled parameters to a given random number. The probability density functions discussed in this section are:

- Binary
- Uniform
- Gaussian (Normal)
- Log-Normal
- Special (e.g., Film-Boiling)

For the Film-Boiling special type probability density functions, the relationship between the probability and the corresponding film-boiling multiplier is provided in Table A-4 and Table A-5 of Reference 2.1.1.

Table A-6 of Reference 2.1.1 provides a listing of each sampled parameter, the type of parameter (model or plant-specific), as well as the type of probability distribution function (PDF) associated with each sampled parameter.

Table A-7 of Reference 2.1.1 provides the probability density functions, including the mean and standard deviation (for Gaussian PDFs), lower and upper bound or tabular values (for binary or uniform PDFs) as appropriate for each model-specific parameter. The mean value, as well as the variance, for each model-specific parameter can be determined by Table A-7 of Reference 2.1.1.

For the plant-specific sampled parameters listed in Table A-6 of Reference 2.1.1, some typical ranges, as well as associated probability density functions, are provided in Appendix B of Reference 2.1.1 as part of the sample problem calculations. Table B-8, Table B-15, and Table B-22 of Reference 2.1.1 provide plant-specific ranges, as well as probability density functions, of sampled parameters for the Westinghouse 3-Loop, Westinghouse 4-Loop, and Combustion Engineering 2x4 Loop sample problems, respectively. The parameter range in Table B-8, Table B-15, and Table B-22 of Reference 2.1.1 allows one to determine some typical mean values, as well as the variance of these values, for some representative plant designs. For each application of the RLBLOCA EM to a plant, the application specific information of these tables will be included within the plant evaluation report.

It is not clear what is meant by limiting value. There is not a unique limiting value to any sampled parameter as the individual case results are a combination of the selected values of all parameters. The ranking of the case results does identify the high probability results for the RLBLOCA application. However, the individual parameter values for the case giving that result should not be considered as limiting values as it is only their combined effect with all other sampled parameters that lead to the result. The range of values over which a parameter may vary has an upper and a lower limit, and that is specified by the probability density function for the parameter.

Reference:

2.1.1 AREVA Topical Report EMF-2103(P) Rev. 3, "Realistic Large Break LOCA Methodology for Pressurized Water Reactors," September 2013.

Table 2.1-1 Uncertainty Parameters and PDFs

[redacted]

2.2 RAI 2:

2.2.1 Statement of RAI 2

Thermal hydraulic system codes, such as RELAP5, have been found to predict asymmetrical results when modeling parallel flow configurations, usually under low-flow conditions. Recognition of such modeling difficulties is presented by G. W. Johnsen, "RELAP5-3D Development & Application Status," Presentation at the 2002 RELAP5 International User's Seminar, September 4-6, 2001, Park City, Utah. In pressurized water reactor (PWR) plant analysis, such flow configurations can be related to parallel flow paths representing the cold legs in the same primary coolant loop of a Combustion Engineering (CE) PWR plant, where liquid can backflow into the steam generators from the cold leg in one of the loops. The potential flow anomaly is also associated with parallel flow channels representing different azimuthal sections of a reactor vessel downcomer including representations of steam generator secondary side volumes or other regions of the reactor system. A possible solution approach in modeling a simple flow problem between parallel pipes is discussed by D. Lucas, "Recirculating Flow Anomaly Problem Solution Method," Proceedings of 8th International Conference on Nuclear Engineering ICONE8, Paper ID 8479, April 2-6, 2000, Baltimore, Maryland.

Please show that S-RELAP5 does not predict anomalous behaviors as described above for other codes when using three-dimensional (3-D) and one-dimensional (1-D) components. As part of the response, present predictions for an illustrative parallel pipe flow problem as implemented in the RELAP5 dual pipe flow input model presented below.

```
=Flow Anomaly Test Problem
*
*-----------------------------------------------------------------------
*crdno              problem type        problem option
0000100                 new                 transnt
*-----------------------------------------------------------------------
*crdno              input units              output units
0000102               british                  british
*-----------------------------------------------------------------------
*crdno    time 1     time 2
0000105   10.        40.     10000.
*-----------------------------------------------------------------------
0000110  nitrogen
*-----------------------------------------------------------------------
*crdno end time  min dt   max dt  control  minor ed  major ed  restart
0000201   5000.   1.0e-6   2.0      3    1       250          500
************************************************************************
************************************************************************
* minor edit requests
************************************************************************
************************************************************************
*
*crdno        variable       parameter
*
301  count    0
302  dt       0
303  dtcrnt   0
304  cputime  0
305  errmax   0
306  emass    0
307  tmass    0
310  mflowj   145010000
311  mflowj   145020000
312  mflowj   716000000
313  mflowj   711000000
314  mflowj   175010000
315  mflowj   175020000
316  tempf    130010000
317  tempf    160010000
318  cntrlvar 1
319  cntrlvar 2
320  testda   2
321  testda   3
322  testda   4
20800001 testda 2
20800002 testda 3
20800003 testda 4
*
********************************************************************
********************************************************************
* hydrodynamic components
********************************************************************
********************************************************************
1300000   pmpsuca2          pipe   * loop a2 rc pump suction
1300001   1
1300101    4.2761  1
1300301        25.956   1
1300401        0.0   1
1300601            -90.   1
1300701     -25.956   1
1300801   .00030          0.    1
1301001    00     1
1301201   3   2200.0   550.0      0.0             0.0       0.0       1
*
1450000   clbrcha2        branch
1450001   2          0
1450101   10.0  5.4064       0.     0. -90.0  -5.4064  .00015      0. 00
1450200   3   2200.0    550.0
1451101   160010000 145000000   4.2761   1.0     1.0    0100
1452101   130010000 145000000   4.2761   1.0     1.0    0100
1451201   0.0       0.0         0.0
1452201   0.0       0.0         0.0
*
```

```
1600000   pmpsuca1          pipe
1600001   1
1600101    4.2761  1
1600301       25.956   1
1600401        0.0   1
1600601           -90.   1
1600701      -25.956   1
1600801   .00030          0.     1
1601001    00     1
1601201   3  2200.0   550.0   0.0                  0.0       0.0       1
*
1750000   clbrcha1        branch
1750001   2         0
*1750101   10.0  5.4064        0.      0. -90.0  -5.4064 .00015       0. 00
1750101   10.0  5.4064        0.      0. -90.0  -5.4064 .01000       0. 00
1750200   3  2200.0   550.0
1751101   175010000 160000000   4.2761   1.0      1.0     0100
1752101   175010000 130000000   4.2761   1.0      1.0     0100
1751201   0.0       0.0         0.0
1752201   0.0       0.0         0.0
*
*
7100000   lpa1hpit        tmdpvol
7100101   1.0e6    10.0 0.0      0.     -90.0  -10.0     0.       0.      00
7100200     3
7100201       0.         2200.0             90.
*
*
7110000   lpa1hpif     tmdpjun
7110101   710010000  175000000         .0246
7110200    1
7110201    0.0     0.0        0.0        0.0
7110202    10.0    96.0       0.0        0.0
*
*
7150000   lpa2hpit        tmdpvol
7150101   1.0e6    10.0  0.0      0.     -90.0  -10.0     0.       0.      00
7150200     3
7150201       0.         2200.0            550.
*
*
7160000   lpa2hpif     sngljun
7160101   145010000  715000000       10.0     1.0 1.0 0
7160201 0     0.0      0.0        0.0
*
20500100  dtempf  sum  1.0 0.0 1
20500101  0.0  1.0 tempf  160010000  -1.0  tempf  130010000
*
20500200  dtempf  sum  1.0 0.0 1
20500201  0.0  1.0 tempf  130010000  -1.0  tempf  160010000
*
.     * end of input stream
```

2.2.2 Response to RAI 2

This response is unchanged from the original response.

AREVA addressed the issue of recirculating flow anomaly in the response to Question 46 of the Revision 0 of the RLBLOCA methodology (Reference 2.2.1, Page 100-107). In addition, AREVA also performed a benchmark of a Multi-Dimensional Flow Testing problem using the EMF-2103(P), Revision 3 methodology, and it is described in Section 8.2.14 of Reference 2.2.2. The purpose of this benchmark is to show that the two-dimensional component functions acceptably. From these studies, AREVA concludes that S-RELAP5 does not predict the anomalous behaviors described in this question.

References:

2.2.1 Framatome ANP, Inc. Letter NRC:02:062, "Responses to a Request for Additional Information on EMF-2103(P) Revision 0 Realistic Large Break LOCA Methodology for Pressurized Water Reactors (TAC No. MB2865)," December 20, 2002.

2.2.2 AREVA Topical Report EMF-2103(P) Rev. 3, "Realistic Large Break LOCA Methodology for Pressurized Water Reactors," September 2013.

2.3 RAI 3:

2.3.1 Statement of RAI 3

In Equations 7.383 and 7.385 what are the conditions at which the properties h_g, h_{fg}, and h_f are determined? What is the sensitivity of the interface heat transfer coefficient, Equation 7.383, to the value of B?

2.3.2 Response to RAI 3

This response is unchanged from the original response.

[
]

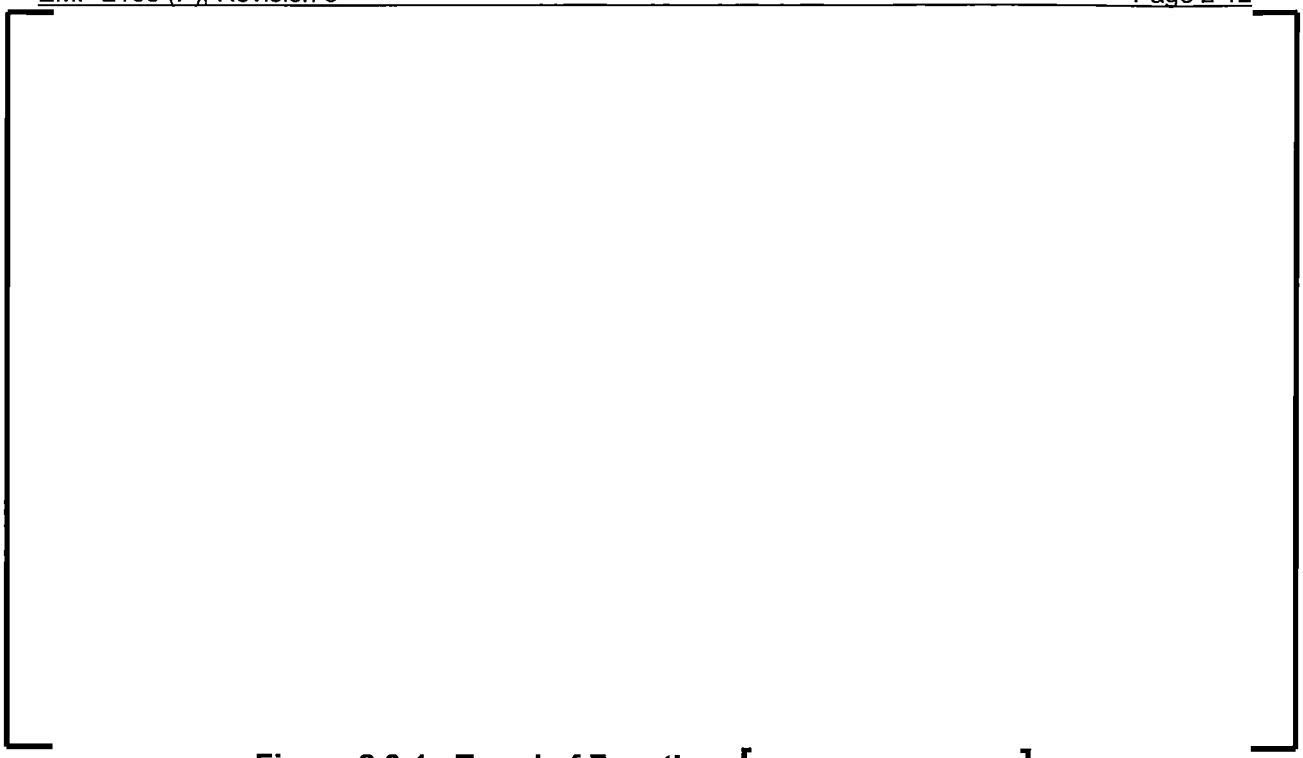

Figure 2.3-1 Trend of Function [ ]

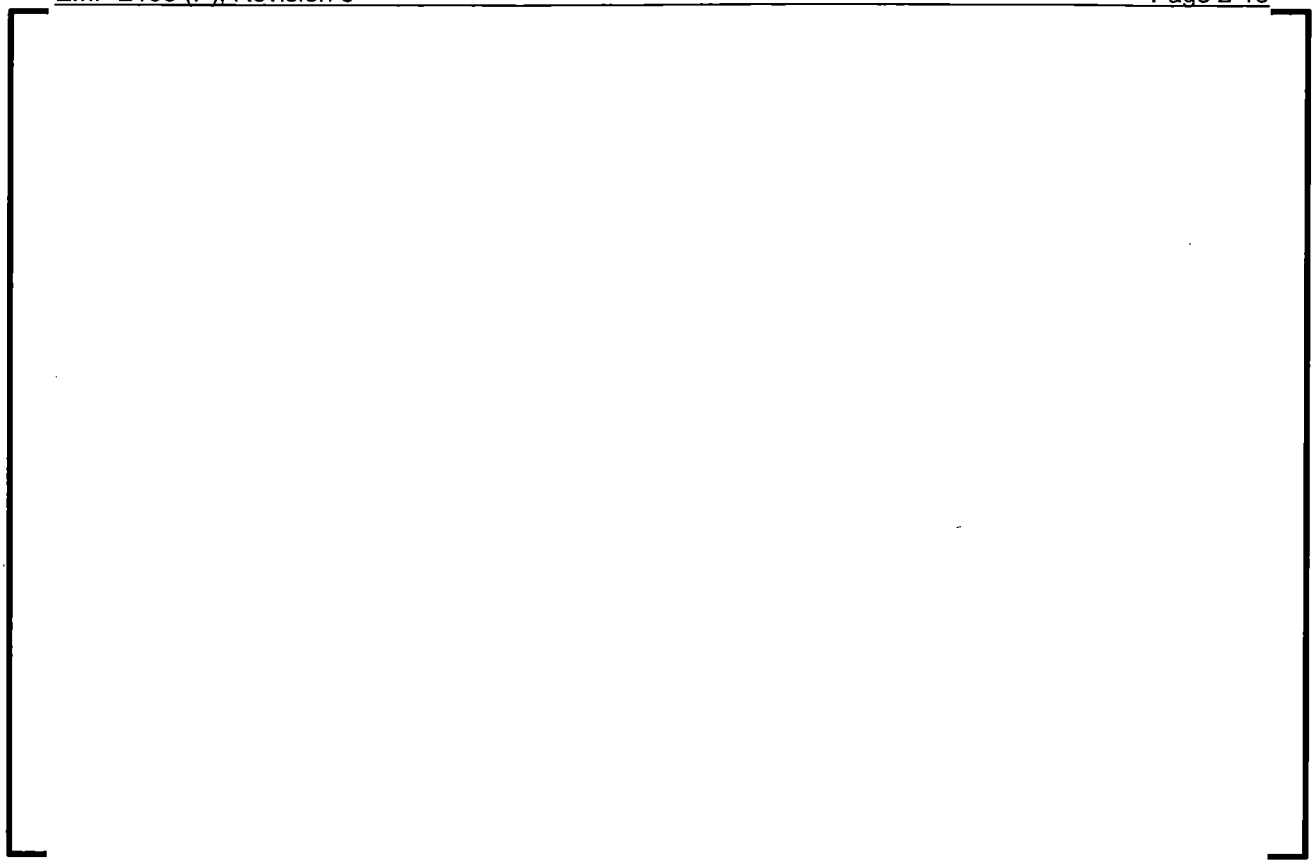

Figure 2.3-2 Comparison of PCT Function of Test Elevation

[ ]

Figure 2.3-3 Comparison of PCT at 78 inch Elevation [ ]

References:

2.3.1 AREVA Topical Report EMF-2103(P) Rev. 3, "Realistic Large Break LOCA Methodology for Pressurized Water Reactors," September 2013.

2.3.2 FLECHT-SEASET Program, PWR FLECHT SEASET Unblocked Bundle, Forced and Gravity Reflood Task Data Report, Volumes 1 and 2, NUREG/CR-1532, EPRI NP-1459, WCAP-9699, June 1980.

2.4 RAI 4:

2.4.1 Statement of RAI 4

Provide the basis for Equation 7.386, Reference 7-81.

2.4.2 Response to RAI 4

This response is unchanged from the original response.

2.4.3 [

]

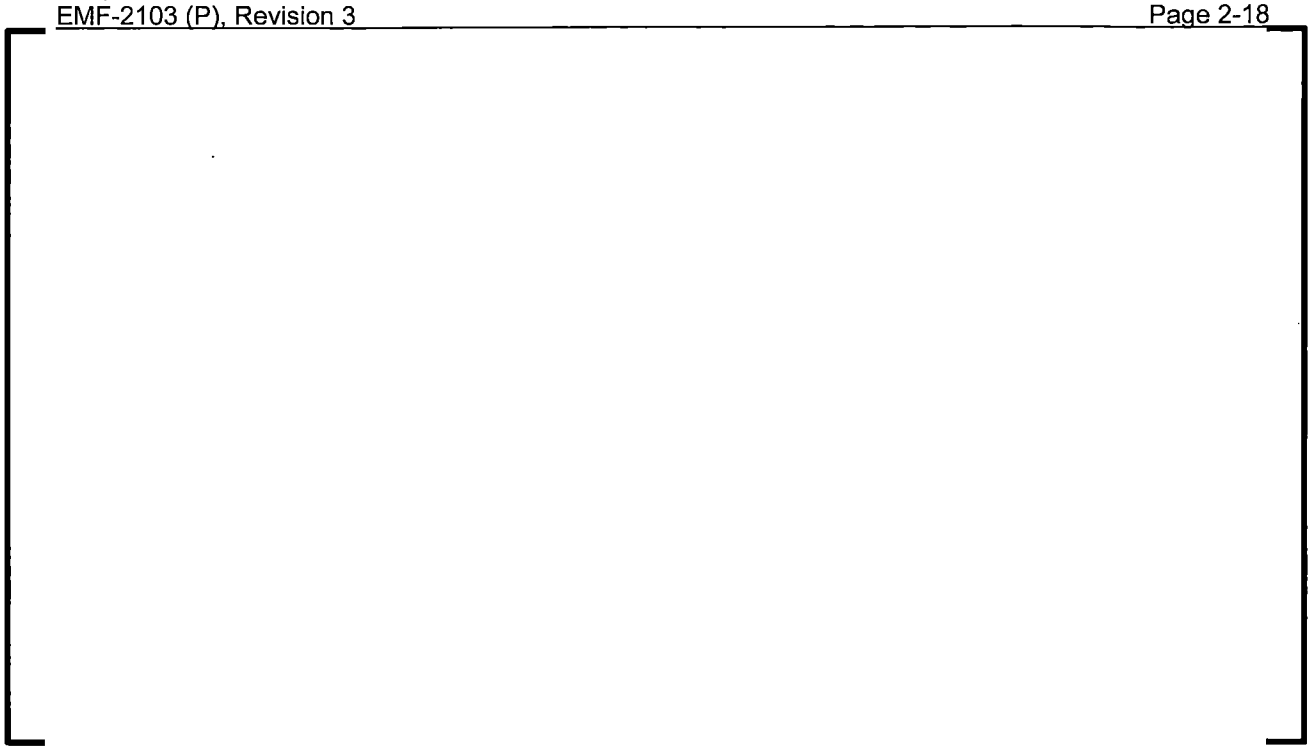

Figure 2.4-1 Comparison of [functions]

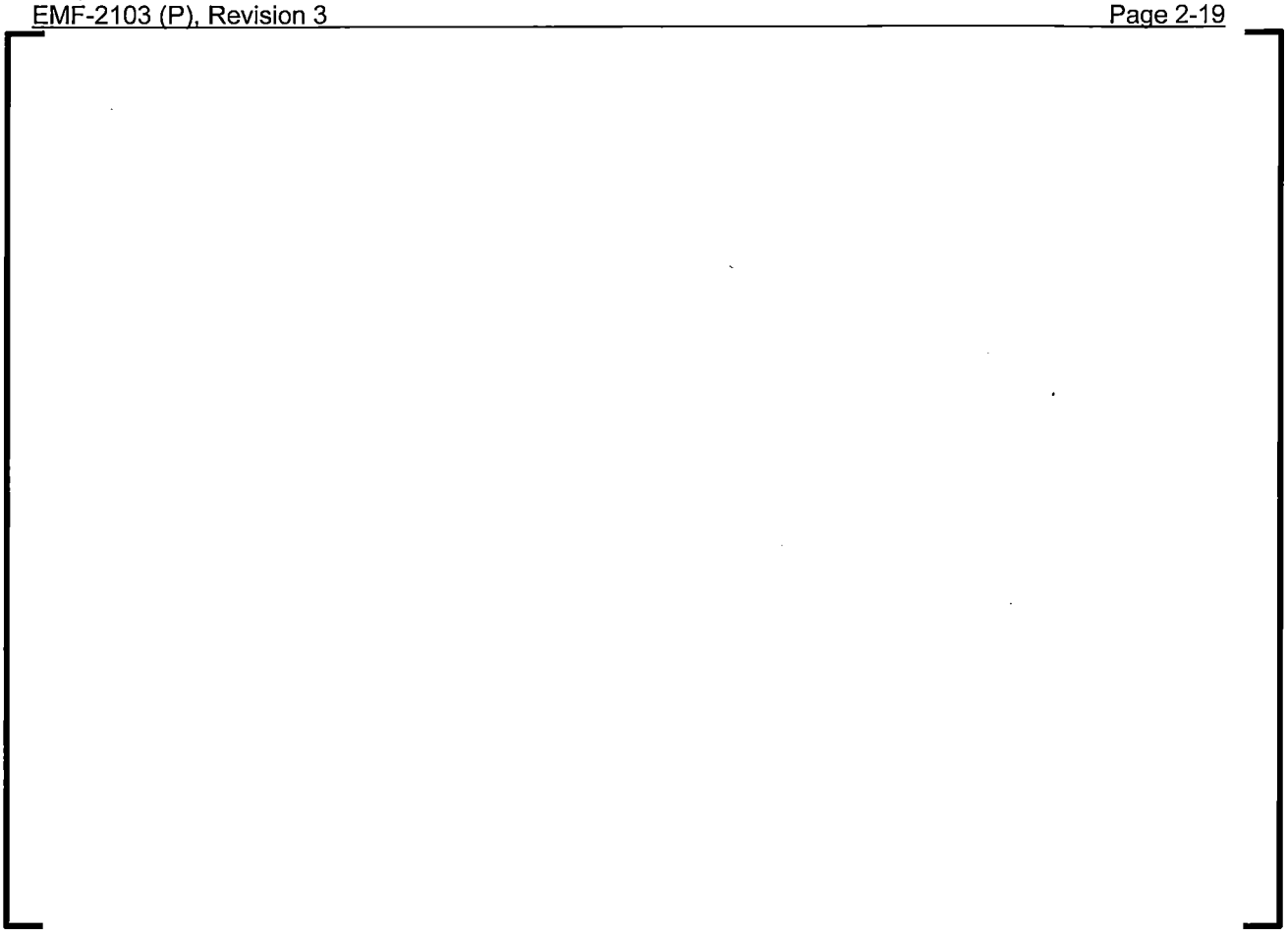

Figure 2.4-2 Comparison of PCT Function of Test Elevation S-RELAP5 [

]

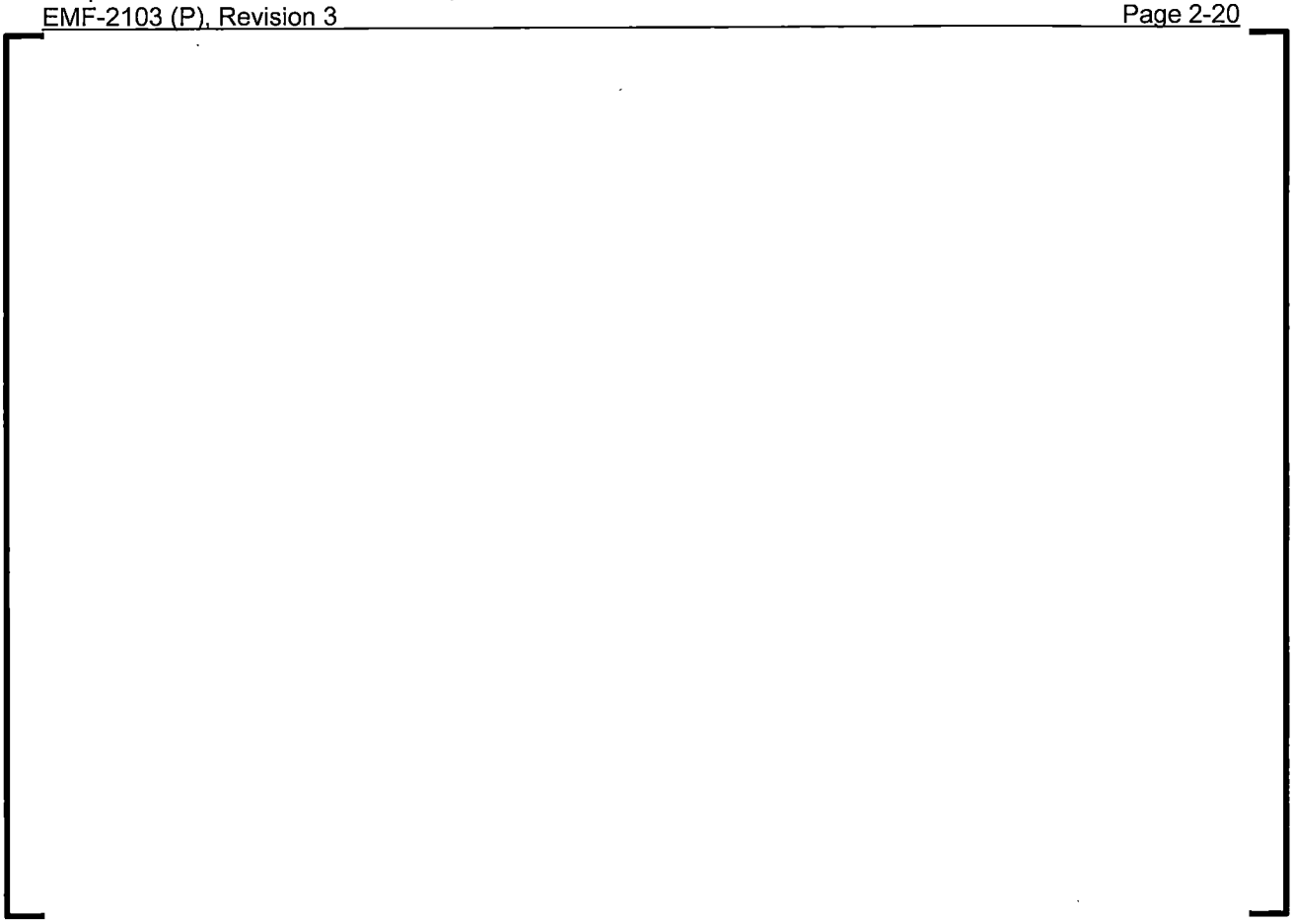

Figure 2.4-3 Comparison of PCT at 78 inch Elevation S-RELAP5

[

]

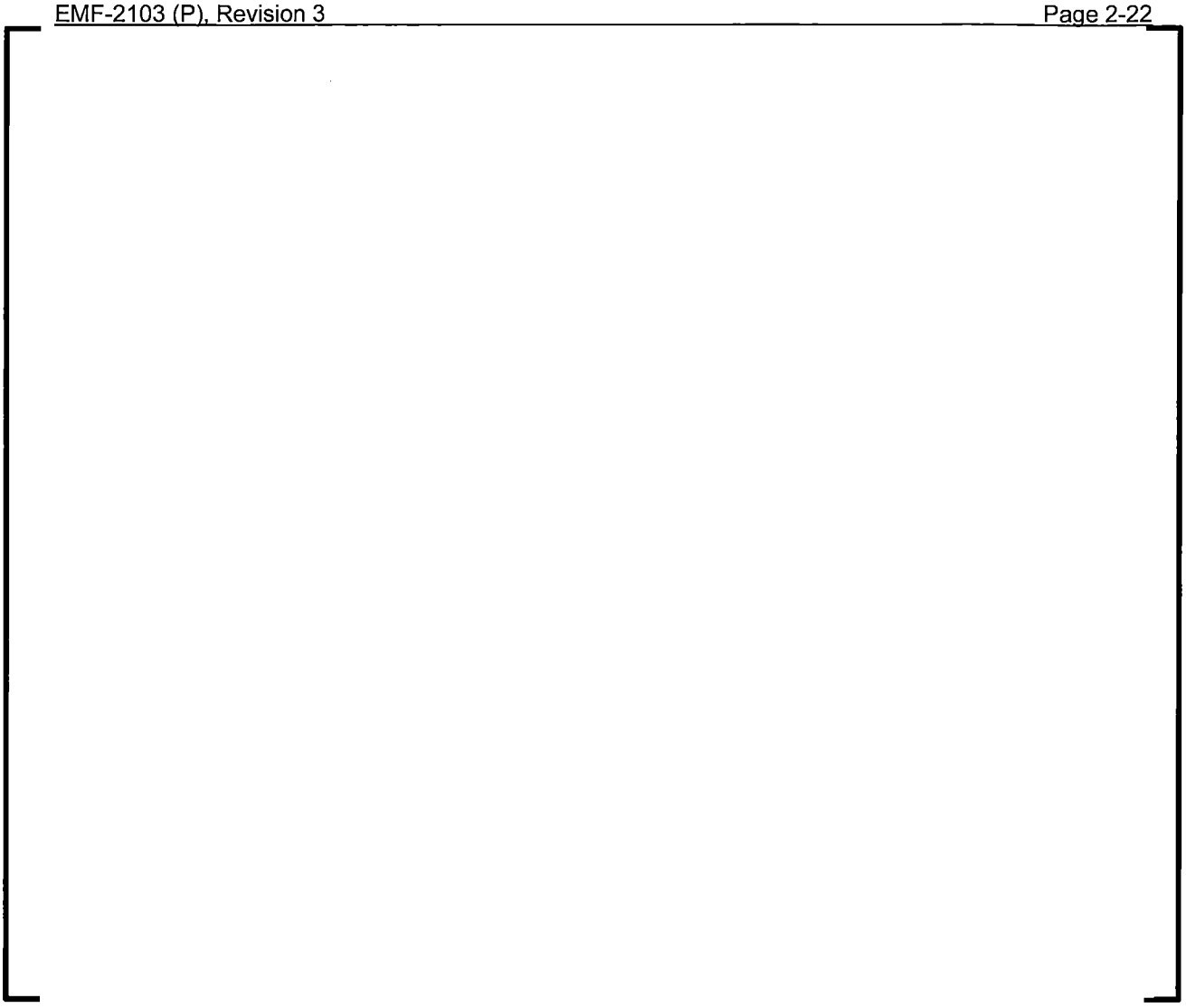

Figure 2.4-4 Trend of Function [ ]

Figure 2.4-5 Comparison of PCT Function of Test Elevation S-RELAP5 [ ]

Figure 2.4-6 Comparison of PCT at 78 inch Elevation S-RELAP5

[ ]

2.5 RAI 5:

2.5.1 Statement of RAI 5

Provide the basis for the minimum drop size used in S-RELAP5 and provide a sensitivity study to the droplet size.

2.5.2 Response to RAI 5

This response is unchanged from the original response.

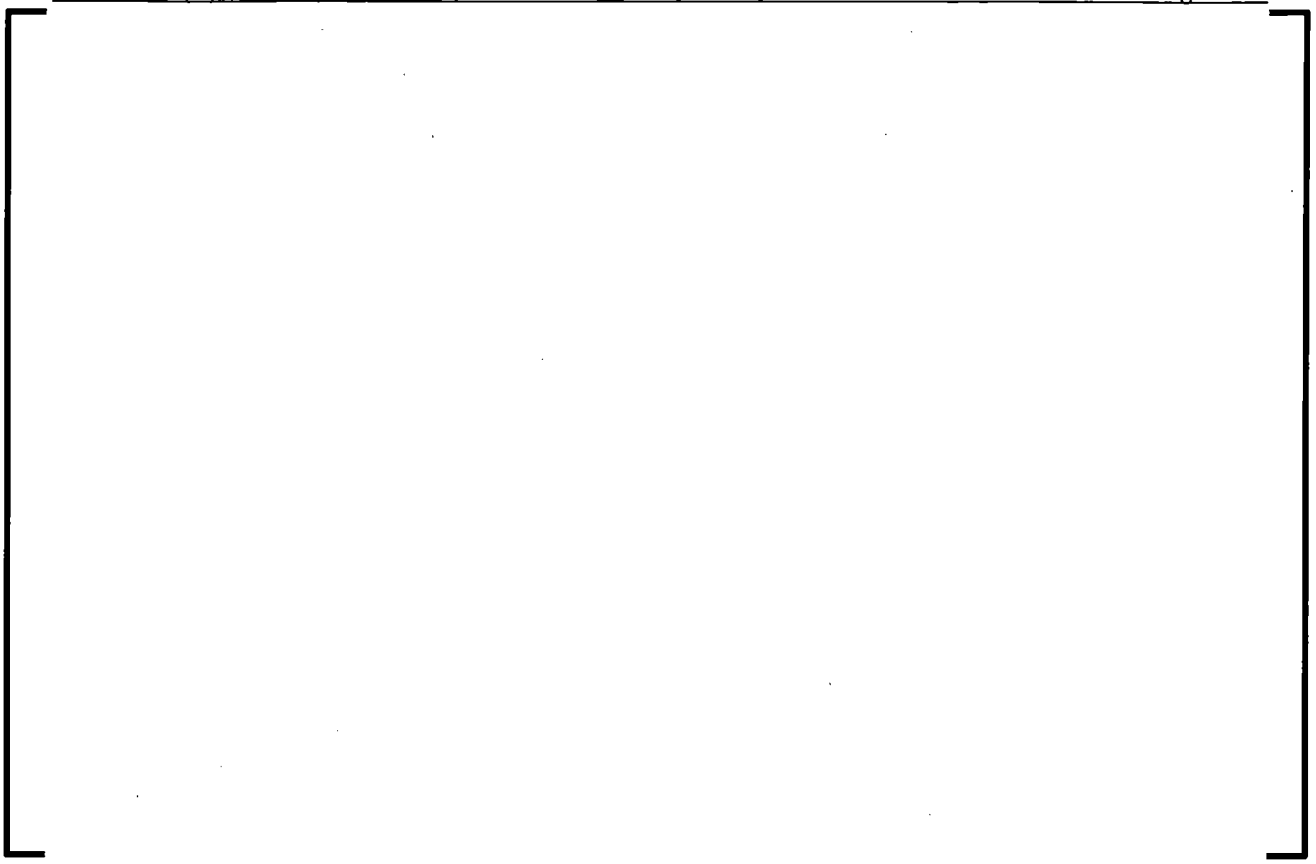

Figure 2.5-1 Comparison of PCT Function of Test Elevation (Minimum Droplet Size Sensitivity)

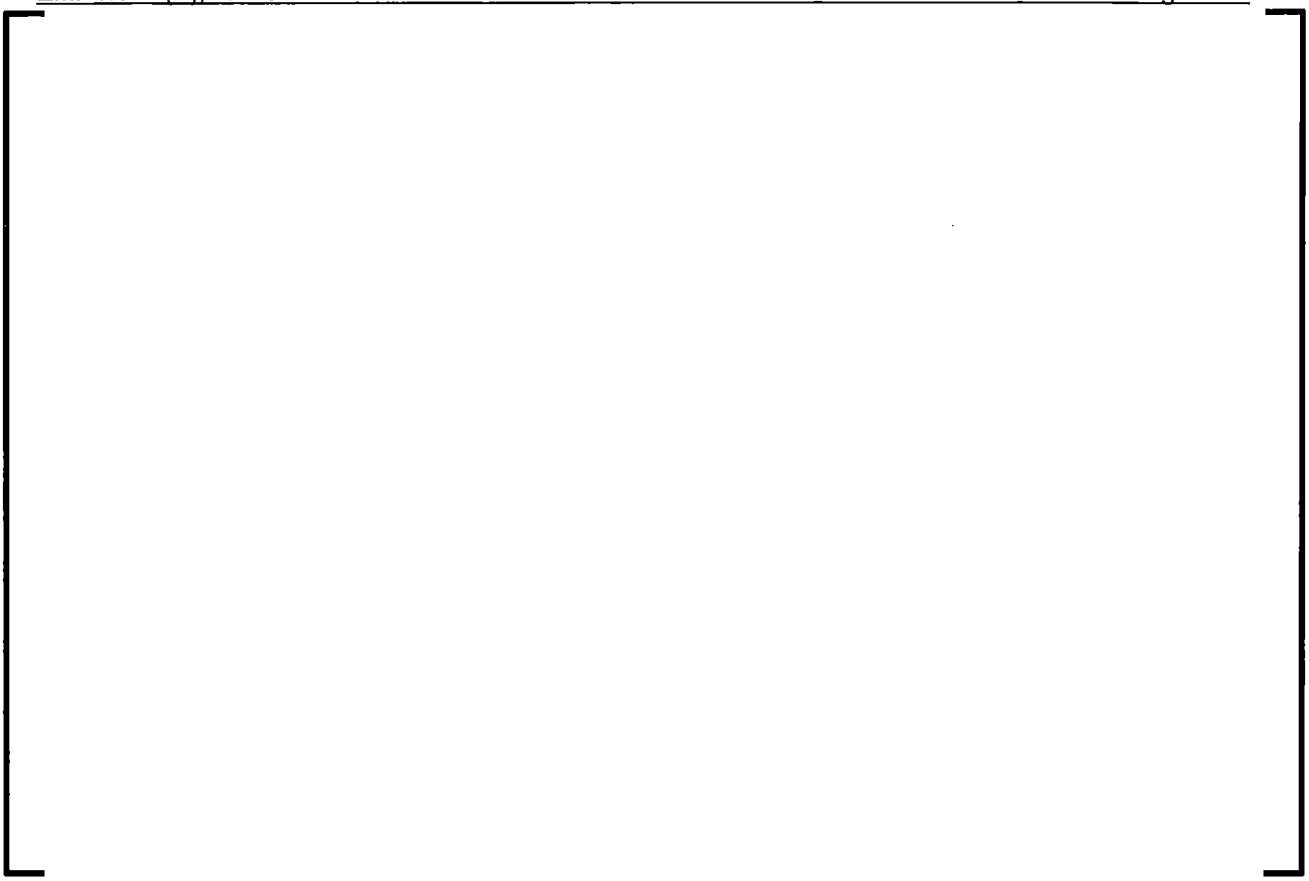

Figure 2.5-2 Comparison of PCT at 78 inch Elevation (Minimum Droplet Size Sensitivity)

References:

2.5.1 AREVA Topical Report EMF-2103(P) Rev. 3, "Realistic Large Break LOCA Methodology for Pressurized Water Reactors," September 2013.

2.5.2 FLECHT-SEASET Program, PWR FLECHT SEASET Unblocked Bundle, Forced and Gravity Reflood Task Data Report, Volumes 1 and 2, NUREG/CR-1532, EPRI NP-1459, WCAP-9699, June 1980.

2.5.3 A.J. Ireland, L.E. Hochreiter, F-B Cheung, Droplet Size and Velocity Measurements in a Heated Rod Bundle, 6th ASME-JSME Thermal Engineering Joint Conference, March 16-20, 2003.

2.5.4 AREVA Topical Report, BAW-10166PA-05, BEACH: Best Estimate Analysis Core Heat Transfer - A Computer Program for Reflood Heat Transfer Analysis During LOCA, November 2003.

2.5.5 C.K. Nithianandan and J.R. Biller, Evaluation of Minimum Droplets Size on Cladding Temperature During Reflood, ANS 2005 Winter Meeting, November 12-17, Washington DC.

2.6 RAI 6:

2.6.1 Statement of RAI 6

Provide a list of the FLECHT tests of Section 8.2.18 and what parameter variations they evaluated. Provide plots of (at peak cladding temperature (PCT) location and 1 node above and below and location of grid):

A. Forced convective heat transfer coefficient to vapor,

B. Grid enhancement multiplier, Fgrid,

C. Two-phase enhancement multiplier, F2ϕ,

D. Radiation heat transfer coefficient to vapor,

E. Radiation heat transfer coefficient to droplets,

F. Interfacial heat transfer coefficient between the drops and the vapor,

G. Droplet number and diameter,

H. Minimum stable film boiling temperature, TMIN.

I. Vapor and liquid temperatures,

J. Droplet diameter, and

K. Rod-to-rod radiation.

2.6.2 Response to RAI 6

This response is unchanged from the original response.

Background:

The FLECHT SEASET and Skewed experiments (Reference 2.6.3) were benchmarked in Section 8.2.3 of Revision 3 of the RLBLOCA Topical Report (Reference 2.6.2). These benchmarks were repeated in Section 8.2.18 of that work to provide a measure of the change in methodology which came about between Revision 2 and 3 of EMF-2103. Additional work has since been performed with the FLECHT SEASET benchmarks, which has extended this work to include a rod-to-rod radiation heat transfer model. As the RAI specifically requested rod-to-rod radiation heat transfer, it was this work that was used as a basis for the response. The FLECHT Skewed benchmarks had not been extended to include this capability, so the original work is plotted for these tests (without rod-to-rod radiation heat transfer).

Results, Summary/Conclusion:

The FLECHT tests discussed in Section 8.2.18 of Reference 2.6.2, along with parameter variations, were identified in Table 8.2-8 of that reference. That table has been repeated here.

References:

2.6.1 NRC letter from J. G. Rowley (NRC) to P. Salas (AREVA), "Request for Additional Information Related to Review of AREVA NP Licensing Topical Report EMF-2103 Revision 3, Realistic Large Break LOCA Methodology for Pressurized Water Reactors" (Accession No. ML14303A385), November 20, 2014.

2.6.2 AREVA Topical Report EMF-2103(P) Rev. 3, "Realistic Large Break LOCA Methodology for Pressurized Water Reactors," September 2013.

2.6.3 FLECHT SEASET Program, "PWR FLECHT SEASET Unblocked Bundle, Forced and Gravity Reflood Task Data Report," Volume 1, NUREG/CR-1532, EPRI NP-1459, WCAP-9699, June 1980.

Table 2.6-1 FLECHT SEASET, FLECHT Skewed Test Conditions

Run	Pressure (psia)	Peak (kW/ft)	Flow Rate (in/s)	Coolant Temp (°F)	Axial Power Profile
FLECHT SEASET Tests Flooding Rate					
31805	40	0.70	0.81	124	Cosine, Center Peak
31203	40	0.70	1.51	126	Cosine, Center Peak
31302	40	0.69	3.01	126	Cosine, Center Peak
31701	40	0.70	6.10	127	Cosine, Center Peak
Pressure Variation					
34209	20	0.72	1.07	90	Cosine, Center Peak
31504	40	0.70	0.97	123	Cosine, Center Peak
32013	60	0.70	1.04	150	Cosine, Center Peak
FLECHT Tests Subcooling Variation					
13609	21	0.70	1.00	87	Skewed, top peak
13914	21	0.70	1.00	223	Skewed, top peak

Plots Generated:

Table 2.6-2 Description of Delivered Parameters

	Requested Parameter	Delivered Parameter	Reference in EMF-2103 Rev 3
A	Forced convective heat transfer coefficient to vapor	Convective heat transfer coefficient to vapor with respect to saturation temperature	Eqn. 7.526
B	Grid enhancement multiplier, F_{grid}	Interphase Surface Area Multiplier	Eqn. 7.442 & 7.443
C	Two-phase enhancement multiplier, $F_{2\varphi}$	Ψ, the dry-wall form of the turbulent two-phase enhancement	Eqn. 7.530
D	Radiation heat transfer coefficient to vapor	Wall-to-vapor radiation heat transfer coefficient with respect to saturation temperature	Eqn. 7.536
E	Radiation heat transfer coefficient to droplets	Wall-to-liquid radiation heat transfer coefficient with respect to saturation temperature	Eqn. 7.536
F	Interfacial heat transfer coefficient between drops and vapor	Vapor side interfacial heat transfer coefficient per unit volume divided by the droplet surface area per unit volume	Section 7.5.4, Pg. 7-123
G	Droplet number and diameter	Droplet density, Liquid volume divided by volume of one droplet	
H	Minimum stable film boiling temperature , T_{MIN}	Input / Sampled Parameter (700 K defined for FLECHT)	
I	Vapor and liquid temperatures	Vapor and liquid temperatures	
J	Droplet diameter	Droplet diameter	Eqn. 7.282
K	Rod-to-rod radiation	Heat flux from the wall to wall radiation model divided by the difference between cladding temperature and saturation.	Section 7.6.8.2, Pg. 7-212.

The additional data was requested "at PCT location and 1 node above and below and location of grid" [

]

Table 2.6-3 FLECHT SEASET Grid Elevations

Grid Number	Distance from Reference Elevation to Top of Grid Reference 2.6.3	Elevation of Grid Bottom Relative to Bottom of Heated Length (ft)
1	2'- 0"	-0.1458
2	3'- 9"	1.6042
3	5'- 5"	3.2708
4	7'- 2"	5.0208
5	8'- 11"	6.7708
6	10'- 7"	8.4375
7	12'- 4"	10.1875
8	14'- 0"	11.8542

The S-RELAP5 bundle nodalization is shown in Table 2.6-4. The exit elevations in bold type show the grid bottom elevations. Note that neither the bottom grid (below the heated length) nor the top grid (at the bundle exit) are considered relevant and have not been modeled.

Table 2.6-4 Cosine Profile Tests Heated Length Nodalization

The plots for FLECHT SEASET Test 31504 for the four nodes requested are presented. The remaining plots will be transmitted under separate cover.

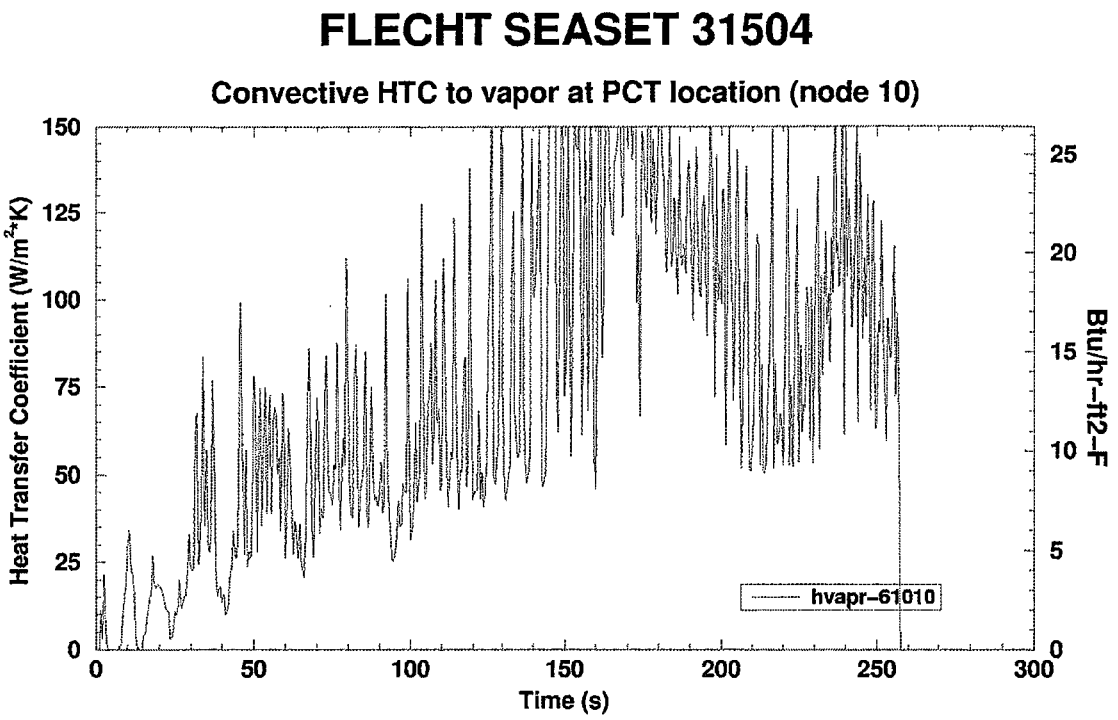

Figure 2.6-1 FLECHT SEASET 31504 Convective HTC to vapor at PCT location (node 10)

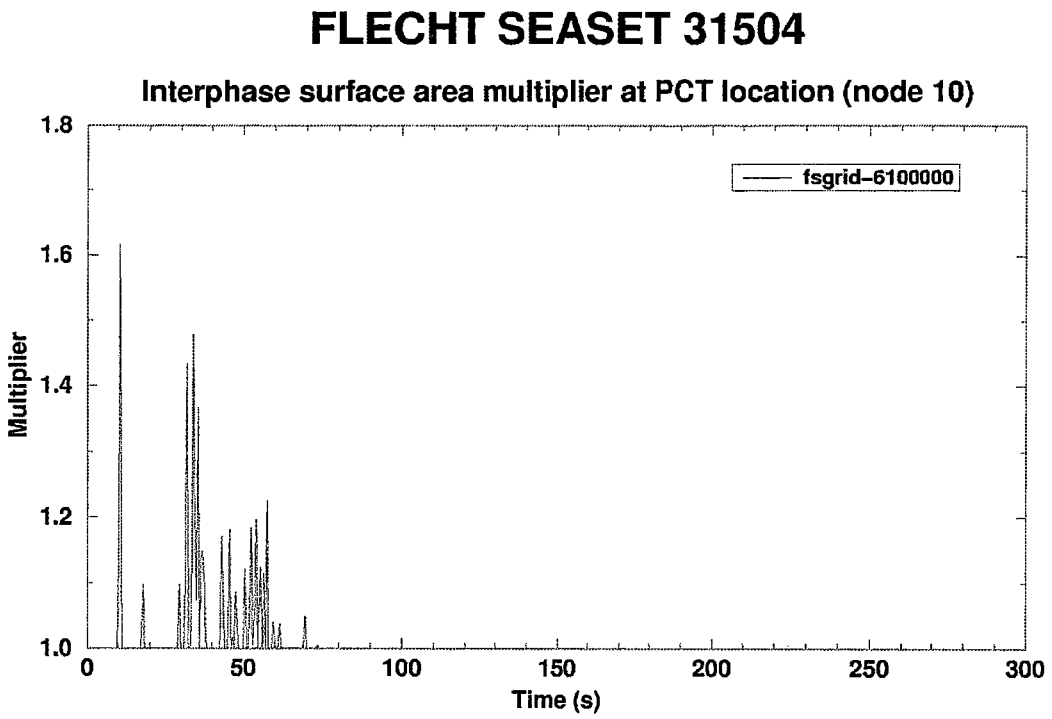

Figure 2.6-2 FLECHT SEASET 31504 Interphase surface area multiplier at PCT location (node 10)

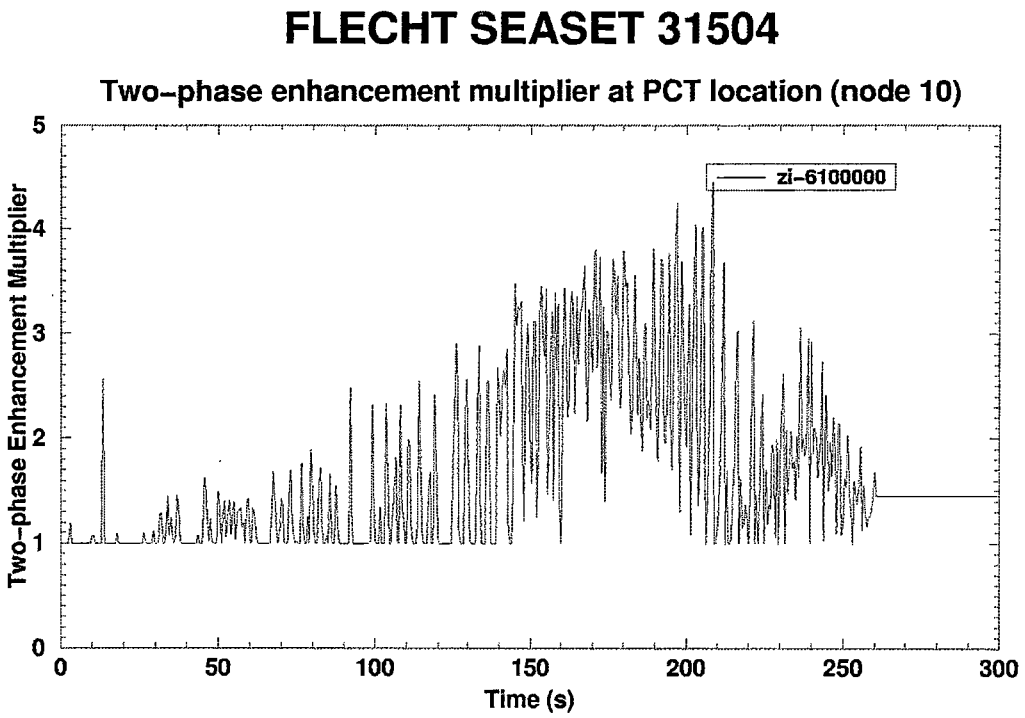

Figure 2.6-3 FLECHT SEASET 31504 Two-phase enhancement multiplier at PCT location (node 10)

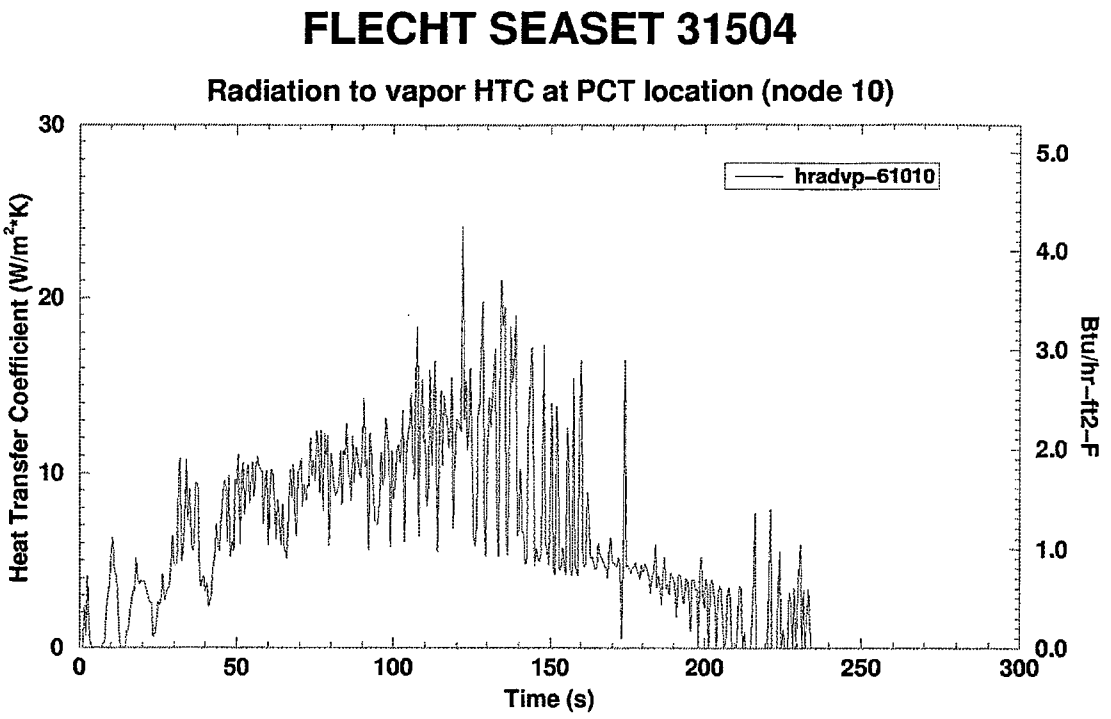

Figure 2.6-4 FLECHT SEASET 31504 Radiation to vapor HTC at PCT location (node 10)

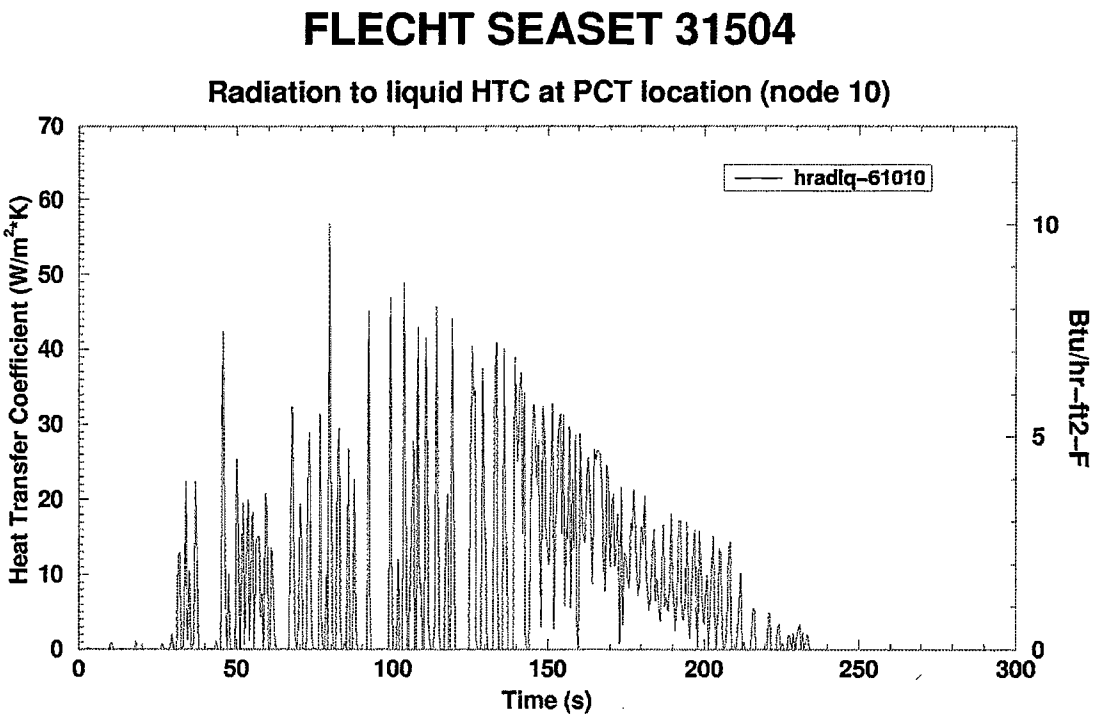

Figure 2.6-5 FLECHT SEASET 31504 Radiation to liquid HTC at PCT location (node 10)

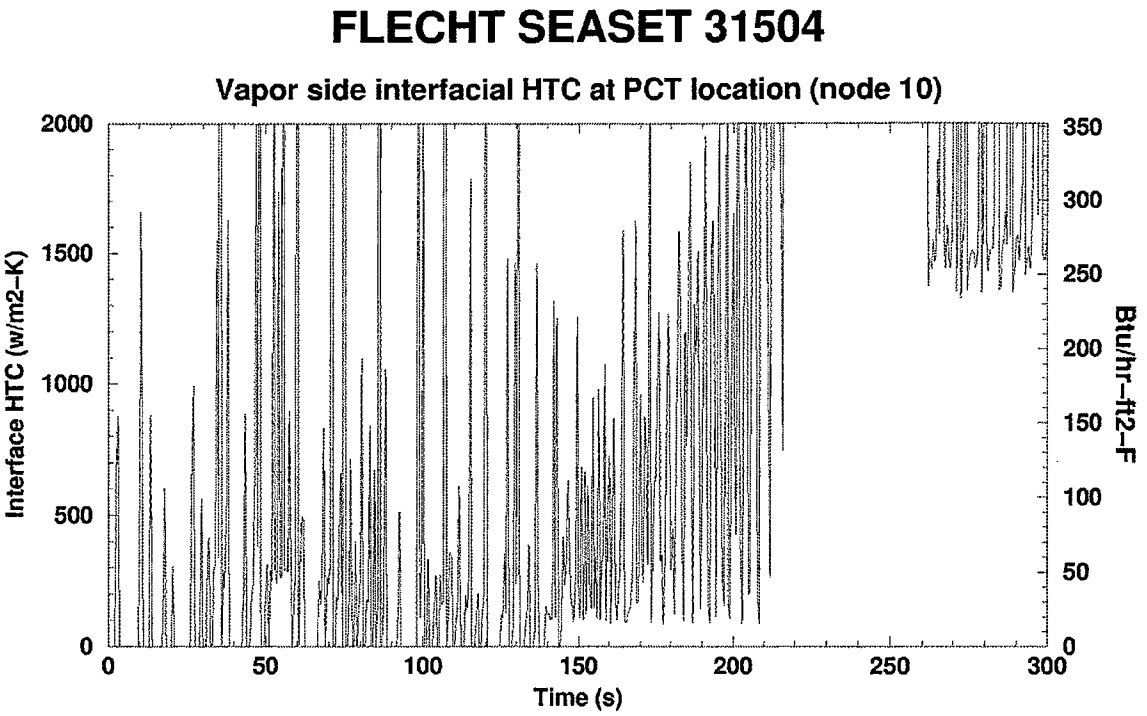

Figure 2.6-6 FLECHT SEASET 31504 Vapor side interfacial HTC at PCT location (node 10)

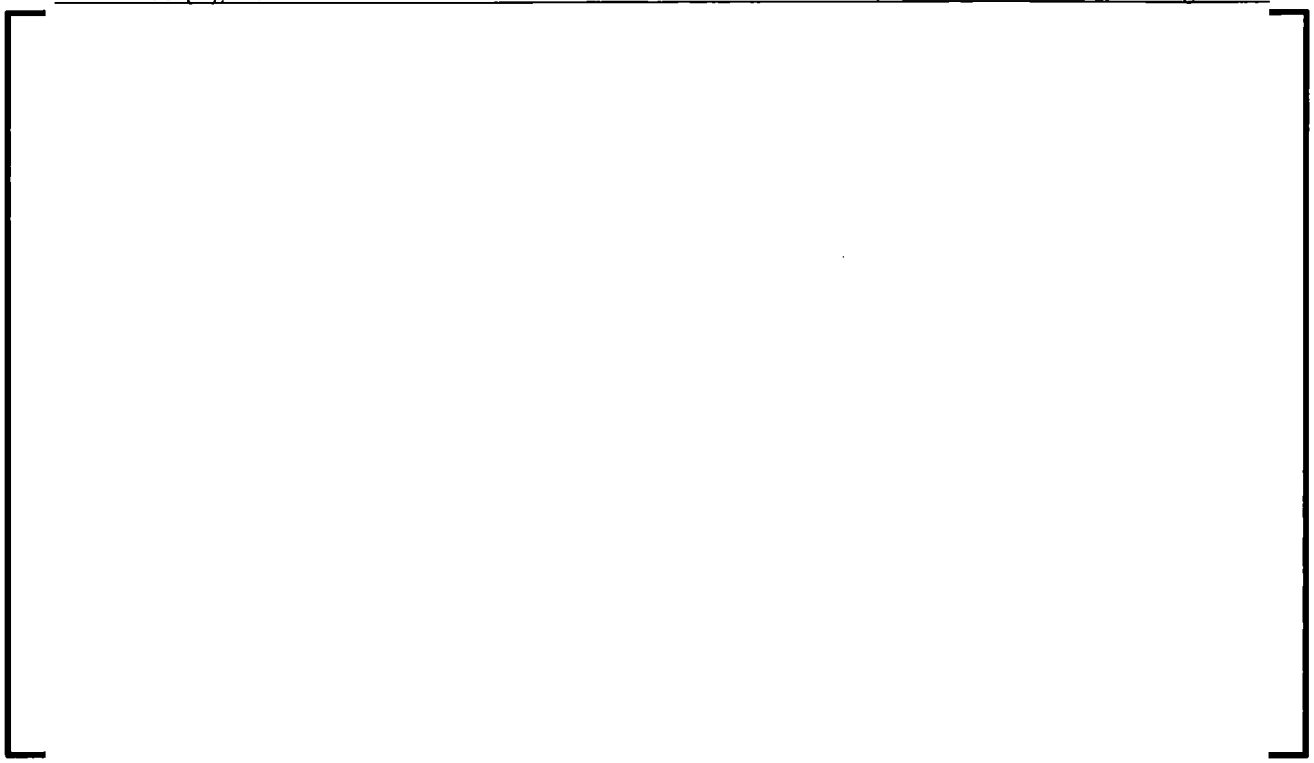

Figure 2.6-7 FLECHT SEASET 31504 Droplet density at PCT location (node 10)

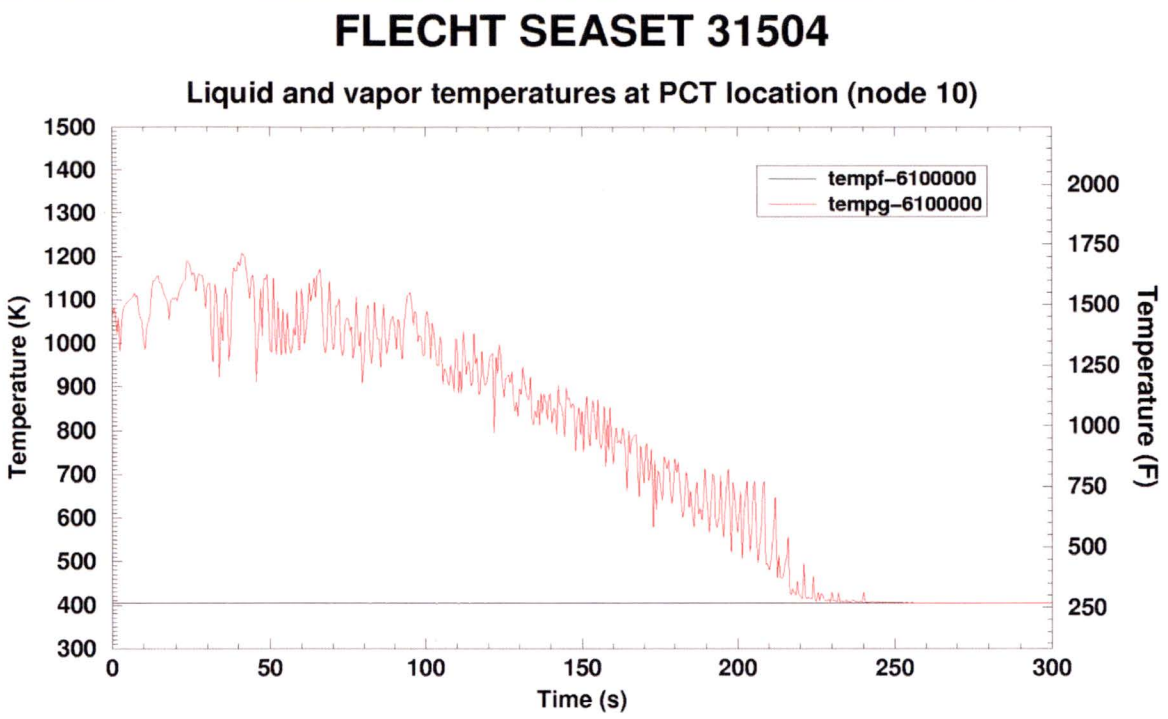

Figure 2.6-8 FLECHT SEASET 31504 Liquid and vapor temperatures at PCT location (node 10)

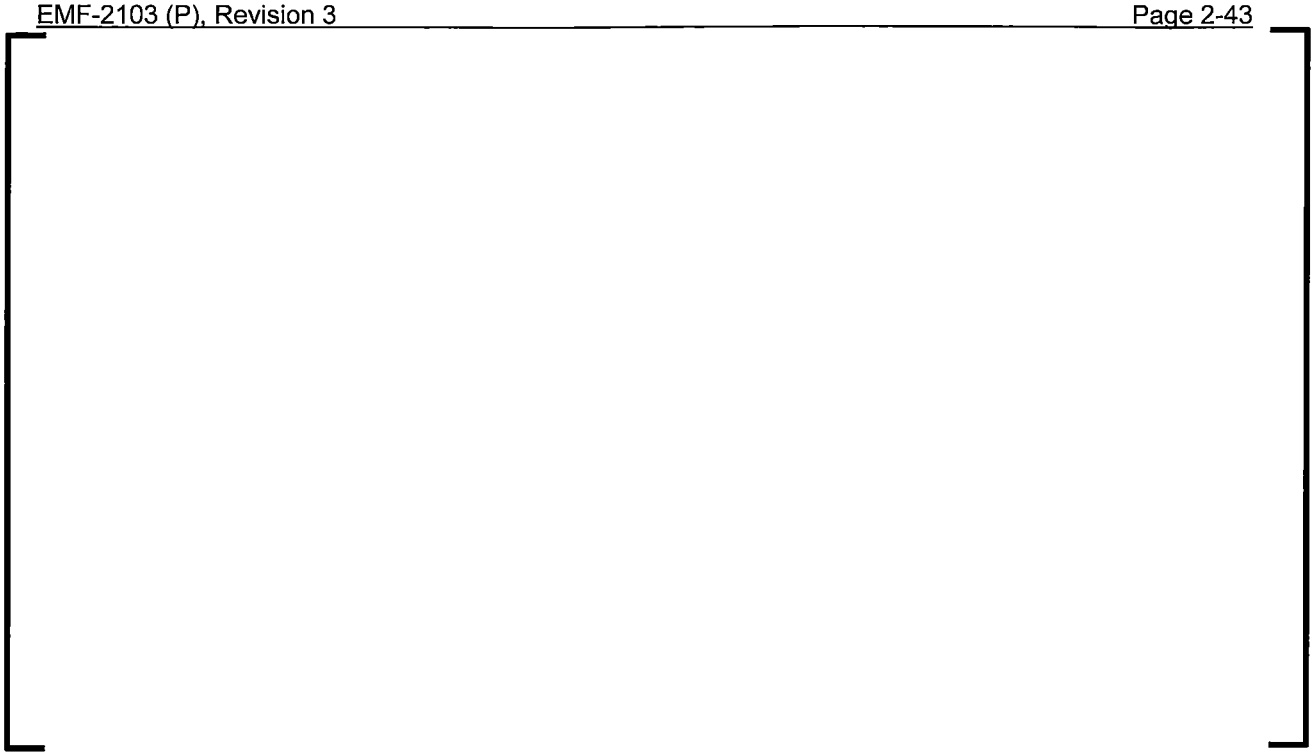

Figure 2.6-9 FLECHT SEASET 31504 Droplet diameter at PCT location (node 10)

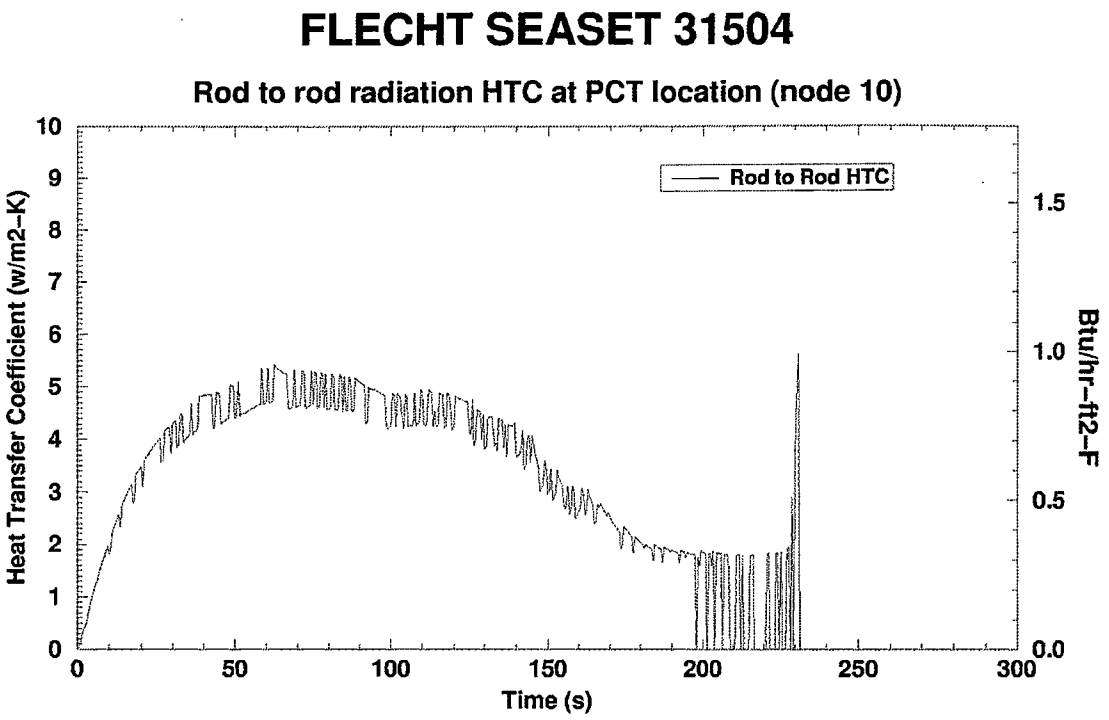

Figure 2.6-10 FLECHT SEASET 31504 Rod to rod radiation HTC at PCT location (node 10)

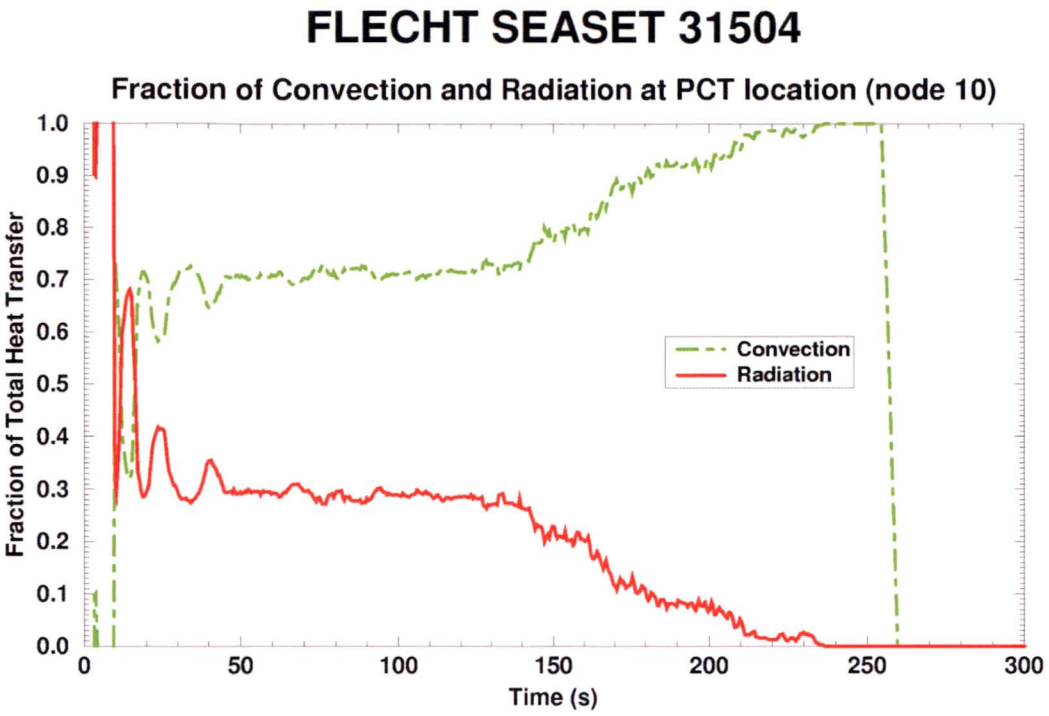

Figure 2.6-11 FLECHT SEASET 31504 Fraction of Convection and Radiation at PCT location (node 10) see note 1

[1] When the heat transfer regime transitions into either nucleate or single-phase boiling the convective heat transfer parameters become zero by definition. Therefore, at approximately 260 s, both convection and radiation heat transfer fractions are also zero.

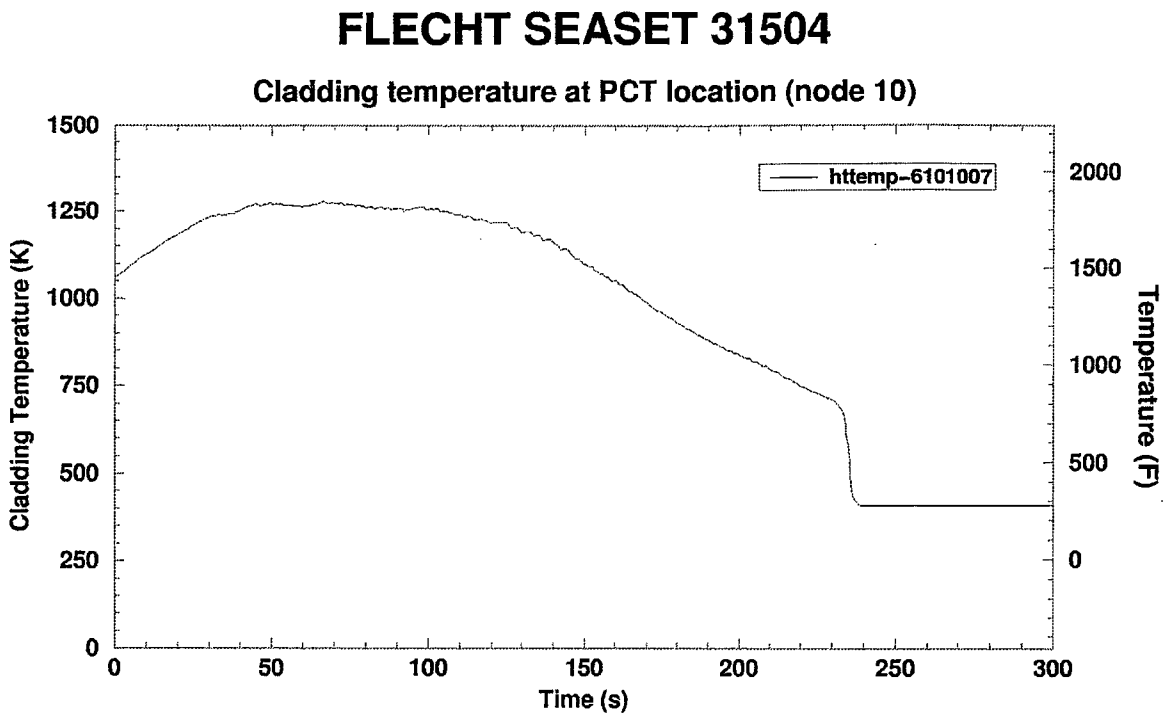

Figure 2.6-12 FLECHT SEASET 31504 Cladding temperature at PCT location (node 10)

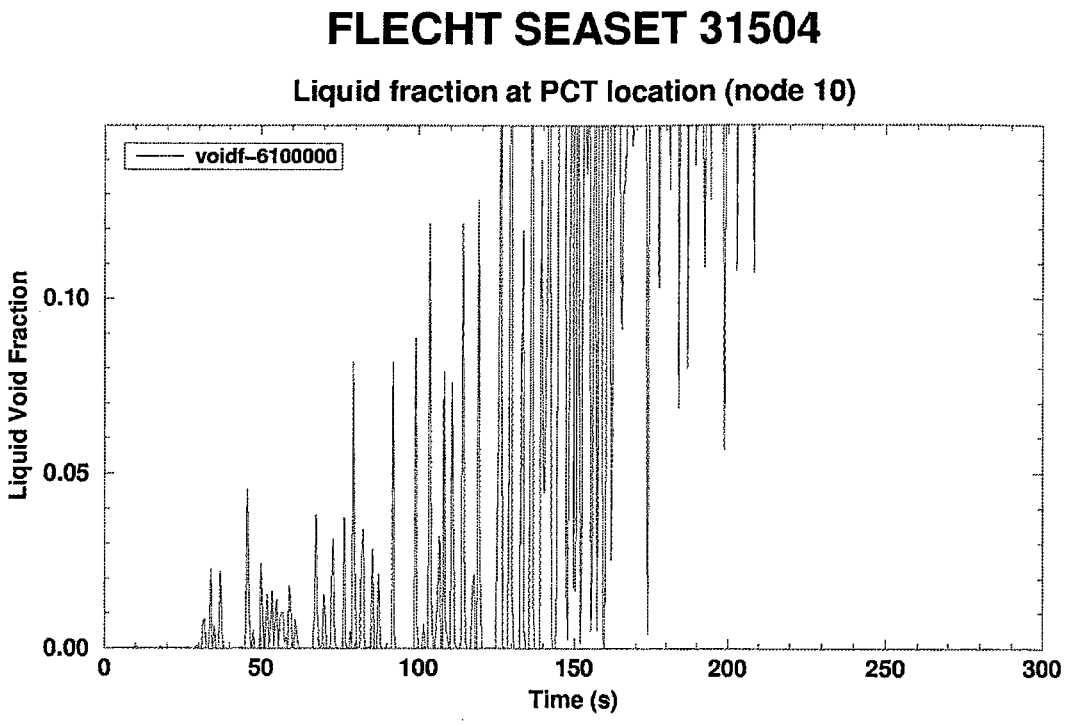

Figure 2.6-13 FLECHT SEASET 31504 Liquid fraction at PCT location (node 10)

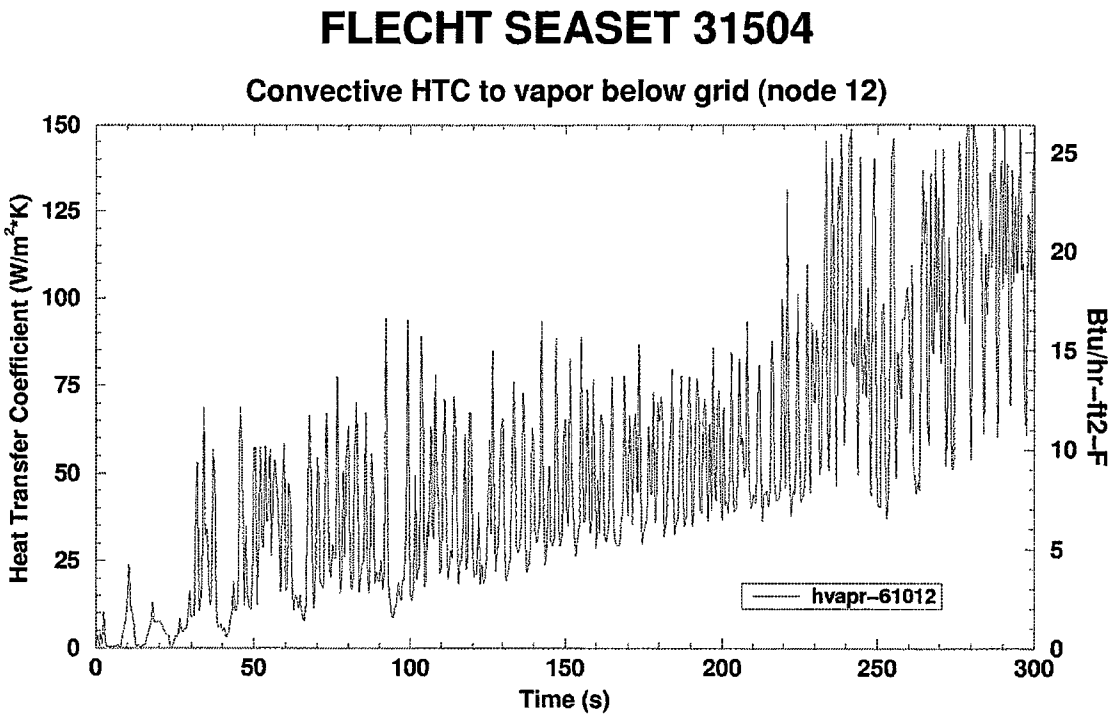

Figure 2.6-14 FLECHT SEASET 31504 Convective HTC to vapor below grid (node 12)

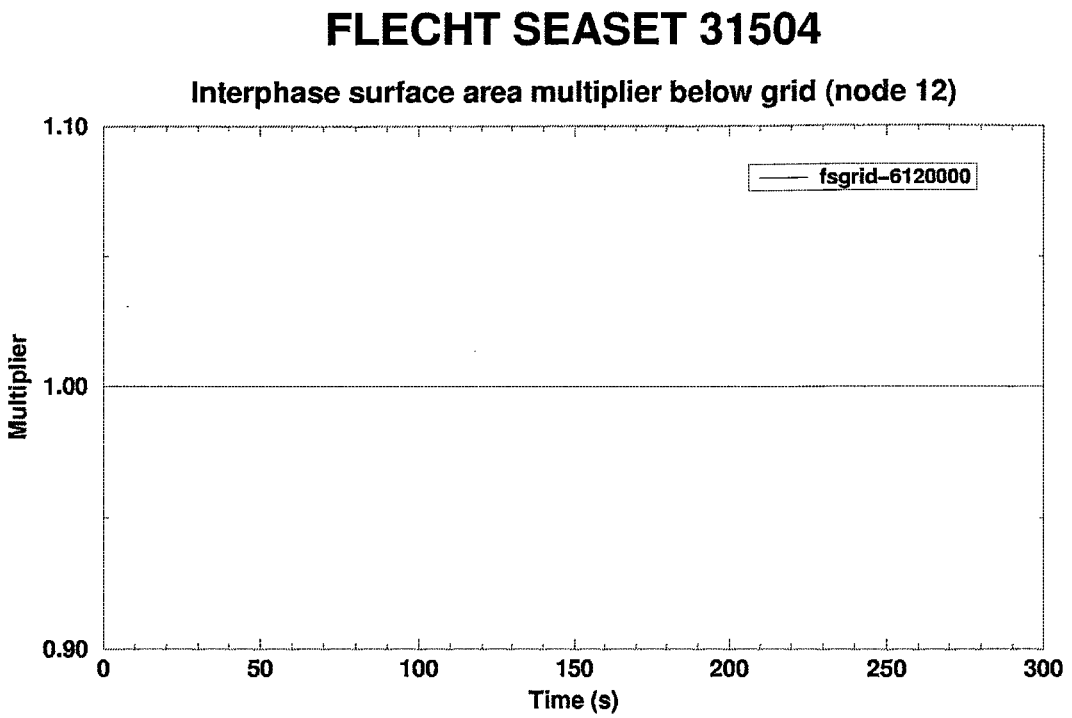

Figure 2.6-15 FLECHT SEASET 31504 Interphase surface area multiplier below grid (node 12)

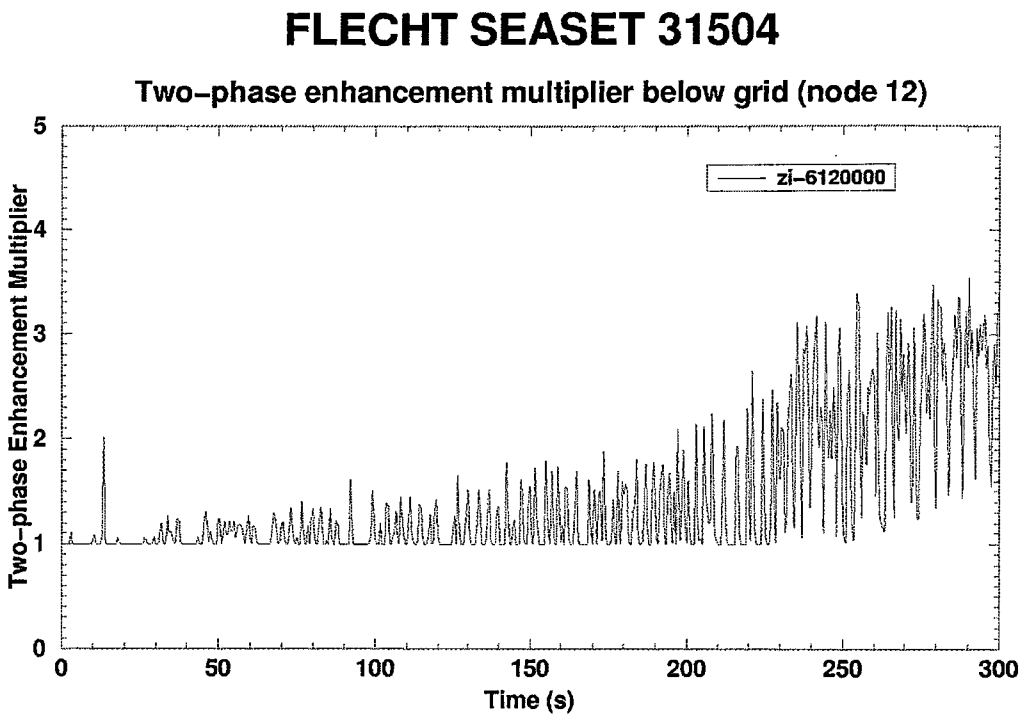

Figure 2.6-16 FLECHT SEASET 31504 Two-phase enhancement multiplier below grid (node 12)

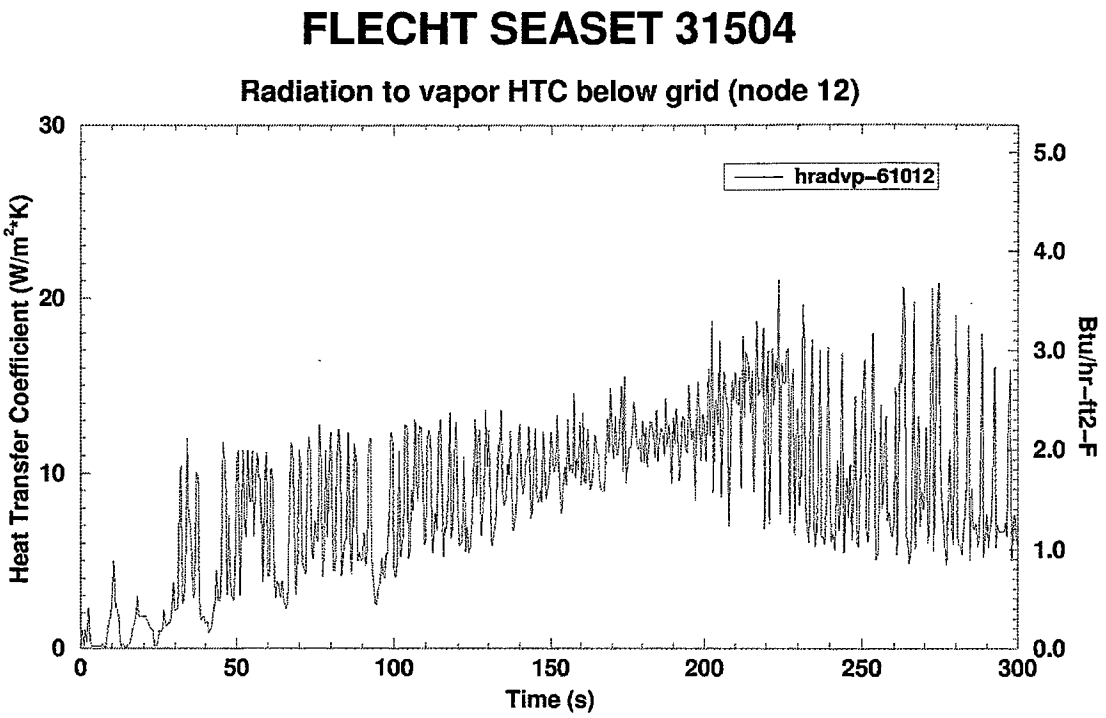

Figure 2.6-17 FLECHT SEASET 31504 Radiation to vapor HTC below grid (node 12)

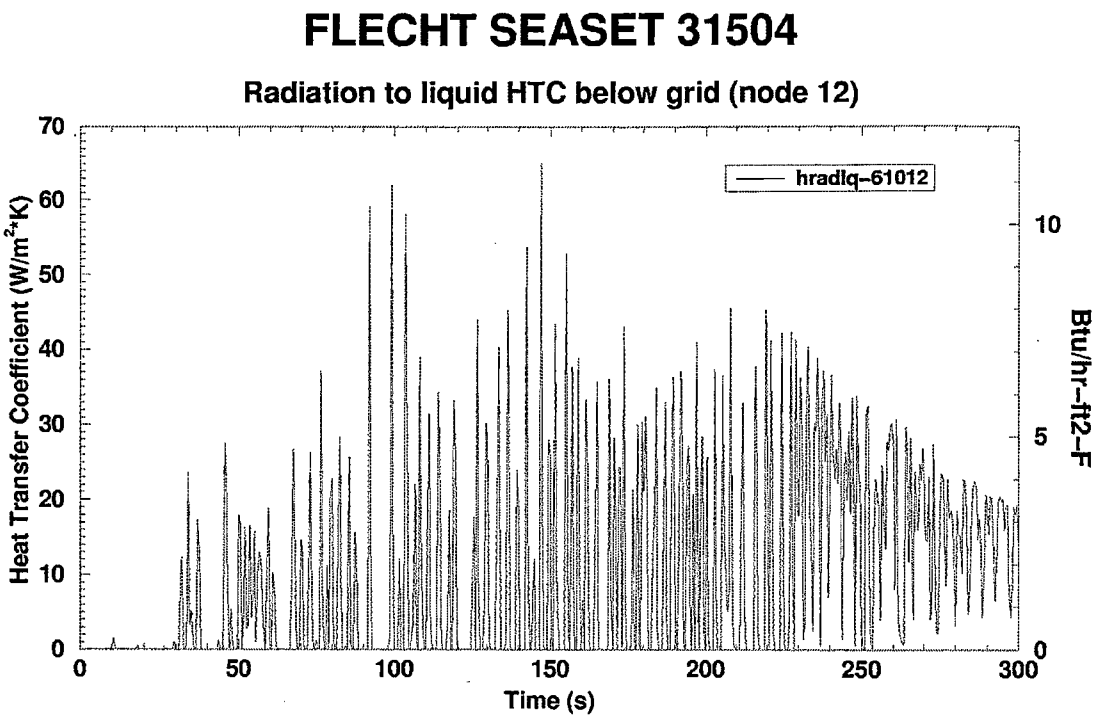

Figure 2.6-18 FLECHT SEASET 31504 Radiation to liquid HTC below grid (node 12)

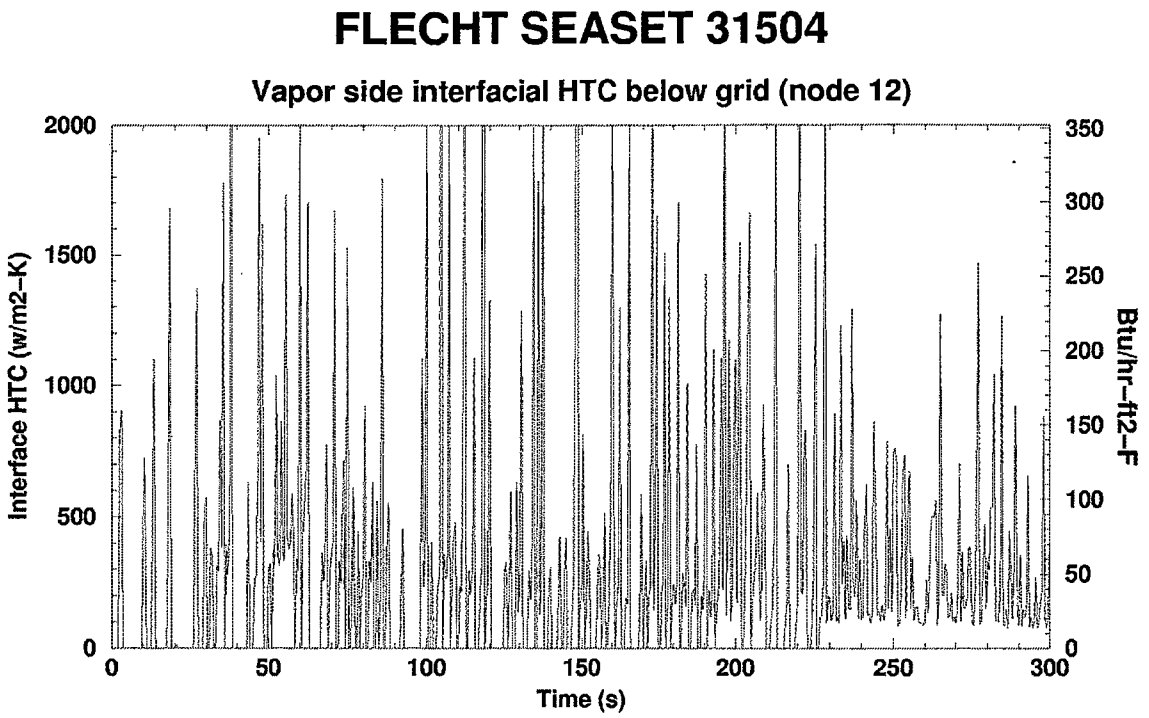

Figure 2.6-19 FLECHT SEASET 31504 Vapor side interfacial HTC below grid (node 12)

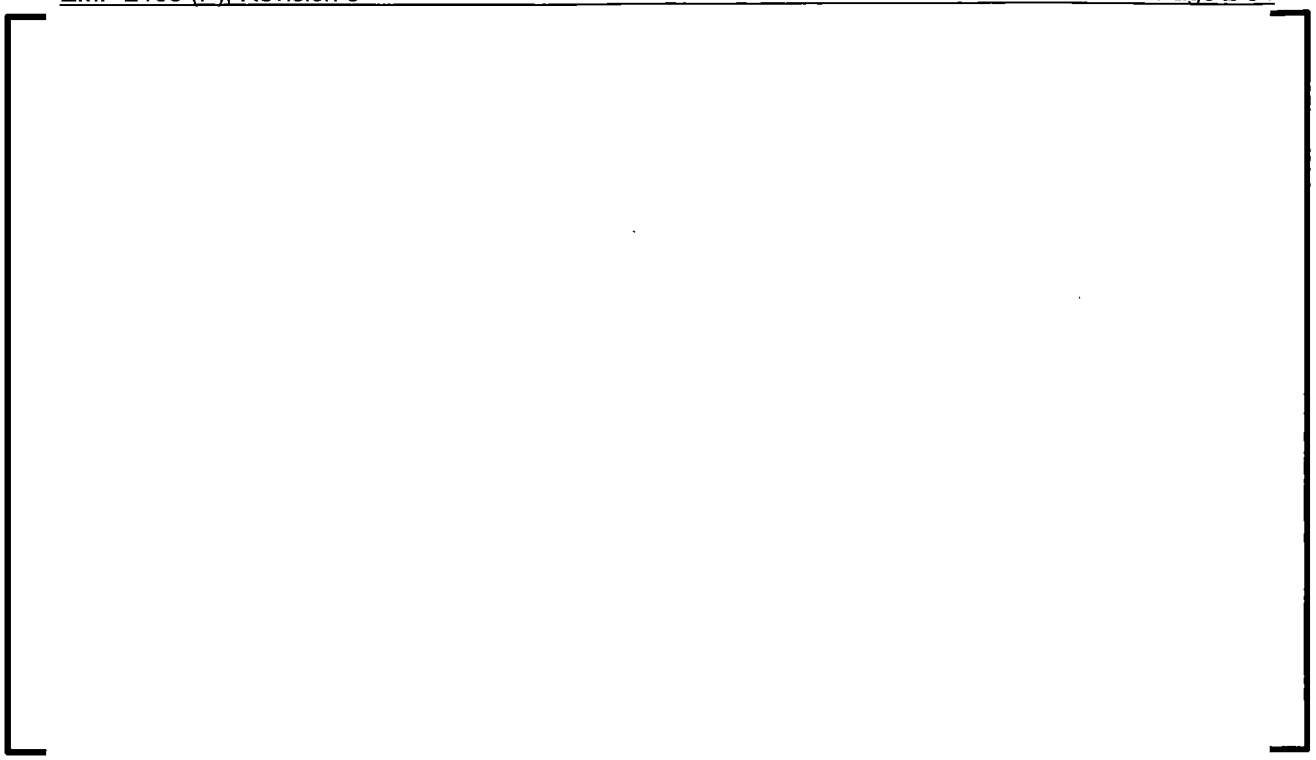

Figure 2.6-20 FLECHT SEASET 31504 Droplet density below grid (node 12)

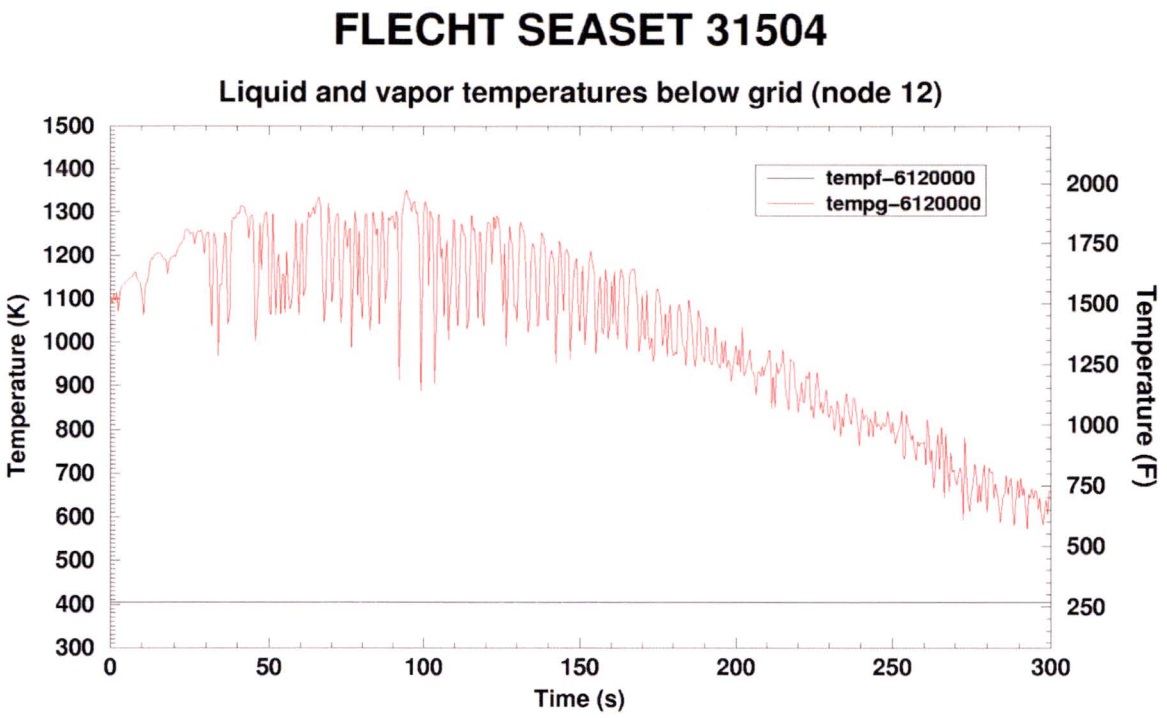

Figure 2.6-21 FLECHT SEASET 31504 Liquid and vapor temperatures below grid (node 12)

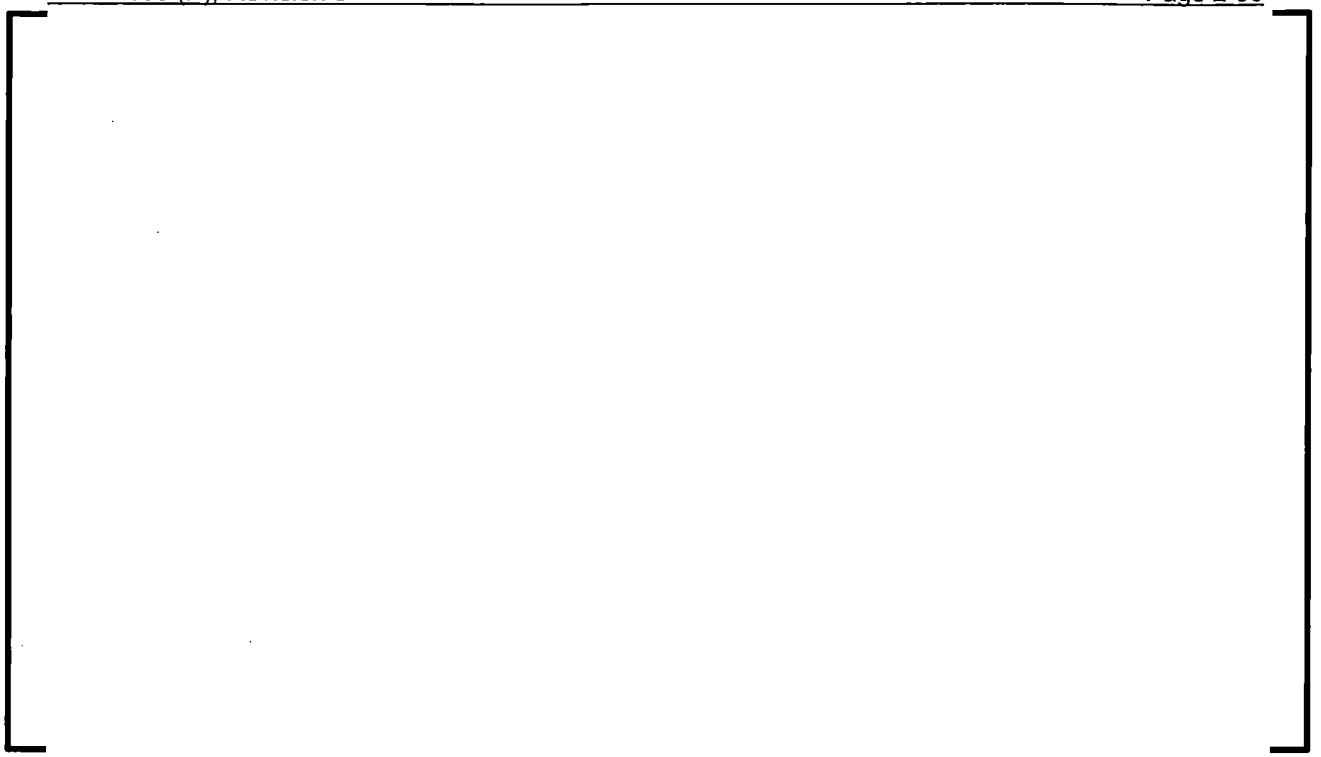

Figure 2.6-22 FLECHT SEASET 31504 Droplet diameter below grid (node 12)

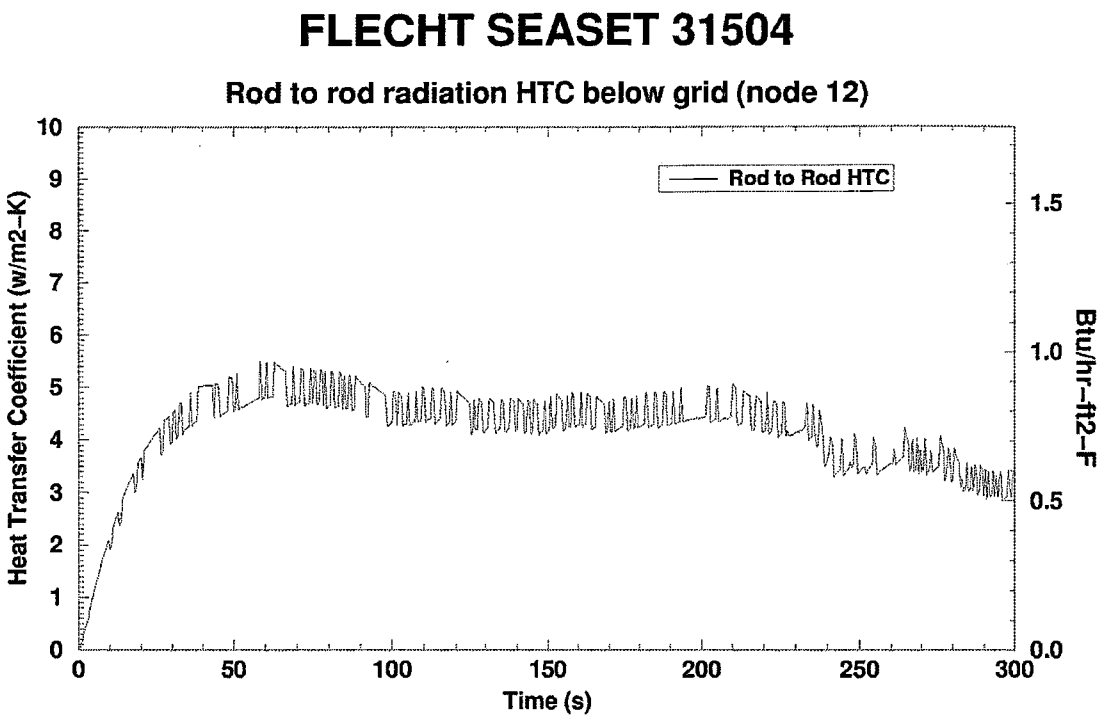

Figure 2.6-23 FLECHT SEASET 31504 Rod to rod radiation HTC below grid (node 12)

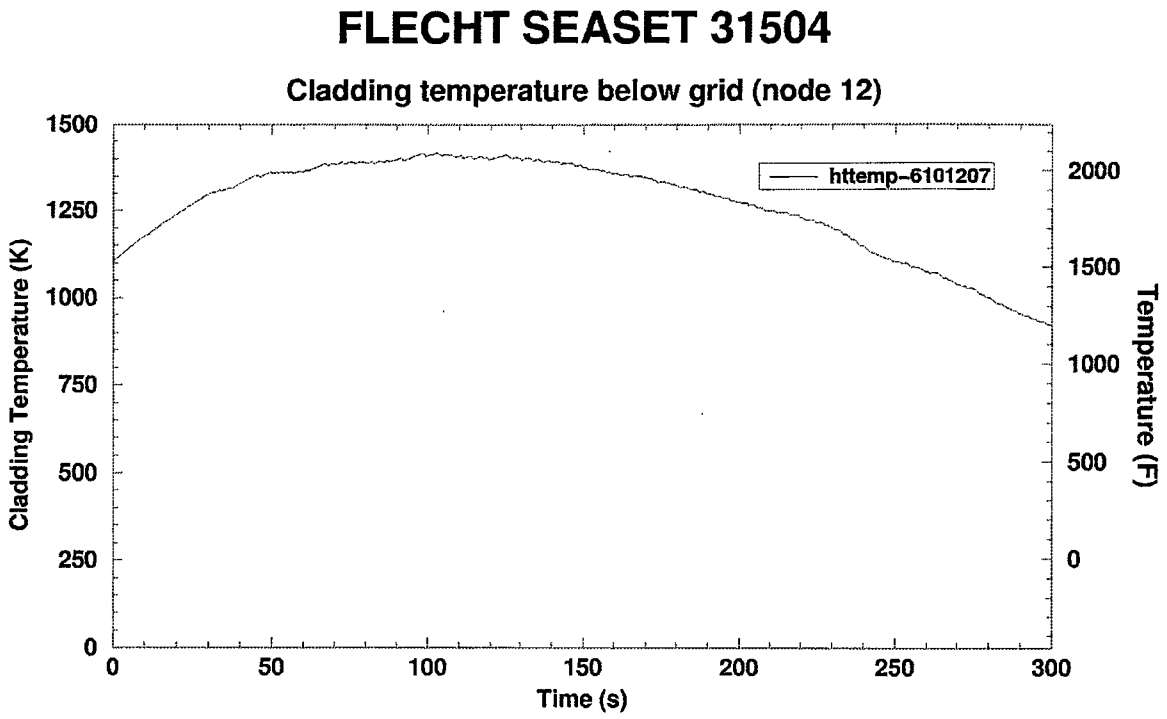

Figure 2.6-24 FLECHT SEASET 31504 Cladding temperature below grid (node 12)

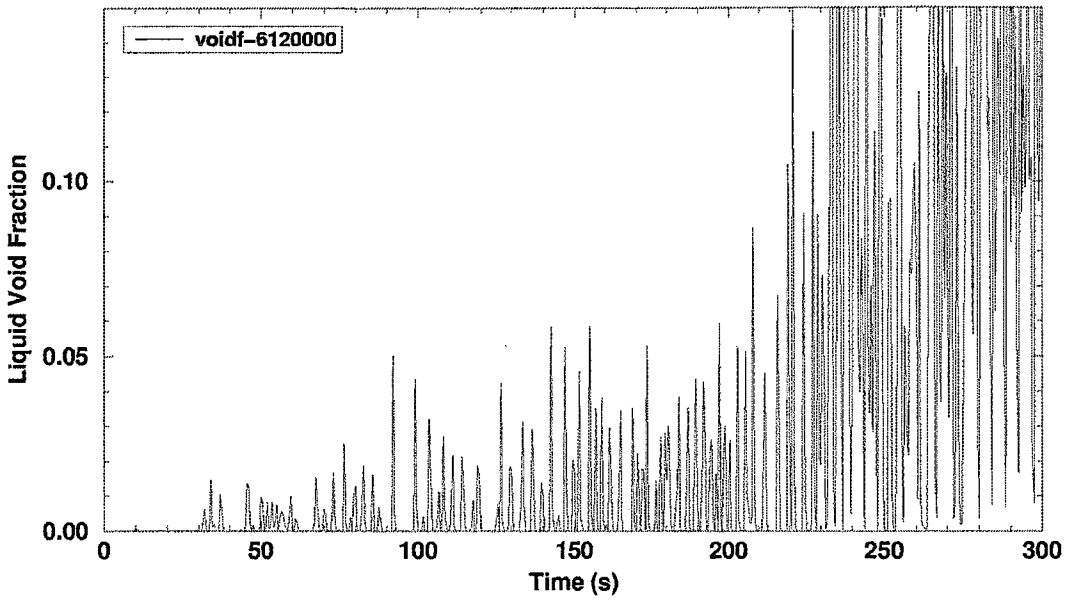

Figure 2.6-25 FLECHT SEASET 31504 Liquid fraction below grid (node 12)

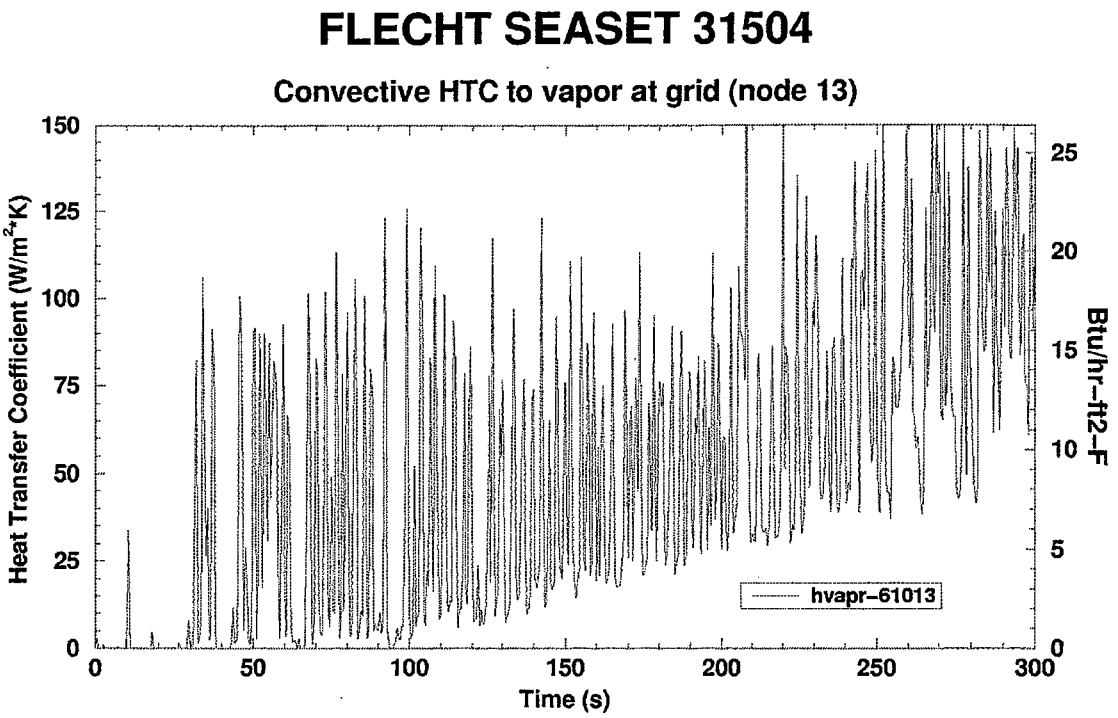

Figure 2.6-26 FLECHT SEASET 31504 Convective HTC to vapor at grid (node 13)

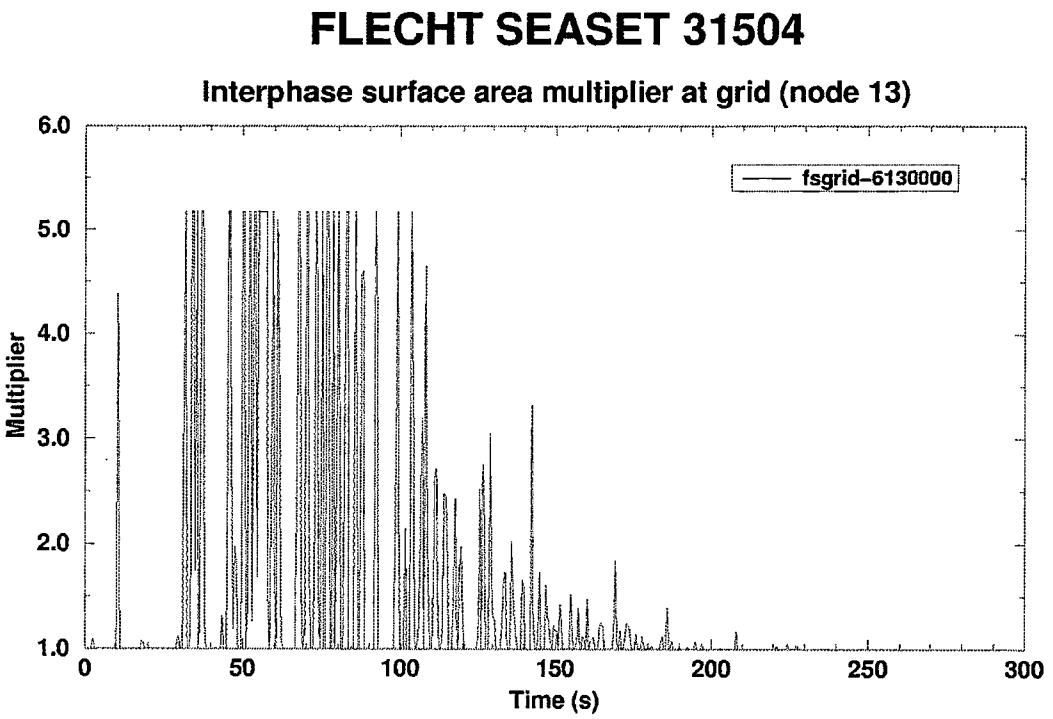

Figure 2.6-27 FLECHT SEASET 31504 Interphase surface area multiplier at grid (node 13)

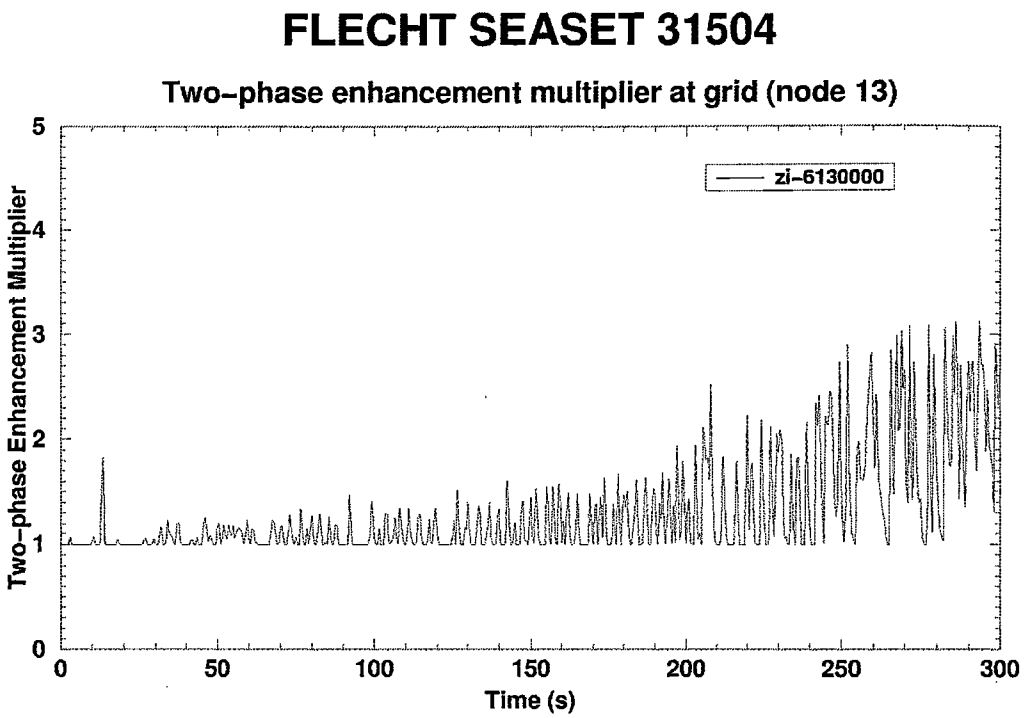

Figure 2.6-28 FLECHT SEASET 31504 Two-phase enhancement multiplier at grid (node 13)

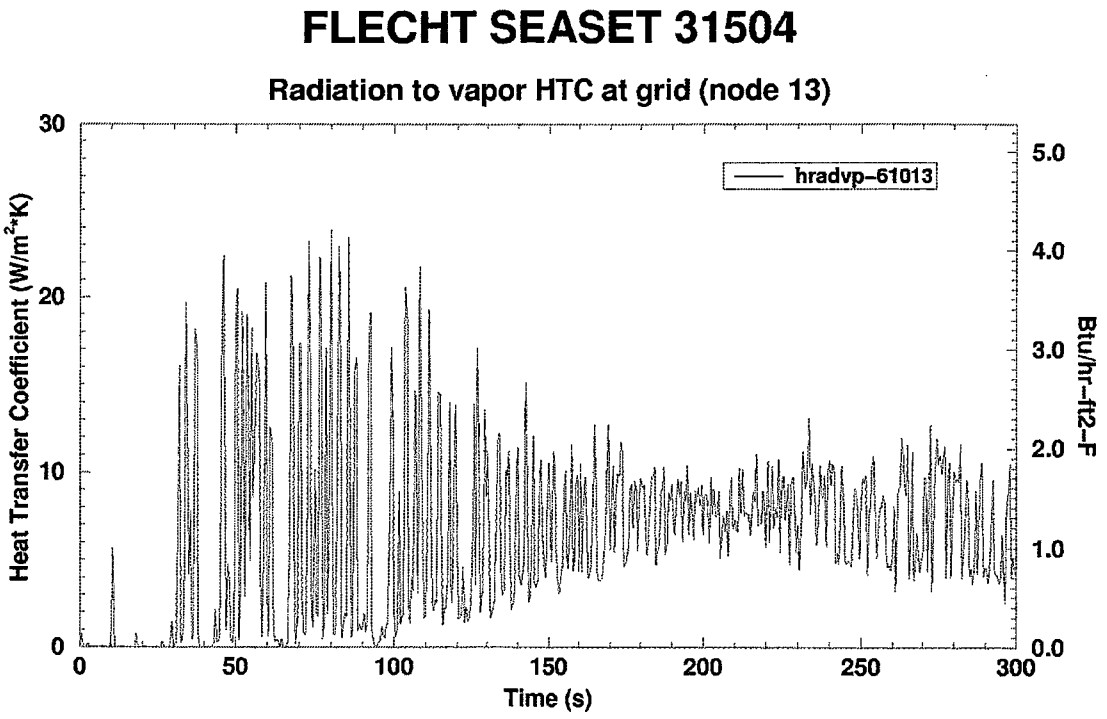

Figure 2.6-29 FLECHT SEASET 31504 Radiation to vapor HTC at grid (node 13)

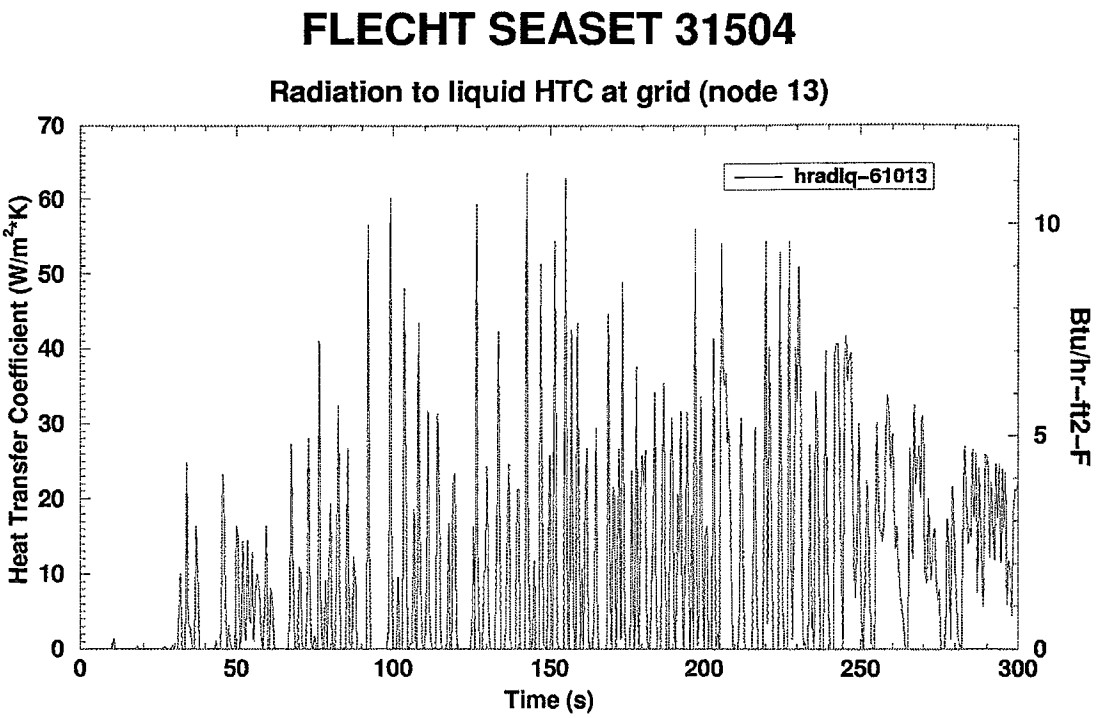

Figure 2.6-30 FLECHT SEASET 31504 Radiation to liquid HTC at grid (node 13)

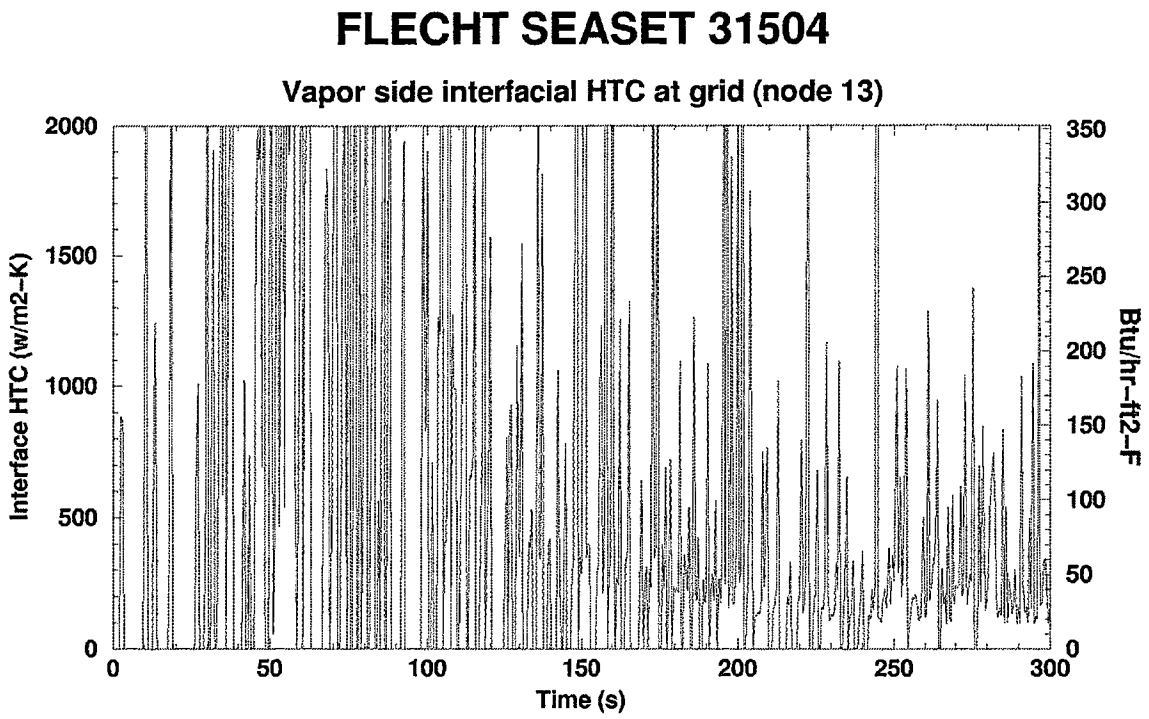

Figure 2.6-31 FLECHT SEASET 31504 Vapor side interfacial HTC at grid (node 13)

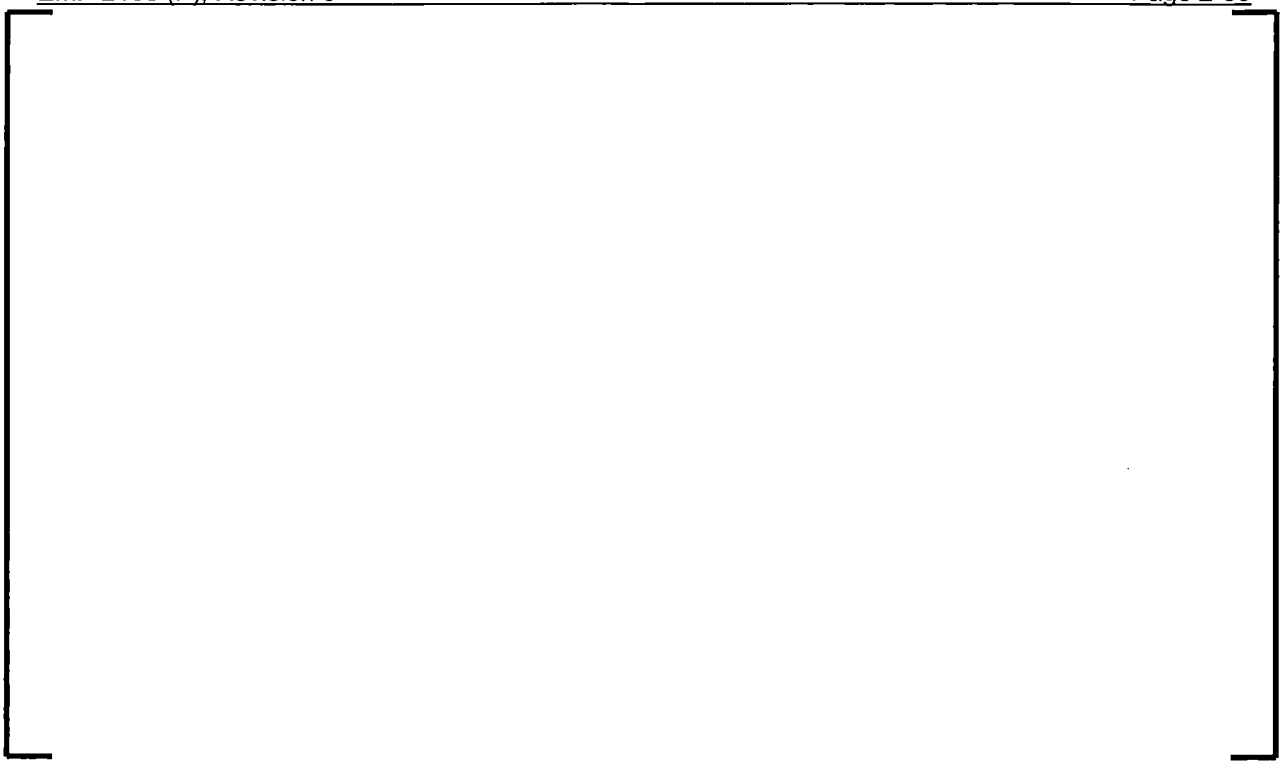

Figure 2.6-32 FLECHT SEASET 31504 Droplet density at grid (node 13)

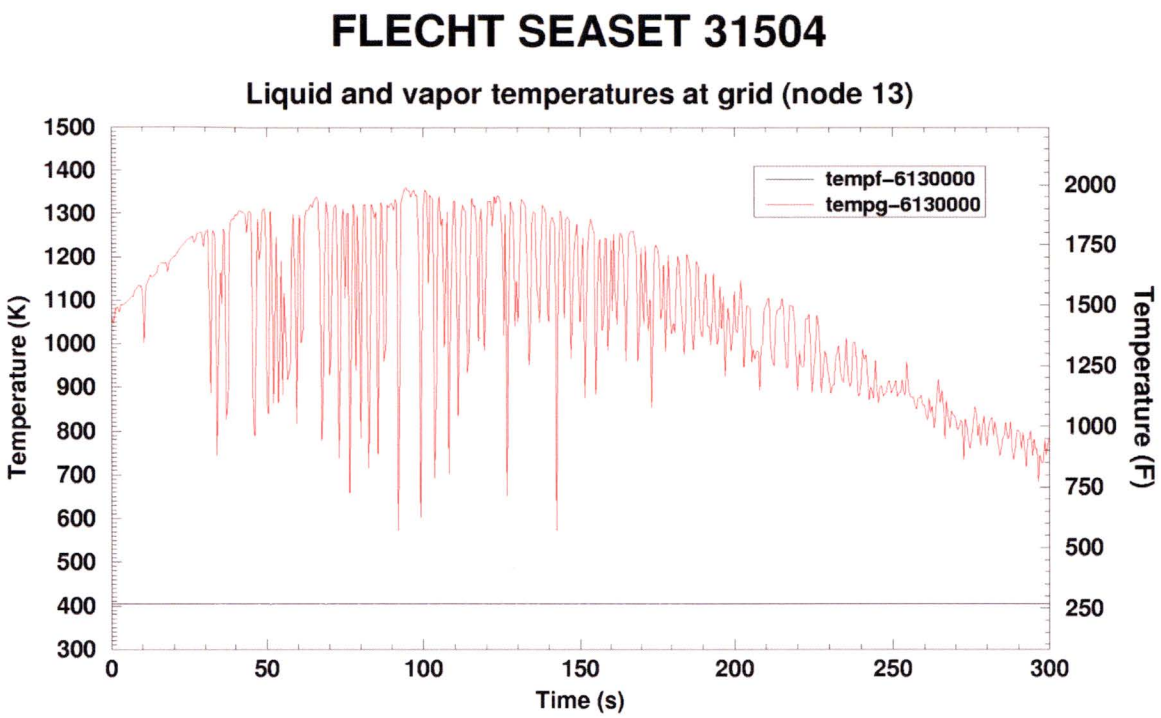

Figure 2.6-33 FLECHT SEASET 31504 Liquid and vapor temperatures at grid (node 13)

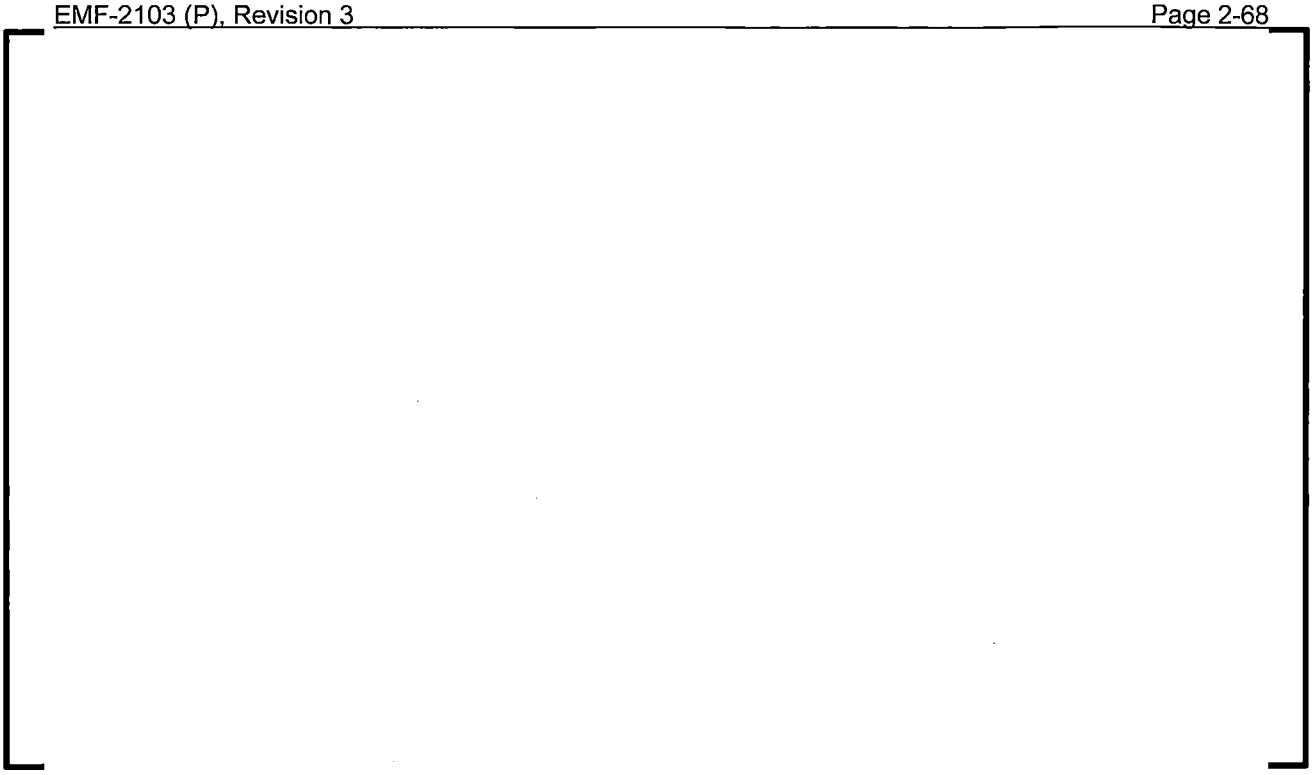

Figure 2.6-34 FLECHT SEASET 31504 Droplet diameter at grid (node 13)

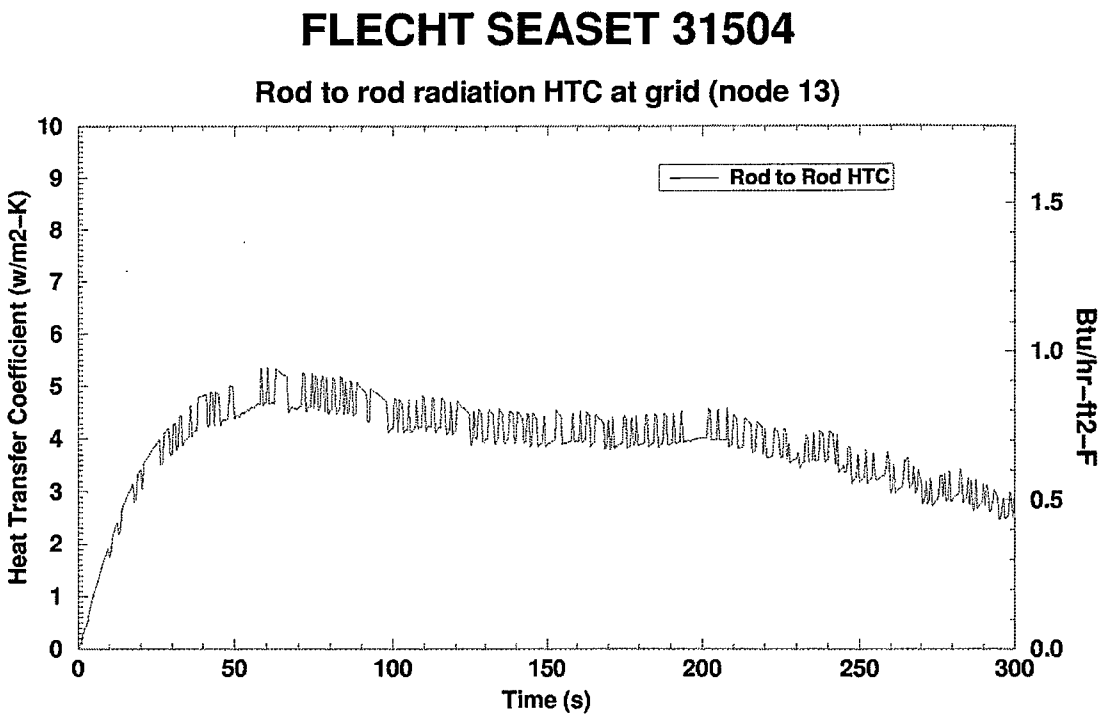

Figure 2.6-35 FLECHT SEASET 31504 Rod to rod radiation HTC at grid (node 13)

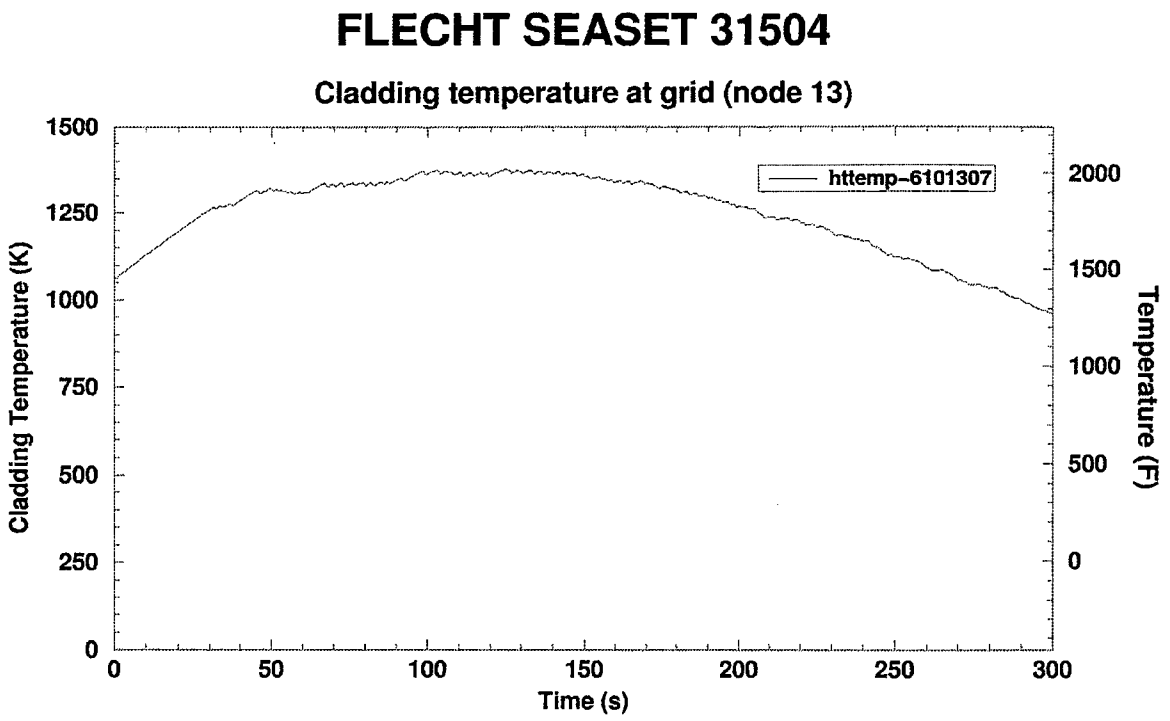

Figure 2.6-36 FLECHT SEASET 31504 Cladding temperature at grid (node 13)

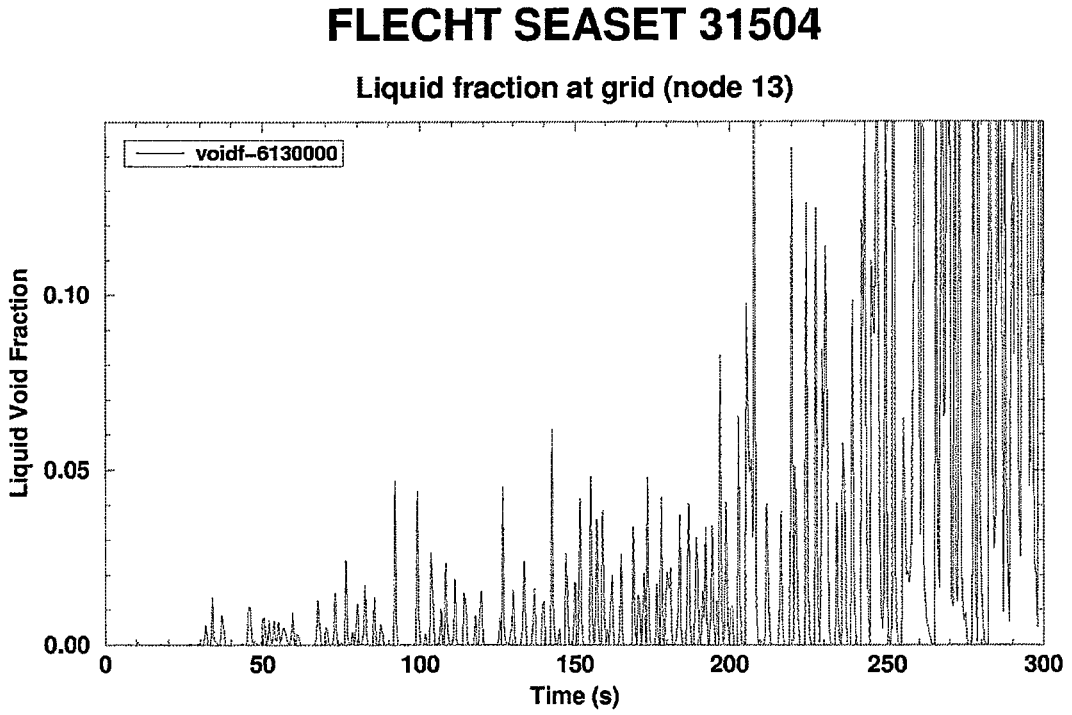

Figure 2.6-37 FLECHT SEASET 31504 Liquid fraction at grid (node 13)

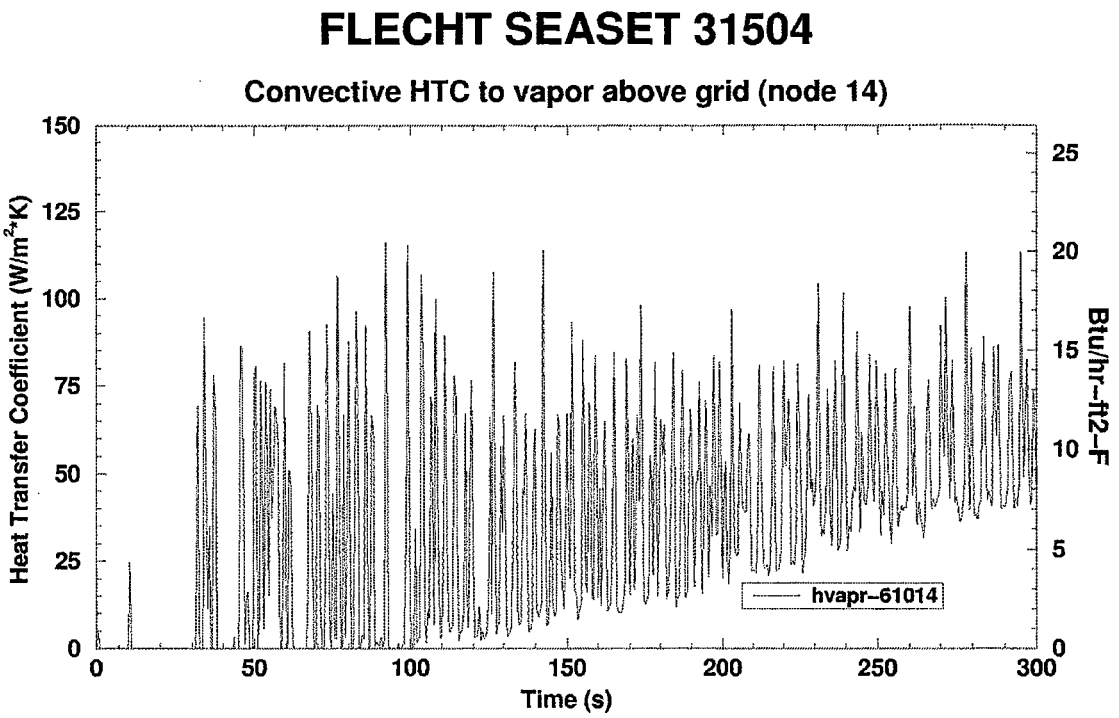

Figure 2.6-38 FLECHT SEASET 31504 Convective HTC to vapor above grid (node 14)

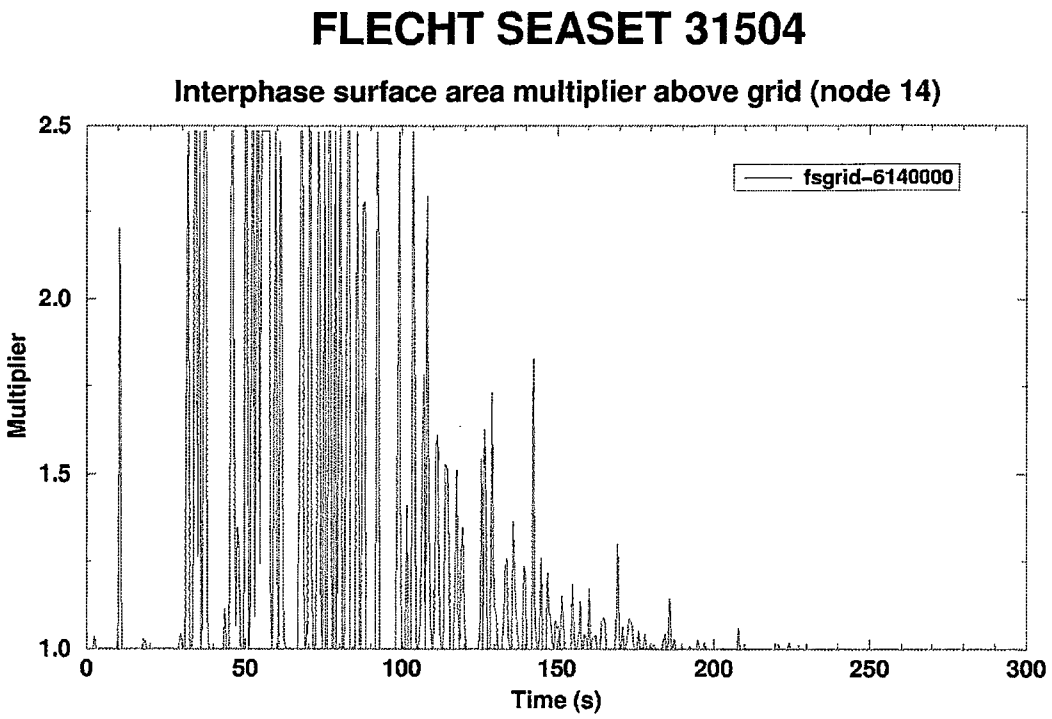

Figure 2.6-39 FLECHT SEASET 31504 Interphase surface area multiplier above grid (node 14)

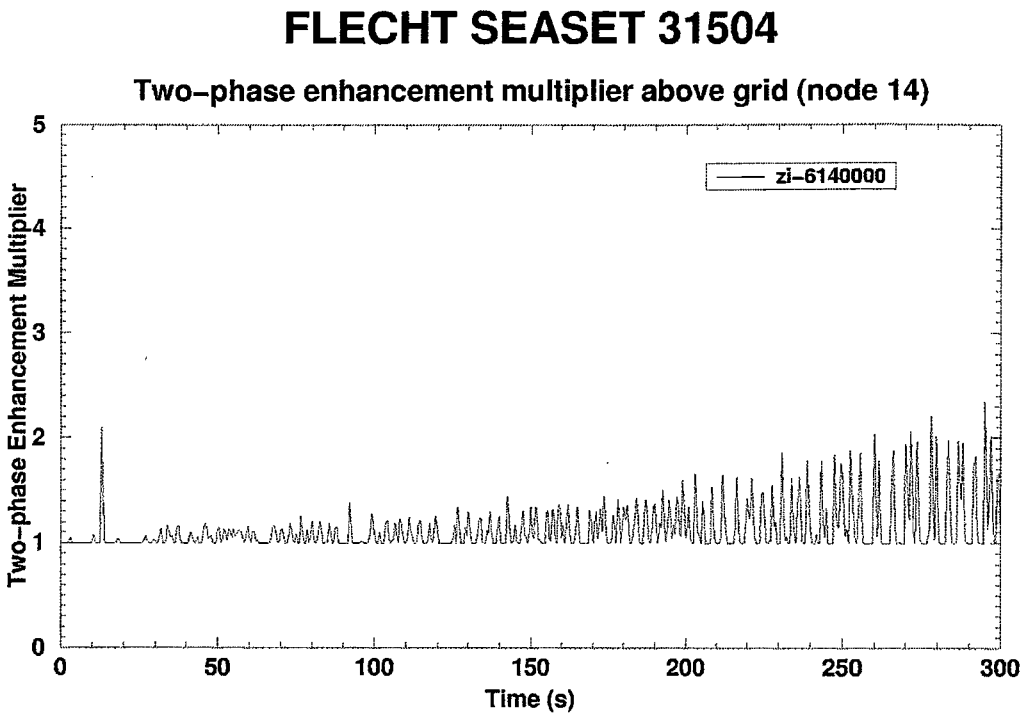

Figure 2.6-40 FLECHT SEASET 31504 Two-phase enhancement multiplier above grid (node 14)

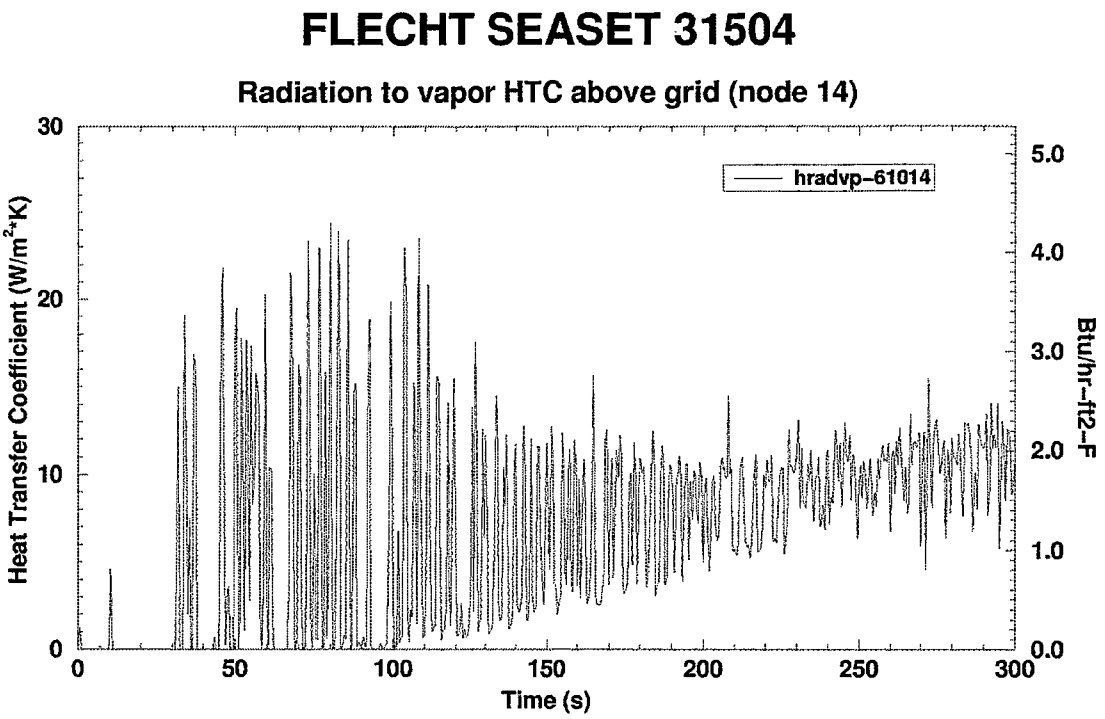

Figure 2.6-41 FLECHT SEASET 31504 Radiation to vapor HTC above grid (node 14)

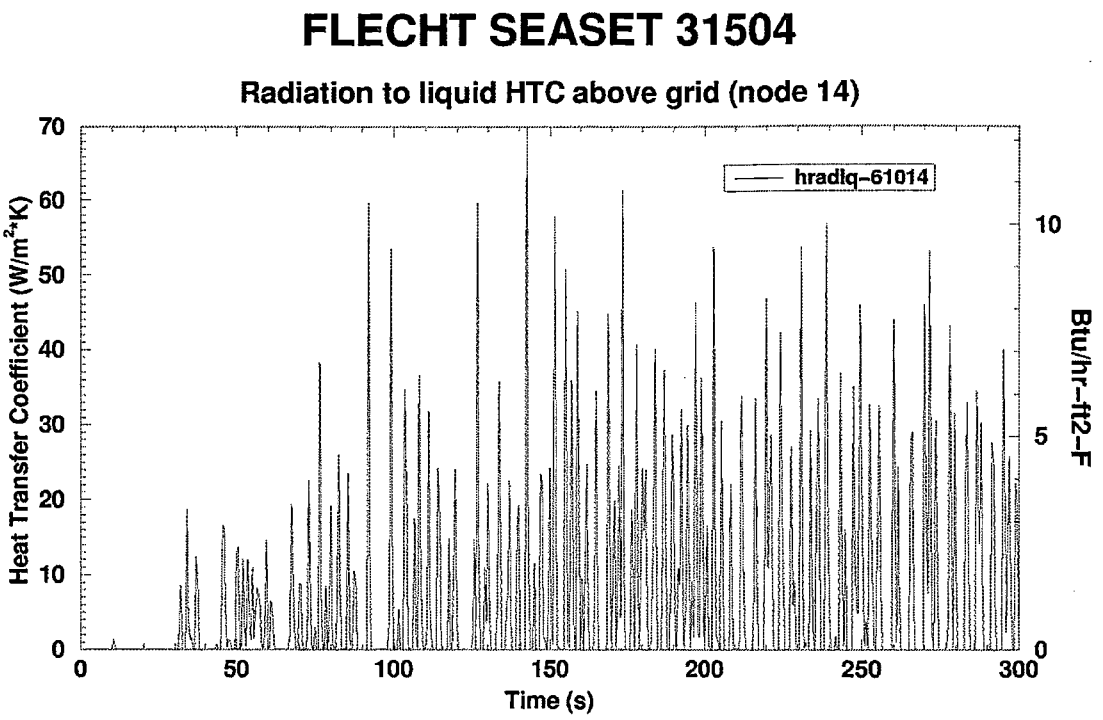

Figure 2.6-42 FLECHT SEASET 31504 Radiation to liquid HTC above grid (node 14)

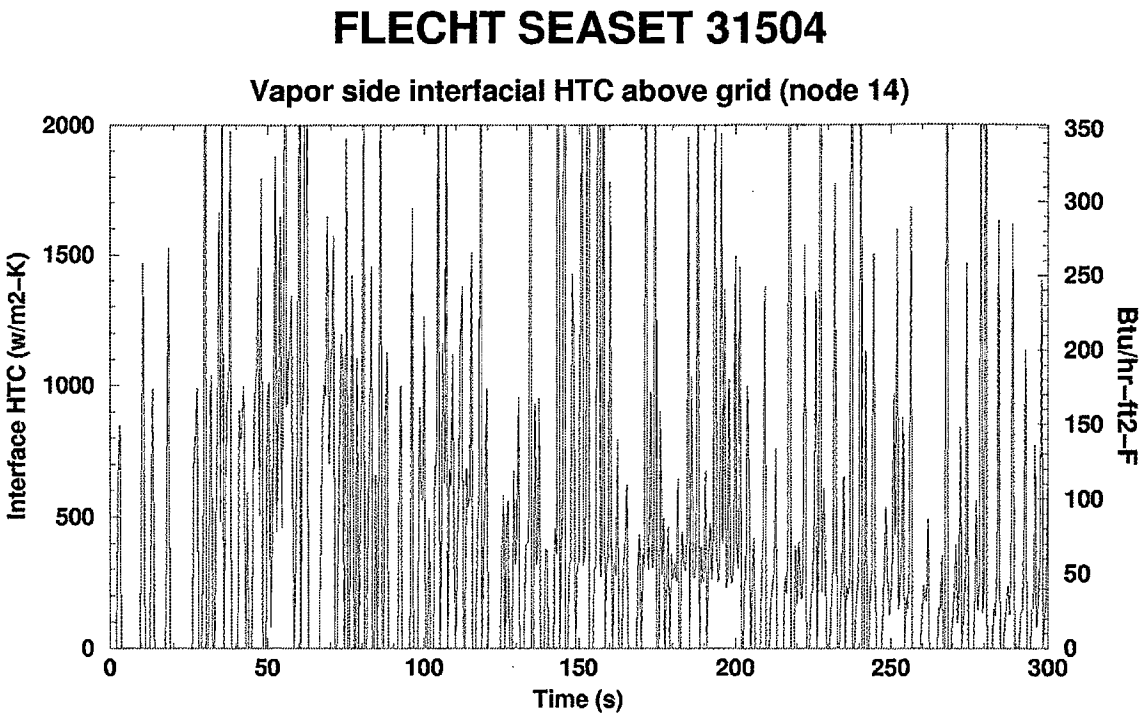

Figure 2.6-43 FLECHT SEASET 31504 Vapor side interfacial HTC above grid (node 14)

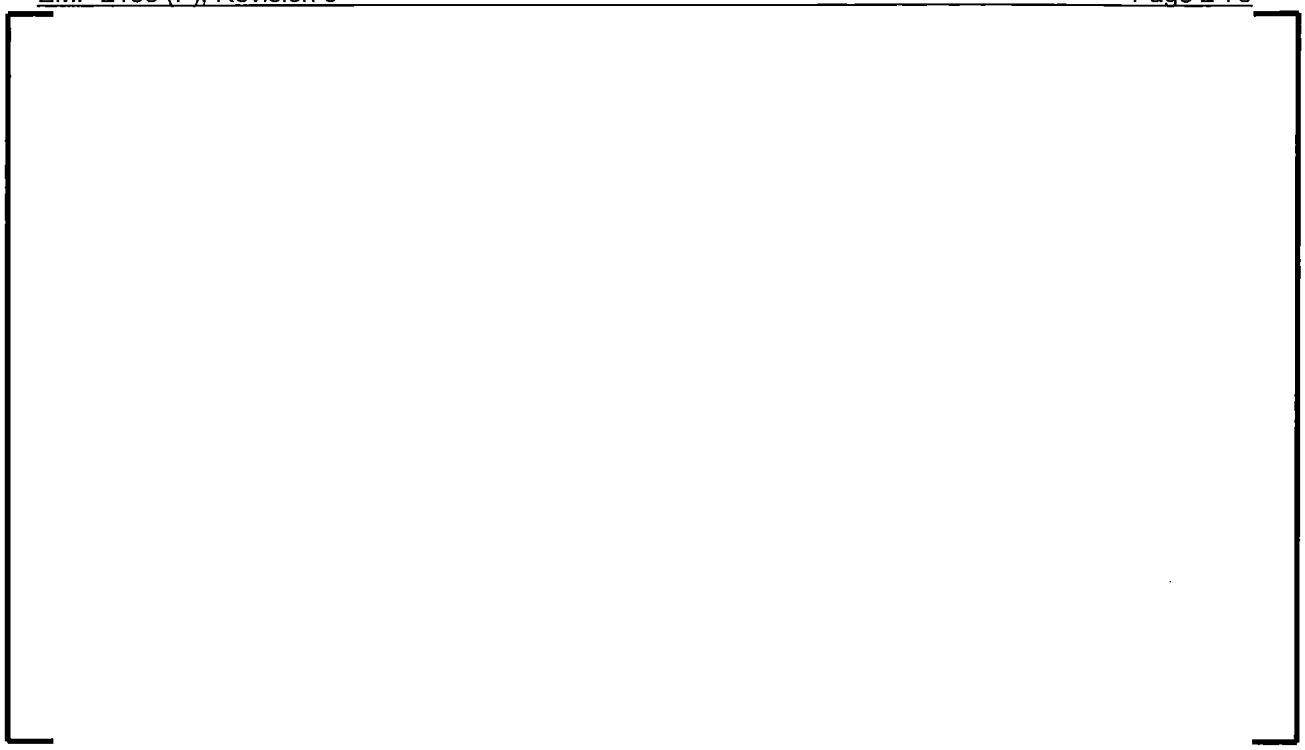

Figure 2.6-44 FLECHT SEASET 31504 Droplet density above grid (node 14)

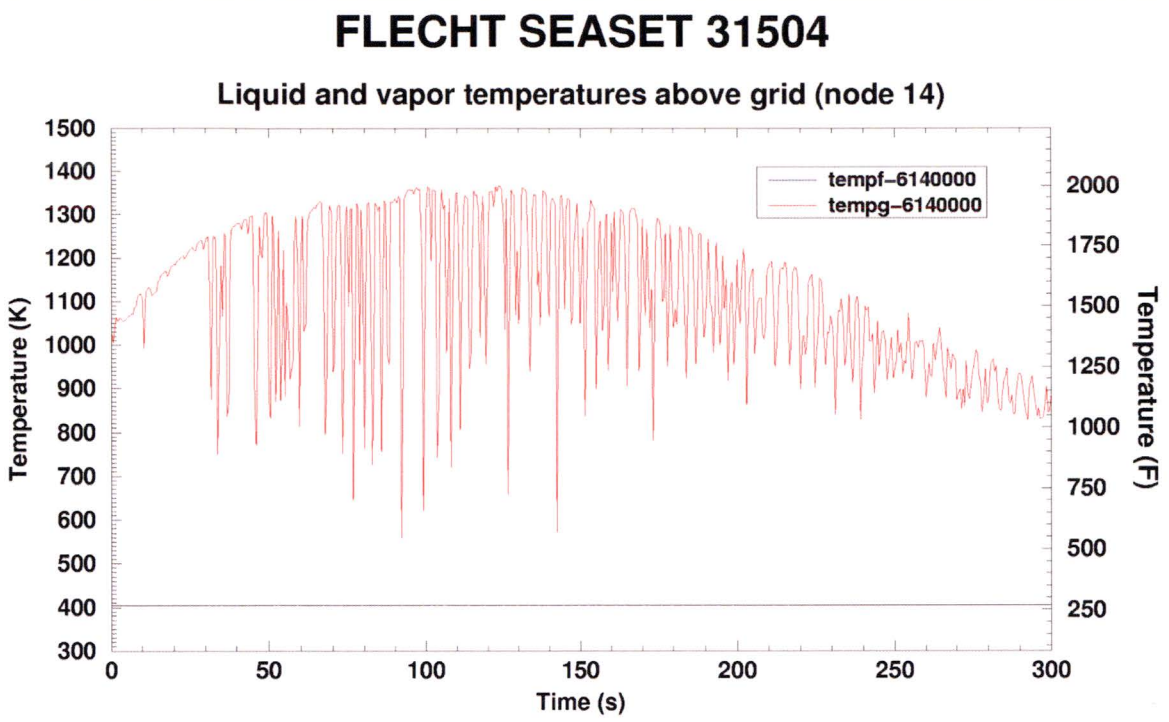

Figure 2.6-45 FLECHT SEASET 31504 Liquid and vapor temperatures above grid (node 14)

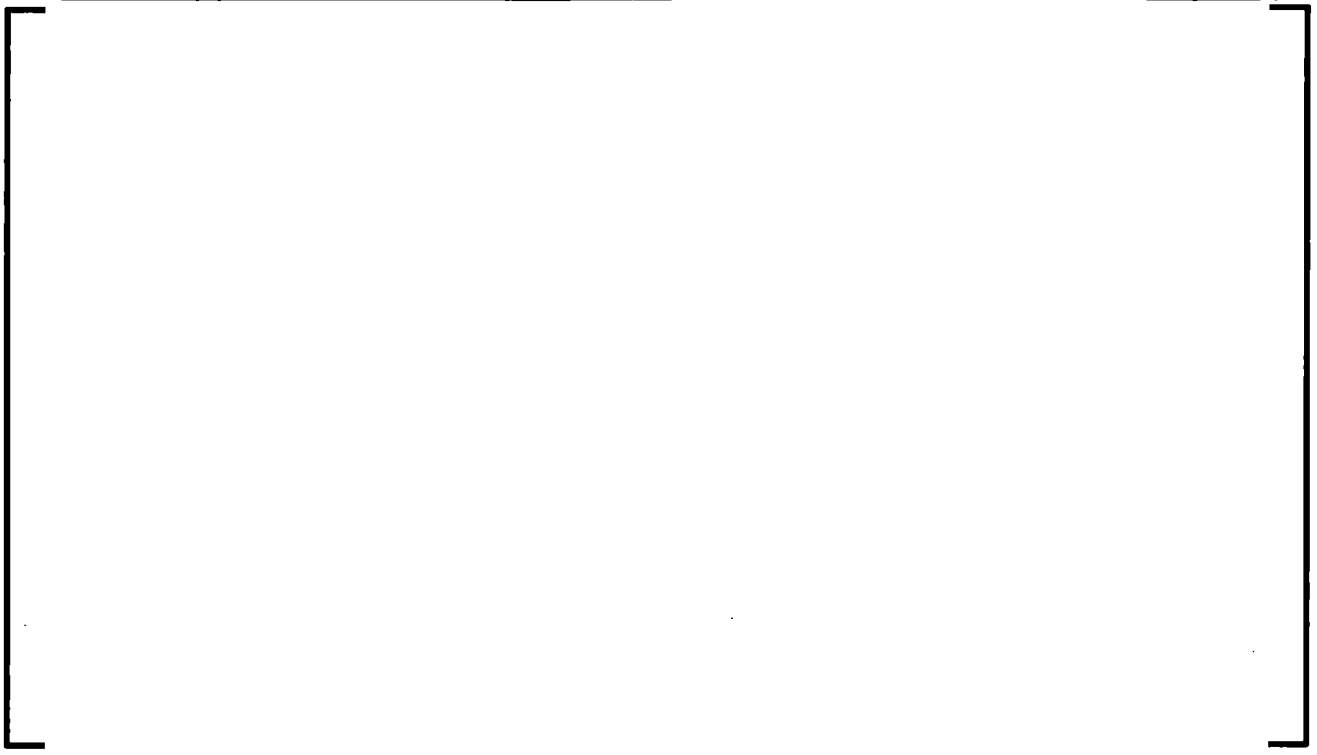

Figure 2.6-46 FLECHT SEASET 31504 Droplet diameter above grid (node 14)

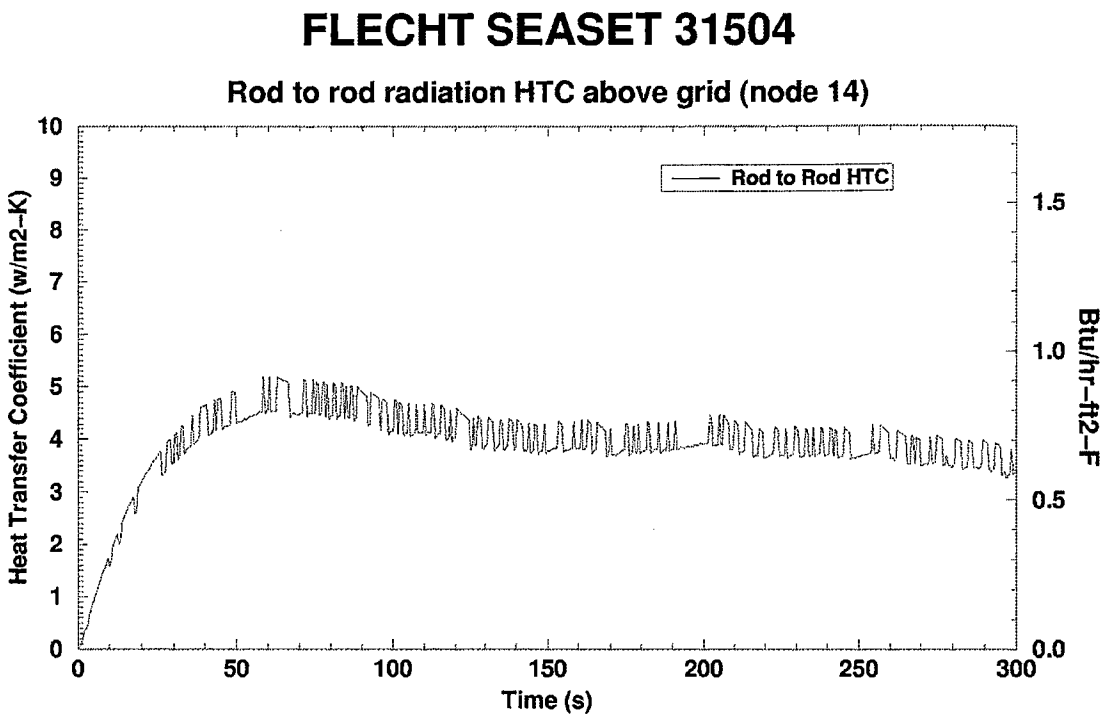

Figure 2.6-47 FLECHT SEASET 31504 Rod to rod radiation HTC above grid (node 14)

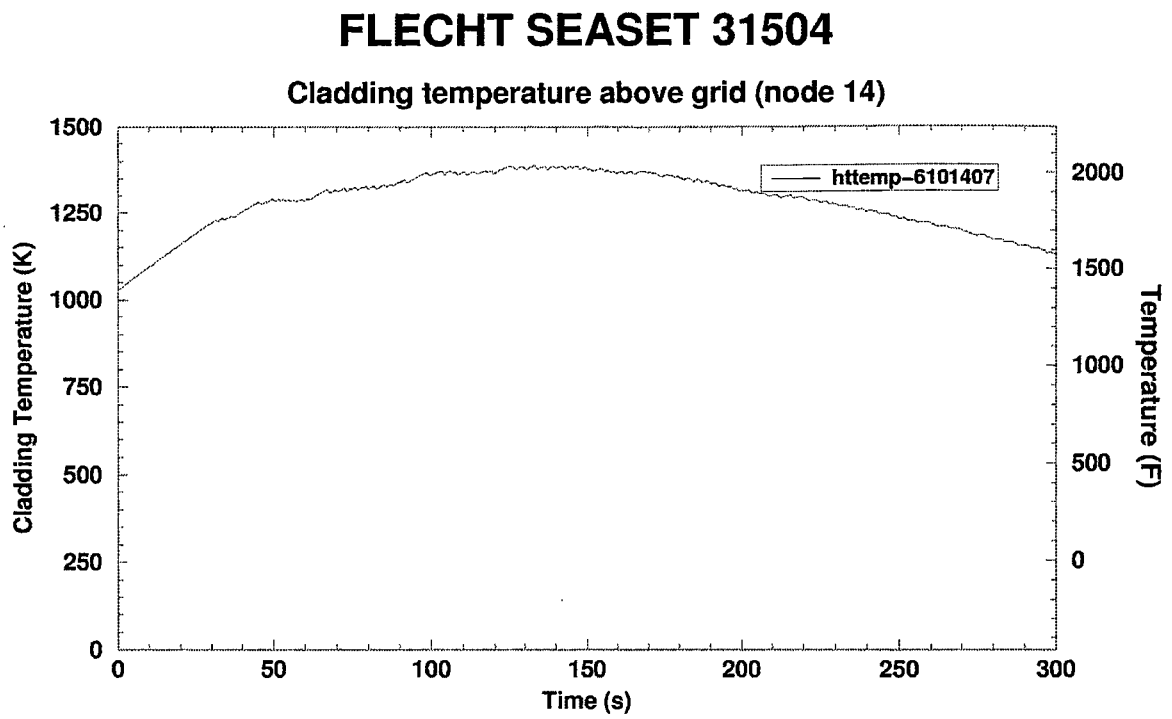

Figure 2.6-48 FLECHT SEASET 31504 Cladding temperature above grid (node 14)

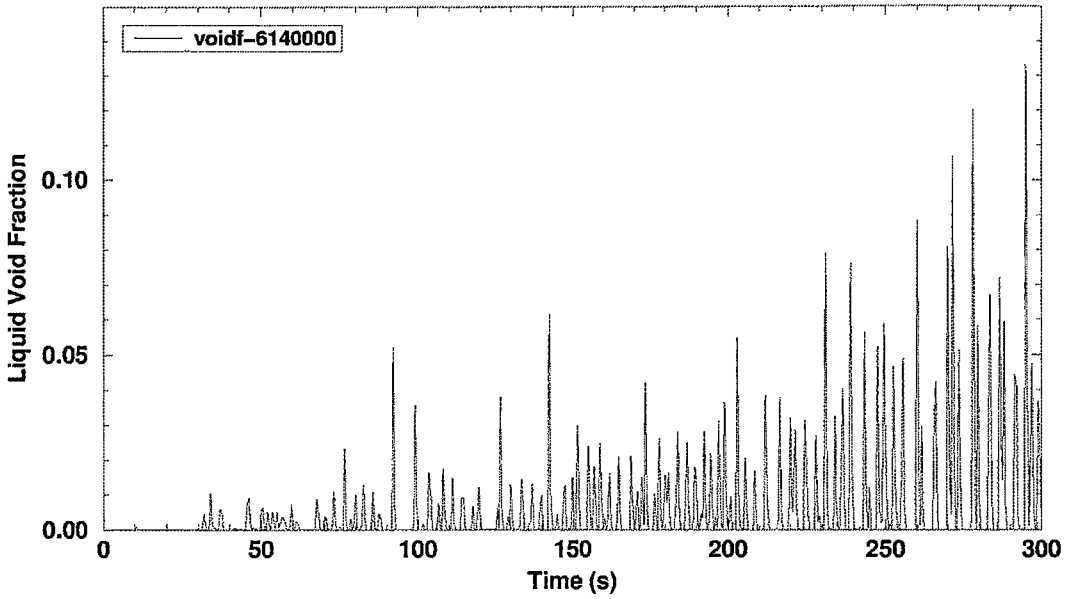

Figure 2.6-49 FLECHT SEASET 31504 Liquid fraction above grid (node 14)

2.7 RAI 7:

2.7.1 Statement of RAI 7

Please apply the statistical analysis method to the test CCTF-62 to show the code capability for simulating a transient. Show the cladding temperatures at the 6, 8, and 10 foot elevations selected as figures of merit. Also show the cladding temperature at the PCT elevation as a figure of merit. Show the distribution for the full case runset and present histograms of the predicted vs measured peak temperatures at each elevation (zero being the PCT and plus or minus temperature difference vs frequency). Identify the parameters that are ranged. Show a plot of the PCT location for all runs against the data.

2.7.2 Response to RAI 7

This response is unchanged from the original response.

An uncertainty analysis of the Cylindrical Core Test Facility (CCTF) CORE-II TEST C2-4 (RUN 62) was performed as a way of demonstrating the capability of the S-RELAP5 code to predict complex phenomena in Integral Effects Test (IETs) and to determine if conservative bias is retained. The results from the uncertainty analysis of a set of [ ] cases are presented below.

The CCTF Test C2-4 Run 62 input model was updated to include all the Revision 3 model upgrades, as follows:

- The core [

  ]
- The core heat structures (heated and unheated rods) were re-nodalized such that [

  ]
- The [ ] input was added to the heat structure input, and the [

  ] were recalculated for the new nodalization [ ]

- The CCTF heater rods have an axial structure in which the material used as insulator is Boron Nitride (BN) in the middle section of the rods and Magnesium Oxide (MgO) at the extremities. An illustration of the CCTF heater rod is provided in Figure 2.7-2. [

  ] The material properties used for the core coupled heat structures [ ] This approach is consistent with other results published in the open literature such as Reference 2.7.1, which used only BN material properties in the JAERI assessment of similar CCTF tests.

- [ ] were added to the model, one for each of the [ ]

- The pressure vessel downcomer heat structure has been modified so that the radial nodalization follows the guideline requirements and includes actual dimensions for the stainless steel cladding, as found in other CCTF Core-II reports.

- A [ ] and the associated [ ] has been implemented in the updated model.

- The control variables affected by the re-nodalization have been updated and a few other control variables have been added to the model.

A reduced order Phenomena Identification and Ranking Table (PIRT) process has been performed in order to select the phenomena relevant to the CCTF Test C2-4 Run 62 and, based on this selection, to determine the parameters to be sampled for this evaluation. The uncertainty parameters used in the CCTF Test C2-4 Run 62 uncertainty analysis and their corresponding Probability Distribution Functions are listed in Table 2.7-1. The random sampled values from the [ ] case set are summarized in Table 2.7-2 and illustrated in Figure 2.7-1. [

]

Figure 2.7-3, Figure 2.7-4, and Figure 2.7-5 show the envelopes of the temperature traces for the hot rod at 6 ft. (1.83 m), 8 ft. (2.44 m), and 10 ft. (3.05 m) elevation, respectively. The PCT elevation in the test data is 6 ft. (1.83 m). In these plots, [

] .

The same plots also include a best-estimate temperature trace which is the calculated temperature from a nominal baseline case. These figures show that the calculated temperature envelope [

] The figures also show [

] A better match between the measured and the calculated temperature traces is obtained [

]

Histograms of the distributions of the predicted vs. measured peak temperatures from the set of [ ] for 6 ft. (1.83 m), 6.68 ft. (2.035 m), 8 ft. (2.44 m), and 10 ft. (3.05 m) elevation are provided in Figure 2.7-6. The figure shows that for the mid-core, high-power elevations, the [

]

Figure 2.7-7 illustrates the results for Hot Rod 210 from the [

]

The results in Figure 2.7-7 show that the code calculated values [

]

A similar depiction of the same vs. elevation results is provided in Figure 2.7-8 - the PCT results are illustrated using box-plots at each node elevation. The box-plots illustrate the numerical data and certain specific quantiles of the samples of calculated PCTs, as explained below:

- [

]

The results depicted in Figure 2.7-8 indicate that, for the mid-core, high-power locations at elevations between 1.12 and 2.55 m elevation, [

] At the peak power location of 1.83 m, [

]

Over the high power elevation range [

]

The results presented above indicate that the application of the EMF-2103, Revision 3 methodology as implemented in the S-RELAP5 code calculations is a good representation of the experimental results in the sense that they provide a good demonstration of the possible LBLOCA outcomes. The results support the conclusion [

]

References:

2.7.1 Y. Murao, K. Fujiki, and H. Akimoto, "Experimental Assessment of Evaluation Model for Safety Analysis on Reflood Phase of PWR-LOCA," Journal of Nuclear Science and Technology, vol. 22, pp. 890–902, November 1985.

2.7.2 AREVA Topical Report EMF-2103(P) Rev. 3, "Realistic Large Break LOCA Methodology for Pressurized Water Reactors," September 2013.

Table 2.7-1 Uncertainty Parameters Ranges for CCTF Run 62 Uncertainty Analysis

Table 2.7-2 Summary of Random Sampled Values for the [ ] Cases in CCTF Test C2-4 Run 62 Uncertainty Analysis

[ ]

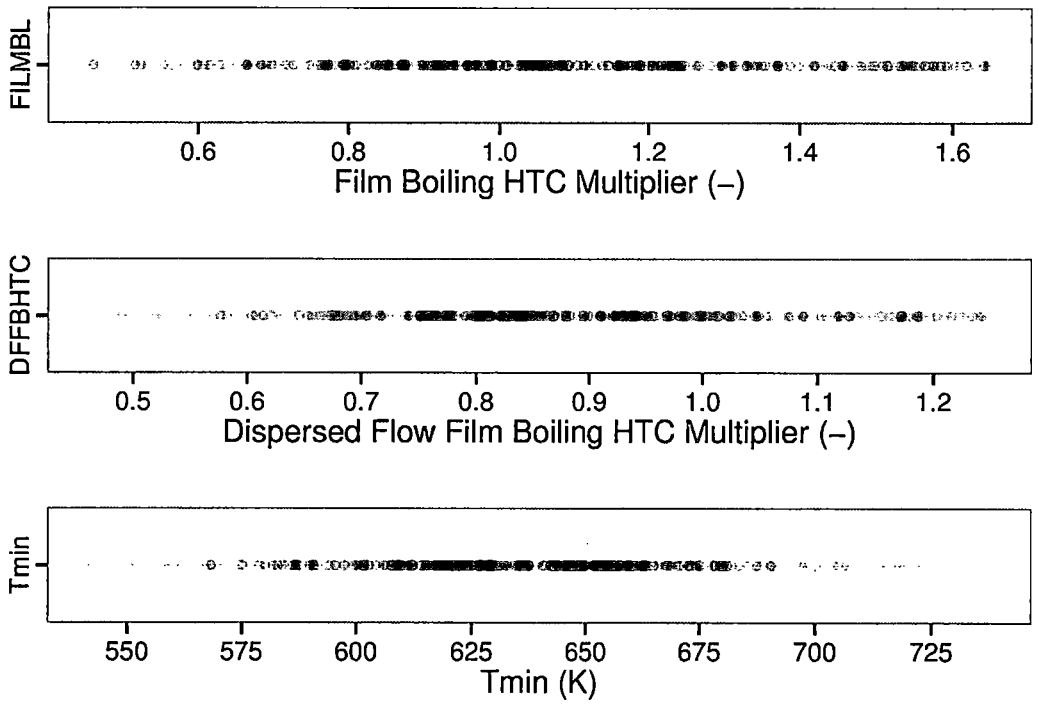

Figure 2.7-1 Scatter Plots of the Random Sampled Parameters for CCTF Test C2-4 Run 62 Uncertainty Analysis

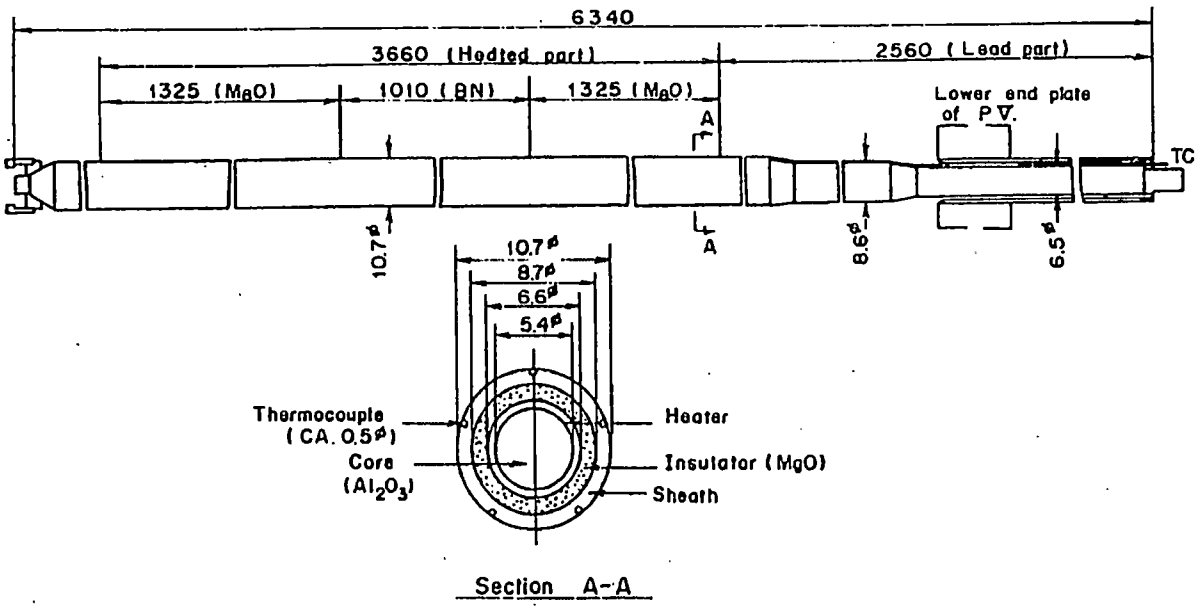

Figure 2.7-2 CCTF Heater Rod (all dimensions in mm)

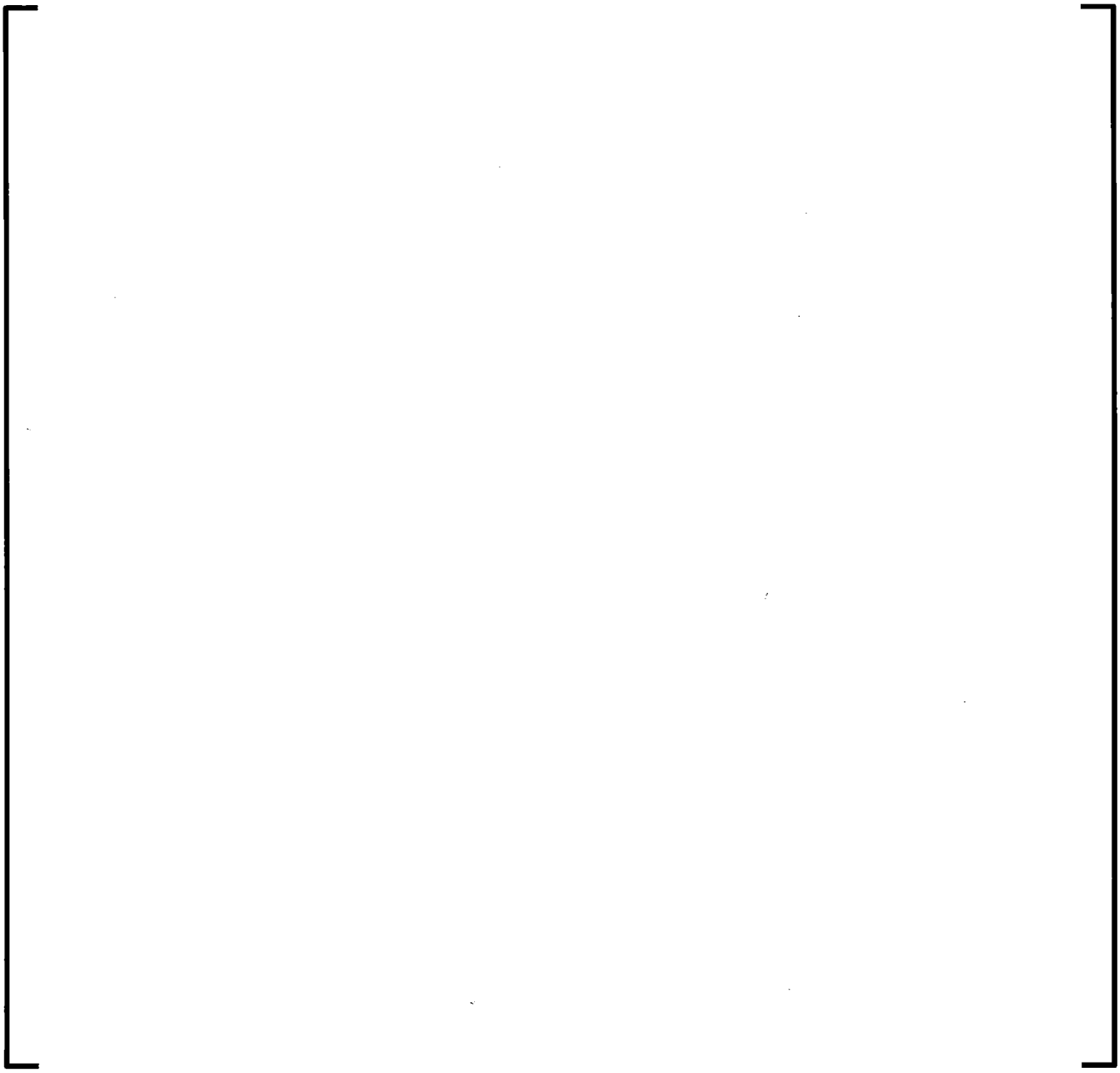

Figure 2.7-3 Rod 210 (BN) Calculated Temperatures Envelope vs. Measured Data at 6 ft. (1.83 m) Elevation for CCTF Test C2-4 Run 62 Uncertainty Analysis

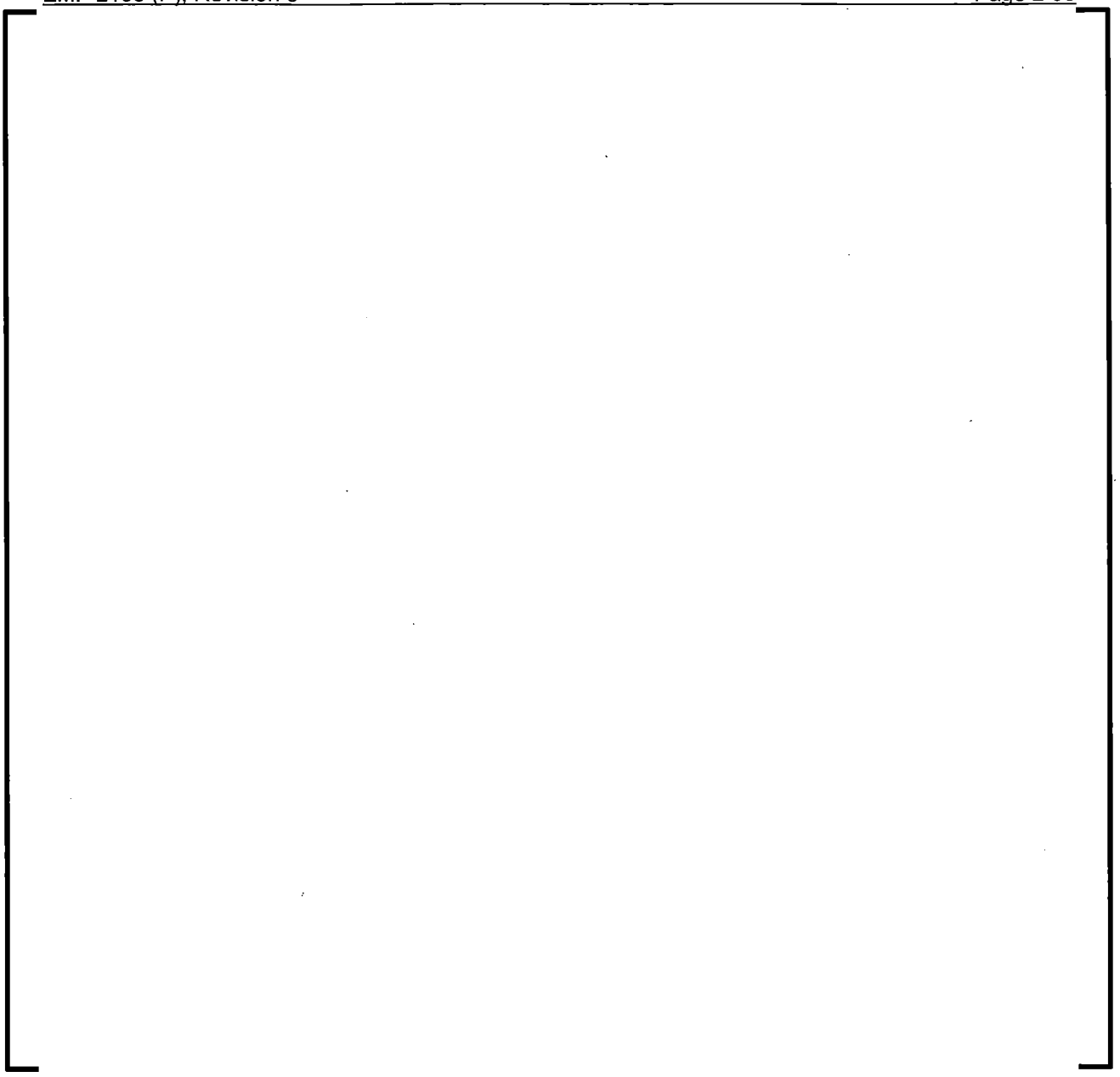

Figure 2.7-4 Rod 210 (BN) Calculated Temperatures Envelope vs. Measured Data at 8 ft. (2.44 m) Elevation for CCTF Test C2-4 Run 62 Uncertainty Analysis

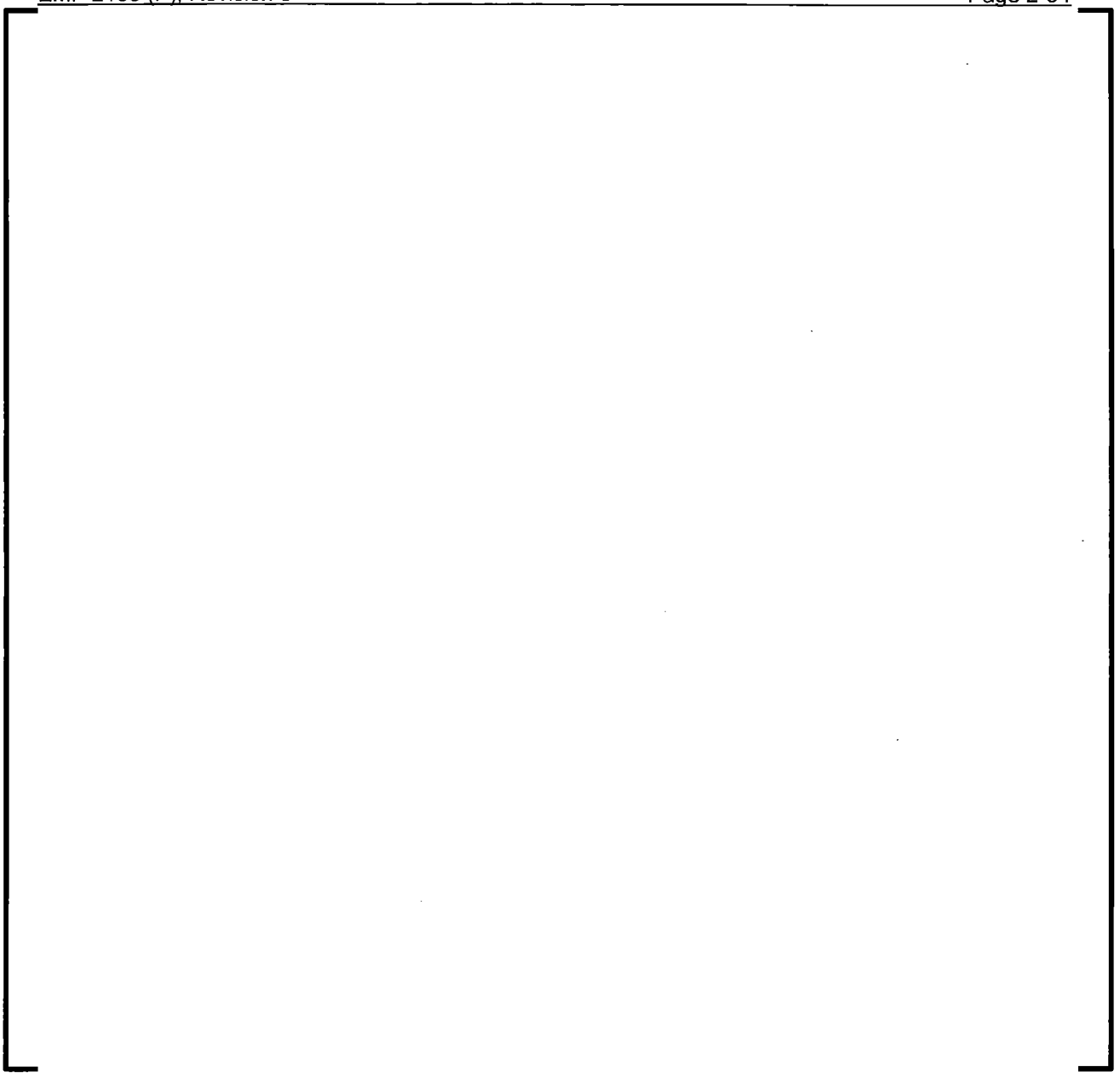

Figure 2.7-5 Rod 210 (BN) Calculated Temperatures Envelope vs. Measured Data at 10 ft. (3.05 m) Elevation for CCTF Test C2-4 Run 62 Uncertainty Analysis

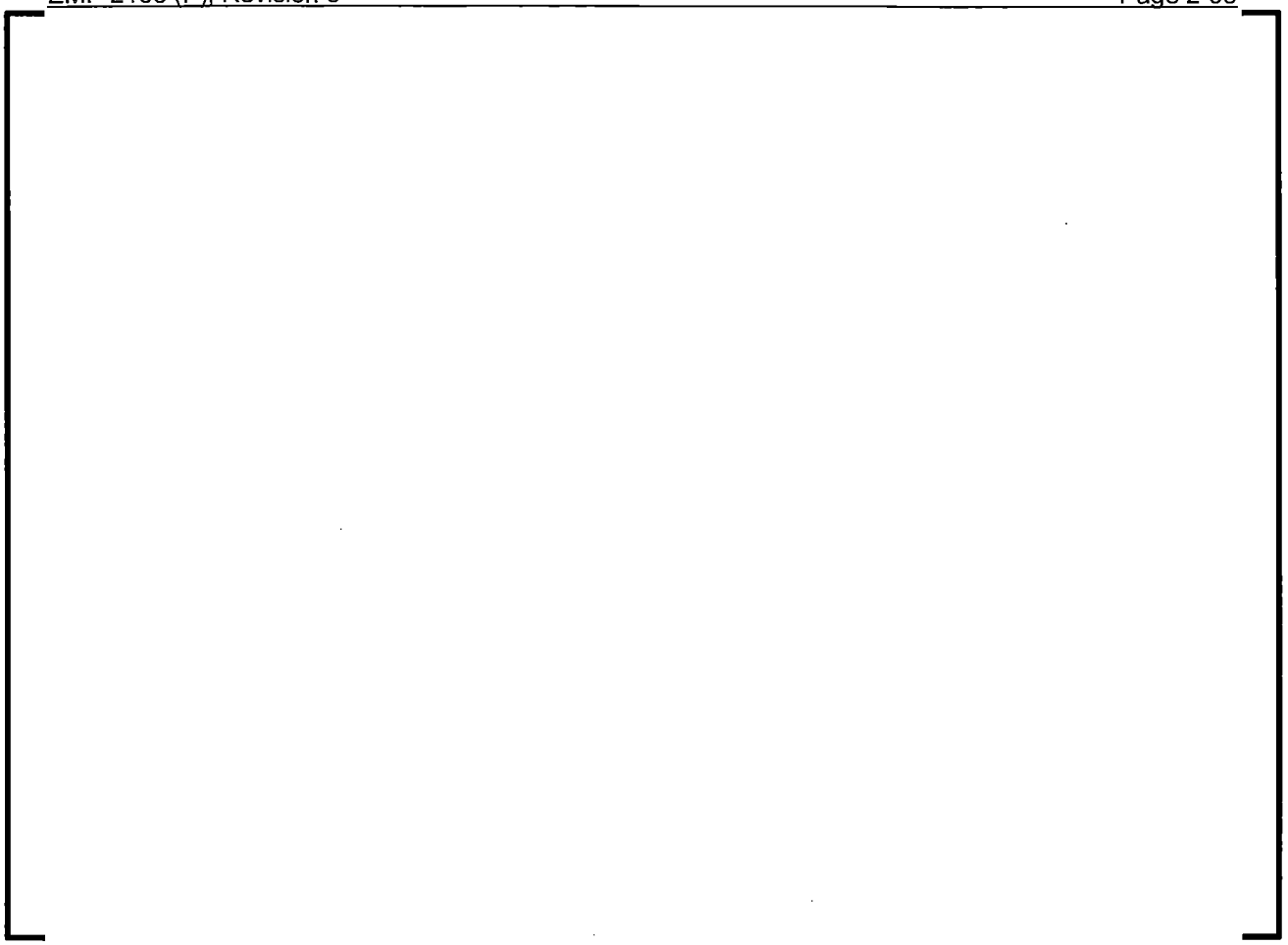

Figure 2.7-6 Histogram of the predicted vs. measured peak temperatures at 6 ft. (1.83 m), 6.68 ft. (2.035 m), 8 ft. (2.44 m), and 10 ft. (3.05 m) elevation for CCTF Test C2-4 Run 62 Uncertainty Analysis

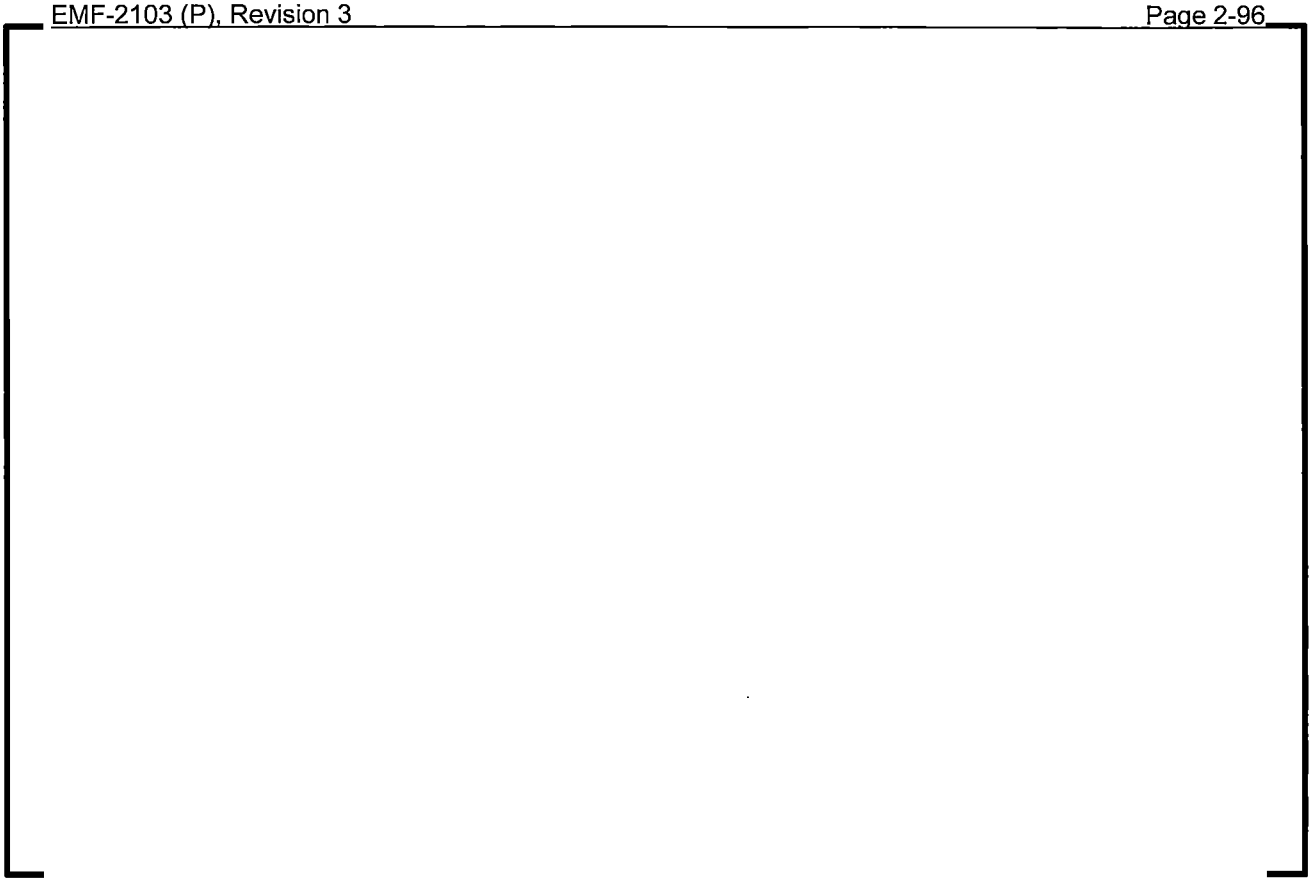

Figure 2.7-7 Peak Cladding Temperature vs. Elevation for Rod 210 (BN) for CCTF Test C2-4 Run 62 Uncertainty Analysis

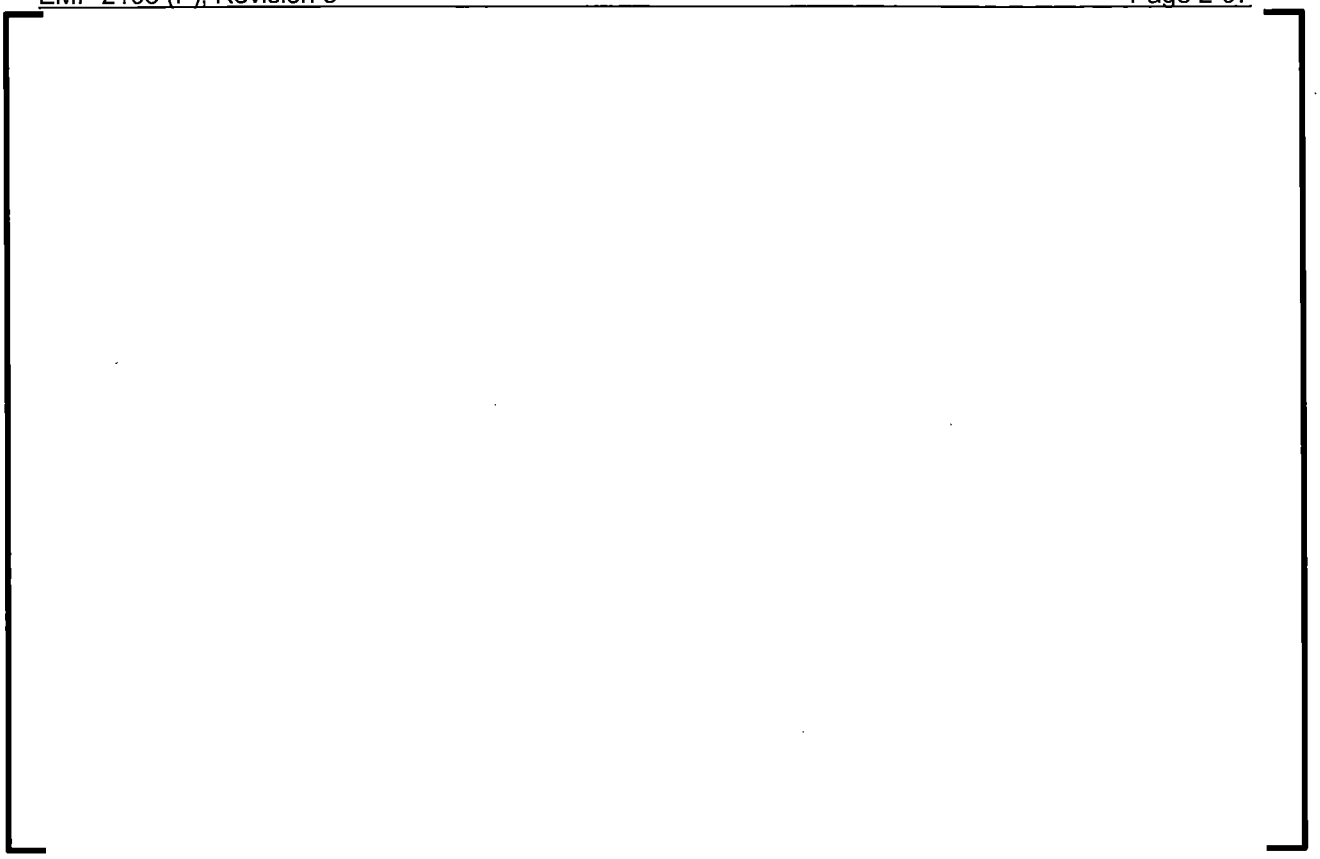

Figure 2.7-8 Boxplot Illustration of the Distribution of Peak Cladding Temperature vs. Elevation for Rod 210 (BN) for CCTF Test C2-4 Run 62 Uncertainty Analysis

2.8 RAI 8:

2.8.1 Statement of RAI 8

Since SRELAP5 is 1-D, the vapor temperature and droplets are distributed evenly across the hot channel. The code computed cross-section average quantities fails to properly capture the very high temperature gradient in the vapor phase boundary layer near the wall so that the distribution of the evaporating water droplets play a fundamental role in the heat transfer process. In particular, interfacial heat transfer is over predicted. This is a major limitation for all 1-D codes. Test data shows that the channel is 3-D with accumulation of drops in the central region and a highly superheated region near the walls. The modeling of this multi-dimensional behavior leads to a substantial reduction in the interfacial heat transfer and limiting of the droplet de-superheating to the central core and not the highly superheated layer near the walls. Since SRELAP5 suffers from this deficiency, please explain what adjustments are made to the dispersed flow film boiling (DFFB) model components to overcome this major discrepancy. That is, the sink temperature is not the average channel temperature for computing single phase heat transfer, an interfacial heat transfer between the drops and the vapor is controlled by the lower vapor temperature in the central core where the drops reside. Furthermore, due to the simplified 1-D averaging of thermodynamic quantities in SRELAP5 and the limited data, it is difficult to quantify all of the component contributions to DFFB. Without the knowledge of all of the contributions to DFFB, how is the magnitude of the droplet contribution verified in the RELAP5 model. Without detailed knowledge of the magnitude of all of the components to DFFB, validation of this model against reflood data may result in including other phenomena/effects that are not pertinent to the heat transfer benefits from the droplet break up model. Lastly it is not clear if coalescence of droplets is modeled.

Please explain how coalescence of droplets is treated and modeled. As reported by Andreani in "Difficulties in Modeling Dispersed –Flow Film Boiling," Warme-und Stoffubertagung 27, 37-49(1992), Springer-Verlag collisions continue to take place one meter above the quench front while the droplet diameter increased with elevation above the quench front by coalescence.

2.8.2 Response to RAI 8

This response is unchanged from the original response.

Background Information:

Dispersed flow film boiling (DFFB) heat transfer (HT) plays an important role in the core thermal response during the reflooding phase of a large-break loss of coolant accident (LOCA) in a PWR. A comprehensive discussion of the reflooding phase of a LOCA is given in Section 6.4 of Reference 2.8.1. A schematic of the flow and heat transfer regimes during reflood is shown in Figure 2.8-1 (Reference 2.8.1). These regimes cover a broad spectrum of conditions. During the reflood phase, a spectrum of droplets exists in the upper region of the bundle, which is created by a complicated thermal-hydraulic process that occurs near the quench front. When the liquid at the quench front is subcooled, with very low void fraction, an inverted flow regime is established just above the quench front (as seen in right side portion of Figure 2.8-1 below). Downstream of this flow regime, the dispersed flow regime is created by a sputtering of liquid at the quench front and by the break-up of the inverted annular liquid core. There is substantial boiling below the quench front, if the liquid at the quench front is saturated (as seen in the left side portion of Figure 2.8-1). Downstream of this flow regime, the dispersed flow regime is created by the bubble burst at the quench front. FLECHT-SEASET test results (Reference 2.8.2) show that during the early reflood phase, a subcooled condition exists near the quench front. As the transient progresses, the addition of heat below the quench front causes the liquid to heat up, and eventually, bulk boiling starts below the quench front. FLECHT-SEASET test (Reference 2.8.2) results show an obvious shift in the quench front propagation rate as the fluid condition at the quench front transitions from subcooled to bulk boiling, as shown in Figure 2.8-2. Further, Ishii observed in his reflood tests (References 7-101 and 7-102 in Reference 2.8.3) that the average droplet diameter of the spectrum of droplets resulting from the bubble burst at the quench front was substantially larger than that for droplets sheared from inverted annular liquid surface.

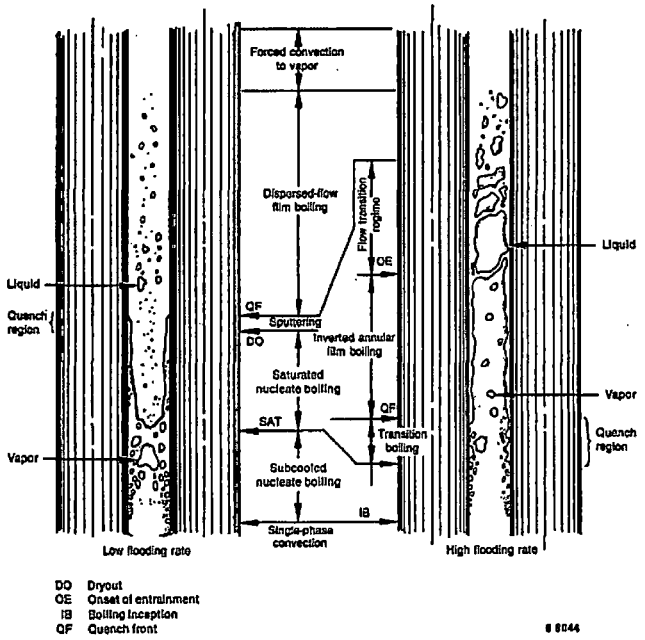

Figure 2.8-1 Flow and Heat Transfer Regimes during Reflood

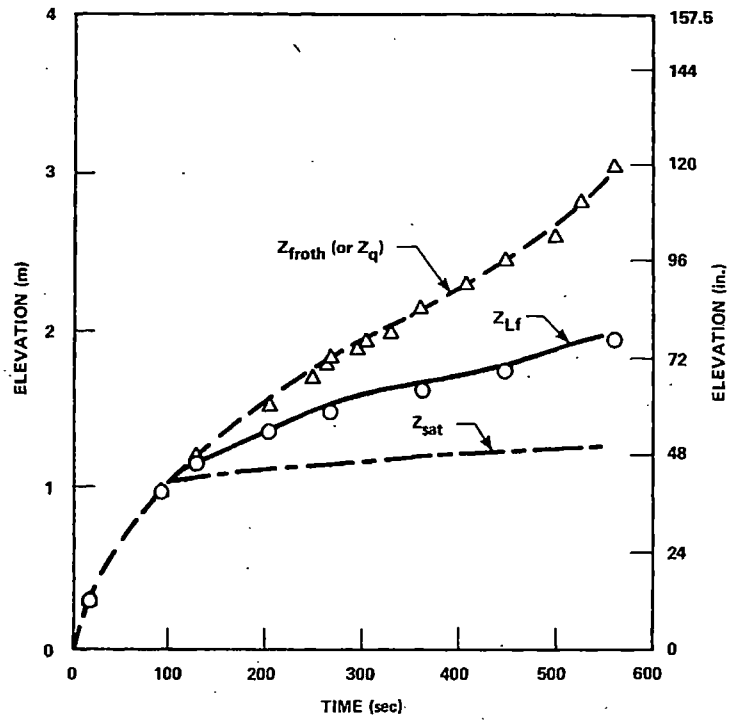

Figure 2.8-2 FLECHT-SEASET Froth Level (Z_{froth}), Collapsed Liquid Level (Z_{Lf}), and Saturation Level (Z_{sat}) Data (Figure 5-1 from Reference 2.8.2)

As the population of the droplets moves upwards in the channel, two phenomena impact the droplet spectrum; the first is the changes due to coalescence of smaller droplets with larger ones, the second is the break-up of larger droplets due to the increase in steam velocities. The presence and design of grid structures (e.g., simple egg crate, mixing vane) in the flow field adds additional complexity to the dispersed flow field. This is due to enhanced vapor turbulence and droplet break-up from drop interaction with the grid spacer structures. Variation in power from one pin to an adjacent pin, variation in power between fuel assemblies (as observed in SCTF (Reference 2.8.4)), and cross flow between assemblies, creates a multi-dimensional flow field in the core region.

Above the quench front, the cladding temperature will be much higher than the quench temperature, which prohibits the potential wall-droplet contact. The higher cladding temperature creates superheated steam, as well as a radial temperature distribution with cooler steam in the middle of the sub-channel. This results in the potential migration of droplets towards the middle of the sub-channel. The net effect is a reduction of thermal potential for droplet evaporation. Simultaneously, the droplet surface heat transfer coefficient increases due to the relatively larger steam velocity in the middle of the sub-channel and due to the increase of the droplet population.

Technical Evaluation:

[
]

[ ]

Summary:

Considering the difficulties in a quantitative modeling of dispersed flow heat transfer, AREVA has benchmarked a set of both separate effects and integral effects tests, which are reported in Section 8.0 of Reference 2.8.3. These tests cover a wide variation of the range of parameters that are important for LBLOCA, and S-RELAP5 predicted acceptable results in all cases. A set of FLECHT-SEASET cases were run with all the models activated including the rod-to-rod-radiation and the grid droplet shattering model, and the uncertainty of the DFFB modeling was determined. The benchmark results from these tests are given in the response to RAI Question 19. It can be seen that the bias in DFFB multipliers is [ ], and the code calculated acceptable results to the benchmarks. In addition, in response to RAI Question 7, CCTF Run 62 was benchmarked applying the statistical analysis method, and the results show that S-RELAP5 calculated conservative cladding thermal response. From these results, it can be concluded that the assumptions and simplifications made in S-RELAP5 are appropriate for calculating the cladding thermal response during an LBLOCA in a PWR.

References:

2.8.1 NUREG-1230 R4, U.S. NRC, "The Compendium of ECCS Research for Realistic LOCA Analysis," December 1988.

2.8.2 N.Lee, S. Wong, H. C. Yeh, and L. E. Hochreiter, "PWR FLECHT-SEASET Unblocked Bundle, Forced and Gravity Reflood Task Data Evaluation and Analysis Report," NUREG/CR-2256.

2.8.3 AREVA Topical Report EMF-2103(P) Rev. 3, "Realistic Large Break LOCA Methodology for Pressurized Water Reactors," September 2013.

2.8.4 NUREG/IA-0126, "2D/3D Program Work Summary Report," June 1993.

2.8.5 M. Andreani and G. Yadigaroglu, "Difficulties in Modeling Dispersed Flow Film Boiling," Warme-und Stoffubertagung 27, 37-49(1992).

2.9 RAI 9:

2.9.1 Statement of RAI 9

It states on Page 2-3 of Topical Report (TR) EMF-2103, Revision 3, that the [ ] correlation is still used for passive metal heat structure heat transfer. Please identify the passive metal heat structure that the model is applied to? Also, does this include spacer grids? Please explain why this model is used for non-fuel rod structures since it is the elevated metal temperature that prevents drops from contacting or wetting the walls. Furthermore, the [ ] correlation is not physically based and contains several flaws that preclude it use on vertical surfaces. Please show the impact of the use of this correlation does not impact PCT following all LBLOCAs.

2.9.2 Response to RAI 9

This response is unchanged from the original response.

In Section 3.6.1.2 of Reference 2.9.1, the [

] As a part of the work to support Reference 2.9.2, the [ ] correlation for film boiling heat transfer was restricted to application outside of the reactor core and only under specific conditions. The correlation was applied only to provide continuity at the transition- film boiling heat transfer response boundary.

Section 7.6.7.1, "Film Boiling for Non-Core Heat Structures" on Page 7-199 of Reference 2.9.2 discusses the correlations for the film boiling heat transfer coefficients used. The reference states that for heat structures which are considered "passive" (those which have the bundle heat transfer option disabled), the convection to liquid during film boiling will use the [ ] correlation. This application has two conditions:

[

]

The uncertainty analysis of a typical Combustion Engineering 2X4 loop PWR plant to be used as a sample problem for submittal of Revision 3 of the AREVA RLBLOCA analysis methodology was examined. Table 2.9-1 lists the heat structures which are considered passive (do not have the bundle heat transfer option enabled), and therefore are subject to the [ ] film boiling correlation. These structures are the heat structures outside the core area. The heat structures that are "active" (have the bundle heat transfer option enabled) and are therefore not subject to [ ] It can be noted that in the RLBLOCA methodology (Reference 2.9.2), [ ]

Table 2.9-1 CE Heat Structures Subject to [ ]

The reactor vessel wall temperatures at three locations are shown in Figure 2.9-1. As shown, all temperatures are below the minimum stable film boiling temperature of [ ] and it is only above the CL nozzle belt that the metal experiences any significant temperature excursion. As described, the [ ] correlation is applied only during film boiling below T_{min}, and only on heat structures outside the reactor core.

Figure 2.9-2 shows the heat transfer mode calculated by S-RELAP5 for the RV wall at the downcomer elevation just above the cold leg nozzle. The code does predict film boiling for short periods of time along the vessel wall.

Figure 2.9-1 RV Wall Temperatures

Figure 2.9-2 Reactor Vessel Wall Heat Transfer Mode

The impact on PCT of completely disabling heat transfer during the time that [ ] would be applied to all susceptible heat structures is shown in Figure 2.9-3. This figure compares the PCT independent of elevation for two calculations; one with [ ] set to zero, and one with [ ] enabled. There is very little impact until approximately 26.5 s. Condensation from SIT tank discharge causes the break fluid flow to decrease and draws non-condensable gas from the break into the cold leg and downcomer. It is reasonable to attribute the difference in PCT response to the arrival of non-condensable gas to the downcomer and to the instability of having zero heat transfer during the short periods of the film-boiling regime when [ ] would be applied. Although small changes in system behavior can be amplified through the system, the application of the [ ] correlation has minimal impact on PCT limits, especially with a statistical methodology.

Figure 2.9-3 Impact of the Removal of the [ ] Heat Transfer on PCT

References:

2.9.1 NRC letter, "Safety Evaluation on Framatome ANP Topical Report EMF-2103(P), Revision 0, "Realistic Large Break Loss-of-Coolant Accident Methodology for Pressurized Water Reactors" (TAC NO. MB7554)

2.9.2 AREVA Topical Report EMF-2103(P) Rev. 3, "Realistic Large Break LOCA Methodology for Pressurized Water Reactors," September 2013.

2.10 RAI 10:

2.10.1 Statement of RAI 10

Section 4.3.3.2.3 of TR EMF–2103 discusses the decay heat standard but does not show the calculated decay curve used in the analyses. Please compare the decay heat model with uncertainty applied to the American National Standards Institute/American Nuclear Society 5.1-1979 standard to show that the S-RELAP5 model predicts or bounds the data in the standard for 2000 seconds. Show a comparison of the integrated decay energy with uncertainty and compare to the standard. How is gamma redistribution uncertainty treated? Please explain.

2.10.2 Response to RAI 10

This response is unchanged from the original response.

Section 4.3.3.2.3 discusses decay heat in EMF-2103(P)(A), Revision 0 (Reference 2.10.1). As part of the NRC approval of Reference 2.10.1, AREVA addressed the comparison of the decay heat model in S-RELAP5 to the ANSI/ANS-5.1-1979 standard in the response to Question 29 of the Revision 0 of the RLBLOCA methodology (Reference 2.10.2, Page 83-84). This response also explains that the diffusion of the decay heat source due to redistribution of the gamma radiation energy is conservatively neglected in the methodology, and no uncertainty is applied due to this effect.

In Revision 3 to EMF-2103(P) (Reference 2.10.3), the application of decay heat is nearly the same as what was applied in Revision 0 (Reference 2.10.1). Where the application of decay heat in Revision 3 (Reference 2.10.3) differs from Revision 0 (Reference 2.10.1), is that the decay heat is [

] Additional discussion of the application of decay heat, as well as the justification of the conservatism of the Revision 3 decay heat, is provided in Sections 3.1.3.2.4 and 8.5.1.17 of Reference 2.10.3. As presented in Section 8.5.1.17 of Reference 2.10.3, the AREVA decay heat curve is the [

] A comparison to itself is not of much interest. However, in Figures 8.5-3 and 8.5-4 of Section 8.5.1.17 (Reference 2.10.3), a comparison to [

]

Although the decay heat comparisons in Section 8.5.1.17 of Reference 2.10.3 do not extend to 2000 seconds, they do extend to 600 seconds, which is well beyond the time of PCT for RLBLOCA analyses.

Gamma radiation energy redistribution is ignored in Revision 3 (Reference 2.10.3), just as it was in Revision 0 (Reference 2.10.1).

References:

2.10.1 Framatome ANP, Inc. Topical Report EMF-2103(P)(A), Revision 0, "Realistic Large Break LOCA Methodology for Pressurized Water Reactors (TAC No. MB7554)," April, 2003.

2.10.2 Framatome ANP, Inc. Letter NRC:02:062, "Responses to a Request for Additional Information on EMF-2103(P) Revision 0 Realistic Large Break LOCA Methodology for Pressurized Water Reactors (TAC No. MB2865)," December 20, 2002.

2.10.3 AREVA Topical Report EMF-2103(P) Rev. 3, "Realistic Large Break LOCA Methodology for Pressurized Water Reactors," September 2013.

2.11 RAI 11:

2.11.1 Statement of RAI 11

Provide a FLECHT steam cooling test benchmark comparison using Sleicher-Rouse and Wong-Hochreiter in S-RELAP5. Include Reynolds Number plot for Wong-Hochreiter.

2.11.2 Response to RAI 11

This response is unchanged from the original response.

Considering convection to vapor at film boiling conditions, the S-RELAP5 core bundle model is designed to be exclusively used in the core region for LOCA scenarios. The model is used in conjunction with the reflood model for large break LOCA analyses.

[

]

[

]

Nu is the Nusselt number, defined as:

$$Nu = \frac{\delta h_{cg}}{k_g} \qquad (2.11.2)$$

where δ, h_{cg} and k_g are the thickness of the thermal boundary layer, the convective heat transfer coefficient at the wall and the thermal conductivity of the vapor, respectively. The vapor Reynolds and Prandtl numbers (Equation 7.511 of Reference 2.11.1) are defined as:

$$\mathrm{Re}_g = \frac{G_g D_h}{\mu_g}; \mathrm{Pr}_g = \frac{C_{pg}\mu_g}{k_g} \qquad (2.11.3)$$

In Equation (2.11.3), G_g represents the vapor mass flux, D_h is the hydraulic diameter, μ_g is the vapor dynamic viscosity, and C_{pg} is the vapor specific heat, respectively. The Wong-Hochreiter correlation uses four different heat transfer coefficients based on the magnitude of the vapor Reynolds number (i.e., on the flow regime). The S-RELAP5 convective heat transfer coefficient, h_{cg}, for the bundle model is determined by using Equation 7.526 of Reference 2.11.1 as:

$$h_{cg} = MAX\left(h_{cg,lam}, h_{cg,nc}, \Psi h_{cg,wh}, \Psi h_{cg,db}\right)F \qquad (2.11.4)$$

For the laminar region, the convective heat transfer coefficient (Equation 7.527 of Reference 2.11.1) is:

$$h_{cg,lam} = 7.86\,\mathrm{Pr}_g^{1/3}\,\frac{k_g}{D_h} \qquad (2.11.5)$$

[ ]

In Equation (2.11.6), g represents the gravity constant, β_g is the volumetric thermal expansion coefficient of the vapor phase, ρ_g is the vapor density, and T_w and T_g are the wall and vapor temperature, respectively. From the Wong-Hochreiter correlation (Reference 2.11.4), the low Reynolds number region that was fitted to steam cooling data was used (Equation 7.528 of Reference 2.11.1):

$$h_{cg,wh} = 0.0797\,\mathrm{Re}_g^{0.6774}\,\mathrm{Pr}_g^{1/3}\,T_{cf}\,\frac{k_g}{D_h} \qquad (2.11.7)$$

where T_{cf} is a temperature correction factor (Equation 7.508 of Reference 2.11.1) accounting for the variation of fluid properties between the thermal boundary layer and the bulk of the fluid due to steep thermal gradients and is defined as:

[ ]

and the exponent n (Equation 7.509 of Reference 2.11.1) is defined as:

The Dittus-Boelter correlation (Reference 2.11.5) is modified to account for the variable properties across the thermal boundary layer when large temperature differences exist (Equation 7.529 of Reference 2.11.1):

$$h_{cg,db} = 0.023 \mathrm{Re}_g^{0.8} \mathrm{Pr}_g^{1/3} T_{cf} \frac{k_g}{D_h} \qquad (2.11.10)$$

Although the Dittus-Boelter correlation typically under-predicts the heat transfer in bundles, it has been successfully used in conjunction with the two-phase turbulent heat transfer enhancement for rod bundles by Drucker and Dhir (Reference 2.11.6) motivating the final form of the bundle heat transfer model where the heat transfer coefficient is defined as the maximum of Wong-Hochreiter and Dittus-Boelter. The Wong-Hochreiter (Reference 2.11.4) vapor convection correlation was used in combination with the grid spacer enhancement model of Yao, Hochreiter and Leech (Reference 2.11.7) and the laminar enhancement due to grid spacers of Meholic et al. (Reference 2.11.8). The Sleicher-Rouse (Reference 2.11.2) correlation (Equation 7.507 of Reference 2.11.1) uses the same definition for T_{cf} given above as the Dittus-Boelter correlation:

The FLECHT-SEASET steam cooling tests 32753, 36160, 36261, 36362, 36463, 36564, 36766 and 36867 (Reference 2.11.4) discussed in Section 8.2.4 of Reference 2.11.1 were rerun with S-RELAP5 using the core bundle model option with either the Wong-Hochreiter vapor convection heat transfer cooling or the Sleicher-Rouse vapor convection heat transfer cooling correlations.

FLECHT-SEASET Test Cases Run with Wong-Hochreiter Correlation:

Using the Wong-Hochreiter vapor convection heat transfer correlation, the FLECHT-SEASET Test cases were run to steady state conditions, as shown by the temperature distribution at the 60 inch elevation plotted for all cases in Figure 2.11-1. The FLECHT-SEASET data/calculated temperature comparison is shown in Figure 2.11-2. The mean of the ratio of measured and calculated temperatures is used as a scale factor to shift the calculated temperatures toward a "best fit to data" condition. A calculated mean of 1.0 implies there is no adjustment to apply (i.e., scale factor of 1.0). The FLECHT-SEASET Test cases run with S-RELAP5 using the Wong-Hochreiter vapor convection heat transfer correlation result in a mean of [ ] and a standard deviation of [ ] (see Figure 2.11-2). A scale factor this close to 1.0 shows that the bundle model gives very accurate results for the temperature (Figure 2.11-1) over the Reynolds number span (see Figure 2.11-3) of the test data considered.

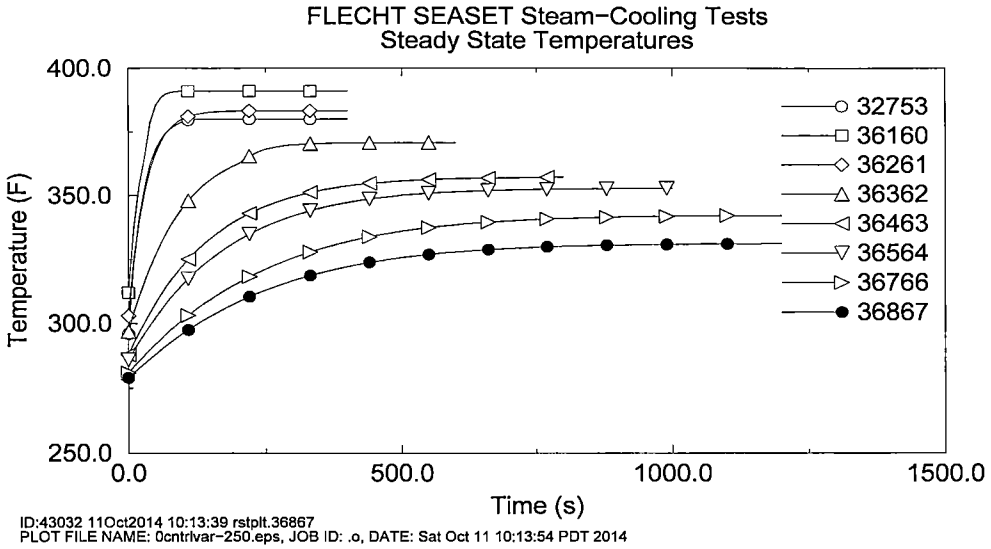

Figure 2.11-1 FLECHT-SEASET Steady State Temperature Distribution (60 inch Elevation) for the Wong-Hochreiter vapor convection correlation

Figure 2.11-2 FLECHT-SEASET Data/Calculated Temperature Comparison for the Wong-Hochreiter vapor convection correlation

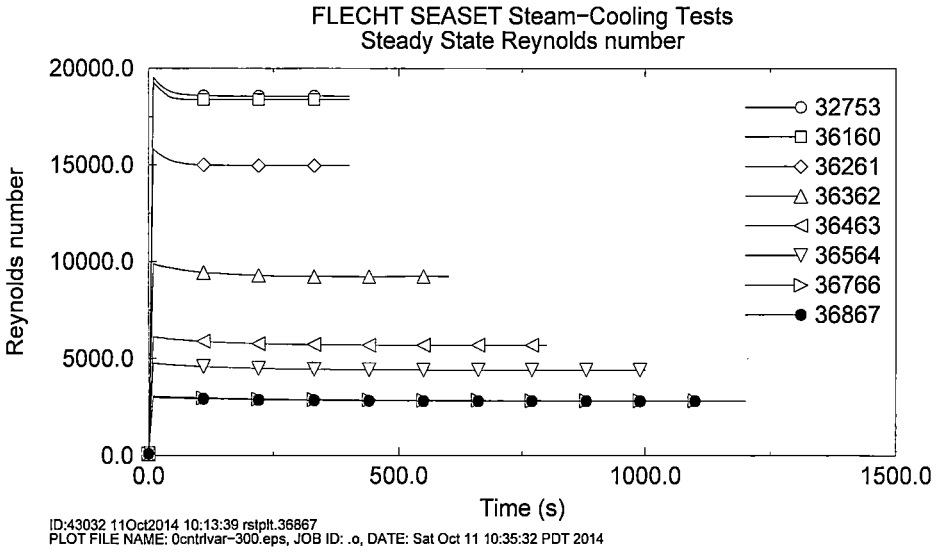

Figure 2.11-3 FLECHT-SEASET Case Tests Exit Section Reynolds number for the Wong-Hochreiter vapor convection correlation

FLECHT-SEASET Test Cases Run with Sleicher-Rouse Correlation:

Using the Sleicher-Rouse vapor convection heat transfer correlation, the FLECHT-SEASET Test cases were run to steady state conditions, as shown in Figure 2.11-4 by the temperature distribution at the 60 inch elevation for all cases. The comparison of FLECHT-SEASET data to calculated temperature is shown in Figure 2.11-5. The FLECHT-SEASET Test cases run with S-RELAP5 using the Sleicher-Rouse vapor convection heat transfer correlation resulted in a mean of [ ] and a standard deviation of [ ] (see Figure 2.11-5) over the Reynolds number span (Figure 2.11-6) of the test data considered.

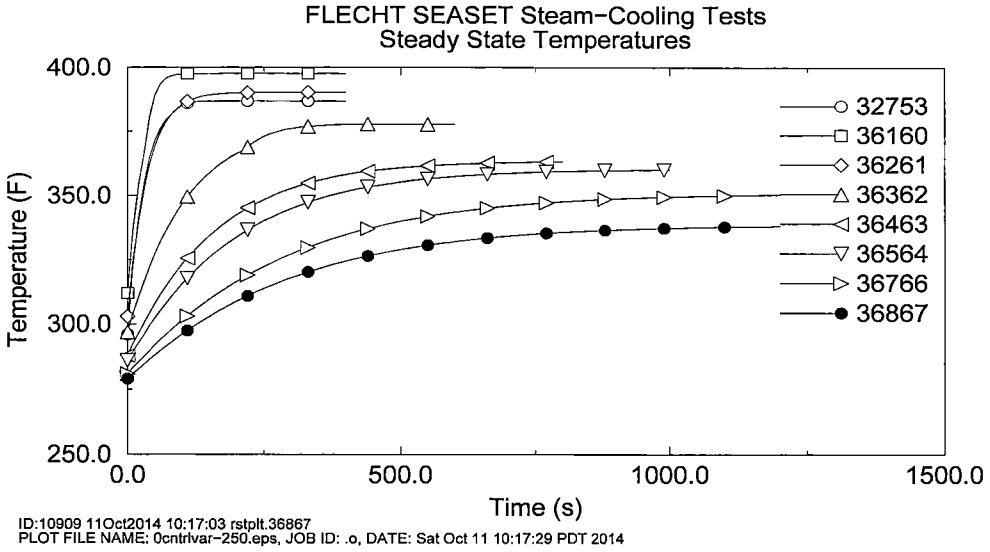

Figure 2.11-4 FLECHT-SEASET Steady State Temperature Distribution (60 in Elevation) for the Sleicher-Rouse vapor convection correlation

[ ]

Figure 2.11-5 FLECHT-SEASET Data/Calculated Temperature Comparison for the Sleicher-Rouse vapor convection correlation

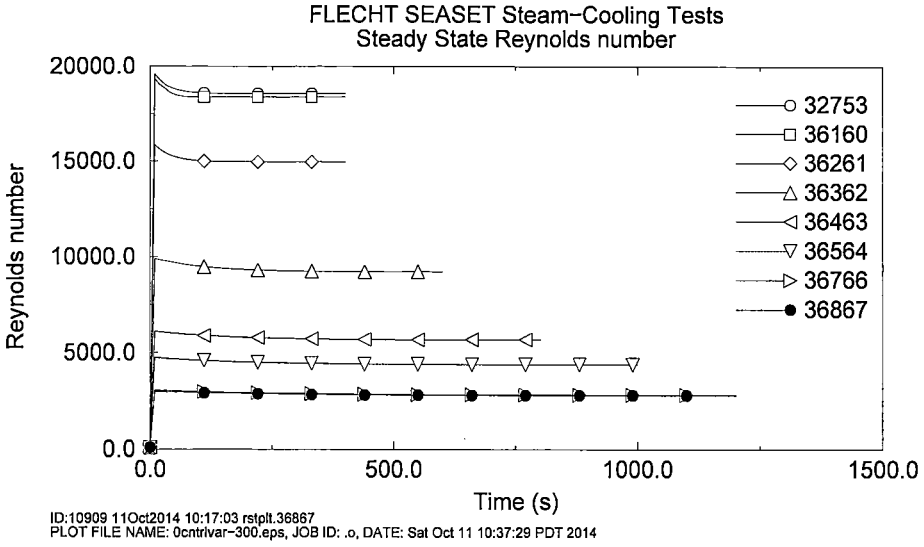

Figure 2.11-6 FLECHT-SEASET Case Tests Exit Section Reynolds number for the Sleicher-Rouse vapor convection correlation

Results and Conclusions:

The FLECHT-SEASET steam cooling test cases 32753, 36160, 36261, 36362, 36463, 36564, 36766 and 36867 (Reference 2.11.4) were simulated by S-RELAP5 using the core bundle model option with either the Wong-Hochreiter vapor convection heat transfer cooling or the Sleicher-Rouse vapor convection heat transfer cooling correlations. The comparison of the calculations to experimental data indicate that when measured cladding temperatures are divided by the S-RELAP5 predicted cladding temperatures using the Wong-Hochreiter vapor convection heat transfer correlation a mean of [ ] and a standard deviation of [ ] is obtained. When the measured data is divided by the S-RELAP5 predicted data using the Sleicher-Rouse vapor convection heat transfer correlation a mean of [ ] and a standard deviation of [ ] are obtained. These results indicate that for FLECHT-SEASET steam cooling tests the Wong-Hochreiter and Sleicher-Rouse vapor convection heat transfer cooling correlations are both in good agreement with the measured data. Since the Wong-Hochreiter correlation was developed using the FLECHT-SEASET bundle tests (Reference 2.11.4), it provides a higher level of confidence for the results obtained when compared to the Sleicher-Rouse correlation.

Re-benchmark of THTF Level Swell Tests:

THTF level swell tests benchmarks, given in the response to self-initiated RAI Question 24, provide additional steam temperature comparisons between the measured and calculated values. These benchmarks cover the range of steam temperatures up to about 1200 °F.

References:

2.11.1 AREVA Topical Report EMF-2103(P) Rev. 3, "Realistic Large Break LOCA Methodology for Pressurized Water Reactors," September 2013.

2.11.2 Sleicher, C.A., Rouse, M.W., "*A Convenient Correlation for Heat Transfer to Constant and variable Property Fluids in Turbulent Pipe Flow*," International Journal of Heat and Mass Transfer, Volume 18, pp. 677-683, 1975.

2.11.3 Forslund, R.P., Rohsenow, W.M., "*Dispersed Flow Film Boiling*," Journal of Heat Transfer, Volume 90 (6), pp. 399-407, 1968.

2.11.4 Wong, S., Hochreiter, L.E., "*Analysis of the FLECHT SEASET Unblocked Bundle Steam Cooling and Boiloff Tests*," NUREG/CR-1533, EPRI NP-1460, WCAP-9729, January 1981.

2.11.5 Dittus, F.W., Boelter, L.M.K., "*Heat Transfer in Automobile Radiators of the Tubular Type*," Publications in Engineering, Volume 2, University of California, Berkeley, pp. 443-461, 1930.

2.11.6 Drucker, M., Dhir, V.K., "*Studies of Single and Two Phase Heat Transfer in a Blocked Four Rod Bundle*," EPRI-NP 3485, Electric Power Research Institute, 1984.

2.11.7 Yao, S.C., Hochreiter, L.E., Leech, W.J., "*Heat Transfer Augmentation in Rod Bundles Near Grid Spacers*," Trans. ASME 104, pp. 76-81, February 1982.

2.11.8 Meholic, M.J., Hochreiter, L.E., Mahaffy, J.H., Spring, J., "Increased Convective Heat Transfer Caused by Spacer Grids in Laminar High Void Fraction Flows," 2008 ANS Winter Meeting.

2.12 RAI 12:

2.12.1 Statement of RAI 12

Provide justification for the Weber numbers used for droplets in dispersed flow (Page 7-91 of TR EMF-2103, Revision 3) and the bubbles.

2.12.2 Response to RAI 12

This response is unchanged from the original response.

Background Information:

S-RELAP5 uses critical Weber numbers of 4.0 and 14.0 for droplets and bubbles, respectively (Section 7.5.2.1 in Reference 2.12.1). [

]

Technical Evaluation:

[redacted]

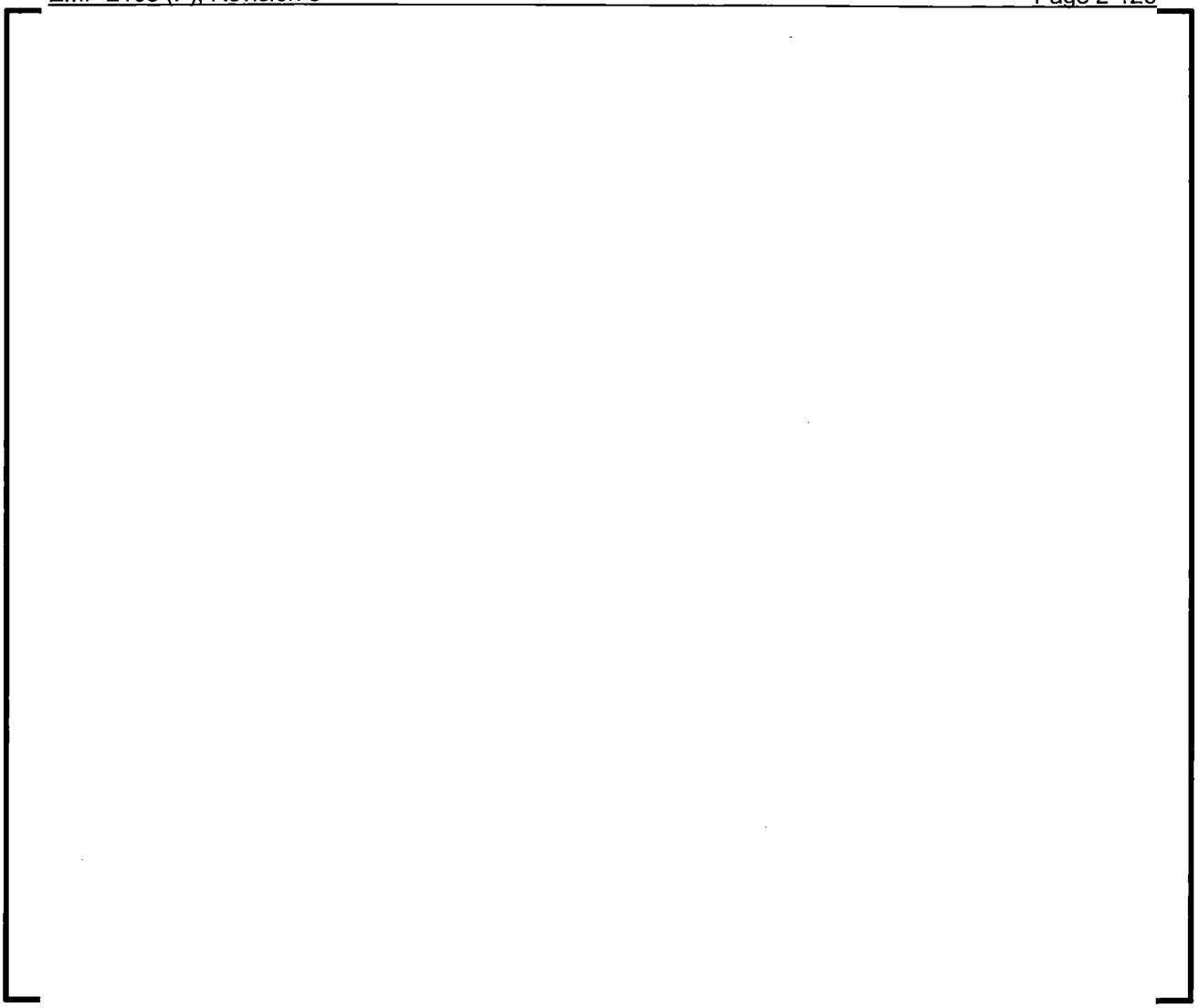

Summary

In summary, the droplet diameter formulation and the minimum droplet diameter limit used in S-RELAP5 provide acceptable cladding thermal response during the dispersed flow film boiling (DFFB) heat transfer in the core region.

Figure 2.12-1 Droplet Weber Number Determined from FLECHT Movies (Reference 2.12.5)

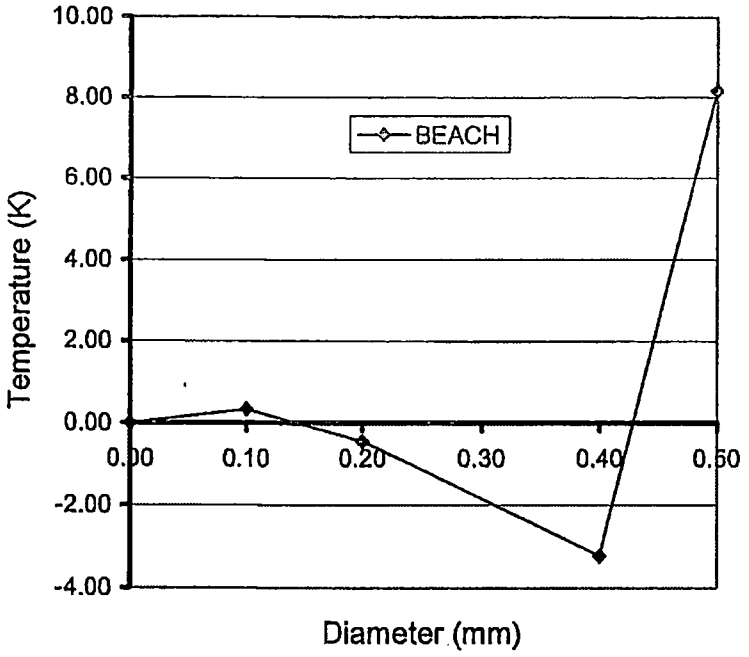

Figure 2.12-2 Peak Cladding Temperature Variations from the Base Case vs. Droplet Diameter (Reference 2.12.8)

References:

2.12.1 AREVA Topical Report EMF-2103(P) Rev. 3, "Realistic Large Break LOCA Methodology for Pressurized Water Reactors," September 2013.

2.12.2 Framatome ANP, Inc. Letter NRC:02:062, "Responses to a Request for Additional Information on EMF-2103(P) Revision 0 Realistic Large Break LOCA Methodology for Pressurized Water Reactors (TAC No. MB2865)," December 20, 2002.

2.12.3 RELAP5-3D Code Manual Volume 1: Code Structure, System Models, and Solution Methods, INEEL-98-00834, Volume 1, Revision 2.4, June 2005.

2.12.4 TRACE Version 5.0 Theory Manual, "Field Equations, Solution Methods, and Physical Models," Accession No. ML071000097.

[

]

2.12.6 N.Lee, S. Wong, H. C. Yeh, and L. E. Hochreiter, "PWR FLECHT-SEASET Unblocked Bundle, Forced and Gravity Reflood Task Data Evaluation and Analysis Report," NUREG/CR-2256.

2.12.7 A. J. Ireland, L. E. Hochreiter, and F. B. Chung, "Droplet Size and Velocity Measurements in a heated Rod Bundles," Paper TED-A-J03-624, The 6th ASME-JSME Thermal Engineering Joint Conference, March 16-20, 2003.

2.12.8 C. K. Nithianandan and J. R. Biller, "Evaluation of Minimum Droplet Size on Cladding Temperature During Reflood," Paper Presented at the ANS Winter Meeting, Washington DC, November 13-17, 2005.

2.12.9 AREVA Topical Report, BAW-10166PA-05, BEACH: Best Estimate Analysis Core Heat Transfer - A Computer Program for Reflood Heat Transfer Analysis During LOCA, November 2003.

2.12.10 AREVA Topical Report BAW-10168PA-03, "RSG LOCA – BWNT Loss-of-Coolant Accident Evaluation Model for Recirculating Steam Generator Plants," December 1996.

2.13 RAI 13:

2.13.1 Statement of RAI 13

A. Explain how other than a uniform distribution that exceeds upper and lower bounds of a technical specification limiting condition of operation-controlled input parameter/initial condition could be applied in an analysis. Provide justification for this treatment.

B. Explain how a licensee and AREVA NP, Inc. (AREVA) will assure that the plant parameter uncertainty treatment used in an application of TR EMF-2103P, Revision 3, is consistent with existing constraints within the facility design and licensing bases. If AREVA believes that such assurances are unnecessary, justify why not.

2.13.2 Response to RAI 13

This response is unchanged from the original response.

Parts A and B of the question will be answered together:

All utilities are required to support their plant's Technical Specifications (TS) with a bases document. This document provides the technical reasoning, method, or calculation supporting a particular licensing limit or technical specification. To what extent the LBLOCA design basis calculation (or any other analysis) supports a plant's licensing basis can vary from plant-to-plant.

While the LBLOCA analysis is a key focal point of plant safety analysis, there is no requirement for it to support every licensing element. AREVA requires the licensee to identify those limits of operation that necessitate support from a LBLOCA calculation through a formal design input transmittal such as an Analytical Inputs Summary or Plant Parameters Document. Since safety analyses provide the strongest support for the licensing basis, the primary goal a licensee has with regard to the performance of safety analysis is to achieve coverage for the relevant limits of operation.

Section A.2.3.7.2 of Reference 2.13.1, Table A-6 provides a list of the typical ranged parameters. While the model parameters are fixed, the plant parameters are not limited to the ones presented in the table, and the licensee has flexibility in defining the plant parameters and ranges to be supported by the RLBLOCA analysis. An example of a table of plant parameters which can be supplied by the plant is provided in Table A-13 of Reference 2.13.1. For each licensing submittal, a table similar to Table B-8 of Reference 2.13.1, will be supplied for NRC review.

All operating ranges used in the analysis are supplied for review by the NRC in a table like Table B-8 of Reference 2.13.1. The applicability of the analysis to support a plant's operating limits is the responsibility of the licensee. Changes by a licensee to the analyzed operating ranges or the assigned uncertainties, such as resulting from new instrumentation, are accommodated provided the sum of the intended range of operation and the uncertainties remains bounded by the limits of the distribution range used in the analysis. Changes that cannot be accommodated within the applied range will require disposition by AREVA, a calculation of the expected impact, or a complete recalculation of the RLBLOCA analysis.

Reference:

2.13.1 AREVA Topical Report EMF-2103(P) Rev. 3, "Realistic Large Break LOCA Methodology for Pressurized Water Reactors," September 2013.

2.14 RAI 14:

2.14.1 Statement of RAI 14

Explain how the evaluation model (EM) will be used to model behavior for non-M5™ fuel cladding. Since this EM will be used to analyze fuel in multiple cycles of operation, consideration should be provided for co-resident, and potentially proprietary, cladding materials such as Westinghouse ZIRLO.

2.14.2 Response to RAI 14

This response is unchanged from the original response.

[
]

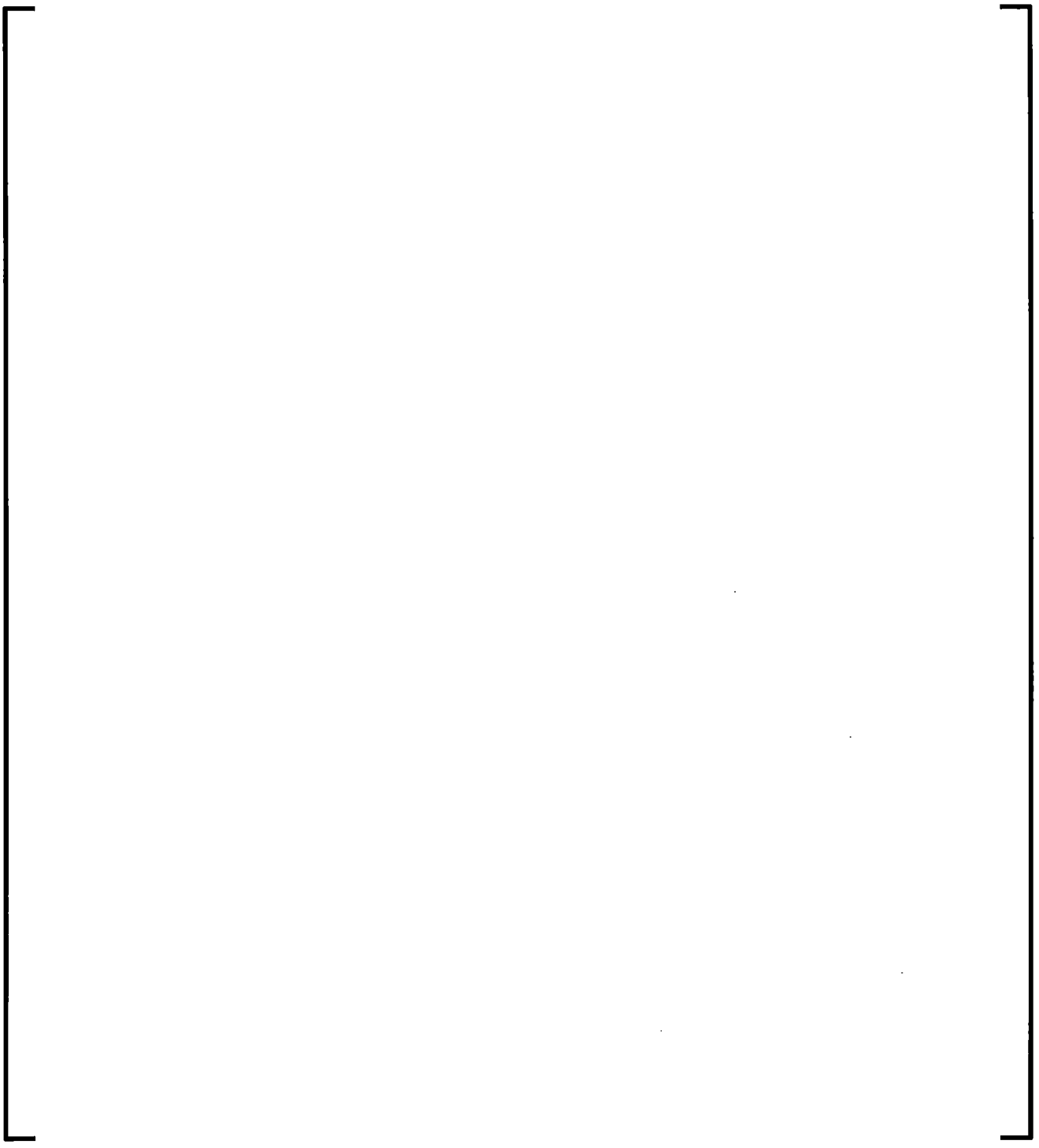

2.15 RAI 15:

2.15.1 Statement of RAI 15

A. Provide additional information to justify the correlation between packing fraction and rupture strain.

B. Explain whether sufficient information exists to determine whether the packing factor is independent from other statistically treated variables, such as fuel burnup.

C. Since uncertainties associated with both rupture strain and packing factor are statistically treated, and the packing factor model is clearly dependent on the rupture strain, justify the validity of the statistical approach taken with regard to sampling both.

D. If the statistical process relied upon to combine uncertainties does not require parametric independence among sampled parameters, explain why not.

2.15.2 Response to RAI 15

This response is unchanged from the original response.

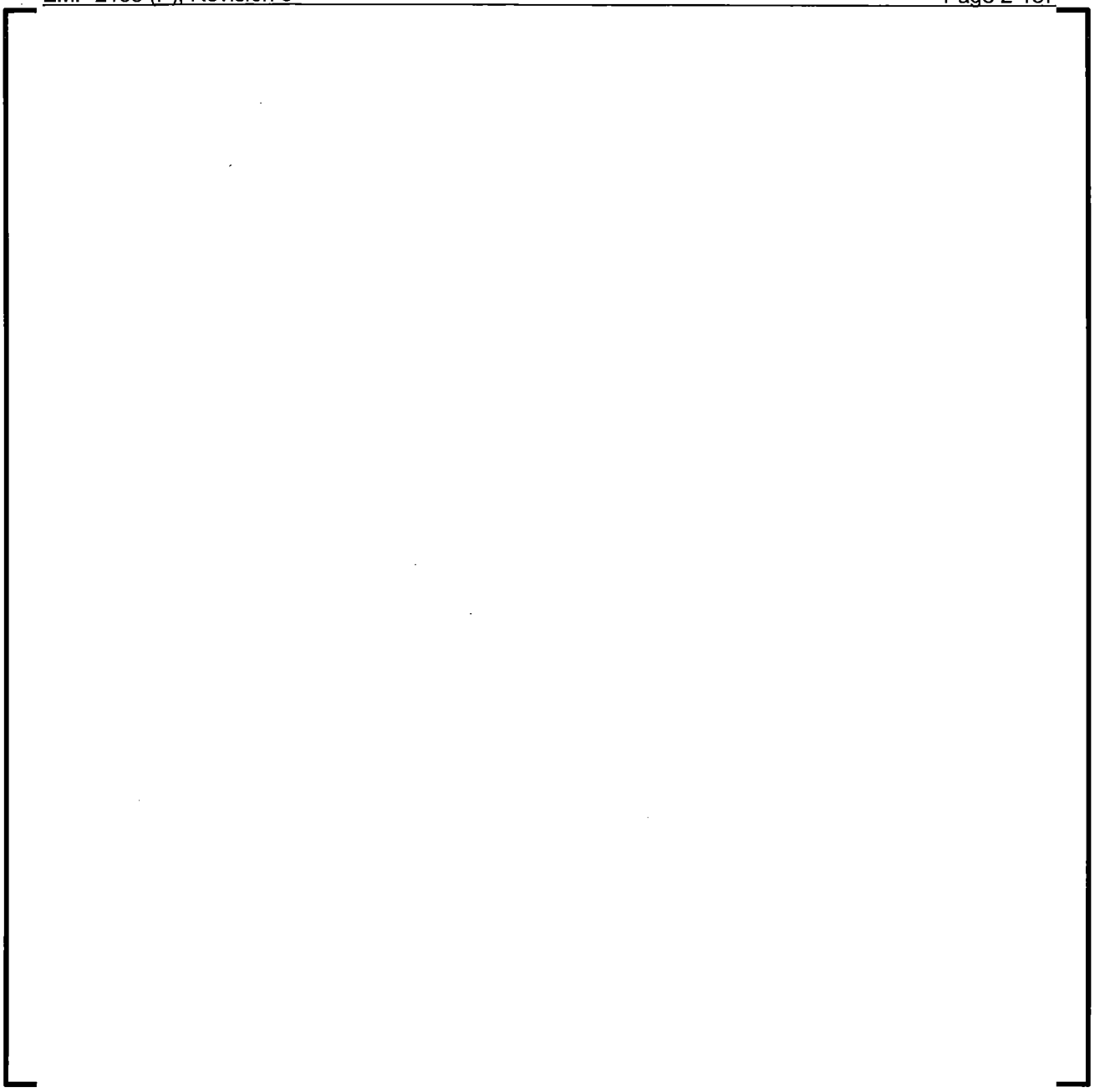

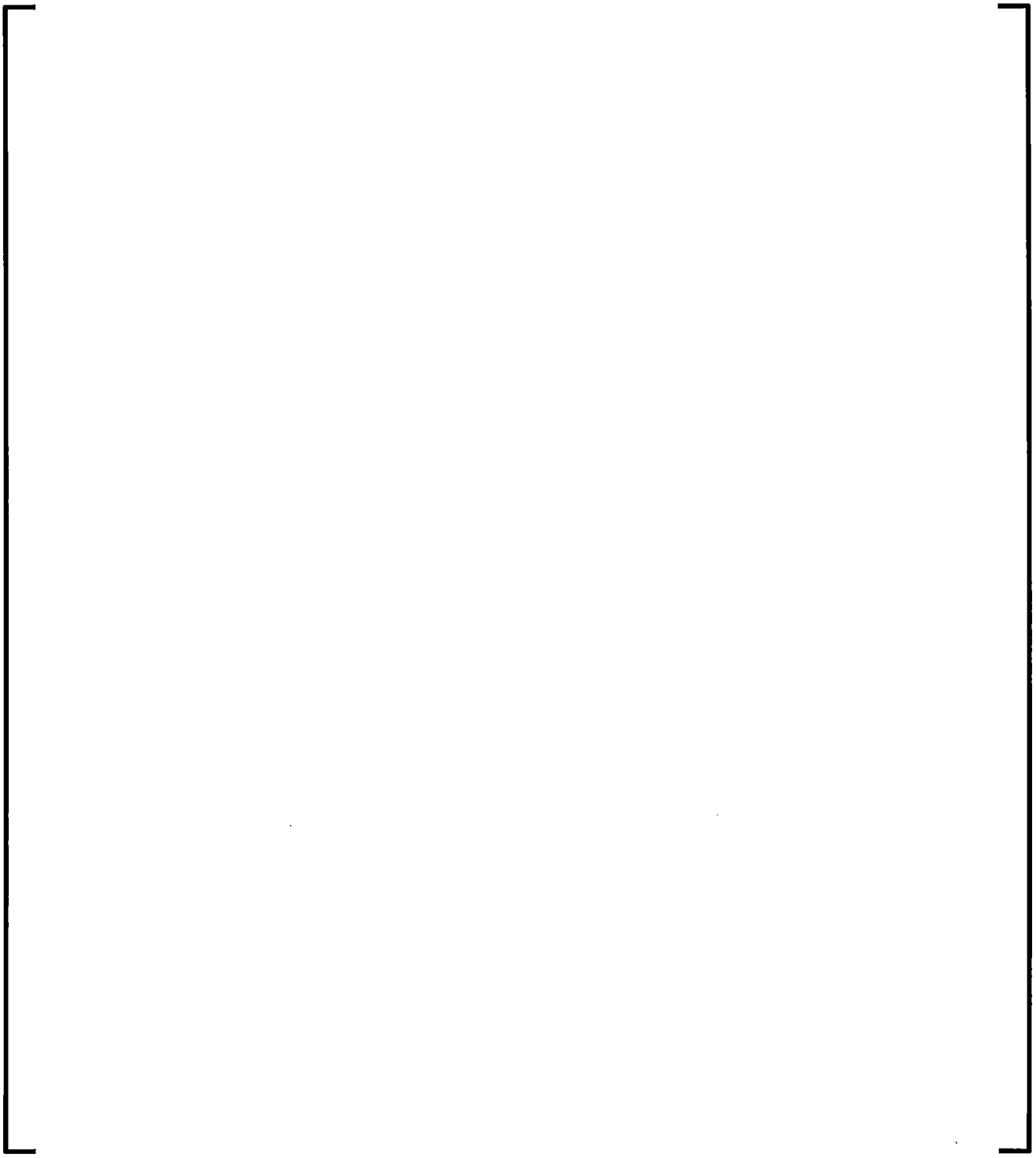

References:

2.15.1 Technical Report SEMCA-2005-313, "STATE-OF-THE-ART REVIEW OF PAST PROGRAMS DEVOTED TO FUEL BEHAVIOR UNDER LOCA CONDITIONS Part One. Clad Swelling and Rupture-Assembly Flow Blockage," Claude Grandjean, IRSN, Saint-Paul-Lez-Durance, France, December 2005.

2.15.2 NUREG-2160, "Post-Test Evaluation Results from Integral, High-Burnup, Fueled LOCA Tests at Studsvik Nuclear Laboratory," Michelle E. Flanagan, U.S. Nuclear Regulatory Commission, Rockville, Maryland, April 2013.

2.15.3 R. Manzel, C.T. Walker; "EPMA and SEM of fuel samples from PWR rods with an average burn-up of around 100MWd/kgHM," Journal of Nuclear Materials 301, pp. 170-182, 2002

2.16 RAI 16:

2.16.1 Statement of RAI 16

A. Explain whether the change described in Section 8.2 is new for Revision 3 of the TR EMF-2103.

B. Provide a detailed description of the rationale discussed in the TR text.

C. Provide an assessment of the adjusted TMINK value using FLECHT-SEASET tests with different flooding rates to show the general effect of changing the value. If this assessment is provided in response to another RAI question, it would be sufficient to reference that RAI response.

2.16.2 Response to RAI 16

This response is unchanged from the original response.

Background Information:

[
]

References:

2.16.1 Framatome ANP, Inc. Topical Report EMF-2103(P)(A), Revision 0, "Realistic Large Break LOCA Methodology for Pressurized Water Reactors (TAC No. MB7554)," April 2003.

2.16.2 AREVA Topical Report EMF-2103(P) Rev. 3, "Realistic Large Break LOCA Methodology for Pressurized Water Reactors," September 2013.

2.17 RAI 17:

2.17.1 Statement of RAI 17

A. Explain how the enhancement factors applied in the reflood assessments differ from those implemented for routine S-RELAP5 emergency core cooling system evaluations.

B. Provide a basis for their development, including an assessment of the implementation within the EM.

2.17.2 Response to RAI 17

This response is unchanged from the original response.

Background Information:

The grid spacer enhancement factors described in Section 8.2.3.5 of Reference 2.17.1 are calculated using the Yao, Hochreiter, and Leech correlation and modified by Meholic et al. These correlations are described in Section 7.6.7.2 and are given by Equations 7.531 through 7.534 of Reference 2.17.1. The Rod Bundle Heat Transfer (RBHT) test facility was used to develop these correlations, and the bundles in RBHT used prototypical mixing vane grids; these correlations are applicable for fuel assemblies that have non-mixing vane grids as well as mixing vane grids.

The enhancement factors, F1 and F2, depend on the [

]

(Reference 2.17.1, Page 7-206). In the input model, the enhancement factors for a given node within a grid span are calculated as a mean value as described on page A-69 of Reference 2.17.1.

In the FLECHT-SEASET tests, as well as in the FLECHT skewed power test bundles, simple egg-crate-type grid spacers (no mixing vanes) with a blockage factor of 29 percent are used. This value for the blockage factor is used in calculating the grid turbulence enhancement factors in the FLECHT-SEASET and the FLECHT skewed power test benchmarks reported in Section 8.2.3 and in Section 8.2.18 of Reference 2.17.1. The benchmarks reported in Section 8.2.18 were also used to validate the grid droplet shatter model described in Section 7.5.4.10.1 of Reference 2.17.1. A blockage factor of [ ] percent was also used in the development of the droplet shatter input parameters used in these benchmarks.

The grids used in the CCTF test bundle had a blockage factor that was [ ] percent. This value was used in the CCTF Run-62 benchmark given in the response to RAI Question 8 for the grid turbulence and the grid droplet shattering models.

Response:

The droplet shatter model, as well as the turbulent enhancement factors, was validated for grid blockages up to [ ] percent based on the test facility benchmarks. In the plant cases, AREVA will limit the fuel assembly grid blockage values [ ] percent until AREVA provides additional justification to use values above [ ] percent.

References:

2.17.1 AREVA Topical Report EMF-2103(P) Rev. 3, "Realistic Large Break LOCA Methodology for Pressurized Water Reactors," September 2013.

2.18 RAI 18:

2.18.1 Statement of RAI 18

Demonstrate the integral effects of the proposed model revisions by providing an updated analysis to compare alongside a recently completed analysis using a previously acceptable version of the EM. Specific comparisons should be provided for results that include a variety of PCTs and event sequences.

2.18.2 Response to RAI 18

This response is unchanged from the original response, with the exception of the addition of a missing reference.

Background:

Several model improvements are incorporated in the Revision 3 methodology which are not present in the Revision 0/Transition methodology. These are described in Section 1.1 and Section 2.3 of EMF-2103 (Reference 2.18.3). The major improvements that are expected to reduce the PCTs are as follows.

1. Rod-to-rod-radiation: In Reference 2.18.2, using a computer program R2RRAD provided by the NRC, AREVA showed that the PCT is reduced by the addition of rod-to-rod-radiation when the PCT is greater than approximately [ ]

   Calculations were performed with R2RRAD using FLECHT-SEASET data and estimating the effect on a similar 17x17 fuel assembly in an operating plant. The following Figure 2.18-1 shows the results for two FLECHT-SEASET sets and for the plant set. The figure shows that for PCTs greater than about [ ] the hot rod thermal radiation in the plant cases exceeds that of the same component within the experiments.

Figure 2.18-1 Rod Thermal Radiation in FLECHT-SEASET Bundle and in a 17x17 FA

2. Grid cooling due to droplet shatter (Reference 2.18.3, Section 7.5.4.10.1): The grid spacer droplet shatter model was added in Revision 3 to reduce the PCTs above the mid-plane of the FAs. The FLECHT-SEASET and FLECHT skewed-power test benchmarks show PCT reductions of more than [

] , as discussed in the response to RAI Question 19.

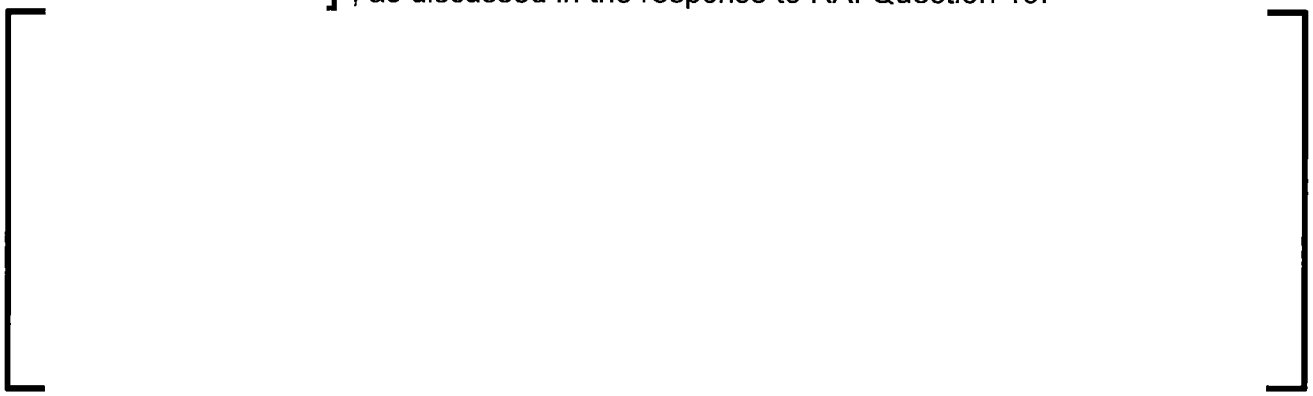

[ ]

Comparison of Transition to Revision 3:

Differences in the random sampling of parameters, the use of the COPERNIC rather than RODEX3A fuel models, and addition of new models to S-RELAP5 make a direct comparison of cases from the new methodology to cases from the approved methodology very difficult. There are no individual cases in either calculation that will produce easily comparable results. The statistical results from Transition analysis in Reference 2.18.1 are as follows:

[ ]

While the conditions are not identical for the limiting cases, they are somewhat similar. A summary of conditions for each case is shown below.

Table 2.18-1 Comparison of 95/95 Limiting Cases

Figure 2.18-2 Peak Clad Node Temperature Comparison

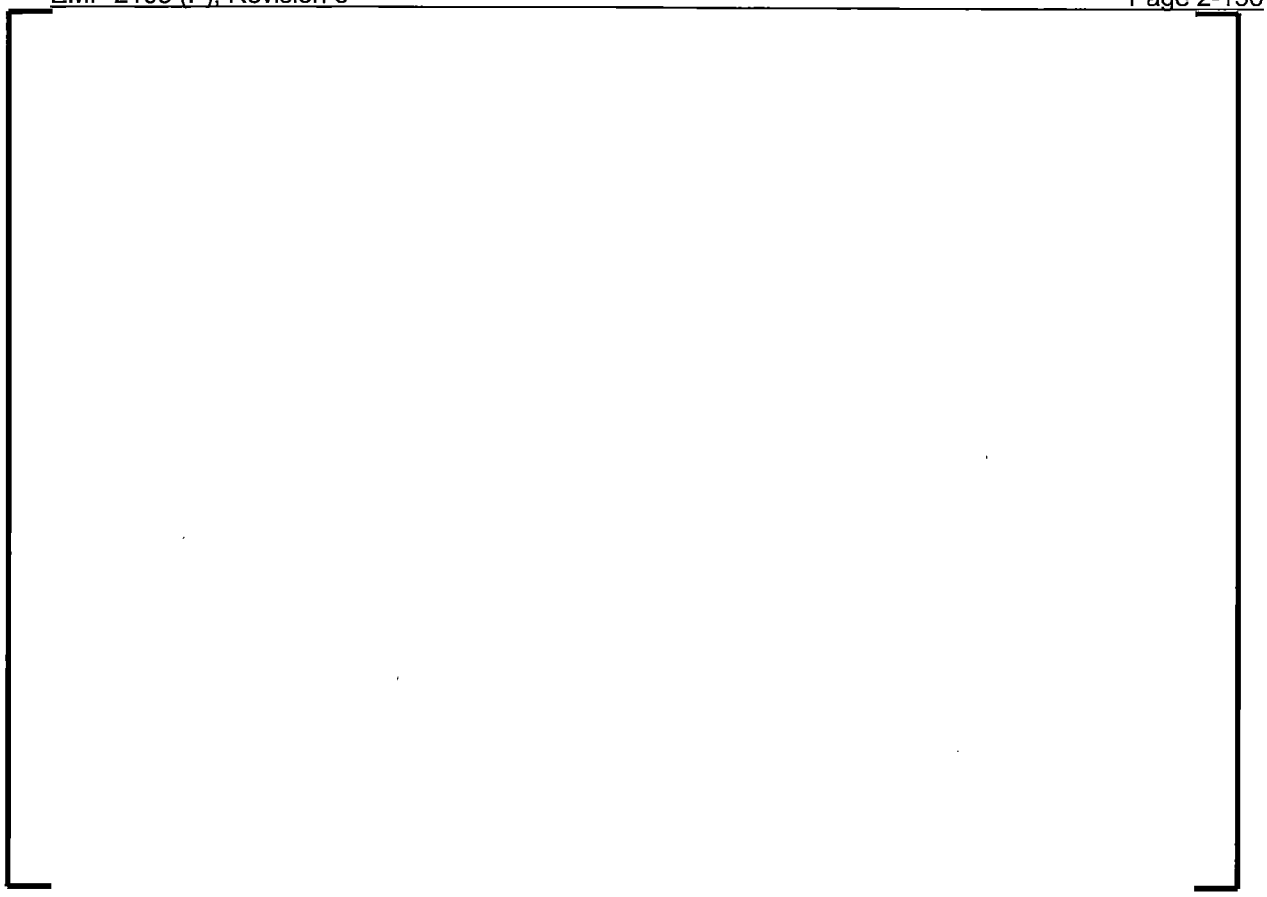

Figure 2.18-3 Normalized Axial Factor Comparison

Figure 2.18-4 shows the clad surface temperature at each axial node for the PCT rod at the time of PCT. Although both models have [

]

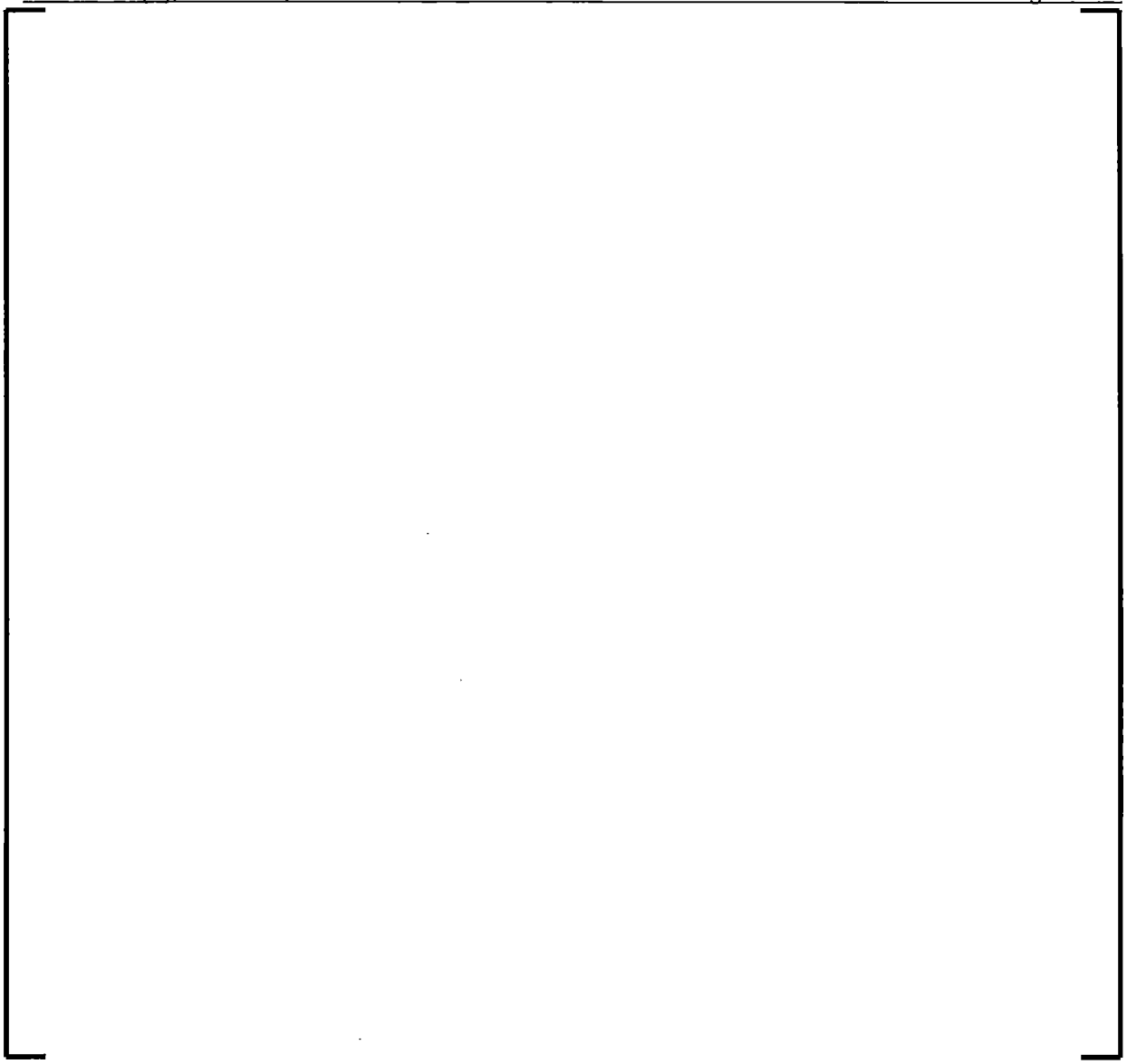

Figure 2.18-4 PCT Rod Temperature versus Elevation at Time of PCT

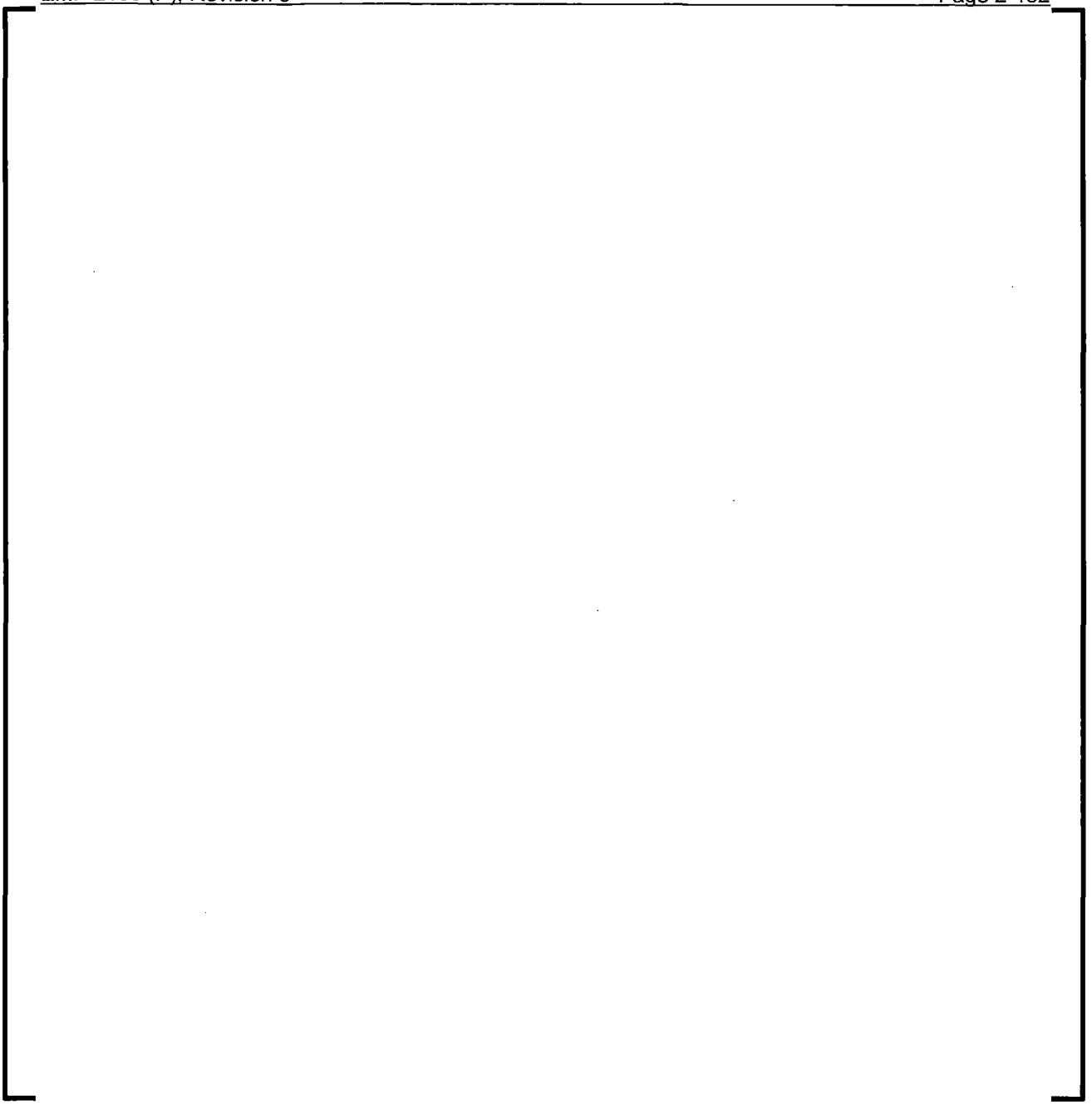

Figure 2.18-5 Comparison of PCT Margin for All Cases

Figure 2.18-6 PCT Versus Break Area

The top 5 PCT results for each set are shown in Table 2.18-2. The Revision 3 cases are from the 95/95 set (starting with the sixth case in the analysis).

Table 2.18-2 Ranking of Top 5 Cases

[ ]

The peak node temperature for each of these top 5 cases is shown on Figure 2.18-7. All of the Revision 3 cases in this plot showed a hot rod rupture, in part explaining the lower temperatures at the peak node.

[ ]

Figure 2.18-7 Peak Node Temperature for Top 5 PCT Cases

Figure 2.18-8 shows the reactor vessel mass for these top 5 cases from each analysis. The x-axis is expanded to show just the first 100 seconds of the transient. [

]

Figure 2.18-8 Reactor Vessel Mass for Top 5 PCT Cases

In summary, as expected, the Revision 3 results show a reduction in the PCT compared to the currently acceptable methodology.

References:

2.18.1 AREVA Topical Report ANP-3237P Rev 0 "Harris Nuclear Plant Unit 1 Realistic Large Break LOCA Analysis."

2.18.2 AREVA Topical Report ANP-2655(NP), Revision 1, "Sequoyah Nuclear Plant Unit 2 Realistic Large Break LOCA Analysis."

2.18.3 AREVA Document EMF-2103(P), Revision 3, "Realistic Large Break LOCA Methodology for Pressurized Water Reactors."

2.18.4 Code of Federal Regulations Title 10, Pt. 50.46, "Acceptance criteria for emergency core cooling systems for light-water nuclear power reactors."

2.19 RAI 19:

2.19.1 Statement of RAI 19

A. Provide a comprehensive set of the FLECHT benchmarking related to the updated EM.

B. For each model upgrade, or each set of upgrades that improve modeling capability with respect to a single phenomenon or process, provide an independent assessment that shows how the model upgrade performs relative to the previously approved model, and relative to its applicable assessment data set.

2.19.2 Response to RAI 19

This response is unchanged from the original response.

Background:

Section 8.2.3 of EMF-2103, Revision 3 presents the S-RELAP5 benchmarks of FLECHT SEASET tests 31504, 31701, 31302, 31203, 31805, 32013, and 34209, and FLECHT Skewed tests 13609 and 13914. Those benchmarks were performed under Revision 2 of the methodology and consist of a 20 node core without the grid cooling (GC) or rod-to-rod (RTR) radiation models. The main features of that model can be found in Section 8.2.3.5. Following this work, minor S-RELAP5 code changes and error corrections were made as discussed in Section 8.1.5; however, the benchmarks were not rerun because the impact of the changes was deemed negligible. The methodology was then updated from Revision 2 to Revision 3, at which point the FLECHT SEASET and Skewed benchmarks were repeated in Section 8.2.18 in order to show the effects of incorporating the EM changes described in Section 8.1.5. These changes, particularly the addition of the grid cooling model, required a re-nodalization from 20 to 21 core nodes.

The work necessary to develop the probability density functions for the film boiling and dispersed flow film boiling heat transfer multipliers in Section 8.4.1.4 required the reanalysis of all FLECHT SEASET tests but not the Skewed test. These benchmarks therefore include all of the Revision 3 modifications discussed previously as well as the rod-to-rod (RTR) radiation model.

Following the work of Section 8.4.1.4, it was found that the pressure limit of 150 psia on the vapor absorptivity coefficient of vapor and droplets (Equation 7.540) was more appropriately modeled using a limit of [ ]. Since all but one of the FLECHT tests were operated [ ], this change only has the potential to impact test 32013, which operated at 60 psia. Therefore, rather than re-analyzing all tests using this change, only test 32013 incorporates this change in the following results.

The FLECHT Skewed tests were performed in Section 8.2.3 under the Revision 2 model, and have since been performed again with all Revision 3 changes except the RTR radiation model.

In the figures below, the results labeled as Rev. 3 reflect the final EMF-2103, Revision 3 model, which includes the 21 node core, grid cooling model, rod-to-rod radiation, and pressure limit changes. Any results that do not contain all of these changes are identified as being subtracted from the final Revision 3 model.

Discussion of Results:

The figures below present the results of FLECHT SEASET tests 31203, 31302, 31504, 31701, 31805, 32013, and 34209, performed according to the current evaluation model. Figure 2.19-1 through Figure 2.19-5 demonstrate the progression from Revision 0 of EMF-2103 (Reference 2.19.1) to the updated Revision 3, using the maximum cladding temperature results of test 31504. Specifically, Figure 2.19-1 compares the Revision 0 methodology against the Revision 2 methodology from Section 8.2.3, showing that the implementation of the new drag package and Wong-Hochreiter bundle option results in a more accurate PCT prediction, particularly in the upper elevations of the core. Figure 2.19-2 then compares the Revision 2 methodology with and without the minor error corrections discussed in Section 8.1.5, showing a negligible impact. Figure 2.19-3 then compares the error corrected Revision 2 methodology to the base Revision 3 methodology with a 21 node core model. The finer nodalization again results in a small but more favorable PCT response, closer to the experimental data. Figure 2.19-4 then compares that 21 node core model to the same model but with the addition of grid cooling, improving the PCT prediction above the middle elevation of the core. Figure 2.19-5 then completes the progression by comparing results against the Revision 3 methodology which also includes RTR radiation, an effect which increases the PCT prediction at the upper core elevations.

Figure 2.19-6 through Figure 2.19-103 each provide a comparison between the Revision 2 results presented in Section 8.2.3 of EMF-2103 and that with the addition of core re-nodalization, grid cooling model, and RTR radiation model, giving insight into the integrated effects of these models on the FLECHT SEASET tests, as well as comparing those results against experimental data. In other words, they reflect the changes shown between Figure 2.19-2 and Figure 2.19-5.

[

]

The FLECHT Skewed tests are presented in Figure 2.19-105 through Figure 2.19-124. They differ slightly from the non-skewed cases in that the latest runs do not include a model for RTR radiation, but they do include the pressure limit on the vapor absorptivity coefficient.

The overall trends in these comparisons are consistent with the effects of each model change shown by Figure 2.19-1 through Figure 2.19-5. In general, cooling above the mid-plane of the core is improved, and the RELAP calculations more closely predict the experimental data while still maintaining conservatism.

References:

2.19.1 Framatome ANP, Inc. Topical Report EMF-2103(P)(A), Revision 0, "Realistic Large Break LOCA Methodology for Pressurized Water Reactors (TAC No. MB7554)," April, 2003.

Figure 2.19-1 Influence of New Drag Package and Use of Wong-Hochreiter Bundle Option

Figure 2.19-2 Influence of Code Error Corrections

Figure 2.19-3 Influence of Core Re-nodalization

Figure 2.19-4 Influence of Grid Cooling Model

Figure 2.19-5 Influence of Rod-to-rod Radiation

Figure 2.19-6 FLECHT SEASET Test 31203, Max Clad Temperature

Figure 2.19-7 FLECHT SEASET Test 31203, Rod Surface Temperatures at 48 in

Figure 2.19-8 FLECHT SEASET Test 31203, Rod Surface Temperatures at 78 in

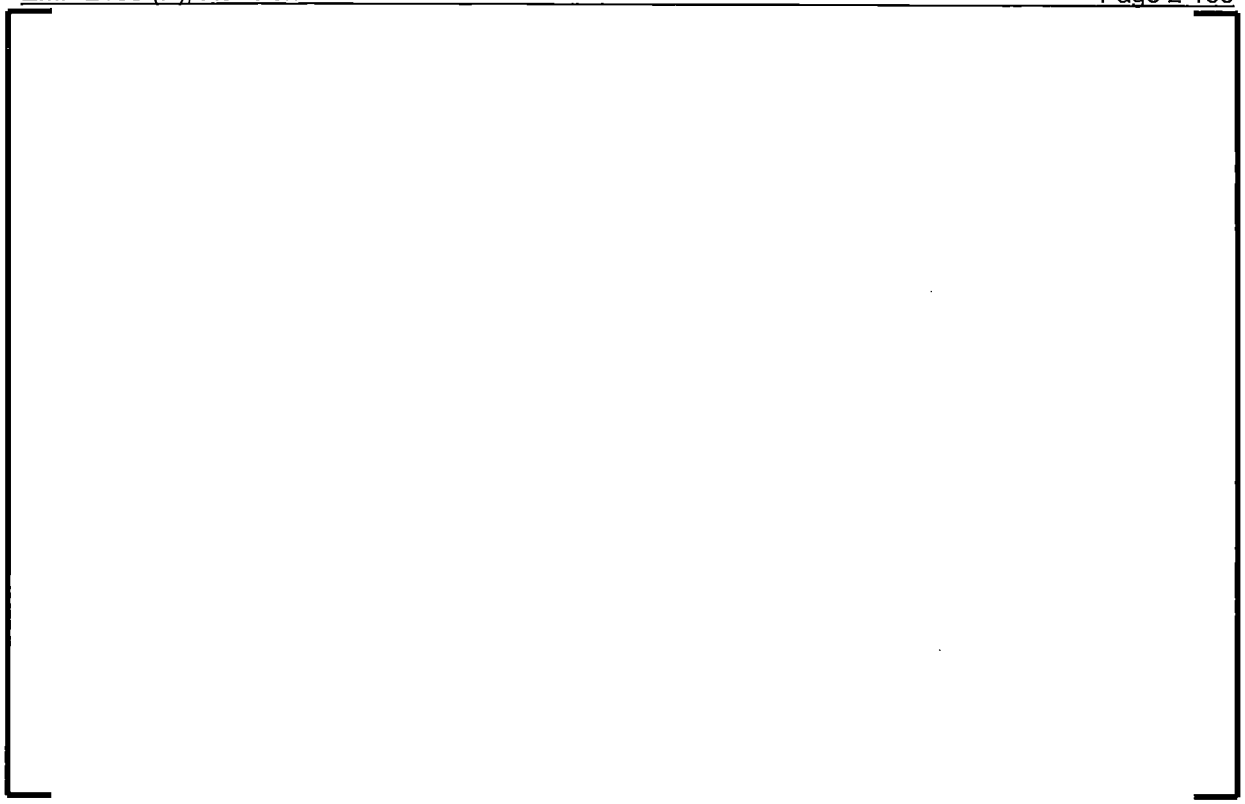

Figure 2.19-9 FLECHT SEASET Test 31203, Rod Surface Temperatures at 90 in

Figure 2.19-10 FLECHT SEASET Test 31203, Rod Surface Temperatures at 111 in

Figure 2.19-11 FLECHT SEASET Test 31203, Differential Pressure Between 72 in and 84 in

Figure 2.19-12 FLECHT SEASET Test 31203, Heat Transfer Coefficient

Figure 2.19-13 FLECHT SEASET Test 31203, Accumulated Water Mass in Test Section

Figure 2.19-14 FLECHT SEASET Test 31203, Total Liquid Carryover from Test Assembly

Figure 2.19-15 FLECHT SEASET Test 31203, Steam Temperatures at 72 in

Figure 2.19-16 FLECHT SEASET Test 31203, Steam Temperatures at 78 in

Figure 2.19-17 FLECHT SEASET Test 31203, Steam Temperatures at 84 in

Figure 2.19-18 FLECHT SEASET Test 31203, Steam Temperatures at 90 in

Figure 2.19-19 FLECHT SEASET Test 31203, Steam Temperatures at 96 in

Figure 2.19-20 FLECHT SEASET Test 31302, Max Clad Temperature

Figure 2.19-21 FLECHT SEASET Test 31302, Rod Surface Temperatures at 48 in

Figure 2.19-22 FLECHT SEASET Test 31302, Rod Surface Temperatures at 78 in

Figure 2.19-23 FLECHT SEASET Test 31302, Rod Surface Temperatures at 90 in

Figure 2.19-24 FLECHT SEASET Test 31302, Rod Surface Temperatures at 111 in

Figure 2.19-25 FLECHT SEASET Test 31302, Differential Pressure Between 72 in and 84 in

Figure 2.19-26 FLECHT SEASET Test 31302, Heat Transfer Coefficient

Figure 2.19-27 FLECHT SEASET Test 31302, Accumulated Water Mass in Test Section

Figure 2.19-28 FLECHT SEASET Test 31302, Total Liquid Carryover from Test Assembly

Figure 2.19-29 FLECHT SEASET Test 31302, Steam Temperatures at 72 in

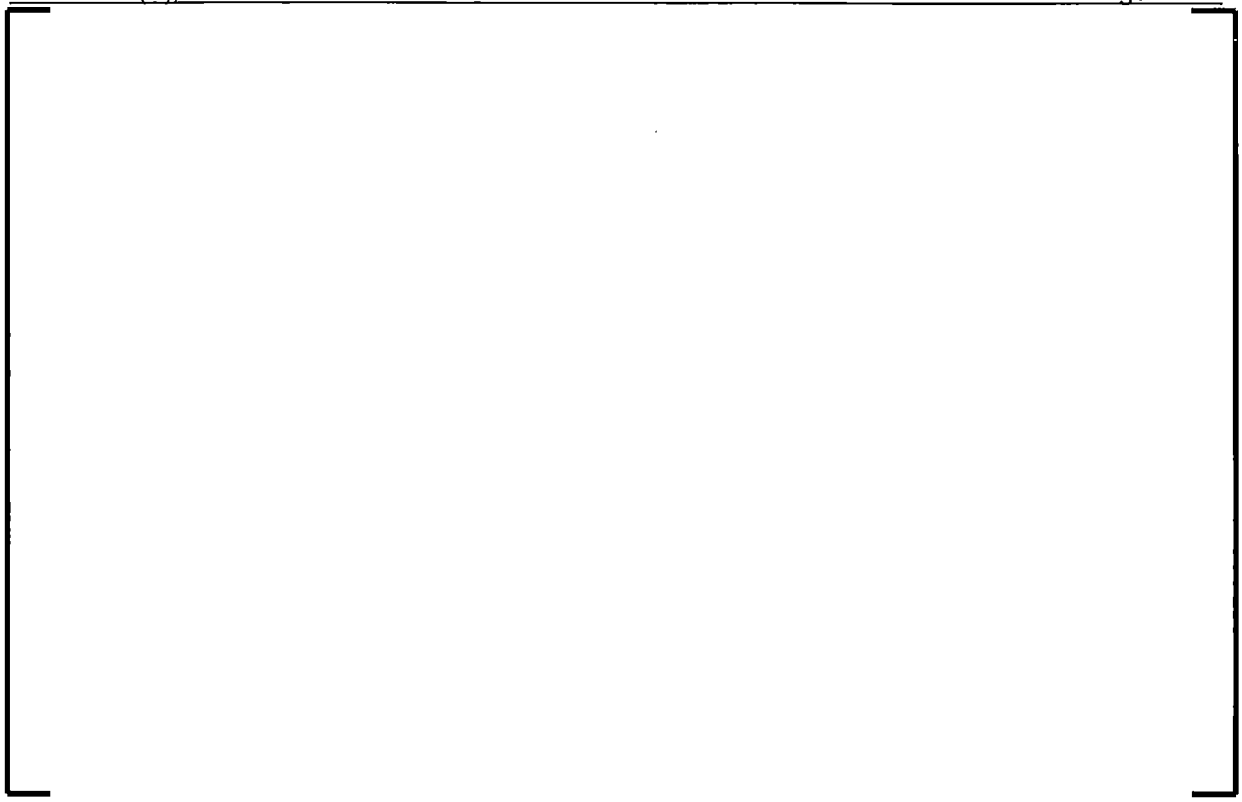

Figure 2.19-30 FLECHT SEASET Test 31302, Steam Temperatures at 78 in

Figure 2.19-31 FLECHT SEASET Test 31302, Steam Temperatures at 84 in

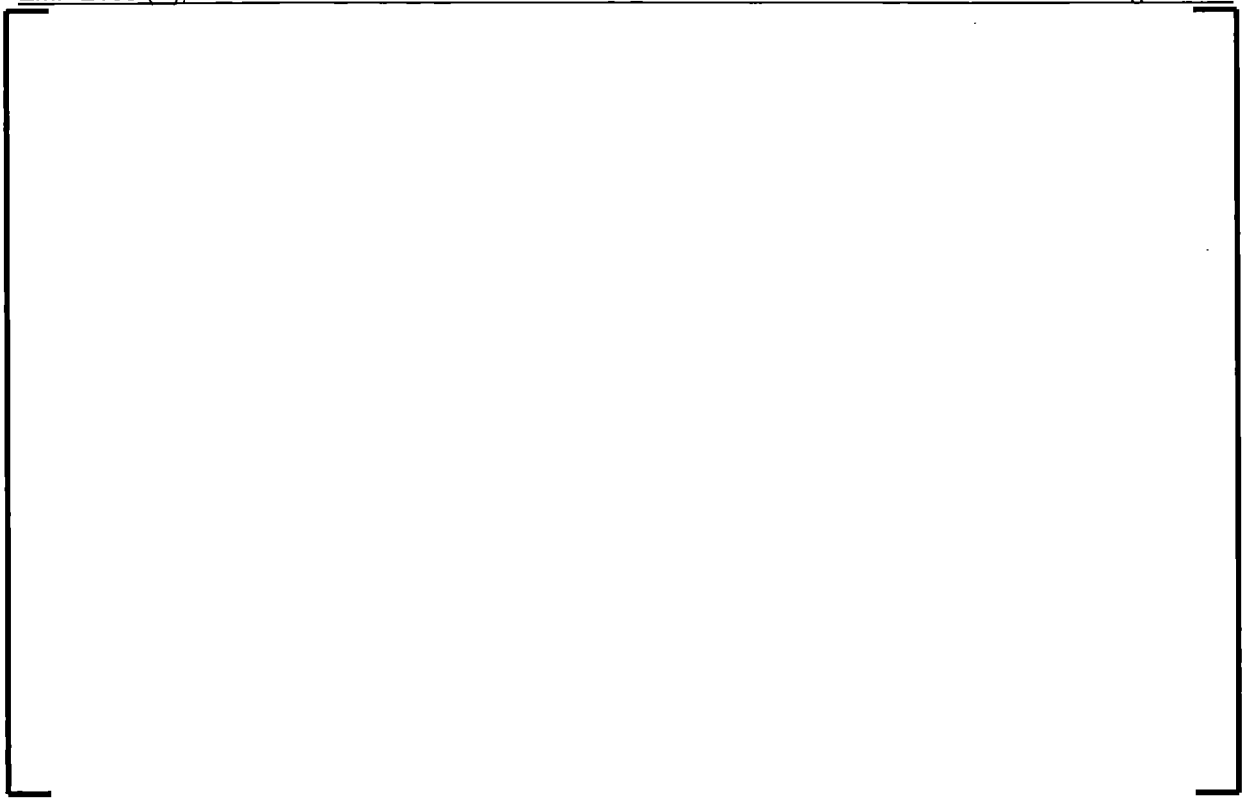

Figure 2.19-32 FLECHT SEASET Test 31302, Steam Temperatures at 90 in

Figure 2.19-33 FLECHT SEASET Test 31302, Steam Temperatures at 96 in

Figure 2.19-34 FLECHT SEASET Test 31504, Max Clad Temperature

Figure 2.19-35 FLECHT SEASET Test 31504, Rod Surface Temperatures at 48 in

Figure 2.19-36 FLECHT SEASET Test 31504, Rod Surface Temperatures at 78 in

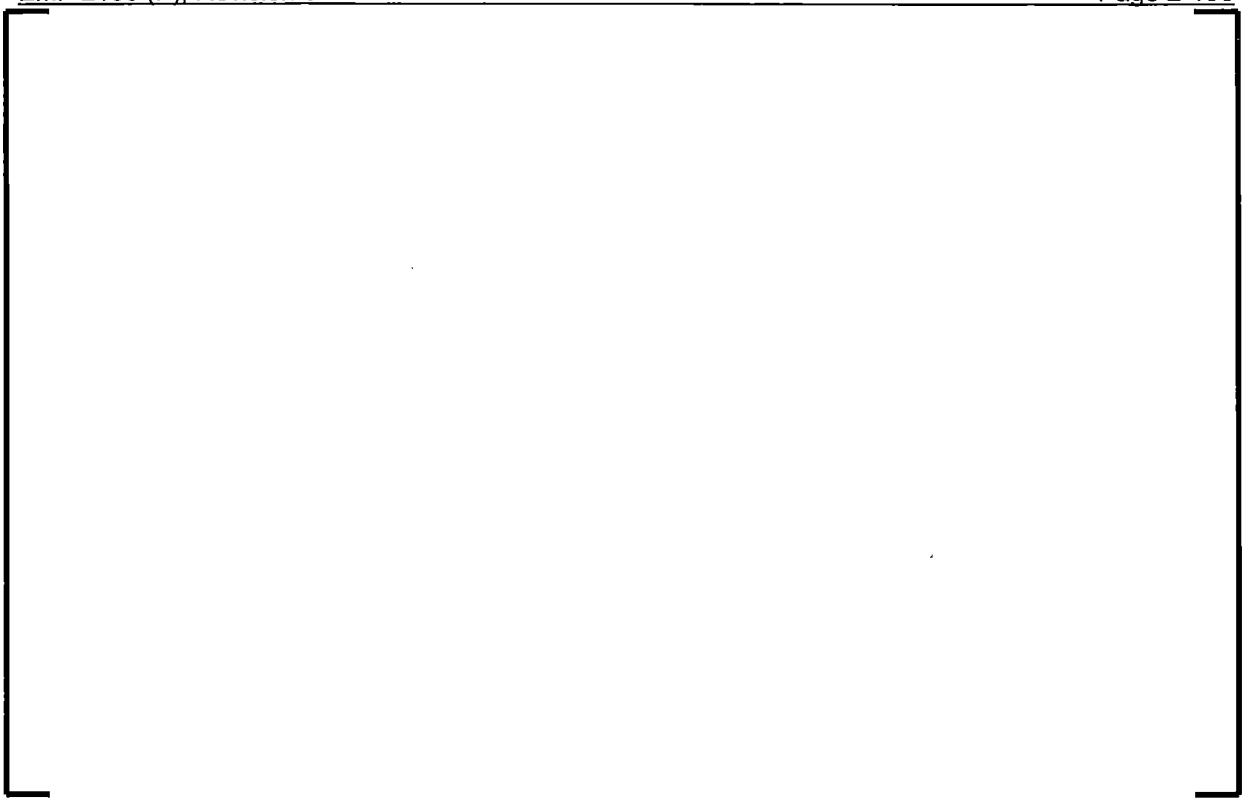

Figure 2.19-37 FLECHT SEASET Test 31504, Rod Surface Temperatures at 90 in

Figure 2.19-38 FLECHT SEASET Test 31504, Rod Surface Temperatures at 111 in

Figure 2.19-39 FLECHT SEASET Test 31504, Differential Pressure Between 72 in and 84 in

Figure 2.19-40 FLECHT SEASET Test 31504, Heat Transfer Coefficient

Figure 2.19-41 FLECHT SEASET Test 31504, Accumulated Water Mass in Test Section

Figure 2.19-42 FLECHT SEASET Test 31504, Total Liquid Carryover from Test Assembly

Figure 2.19-43 FLECHT SEASET Test 31504, Steam Temperatures at 72 in

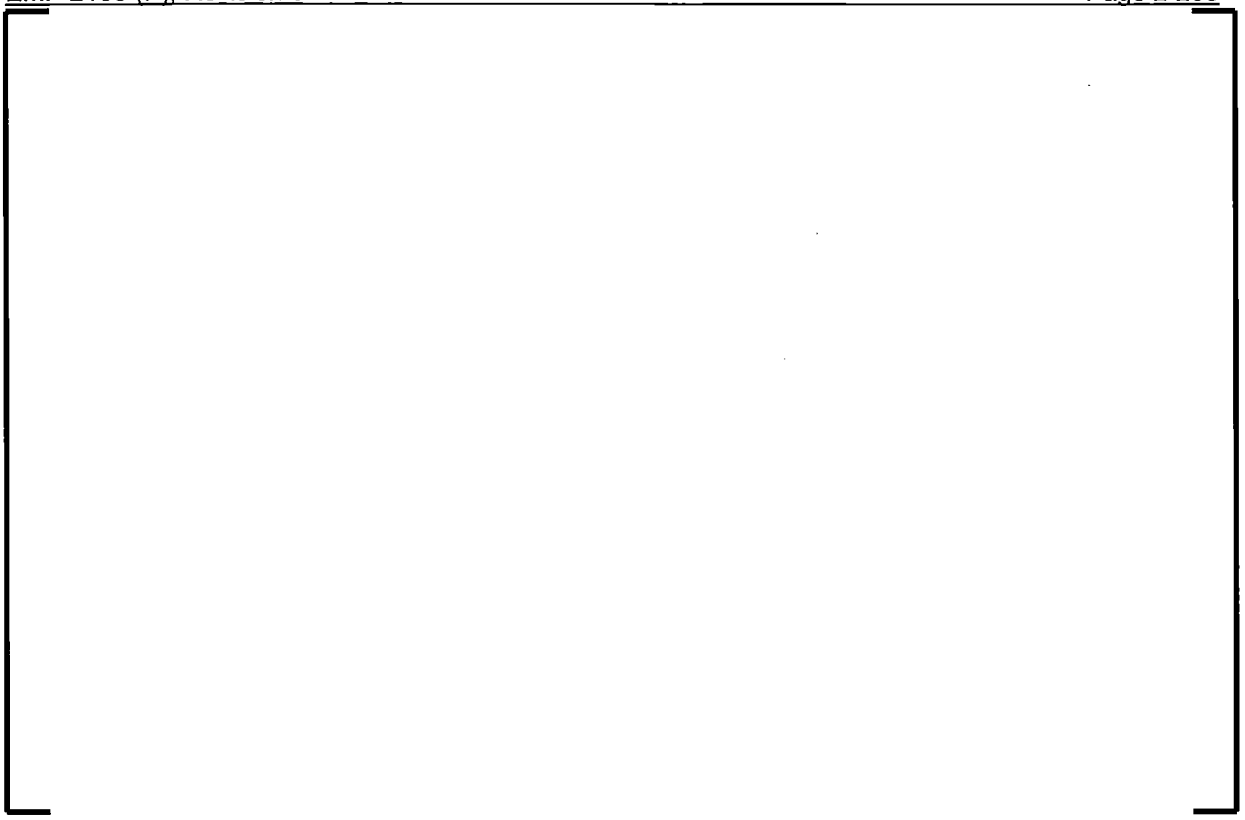

Figure 2.19-44 FLECHT SEASET Test 31504, Steam Temperatures at 78 in

Figure 2.19-45 FLECHT SEASET Test 31504, Steam Temperatures at 84 in

Figure 2.19-46 FLECHT SEASET Test 31504, Steam Temperatures at 90 in

Figure 2.19-47 FLECHT SEASET Test 31504, Steam Temperatures at 96 in

Figure 2.19-48 FLECHT SEASET Test 31701, Max Clad Temperature

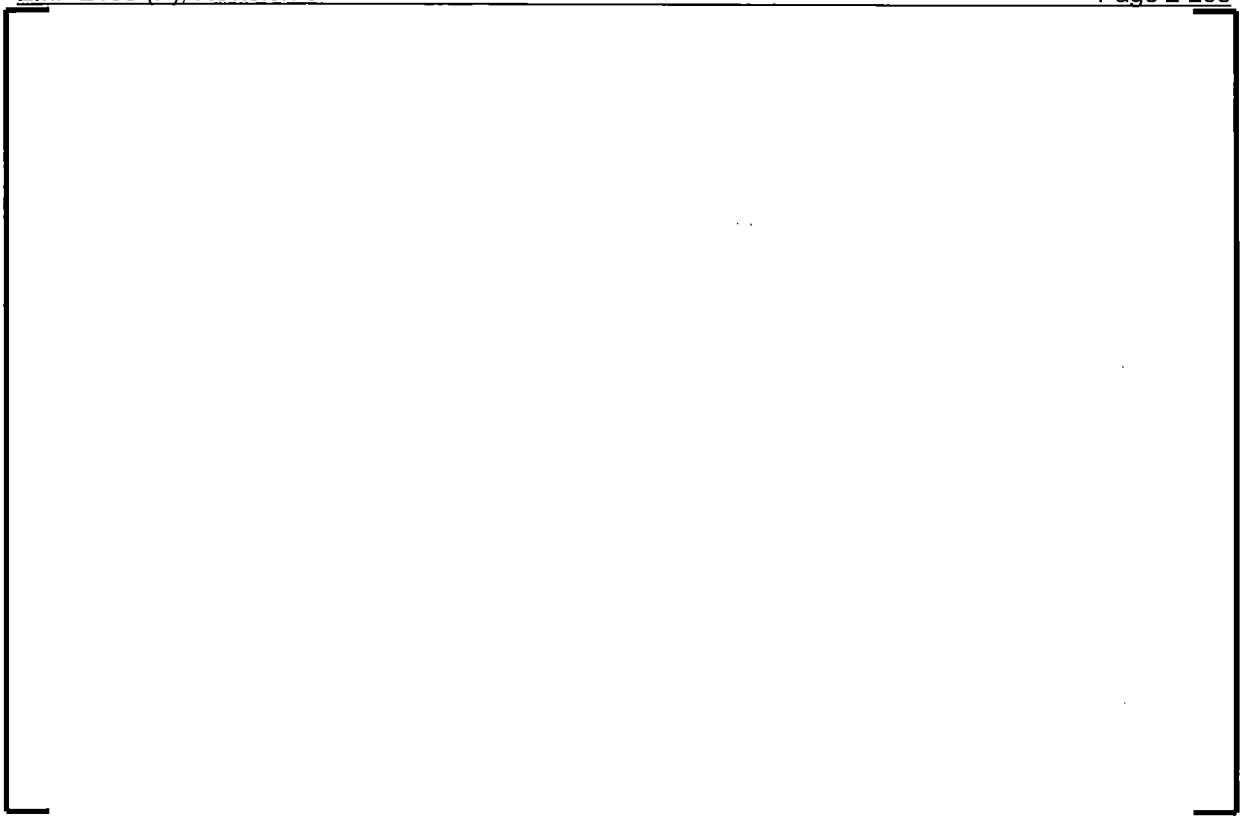

Figure 2.19-49 FLECHT SEASET Test 31701, Rod Surface Temperatures at 48 in

Figure 2.19-50 FLECHT SEASET Test 31701, Rod Surface Temperatures at 78 in

Figure 2.19-51 FLECHT SEASET Test 31701, Rod Surface Temperatures at 90 in

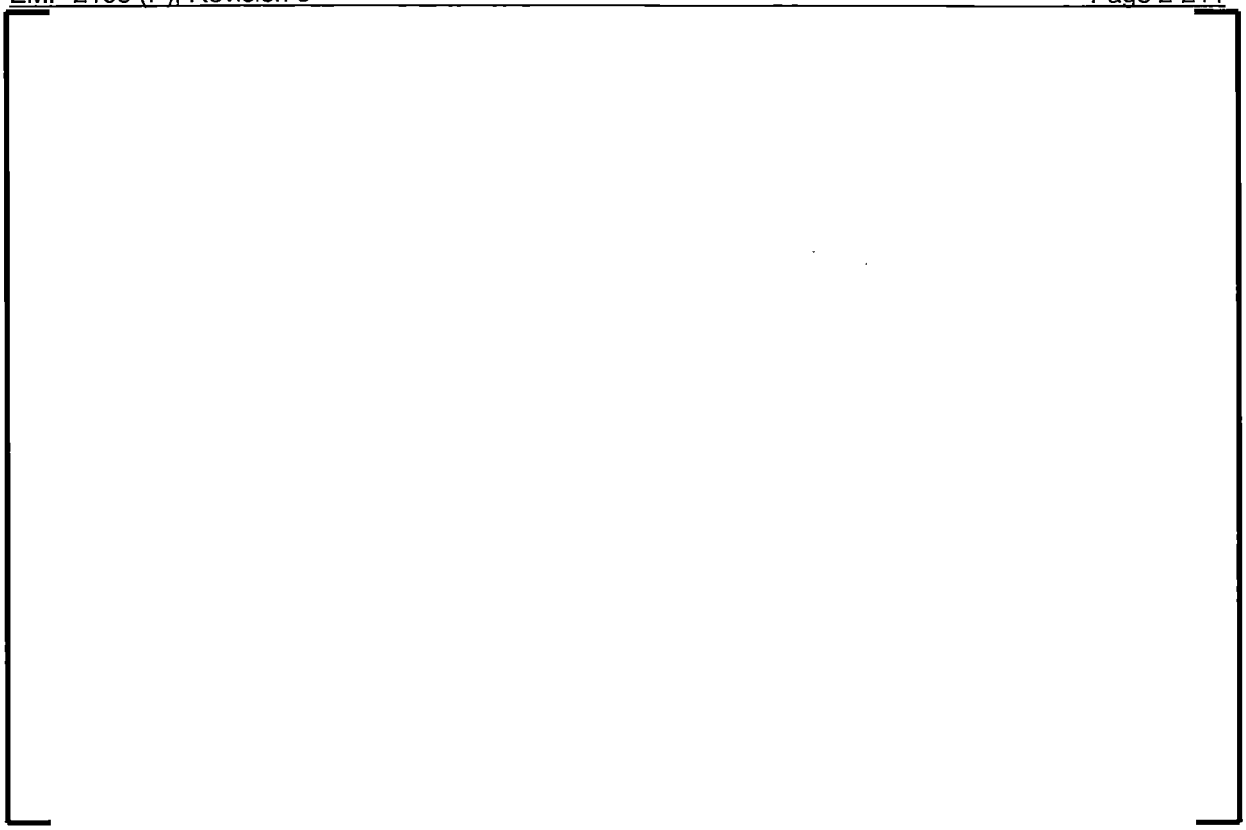

Figure 2.19-52 FLECHT SEASET Test 31701, Rod Surface Temperatures at 111 in

Figure 2.19-53 FLECHT SEASET Test 31701, Differential Pressure Between 72 in and 84 in

Figure 2.19-54 FLECHT SEASET Test 31701, Heat Transfer Coefficient

Figure 2.19-55 FLECHT SEASET Test 31701, Accumulated Water Mass in Test Section

Figure 2.19-56 FLECHT SEASET Test 31701, Total Liquid Carryover from Test Assembly

Figure 2.19-57 FLECHT SEASET Test 31701, Steam Temperatures at 72 in

Figure 2.19-58 FLECHT SEASET Test 31701, Steam Temperatures at 78 in

Figure 2.19-59 FLECHT SEASET Test 31701, Steam Temperatures at 84 in

Figure 2.19-60 FLECHT SEASET Test 31701, Steam Temperatures at 90 in

Figure 2.19-61 FLECHT SEASET Test 31701, Steam Temperatures at 96 in

Figure 2.19-62 FLECHT SEASET Test 31805, Max Clad Temperature

Figure 2.19-63 FLECHT SEASET Test 31805, Rod Surface Temperatures at 48 in

Figure 2.19-64 FLECHT SEASET Test 31805, Rod Surface Temperatures at 78 in

Figure 2.19-65 FLECHT SEASET Test 31805, Rod Surface Temperatures at 90 in

Figure 2.19-66 FLECHT SEASET Test 31805, Rod Surface Temperatures at 111 in

Figure 2.19-67 FLECHT SEASET Test 31805, Differential Pressure Between 72 in and 84 in

Figure 2.19-68 FLECHT SEASET Test 31805, Heat Transfer Coefficient

Figure 2.19-69 FLECHT SEASET Test 31805, Accumulated Water Mass in Test Section

Figure 2.19-70 FLECHT SEASET Test 31805, Total Liquid Carryover from Test Assembly

Figure 2.19-71 FLECHT SEASET Test 31805, Steam Temperatures at 72 in

Figure 2.19-72 FLECHT SEASET Test 31805, Steam Temperatures at 78 in

Figure 2.19-73 FLECHT SEASET Test 31805, Steam Temperatures at 84 in

Figure 2.19-74 FLECHT SEASET Test 31805, Steam Temperatures at 90 in

Figure 2.19-75 FLECHT SEASET Test 31805, Steam Temperatures at 96 in

Figure 2.19-76 FLECHT SEASET Test 32013, Max Clad Temperature

Figure 2.19-77 FLECHT SEASET Test 32013, Rod Surface Temperatures at 48 in

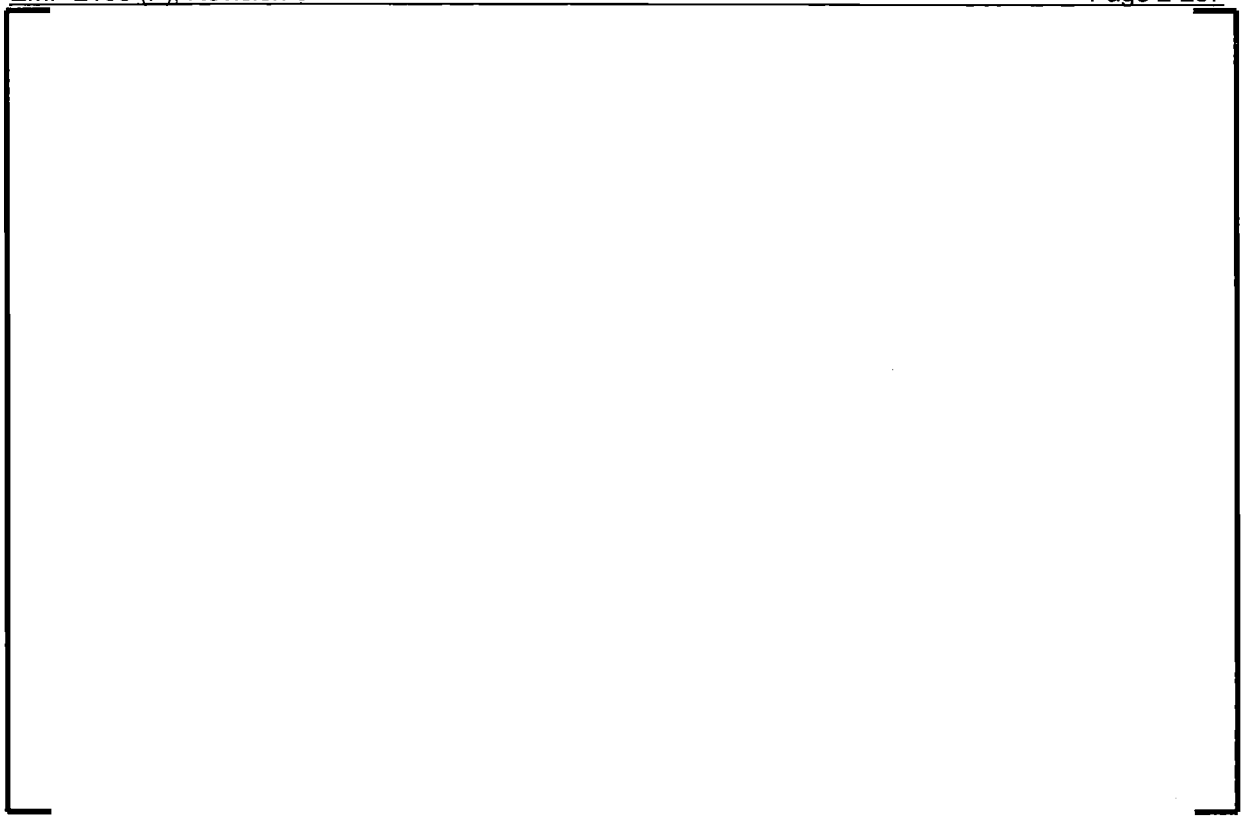

Figure 2.19-78 FLECHT SEASET Test 32013, Rod Surface Temperatures at 78 in

Figure 2.19-79 FLECHT SEASET Test 32013, Rod Surface Temperatures at 90 in

Figure 2.19-80 FLECHT SEASET Test 32013, Rod Surface Temperatures at 111 in

Figure 2.19-81 FLECHT SEASET Test 32013, Differential Pressure Between 72 in and 84 in

Figure 2.19-82 FLECHT SEASET Test 32013, Heat Transfer Coefficient

Figure 2.19-83 FLECHT SEASET Test 32013, Accumulated Water Mass in Test Section

Figure 2.19-84 FLECHT SEASET Test 32013, Total Liquid Carryover from Test Assembly

Figure 2.19-85 FLECHT SEASET Test 32013, Steam Temperatures at 72 in

Figure 2.19-86 FLECHT SEASET Test 32013, Steam Temperatures at 78 in

Figure 2.19-87 FLECHT SEASET Test 32013, Steam Temperatures at 84 in

Figure 2.19-88 FLECHT SEASET Test 32013, Steam Temperatures at 90 in

Figure 2.19-89 FLECHT SEASET Test 32013, Steam Temperatures at 96 in

Figure 2.19-90 FLECHT SEASET Test 34209, Max Clad Temperature

Figure 2.19-91 FLECHT SEASET Test 34209, Rod Surface Temperatures at 48 in

Figure 2.19-92 FLECHT SEASET Test 34209, Rod Surface Temperatures at 78 in

Figure 2.19-93 FLECHT SEASET Test 34209, Rod Surface Temperatures at 90 in

Figure 2.19-94 FLECHT SEASET Test 34209, Rod Surface Temperatures at 111 in

Figure 2.19-95 FLECHT SEASET Test 34209, Differential Pressure Between 72 in and 84 in

Figure 2.19-96 FLECHT SEASET Test 34209, Heat Transfer Coefficient

Figure 2.19-97 FLECHT SEASET Test 34209, Accumulated Water Mass in Test Section

Figure 2.19-98 FLECHT SEASET Test 34209, Total Liquid Carryover from Test Assembly

Figure 2.19-99 FLECHT SEASET Test 34209, Steam Temperatures at 72 in

Figure 2.19-100 FLECHT SEASET Test 34209, Steam Temperatures at 78 in

Figure 2.19-101 FLECHT SEASET Test 34209, Steam Temperatures at 84 in

Figure 2.19-102 FLECHT SEASET Test 34209, Steam Temperatures at 90 in

Figure 2.19-103 FLECHT SEASET Test 34209, Steam Temperatures at 96 in

Figure 2.19-104 FLECHT SEASET Test 32013, Max Clad Temperature with PVAB Limit

Figure 2.19-105 FLECHT SEASET Test 13609, Max Clad Temperature

Figure 2.19-106 FLECHT SEASET Test 13609, Rod Surface Temperatures at 36 in

Figure 2.19-107 FLECHT SEASET Test 13609, Rod Surface Temperatures at 60 in

Figure 2.19-108 FLECHT SEASET Test 13609, Rod Surface Temperatures at 84 in

Figure 2.19-109 FLECHT SEASET Test 13609, Rod Surface Temperatures at 108 in

Figure 2.19-110 FLECHT SEASET Test 13609, Differential Pressure Between 72 in and 84 in

Figure 2.19-111 FLECHT SEASET Test 13609, Heat Transfer Coefficient

Figure 2.19-112 FLECHT SEASET Test 13609, Accumulated Water Mass in Test Section

Figure 2.19-113 FLECHT SEASET Test 13609, Total Liquid Carryover from Test Assembly

Figure 2.19-114 FLECHT SEASET Test 13609, Steam Temperatures at 84 in

Figure 2.19-115 FLECHT SEASET Test 13914, Max Clad Temperature

Figure 2.19-116 FLECHT SEASET Test 13914, Rod Surface Temperatures at 36 in

Figure 2.19-117 FLECHT SEASET Test 13914, Rod Surface Temperatures at 60 in

Figure 2.19-118 FLECHT SEASET Test 13914, Rod Surface Temperatures at 84 in

Figure 2.19-119 FLECHT SEASET Test 13914, Rod Surface Temperatures at 108 in

Figure 2.19-120 FLECHT SEASET Test 13914, Differential Pressure Between 72 in and 84 in

Figure 2.19-121 FLECHT SEASET Test 13914, Heat Transfer Coefficient

Figure 2.19-122 FLECHT SEASET Test 13914, Accumulated Water Mass in Test Section

Figure 2.19-123 FLECHT SEASET Test 13914, Total Liquid Carryover from Test Assembly

Figure 2.19-124 FLECHT Skewed Test 13914, Steam Temperatures at 84 in

2.20 RAI 20:

2.20.1 Statement of RAI 20

It is not clear that the proposed treatment of Generic Design Criteria (GDC)-35 will provide assurance that the sampled population reflects analyses of the limiting plant condition with respect to the availability of on- or off-site power. Provide examples to show that the current approach provides assurance of adequate plant capability in either condition stipulated by GDC-35, or propose an alternative approach to provide the requisite assurance.

2.20.2 Response to RAI 20

In the light of the changes to the statistical approach provided in the response to RAI 21 and the revised Section 9.4 of EMF-2103, Rev. 3, the response to the RAI 20 has also been revised to reflect the current approach and to [

] per discussions with the NRC staff.

[
]

In addition to the sections which describe the approach, Appendix B of EMF-2103 Revision 3, which describes the sample problems, will be updated correspondingly.

Table 2.20-1 Comparison of Limiting Values LOOP vs. No LOOP

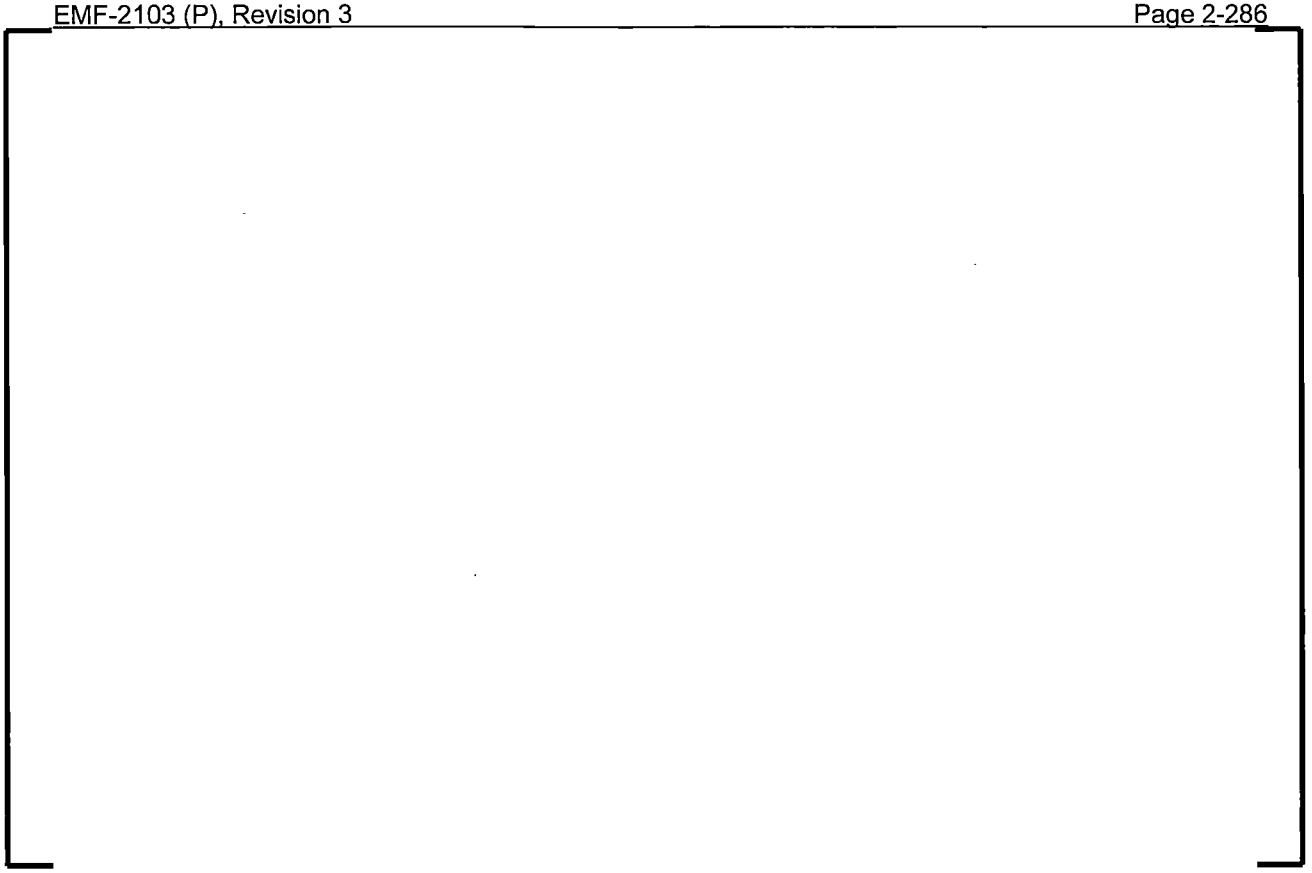

Figure 2.20-1 No LOOP versus LOOP Cases PCT Values

2.21 RAI 21:

2.21.1 Statement of RAI 21

Section 9.4.1, "Statistical Approach," of the TR explains the proposed statistical approach that would effectively collapse the three regulated parameters from Title 10 of the Code of Federal Regulations (10 CFR) 50.46 (b) (i.e., PCT, maximum local oxidation, and core-wide oxidation) into a single figure of merit (i.e., the ratio of the predicted value of the most limiting parameter to its regulatory limit). This single figure of merit would track with and hence indicate the intersection of the events that each of the three parameters is below its regulatory limit. Please address the following issues with this treatment:

A. The existing structure of 10 CFR 50.46 is based on an implicit understanding that licensees will calculate and maintain PCT, maximum local oxidation, and core-wide oxidation as individual figures of merit. These regulatory figures of merit may either be conservatively calculated per 10 CFR 50.46 (a)(1)(ii) and Appendix K to 10 CFR Part 50, or they may be realistically calculated values that reflect applicable uncertainties. However, the staff understood from audit discussions that, while AREVA's approach is proposed as a realistic or best-estimate EM, rather than attempting to compute a realistic figure of merit for each of the criteria in paragraph (b), it would instead appear to be a unique hybrid approach that would produce conservative upper bounds for two of the three parameters. Based upon examples presented during the audit, the staff further observed that (1) the resulting upper bounds for two of the three parameters could contain unrealistic conservatism, potentially well beyond the conservatism imposed by Appendix K, and (2) the calculation of these conservative upper bounds would essentially be divorced from the physical processes governing the behavior of the two bounded parameters.

   Considering that these observations appear contrary to the stated intent of the 1988 revision to 10 CFR 50.46 to permit realistic EMs that reasonably account for uncertainties, please identify whether the proposed approach would provide individual, realistic figures of merit for all three criteria from paragraph (b) of 10 CFR 50.46. If physically based, realistic figures of merit that appropriately reflect uncertainty will not be provided for all criteria in 10 CFR 50.46(b), please provide justification that the proposed approach complies with the regulation.

B. Please provide justification that the proposed figure(s) of merit for PCT, maximum local oxidation, and core-wide oxidation would be sufficient to satisfy the statistical requirements of 10 CFR 50.46. Inasmuch as the proposed statistical approach asserts that [ ] calculations would be sufficient to develop a first-order one-sided tolerance limit for three parameters with 95 percent probability coverage at a 95 percent confidence level (see EMF-2103P, Pages 9-54 and 9-55), please justify the use of terminology such as $PCT_{95/95}$, $MLO_{95/95}$, and $CWO_{95/95}$ (e.g., see EMF-2103P, page 9-49). Over the past 10 to 15 years, a number of authors have debated the required number of calculations to attain a target coverage and confidence level (e.g., 95/95) for multiple parameters at a given estimator grade (e.g., during the audit AREVA showed example calculations using the [ ]. For instance, consider the debate published in Reliability Engineering and System Safety between Guba, Makai, Pal (e.g., 80 (2003) 217-232); Orechwa (e.g., 87 (2005) 133-135); Nutt and Wallis (e.g., 83 (2004) 57-77), etc. In light of these conflicting viewpoints, please provide conclusive evidence that it would not be necessary to perform additional calculations to provide a realistic estimate of a one-sided tolerance limit for each of the three parameters treated separately at a 95 percent probability coverage at a 95 percent confidence level (rather than what AREVA considers to be a conservative upper bound for the upper tolerance limit for two of the parameters).

C. Consider the requirements specified in 10 CFR 50.46 (a)(3) concerning the estimation of the effect of changes or errors in the EM on the PCT and associated reporting requirements. As noted above, the proposed method would provide a realistic figure of merit only for the parameter with minimum margin to its regulatory limit, and conservative upper bounds for the two remaining parameters. Under existent regulations, this treatment would be of particular concern relative to the requirements of 10 CFR 50.46 (a)(3) when PCT is not the parameter with the least margin to its regulatory limit. However, in light of the proposed revision to 10 CFR 50.46, this case is not the only one of concern to the present review. Based on the above discussion, please address the following items:

   i. Please clarify how the effect of changes or errors in the EM would be estimated and tracked, particularly for the two parameters that would be conservatively bounded, and provide justification that the proposed method for estimating and tracking changes and errors complies with 10 CFR 50.46 (a)(3). In particular, please address whether it could become necessary to re-run the entire LOCA analysis to ensure that the limits of 10 CFR 50.46 (b) are satisfied each time there is a need to estimate the effect of a change or error in the EM.

ii. Please provide your interpretation as to how the reporting requirements of 10 CFR 50.46 (a)(3) would apply to the two parameters for which conservative upper bounds would be computed in lieu of realistic figures of merit. In this situation, changes or errors in the calculation of the bounded parameters could be masked by the proposed statistical treatment, even in cases where the magnitude of their effect would exceed a defined threshold of regulatory significance. For example, consider a scenario in which changes or errors result in an increase in peak cladding temperature from 1700 Degrees Fahrenheit (°F) to 1800 °F, while the maximum local oxidation remains constant at 0.14. In addressing this item, please recognize the substantially different weights associated with voluntary commitments, conditions and limitations in safety evaluations, and regulatory requirements.

iii. Please address how the reporting requirements in 10 CFR 50.46 (a)(3) would apply when changes or errors in the EM result in a change in which of the three regulated parameters in paragraph (b) has the least margin to its regulatory criterion. In principle, changes in which parameter has the least margin could perturb the calculated figure(s) of merit for the other two parameters in a manner not directly linked to the physics in the EM, thereby triggering the aforementioned reporting requirements. For example, consider a scenario in which changes or errors result in an increase in maximum local oxidation from 0.12 to 0.14, while the PCT remains constant at 1700 °F.

2.21.2 Response to RAI 21

This response is unchanged from the original response.

Table 2.21-1 Case Summary of Compliance with 10 CFR 50.46

[

]

Table 2.21-2 Characterization of 95/95 Set

[

]

[1] The other two references mentioned in the question focus their debate on an alternative method, titled bracketing method, proposed by Nutt and Wallis in Reference.2.21.7 and discussed in References 2.21.8 and 2.21.9. Since the bracketing method in question is not in consideration here, it is not discussed in our response.

[ ]

References:

2.21.1 AREVA Topical Report EMF-2103(P) Rev. 3, "Realistic Large Break LOCA Methodology for Pressurized Water Reactors," September 2013.

2.21.2 Guba A. et al., Statistical aspects of best estimate method - I, Reliability Engineering and System Safety 80 (2003) 217–232

2.21.3 Wald A., An Extension of Wilks' method for Setting Tolerance Limits, Annals of Mathematical Statistics 14 (1943) 45-55

2.21.4 Wallis G.B., Contribution to the paper 'Statistical aspects of best estimate method-1' by Attila Guba, Mihakly Makai, Lenard Pal, Reliability Engineering and System Safety 80 (2003) 309–311

2.21.5 Regulatory Guide 1.157, Best-Estimate Calculations of Emergency Core Cooling System Performance, U.S. NRC, 1989.

2.21.6 Makai M. and Pál L., Reply to contribution of Graham B. Wallis, Reliability Engineering and System Safety 80 (2003) 313–317

2.21.7 Nutt W.T. and Wallis G.B., Evaluation of nuclear safety from the outputs of computer codes in the presence of uncertainties, Reliability Engineering and System Safety 83 (2004) 57–77

2.21.8 Orechwa Y., Comments on 'Evaluation of nuclear safety from the outputs of computer codes in the presence of uncertainties' by W.T. Nutt and G.B. Wallis, Reliability Engineering and System Safety 87 (2005) 133–135

2.21.9 Wallis, G.B and Nutt W.T., Reply to "Comments on 'Evaluation of nuclear safety from the outputs of computer codes in the presence of uncertainties' by W.T. Nutt and G.B. Wallis," by Y. Orechwa, Reliability Engineering and System Safety 87 (2005) 137–145

2.21.10 Tukey J.W., Non-parametric Estimation II. Statistically Equivalent Blocks and Tolerance Regions – The Continuous Case, Annals of Mathematical Statistics 18 (1947) 529-539

2.21.11 Krishnamoorthy K. and Mathew T., Statistical Tolerance Regions: Theory, Applications and Computation, J. Wiley & Sons, 2009.

2.21.12 Wilks S.S., Determination of sample sizes for setting tolerance limits, Annals of Mathematical Statistics 12 (1941) 91-96

2.21.13 Code of Federal Regulations Title 10, Pt. 50.46, "Acceptance criteria for emergency core cooling systems for light-water nuclear power reactors."

2.21.3 Statement of Follow-Up to RAI 21

i. There remains a gap between the output of the method proposed by AREVA and the staff's interpretation of what the regulation requires. Specifically, the statistical method [

] , which may comply with the joint 95/95 standard; however, this [

]

AREVA separately intends to provide [

] , but these do not appear to be 95/95 values, and it is not clear what they represent statistically. This dichotomy has not been reconciled in the response, and it underlies the majority of the concerns held by the staff regarding the statistical methodology.

ii. The language regarding when a reanalysis would be necessary remains vague and AREVA's recommendation appears inconsistent with the regulatory threshold defined in 50.46.

iii. The responses do not appear to make a clear distinction as to what is legally required and how it is satisfied as opposed to what AREVA's policy would be. In some cases, the responses appear to pass responsibility to a choice of the licensee. But the issue here is that the regulation has reporting requirements, which the utility must meet – there is no choice involved and neither is AREVA a disinterested party. The role of the topical report and associated safety evaluation should be to provide a clear interpretation of the regulatory requirements so that the licensee can fulfill its regulatory obligation. Ultimately, it appears that AREVA is proposing reporting requirements that are based on values that do not appear to meet the 95/95 standard, and aren't necessarily satisfying any clear statistical standard.

2.21.4 Response to Follow-up on RAI 21

Table 2.21-3 Numerical Examples of Results for Hypothetical Top 10 Cases

[
]

Table 2.21-4 Numerical Examples of Ranked Results for Hypothetical Top 10 Cases

References:

2.21.14 AREVA Inc. Letter NRC-15-001, "Response to Request for Additional Information Regarding EMF-2103(P), Revision 3, 'PWR Realistic Large Break LOCA Methodology for Pressurized Water Reactors'," January 16, 2015.

2.22 RAI 22:

2.22.1 Statement of RAI 22

Section 9.4.1, "Statistical Approach," of the TR describes contingency actions to address the potential that the results of the statistical evaluation could exhibit evidence of exceeding regulatory limits. The TR suggests remedies including "a reduction in conservative assumptions" and indicates that the set of statistical simulations will be rerun with new random seeds supplied to the randomized parameters and with an increased number of cases to support the determination of a tolerance interval from a higher-order nonparametric estimator. Please clarify the following information:

A. Please elaborate on and provide examples of the conservative assumptions that may be relaxed by the methodology following a calculated exceedance of regulatory criteria. In particular, the NRC staff understands certain aspects of the proposed EM to be approved *in toto* and further expects the approach to be generally based on realistic or best-estimate modeling.

B. Please justify the stated procedure of generating new random seeds and rerunning calculations with a higher-grade nonparametric estimator. In particular, it is necessary that the calculational procedure contain adequate controls to minimize the potential for rejecting random outcomes demonstrating that regulatory criteria are not satisfied, making non-substantive or insufficient changes to the inputs to the analysis, rerunning statistical simulations, and passing largely on the basis of reshuffling the random numbers used to seed the key analytical parameters rather than the substance of the changes made to the input deck. As such, what process and procedural controls will exist to assure that the substantive effect of changes made to the input deck following a set of unsuccessful statistical simulations is sufficient to justify an *a priori* expectation that a subsequent set of statistical simulations will be successful?

2.22.2 Statement of Follow-up on RAI 22

i. It appears in general that the conservative assumptions that may be relaxed are plant parameters that are in essence constraints on operation that must be satisfied for the analysis to be valid. Exceptions are noted with regard to [

] . Need to confirm understanding, especially concerning [ ] and the process AREVA believes it would be in when making such changes to the evaluation method.

ii. The response discusses an option for [ ] A couple of issues with this statement. First, no criteria are given as to how [ ] is defined. Second, allowing the analyst the option to [ ] introduces selection bias. Third, no specific [ ] was identified. As a result, it appears that the ostensible 95/95 standard would be unattainable via the proposed process. It is further not clear what AREVA means in discussing [ ] For example, if we are considering a [ ] ? And, if a number of values [ ] , in what sense is it reasonable to consider [ ] ? Alternately, if the [ ] is defined based on the [ ] , then why should this approach be justified, as the [ ] ? Recall that we are sampling from an unknown distribution and considering a small subset of the sampled data; determination of what is and what is not [ ] is very much open to subjective interpretation.

2.22.3 Response to RAI 22

Only the AREVA revised response is provided as it is a complete replacement to the response previously provided for the original RAI Question 22.

[
]

2.23 RAI 23:

2.23.1 Statement of RAI 23

The fidelity of statistical conclusions resulting from each plant-specific analysis depends, not only on the final simulation(s) traditionally used to demonstrate that the computed figures of merit comply with regulatory criteria, but also on the integrity of the process used to generate the results. In particular, for the final statistical conclusion of regulatory compliance to be valid, it would appear necessary for the analyst(s) to certify that the computed regulatory figures of merit are the result of a process that is unbiased and representative (e.g., not the result of flipping coins or rolling dice until a favorable conclusion occurs) and create auditable records capable of supporting this conclusion. Auditable records should include, not only (1) the results of the final, successful simulations, but also (2) any statistical simulations that have been performed that did not satisfy one or more acceptance criteria, (3) a description of the changes made to the input deck/EM to support the success of subsequent statistical calculations, and (4) adequate justification that the changes implemented in support of the successful simulations carried a legitimate *a priori* expectation of satisfying regulatory requirements. In light of the discussion above, please address the following requests:

A. Discuss whether calculational procedures clearly define delineation point(s) between preliminary non-statistical scoping calculations and statistical calculations of record and provide justification if not,

B. Describe procedural requirements that would be in effect for conducting, logging, and documenting all statistical calculations for a particular plant, including any statistical calculations that did not satisfy regulatory criteria,

C. Provide justification that the process for conducting, logging, and documenting statistical calculations is sufficient to demonstrate that unbiased and representative statistical conclusions can be made regarding regulatory compliance,

D. Describe and provide justification for the level of information that will be included in plant-specific applications submitted to the NRC concerning initial statistical calculations that did not satisfy regulatory criteria and the changes made to the EM to support satisfaction of regulatory criteria in subsequent statistical calculations, and

E. Discuss whether analysts will be required to certify, not only that they concur on the final plant-specific calculations applying the proposed EM, but further, that they affirm that the calculated results derive from a statistically representative calculational process that was executed in an unbiased manner.

2.23.2 Follow-up on RAI 23

Staff considers a number of the proposals discussed in the responses reasonable. However, several issues remain, including:

A. [ ] Need to discuss further to ensure common understanding. What the customer requests appears somewhat extraneous in that an acceptable method should specify controls that preclude customer requests from violating either the physical or statistical integrity of the method. This is exactly what the RAI was seeking to establish, regardless of the origin of the change request.

B. Clarify what is meant by "intermediate calculations." Appears to be calculations that were intended to be final calcs, but which were subsequently revised further and hence ended up not being the final analysis. Understand the documentation that will be provided in plant-specific submittals in this regard. A reviewer should be able to determine the number of intermediate iterations and gauge whether changes made to inputs for intermediate calculations were substantive and carried a legitimate *a priori* expectation of success. Unlike Appendix K, the integrity of the process is important, rather than just the final analysis of record.

C. Not clear why [ ] Again, the potential for selection bias is introduced – note in particular, the response says "can… only" and not "must". Also, the linkage between the [ ] cannot be understood. As such, the option (or even if it were specified as a requirement) for choosing [ ] seems a disconnected and unnecessary complexity.

D. The statement to be added to Appendix A appears narrow and may not adequately capture all concerns regarding statistical fidelity raised by the staff.

2.23.3 Response to RAI 23

This revised response fully replaces the previous response to RAI 23. The revised response, based on NRC reviewer comments, for RAI 23 is presented below.

[

]

References:

[

]

2.24 Self-Initiated RAI 24:

2.24.1 Statement of RAI 24

Please provide justification for the use of 150 psia as an upper limit for pressure in Equation 7.540.

2.24.2 Response to RAI 24

This response is unchanged from the original response.

Background:

The Thermal-Hydraulic Test Facility (THTF) mixture level swell tests benchmarks reported in Section 8.2.1 of Reference 2.24.1 was originally used to validate the interphase drag model only, by comparing the axial void profile for these tests. Figure 8.2-10 through Figure 8.2-12 in Reference 2.24.1 show the results for Tests 3.09.10j, 3.09.10m, and 3.09.10dd, respectively. In the wall to vapor radiation heat transfer described in Section 7.6.8.1 of Reference 2.24.1, the correlation for vapor absorption coefficient is given by Equation 7.540, and it was taken from the FLECHT-SEASET data evaluation report (Equation 6-6, Reference 7-188 in Reference 2.24.1). It was found that this correlation over-predicts the vapor absorptivity at higher pressures. [

] The THTF level swell tests were rerun, and it was found that S-RELAP5, with this pressure limit, predicts proper cladding thermal responses above the mixture level. The technical basis for this pressure upper limit and the results for the revised THTF level swell benchmarks are discussed below.

Technical Basis:

[
]

[

]

Re-benchmark of THTF Level Swell Tests:

THTF Level Swell Tests 3.09.10j and 3.09.10m were rerun using [

] respectively. Test 3.09.10dd was not re-run because in this test the mixture level was almost near the top of the bundle. The following plots show the axial void profile, vapor temperature, and rod surface temperatures for the two tests. As expected, the pressure limit has no effect on the void profiles shown in Figure 2.24-1 and Figure 2.24-2, and the results are the same as that given in Section 8.2.1 of Reference 2.24.1. Figure 2.24-3 and Figure 2.24-4 show S-RELAP5 calculated steam temperatures are slightly higher than the data and have no effect of the pressure limit, because both tests are steady-state tests. Figure 2.24-5 and Figure 2.24-6 show that S-RELAP5 calculated rod surface temperatures above the mixture level are closer to data when [

]

Summary:

S-RELAP5, with [ ] in Equation 7.540, will calculate proper wall to steam radiation heat transfer. Sections 2.3, 7.6.8.1, 8.1.5, and 8.2.1.6 of Reference 2.24.1 will be updated to reflect the changes due to this RAI response

Figure 2.24-1 Measured and Predicted Void Fraction: THTF Test 3.09.10j

Figure 2.24-2 Measured and Predicted Void Fraction: THTF Test 3.09.10m

Figure 2.24-3 Measured and Predicted Vapor Temperature: THTF Test 3.09.10j

Figure 2.24-4 Measured and Predicted Vapor Temperature: THTF Test 3.09.10m

Figure 2.24-5 Measured and Predicted Rod Surface Temperature: THTF Test 3.09.10j

Figure 2.24-6 Measured and Predicted Rod Surface Temperature: THTF Test 3.09.10m

References:

2.24.1 AREVA Topical Report EMF-2103(P) Rev. 3, "Realistic Large Break LOCA Methodology for Pressurized Water Reactors," September 2013.

2.24.2 C. L.Tien, "Thermal Radiation Properties of Gases," in T.F. Irvine Jr., and J. P. Hartnett: (eds), "Advances in Heat Transfer," vol. 5, pp. 253-324, Academic Press Inc., New York, 1968.

2.24.3 H. C. Hottel and A. F. Sarofim, "Radiative Heat Transfer," McGraw Hill Book Company, New York, St. Louis, San Francisco, Toronto, London, Sydney, 1967.

2.24.4 J. W. Spore, et al., "TRAC-BD1/MOD1: An Advanced Best Estimate Computer Program for Boiling Water Reactor Loss-of-Coolant Accident Analysis, Volume 1: Model Description," NUREG/CR-3633(EGG-2294), April 1984.

2.24.5 J. W. Spore, M. M. Giles and R. W. Shumway, "A Best Estimate Radiation Heat Transfer Model Developed for TRAC-BD1," ASME Publication 81-HT-68 for the 20th Joint ASME/AIChE National Heat Transfer Conference, Milwaukee, Wisconsin, August 2-5, 1981.

2.24.6 R. Siegel and J. R. Howell, "Thermal Radiation Heat Transfer," Hemisphere Publishing Corporation, Second Edition, 1981.

2.24.7 M. M. Abu-Romia, and C. L. Tien, "Appropriate Mean Absorption Coefficients for Infrared Radiation of Gases," ASME J. of Heat Transfer Vol. 89, November 1967, pp. 321-327.

2.24.8 S. Yao, L.E. Hochreiter and C. E. Dodge, "A Simple Method for Calculating Radiative Heat Transfer in Rod Bundles with Droplet and Vapor as Absorbing Media," ASME J. of Heat Transfer, Vol. 101, November 1979, pp. 736-739.

2.24.9 D. E. Burch, E. B. Singleton, and D. Williams, "Absorption Line Broadening in the Infrared," Appl. Opt., Vol. 1, No. 3, pp. 359-363, 1962.

2.24.10 D.K. Edwards, "On the Use of Total Radiation Properties of Gases," ANL/RAS 75-12, April 1975.

2.24.11 S. S. Penner, "Quantitative Molecular Spectroscopy and Gas Emissivities," Addison-Wesley Publishing Company Inc., Reading, Massachusetts, USA.

2.25 Self-Initiated RAI 25:

2.25.1 Statement of RAI 25

Please describe whether or not there is an upper limit to the calculation of the rupture node vapor temperature, T_g*, used in the [

]

2.25.2 Response to RAI 25

This response is unchanged from the original response.

[

]

Reference:

2.25.1 AREVA Topical Report EMF-2103(P) Rev. 3, "Realistic Large Break LOCA Methodology for Pressurized Water Reactors," September 2013.

Table 2.25-1 Overall Case PCT Comparison with and without T_g* Limitation

[
]

Figure 2.25-1 W3 Case 039 – Limited T_g* Case vs. Sample Problem

Figure 2.25-2 W4 Case 138 – Limited T_g* Case vs. Sample Problem

Figure 2.25-3 CE Case 065 – Limited T_g* Case vs. Sample Problem

2.26 Self-Initiated RAI 26:

2.26.1 Statement of RAI 26

Please describe the random number generator, as well as the seeding process, documented in Sections A.2.3.3 and A.2.3.5.

2.26.2 Response to RAI 26

This response is unchanged from the original response.

The initial automation calculations used for EMF-2103, Rev. 3 (Reference 2.26.1) used the Linux workstation system functions srand48() and drand48() to generate the pseudo-random numbers for the uncertainty analysis as described in Section A.2.3.3 in Reference 2.26.1.

The previous seeding process created a list of initial seeds (one for each case) and that seed fed the srand48() function. It was determined that although unlikely, there was a slight possibility that the same case could be repeated in a given case set if one was to reseed the pseudo-random number generator in this fashion. The probability of this occurrence is estimated at approximately 1/300,000.

To improve the randomness and prevent the possibility of a repeated case within a given RLBLOCA case set, three improvements have been made:

[

]

Additional procedural requirements and discussions are detailed in the response to RAI Question 23.

The text in Sections A.2.3.3 and A.2.3.5 of EMF-2103, Revision 3 (Reference 2.26.1) will be revised to reflect this improvement.

References:

2.26.1 AREVA Topical Report EMF-2103(P) Rev. 3, "Realistic Large Break LOCA Methodology for Pressurized Water Reactors," September 2013.

2.27 RAI 27:

2.27.1 Statement of RAI 27

Provide additional information to justify the sampling range for the [ ], as defined in Section 7.9.3.3.1 of EMF-2103P, Revision 3. Based on the U.S. Nuclear Regulatory Commission (NRC) staff review of the database supporting the correlation to which this parameter is applied, it would appear that the sampling range provided in the topical report should be doubled to provide better coverage of the available data.

2.27.2 Response to RAI 27

[
]

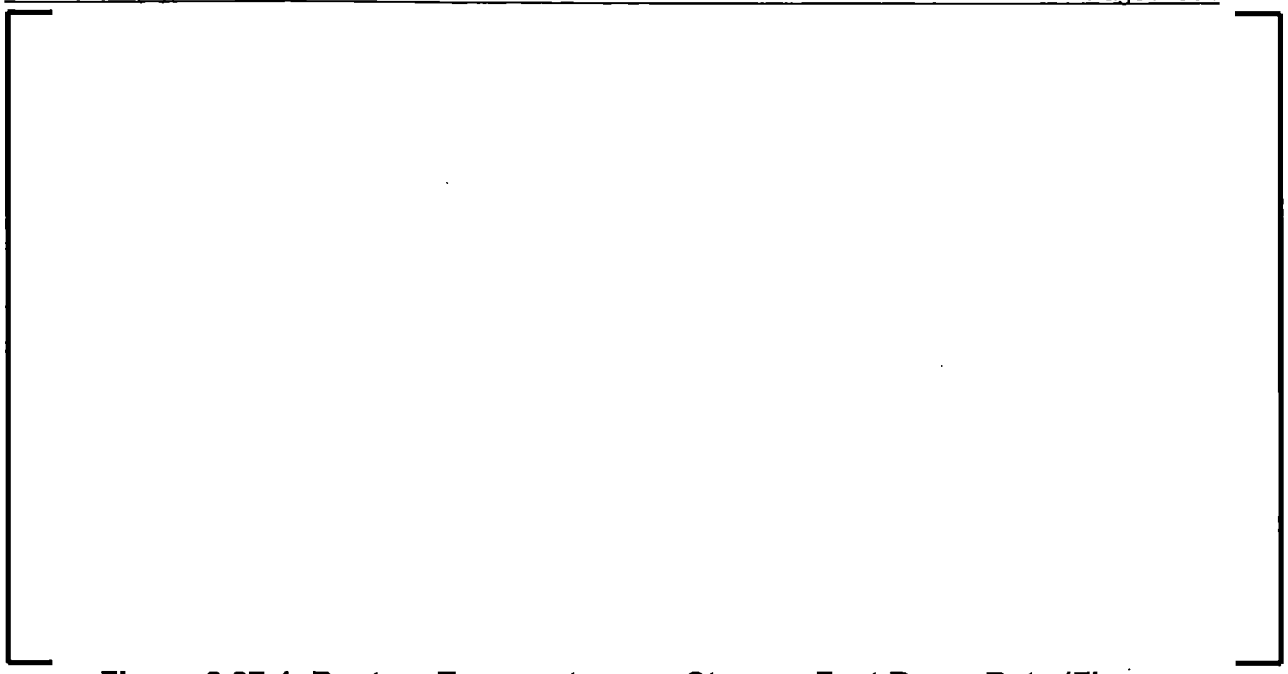

Figure 2.27-1 Rupture Temperature vs. Stress – Fast Ramp Rate (Fig. 2, Ref. 2.27.1)

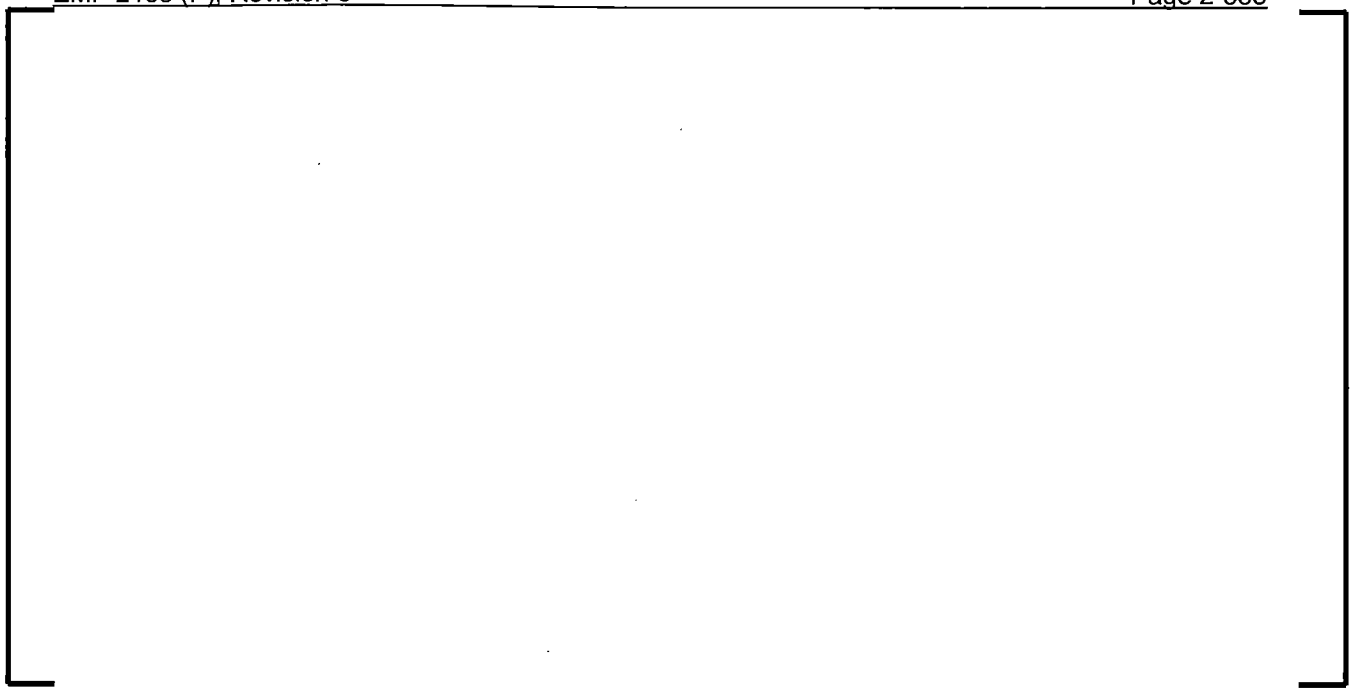

Figure 2.27-2 Rupture Temperature vs. Stress – Various Ramp Rates (Fig. 3, Ref. 2.27.1)

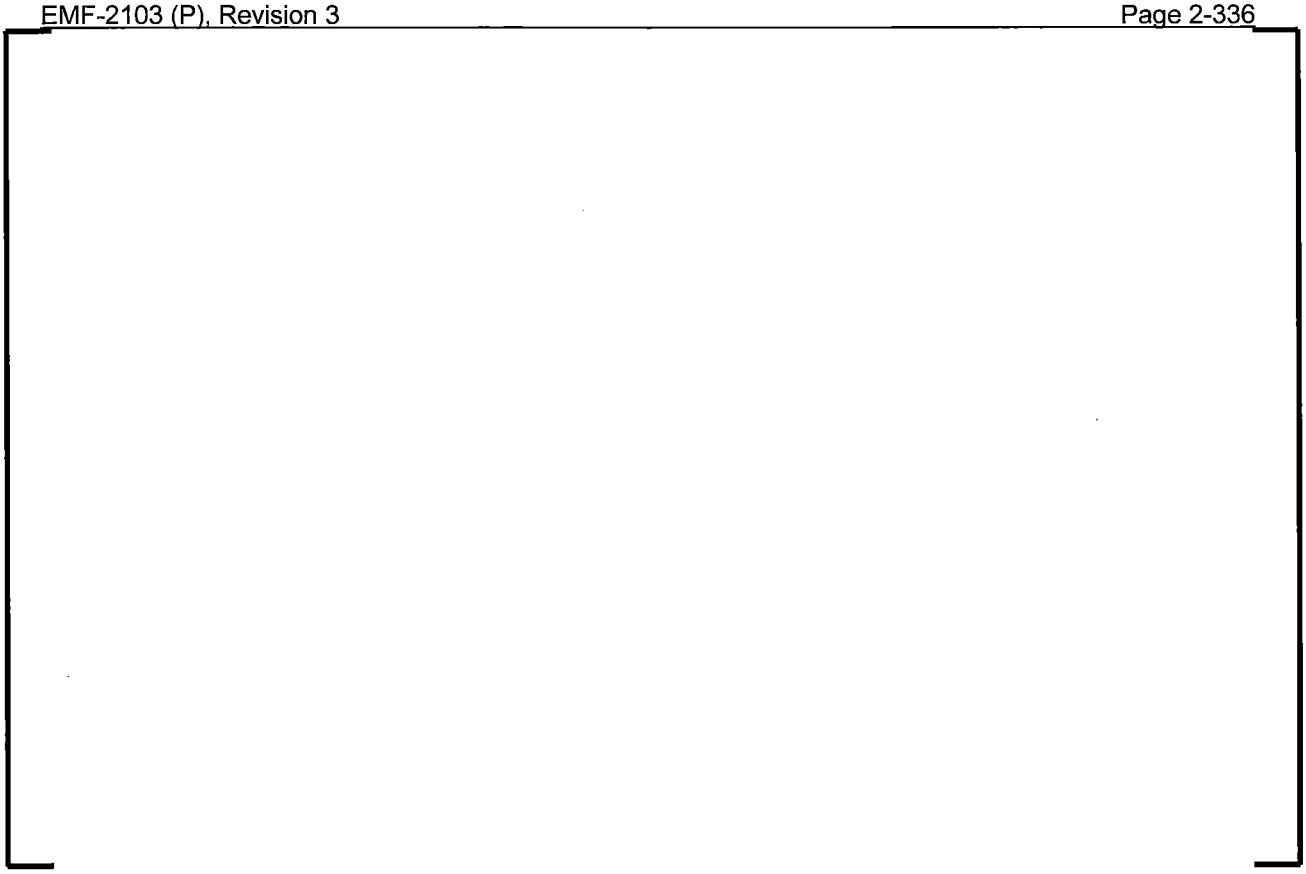

Figure 2.27-3 Rupture Temperature vs. Stress – Slow Ramp Rate (Fig. K-5.11, Ref. 2.27.2)

Figure 2.27-4 Rupture Temperature vs. Stress – Fast Ramp Rate (Fig. K-5.12, Ref. 2.27.2)

References:

2.27.1 NUREG-0630, "Cladding Swelling and Rupture Models for LOCA Analysis," D.A. Powers and R.O. Meyers, US NRC, Washington DC, April 1980.

2.27.2 AREVA Topical Report BAW-10227P-A, Rev. 1, "Evaluation of Advanced Cladding and Structural Material (M5) in PWR Reactor Fuel," June 2003.

2.27.3 AREVA Topical Report EMF-2103(P) Rev. 3, "Realistic Large Break LOCA Methodology for Pressurized Water Reactors," September 2013.

2.28 RAI 28:

2.28.1 Statement of RAI 28

Justify the approach for treating uncertainty in the [ ]
Show that treating the [ ] is appropriate in light of the data used to develop [ ]. Consider alternative statistical distributions and include goodness-of-fit analyses, and as justification for use of a [ ], explain why added numerical dispersion at both tails of the actual distribution introduces conservatism.

2.28.2 Response to RAI 28

[
]

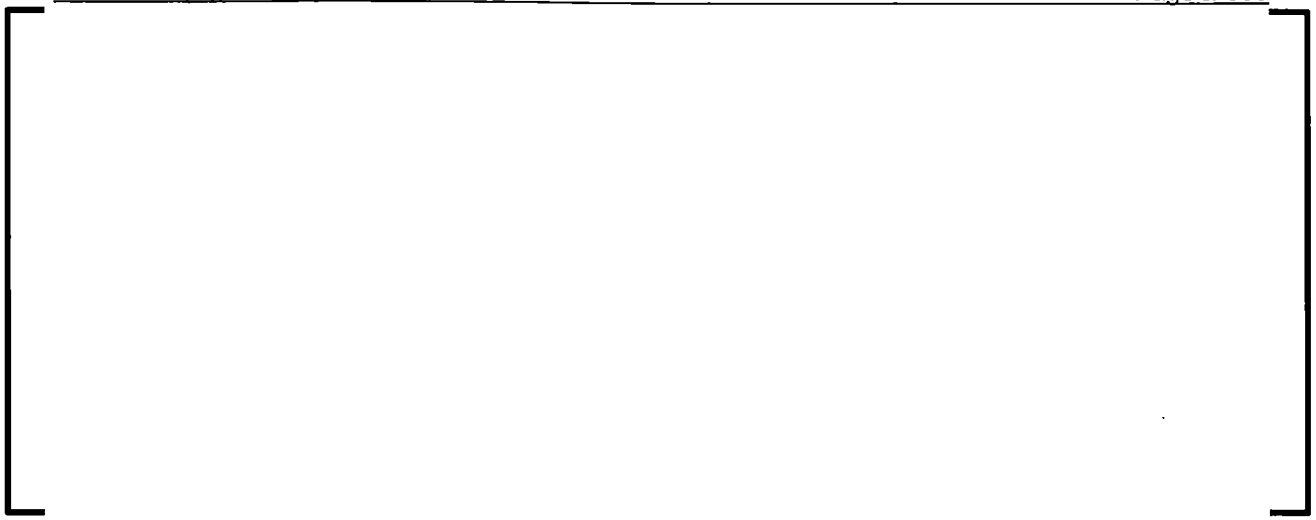

Figure 2.28-1 Circumferential Strain vs. Rupture Temperature (Fig. 4 of Ref. 2.28.2)

Figure 2.28-2 M5 Slow Ramp Correlations with Supporting Rupture Strain Data (Figure 8.5-6 of Ref. 2.28.1)

Figure 2.28-3 M5 Fast Ramp Correlations with Supporting Rupture Strain Data (Figure 8.5-7 of Ref. 2.28.1)

Table 2.28-1 Case Summary – W3 Sample Problem (PCT Rod)

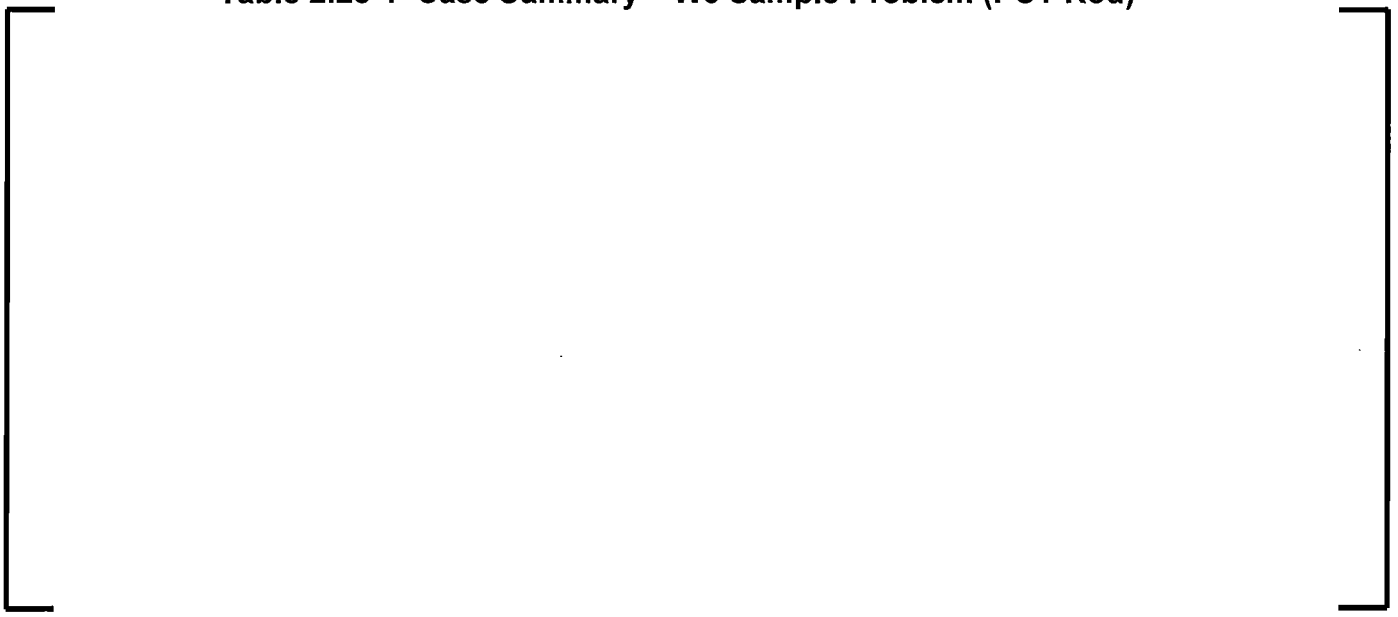

Table 2.28-2 Results of Sensitivity Study (PCT Rod)

Figure 2.28-4 [ ]

References:

2.28.1 AREVA Topical Report EMF-2103(P) Rev. 3, "Realistic Large Break LOCA Methodology for Pressurized Water Reactors," September 2013.

2.28.2 NUREG-0630, "Cladding Swelling and Rupture Models for LOCA Analysis," D.A. Powers and R.O. Meyers, US NRC, Washington DC, April 1980.

2.28.3 NUREG/CR-5249, "Quantifying Reactor Safety Margins, Application of Code Scaling, Applicability, and Uncertainty Evaluation Methodology to a Large Break, Loss-of-Coolant Accident," December 1989.

2.28.4 Letter, Pedro Salas (AREVA Inc.) to Document Control Desk (NRC), "Errata and Revised Sample Problems for EMF-2103P, Revision 3, 'Realistic Large Break LOCA Methodology for Pressurized Water Reactors'," NRC:15:005, January 16, 2015.

2.29 RAI 29:

2.29.1 Statement of RAI 29

Provide a brief explanation of the treatment of [ ] for cases where the [ ] On what basis does AREVA NP, Inc. (AREVA) conclude that this model replicates observed [ ] behavior?

2.29.2 Response to RAI 29

[
]

Figure 2.29-1 Maximum Diametrical Expansion vs. Temperature (Ref. 2.29.1)

[ ]

References:

2.29.1 D. G. Hardy (AECL), "High Temperature Expansion and Rupture Behavior of Zircaloy Tubing", Topical Meeting on Water-Reactor Safety, Salt Lake City, Utah, Sponsored by American Nuclear Society; March 1973.

2.30 RAI 30:

2.30.1 Statement of RAI 30

Provide an explanation for the collection of [ ] data as documented in BAW-10227P-A. The M5 LTR appears to contain little justification or explanation concerning the concept that [ ], especially given that, as shown in NUREG-2160, rupture shape and size tends to be somewhat stochastic.

2.30.2 Response to RAI 30

[
]

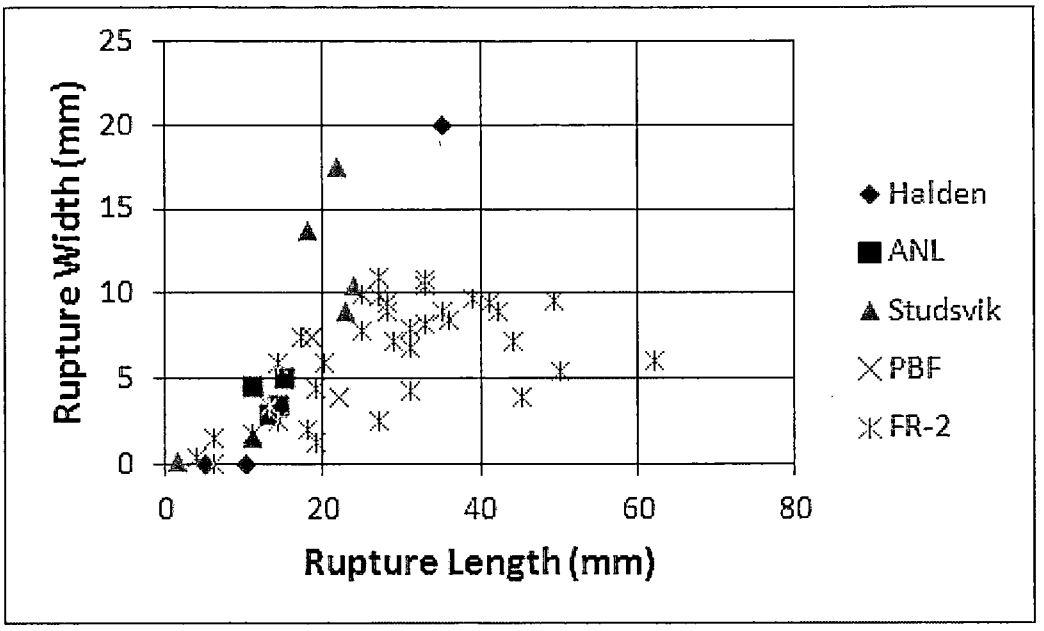

Figure 2.30-1 Rupture Width vs. Rupture Length (Figure 4-56 of Ref. 2.30.2)

[ ]

References:

2.30.1 NUREG-2160, "Post Test Examination Results from Integral, High-Burnup, Fueled LOCA Tests at Studsvik Nuclear Laboratory," Michelle E. Flanagan, US NRC, Rockville, MD, August 2013.

2.30.2 NUREG-2121, "Fuel Fragmentation, Relocation, and Dispersal during the Loss-of-Coolant Accident," Patrick A. C. Raynaud, US NRC, Rockville, MD, March 2012.

2.30.3 AREVA Topical Report BAW-10227P-A, Rev. 1, "Evaluation of Advanced Cladding and Structural Material (M5) in PWR Reactor Fuel," June 2003.

2.31 RAI 31:

2.31.1 Statement of RAI 31

Provide a general description of the way the fuel clad swelling model is implemented in the axial (z) direction.

2.31.2 Response to RAI 31

[
]

[ ]

Figure 2.31-1 Schematic of Liquid Droplet Distribution around a Blockage during an ACHILLES Reflood Test (Fig. 10 in Reference 2.31.8)

Figure 2.31-2 Cladding Temperature and Internal Rod Pressure of a Burst Rod in REBEKA-6 Test (Figs. 7 and 8 in Reference 2.31.9)

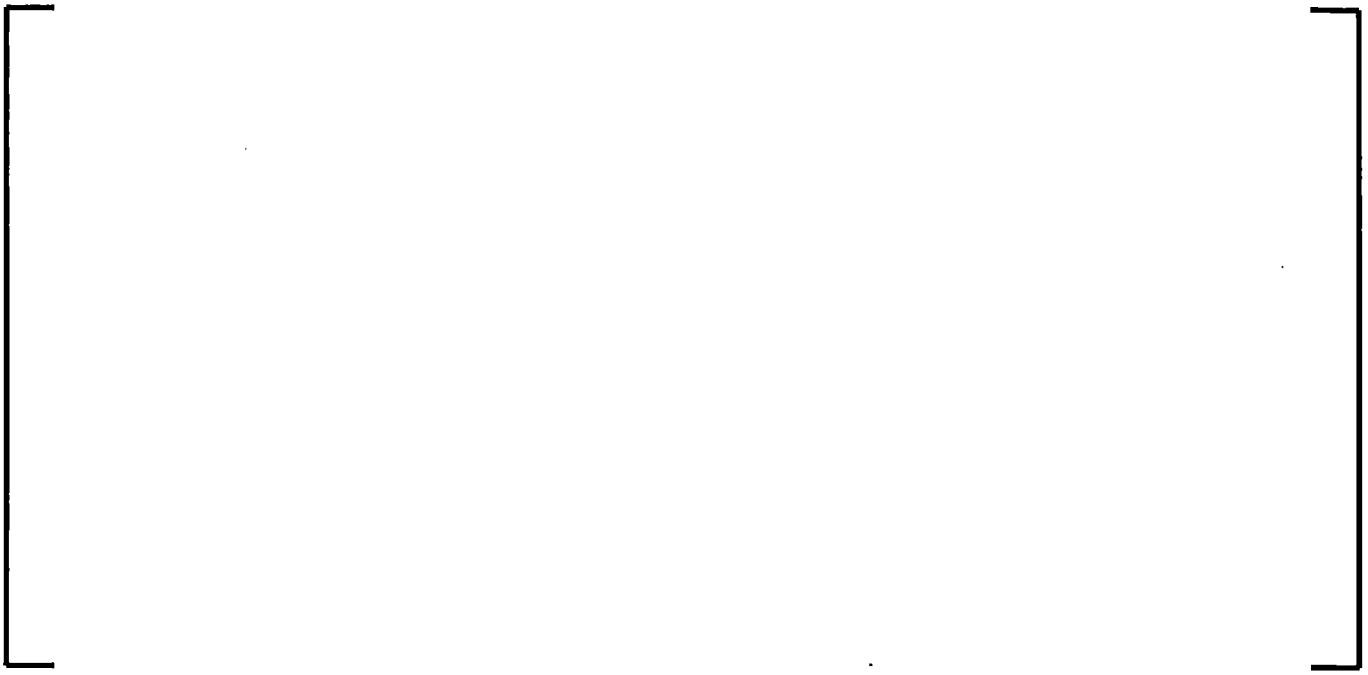

Figure 2.31-3 Temperature and Pressure Transients of REBEKA-7 Rod Bundle (70% Blockage) (Fig. 13 in Reference 2.31.3)

Figure 2.31-4 Burst Strain vs. Azimuthal Temperature Difference (Fig.9 in Reference 2.31.3)

References:

2.31.1 Chapman, R. H., Crowley, J. L., and Longest, A. W.,"Effect of Bundle Size on Cladding Deformation in LOCA Simulation Tests," Zirconium in the Nuclear Industry: Sixth International Symposium, ASTM STP 824, pp. 693-708, 1984.

2.31.2 NUREG/CR-103, ORNL/NUREG/TM-200, "Multirod Burst Test Program Progress Report for July-December 1997," US Nuclear Regulatory Commission, Washington DC.

2.31.3 F. J. Erbacher, H. J. Neitzel, K. Wiehr, "Cladding Deformation and Emergency Core Cooling of a Pressurized Water Reactor in a LOCA," Summary Description of the REBEKA Program, KfK 4781, August 1990.

2.31.4 K. Wiehr, and U.Harten, "Datenericht REBEKA-6," KfK 3986, March 1986.

2.31.5 K. Wiehr, "REBEKA-Bundelversuche Untersuchungen zur Wechselwirkung zwischen aufblahenden Zircaloyhullen und einsetzender Kernnotkuhlung," KfK 4407, Mai 1998.

2.31.6 P. Ihle, and K. Rust, "FEBA – Flooding Experiments with Blocked Arrays Evaluation Report," KfK 3657, March 1984.

2.31.7 Fairbairin, F. A, and Piggott, B. D. G.,"Studies on the Effects of Blockage Upon LWR Emergency Core Cooling Systems," Proceedings of a Seminar on the Results of the European Communities' Indirect Action Research Programme on Safety of Thermal Water Reactors held in Brussels, October 1-3, 1984.

2.31.8 P. Dore, and K.G. Pearson, "ACHILLES Ballooned Cluster Experiments," AEEW-2590, July 1991.

2.31.9 F. J. Erbacher, P.Ihle, K. Rust, and K. Wiehr, "Temperature and Quenching behavior of Undeformed, Ballooned and Burst Fuel Rods in a LOCA," Fifth International Meeting on Thermal Nuclear Reactor Safety, Held in Karlsruhe, FRG, September 9-13, 1984.

2.31.10 AREVA Topical Report EMF-2103(P), "Realistic Large Break LOCA Methodology for Pressurized Water Reactors," September 2013.

2.31.11 Letter, Pedro Salas (AREVA Inc.) to Document Control Desk (NRC), "Errata and Revised Sample Problems for EMF-2103P, Revision 3, 'Realistic Large Break LOCA Methodology for Pressurized Water Reactors'," NRC:15:005, January 16, 2015.

2.31.12 AREVA Topical Report, BAW-10227P-A, Rev. 1 "Evaluation of Advanced Cladding and Structural Material (M5) in PWR Reactor Fuel," June 2003.

2.32 RAI 32:

2.32.1 Statement of RAI 32

Explain whether the same models described in the discussion about fuel rod swelling, rupture and relocation are the same as those used to [

] . This discussion could be well informed with a cartoon of the model as implemented for a severely strained section of fuel.

2.32.2 Response to RAI 32

[
]

References:

2.32.1 AREVA Topical Report EMF-2103(P) Rev. 3, "Realistic Large Break LOCA Methodology for Pressurized Water Reactors," September 2013.

2.32.2 Letter, Pedro Salas (AREVA Inc.) to Document Control Desk (NRC), "Errata and Revised Sample Problems for EMF-2103P, Revision 3, 'Realistic Large Break LOCA Methodology for Pressurized Water Reactors'," NRC:15:005, January 16, 2015.

2.32.3 P. Dore, K.G. Pearson, "ACHILLES Ballooned Cluster Experiments," AEEW-2590, July 1991.

2.33 Self-Initiated RAI 33:

2.33.1 Statement of RAI 33

Please provide a justification for the change in the constant multiplier for Equation 7.540 in the EMF-2103(P) Revision 3 Topical Report.

2.33.2 Response to RAI 33

[ ]

References:

2.33.1 AREVA Topical Report EMF-2103(P), Revision 3, "Realistic Large Break LOCA Methodology for Pressurized Water Reactors," September 2013.

2.33.2 Framatome ANP, Inc. Topical Report EMF-2103(P)(A), Revision 0, "Realistic Large Break LOCA Methodology for Pressurized Water Reactors (TAC No. MB7554)," April, 2003.

2.33.3 AREVA Topical Report EMF-2100(P), Revision 4, "S-RELAP5 Models and Correlations Code Manual", January 2001.

2.33.4 AREVA Topical Report, BAW-10166PA-05, "BEACH: Best Estimate Analysis Core Heat Transfer - A Computer Program for Reflood Heat Transfer Analysis During LOCA", November 2003.

2.34 Self-Initiated RAI 34:

2.34.1 Statement of RAI 34

Please provide a summary of the modifications made to the interfacial drag model as part of the EMF-2103(P), Revision 3 methodology.

2.34.2 Response to RAI 34

Two-phase flow regimes and the associated interphase drag and heat transfer play an important role in the core thermal response during a large-break LOCA in a PWR. A schematic of the flow and heat transfer regimes during reflood is shown in Figure 6.4-3 of Reference 2.34.1 and is shown below as Figure 2.34-1. These regimes cover a broad spectrum of conditions. During the reflood phase, a spectrum of droplets exists in the upper region of the bundle, which is created by a complicated thermal-hydraulic process that occurs near the quench front. Ishii and De Jarlais (Reference 2.34.2) discuss in detail various flow regimes and the flow regime transition criteria. Various flow regimes that can exist in the boiling channel in the pre-CHF region and the flow regime transition criteria developed by various researchers are shown in Figure 1 from Reference 2.34.2. This figure is shown below as Figure 2.34-2.

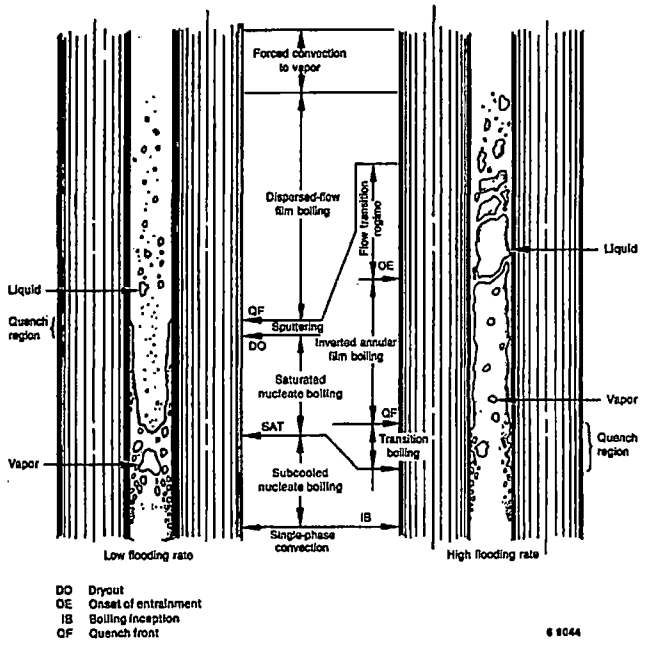

Figure 2.34-1 Flow and Heat Transfer Regimes during Reflood

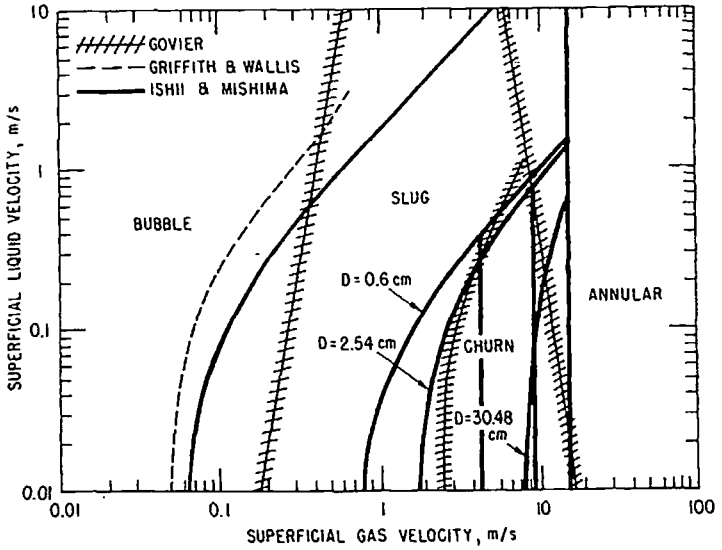

Figure 2.34-2 Wet Wall Flow Regime Map (Figure 1 in Reference 2.34.2)

Technical Evaluation

[
]

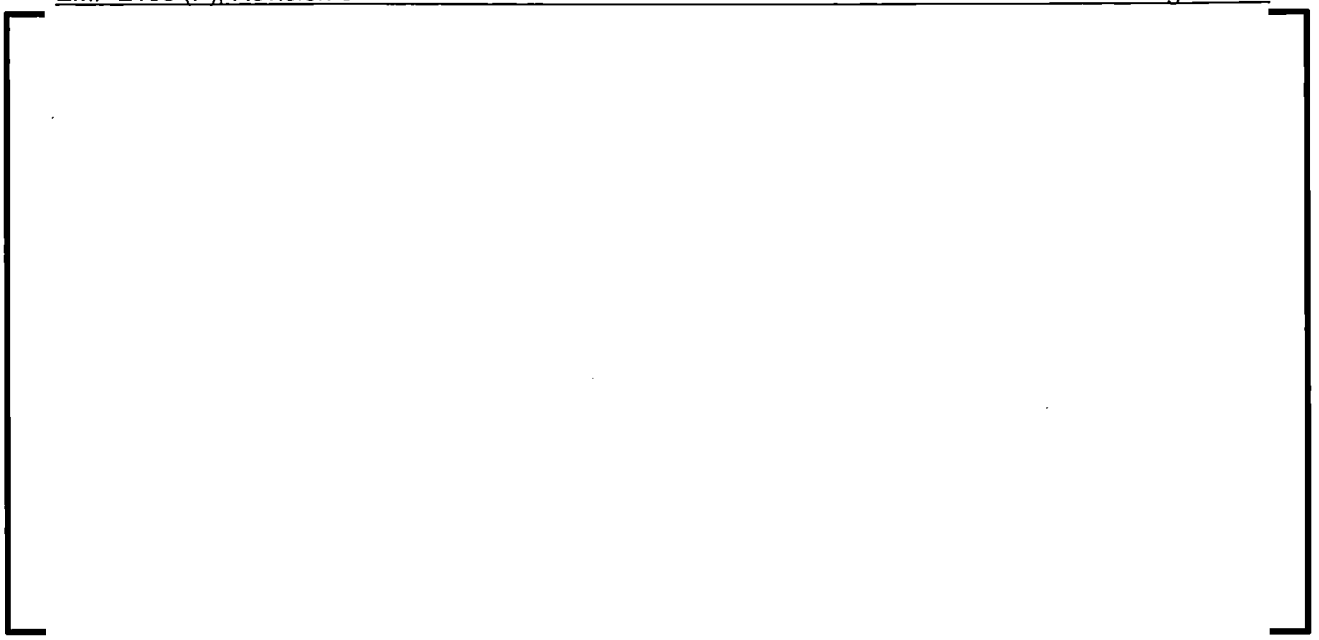

Figure 2.34-3 Vertical Flow Regime Map with Hatches Indicating Transition Regions

Table 2.34-1 FILMBL and DFFBHTC Heat Transfer Multipliers

[ ]

EMF-2103, Revision 3 Drag Changes (Section 7.5.2 in Reference 2.34.3)

[ ]

Maximum droplet diameter limit in the inverted annular flow regime

[ ]

Interphase shape factor (S_F) modification

The minimum number of particles per unit volume, N_p in the mist flow regime

Slug Flow Regime Drag Changes (Section 7.5.2.2 in Reference 2.34.3)

Figure 2.34-4 Combined FRIGG-2, FRIGG-3 and KATHY Void Distribution Tests Calculated Minus Measured Void Fraction

Junction Interphase Drag Modification (Section 7.5.2.7 in Reference 2.34.3)

[ ]

References:

2.34.1 NUREG-1230 R4, U.S. NRC, "The Compendium of ECCS Research for Realistic LOCA Analysis," December 1988.

2.34.2 M. Ishii and G. De Jarlais, "Flow Regime Transition and Interfacial Characteristics of Inverted Annular Flow," Nuclear Engineering and Design, **95**, pp. 171-184, 1986.

2.34.3 AREVA Topical Report EMF-2103(P), Revision 3, "Realistic Large Break LOCA Methodology for Pressurized Water Reactors," September 2013.

2.34.4 Framatome ANP, Inc. Topical Report EMF-2103(P)(A), Revision 0, "Realistic Large Break LOCA Methodology for Pressurized Water Reactors (TAC No. MB7554)," April 2003.

2.34.5 AREVA Topical Report EMF-2100(P), Revision 4, "S-RELAP5 Models and Correlations Code Manual", January 2001.

2.35 Self-Initiated RAI 35:

2.35.1 Statement of RAI 35

Please verify the FILMBL and DFFBHTC heat transfer multipliers used in the benchmarks in Sections 8.2 – 8.5 of the EMF-2103(P), Revision 3 Topical Report.

2.35.2 Response to RAI 35

Section 8.4.1 of EMF-2103(P), Revision 3 (Reference 2.35.1) discusses the determination of the FILMBL and DFFBHTC heat transfer multipliers and PDF of the multipliers developed with the EMF-2103(P), Revision 2 (Reference 2.35.2) methodology. Table 8.5-4 of Reference 2.35.1 provides the FILMBL and DFFBHTC multiplier values used for the benchmark cases discussed in Section 8.2 and Section 8.3 of Reference 2.35.1. Table 8.5-5 and Table 8.5-6 of Reference 2.35.1 give the PDF of FILMBL and DFFBHTC multipliers, respectively.

In order to provide additional clarity on the use of the FILMBL and DFFBHTC heat transfer multipliers, several footnotes and additional clarifying information were added throughout the EMF-2103(P), Revision 3 Topical Report as part of the errata pages provided in Reference 2.35.3.

Table 2.35-1 provides the FILMBL and DFFBHTC heat transfer multipliers developed with the EMF-2103(P), Revision 2 (Reference 2.35.2) methodology and the FILMBL and DFFBHTC heat transfer multipliers developed with the EMF-2103(P), Revision 3 (Reference 2.35.1) methodology, respectively.

Table 2.35-2 provides the PDF of the FILMBL heat transfer multiplier developed with the EMF-2103(P), Revision 2 (Reference 2.35.2) methodology and the PDF of the FILMBL heat transfer multiplier developed with the EMF-2103(P), Revision 3 (Reference 2.35.1) methodology, respectively.

Table 2.35-3 provides the PDF of the DFFBHTC heat transfer multiplier developed with the EMF-2103(P), Revision 2 (Reference 2.35.2) methodology and the PDF of the DFFBHTC heat transfer multiplier developed with the EMF-2103(P), Revision 3 (Reference 2.35.1) methodology, respectively.

Table 2.35-1 FILMBL and DFFBHTC Heat Transfer Multipliers

Table 2.35-2 PDF of FILMBL Heat Transfer Multiplier

Table 2.35-3 PDF of DFFBHTC Heat Transfer Multiplier

As addressed in Section 8.4.1.4 of Reference 2.35.1, Section A.2.3.6.5 discusses the reevaluation of the film boiling multipliers and their PDF using the Revision 3 methodology. The reevaluated FILMBL and DFFBHTC multipliers and their associated PDF are given in Sections A.2.3.6.5.1 and A.2.3.6.5.2 of Reference 2.35.3, respectively. Table 2.35-4 summarizes the FILMBL and DFFBHTC multipliers used throughout EMF-2103(P), Revision 3 supporting calculations.

Table 2.35-4 FILMBL and DFFBHTC Heat Transfer Multipliers Used

References:

2.35.1 AREVA Topical Report EMF-2103(P), Revision 3, "Realistic Large Break LOCA Methodology for Pressurized Water Reactors," September 2013.

2.35.2 AREVA Topical Report EMF-2103(P), Revision 2, "Realistic Large Break LOCA Methodology for Pressurized Water Reactors," November 2010.

2.35.3 Letter, Pedro Salas (AREVA Inc.) to Document Control Desk (NRC), "Errata and Revised Sample Problems for EMF-2103P, Revision 3, 'Realistic Large Break LOCA Methodology for Pressurized Water Reactors'," NRC:15:005, January 16, 2015.

3.0 REFERENCES

1. AREVA Topical Report EMF-2103(P) Rev. 3, "Realistic Large Break LOCA Methodology for Pressurized Water Reactors," September 2013.

2. NRC letter from J. G. Rowley (NRC) to P. Salas (AREVA), "Request for Additional Information Related to Review of AREVA NP Licensing Topical Report EMF-2103 Revision 3, Realistic Large Break LOCA Methodology for Pressurized Water Reactors" (Accession No. ML14303A385), November 20, 2014.

3. NRC letter from J.G. Rowley (NRC) to G. Peters (AREVA), "Request for Additional Information Related to Review of AREVA NP Licensing Topical Report EMF-2103 Revision 3, Realistic Large Break LOCA Methodology for Pressurized Water Reactors" (ML15348A140), January 13, 2016.

4. Letter, Pedro Salas (AREVA Inc.) to Document Control Desk (NRC), "Response to Request for Additional Information Regarding EMF-2103(P), Revision 3, 'PWR Realistic Large Break LOCA Methodology for Pressurized Water Reactors'," January 16, 2015.